VSB - Technical University of Ostrava

The Conference Proceedings of the

# Knowledge in Telecommunication Technologies and Optics

## KTTO 2010

Editors: Miroslav VOZNAK, Jan SKAPA

Knowledge in Telecommunication Technologies and Optics 2010 KTTO 2010

Department of Telecommunications, Faculty of Electrical Engineering and Computer Science,
VSB—Technical University of Ostrava, 17. listopadu 15, 708 33 Ostrava—Poruba,
Czech Republic

Authors: collective of authors

First published: Ostrava, 2010, 1st edition
Page count: 224
Publisher: VSB-Technical University of Ostrava
Printed by: VSB-Technical University of Ostrava
Impression: 60 pieces

Not for sale

**ISBN 978-80-248-2330-0**

# Preface

The 10th International Conference on Knowledge in Telecommunication Technologies and Optics took place in Ostrava in December 2010. This event provided a great forum for researchers and scholars who talked about the latest challenges and discussed about their outlooks. Selected papers were accepted for this conference proccedings and the conference provided a chance for attendees to up-to-date on the latest advances in telecommunications and optics.

Miroslav Voznak

KTTO 2010 chairman

# Table of Contents

### *Security in Communications*



### *Network technologies and Services*



### *Applied Electronics in Telecommunications*

# Multimedia

# Asterisk - video recording and playback

## Asterisk multimedia gateway

Lukas Kapicak, Jaroslav Zdralek, Pavel Nevlud
Department of Telecommunications
VSB – Technical University of Ostrava
17. listopadu 15, 708 33 Ostrava, Czech Republic
lukas.kapicak.st@vsb.cz, jaroslav.zdralek@vsb.cz, pavel.nevlud@vsb.cz

***Abstract* — Asterisk is very famous communication server and it is mainly used for audio and video calls but it could have many others applications. We used asterisk features for video calls but our primary object is not switching video calls but automatic recording of these video calls. We are able to record and play video calls as well as we are able to save video calls directly on server. For recording and playback could be used client´s desktop but our primary equipment are mobile end-user devices.**

***Keywords - asterisk; video calls; streaming; recording; playback; 3G networks; smartphones***

## I. INTRODUCTION

Asterisk [1] is open source telephone exchange [5] which brings capability for audio and video calls. Asterisk is software that could be installed on ordinary personal computer and then it turns into communication server. Main functions of Asterisk are establishing audio and video calls, voicemail VOIP gateway etc. [5].

For transmitting video calls Asterisk has native support and it is possible to establish video transmission between two or more sides. Recording videos and playback is not supported by Asterisk. Asterisk has native support for many video codecs for example H.263, H.263p and H.264.

In our configuration we use Asterisk like multimedia video server. Our modified Asterisk has capabilities for saving video calls into the file and afterwards replaying these files to other users through their terminals which support video calls. For completion of user´s terminals could be used desktop computers or mobile devices with appropriate software.

We are able to connect IP cameras with end-users terminals and perform to them streamed video from these cameras. Users are able to watch video captured via their users devices like smartphones or softphones installed on their personal computers.

Our solution is suitable for users in office which apply personal computers for video calls but primary our solution will be addressed to customers using smartphones. Mobile devices support video calls through video service in 3G network [4] but quality of these video calls is not adequate to hardware which are mobile devices equipped. Video quality is poor too.

Mobile devices with open operating system could be upgraded with third party software. Among this software belong VOIP clients and with these VOIP clients we could be directly connected to the Asterisk without any gateways. We could use Wi-Fi connection for access to Asterisk but Wi-Fi does not cover such large areas. For audio and video transmission we could use UMTS networks. These networks have qualities which perform possibility for using VOIP or video calls.

Asterisk with capabilities for recording and playback of video files has PULL and PUSH functions. PULL function needs interaction of end-user, who will choose video on demand. PUSH function on the other side brings capability to other user to choose specific video file and consequently route this video file to the specific end-user or group of the end-users.

## II. TESTING CONFIGURATION

For testing of our solution we have decided to choose only open source software. Operating system is Ubuntu in version 9.10. For testing purposes we have chosen version of Ubuntu for desktop computers, but it could be replaced by a server version.

Communication server was Asterisk in version 1.6.2.6. Ubuntu and Asterisk have not capabilities for playback video files and it is necessary to install FFmpeg. FFmpeg is a complete, cross-platform solution to record, convert and stream audio and video. [6]

Other software, which is necessary for streaming video context, is MPEG4IP. MPEG4IP provides a standards-based system for encoding, streaming, and playing encoded audio, video and text. [7]

FFmpeg and MPEG4IP extend operating system for supporting of multimedia context. For connection Asterisk with FFmpeg and MPEG4IP is needed to install into the Asterisk extension called app_mp4.c. This extension has two parts. One part is mp4play, which brings ability to play video files directly to the end-users device. On the other hand, the second part called mp4save has ability to save video files on the host´s disk or on other storage.

Streaming multimedia contents provide extension called app_rtsp.c. With this extension we are able to connect

streaming contents from IP cameras or VLC player [8] with end-user devices. For our testing purposes we did not use video call service [4] which offers 3G networks. This service has limitations in video quality and resolution of transmitted video contents. We used data connection which offers UMTS networks. Data bandwidth and latency bring us ability to record and play video files with higher resolution compare to video call service [4] implemented in UMTS networks.

## III. CONFIGURATION FOR VIDEO PLAYBACK, RECORD AND STREAMING

Configuration for video playback and a record is similar. We installed Asterisk communication server on personal computer with Ubuntu operating system and end-user devices were connected to this server via local computer network. Smartphones were connected with server via Wi-Fi or UMTS network.

### *A. Video record configuration*

For video record we used smartphone with Android operating system [9] and Ekiga [10] softphone installed on personal computer. Ekiga is multiplatform application and it could be installed on personal computers with Linux and Windows operating systems. Ekiga supports H.261, H263, H263p, H.264, theora and MP4V-ES video codecs. For Android operating we have chosen application IMSDroid [11]. This application has support for the same video codecs like Ekiga softphone.

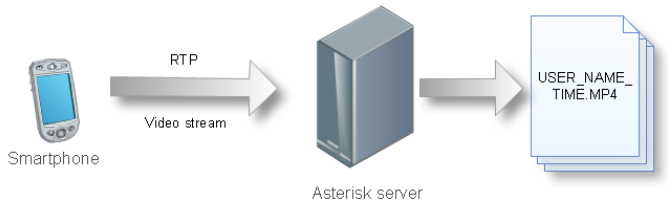


Figure 1: Saving video to file

In Figure 1 you can see our testing configuration for video recording. In our configuration was destination our Asterisk server. In Figure 2 you can see how we set up extension.conf for automatic recording all video files. Recorded video files are tagged with caller ID and time in which was video call established.

```
exten => 784,1,Answer()
exten => 784,2,mp4save(/tmp/${CALLERID(num)}${EPOCH},,D%d:M%m-%H:%M:%S_%$}.mp4)
exten => 784,3,Hangup()
```

Figure 2: extension.conf for saving video to file

If user chooses function “send video”, it is automatically established RTP relation between end-user device and Asterisk and video is saving to the defined storage in extension.conf how it is shown in Figure 2. extension.conf is possible to configure for playback video file which user saves into the server defined storage. For choosing this video file user could use DTMF dialing.

### *B. Video playback configuration*

Video playback could be initiated from two sides. Figure 3 show initialization from user side. End-user could choose video file throw DTMF dialing. This technique has limitations in number of possible choices. If database is too large, the user can not choose video file what he need but it is possible to offer him for example last 10 video files.

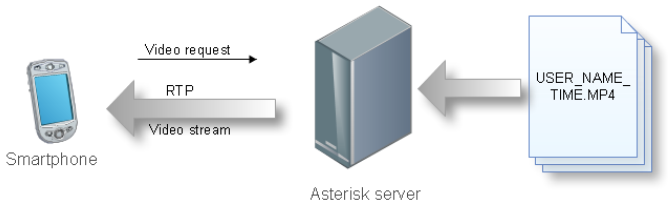


Figure 3: PULL video playback

Configuration file extension.conf for video playback is shown in Figure 4. This configuration file contains information about number which user will call for video playback from server side.

```
exten => 782,1,Answer()
exten => 782,2,mp4play(/tmp/video.mp4)
exten => 782,3,Hangup
```

Figure 4: extension.conf for one file video playback

Figure 5 shows a concept on what we are working at the moment. Choosing of video files will be initiated via the Internet pages and some coordinator could choose demanded video file and this video file PUSH to the end-user device.

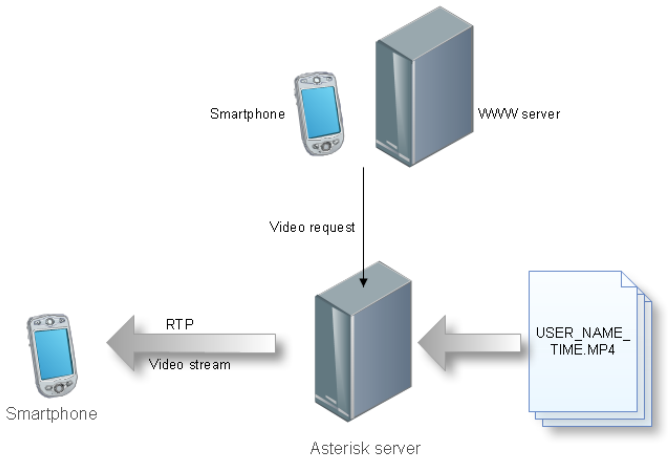


Figure 5: PUSH video playback

End-users with softphones and smartphones will be able to sort out video from database via their web browser and PUSH the video files to their end-user device or they could select device from someone else.

Recorded video is saved in storage in native format with standard codecs. Mobile devices are able to play this video files so user could download this video files to their local storage and then play this video files.

### C. *Streaming video via Asterisk*

Configuration for video streaming is shown in Figure 6 and in extension.conf in Figure 7. For streaming video we need source of streaming content. Between sources of streaming content belong IP cameras or media players with streaming support. Between these media players belongs for example VLC media player [8]. IP cameras and media players have to support streaming in codecs which support Asterisk and VOIP clients in their end-user devices.

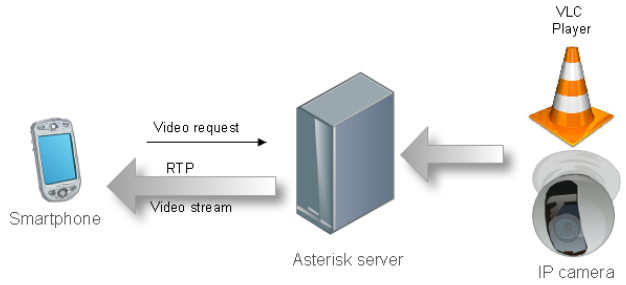


Figure 6: PULL initialized streaming to host

```
exten => 783,1,Answer()
exten => 783,2,Rtsp(rtsp://192.168.1.41/live.sdp)
exten => 783,3,Hangup
```

Figure 7: extension.conf for PULL initialized video streaming to host

In Figure 8 you can see that Asterisk could perform streaming content to more end-users. End-users could select specific IP camera or media player through dialed number. Thanks to web pages it is possible to initialize PUSH technology and send video from specific IP camera or multimedia player to end-users devices.

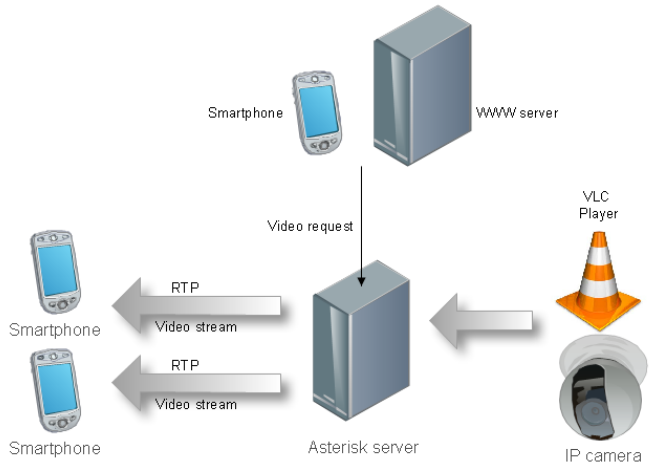


Figure 8: PUSH initialized streaming to multiple hosts

## IV. RECORD, PLAYBACK AND STREAMING IN MOBILE NETWORK

Smartphones or mobile phones support video calling in 3G networks. Resolution and quality of these video calls has limitations because video call is standardized service with channel capacity only 64 kbps. If we want to transmit video like a 3G video call between Asterisk and end user devices, we need gateway to PSTN [3] network.

For video transmission we do not use 3G video call service. We use only data transmission. UMTS networks have enough network capacity for video transmission [4].

With our solution we are able to transfer video in 2G networks via EDGE [2] [3].

## V. CONCLUSION

Asterisk is very famous communication server. It has the support for switching voice and video calls through number of audio and video codecs. Unfortunately, Asterisk has no capabilities for recording and playback video files.

Our solution is primary designed for customers using smartphones. These customers could apply their end-user devices for recording video and immediately save this video files to server. In end-user devices is not necessary a large storage memory because video is not saving into their storage but it is saving directly on the server side. Other users have this video immediately available.

Asterisk with program mp4play could play video files saved on server storage directly in the end user equipment. From Asterisk log we even know if user received this video and then we have backwards control if user received video call from server.

Now we are working on connection between Asterisk and web server. With this connection it will be easy to choose video from database and PUSH this video directly to the end user device.

The paper focuses mainly on video transfer to or from the mobile end user devices over a wireless network. The video quality is important for end users, so the next challenge will be to assess the quality of transmitted video.

## ACKNOWLEDGMENT

The research leading to these results has received funding from the European Community's Seventh Framework Programme (FP7/2007-2013) under grant agreement no. 218086.

## REFERENCES

[1] Jim Van Meggelen, Jared Smith, Leif Madsen, “Asterisk: The Future of Telephony,” O'Reilly Media, pp. 15 - 48, September 2005. ISBN 978-0-596-00962-5.

[2] Timo Halonen, Javier Romero, Juan Melero, “GSM, GPRS and EDGE Performance Evolution Towards 3G/UMTS,” 2.edition, West Sussex, England: John Wiley & Sons, Ltd, 2003, pp. 11, 14, 49. ISBN 0-470-86694-2.

[3] Jörg Eberspächer, Hans-jörg Vögel, Christian Bettstetter, Christian Hartmann, “GSM-Architecture, Protocols and Service,” 3.edition, West Sussex, England: John Wiley & Sons, Ltd, 2002, pp. 58, 108, 139, 212, 234, 264, 266. ISBN 978-0-470-03070-7.

[4] Holma, Toskala, “HSDPA/HSUPA for UMTS,” 1. edition, West Sussex, England: John Wiley & Sons, Ltd, 2006, p. 31 and 61. ISBN 0-470-01884-4.

[5] Asterisk; Asterisk: Open source communication, asterisk.com. http://www.asterisk.org/applications (2010-11-15)

[6] FFmpeg; FFmpeg cross platform video solution: documentation. http://www.ffmpeg.org/about.html (2010-11-15)

[7] MPEG4IP Project; MPEG4IP Project documentation. http://mpeg4ip.sourceforge.net/documentation/index.php (2010-11-15)

[8] VLC Player; Video LAN features. http://www.videolan.org/vlc/features.html (2010-11-15)

[9] Android developers; Core media formats; Android developers. http://developer.android.com/guide/appendix/media-formats.html (2010-11-15)

[10] Ekiga softphone; Ekiga softphone features. http://ekiga.org/ekiga-softphone-features (2010-11-15)

[11] IMSDroid; IMSdroid features. http://code.google.com/p/imsdroid/ (2010-11-15)

# Possibilities of Using an Embedded Accelerometer in Mobile Device Applications

Ondrej Krejcar, Jindrich Cernohorsky
Department of Measurement and Control, Center for Applied Cybernetics,
Faculty of Electrical Engineering and Computer Science
VSB Technical University of Ostrava
*17. Listopadu 15, 70833,*
*Ostrava-Poruba, Czech Republic*
*ondrej.krejcar@remoteworld.net,*
*jindrich.cernohorsky@vsb.cz*

Martin Vanek
Department of Measurement and Control,
Faculty of Electrical Engineering and Computer Science
VSB Technical University of Ostrava
*17. Listopadu 15, 70833,*
*Ostrava-Poruba, Czech Republic*
*martin.vanek@vsb.cz*

***Abstract -*** The purpose of this project is to utilise an accelerometer integrated into mobile systems. The accelerometer is a motion sense module which is placed i.e. inside a mobile phone. This mobile phone is then able to recognize self in which position it is located. Consequently, it is capable of i.e. turning the display portrayal by 90 degrees. The desirable outcome of this project is a methodology which describes an implementation of accelerometer module into new developed application that enables the access to data which the accelerometer provides. On the basis of this received data i.e. the location of the mobile system could be obtained. This knowledge may be used in a various case of ubiquitous information systems to improve user's state base as well as to support some kind of decision methods implemented in.

***Keywords - accelerometer; gravitation chip; G-senzor; motion sensor;***

## I. INTRODUCTION

The accelerometer is a sensor which uses the mass momentum for measuring the difference between kinematic acceleration (with regard to a specific inertial space) and gravity acceleration [1]. In articles, terms such as gravity chip, accelerometer, G-sensor or motion sensor are to be found. However, it is still the same matter. Furthermore, the most accurate term is still the accelerometer. This term may be freely translated as a measuring instrument (or sensor) of acceleration.

The accelerometer is an apparatus which measures vibrations or acceleration during the movement of structures. The force that inflicts the vibrations or change in movement (acceleration) takes effect on the mass of transducer which compresses piezoelectric element that generates electric charge which is comparable to compression. The electric charge is proportional to force and the mass of transducer are constant. Therefore, the electric charge is also proportional to the acceleration.

Several types of accelerometers which function on variety of principles and are produced by different production technologies may be found in stores nowadays.

Owners of communicators may use the advantages of accelerometer i.e. through using Opera Mobile or while browsing images. Due to mobile Windows, other applications and utilities start to appear. These shift the options of motion sensor further.

## II. HTC LIBRARY

The accelerometer is widely used in Apple iPhone, where it is applied in mobile entertainment and therefore, several games use it. This is the same for Windows Mobile.

Library HTCSensorSDK.dll is used for working with G-sensor. Beside the availability of this library a great help while solving this assignment was the code listed on the internet blog http://blog.enterprisemobile.com [2].

It is necessary to mention that an algorithm which uses the library that arranges data from motion sensor of an apparatus is functioning only on the basis of operating system Windows Mobile 6. Compilation and running of this application was not successful in previous versions.

A class HTCGSensor is a component of the code mentioned above. This class enables us to pick up and use the status of G-Sensor in a device.

The following section of the code is major for gaining data from sensor.

```
[DllImport("HTCSensorSDK")]
extern static IntPtr HTCSensorOpen(HTCSensor
sensor);
[DllImport("HTCSensorSDK")]
extern static void HTCSensorClose(IntPtr
handle);
[DllImport("HTCSensorSDK")]
extern static IntPtr
HTCSensorGetDataOutput(IntPtr handle, out
HTCGSensorData sensorData);
IntPtr hEvent = CreateEvent(IntPtr.Zero,
true, false, "HTC_GSENSOR_SERVICESTOP");
SetEvent(hEvent);
CloseHandle(hEvent);
```

```
IntPtr hEvent = CreateEvent(IntPtr.Zero,
true, false, "HTC_GSENSOR_SERVICESTART");
SetEvent(hEvent);
CloseHandle(hEvent);
```

With the help of this algorithm we are capable of running the application for reading information. The information is gained on the basis of the indicator that shows the position in memory, where this information is stored. After reading required data the application is closed. It is very important to reinstate everything after closing the application. This means to reset all used variables.

Obtained information is only sequences of bytes, which is why this information is later decoded.

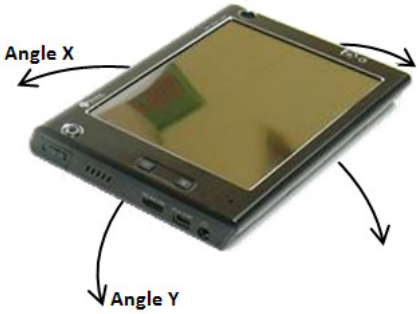


Fig. 1.: Rotation of device with shoved angles.

By using the mentioned method GetRawSensorData, we can get the measures directly from the motion sensor in the range from approximately -1000 to 1000, which this method returns back. This method then returns the values of axis X, Y and Z.

Nevertheless, the output values of the acceleration in particular axis in the range from -1000 to 1000 are not very concrete and it is hard for anyone to imagine a particular acceleration. Therefore, received data in this code from G-sensor were given sense of the real world and gained measures are transferred into appropriate gravity acceleration in m $s^{-2}$ units. If the apparatus is at rest, it returns the vector length 9,8, which is an approximate value of gravity acceleration that has the theoretical value of 9,823 m $s^{-2}$ on the world's surface. The size of gravity acceleration is slightly different (in hundredths of m $s^{-2}$) in various places; its value on the equator is smaller and towards Poles becomes bigger. This is caused by the size of the centrifugal force which is formed by world's rotation that is the greatest on the equator and smallest on Poles. The negotiated middle value of gravity acceleration, which means normal gravity acceleration is g = 9,80665 m $s^{-2}$.

Aside from these three outputs GetRawSensorData method offers also values of an angle displacement of apparatus for axis X and Y. The value of a tilt angle of apparatus for axis X and Y changes as follows:

- If the apparatus lies on a horizontal base with its display upwards (position FaceUp), the method GetRawSensorData returns the angles' zero values for both axis.
- If the apparatus is held as shown on the image 1. and is gradually turned in a direction of the arrow to the right, the value of an angle X would be increasing from 1° to 360°. On the image 2. an apparatus is shown which is turned approximately by an angle 295° in the direction of axis X.
- If the apparatus is turned forward, the value of an angle Y would be increasing from 1° to 360°.


Fig. 2.: Rotation of device - angel = 295°.

This method is also used by method GetGVector. Class HTVGSensor also offers following methods, characteristics and occurrences:

**GetGVector**

It returns the length of the vector which describes the direction of gravity acceleration in relation to the display of the apparatus. This method then returns the value of gravity acceleration due to particular axis X,Y and Z. In order to get data from sensor, it uses the previous algorithms and just adjusts them into an interval between –9,8 and +9,8.

If the apparatus is faced upward (by its main display) on a horizontal base (Fig. 3), the method would return values 0, 0, -9,8. The value for Z = -9,8 means that acceleration is in an opposite direction in relation to the orientation of the screen.

If the apparatus is held in a vertical position, this method returns values 0, -9,8, 0 (Fig. 4). The value for Y = -9,8 means that the apparatus speeds up in the direction from the bottom part of the screen.

On the other hand, if the apparatus is held in a vertical position, so the upper part is facing down, the method returns 0, 9,8, 0.

The returned vector has a measured length in units of gravity acceleration, thus in square meter per second (m $s^{-2}$).

In an ideal case, where the apparatus is motionless, the value of the length of the returned vector should be 9,8, thus the constant of gravity acceleration. Nevertheless, the sensor is not extremely accurate, therefore this case almost never

happens and the length of the returned vector's direction of acceleration would be around the value 9,8.

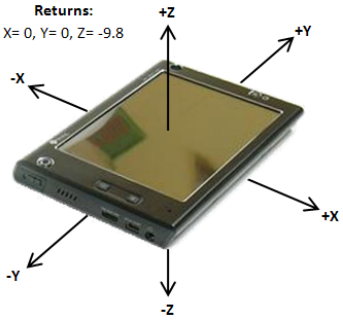


Fig. 3.: Device in face up mode.

**Orientation**

Actual obtained orientation of an apparatus returns one of the following listings of basic orientations:

- Landscape,
- ReverseLandscape,
- Portrait,
- ReversePortrait,
- FaceDown,
- FaceUp.

**OrientationChanged**

This occurrence is evoked always when the apparatus changes its orientation.

Class GSensor, which provides methods described in a previous part of the text, was necessary to add to references of the testing system while creating the application for testing.

The testing application whose appearance is shown in (Fig. 6. 7.), uses previously mentioned methods and excerpts them on the apparatus's display. User has the possibility to choose which values of accelerometer he wants to portray. User might choose among values directly excerpted from sensor or values converted to gravity acceleration.

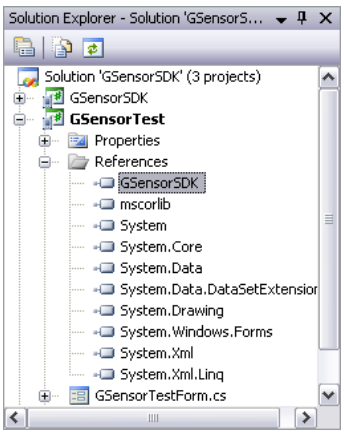


Fig. 5.: References of test application

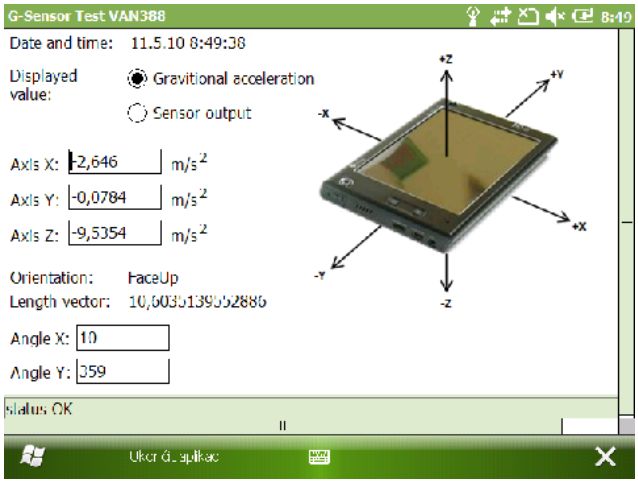


Fig. 6.: Test application in runing mode

Fig. 7.: Test application

Aside from the excerpt of the received values from accelerometer on display of the apparatus, saving of these values into the set GSensor_log.csv happens in regular time periods.

CSV (Comma-separated values) is a simple file format dedicated for the exchange of table data. The file in CSV format is made of rows in which particular elements are separated by a sign comma (,). Values of elements might be closed into quotation marks ("), which enables the text of the element to contain comma.

The option with semi-colon (but still called CSV) is used by i.e. Microsoft Excel in a Czech version Microsoft Windows. This option is used in a testing application.

| | A | B | C | D | E | F | G | H |
|---|---|---|---|---|---|---|---|---|
| 1 | Date, Time | Screen orientation | Output - Axis X | Output - Axis Y | Output - Axis Z | Output type | Angle X | Angle Y |
| 2 | 10.5.2010 22:08 | FaceUp | -0,1274 | -0,0196 | -10,0156 | Grav. Accelration | 0 | 359 |
| 3 | 10.5.2010 22:09 | FaceUp | -0,1274 | -0,0196 | -10,0254 | Grav. Accelration | 0 | 359 |
| 4 | 10.5.2010 22:09 | FaceUp | -0,1274 | -0,0196 | -10,0058 | Grav. Accelration | 0 | 359 |
| 5 | 10.5.2010 22:09 | FaceUp | 3,5868 | -0,1274 | -9,3492 | Grav. Accelration | 11 | 359 |
| 6 | 10.5.2010 22:09 | FaceUp | -1,519 | -0,0098 | -10,9564 | Grav. Accelration | 0 | 347 |
| 7 | 10.5.2010 22:09 | FaceUp | 0 | 0 | -1022 | Sensor output | 12 | 14 |
| 8 | 10.5.2010 22:09 | FaceUp | 108 | 0 | -1001 | Sensor output | 346 | 346 |
| 9 | 10.5.2010 22:09 | Landscape | 541 | 4 | -780 | Sensor output | 315 | 0 |
| 10 | 10.5.2010 22:09 | Landscape | 728 | 6 | -600 | Sensor output | 305 | 0 |
| 11 | 10.5.2010 22:09 | Landscape | 871 | 7 | -420 | Sensor output | 291 | 0 |
| 12 | 10.5.2010 22:09 | FaceUp | -11 | -3 | -1022 | Sensor output | 0 | 359 |
| 13 | 10.5.2010 22:09 | FaceUp | -12 | -3 | -1022 | Sensor output | 0 | 359 |
| 14 | 10.5.2010 22:09 | FaceUp | -13 | -2 | -1023 | Sensor output | 0 | 359 |
| 15 | | | | | | | | |

Fig. 8.: Formated output - GSensor_log.csv

On the image 8, an example of an output to a file GSensor_log.csv is shown. The example shown on the picture is already formatted using SW Microsoft Office Excel and gained basic information is there. On the last rows the output of accelerometer is shown in a time, when the apparatus lies on almost horizontal base faced upward.

## III. Possibilities of Using Embedded Accelerometer in Mobile Device Applications

Previous chapters deals with a accelerometers theory and implementation issues in managed code by previous chapters deals with a accelerometers theory and implementation issues in Visual Studio by managed code in C# language.

Authors in several journal papers [3], [4], [5] describes an implementation and theory of accelerometers in biomedical area. Therefore they describe a biomedical signal processing; accelerometers can play as a type of biomedical signal too [9].

Embedded or remote accelerometers can be used in embedded platforms for data measuring or as another source information of satellite images as described in [11] resp. [10].

Due to a fact, that accelerometers are embedded in modern mobile devices (along with proximity sensors, light sensors etc.) they can play a stronger role in near future by use a genetic algorithms [6].

Mobile device equipped with embedded accelerometers can be use in outdoor area in electrical distribution networks [7] or in public lighting area [8] for detection of possible vibrations in some extreme cases.

## IV. Conclusions

A methodology which describes an implementation of accelerometer module into new developed application that enables the access to data which the accelerometer provides was described. A special HTC library was also covered with a focus to their use in program code. In real project is therefore possible to obtain the location of the mobile system on the basis of received data. This knowledge may be used in a various case of ubiquitous information systems to improve user's state base as well as to support some kind of decision methods implemented in.

## References


[1] Using HTC Diamond's Accelerometer/Sensor SDK from Managed Code by Enterprise Mobile. [online]. 2010 [accessed 2010-04-20]. <http://blog.enterprisemobile.com/2008/07/using-htc-diamonds-sensor-sdk-from-managed-code/>.

[2] Akcelerometr: RobotWiki. [online]. [accessed 2010-04-19]. < http://wiki.kn.vutbr.cz/robot/index.cgi?akcelerometr >.

[3] Idzkowski A., Walendziuk W. (2009) Evaluation of the static posturograph platform accuracy, Journal of Vibroengineering, Volume 11, Issue 3, 2009, pp.511-516, ISSN 1392 - 8716

[4] Idzkowski A., Walendziuk W. (2009) Portable acquisition system for domiciliary uroflowmetry, Journal of Vibroengineering, Volume 11, Issue 3, 2009, pp.592-596, ISSN 1392 – 8716

[5] Vasickova, Z., Augustynek, M., New method for detection of epileptic seizure, Journal of Vibroengineering, Volume 11, Issue 2, 2009, pp.279-282, (2009) ISSN 1392 - 8716

[6] Kromer P, Snasel V, Platos J, Husek D. GENETIC ALGORITHMS FOR THE LINEAR ORDERING PROBLEM, NEURAL NETWORK WORLD, Vol. 19, Issue 1, pp. 65-80, 2009 ISSN: 1210-0552

[7] Gono R., Kratky M., Rusek S., Analysis of Distribution Network Failure Databases, PRZEGLAD ELEKTROTECHNICZNY, Vol. 86, Issue 8, pp. 168-171, 2010 ISSN: 0033-2097

[8] Litschmannova M., The methodology for the evaluation of energy savings' states of the public lighting, PRZEGLAD ELEKTROTECHNICZNY, Vol. 84, Issue 8, pp. 65-67, 2008 ISSN: 0033-2097

[9] Peterek, T., Zurek, P., Augustynek, M., Penhaker, M (2009) Global courseware for visualization and processing biosignals, WORLD CONGRESS 2009 - MEDICAL PHYSICS AND BIOMEDICAL ENGINEERING, Munchen

[10] Brad, R., Satellite Image Enhancement by Controlled Statistical Differentiation, In INNOVATIONS AND ADVANCED TECHNIQUES IN SYSTEMS, COMPUTING SCIENCES AND SOFTWARE ENGINEERING, International Conference on Systems, Computing Science and Software Engineering, ELECTR NETWORK, DEC 03-12, 2007, pp. 32-36

[11] Machacek, Z, Srovnal, V., "Automated system for data measuring and analyses from embedded systems", In 7th WSEAS International Conference on Automatic Control, Modeling and Simulation, Mar 13-15, pp. 43-48, Prague, Czech Republic (2005)

# Web-based Call Forwarding Management

Jiri Vychodil, Karel Tomala, Filip Rezac, Jan Rozhon, Miroslav Voznak
Department of Telecommunications
VSB – Technical University of Ostrava
Ostrava – Poruba, Czech Republic
jiri.vychodil@vsb.cz, karel.tomala@vsb.cz, filip.rezac@vsb.cz, jan.rozhon@vsb.cz, miroslav.voznak@vsb.cz

*Abstract*— **A lot of companies offer a full-time support for their customers and specified phone numbers are reserved for this purpose. Because the service is often served by different employee during the day, there is a need of a service-desk, which offers a redirection of customer's calls. A majority of big companies use their own systems which can ensure this. But many small ones can use simpler and cheaper systems based on Asterisk. We have developed a redirection system, which is created by a PBX Asterisk and webserver Apache. The system offers call redirection and a voicemail with possibility to set up conditions when the voicemail should be used. We consider future improvement and another possibilities of the created service desk at a conclusion.**

***Keyword: Asterisk; Call redirection; Voicemail; Management; Call forwarding***

## I. INTRODUCTION

Currently, voice services are increasingly carried out and grouped into complete communication solutions. PBX is used to process local calls within the organization and distribute calls to each participant. The basic advantage of the system based on the PBX is an optimal processing of incoming calls when the calls are always routed to the competent party. These systems must ensure the optimum balance between functionality, scalability and quality on the one hand, and the system cost on the other. Telephone PBXs are commonly used in both small and large businesses, offices, schools and so on.

These institutions also often use access directory servers using Lightweight Directory Access Protocol (LDAP). Access names and passwords for each user are stored in them. LDAP offers more options as imposing residence, birth dates, telephone numbers, and many other records. It is a phone number, what is crucial for our work. This paper brings a solution where a typical user can easily set up his voicemail service for phone records and eventually send a mail with the recorded entry in the attachment.

## II. STATE OF ART

There are many ways how to realize software voicemail which could be controlled by user. We can use solutions that are provided by already created systems, or it is possible to create our own. Each way has its advantages and disadvantages. The greatest asset of the already developed ones is their easy implementation without having to implement anything. FreePBX tool uses a web portal ARI (Asterisk Recording interface) that allows users to configure many features of their assigned numbers. ARI allows call forwarding and system settings, including sending an email alert with voice entry.

Unfortunately, there is a disadvantage in this solution, because integrated voicemail service is subject to higher overhead of the superior systems and configuration may not always be easy. In terms of convenience, it is better to integrate these services into one system, which is certainly used by every institution. This is the goal of our work. Our solution is not integrated into any bigger information system, but implements a simple solution to control services. When using an appropriate interface between the PBX and information system (IS), there is a possibility to link these two units and create a solution tailored to each. And IS developers do not have to know the details and problems of routing calls, data logger settings etc.

## III. DESIGN METHODOLOGY AND OBJECTIVES

The system uses the LAMP as a Web user interface as well as connections to the Asterisk PBX (PBX) and the LDAP server [1-6]. LAMP is an acronym for free software used as a platform for implementing dynamic Web site (Linux, Apache, MySQL, PHP). At this stage of development, however, MySQL database is not used. LDAP server is used external, we do not record, edit nor add any enters into the database, we just use it. We can imagine LDAP like a protocol for storing and accessing data on a directory server. Under this protocol, the individual items are stored in the form of records arranged in a tree structure.

The most significant feature of LDAP is the authentication function. We assume that the records contain the login name, password, email address, private and business telephone number. One business number can be assigned to more than one person. The advantage is that the user name and password can be used to access to multiple services.

Furthermore, we assume that there is a complete routing dialplan created including the public telephone network in the PBX. Asterisk Dialplan is the core. It is a configuration that specifies how Asterisk should handle calls. Dialplan is stored in a file */etc/asterisk/extension.conf*. This file is independent of the technology, which is one of the strengths of Asterisk. We will not deal with developing of this plan, we only modify parts needed to build the system [1], [2], [9].

## IV. Features Of Implementation

The system is designed with an emphasis on comfort and ease of use. After logging into the system via a Web interface using your username and password, the list of business phone numbers is shown. It is also displayed if any number is redirected to a private number or to voicemail. The user can set the following divert alternatives for each number:

- Do not redirect
- Redirect to private number
- Hang up if not available
- Redirect to voice mail if not available
- Redirect to voicemail unconditional

It is clear that if one phone number is shared by several people, such as there is only one telephone line in the office, this number could not be forwarded. The question is, what number will be allowed to divert. One answer is: any that the system recognizes as valid. Our implemented solution allows users to redirect calls only on a users private number stored in LDAP. However, this decision may be relatively simply changed in the PHP code. Figure 1 shows the basic concept of a Service Desk.

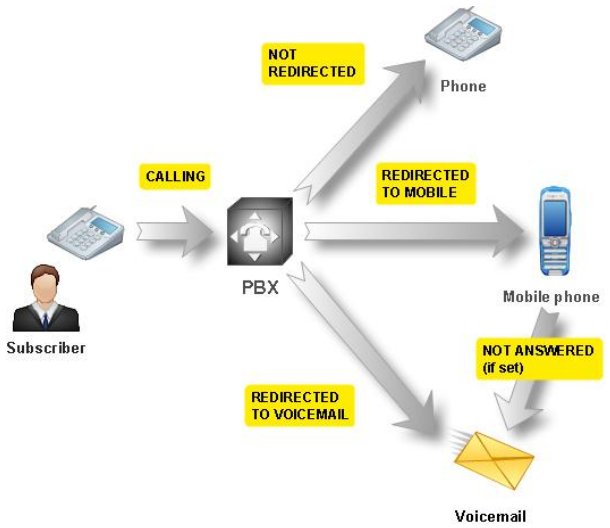


Figure 1. Scheme of service desk

If the situation shown in Figure 1 occurs - the call forwarded to mobile number will not be answered; the PBX routes a caller to the answering machine so the caller can record a message. After the calling party leaves a message on the answering machine, the Asterisk PBX will send an email with an attachment to unavailable subscriber (see Figure 2).

## V. Methods

How the webserver works: as mentioned hereinbefore, the server does not use its own database, but get the user information from the LDAP server. Server enters commands to the PBX via the PBX's command line. These commands represent entering data for the PBX database. The server does not change the PBX configuration files in any case.

Calls are managed through the PBX dialplan. For each incoming call, the server confirms whether there is a record in a database to redirect. According to the record, the server redirects the call either to number or to voicemail.

Example of *extensions.conf*:

```
exten => _1XXX,1,Set(called=${EXTEN})
exten =>
 _1XXX,n,Set(number_to=${DB(redirect/${cal
 led}/number)})
exten =>
 _1XXX,n,GotoIf($[$[number_to]]?redirect)
exten =>
 _1XXX,n,Set(voicemail=${DB(redirect/${cal
 led}/voicemail)})
exten =>
 _1XXX,n,GotoIf($[$[voicemail]]?voicemail)
exten => _1XXX,n,Macro(dial,${called})
exten =>
 _1XXX,n(redirect),Macro(redirect,${number
 _to})
exten =>
 _1XXX,n(voicemail),Macro(voicemail,${call
 ed})
```

The institution has a four-digit service numbers starting with the “1”. When a call is initiated to this number, the number is stored in the variable "called". The variable "number_to" should have a value of number read from database, where the Call is forwarded to. If no such record exists, the variable will be blank. If it exists, in the next step, the condition is valid and dialplan goes to a label "redirect". Then macro named “redirect” serves call according to forwarding settings. Similary dialplan works in the case where the call is routed directly to the voicemail, or if no redirect is set.

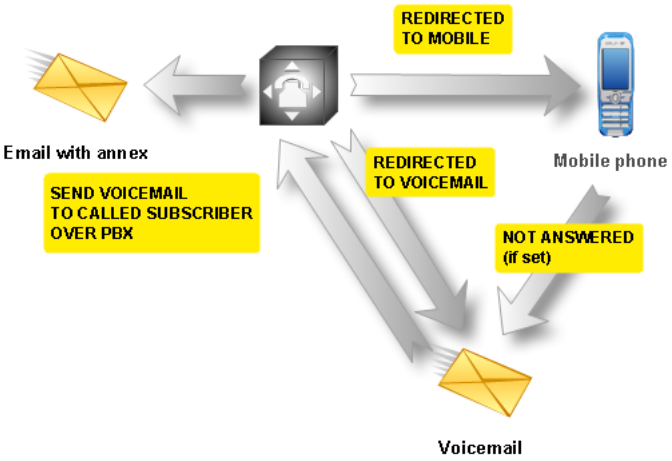


Figure 2. Transfer of voicemail

Figure 3 shows a graphical diagram that describes the principle of routing using the database.

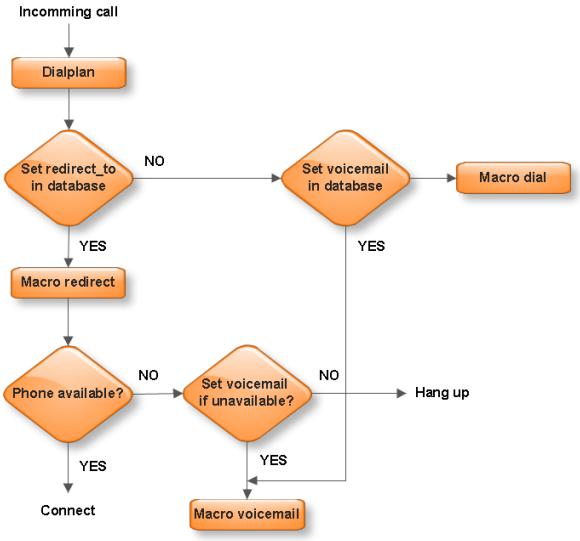


Figure 3. Diagram of call transfer

Example of *voicemail.conf*:

```
1203 => 6520, Jan Novak,
 jan.novak@email.com, ,attach=yes|
 delete=yes
```

Mr. Novak's voicemail. Mr. Novak does not use the password "6520" to access the mailbox, the message will be send by mail as an attachment and immediately deleted from the voicemail. This box must be created for all persons in LDAP, which can divert the calls.

Example of database:

```
/redirect/1203/number_to    420728457142
/redirect/1541/voicemail          yes
```

The user with number 1203 has redirected his calls to 42072857142, the user with number 1541 set that his incoming calls will be forwarded directly into his voicemail. His e-mail address is not stored in the database.

After the user set the redirection, web server execute command:

```
exec("sudo asterisk -rx 'database put
 redirect $redirect[number]
 $redirect[number_to]'");
```

which put an information into the asterisk's database, that "number" is redirect to "number_to". Users using a web interface have no rights to interfere in Asterisk PBX.

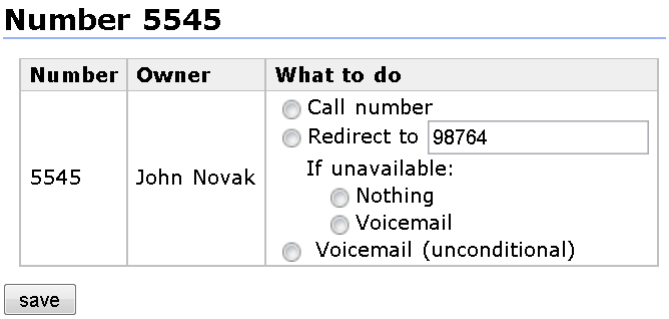


Figure 4. Web interface of setting up the redirection

All official telephone numbers are created in configuration *sip.conf* file as "extensions". To be able to transfer the call to voicemail, this extension must have the mailbox created in a *voicemail.conf* file. The system itself does not ensure this, a PBX administrator has to make these steps. This is strongly recommended to take into account only data from the LDAP server when creating these configuration files. This will ensure the integrity of the system and management will be easier.

## VI. Conclusion

We developed a system that provides to users of a corporate phone system possibility to easy redirect calls routed to their phone company. Settings are done via a simple web interface using a login name and password verified against the LDAP server. This system was already implemented and applied in a company, which offer full-time support for its customers. The operator of the company can set the redirection based on which of the employee is on duty and users can add a phone numbers of their choice. The advantage is that they do not have to contact the administrator. There is a possibility of extension for the voice mailbox for the customers. They could choose whether they want to send a message in email attachment or just send an email to notify new messages in the mailbox or not to send any notification.

From the system implementation point of view, it would be great for PBX administrators when the system will be connected to LDAP directly. For example the administrator could find the system user name in LDAP and through the Web interface create an account and voicemail. If the PBX administrator manages the LDAP, he could establish extension number in a dialplan and in LDAP at the same time. There is also a possibility of using an Asterisk Realtime Architecture (ARA). In this case, no settings are saved in configuration files, but in the database (eg. MySQL). PHP cooperation and PBX could be improved because for the larger settings, the changes would be implemented in the database, which is far easier than edit files. Another possible improvement of the system is voice recognition integration. This would lead to more options when recorded messages could be sent to the user in text form via email or only via SMS alert just with the beginning of the message.

Integration with another system, which is already used by any company is also possible. It would increase convenience for users who do not have to use another web portal.

Our solution is made fully operational, however, offers many directions for expansion.

## ACKNOWLEDGMENT

The research leading to these results has received funding from the European Community's Seventh Framework Programme (FP7/2007-2013) under grant agreement n° 218086.

## REFERENCE

[1] MEGGELEN, J., SMITH J., MADSEN L. *Asterisk The Future of Telephony.* 2nd ed. O'Reilly Media, 2007.

[2] CHOCHELINSKU, R., BARONAK,I. *Private Telecommunication Network Based on NGN*, 32nd International Conference on Telecommunications and Signal Processing, AUG 26-27, 2009 Dunakiliti, HUNGARY.

[3] NIXON, R. *Learning PHP, MySQL, and JavaScript*, 1st ed. O'Reilly Media, 2009.

[4] CARTER, G. *LDAP System Administration,* 1st ed. O'Reilly Media, 2003.

[5] BOWEN, R. Apache Cookbook, 2rd ed. O'Reilly Media, 2007. s. ISBN 978-0-596-52994-9.

[6] DUBOIS, P. *MySQL Cookbook.* 2nd ed. O'Reilly Media, 2007. s. ISBN 978-0-596-00145-2.

[7] PRAVDA, I., VODRAZKA, J., *Voice quality planning for NGN including mobile networks*, 12th International Conference on Personal Wireless Communications (PWC 2007), SEP, 2007 Prague, CZECH REPUBLIC

[8] KOCUR,Z.,MACHULA,V.,KULDA,J.,VOJTECH,J. *Analysis of Influence of Disturbance Level on Data Transmission in Wireless Networks.* In TSP 2010 - 33rd International Conference on Telecommunications and Signal Processing. Budapest: Asszisztencia Szervező Kft., 2010, p. 292-296.

[9] VOZNAK,M. , RUDINSKY,J. *Alternative Methods of Intelligent Network Service Implementation in IP Telephony*, The 14th WSEAS International Conference on COMMUNICATIONS ,p.204-207, Corfu, July 23-25,2010

# Speech Quality

# Erlang Formulas and Next Generation Networks

Erik Chromy
Department of Telecommunications, Faculty of Electrical Engineering and Information Technology
Slovak University of Technology
Bratislava, Slovak Republic
chromy@ktl.elf.stuba.sk

*Abstract*— **The paper deals with the possibility of the Erlang B and Erlang C formula utilization in Next Generation Networks (NGN). Based on the common properties of synchronous and asynchronous networks it is possible the utilization of Erlang formulas also for asynchronous networks. It is possible to describe traffic in NGN networks by calculation of following parameters – loss, link utilization and bandwidth.**

***Keywords-Erlang B formula; Erlang C formula; Next Generation Networks; QoS***

## I. INTRODUCTION

Much attention is focused on description of traffic in asynchronous packet networks (represented by ATM and IP networks). There are various methods for traffic description. Many of them are complex with high computational requirements. The description by Markov chains is one of them. Therefore the Erlang formulas can be very efficient and simple way how we can describe traffic parameters in asynchronous networks.

Erlang formulas use traffic parameters such as loss, probability of delay, bandwidth and link utilization. These parameters are especially important from the Quality of Service (QoS) [8], [10] providing point of view. Hence the Erlang formulas seem to help us in the field of Quality of Service in Next Generation Networks (NGN). This paper focused on ATM and IP networks [7] today used mainly as backbone networks for NGN.

Erlang theory is described in detail in [3], [4], [13], [16].

## II. ATM NETWORKS

Asynchronous Transfer Mode (ATM) was the emerging network technology in the beginning of 90-ties. The main reasons for ATM development were:

- Increasing demand for telecommunication and information technologies and services.
- Convergence of data and voice communication.

ATM networks are connection oriented networks. ATM technology combines fast packet transfer with synchronous transfer through virtual circuits and virtual paths. It is cell switching mode which offers low transfer latency with high level of Quality of Service and ensures the support for voice, data and video service with high transfer rates.

## III. IP NETWORKS

Networks based on Internet Protocol (IP) provide datagram service. IP transfer is non-connection oriented and its main feature is that it is best effort service. It means that the packet will be transferred in the best way, without forced delay and without unnecessary packet losses. The transfer of IP datagrams is done without guarantee of packet delivery [2], [6].

Services such as voice and real-time video are very sensitive on particular traffic parameters. The main of these parameters are delay, loss and error rate. We have to note that various types of services have also different bandwidth requirements. Therefore there is need for guarantee of these parameters. This guarantee is called Quality of Service.

QoS requirements are: end-to-end delay, jitter, packet losses, bandwidth, link utilization.

## IV. ERLANG FORMULAS

Two Erlang formulas (B and C) are used to describe the traffic in asynchronous networks. Calculations were performed in Matlab environment.

### A. The Erlang B Formula

The Erlang B formula represents the ratio of lost calls. Therefore it is sometimes called “loss Erlang formula”. It is defined as follows:

$$B = \frac{\frac{A^N}{N!}}{\sum_{k=0}^{N}\frac{A^k}{k!}} = \frac{A^N}{N!}\cdot\frac{1}{1+A+\frac{A^2}{2!}+\frac{A^3}{3!}+\ldots+\frac{A^N}{N!}} \qquad (1)$$

where:

$B$ - ratio of lost calls [%],

$A$ - total offered traffic [Erl],

$N$ - number of channels (links).

The first Erlang formula can be written also in the following form:

$$B = \frac{1}{1+\sum_{k=1}^{m}\left(\frac{N}{A}\right)\cdot\left(\frac{N-1}{A}\right)\cdots\left(\frac{N-k+1}{A}\right)} \quad (2)$$

The use of the equation (2) can significantly decrease the computational requirements and we can also calculate the load of the system with the higher values [3, 4].

The following conditions must be met for the first Erlang formula:

- The flow of requests (calls) originates randomly with exponential distribution of incoming requests, which means the higher distance between requests, the lower number of these cases.
- Service time has similar distribution, i.e. exponential decreasing of requests with higher service time.
- The flow of requests is steady, as if it comes from infinite number of request sources.
- There is full availability of requests to all served links.
- Rejected requests do not return to incoming flow, therefore there are not repeated requests.
- No two requests will originate together [3].

IP traffic brings radical changes into telephone networks. The condition 2 is not fulfilled. And because the traffic from one source is considerable increasing, also the condition 5 can not be met.

### *B. The Erlang C Formula*

The Erlang C formula also assumes infinite number of traffic sources. These sources generate the traffic A for N lines. The incoming request is inserted into waiting queue if all links N are occupied. Waiting queue can store infinite number of requests concurrently. This Erlang formula calculates probability of creation of waiting queue in the case of traffic A, and if it is assumed that the blocked calls will remain in the system until they are served [3].

$$C = \frac{\frac{A^N}{N!}\cdot\frac{N}{N-A}}{\sum_{k=0}^{N-1}\frac{A^k}{k!}+\frac{A^N}{N!}\cdot\frac{N}{N-A}}, \text{ where } N>A \quad (3)$$

where:

$A$ - total offered traffic [Erl],

$N$ - number of channels (links),

$C$ - probability of waiting for service.

The Erlang C formula (3) can be simplified through following modifications:

- Dividing numerator and denominator by $\sum_{k=0}^{N}\frac{A^k}{k!}$ and
- consecutive use of Erlang B equation (1).

$$C = \frac{N\cdot B}{N - A\cdot(1-B)} \quad (4)$$

### *C. Common Characters of Asynchronous and Synchronous Networks*

Erlang formulas were primary intended for traffic description in synchronous networks. The idea is to use these formulas also for asynchronous networks.

| **Synchronous network** | | **Asynchronous network** | |
|---|---|---|---|
| B [%] | Lost calls ratio | B [%] | Loss rate |
| C | Probability of waiting for service | C | Probability of delay |
| A [Erl] | Total offered traffic | A [%] | Link utilization |
| N | Number of channels (links) | N [Mbit/s] | Bandwidth |

Probability of delay C for asynchronous networks represents the latency which occurs during transmission in the case of the heaviest traffic. This delay occurs in IP networks due to waiting queues in buffers in network nodes. Unfortunately, there is no similar parameter for jitter in synchronous networks, hence through Erlang formulas it can not be estimated.

## V. RESULTS FOR ERLANG B FORMULA

This part represents results obtained by calculations through Erlang B formula. Input parameters were given as follows:

- One of parameters is constant.
- Other parameter was increased in given step sequence.

It is known that we can calculate the loss $B$ through Erlang B formula if we have given link utilization $A$ and bandwidth $N$. But it is also possible to calculate the link utilization $A$ by method of bisection, if we know the bandwidth $N$ and loss $B$ [4].

### *A. Bandwidth and Loss in the Case of Constant Link Utilization*

The tendencies are following:

- The loss $B$ is decreasing if the bandwidth is increasing and link utilization is constant.
- The loss $B$ is increasing if the link utilization $A$ is increasing.

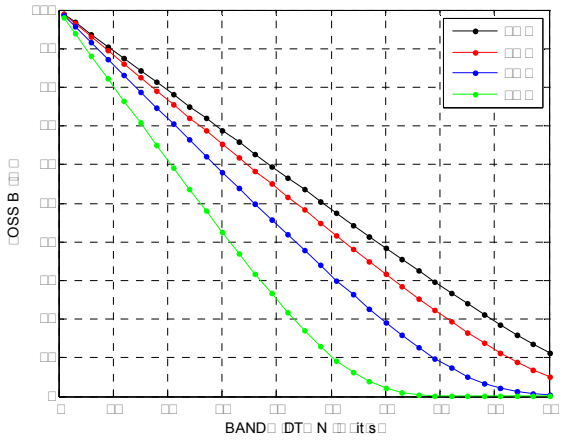

Figure 1. Dependency between loss and bandwidth in the cases of constant link utilization.

### B. *The Loss and Link Utilization in the Case of Constant Bandwidth*

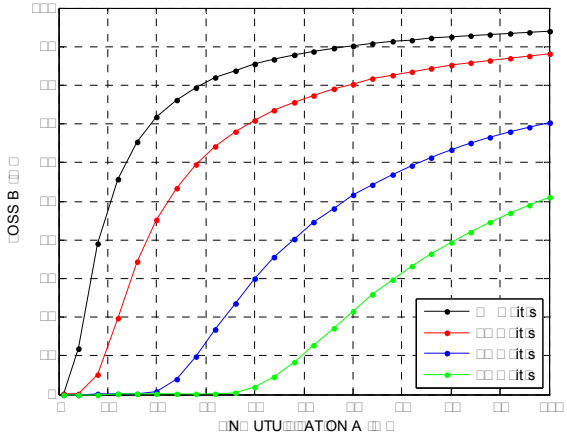

Figure 2. Dependency between loss and link utilization in the cases of constant bandwidth.

The tendencies are following:

- By increasing link utilization *A* the loss *B* is also increasing if the bandwidth *N* is constant.
- By increasing bandwidth *N* the loss *B* is decreasing if the link utilization *A* is constant.

## VI. Results for Erlang C Formula

This part represents the results obtained by calculations through Erlang C formula (4). By this equation we can calculate the possibility of delay *C* and loss *B* if we know the two parameters – the link utilization *A* and bandwidth *N*. Also in this case the input parameters were given as follows:

- One of parameters is constant.
- Other parameter was increased in given step sequence.

### A. *Link Utilization and Probability of Delay in the Case of Constant Bandwidth*

The tendencies are following:

- In the case of constant probability of delay *C* and increasing bandwidth *N* the link utilization *A* can be higher.
- In the case of constant link utilization *A* and increasing bandwidth *N* the probability of delay *C* is decreasing.
- In the case of increasing link utilization *A* and constant bandwidth *N* the probability of delay *C* is increasing.

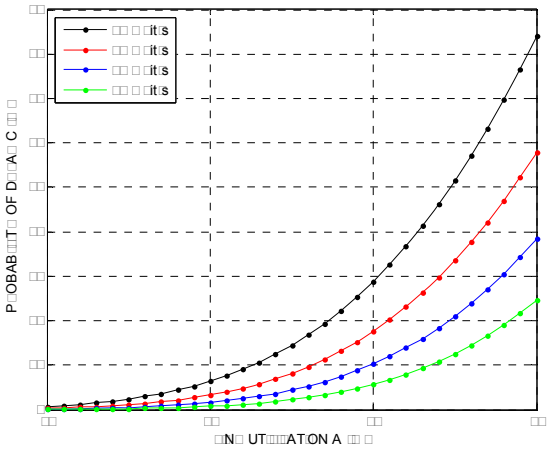

Figure 3. Probability of delay in the case of constant bandwidth and increasing link utilization.

### B. *Link Utilization and Bandwidth in the Case of Constant Probability of Delay*

By use of the Erlang B formula (4) and the method of bisection is possible to obtain the dependency of the link utilization *A* if the probability of delay *C* is constant and bandwidth *N* is increasing. The results are depicted in the Fig. 4.

The tendencies are following:

- In the case of constant link utilization *A* and increasing bandwidth *N* the probability of delay *C* is decreasing.
- In the case of constant bandwidth *N* and increasing probability of delay *C* the link utilization *A* is increasing.
- In the case of increasing bandwidth *N* and constant probability of delay *C* the link utilization *A* is increasing.

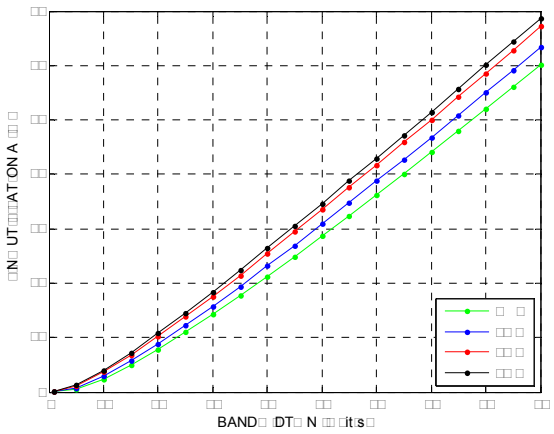

Figure 4. Link utilization in the case of constant probability of delay and increasing bandwidth.

### C. *Probability of Delay and Loss if the Link Utilization and Bandwidth are changing*

By use of the Erlang C formula (4) is possible to obtain dependencies of probability of delay C and loss B if the bandwidth N and link utilization A were changing. The obtained results are shown in the Fig. 5 and 6.

The tendencies are following:

- In the case of increasing link utilization *A* together with decreasing bandwidth *N* the loss *B* and probability of delay *C* are increasing.
- In the case of constant bandwidth *N* together with increasing link utilization *A* the loss *B* and probability of delay *C* are increasing.
- In the case of constant link utilization *A* together with increasing bandwidth *N* the loss and probability of delay *C* are decreasing.

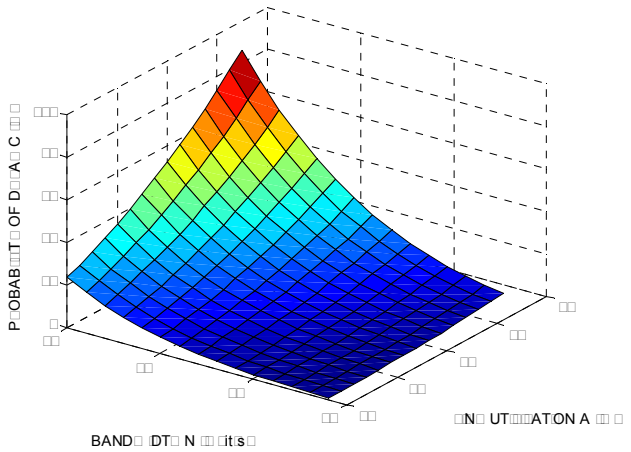

Figure 5. Dependency between probability of delay, bandwidth and link utilization.

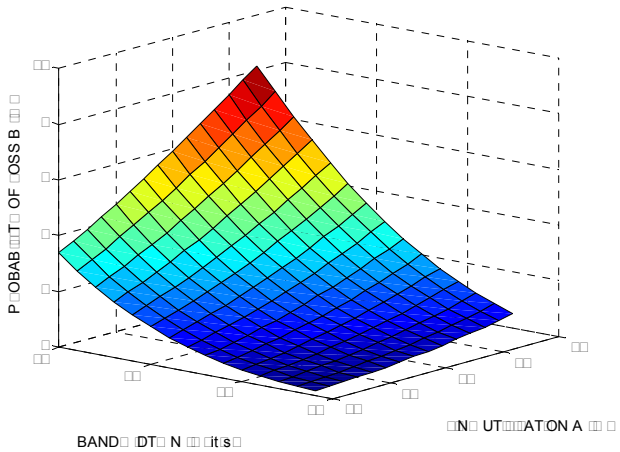

Figure 6. Dependency between loss, bandwidth and link utilization.

## VII. Results for Erlang B Formula

The paper proposes the idea of utilization of Erlang B and Erlang C formulas for description of traffic in NGN networks. All obtained tendencies through the calculations suggest the possibility of the Erlang formulas use in NGN networks (transport layer is represented through the ATM or IP network). Erlang B formula does not contain parameter for probability of delay, therefore this formula is more suitable for ATM network, because the probability of delay in this network is omissible. Through the Erlang C formula is possible to estimate the probability of delay, which usually occurs in IP networks. Description of traffic gives the opportunities to monitor the Quality of Service parameters in NGN networks. It seems that simplicity and unpretentiousness of Erlang formulas can be their strong advantage against other methods for traffic description in asynchronous networks, but the more future research is necessary in this field.


## Acknowledgment

*This work is a part of research activities conducted at Slovak University of Technology Bratislava, Faculty of Electrical Engineering and Information Technology, Department of Telecommunications, within the scope of the projects VEGA No. 1/0565/09 „Modelling of traffic parameters in NGN telecommunication networks and services“ and the partial result of the Research & Development Operational Programme for the project Support of Center of Excellence for Smart Technologies, Systems and Services, ITMS 26240120005, co-funded by the ERDF.*


## References


[1] MULLER, N. J.: Desktop Encyclopedia of Telecommunications. Edition: 3, *McGraw-Hill Professional*, 2002, ISBN 0071381481.

[2] PUŽMANOVÁ, R.: Modern communication networks from A to Z. *Computer Press Brno*, 2006, ISBN 80-2511278-0.

[3] KLIKA, O.: Theory and experience of operation load in telecommunications. Praha, 1973, OS-31-047-73.

[4] COOPER, R. B.: Introduction to Queueing Theory: 2nd Edition, *Elsevier*, 1980, ISBN 0444010653.
[5] KRAUSE, M., TIPTON, H. F.: Information Security Management Handbook. Edition: 4, *CRC Press*, 1999, ISBN 0849308003.
[6] TAYLOR, T.: QoS in Packet Network. *Springer*, 2004, ISBN 038723389.
[7] VOZŇÁK, M.: *Advanced Implementation of IP Telephony at Czech universities*, WSEAS TRANSACTIONS on COMPUTERS, Issue 1, Volume 9, September 2010, ISSN: 1109-2750, pp. 679-693,
[8] BALOGH, T., MEDVECKÝ, M.: Performance Analysis of Priority Queuing Based Scheduling Algorithms. In: 33rd International Conference on Telecommunications and Signal Processing - TSP 2010, August 17-20, 2010, Baden near Vienna, Austria, pp. 228 – 233, ISBN 978-963-88981-0-4
[9] HALÁS, M., KYRBASHOV, B., KOVÁČIK, M.: Influence of Encryption on VoIP Connection Quality, In *RTT 2008. Research in Telecommunication Technology: 9th International Conference*. Vyhne, Slovak Republic, 10.-12.9.2008, pp. 50-53, ISBN 978-80-227-2939-0.
[10] LUKNÁROVÁ, D., MEDVECKÝ, M.: Investigation of A-RIO, RB-nRED and WRED algorithms from the point of QoS support. In: 33rd International Conference on Telecommunications and Signal Processing - TSP 2010, August 17-20, 2010, Baden near Vienna, Austria, pp. 438 – 443, ISBN 978-963-88981-0-4.
[11] QIAO, S. *A Robust and Efficient Algorithm for Evaluating Erlang B Formula*. Hamilton, Ontario Canada : McMaster University, 1998. http://www.cas.mcmaster.ca/~qiao/publications/erlang.pdf
[12] Diagnostic Strategies. *Traffic Modeling and Resource Allocation in Call Centers*. : Needham (Mass., USA) : Diagnostic Strategies, 2003. http://www.fer.hr/_download/repository/A4_1Traffic_Modeling.pdf.
[13] Westbay Engineers Ltd. *The Extended Erlang B Traffic Model*. : Westbay Engineers Ltd., 2008. http://www.erlang.com/calculatormanual/index.html?the_extended_erlang_b_traffic_model.htm
[14] FREEMAN, R.: Fundamentals of Telecommunications, Second Edition. John Wiley & Sons, Inc. Hoboken, New Jersey, IEEE Press, 2005, ISBN 0-471-71045-8
[15] KAVACKÝ, M., ZOLNAY, A.: IP Videokonference in Learning Process. In *ICETA 2010 : 8th International Conference on Emerging eLearning Technologies and Applications. Stará Lesná, Slovakia, 28.-29.10.2010.* Košice: Elfa, 2010, s. 137--140. ISBN 978-80-8086-166-7.
[16] MIŠUTH, T., BAROŇÁK, I.: Performance Forecast of Contact Centre with Differently Experienced Agents. In: Elektrorevue – Electrotechnic magazine, 2010/97 – 16.11.2010, pp. 97-1 - 97-7, ISSN 1213-1539.

# High-speed Data Transmission in Wireless and Mobile Networks

Tomas Macha, Lubos Nagy, Jan Ochodnicky
Department of Telecommunications
Brno University of Technology
Brno, Czech Republic
tomas.macha@phd.feec.vutbr.cz, lubos.nagy@phd.feec.vutbr.cz, xochod00@stud.feec.vutbr.cz

***Abstract*—This article describes the comparison of Voice over IP (VoIP) calls between two different access points. The first case is focused on ordinary Wi-Fi access point enabling wireless connection to hardware and software IP phones. The second scenario is similar, except the Wi-Fi router is replaced by a Wi-Fi hotspot created from a HTC mobile phone with Android 2.1 operating system. The goal of the research was to examine high-speed data transmission in wireless and mobile networks. Different plots of delay and jitter are analyzed and shown in the article.**

***Keywords- Wi-Fi; hotspot; VoIP; SIP; 3G***

## I. INTRODUCTION

New mobile phones offer new possibilities in effective data transfer. One of them is the opportunity to configure the mobile phone to a Wi-Fi hotspot. For our experimental network, the HTC Desire mobile phone was used. This mobile phone enables Wi-Fi hotspot setup. The configuration can be used by three different devices at the same time.

The idea was to connect Wi-Fi-based devices, such as Wi-Fi phones mutually or with notebooks containing Wi-Fi module and installed software IP phone. One hardware IP phone was added for the possibility of comparison. All mentioned software or hardware IP phones were based on Session Initiation Protocol (SIP). User's accounts were created in a SIP-based software exchange. This exchange is described in the next chapter.

The experimental network was located at Department of Telecommunications at Brno University of Technology. The HTC mobile phone contained an O2 SIM card. In this area, the O2 operator offers 3G telecommunications network for the wireless transmission of data through radio signals with real speeds of 3Mbit/s.

The Wi-Fi router was an N Gigabit router (802.11n) compliant device providing high-speed Internet access.

### *A. 3G WiFi Hotspot*

The goal of a hotspot is to cover a public area with an 802.11 signal. The hotspot is a site that offers an Internet access over a Wireless Local Area Network (WLAN) [1] with the help of a device connected to an Internet service provider. Wi-Fi technology is typically used for hotspots. The HTC Desire phone can be used as a portable Wi-Fi hotspot enabling phone's internet connection to any other device in range via a Wi-Fi connection. It connects to CDMA [2] networks at 3G speeds. HTC Desire manages three devices connected to Wi-Fi hotspot.

### *B. 3CX PBX exchange*

3CX Phone System for Windows OS is a software-based private branch exchange based on the SIP standard. This PBX is installed and managed via web interface. It supports IP hardware and software phones [3].

## II. EXPERIMENTAL NETWORK TOPOLOGY FOR HOTSPOT

The experimental network was created of several wired and wireless end devices. However, only two of them were connected to each other for VoIP connection. No conference call was originated. Table 1 defines all used devices for the experimental network. The IP address of Linksys 1 was assigned by the network. The other IP addresses were fixed.

TABLE I. EXPERIMENTAL NETWORKS SETUP

| Device | Tel. number | IP address |
|---|---|---|
| Linksys 1 | 100 | 85.160.188.105 |
| Linksys 2 | 101 | 147.229.151.210 |
| VIP-153T | 102 | 147.229.151.71 |
| Notebook | 104 | 147.229.151.100 |
| 3CX PBX | - | 147.229.151.105 |
| HTC Desire | - | - |

### *A. SIP phone to Wi-Fi phohe connection*

The first connection was established between a SIP phone (VIP-153T) and a Wi-Fi phone (Linksys 1). The logical topology is shown in Figure 1.

The mobile phone with Android OS represented a Wi-Fi hotspot. In this scenario, one device was connected to the hotspot, namely Wi-Fi phone Linksys. The Android phone used 3G connection for data transmission over the O2 operator. Afterwards was the data transmission processed through the Brno University of Technology network up to the PBX software SIP exchange 3CX PBX. This PBX represented an

Asterisk solution for OS Windows. The PBX exchange contained users account information. To the exchange was also linked the hardware SIP phone.


Figure 1 The logical topology of SIP to Wi-Fi phones connection using hotspot

### B. *SIP phone to Wi-Fi phone connection*

The second scenario was focused on connection between the software IP phone (X-Lite) and the SIP phone VIP-153T. The logical topology of this established connection is shown in Figure 2.

The second topology is very similar to the previous one except one device change. The Linksys phone was replaced by a computer with installed software IP phone called X-Lite. The software phone user account was also controlled by the 3CX PBX.

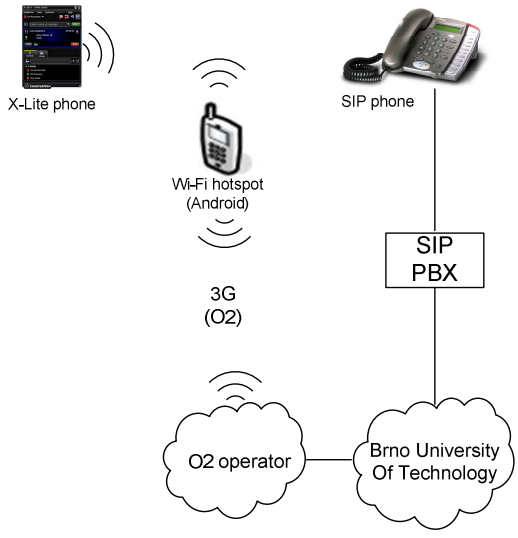


Figure 2 The logical topology of X-Lite to SIP phones connection using hotspot

### C. *Wireless software IP phone to Wi-Fi phone connection*

The last scenario of this type of experimental network was focused on connection between the software IP phone (X-Lite) installed on the notebook (wireless connection) and the Wi-Fi phone Linksys. The logical topology of this established connection is shown in Figure 3.

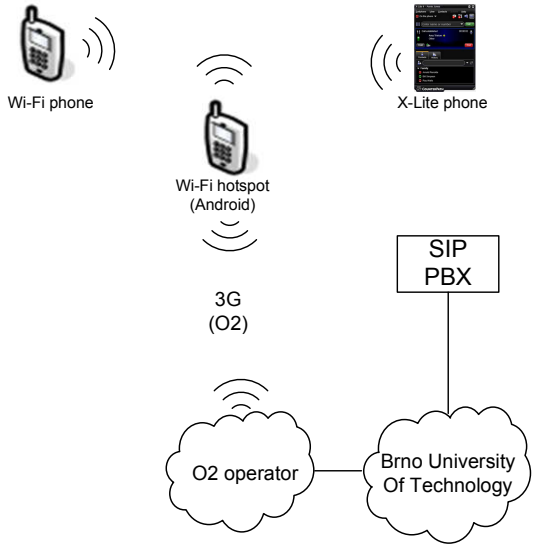


Figure 3 The logical topology of two wireless end devices connected to the Wi-Fi hotspot

## III. EXPERIMENTAL NETWORK TOPOLOGY FOR WI-FI ROUTER

This type of network used an ordinary Wi-Fi router for data transmission between end users and SIP PBX. Another three scenarios were measured. These scenarios are similar to the previous ones. The difference is in the access point. The HTC hotspot was replaced by the Wi-Fi router mentioned before.

### A. *SIP phone to Wi-Fi phohe connection*

Figure 4 illustrates the configured network for another type of call. In this case, one end device, namely SIP phone was linked to the exchange and the second one (Linksys) represented the wireless connection.

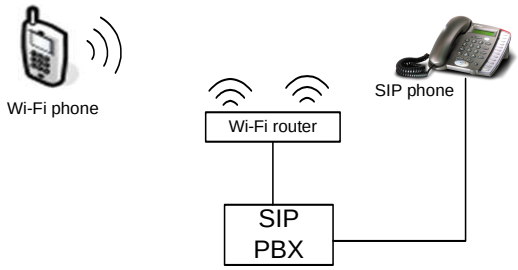


Figure 4 The logical topology of SIP phone to Wi-Fi phone connection using Wi-Fi router

### B. *Wireless software IP phone to SIP phohe connection*

Figure 5 illustrates the second scenario for Wi-Fi router. SIP phone is connected to the X-Lite software via Wi-Fi router and the users are controlled by the PBX.

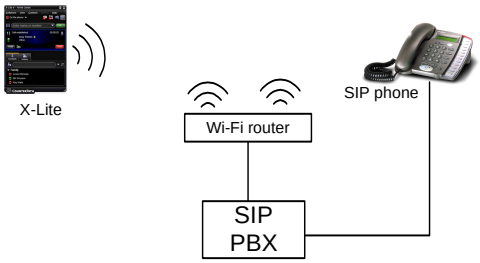


Figure 5 The logical topology of VIP-153T phone to software IP phone connection using Wi-Fi router

### C. *Wireless software IP phone to Wi-Fi phone connection*

Figure 6 illustrates the network configuration of a connection between wireless end devices, namely the Wi-Fi IP phone and the X-Lite software IP phone.

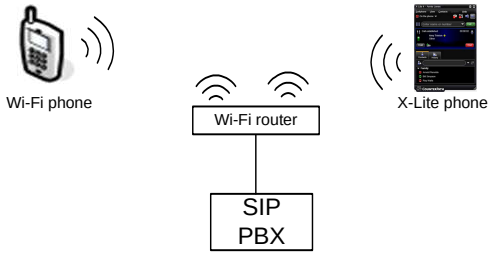


Figure 6 The logical topology of X-Lite to Wi-Fi phones connection using Wi-Fi router

## IV. RESULTS AND COMPARISONS

For each one scenario were performed three calls for more accurate measurement. One call took 30 seconds. Delay and jitter plots of all scenarios are illustrated in results. The established connections were monitored and investigated through a packet analyzer Wireshark.

As mentioned before, HTC desire contained O2 SIM card. The information about serving cell follows in Table 2.

TABLE II. O2 SERVING CELL

| Name: | Value: |
|---|---|
| Operator | O2 |
| Type | UMTS |
| LAC | 3811 |
| CID | 40238 |
| PSC | 3801 |
| Signal | -83dBm |

For the hotspot scenarios, the maximal delay was around 60ms. There were some packets which got over 1s but this disruption was caused by the load along the path of packets. The packet lost was 0.0%. The maximum jitter was 35ms and the mean jitter around 5.8ms. According to ITU-T specification [5] for voice quality is the network configuration good for voice transmission.

For the Wi-Fi router scenarios, the maximal delay was around 22ms. Some small inaccuracies were detected, but it was probably caused by the network background load. The packet lost was 0.0%. The maximum jitter was 16ms and the mean jitter around 3.7ms.

These measured values are noted for good quality of voice over data networks according to ITU-T specifications [5]. Good results were expected because of minimal network load and the effective use of the network.

### A. *SIP phone to Wi-Fi phohe connection results*

Figure 7 illustrates the plot of measured delay for SIP phone and Wi-Fi phone Linksys. A red curve indicates average delay for calls processed via Wi-Fi router and a blue curve indicates the average delay for calls via hotspot. It can be seen that the red curve runs around 20ms of delay. The blue curve noted expected fluctuation caused by the load and along the packet's path through the network. Also according to expected results, the jitter (Figure 8) noted steady state for Wi-Fi router and fluctuated state for hotspot calls. The jitter is caused by queuing, contention and serialization effects on the path through the networks.

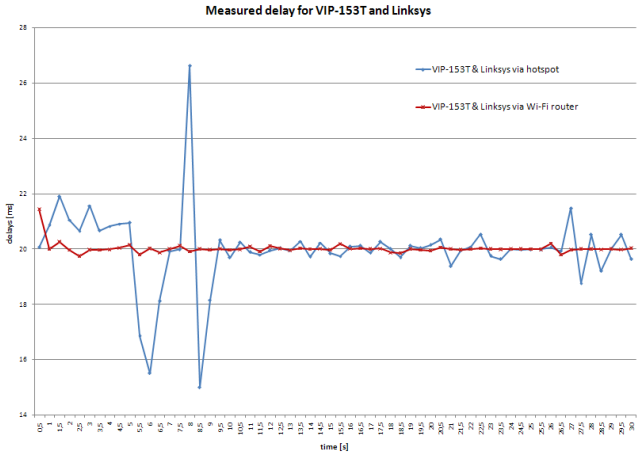


Figure 7 The comparison of measured delay for SIP phone and Wi-Fi phone

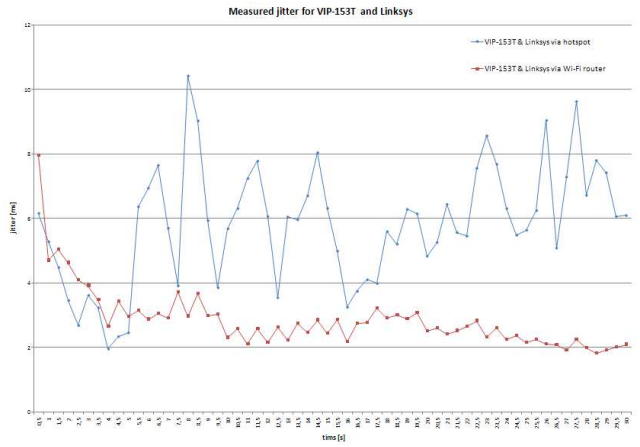


Figure 8 The comparison of measured jitter for SIP phone and Wi-Fi phone

### B. *Wireless software IP phone to SIP phohe connection results*

Figure 9 shows the measured delay for SIP phone and software X-Lite phone. A red curve indicates average delay for calls processed via Wi-Fi router and a blue curve indicates the average delay for calls via hotspot. It can be seen that the red curve is steady around 20ms of delay. The blue curve noted expected fluctuation. Figure 10 depicts the jitter

according to expected results. Performed calls via hotspot noted increased and fluctuated jitter.

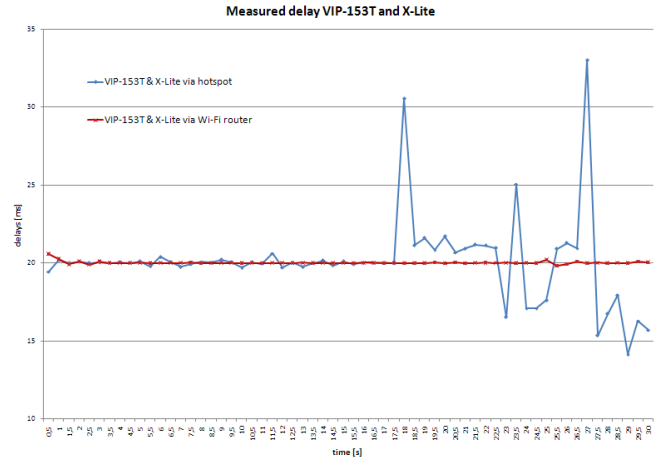


Figure 9 The comparison of measured delay for SIP phone and X-Lite phone

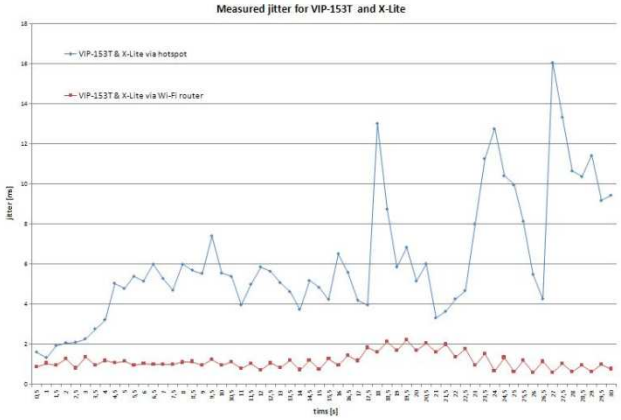


Figure 10 The comparison of measured jitter for SIP phone and X-Lite phone

### C. *Wireless software IP phone to Wi-Fi phone connection results*

This scenario is very similar to the previous ones. Again, the red curve indicates calls through the Wi-Fi router and the blue curve indicates calls through the hotspot. The average delay (Figure 11) is about 20ms and average jitter (Figure 12) did not cross over 6ms.

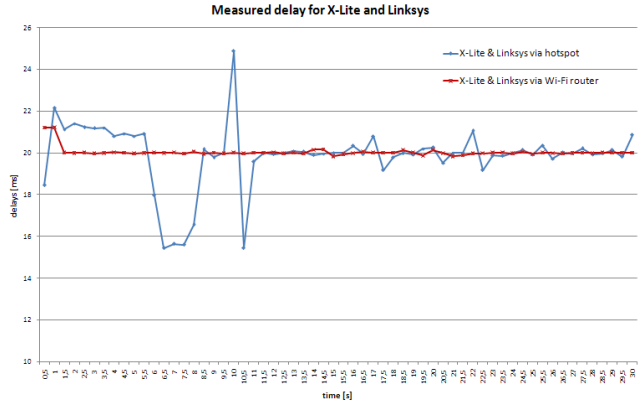


Figure 11 The comparison of measured delay for Wi-Fi phone and X-Lite phone

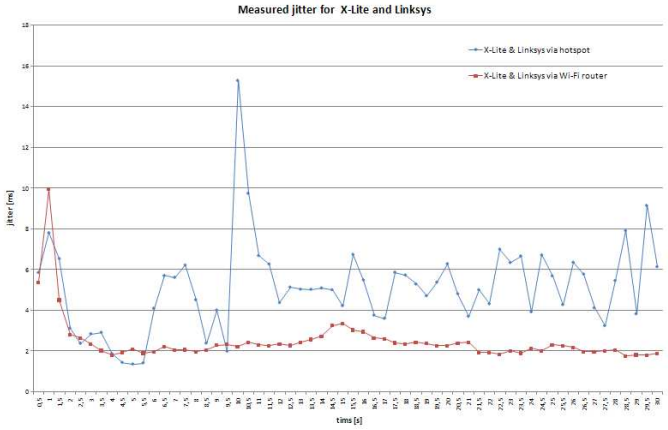


Figure 12 The comparison of measured jitter for Wi-Fi phone and X-Lite phone

## V. CONCLUSION

The real-time multimedia services for transmitting information under the certain QoS parameters are one of the most actual issues in telecommunication world. In this article, the comparison of two different types of networks is described. The first one is focused on 3G Wi-Fi hotspot created from a special mobile phone. The second one is represented by an ordinary Wi-Fi router.

The issue of QoS refers mainly to the quality of the packet network. The ability of the network to provide required QoS to the user depends on particular parts of the network. It means that the QoS depends on the weakest element of the network.

The delay and jitter for hotspot scenario calls were characterized by fluctuation caused by different actions and load in the network along the packet's path, especially in 3G network. On the other hand, the delay and jitter for Wi-Fi router scenario calls remained steady without any disturbance. There were no Mean Opinion Score (MOS) measurements but according to objective perception, the Wi-Fi router calls were characterized by higher quality.

The real measurements follow expected results. Both types of scenarios offer good voice quality according to ITU-T.

## ACKNOWLEDGMENT

This project was supported by the FRVŠ 2986/2010.

## REFERENCES

[1] J. Ross, "The book of Wi-Fi: install, configure and use 802.11b wireless networking," San Francisco, 245p., 2003. ISBN: 1-886411-45-X.

[2] H. Holma, A Toskala, "WCDMA for UMTS: HSPA evolution and LTE" 5th ed., Wiley, 2010, 597p. ISBN: 978-0-470-68646-1.

[3] 3CX PBX Brochure. 2010. www.3CX.com.

[4] T. Macha, "Analýza komunikace při realizaci VoIP spojení." Elektrorevue - Internetový časopis (http://www.elektrorevue.cz), 2008, roč. 2008, č. 12, s. 1-11. ISSN: 1213- 1539.

[5] ITU-T. Series G: Transmission systems and Media, Digital Systems and Networks. International telephone connections and circuits – General Definitions. The Emodel, a computational model for use in transmission planning. Recommendation ITU-T G.107. May 2000.

# Analysis of Influence of Network Performance Parameters on VoIP Call Quality

Adrian Kovac, Michal Halas
Department of Telecommunications
Slovak University of Technology
Bratislava, Slovakia
fotoadrian@gmail.com, halas@ktl.elf.stuba.sk

*Abstract* — **The paper deals about the measurement of the packet-oriented networks transmission QoS parameters impact to the VoIP call quality. Theoretical calculation of MOS call quality assessment for the selected audio codec is implemented using the E-model. The main input QoS parameters for E-model are especially packet loss and delay. Practical VoIP calls simulation examines the impact of fluctuations in network delay – jitter, in the resulting call quality MOS. The aim is to analyze the usability of audio codecs for different values of loss, delay and jitter in the transmission network and quantification of estimation error in the E-model for raising jitter.**

***Keywords – E-model; QoS; MOS; Jitter; Delay***

## I. INTRODUCTION

In proposed article we analyze and measure the influence of packet network performance parameters and their influence on VoIP call quality. Degradation of network performance causes inhomogeneous packet data stream which translates into speech impairments of transferred VoIP calls. Theoretical call quality estimate for selected codecs is performed via E-model and MOS score. Main input parameters for E-model are packet loss, network delay and codec impairment factors. Real simulation of VoIP calls is used to determine influence of delay jitter and receiver's input size on final MOS score. Aim of the article is to quantify codec performance at various network conditions and to analyze influence of jitter on E-model MOS estimate.

## II. QOS PARAMETERS IN VOIP PACKET NETWORKS

VoIP technology uses set of objectively measurable network parameters to calculate actual performance of network. The greatest influence on QoS performance has the following parameters:

- Network delay [ms];
- Network delay jitter [variance σ in ms];
- Network packet loss [%];
- Echo [ΔT in ms, level in dB].

### A. Network Delay

Voice delay is the first observable quality parameter to describe call quality. According to the ITU-T G.114 recommendation the maximum recommended one-way delay $T_a$=*150 ms*. This value is an outcome of human psycho-acoustic model. After saying a sentence or asking a question a human intuitively awaits response after a certain short moment, because listener has to hear, process and reply to the question which would be roughly the return delay of additional $T_a$ = *150 ms* in our example. Total transmission time for information is the sum of forward and backward time called the *RTT (Round Trip Time).* RTT can be calculated as follows in eq. 1:

$$T_{RTT} = 2\ T_a \quad [\text{ms}] \tag{1}$$

Delay has a cumulative character and is a sum of partial delays originated in all transmission chain network elements as in eq. 2:

$$T_a = 2.T_{alg} + T_{packet} + T_{ser} + T_{prop} + T_{comp} + T_{dejitter}\ [\text{ms}] \tag{2}$$

*1) Algorithmic delay:*

$T_{alg}$ is delay imposed by implemented audio codec. Audio compression codec needs to cumulate audio samples for certain periods, group and encode them to be sent as one packet. Grouped time interval of voice samples is $T_{packet}$ Compression process also takes up some time. $T_{packet}$ represents length of packet in output audio stream.

*2) Packetization Delay*

$T_{packet}$ occurs when packing audio samples into RTP packets. Grouping audio packets in larger packets saves bandwidth by reduction of control data overhead. Frequency of packet transmission is usually 50 per second (e.g. G.721 codec) or 33,3 per second (e.g. G.723 codec) what represents packetization delay of 20 or 30 ms. Application packet assembly layer waits for all samples to be generated and only then packs samples into packet, what produces additional delay $T_{packet}$.

*3) Serialization Delay*

$T_{ser}$ represents delay occurring at physical level when packet is being placed onto serial medium with certain finite

transmission speed. Serialization delay is given by length of the frame and serial data transfer speed of the medium as in eq. 3:

$$T_{ser} = 8\, l_{packet} / v_{transmission}\ [\text{ms}] \qquad (3)$$

where $l_{paket}$ is overall packet length including control information, headers and trailers in bytes and $v_{transmission}$ is link speed in kb/s. Serialization delay has additive nature. When packet travels across multiple network devices, mostly active ones, where processing or transcoding on different link type occurs, serialization delay sums up and packet delay increases.

*4) Propagation Delay*

$T_{prop}$ represents delay caused by physical propagation of signal on physical media (e.g. air, optical fiber, copper wire). Propagation delay can become observable mainly on long distance network segments in orders of hundreds of kilometers and more. For example propagation delay of space satellite radio links becomes a large concern when making real-time calls through satellite networks as Thuraya and Iridium or when crossing transatlantic link. One-way delay on these links can reach values in order of tenths to hundreds of milliseconds what becomes a limiting factor in design of other VoIP communication link components. Propagation delay $T_{prop}$ can be expressed through eq. 4.:

$$T_{prop} = d_{ef} / \lambda_{prop}\ [\text{s}] \qquad (4)$$

where $d_{ef}$ [km] is an effective distance of traversed physical media multiplied by 2 for calculation two-way RTT delay. $\lambda_{prop}$ is propagation speed of signal in physical medium in [km/s].

*5) Component Delay*

$T_{comp}$ is a delay imposed by packet processing on active network elements occurring during switching and routing. Switching delays are mostly negligible (below 1ms), but processing and queuing with prioritization on routers can significantly increase overall component delay $T_{comp}$. During active traffic shaping $T_{comp}$ can reach values up to 10 ms in Ethernet networks.

*6) Memory buffer delay*

Presents delay of audio samples occurring at packet input memory buffer at receiving device and equals roughly the half of the total buffer length. Input buffer reduces effects of jitter that is the fluctuation of packet arrival time in packet networks with stochastic asynchronous access methods as IP networks are. At price of increased total delay by $T_{dejitter}$ in order of 10 to 100 ms, effective packet loss can be minimized. End-to-End delay of VoIP traffic and packet interarrival times can successfully be modeled by Pareto distribution [11].

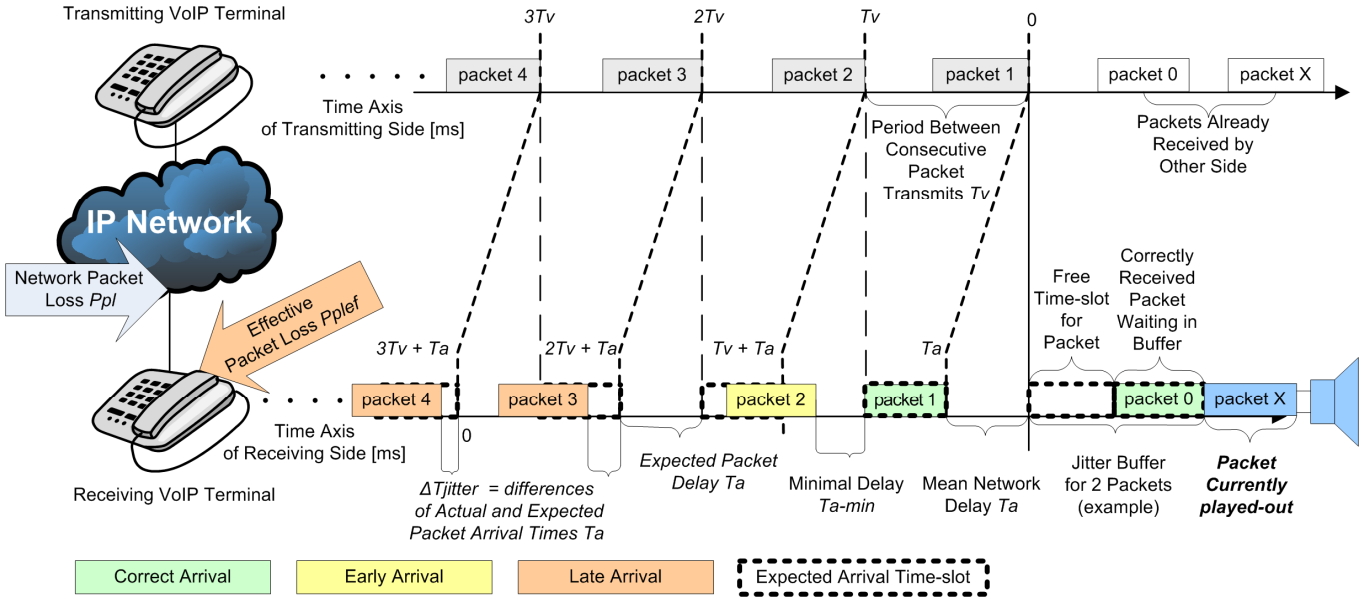


Figure 1. Effects of jitter and memory buffer on packet delay and interarrival time

## B. Network Delay Fluctuations - Jitter

When packets travel across IP packet network with stochastic nature of traffic multiplexing, it is not possible to make accurate estimates of momentary condition of the network. These momentary short-term fluctuations cause variations in delay $T_{comp}$ as well as $T_a$. Packets reach their destination mostly at time $T_a$ but with nonzero probability they can arrive earlier or much later than expected by the receiver. Let the difference between expected and real arrival time be $\Delta T$ as an absolute value. Influence of arrival time fluctuations are shown at figure 1.

*1) Network Delay Lower Bound*

Network delay as the shortest time in which a packet can traverse the network is given bz eq. 2 when $T_{comp} \rightarrow 0$.

*2) Network Delay Upper Bound*

Maximum packet travel time thorough the network is unbounded and in case of lost packet reaches infinity from the receiver's point of view. Delay variation $\sigma_{Ta}$ [ms] is given as a variance of network delay with mean value of $T_a$. Mean value of jitter itself is $\sigma_{Ta} = 0$. Based on our testing and simulations with standard codec's and jitter buffer configuration (receiver's buffer for two packets), delay variance up to 20 ms can be considered acceptable for VoIP traffic, VoIP communication on networks with jitter up to 40 ms is feasible and jitter higher than 50 ms caused significant speech impairments that are unacceptable for real-time VoIP phone calls.

## C. Network Packet Loss

When packets traverse through communication network as a whole, some of them can be lost at various segments of the network due to stochastic access control to media, traffic shaping, congestions, broken links etc. For fluent VoIP phone call communication it is not desired to wait for a voice packet to be retransmitted because the synchronicity would be lost and overall delay would after a few retransmissions grow to unacceptable extent. It is less disturbing to miss the packet and let the gap in voice stream to be masked or simply be empty. Various PLC (packet loss concealment) methods acoustically reconstruct samples in dropped voice packets up to chain of 3 subsequent packets with great success so the listener may not even notice that any drop has occurred. This approach increases overall perceived MOS of voice calls. Most threatening packet losses are in form of bursts, when more than 2 subsequent packets are lost. This behavior of internet packet traffic can be described by Gilbert model of On-Off source as in [11].

Real packet loss at receiver's side on decoder input is composed of network packet loss as measured by network management tools and of additional packet loss on jitter buffer memory because of overly delayed packets. When we describe the receiver input queue by Kendall classification as Pareto/D/1/K system [8, 10] the probability of packet loss is equal to probability that there would be more packets on the input than the maximum buffer memory size K (figure 2).

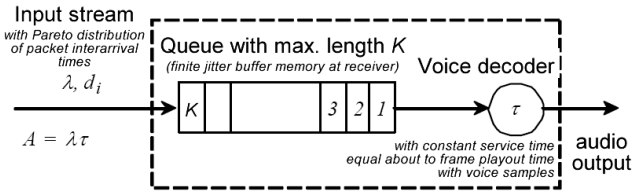


Figure 2. Packet arrival stream and input buffer function

## D. Echo

Echo is an acoustic effect caused by feedback at the far end of communication line. Listener can hear his own voice delayed by RTT time $T_{RTT}$ (eq. 1) and attenuated. Echo suppression can be performed by hardware or software at speaker's side by various methods of signal subtraction which are called echo cancellation methods.

TABLE I. MOS SCORE RELATION TO R-FACTOR VALUE AND VERBAL QUALITY EVALUATION

| ***R–faktor* lower bound** | **MOS lower bound** | **Word evaluation of MOS score** | **User satisfaction level** |
|---|---|---|---|
| 90 | 4.34 | **5 – excellent** | Very satisfied |
| 80 | 4.03 | **4 – good** | Satisfied |
| 70 | 3.60 | **3 – fair** | Some users dissatisfied |
| 60 | 3.10 | **3 - fair** | Many users dissatisfied |
| 50 | 2.58 | **2 – poor** | Most users dissatisfied |
| < 50 | < 2,58 | **1 – bad** | Most users dissatisfied |

# III. MOS MEASUREMENTS AND SIMULATIONS

Measurement and simulation of MOS score was performed for following varying network parameters and following set of codecs:

- One-way network delay $T_a \in \{0, 20, 50, 100, 150, 200, 300, 400\}$ [ms];
- Network packet loss $P_{pl} \in \{0, 1, 2, 3, 5, 7, 10, 15, 20\}$ [%];
- Codecs G.711 with and without PLC, G.723.1 ACELP, G.723.1 MPMLQ, G.726, G.729.

Packetization interval for codecs G.711 with and without PLC, G.726 and G.729 was set to 2 = 20 ms of voice samples per audio packet. Jitter buffer size at receiver was set to default value of 2 packets = 40 ms of audio.

Packetization interval for codecs G.723.1 ACELP and G.723.1 MPMLQ was set to 1 = 30 ms of voice samples per audio packet. Jitter buffer size at receiver was set to default value of 2 packets = 60 ms of audio. We have selected static jitter buffer to abstract from performance gain of dynamic jitter buffers to obtain worst case data points. All codecs except from G.711 without PLC had their PLC masking method active by default. Network delay, jitter and loss were set only in one way from sender to receiver. Backward link was used for data collection and was implemented without impediments.

As VoIP traffic generator the IxChariot v. 6.3 including endpoints v. 7.2 was used. As an operating system Linux Ubuntu 9.04 was used. Computers were three, one was the traffic generator, the second in chain was traffic degradator with selected simulation parameters running WANem v 2.1 and the third computer was the receiver endpoint which collected data. All computers were connected in chain by 100 BASE TX cable full duplex Ethernet.

# IV. CALCULATIONS AND SIMULATION RESULTS

## A. Additional Jitter Buffer Packet Loss

We propose to use effective packet loss *Pplef* instead of network packet loss *Ppl* in E-model to obtain more realistic results of MOS estimate mainly in environment with greater jitter. We substitute *Ppl* for *Pplef* where *Pplef* can be expressed by equation 5:

$$Pplef = 1 - (1 - Ppl)(1 - Pdejitter) \quad \in <0,1> \qquad (5)$$

After modification we obtain packet loss caused by jitter buffer overflow *Pdejitter,* expressed as equation 6:

$$Pdejitter = \frac{Pplef - Ppl}{1 - Ppl} \quad \in <0,1> \qquad (6)$$

Afterwards we have analyzed net network packet loss from obtained simulation and measurement data, marked as *P(ef)*. We have known the net network packet loss set on WANem (*Ppl*) and with formula in eq. 7 derived from eq. 6 we calculated real contribution of excessive packet loss caused by jitter for certain jitter and buffer size.

$$P(\,jitter\,) = \frac{P(ef\,) - P(\,pl\,)}{1 - P(\,pl\,)} \qquad (7)$$

where *P(ef)* can be calculated as *an_average_number_of_lost_bytes* divided by *an_average_number_of_received_bytes.* All measurements were performed individually for 20, 40 and 80 ms jitter, for each network packet loss and individually for codecs with 40 and with 60 ms jitter buffer. Result is the table of average packet losses that occurred on jitter buffer (table 2.). Based on these values we have searched for best $\sigma$, $\xi$ and $\mu$ parameters of Pareto distribution function, that would describe jitter effects on MOS in best way. We have used MSE optimization. Average losses were grouped by codec jitter buffer size, that is 40 ms codecs (G.711 with PLC, G.711 without PLC, G.726, G.729) and 60 ms codecs (G.723.1 ACELP and MPMLQ) formed separate groups. Table 2 lists all values of excess packet loss caused by jitter buffer effects, which originates outside transport network itself. Values are result of simulation and measurements.

TABLE II. REAL AVERAGE PACKET LOSSES AT DECODER INPUT CAUSED BY NETWORK PACKET LOSS AND JITTER EFFECTS AT INPUT BUFFER

| **Jitter [ms]** | **Jitter buffer size [ms]** | **Average packet loss *P(jitter,dejitter)*** | ***Complement to packet loss F(jitter,dejitter)* = transmission** |
|---|---|---|---|
| 20 | 40 | 0,116114 | 0,883886 |
| 20 | 60 | 0,029393 | 0,970607 |
| 40 | 40 | 0,307519 | 0,692482 |
| 40 | 60 | 0,180276 | 0,819725 |
| 80 | 40 | 0,509000 | 0,399790 |
| 80 | 60 | 0,399790 | 0,600206 |

Sought for complementary values to packet loss called transmission and marked as $F_{(jitter,dejitter)}$, where „dejitter“ index = size of codec jitter buffer and „jitter“ = certain value of network jitter, represent values of cumulative distribution function describing probability of reception and processing packets without loss. Function $F_{(\xi,\mu,\sigma)}$ (eq. 8) was adapted to this function by regression and finding coefficients with lowest MSE.

$$F_{(\xi,\mu,\sigma)}(x) = 1 - \left(1 + \frac{\xi(x-\mu)}{\sigma}\right)^{-\frac{1}{\xi}} \qquad (8)$$

We make an assumption of jitter behavior depicted in figure 1. In calculations, our interest lies not in an absolute delay of packet, but only in time difference ΔT which represents only difference between expected average arrival time („virtual timeslot“) and actual delay influenced and varied by jitter. Virtual timeslot has a delay equal to the lower bound of possible network delay on given network = $T_a = 2T_{alg} + T_{packet} + T_{ser} + T_{prop} + T_{comp} + T_{jitter}$ according to eq. 2. $T_a$ lower bound can be calculated when we put all delays except from algorithmic $T_{alg}$ and propagation $T_{prop}$ equal to zero. Eq. 2 simplifies to $T_a = 2T_{alg} + T_{prop}$.

For choosing the correct function for jitter buffer behavior description we make following considerations:

- When jitter is present and delay fluctuations are not larger than packet transmission interval *Tv* the probability, that packet reordering occurs, is zero.
- When packet arrives disordered, jitter buffer of software used in our simulations does not reorder the packets and the packet is dropped.
- We put the position parameter $\mu$ for PDF of packet arrival times = 0, because we are only interested in relative deviations from expected timeslot.

### *B. Additional Packet Loss Calculation*

Calculation has shown lowest MSE of packet transmission to be 12% of transmission value when $\xi = -0,1$. σ is substituted by actual network jitter and μ = 0. Function value at point *x* represents probability of successful packet transmission through jitter buffer without loss. To calculate probability *Pdejitter* in eq. 6 we needed to recalculate *Pjitter* to *Pdejitter* according to eq. 9, which is derived from autocorrelation of PDF function in point μ = 0. Value is squared and divided by 2. Extrapolated values of jitter buffer losses are shown at figure 5 for 20, 40 and 80 ms jitter.

$$Pdejitter = \frac{(1 - F(x,\mu,\xi,\sigma))^2}{2} \quad \in <0;0,5> \qquad (9)$$

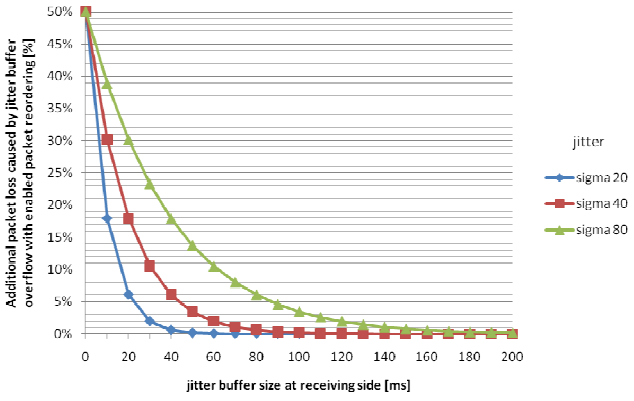


Figure 3. Relation between excess packet loss on jitter buffer (in %) and jitter of 20, 40 and 80 ms

Table 3 shows MOS performance comparison of tested codecs at various network parameters. From the results we can observe significant voice quality degradation with increasing jitter with constant jitter buffer.

TABLE III. CODECS' MEASURED MOS PERFORMANCE COMPARISON

| | Jitter [ms] | *Ta* = 20 ms, *Ppl* = 0 % | *Ta* = 50 ms, *Ppl* = 1 % | *Ta* = 100 ms, *Ppl* = 3 % | *Ta* = 200 ms, *Ppl* = 7 % |
|---|---|---|---|---|---|
| G.711 without PLC | | | | | |
| | 20 | 4,36 | 4,33 | 2,34 | 1,00 |
| | 40 | 2,33 | 1,72 | 1,00 | 1,00 |
| | 80 | N/A | 1,10 | 1,00 | 1,00 |
| G.711 with PLC | | | | | |
| | 20 | 4,36 | 4,36 | 4,14 | 3,71 |
| | 40 | 4,34 | 3,98 | 3,60 | 3,09 |
| | 80 | N/A | 2,81 | 2,36 | 2,32 |
| G.723.1 ACELP | | | | | |
| | 20 | 3,62 | 3,62 | 2,85 | 2,06 |
| | 40 | 3,60 | 3,28 | 2,64 | 1,88 |
| | 80 | N/A | 2,52 | 1,61 | 1,39 |
| G.723.1 MPMLQ | | | | | |
| | 20 | 3,80 | 3,80 | 3,12 | 2,21 |
| | 40 | 3,78 | 3,51 | 2,83 | 1,98 |
| | 80 | N/A | 2,74 | 2,04 | 1,46 |
| G.726 | | | | | |
| | 20 | 4,16 | 4,15 | 2,28 | 1,69 |
| | 40 | 2,90 | 2,84 | 1,56 | 1,00 |
| | 80 | N/A | 1,53 | 1,00 | 1,00 |
| G.729 | | | | | |
| | 20 | 4,01 | 4,01 | 3,44 | 2,80 |
| | 40 | 3,45 | 3,10 | 2,65 | 2,27 |
| | 80 | N/A | 2,09 | 1,00 | 1,00 |

*note: *Ta* = one-way delay of transport network; *Ppl* = network packet loss excluding packet drops on input jitter buffer memory.

## V. RESULTS

Expected negative effect of increasing network jitter was proved right. MOS degradation with increasing jitter was proved by simulation and by calculation. Increasing jitter appears as increased packet loss at jitter buffer input of receiver due to too early or too late packet arrivals, packet disorders and limited buffer size. Effective packet loss is greater than measured network packet loss. Increased memory buffer results in lower effective packet loss but in increased network delay. Original E-model as defined by ITU-T G.107 takes in its MOS calculations in account only network packet loss *Ppl,* which we substitute for effective packet loss *Pplef* in our calculations. *Pplef* accounts for additional two input parameters – network jitter and receiver buffer size in milliseconds. Our MOS estimate proves to obtain more accurate not so optimistic results as original E-model mainly on networks with jitter greater than 20 ms.


## ACKNOWLEDGMENTS

This work was a part of research activities conducted at Slovak University of Technology Bratislava, Faculty of Electrical Engineering and Information Technology, Department of Telecommunications, within the scope of the project VEGA No. 1/0565/09 „Modeling of traffic parameters in NGN telecommunication systems and networks “.


## REFERENCES


[1] ITU-T G.107, The E-model, a computational model for use in transmission planning, *ITU-T Recommendation G.107, ITU-T.* Geneva, Switzerland: May 2000.

[2] ITU-T G.107, The E-model, a computational model for use in transmission planning, *ITU-T Recommendation G.107, ITU-T.* Geneva, Switzerland: 2002.

[3] ITU-T G.107 – Amendment 1, Provisional Impairment Factor Framework for Wideband Speech Transmission, *ITU-T Recommendation G.107, ITU-T.* Geneva, Switzerland: June 2006.

[4] ITU-T G.109, Definition of categories of speech transmission quality, *ITU-T Recommendation G.109, ITU-T.* Geneva, Switzerland: September 1999.

[5] ITU-T G.133, Appendix I: Provisional planning values for the equipment impairment factor Ie and packet-loss robustness factor Bpl, *ITU-T Recommendation G.133, ITU-T.* Geneva, Switzerland: September 1999.

[6] ITU-T G.722, *7 kHz Audio – Coding within 64 kbit/s. ITU-T Recommendation G.722.* Geneva, Switzerland: September 1993.

[7] ITU-T STUDY GROUP 12 – DELAYED CONTRIBUTION 106: *Estimates of Ie and Bpl parameters for a range of CODEC types.* Geneva, Switzerland: 27-31 January 2003.

[8] KOH, Y., KISEON K.: Loss probability behavior of Pareto/M/1/K queue. In: *Communications Letters, IEEE*, vol.7, no.1, p. 39-41, January 2003. DOI: 10.1109/LCOMM.2002.806469

[9] KOTULIAKOVÁ, J., ROZINAJ, G.: *Číslicové spracovanie signálov.* Bratislava: STU Bratislava, 2001. 174 s. ISBN 80-227-1470-4

[10] MIRTCHEV, S., GOLEVA, R.: Evaluation of Pareto/D/1/K Queue by Simulation. In: *International Book Series "Information Science and Computing"*. Technical University of Sofia. Sofia, Bulgaria: June 2008.

[11] DANG, T.D.,SONKOLY, B., MOLNÁR, S.: Fractal analysis and modeling of VoIP traffic, *Telecommunications Network Strategy and Planning Symposium. NETWORKS 2004, 11th International* , vol., no., pp. 123- 130, 13-16 June 2004.

[12] TISOVSKÝ, A. - KLÚČIK, S. - KOVÁČIK, M. Modelling the Throughput of Mixed Traffic for a Computationally Intensive IPsec Process, *RTT 2010, Velké Losiny; Ostrava*, VUTBR, 8-10 September 2010, ISBN 978-80-248-2261-7. pp. 76-81

[13] KYRBASHOV, B. – BAROŇÁK, I. - KOVÁČIK, M. - JANATA, V. Vyhodnotenie oneskorenia v sieťach VOIP. *EE časopis pre elektrotechniku a energetiku*. - ISSN 1335-2547. - Roč. 16, mimoriadne č (2010), s. 152-159

# Optical Communications

# Fog model for Free Space Optics Link

Jan Vitásek, Artem Ganiyev, Jan Látal
Department of Telecommunications
VŠB – Technical University Ostrava
Ostrava, Czech Republic
jan.vitasek@vsb.cz, artem.ganiyev.st@vsb.cz, jan.latal@vsb.cz

***Abstract*—Atmospherical phenomena attenuate a laser beam which propagates through atmosphere. Fog causes the biggest attenuation. For design of free space optics links we use software OptiSystem. A component for fog simulation is missing therefore it was created.**

***Keywords-fog; FSO; attenuation; Kim model***

## I. INTRODUCTION

Fog is water that has condensed close to ground level, producing a cloud of very small droplets that reduce visibility [1]. It consists of small water droplets or tiny ice crystals suspended in the air. These small droplets cause dispersion of laser beam therefore all transmitted power can not be received by receiver. This effect is more significant by fog than by rain because the droplet size of fog is considerably smaller than droplet size of rain. A diameter of fog droplet can be from 1 to 20 μm.

## II. MATHEMATICAL MODELS

### A. Mathematical model of fog

The theoretical background of fog attenuation is based on Mie scattering. There are several models which allow calculate a specific attenuation for different optical wavelengths based on visibility data. The two most widely used models are the Kruse model and the Kim model [2]. Kim model is described by equation

$$\alpha_{fog} = \frac{17}{V_m \cdot \left(\frac{\lambda_r}{\lambda_0}\right)^q}, \quad (1)$$

where $\alpha_{fog}$ is an attenuation of fog, unit is dB/km. $V_m$ is a meteorological visibility, unit is km, $\lambda_r$ is reference wavelength (555nm) and $\lambda_0$ is a wavelength of laser beam, unit is nm. Meteorological visibility is defined as a distance for which a transmission is $T = 0.02 = 2\%$. The transmission $T$ is described as

$$T = \frac{I_{output}}{I_{input}} = 0.02. \quad (2)$$

The last parameter in (1) is $q$, which is given in table. $q$ is an empirical value [3].

TABLE I. TABLE OF Q VALUES [3]

| Table of $q$ values | |
|---|---|
| $V_m$ [km] | $q$ |
| $V_m > 50$ km | 1.6 |
| 6 km $< V_m \leq 50$ km | 1.3 |
| 1 km $< V_m \leq 6$ km | $0.16\,V_m + 0.34$ |
| 0.5 km $< V_m \leq 1$ km | $V_m - 0.5$ |
| $V_m \leq 0.5$ km | 0 |

### B. Propagation attenuation

When a laser beam propagates through an atmosphere the power of beam is attenuated because atmosphere is not vacuum. In the clear atmosphere the attenuation is called propagation attenuation. Propagation attenuation $\alpha_p$ is described by equation

$$\alpha_p = 20 \cdot \log\left(\frac{L_0}{L_d + L_0}\right) [3]. \quad (3)$$

The unit of $\alpha_p$ is dB/km. $L_d$ is communication distance, unit is km. $L_0$ is an additional distance. It can be expressed as

$$L_0 \approx \frac{D_{Tr}}{\varphi_{Tr}}, \quad (4)$$

where $D_{Tr}$ is diameter of transmitted optical aperture and $\varphi_{Tr}$ is a beam divergence [3].

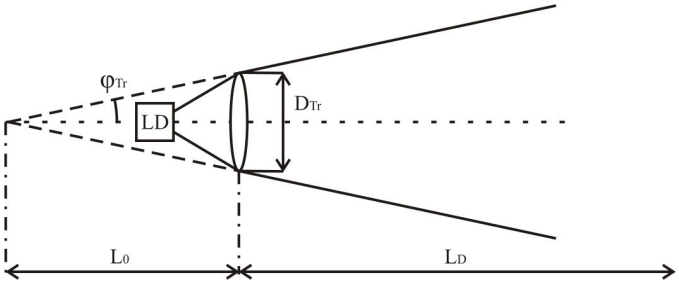


Figure 1. Additional distance $L_0$ [3]

In the clear atmosphere the propagation attenuation $\alpha_p$ achieves a value in range 0.5 – 1 dB/km [3].

## III. FSO LINK WITH FOG MODEL

### A. *OptiSystem Software*

Optical communication systems are increasing in complexity on an almost daily basis. The design and analysis of these systems, which normally include nonlinear devices and non-Gaussian noise sources, are highly complex and extremely time-intensive. As a result, these tasks can now only be performed efficiently and effectively with the help of advanced new software tools [4].

OptiSystem is an innovative optical communication system simulation package that designs, tests, and optimizes virtually any type of optical link in the physical layer of a broad spectrum of optical networks, from analog video broadcasting systems to intercontinental backbones [4].

OptiSystem is based on graphic language. Active and passive components are put in layout from the large library. Components are made according real parameters [4].

Benefits of OptiSystem [4]:

- rapid, low-cost prototyping,
- global insight into system performance,
- straightforward access to extensive sets of system characterization data,
- automatic parameter scanning and optimization,
- assessment of parameter sensitivities aiding design tolerance specifications,
- dramatic reduction of investment risk and time-to-market,
- visual representation of design options and scenarios to present to prospective customers.

### B. *FSO Link*

It was created a FSO link which contains a transmitter, a clear atmosphere, a fog and a receiver. This situation in Figure 2 can appears, when the laser beam propagates over some water source like river or lake. Close water source fog appears more often.

As transmitter was chosen CW laser, wavelength 632.8nm, power 5mW, beam diameter 0.8mm, beam divergence 1mrad [5].

As receiver was chosen PIN photodetector with wavelength range 400-1100nm and optical power working range 50nW–50mW [6].

The fog was created by Matlab component in OptiSystem. Matlab component uses a script written in Matlab [7]. The script includes equations to calculate parameters of transmitted beam. The user defines input variables by adding User parameters. These User parameters are easy changeable therefore different conditions can be simulated. It was created User parameters Visibility [km] and FogWidth [km].

Matlab chooses the parameter $q$ according the table I. Wavelength $\lambda_0$ is load by command "lambda = 299792458/InputPort1.Parameterized.Frequency". Matlab calculates the attenuation according equation (1).

The clear atmosphere was created by Matlab component too. The User parameters are Distance [km] and Attenuation [dB/km].

In the arrangement in Figure 4 the power can be measured at any point of FSO link. It allows know the energy budget which is very important for FSO link design. In the Figure 4 is measured power of laser and power before receiver.

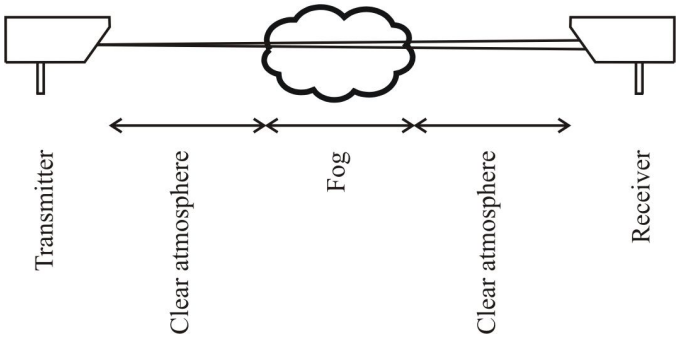


Figure 2. FSO Link with fog

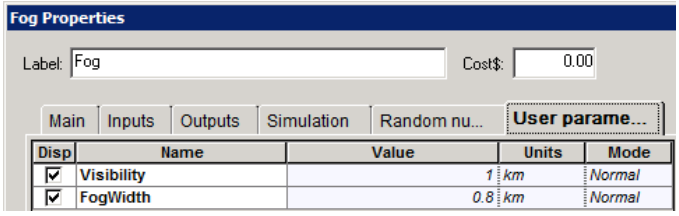


Figure 3. User parameters

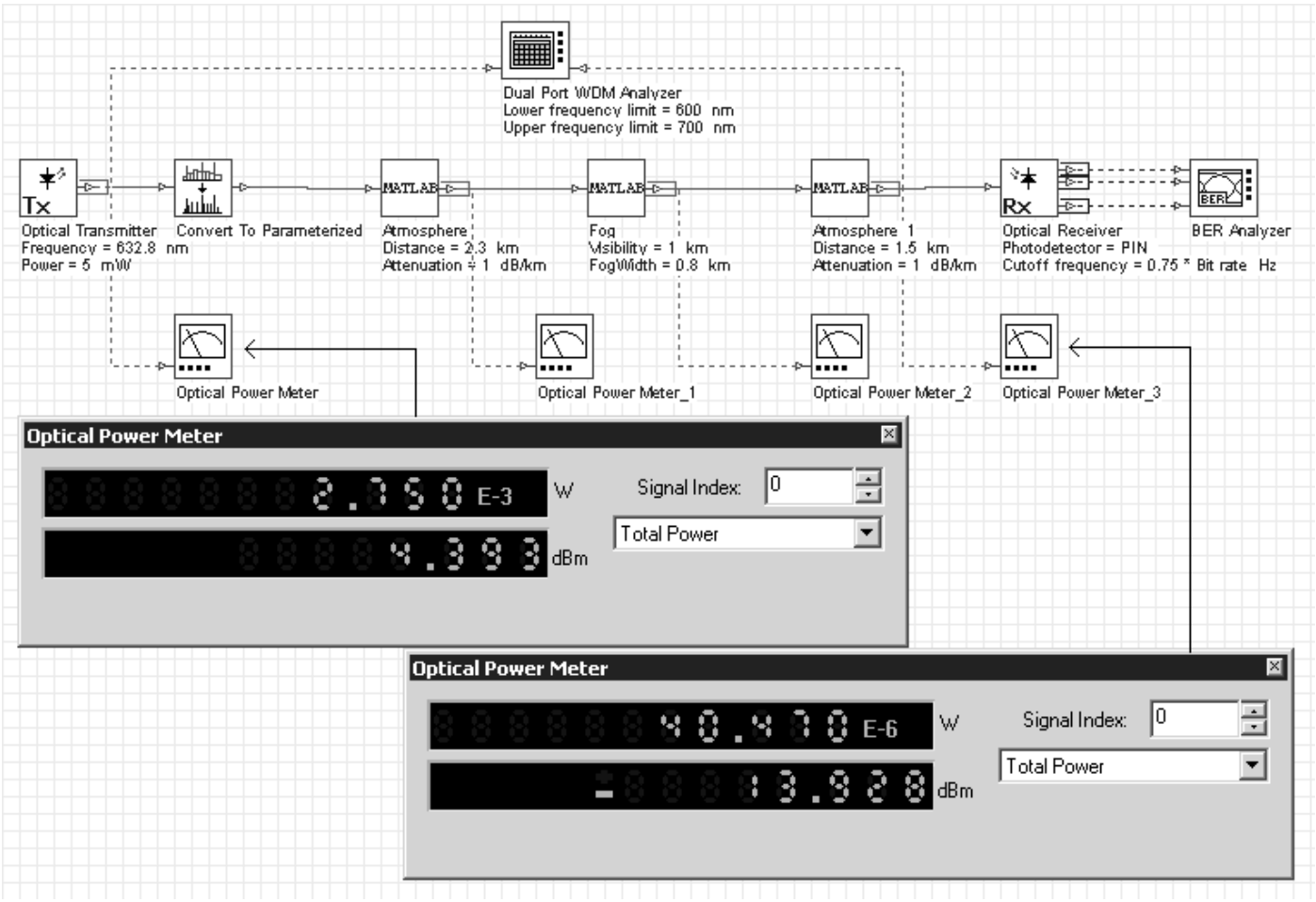


Figure 4. FSO link in OptiSystem

## IV. CONCLUSION

OptiSystem is software which includes a lot of components, allows simulate many designs and is very sophisticated. But it does not include fog component that is why it was created. As it was mentioned above, fog very influences transmitted beam therefore this component is useful.

## ACKNOWLEDGMENT

This project has been supported by a Czech Science Foundation GA102/09/0550 and CESNET 337/2010, SP/2010185.

## REFERENCES

[1] *National Weather Service* [online]. 2010 [cit. 2010-11-18]. Terms used by meteorologists, forecasters, weather observers, and in weather forecasts. http://www.erh.noaa.gov/er/box/glossary.htm.

[2] SHEIKH MUHAMMAD, S.; KÖHLDORFER, P.; LEITGEB, E. Channel Modeling for Terrestrial Free Space Optical Links. In *7th International Conference on Transparent Optical Networks* [online]. Barcelona : IEEE, 2005 [cit. 2010-11-16]. <http://www.scribd.com/doc/36340567/Channel-Modeling-for-Terrestrial-FSO>.

[3] WILFERT, Otakar. *Fotonika a optické komunikace - přednášky*. Brno : Vutium, 2000. 122 s. ISBN 978-80-214-3537-7.

[4] OptiSystem : Getting Started. Kanada : OptiSystem, 2010.

[5] *Melles Griot* [online]. 2010 [cit. 2010-11-17]. CVI Melles Griot. <http://www.cvimellesgriot.com/Products/Red-632.8-nm-Cylindrical-Helium-Neon-Laser-Systems.aspx>.

[6] *Thorlabs* [online]. 2010 [cit. 2010-11-17]. Standard Power Sensor, Si, 400 - 1100 nm, 50 mW. <http://www.thorlabs.de/thorProduct.cfm?partNumber=S120C>.

[7] OptiSystem : Component Library. Kanada : OptiSystem, 2010.

# The Optical Burst Switching OMNET++ Simulator Model Extension with The Polarisation Multiplex

Miloš Kozak
Faculty of Electrical Engineering, Department of telecommunication technology
Czech Technical University in Prague
Prague, Czech Republic
milos.kozak@fel.cvut.cz

Leos Bohac
Faculty of Electrical Engineering, Department of telecommunication technology
Czech Technical University in Prague
Prague, Czech Republic
bohac@fel.cvut.cz

*Abstract* — **This paper deals with the simulations of the optical communication systems. The main focus of the simulations is on OMNeT++ simulation environment and the telecommunication fibre optics. The optical burst switching technique is considered and further extended with the polarisation multiplex.**

***Keywords-Optical models; OBS; Bursts, Routing, Polarisation multiplex***

## I. INTRODUCTION

The massive deployment of the access technologies such as Asymmetric Digital Subscriber Line (ADSL), wireless networks or even passive optical networks in cities have facilitated a variety of new multimedia services such as YouTube, Skype, etc. But the deployment of these services led to a significant increase in the data traffic. As a result the transmission and switching systems must be modernised to handle this massive amount of user data transmitted to and from data centrums where servers of these services are located.

A number of new technologies have recently emerged to tackle the aforementioned problems. The first one is the wavelength division multiplexing (WDM) which is based on using more channels in one fibre. The foreseen speed limitations of the electronic switching and routing systems have stimulated active research on promising technologies like the optical packet switching (OPS) and optical burst switching (OBS). The main focus of this article is on the optical burst switching network modelling in simulation environment of OMNeT++ and the proposition of new bandwidth extension method using polarisation multiplex. The OMNeT++ simulator and its usage in the field of the optical networks is briefly summarized in the chapter II. Chapter III describes main aspects of current state of OBS. Description of models that can be used for the simulations is carried out in paragraph a). Chapter IV proposes extension of OBS models to allow polarization multiplexing.

## II. THE OPTICAL NETWORK SIMULATIONS IN OMNET++

The simulations are very useful for understanding of system behaviour, because it is possible to easily specify input variables and make a very comfortable post-evaluation of the system after a simulation was carried out. The simulation is indispensable tool in situations where the real systems are not yet on the market or where their testing would be very expensive, impractical or time consuming. The simulations, if well done, change the development process where the system or network is first simulated, checked for correct functionality and then actually built and manufactured. The domain of optical burst switching networks is just one example because only a few laboratory test beds exist around the world now. As a result the majority of proposals in the area of optical burst switching concepts came out from the simulations.

The simulations costs are cut because the system function is simulated in software running on a computer and thus it is not necessary to build the equipment or network itself to test on. Through the simulations it is more flexible to change some of the parameters of the model in contrast to the real situations where more complicated hardware interventions are sometimes required. Also a special working environment can be simulated that is difficult to achieve in the practice. However, the true test bed gives more relevant results, because it is still difficult to simulate some stochastic processes accurately in software only.

The various software packages are available for the simulation of data networks. One of them is OMNeT++, an object-oriented modular discrete event network simulation framework that allows simulation of a broad range of the communication systems from the wireless to the optics. In the area of optics it is not extensible used as in the other fields because of less interest in the optical switching simulations and the existence of other commercial simulators that are capable to simulate propagation effects on the physical optical signal as it propagate in the fibre (1st RM-OSI layer). And as to the less interest in optical simulations in OMNeT++, a possible reason may be in unavailability of optical models which could be used for the optical system simulations. The OMNeT++ simulation environment uses C++ programming language as the main language in addition to two meta-languages that are used for the message and network topology description. Both meta-languages are processed using tools which are shipped with OMNeT++ simulation environment. Names and usage of these tools are depicted in Figure 1.

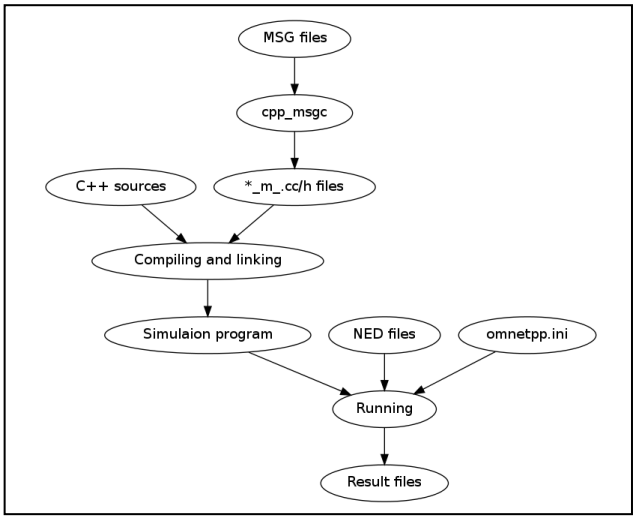


Figure 1. OMNeT++ simulation build proces.

The OMNeT++ can be easily used for the simulations of both metropolitan and wide area networks containing optical nodes.

## III. OPTICAL BURST SWITCHING

The optical burst switching is an all-optical switching technology considered as a candidate for the next-generation transmission systems. The slow speed of recent all-optical switching elements and processing units prohibits full optical processing. As a consequence it is still necessary to evaluate the content of the switching header in real time and drive the optical switching elements as quickly as possible to avoid losing the data content of the packet that goes immediately after the header. It is not yet possible in contrast to the electronics to delay an optical packet arbitrarily in buffer for a period of time as we do not have an optical memory.

What seems to be feasible today is to use in-advance reservation mechanism. In this case the lightpath is set before an optical burst is sent into the network and torn down if it is not needed any more. It means no optical buffering is needed. An optical burst is usually defined as a number of continuous packets destined to a common egress point [2]. The burst size can vary from a single IP packet to a large data set at milliseconds time scale. The small time scale allows fine grained multiplexing over a single wavelength. Every optical burst is preceded by burst control packet (BCP) which is set onto a different wavelength and is used for signalling. BCP carries significant information for switching node to set an appropriate optical cross connects (OXC) to appropriate state to satisfy reservation and routing demands. Fundamental parts of switching node are depicted in Figure 2. From Figure 2. it is clear there are two different plains, control and data plane. The control plane is the point-to-point and the optical-electrical-optical conversion is used because BCP processor is an ordinary electronic device conducting OXC function.

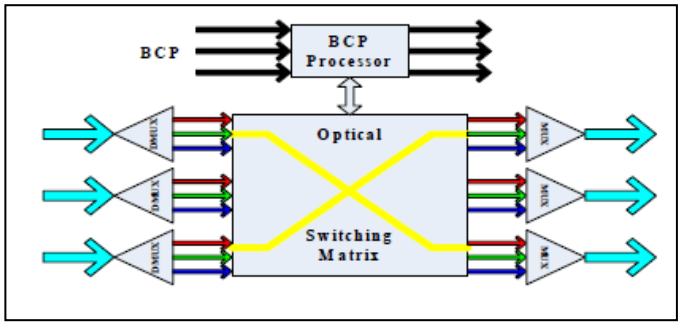


Figure 2. Basic concept of OBS core node.

The OBS network performance depends on signalling strategy. The most appropriate strategy can be achieved through the graph theory. If is given a topology *G(N,L)* where *N* - number of nodes, *L* - number of links. Blocking probability between any two nodes is denoted by (1).

$$1 - B_{f_j} = \prod_{i \in f_j} \left(1 - B_{l_i}\right), \quad j = 1, \ldots, N^2 \tag{1}$$

Where $f_j$ stands for *j*-th lightpath and $B_{l_j}$ is blocking of *j*-th link, $B_{f_j}$ is blocking of *j*-th lightpath.

$$I_{l_i} = \sum_j I_{f_j} \prod_k \left(1 - B_{l_k}\right) \tag{2}$$

Where $I_{l_i}$ denotes offered traffic carried by an individual link and $B_{l_k}$ denotes blocking of link and $I_{f_j}$ denotes offered traffic of a lightpath. Blocking of a links is obtained from (3), where $M_i$ denotes a number of wavelengths of the *i*-th link.

$$B_{l_i} = E_B\left(I_{l_i}, M_i\right) \tag{3}$$

Finally if the (3) is substituted back into (1) the blocking probability of the link can be computed.

### A. Simulation of OBS networks

The simulations of networks using OBS can be performed using several software packages, for example using OMNeT++ simulator. To perform simulations it is highly desirable to use a library of OBS network models. This library is freely available [3]. The name of this library is *OBSModules* and can be run under OMNeT++ v3.3 and INET 20061020. Models included in this library provide only basic functionality of OBS network nodes. The JET signalisation [4],[5], static routing only with no polarisation multiplex (PolMUX) and wavelength conversion are currently implemented. On the other hand there is full implementation of EdgeNode and CodeNode model, see Figure 3.

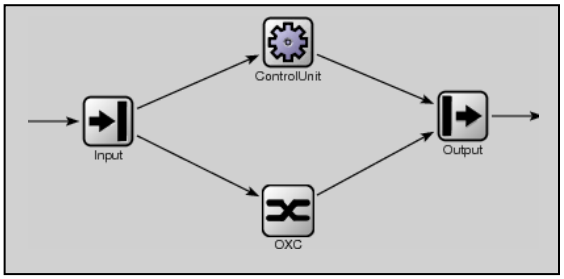


Figure 3. CoreNode definition in NED language.

EdgeNode model is used as the ingress to the network formed of CoreNodes. EdgeNode model is based on the Router model contained in INET framework and extends it with the optical burst interface. The CoreNode consists of the input and output components that must decide whether an arriving message is BCP or the optical burst in relation to the corresponding switch and drive ControlUnit or OXC. The ControlUnit implements Control Plane mechanisms.

## IV. The Extension with the Polarisation Multiplex

The PolMUX facilitates achieving of higher throughput and decreases blocking probability (1). The PolMUX introduces two orthogonal polarizations each carrying different control and data [2]. The polarizations are identified as the in-phase and quadrature [6] and can be considered as two non-interfering channels.

Blocking probability of the system can be obtained through evaluation of (3), (1) but parameter $M_i$ in (3) must be doubled and two more channels must be considered in calculations. Resulting blocking probability difference between PolMUX and ordinary transmission system is depicted in Figure 4. The graph is parameterised with the offered load in Erlangs and exhibits blocking gap where ordinary system is blocked but PolMUX system is not.

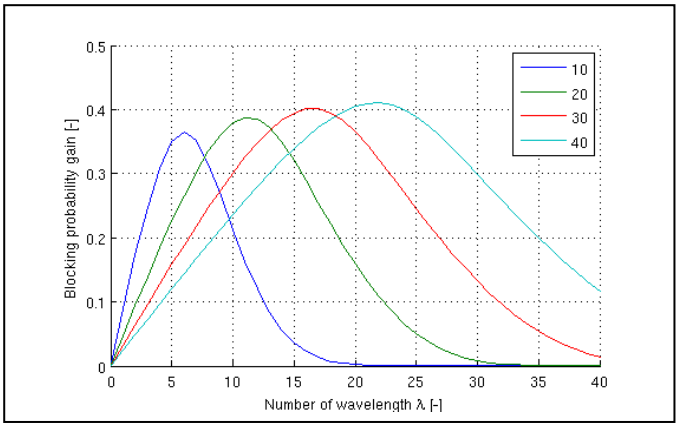


Figure 4. Blocking probability gain.

It is clear the PolMUX brings better utilization of current transmission system, but new driving systems must be installed to perform polarisation changes. Before installation of these systems the complete transmission system must be simulated to find the most appropriate input parameters. These optimal parameters can be find out with the simulations. Aforementioned library does not include a PolMUX facility, so must be implemented first.

Bringing PolMUX into OBSModules denotes a lot of code changes in the messages, component description and in model implementation of both EdgeNode and CoreNode. The most significant change is the integration of information about the polarization in the messages used for BCP and an optical burst see Table I. Parameter *inPhase* is also significant for OXC and ControlUnit model because it describes the optical burst. Based on this parameter optical burst can be dropped if polarization does not match predefined state on OXC. It means the ingress port is filtered. Filtering must have been newly implemented in OXC model using C++ language.

TABLE I. OMNeT++ messages extended with PolMUX parameter a) BCP, b)Optical burst.

```
message OBS_BurstControlPacket
{
   int msgColour;
   simtime_t burstArrivalTime;
   int burstColour;
   int label;
   int burstfierId;
   int numSeq;
   int senderId;
   int burstSize;
    bool inPhase;
}
```

```
message OBS_Burst
{
  properties:
   customize = true;
  fields:
   cQueue messages;
   int numPackets;
   simtime_t minOffset;
   simtime_t maxOffset;
   int lambda;
   int label;
   int burstfierId;
   int numSeq;
   int senderId;
   bool inPhase;
};
```

Proposal of a new OXC component description is denoted in Table II. A new *inPhase* parameter is introduced and in the model implementation is used for making a decision whether or not to drop that burst. Dropping itself is done by OXC model. The parameter is set in simulation configuration file.

TABLE II. OMNeT++ OXC component description.

```
simple OBS_OpticalCrossConnect
  parameters:
    switchingDelay: const;
    inPhase;
  gates:
    in: in[];
    out: out[];
endsimple;
```

CoreNode with support of PolMUX is depicted in Figure 5, only one ControlUnit is used thanks to OMNeT++'s parallel processing facility. Two building blocks of OXC were used, both terminating the same optical signal moreover both are filtering the signal of improper polarization burst.

This PolMUX implementation decreases blocking probability but increases memory consumption of simulation [3].

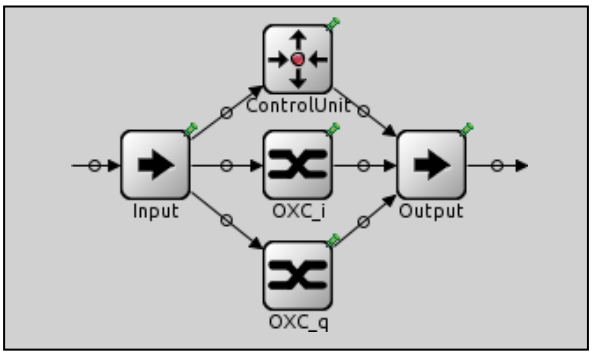


Figure 5. OMNeT++ proposed CoreNode definition in NED language.

## V. CONCLUSION

The motivation for writing this paper was the lack of articles dealing with this topic, in the time of writing this article. Secondly it was challenge of lower blocking probability and increasing of throughput. This proposal cannot be used with systems using similar 1st RM-OSI modulations as 100 Gbit/s Ethernet standard, which uses two polarizations for description of one modulation symbol. Additionally PMD must be taken into account because uncompensated PMD can introduce polarization cross talk and so decrease throughput and increase bit error ratio.

This article introduces a new proposal of PolMux for optical burst switching networks, supply informations important for PolMUX implementation in *OBSModule*ses CoreNode for OMNeT++. The article does not contain all informations useful for PolMUX implementation of EdgeNode, but all informations contained in this article are valid for EdgeNode as well.

## VI. ACKNOWLEADGEMENT

The work was supported by grant The Research in the Area of the Prospective Information and Communication Technologies under project MSM6840770014

## VII. REFERENCES

[1] RUMLEY, S, et al. Towards Digital Optical Networks. Germany : Springer, 2009. Software Tools and Methods for Research and Education in Optical Networks, s. 362. ISBN 0302-9743.

[2] https://www.tlm.unavarra.es/investigacion/proyectos/strrong/soft/obsmodules/

[3] ESPINA, Felix, et al. OBS network model for OMNeT++: A performance evaluation. OMNeT++ 2010 March. 2010, 5, s. 134-142. ISSN 78-963-9799-87-5.

[4] Y. Chen, C. Qiao, and X. Yu. Optical burst switching: a new area in optical networking research. Network, IEEE, 18(3):16–23, May-June 2004.

[5] VAN DEN BORNE, Dick, et al. POLMUX-QPSK modulation and coherent detection: the challenge of long-haul 100G transmission. ECOC. 2009, s. 123-127. Dostupný také z WWW: <[5] http://alexandria.tue.nl/openaccess/Metis233169.pdf>. ISSN 978-3-8007-3173-2.

**Miloš Kozák** received the M.S. degree in electrical engineering from the Czech Technical University, Prague, in 2009. He participates in teaching of course of optical communication systems. His research interest is on the application of high-speed optical transmission systems in a data network. Currently he is activaly involed in some of the projects on high speed optical modulations and Communication of Czech Antarctic Station.

**Leoš Boháč** received the M.S. and Ph.D. degrees in electrical engineering from the Czech Technical University, Prague, in 1992 and 2001, respectively. Since 1992, he has been teaching optical communication systems and data networks with the Czech Technical University, Prague. His research interest is on the application of high-speed optical transmission systems in a data network. He has also participated in the optical research project CESNET - the academic data network provider to help implement a long-haul high-speed optical research network. Currently he is actually involved in and leads some of the projects on optimal protocol design, routing, high speed optical modulations and Turbo codes for future data and optical networks.

# *System for Evaluating Impulse Signals*

Radek Novak, Vladimir Vasinek
Department of Telecommunications
VŠB TU Ostrava, 17.Listopadu 15
Ostrava, Czech Republic
radek.novak@vsb.cz, vladimir.vasinek@vsb.cz

*Abstract*— **In our Department of Telecommunications is solved science grant GA102/06/1202 „Optical Microcell Fiberless Aproach Networks“ . There are 4 sources of light in described system. These sources are synchronously sending the same information in form short flashes of lightning. On the board of movable car are placed 4 photoelectric sensors producing globally 4 output signals. These signals are evaluated by described circuits.**

***Keywords - Optical microcell fiberless aproach network; microelectronics; photosenzor; microcontroller; flip – flop; sample-hold circuit.***

## I. Introduction – short description of the system

There are 4 sources of light in described system. These sources are synchronously sending the same information in form short flashes of lightning [1] [3]. On the board of movable car are placed 4 photoelectric sensors producing globally 4 output signals i3, i2, i1, i0. The sensors are of type DET10C/M(THORLABS). Because sensors are in different distance from their individual light sources, so final impulses have shapes see pic. 1.

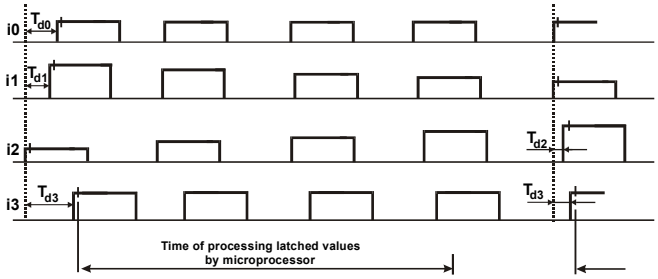


Pic. 1 Evaluated impulses i0 – i3

So impulses differ in amplitude and also in time-delay. The task for microprocessor [5] in described system is to evaluate amplitudes and time-delays of signals i3, i2, i1, i0. It is only one of tasks solved in the mentioned grant. Microprocessor must decide which of the signals i3, i2, i1, i0 is dominant, which is too small(this one will be ignored), which of them will be added. Outputs of microprocessor are only four discrete signals giving information which channels continues to next circuits, and which channels are ignored. The task is not time-critical, existing time of processing (Pic.1) is not problem, because impulses can't dramatically change. Block schema of realized system is on pic. 2.

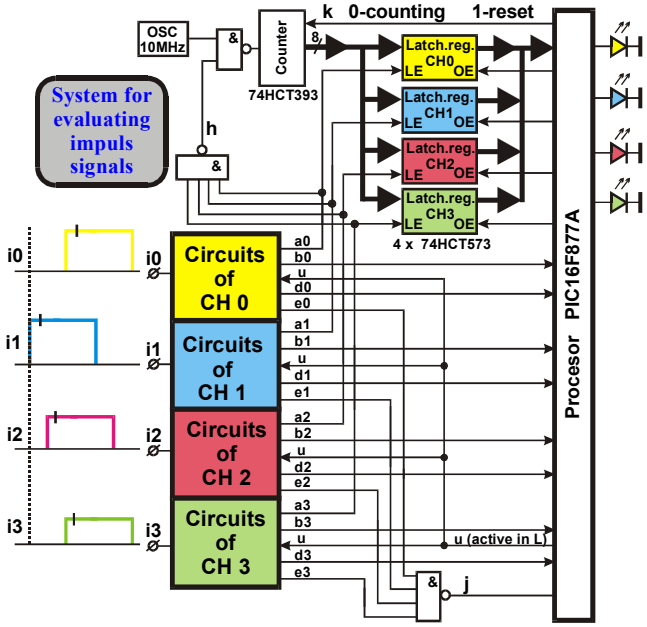


Pic. 2 Block schema of system

Described solution consists in measuring of amplitudes and time-delays Td . Amplitude is memoried by Sample/Hold circuit (Analog Devices AD781) and consequently digitized in microprocessor [5]. The amplitude is memoried 1ms after rising edge of impuls, it is given by the Monostabil flip-flop. Time-delay is measured by common counter, started by the first rising edge. It counts 10MHz signal from oscillator. Time-delay is latched internally by latch register 74HCT573 as value of counter at moment of rising edge.

## II. Details of the solution

### *A. Measuring of Amplitude*

Detail schema for example of Channel_3 is on pic.3. Signal i3 is formatted by comparator MAX913 having two outputs. Compare level is given by resistor divider connected

to inverting input. At rising edge of i3 a negative impuls appears in signal m3, it is generated by Monostabil flip-flop. At moment of rising edge of m3 an actual amplitude of i3 is held by the Sample/Hold circuit AD781 as d3 signal, it is coupled to A/D converter of microprocessor [3][5].

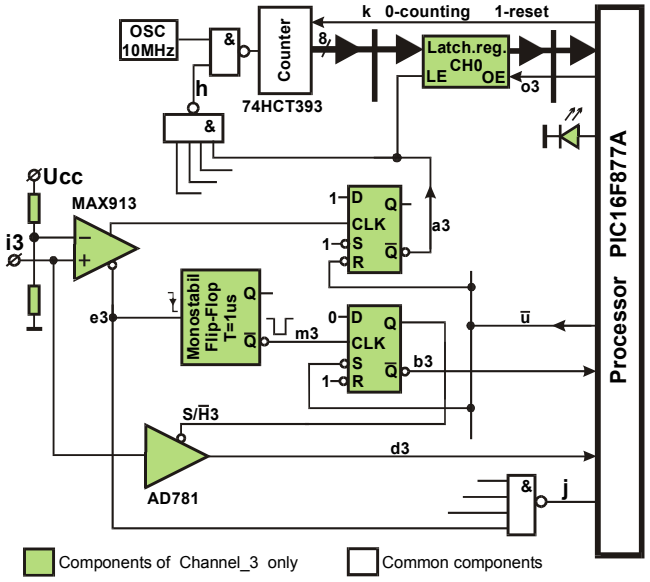


Pic.3 Circuits of Channel_3, detail schema

Logical „1“ in signal b3 means „new value of amplitude is present in output of sample-hold circuit“ , and the processor can carry out A/D conversion, and read latched value from latch register. When all channels are processed, so processor resets the circuits - activates u signal(active in 0), and also resets counter by k signal. This u signal After it processor waits for situation „no impuls in any channel“, it is idicated by „0“ in signal j . If it is recognized, then processor pasivates u signal.

### *B. Measuring of time - delay*

At rising edge of i3 the „0“ is created by D flip-flop in signal a3(falling edge). The gating signal „h“ is forced to H, NAND gate stays transparent, and oscillator signal is counted by counter. The same falling edge of a3 serves to memorying of momental value of counter internally in latch register 74HCT573. All the solution is based on fact, that not every group of impulses must be processed, because their amplitudes and time-delays can’t change very dynamicly. Measure cyclus starts by initial state, this is created by L in control signal “u”. After it microprocessor waits for 0 in all the impuls signals i0 – i3. If all of them are 0, then “j” is 0, so microprocessor waits for transition from 1 to 0 in this signal. After this transition control signal “u” is pasivated, level H. Now microprocessor is waiting for situation “all impulses have come”, it is indicated by level H in all the signals b0 – b3. If it appears, then microprocessor succesive reads holded amplitudes and latched time-delays, and processes them. Criterium of evaluating : If one of impulses is dominant by its amplitude(all rest signals are less than 80% of this amplitude), so only this signal is transfered to consequent circuits. If this rule is False, so signal with maximal amplitude and signal with minimal time-delay will be added and transferred to consequent circuits. Final results are indicated by four LEDs. Limitating component in described solution is Sample/Hold AD781, it has acquisition time 700ns. It determines maximal frequency of measured signal.

## III. MEASURED DIAGRAMS

There are four impulse signals from four photosensors in pic. 4.

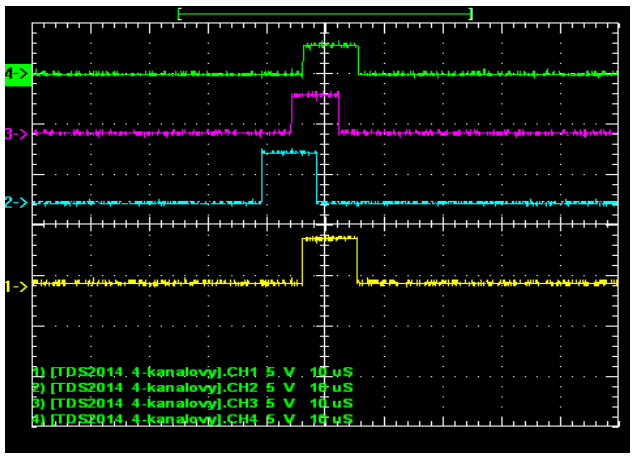


Pic. 4 Processed impulses (scale 10µs/el.)

4(green)……..impulse signal i3

3(red)……..impulse signal i2

2(blue)……....impulse signal i1

1(yellow)…....impulse signal i0

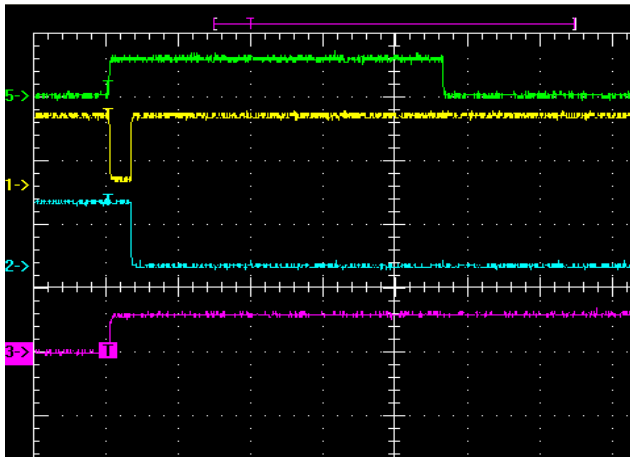


Pic.5 Detail view to Channel 3 signals (scale 2,5µs/el.)

5(green)……..impulse signal i3

1(yellow)……signal m3(output of monostabil Flip-Flop)

2(blue)……....signal S/H3 ( control signal for S/H circuit )

3(red)……....signal d3(output of S/H circuit)

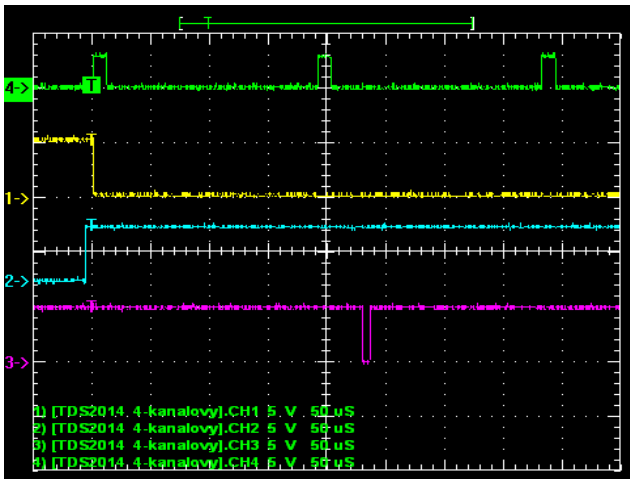


Pic. 6 Other signals of Channel 3 (scale 50ms/el.)

4(green)……impulse signal i3

1(yellow)…..signal a3 ( Q-NON output of D Flip-Flop )

2(blue)…...…signal h ( output of NAND gate )

3(red)……signal o3(OE-Output Enable for latch register, generated by microprocessor )

Next intended way in impulses processing will consist in different princip of evaluating, very fast A/D converters ADC08100 and Xilinx Spartan XC3S1200E circuits will be used.

## References


[1] VAŠINEK, V. : Analyzis of Solution Grant Project and Summary. Report on solution grant project GA102/06/1202 „Optical Microcell Fiberless Aproach Networks“. Grant Agency of Czech Republic, Prague, 2009.

[2] NOVÁK, R. : ELECTRONIC DEVICE TCW4. In 6th International Conference RTT 2005, Hradec nad Moravici, FEI VSB-TUO, ISBN 80-248-0897-8.

[3] Koudelka, P., Látal, J., Hanáček, F., Vašinek, V.: Optofibre Distribute Systems Applied Into Industry. In Optické komunikace 2009, Praha, ISBN 978-80-86742-28-1.

[4] LÁTAL, J., KOUDELKA, P., ŠIŠKA, P., HANÁČEK, F., SKAPA, J., VAŠINEK, V.: Passive fiber rings as a basic part of fiber optic sensors, In conference SPIE Photonics West 2010, USA, SPIE--The International Society for Optical Engineering, 2010.

[5] PIC16F87XA Data Sheet [online] c2008 [cit. 2009-12-12]. http://ww1.microchip.com/downloads/en/DeviceDoc/39582b.pdf

[6] KOUDELKA, P., LÁTAL, J., SKAPA, J., VAŠINEK, V., HANÁČEK, F., ŠIŠKA, P.: Vláknově optické senzory - hudba budoucnosti. In Automatizace, Praha. Ed. Bc.Ivana Klimtová, 09/2009, s. 577-579, ISSN 0005-125X.

# Radio Networks and Wireless Communications

# Synthetic Coordinate System in Wireless Sensor Networks

Patrik Moravek, Dan Komosny, Pavel Vajsar
Department of Telecommunication
Brno University of Technology
Brno, Czech Republic
moravek@phd.feec.vutbr.cz, komosny@feec.vutbr.cz, xvajsa01@stud.feec.vutbr.cz

***Abstract* — The paper presents a possibility of synthetic coordinate system viability for localization purposes in wireless sensor networks. It is very challenging to employ synthetic coordinate localization algorithms proposed for IP based networks in energy constraint networks. We proposed modified version of Vivaldi localization algorithm with 2D plus height system and developed a simulator tool for initial investigation of its function in WSN based networks.**

***Keywords - WSN; localization; synthetic coordinates; Vivaldi***

## I. INTRODUCTION

Wireless sensor networks are an emerging network technology with promising perspective in the future. The networks consist of small low-cost, low-powered devices capable of sensing surrounding quantities and monitor the environment. The devices called sensor nodes are equipped with radio interface for wireless communication. Standard that describes physical and link layer of such communication is IEEE 802.15.4 [1], for addressing, routing and other functions on higher levels Zigbee standard is often used [2].

WSN covers broad band of applications ranging from military projects (the historical origin of this technology) to medical surveillance including habitat monitoring, storehouse management or building automation.

In a lot of applications self-localization of network nodes is a high desirable feature. Sensed data without location information are meaningless. Moreover, other processes run in WSN can advantageously exploit the position knowledge for better and more efficient function. Geographical routing, hierarchical aggregation, multicast and data gathering can be mentioned as examples of such processes [3].

Because of a high variety of application in different fields and with different features, there are also a lot of different requirements on localization process. Some of the applications need a precise localization with an error less than 10 % and for other coarse grained localization is sufficient. However, in general, WSN nodes are equipped with limited energy sources and thus each process in WSN should be energy aware.

One of the approaches increasing accuracy of localization in IP based network contains synthetic coordinate system. This approach

The rest of the paper is organized as follows. Section II gives a brief overview of localization techniques and approaches, section III introduces synthetic coordinate systems and their representatives. The discussion of viability of synthetic coordinates and necessary modification of Vivaldi algorithm for use in WSN follow in section IV. New simulator designed for simulation of Vivaldi and its modification is described in section V, which precede the last summarizing section VI.

## II. LOCALIZATION

The term of localization relates to finding a position of an object in a defined area, generally. In IP based networks, the localization mainly means locating the station within the network. However, since a lot of application provides surveillance, localization in WSN can also include locating an object, which is not a component of a network topology. This is called tracking and we do not consider it in this paper.

Localization protocols incorporate a localization algorithm to estimate the location of sensor node without previous knowledge of its coordinates. The localization can be relative to other nodes in a network or absolute in a determined coordinate system. If the network contains certain percentage of nodes with known position (called anchors), the unknown nodes (nodes have no knowledge of their position) use a certain measurement technique to estimate distance to these nodes and calculate their own position using determined localization algorithm. Anchor nodes can obtain their coordinates from GPS or by manual assignment. However, both approaches have their shortcomings either in higher energy cost or demanding initial process. The coordinate system of anchors is then applied to other nodes as well. The brief taxonomy of WSN localization is given in [4].

Localization algorithms require certain input information for position determination. They work with information including mainly distances or angles. To obtain this information, specific measurement techniques are used. These techniques can be categorized into three main classes: RSS (received signal strength), TOA (time of arrival) and AOA

(angle of arrival) based techniques [5]. Direct measurement is another technique, which is however impossible to use in most of applications.

RSS based method of distance estimation infers the distance from signal strength measured in a receiver. There are several signal propagation models that approximate the real radio channel and allow to relate received signal strength to the distance between transmitter and receiver. It is inexpensive and easy method of estimation in WSN since no extra hardware is required. However, several negative influences affect the measurement and cause estimation errors [6][7].

Next category of measurements is based on measurement of signal propagation time. One-way measurement infers the distance between two nodes from sending and receiving time of the nodes. It requires precise clock at each node and complex time synchronization of all nodes. To overcome this inconveniences, round-trip delay (RTT) can be calculated. The difference between sending and receiving time is measured at the same node and thus the synchronization is not necessary. However, a processing delay (to handle a packet) of the other node is included in the measured value. TDOA (time difference of arrival) is another category, which computes the position of the transmitter from the delay measured at several different nodes with known position.

The last class of measurement techniques employs a system of angle measurement. If the unknown node knows at least the coordinates of two transmitting nodes and their directions, it is able to calculate its own position. For more detailed information about localization techniques and algorithms please refer to [5].

## III. SYNTHETIC COORDINATE SYSTEMS

To solve a localization problem in IP based network, the problem of distance estimation between network stations was transferred into an artificial multidimensional coordinate system. Generally, RTT measurement was performed to estimate the distance between two stations. There is no need to measure the RTT between each pair of stations in localization algorithm based on a synthetic coordination system. Instead, the measured value between two stations is estimated from their known coordinates in a predefined synthetic coordinate system. The measured value refers to the calculated distance between stations in the coordinate system. Provided that communication networks work ideally (there are no delays), a geographical coordinate system with longitude and latitude would be the appropriate choice as a coordinate system for localization purposes. Unfortunately, this condition is not accomplished in any real communication network – packets are transmitted via more direct links, delayed in intermediate nodes, etc. Therefore, it is not possible to use a simple 2D coordinate system for RTT value prediction of network nodes. As a result, new artificial coordinate systems were proposed to meet real conditions in IP based networks. There is no limitation in the number of dimensions or the type of coordinate system. Besides the standard Euclidian system, other coordinate systems (spherical, toroid, hyperbolic) were investigated (for more details see [8]). However, the Euclidian coordinate system is used the most because it offers the most suitable possibilities for this purpose.

There are proposed several algorithms using synthetic coordinate system (GNP, Lighthouse system, Vivaldi etc.). GNP [9] is a centralized algorithm with reference stations, which form a matrix of distances between themselves in the first phase and the rest of nodes is localized in the following step.

Lighthouse system presented in [10] uses reference station as well (called lighthouses). Contrary to GNP, it uses simpler mathematical operations and features more scalability thanks to employing recently localized nodes into a reference nodes infrastructure in each iteration step.

### A. *Vivaldi algorithm*

The Vivaldi algorithm proposed by Dabek et al. in [11] is a favourite localization algorithm used to obtain the position of stations in a network using the synthetic coordinate system. The algorithm uses synthetic coordinates with Euclidian distances; two standard dimensions and one extra dimension called height are defined in the new coordinate system. Communication delay in an access network is covered by the third dimension (as the main purpose of this dimension) while delay in a distribution network is expressed by coordinates.

The new coordinate system, 2D Euclidian system with height, is described by the following equations:

$$x - y = (x_1 - y_1, x_2 - y_2, x_h + y_h), \quad (1)$$

$$\|x\| = \sqrt{x_1^{\,2} + x_2^{\,2}} + x_h, \quad (2)$$

$$ax = (ax_1, ax_2, ax_h). \quad (3)$$

Coordinates of nodes are taken as vectors in the whole following text. The difference between standard 3D, 2D system and 2D coordinate system with height is depicted in Fig. 1.

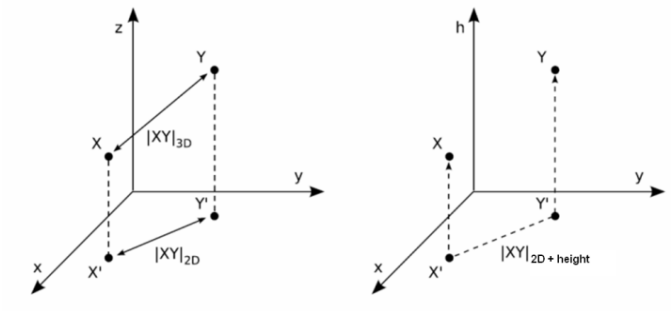


Fig. 1: Distance in 2D, 3D and 2D with height coordinate system

The Vivaldi algorithm is a distributed and decentralized algorithm working without any infrastructure (such as reference stations). All nodes are equivalent in the system.

Finding node coordinates that minimize the error in predicted round-trip latency between arbitrary two nodes in a network is the basic principle of the Vivaldi algorithm. The idea of the algorithm comes from the analogy to a physical

mass-spring system described in [12]. As a spring tends to maintain its length with minimum energy, distances between nodes in a network are set such that minimum predicted latency error is achieved. Findings the energy minimum in the system of springs corresponds to finding the minimum error in the position estimation. Searching for node position is simulated as a movement of nodes connected with springs, see Fig. 2.

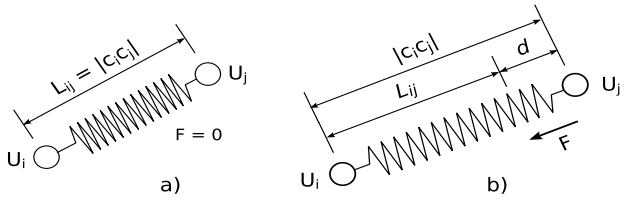


Fig. 2: Spring analogy to predicted latency; a) errorless prediction b) prediction with error

Nodes in a network are moved in a way in order to minimize the error function *E:*

$$E = \sum_i \sum_j (L_{ij} - \left\| \vec{c_i} - \vec{c_j} \right\|), \tag{4}$$

where $L_{ij}$ is the real latency between nodes *i* and *j* and $\vec{c_i}$ and $\vec{c_j}$ are their coordinates in the synthetic coordinate space. This equation corresponds to a spring between *i* and *j* nodes with a length of $L_{ij}$.

The principle of minimizing the error function is derived from the impact of a spring placed between two nodes. According to the Hook law

$$\vec{F} = -k\vec{d}, \tag{5}$$

the stretched or compressed spring affects the surrounding nodes, which are linked by the spring, by the force $\vec{F}$ in the opposite direction to this stretch or compression. This force is proportional to the length of the stretch (compression) described by the vector $\vec{d}$ and the spring constant k. In the Vivaldi algorithm, the force $\vec{F}_{ij}$ affecting the nodes *i* and *j* is

$$\vec{F_{ij}} = (L_{ij} - \left\| \vec{c_i} - \vec{c_j} \right\|)\vec{u}(\vec{c_i} - \vec{c_j}), \tag{6}$$

where $\vec{u}(\vec{c_i} - \vec{c_j})$ is the unit vector with the same direction as the vector $\vec{c_i} - \vec{c_j}$.

The resultant vector $\vec{F}_i$ of a node *i* is the summation of partial vectors $\vec{F}_{ij}$ affecting the node *i* (from all springs connected to the node *i*). In the one iteration step of the computational process the time interval δ of the affecting force $\vec{F}_i$ is considered. The node *i* is subsequently moved to a new position $\vec{c_i}$ in the direction of force $\vec{F}_i$ according to the equation

$$\vec{c_i} = \vec{c_i} + \delta\vec{F_{ij}}. \tag{7}$$

Since the Vivaldi algorithm is a decentralized localization algorithm, the presented idea is performed at all nodes in a network. Each node then individually simulates its movement. The direction and the length of movement are computed from the latency values $L_{ij}$ and coordinates $\vec{c_j}$ received from nodes *j*.

The decentralized character of the algorithm means also that the coordinates received do not have to be reliable. The node with the coordinate $\vec{c_j}$ can be, for example, a new node at the beginning of the localization process or a node that cannot determine its position for whatever reason, and its coordinate oscillates.

The negative impact of the situations described is reduced in the Vivaldi algorithm with an adaptive timestep by assigning a specific error $e_j$ to each node. This error is sent by node with its coordinate.

The complete process of algorithm for node *i* is described in five steps below.

1) the weight *w* is computed from the estimated errors in coordinate calculation at the local node *i* and a distant node *j*

$$w = \frac{e_i}{e_i + e_j} \tag{8}$$

2) the relative error $e_s$ of latency measurement calculation

$$e_s = \frac{L_{ij} - \left\| \vec{c_i} - \vec{c_j} \right\|}{L_{ij}} \tag{9}$$

3) the weighted moving average of local error $e_i$ is updated

$$e_i = e_s c_e w + e_i(1 - c_e w) \tag{10}$$

4) timestep δ calculation

$$\delta = c_c w \tag{11}$$

5) the node coordinate is updated

$$\vec{c_i} = \vec{c_i} + \delta(L_{ij} - \left\| \vec{c_i} - \vec{c_j} \right\|)\vec{u}(\vec{c_i} - \vec{c_j}) \tag{12}$$

One modification of the Vivaldi algorithm implements also the timestep δ adapted by multiplication by the constant $c_c$ and the weight *w* (step 4). The weight *w* depends on both local error $e_i$ and distant error $e_j$. If the error $e_j$ is greater related to local error $e_i$ the weight *w* is smaller and the node *j* has small relevance in position calculation. On the contrary, if the error $e_j$

is small, the weight $w$ is close to one and the node $j$ impacts on position calculation significantly.

The error $e_i$ in coordinate estimation is calculated in step 3 as a weighted moving average of relative latency error $e_s$. The value of this average can be changed by a tune constant $c_e$. If the constant $c_e$ is close to one, the error $e_i$ is affected the most by the current error $e_s$. With decreasing value of $c_e$ the previous value of $e_i$ plays a more significant role in the calculation.

Besides the above described algorithm two simpler variants exist [11]. The main difference is that the timestep $\delta$ is a constant or a slowly decreasing value instead of dynamically adapting in these modifications.

## IV. Synthetic coordinates in WSN

Since synthetic coordinate systems were proposed for IP based networks, there are several inconveniences rising from their usage in WSN networks. Algorithms described in previous section are very demanding; especially from the energy point of view. We have to be always aware of strict energy constraints dealing with wireless sensor networks. Sensor nodes are relatively simple devices with weak microcontroller and very limited energy source. And provided that we use synthetic coordinate system, we affect both. There is higher computation cost and because of frequent communication, the energy consumed by radio part also increases. Moreover, system management and control require certain amount of energy too. On the other hand, the synthetic coordinate system offers indisputable advantages. Decentralized feature of a localization algorithm means that the system is less vulnerable to system collapse because of node dysfunction or local error. There is an option to start localization without anchor nodes and form completely relative map. But mainly, it provides more accurate position estimation based on cooperation of all nodes. The synthetic coordinate algorithms are able to eliminate or minimize error caused by measurement methods, which is serious problem in range based localization. The optimization of accuracy is based on iterative approximation. However, this means the undesirable increase of energy cost, since each iteration requires updated information about others node position and new measurement of distance.

All the mentioned facts infer that we have to accept a certain trade-off considering the use of synthetic coordinate systems in WSN. Also, application requirements set the important conditions and limitations. Therefore, we proposed following modification of Vivaldi algorithm to adapt it for wireless sensor networks. The modification is called EAVA (Energy Aware Vivaldi Algorithm) and we will refer to it in the following text.

First, we decided to use two dimensional system with height (2D+h) with possible extension to 4D+h system, which can have better results (as stated in [13]). In IP based networks $h$ is a positive value since it represents delay between two stations. In WSN, $h$ can be related to general error caused by measurement method. Thus, it can be either positive or negative.

Distances are derived from RTT measurement in IP based networks. However, this is hardly possible in WSN. Time measurement requires precise time synchronization, which means precise clock embedded in each device. Moreover, time synchronization process and its control is difficult task and additional energy costs. In low-cost applications, mostly RSS based distance estimation is used. So, we recommend to use RSS measurement for distance estimation instead of time based measurement. In proposed simulations with EAVA we consider RSS measurement as well.

The initial setting of a network depends on the presence of anchor nodes. If there are some, they can be either equipped with GPS receiver to set the coordinates or manual setting is possible. Then, the third coordinate $h$ states for the error of GPS estimation. The other two coordinates relates to standard 2D geographical system. With this initial setting of anchor nodes, triangulation or maximum likelihood method is performed to obtain rough position estimation of all nodes.

Provided that there are no anchor nodes in the network, all nodes are set with certain determined initial coordinates (such as $x_i=0$, $y_i=0$, $h_i=0$, for example). The localization process then starts from the very beginning and there is naturally slower convergence requiring more iteration steps, which consumes subsequently more energy.

To save energy during communication before each iteration step, only RSS measurement and communication with neighbours is performed. In case of high node degree, only a subset of neighbours can be involved.

The most crucial parameter of the localization is energy cost, highly dependent on the number of iterations and speed of convergence. Therefore, the setting of a shift constant $\Delta$ analogical to timestep $\delta$ is highly important. However, there are other conditions and parameters, which considerably influence the convergence and thus energy depletion and they have to be investigated. For parameters adjustment purposes certain simulations were proposed.

## V. Simulations

The transfer and the adjustment of protocols developed for a certain kind of a network to an environment with totally different main features is always a challenging process. It is difficult to predict the function and reliability of the protocol under different conditions. Although a protocol works well in IP networks, it can totally fail in WSN networks. The energy depletion is the most problematic is in this case, which is not considered in networks of mains-operated stations. Therefore, it is necessary to run certain simulations to verify the viability of a transferred protocol in new networks. Simulations can answer the question if it is reasonable to use the protocol without changes, with changes or if the protocol is totally inapplicable and a new one should be proposed.

For the purposes of simulations of synthetic coordinate algorithms Vivaldi and EAVA, we proposed and developed a new simulation tool [14][15]. The simulator is a JAVA based application implementing Vivaldi algorithm and its modified versions. The base coordinate system is 2D with height but can

be easily upgraded to 4D with height system. The main simulator window can be seen in Fig. 3.

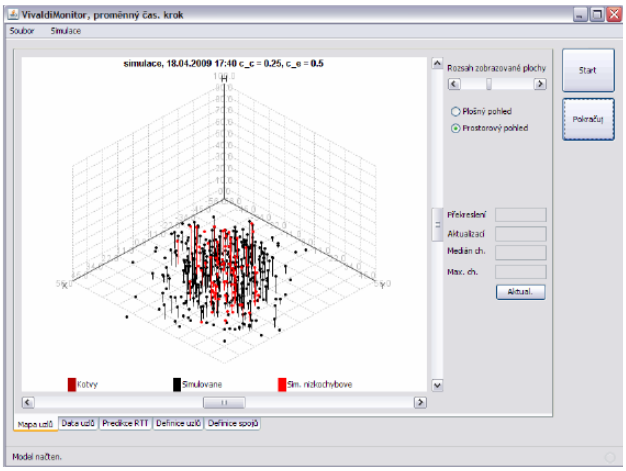


Fig. 3: Graphic user interface of developed simulation tool

The simulator displays the convergence process of localization by updating the main window. There are three types of network nodes distinguished in the figure; anchors, unknown nodes with position error under threshold (0.15 default) and nodes with higher position error.

The other modules of the simulator offer the graphical representation of position and error evolution. The example of a position convergence simulation is depicted in Fig. 4.

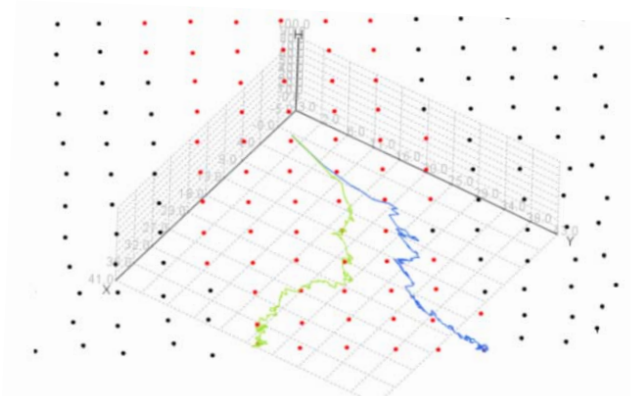

Fig. 4: Convergence of position of two nodes

Besides that the simulator incorporates the embedded editor of simulated topologies with import and export functions. Moreover, the various quantities and their evolution are presented in clearly arranged graphs with the possibility of subsequent export of all data into a Matlab environment. History of coordinates is also a useful feature.

So far, the simulator works perfectly for static topologies in general networks without WSN characteristic features. Nowadays, we work on the library implementing proposed algorithm EAVA and a module of the simulator following the main features of energy constrained networks.

## VI. Conclusion and Future Work

Localization in WSN is a challenging task and there is a broad variety of current approaches. Because of the particularity of these networks it is very difficult to simply implement protocols from different networks. However, although it is impossible to transfer protocols directly, it is promising to use at least some their features, which allowed their successful deployment in IP based networks. Therefore, we proposed modified version of Vivaldi algorithm called EAVA, which is adjusted to WSN. The protocol considers RSS measurement for distance estimation and strictly controls the energy consumption during localization. The main idea is to exploit cooperation of nodes based on mass spring principle and at the same time use as little energy as possible. In IP based networks the Vivaldi algorithm features promising results but at the cost of high communication. This is not acceptable in WSN, so radical change has to be done.

For the simulation purposes, we proposed and developed a new simulator tool VivaldiMonitor. It implements successfully Vivaldi algorithm and its modification into static networks. It offers modularity and elaborated graphical output with user-friendly interface with data export and import option. The next phase is devoted to development of library implementing EAVA and modification of simulator for WSN specific features with development of energy module to control an energy depletion during localization.

## Acknowledgment

This work was supported by Ministry of Education of the Czech Republic project No. MSM0021630513, Ministry of Industry and Trade of the Czech Republic - project No. MPO FR-TI2/571.

## References

[1] IEEE Standard for Information Technology Part 15.4: Wireless medium access control (MAC) and physical layer (PHY) specifications for low-rate wireless personal area networks (WPANs), *IEEE Std 802.15.4-2006* (Revision of IEEE Std 802.15.4- 2003), pp. 1–305, 2006.

[2] Zibee Alliance, [online], URL: www.zigbee.org.

[3] I.F. Akyildiz, W. Su, Y. Sankarasubramaniam, and E. Cayirci, “Wireless sensor networks: A survey”, *Computer Networks J.* , 38(4), 393–422, 2002.

[4] Wenhao Huang; Yu Wang; Haoran Guan; , "The Current Situation and Prospect of Localization in Wireless Sensor Network," *Computer Science and Engineering, 2009. WCSE '09. Second International Workshop on* , vol.1, no., pp.483-487, 28-30 Oct. 2009.

[5] Guoqiang Mao, Baris Fidan, Brian D.O. Anderson, “Wireless sensor network localization techniques“, Computer Networks, Volume 51, Issue 10, Pages 2529-2553, ISSN 1389-1286, 2007.

[6] Moravek, Patrik, Komosny, Dan, Sala, David Girbau, Guillen, Antoni Lazaro, "Received signal strength uncertainty in energy-aware localization in wireless sensor networks," *Environment and Electrical Engineering (EEEIC), 2010 9th International Conference on* , vol., no., pp.538-541, May 2010.

[7] Moravek, P., Komosny, D., Simek M., Jelinek, M., Girbau, D., Lazaro, A. “Signal Propagation and Distance Estimation in Wireless Sensor Networks”, In *The 33rd International Conference on Telecommunication and Signal Processing, TSP 2010.* s. 35-40, 2010.

[8] Shavitt, Y., Tankel, T. “On the curvature of the Internet and its usage for overlay construction and distance estimation” INFOCOM 2004 - Twenty-third Annual Joint Conference of the IEEE Computer and Communications Societies. IEEE, 2004.

[9] Ng, E., Hui, Z. “Predicting Internet network distance with coordinates-based approaches” In INFOCOM 2002. Twenty-First Annual Joint Conference of the IEEE Computer and Communications Societies. Proceedings. IEEE, Vol. 1, 2002.

[10] Pias, M., Crowcroft, J., Wilbur, S., Harris, T., Bhatti, S. ”Lighthouses for Scalable Distributed Location” Lecture Notes in Computer Science. Springer Berlin / Heidelberg, 2003.

[11] Dabek, F., Cox, R., Kaashoek, F., Morris, R. “Vivaldi: a decentralized network coordinate system” ACM SIGCOMM Computer Communication Review. Association for Computing Machinery, 2004.

[12] Fruchterman, T., Reingold, E. “Graph Drawing by Force-directed Placement. Software - Practice and Experience (SPE)”, November 1991.

[13] Ledlie, J., Gardner, P., Seltzer, M. “Network Coordinates in the Wild” In Proceedings of NSDI 2007. [online] Cambridge (USA): Harvard School of Engineering and Applied Sciences and Aelitis, 2007. URL: http://www.eecs.harvard.edu/ syrah/nc/wild07.pdf.

[14] Moravek, P., Komosny, D., Simek M., Sveda, J., Handl, T. “Vivaldi and other localization methods” In *TSP 2009*. s. 1-5. 2009.

[15] Moravek, P., Komosny, D., Burget R.., Sveda, J., Handl, T. “Study and Performance of Localization Methods in IP Based Networks: Vivaldi Algorithm” *Journal of network and computer applications*, roč. 34, č. 1, s. 1-17, 2010.

# The Proposal of System for Distance Measurement and 2-D Location Services Using CC2420

Ľuboš Nagy, Jan Karásek, Petr Vychodil
Department of Telecommunications
Faculty of Electrical Engineering and Communication
Brno University of Technology
Brno, Czech Republic
{lubos.nagy, karasek.jan, petr.vychodil}@phd.feec.vutbr.cz

Pavel Holešinský
pavel.holesinsky@gmail.com

*Abstract*—**The paper presents an implementation of designed system for distance measurement and 2-D location using radio chip CC2420 in Wireless Sensor Network (WSN) and describes the measurement of distance and simulations of localization algorithm in indoor and outdoor areas. The objective of this article is to design a system for localizing sensors for a medium-sized distance (approximately 15 meters). Finally, the figures of measured distance with an error of the used method are shown. Also, the error of the simulated localization algorithm is shown. The simulations were tested with the help of Matlab.**

***Keywords-CC2420; WSN; 2-D localization; trilateration; RSSI; error of the trilateration; error of measured distance.***

## I. INTRODUCTION

The wireless sensor networks, better known as WSN, are usually used to monitor physical variables, such as pressure, vibration or temperature. In general, the WSN is divided into two main parts: the sensor nodes and the base stations. In the first case, the device is used to process values (i.e. pressure). Then, the information is sent to the base station. The base station is used to collect data from sensor nodes and for further processing of information.

For an advanced evaluation of the information collected from sensors it is often necessary to know the position of nodes in WSN. This paper describes the possibility of finding the coordinates of sensors in R2 environment with the help of trilateration algorithm. In this paper, the distance between sensors will be calculated using RSSI method (Received Signal Strength Indication). Other possibilities how to estimate the unknown distance in wireless sensor networks between sensors for determination of the position nodes are described for example in [1], [2], [3] or [4].

The structure of this article is as follows: related work is presented in the second part of the paper. The implementation of proposed system with RSSI method is described in the third section. Also, this part briefly describes the localization method based on the trilateration (in subsection B). In the fourth section, the measured scenarios for analysis of distance measurement (in the subpart A) and simulated scenarios for analysis of trilateration (in the subpart B) are described. The examination of proposed system is discussed in the last section of the paper.

## II. IMPLEMENTATION

The system (see Figure 1. ) for 2-D location service in WSN consists of J2ME applications (run on sensor nodes), J2SE application (executed on base station) and database of all nodes in WSN (used as the information storage). The SPOT (Small Programmable Object Technology) sensors with CC2420 radio chip with the integrated antenna are used as nodes in the designed system.

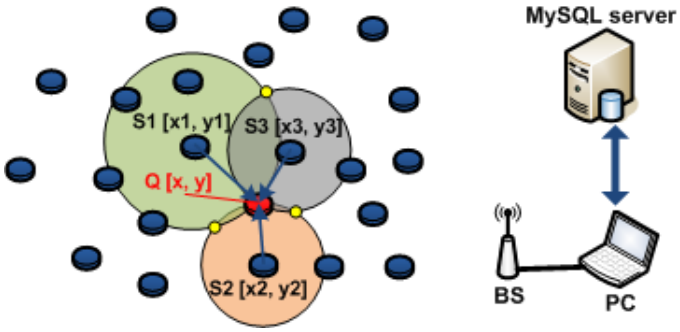


Figure 1. The topology of WSN (yellow points – intersection of the circles, red node (Q) – target node, blue nodes – localized sensors, BS – base station, PC – personal computer).

### A. The measurement of distance in the system

In the system, the RSSI method is used to determine unknown distances (see d in (1)) between the target and anchor sensors in WSN [4], [5], [6].

$$PL(d) = PL_0 + 10n\log_{10}\left(\frac{d}{d_0}\right) + X_\sigma\ [dBm] \qquad (1)\ [5]$$

where PL are path-loss parameters, that is PL(d) for the unknown distance d and PL0 for the reference distance d0. The recommended values of Gauss's constant (Xσ) and path-loss exponent (n) are shown in TABLE I. The parameter PL(d) is defined with the help of RSSI and Pt values (see (2)). The computing of reference PL0 is illustrated in (4).

$$RSSI' = P_t - PL_{(d)}\ [dBm] \qquad (2)\ [5]$$

where RSSI' is the calculated value from (3) [dBm] and Pt is the transmission power [dBm].

$$RSSI' = RSSI - RSSI_{OFFSET}[dBm] \qquad (3)\ [5]$$

where RSSI is the measured value of received signal strength in dBm and RSSIOFFSET is the offset of RSSI [dBm], for used sensors it is approximately -45 dBm.

$$PL_0 = 20\log_{10}\left(\frac{4\pi f d_0}{c}\right)\ [dBm] \qquad (4)\ [5]$$

where f [Hz] is the frequency and c is the speed of light in vacuum [m/s].

TABLE I. THE TYPICAL VALUES OF PARAMETERS FOR (1) [5], [6].

| **Parameters** | **The range of recommended values** | | |
|---|---|---|---|
| Path-loss exponent – n [-] | Outdoor | free area | 2 |
| | | occupied area | 2.7-5 |
| | Indoor | without obstacle | 1.6-1.8 |
| | | with obstacle | 4-6 |
| Gauss's constant - $x_\sigma$ [-] | 4 – 12 | | |

### B. *Localization of the nodes in the system*

In the designed system, the trilateration algorithm is used to find the position of the sensors located in Cartesian coordinate system. This algorithm is based on the Pythagoras' theorem. The principle of localization in the Cartesian coordinate system is illustrated in Figure 1. and in (5).

In Figure 1. , the points S1-3 define the position of anchor nodes (see [xn, yn] in (5)) and point Q is the target node with unknown coordinates (see [x, y] in (5)). In (5), the unknown distance between the target and anchor nodes is shown as rn.

$$r_n^2 = (x - x_n)^2 + (y - y_n)^2\ [m] \qquad (5)$$

The principle of communication between the target node and other nodes (motes or base stations) is illustrated with the help of the sequence diagram in Figure 2. After turning the sensors on, the nodes send the message to the base station. This message consists of ID (the 64-bit IEEE address of device loaded from the nodes). The nodes determine if the node is localized or not according to the answer from the base station. If the node has not yet been localized, this sensor will send the broadcast message with the request coordinates to others localized nodes. When the target node receives the necessary number of messages for localization algorithm, the node calculates its coordinates. These coordinates are stored in the database of sensors.

The fundamental of trilateration for 3D localization is described in [7].

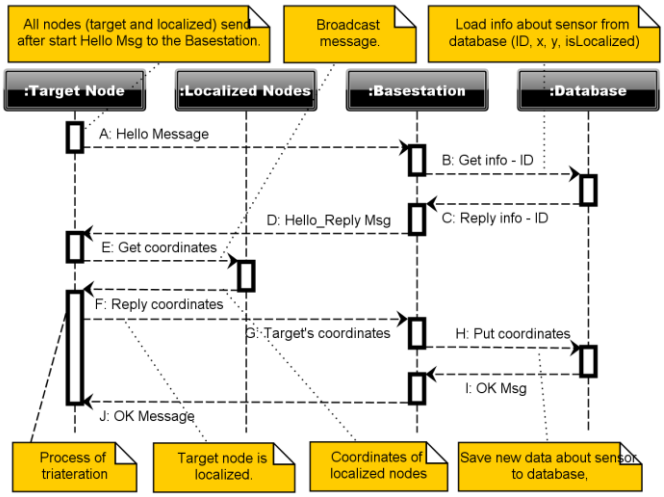


Figure 2. The sequence diagram of designed system.

## III. MEASURED AND SIMULATED RESULTS

Three scenarios were simulated and measured. In the first and the second scenarios, the distances of sensor nodes were tested in the building. In the first scenario (Figure 3. - on the left), the sensors are situated in the vestibule. In the second situation (Figure 3. - on the right), the nodes are placed in the corridor. In the last scenario, the sensors were located in the occupied outdoor environment. For high accuracy, 80 values of RSSI were measured (Figure 4. ). In case of two scenarios in the building, the maximum measured distances were 18 m, in the outdoor area the maximum distance was 25 m. The next section describes the results of measured distance.

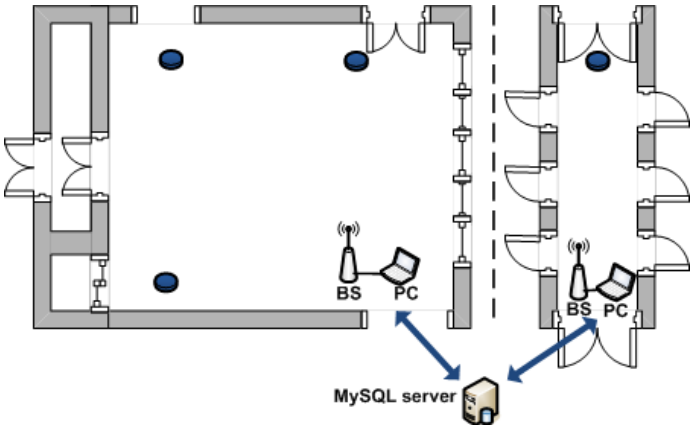


Figure 3. The indoor locations for distance measurement (on the left: vestibule, on the right: corridor).

### A. *Results of Measured Distance*

In the graph (see Figure 4. ), the characteristics of RSSI within measured distance and the number of measurements in outdoor environment are shown. It can be seen that the values are almost invariable for each of the studied measurements. The measured RSSI values are calculated using formula (6).

$$RSSI = \sum_{k=1}^{n} \frac{\mathrm{RSSI_n}}{\mathrm{n}} \, [dBm] \qquad (6)$$

In (6), the RSSI represent RSSI value for (3), RSSIn the measured values and n is the number of measurements.

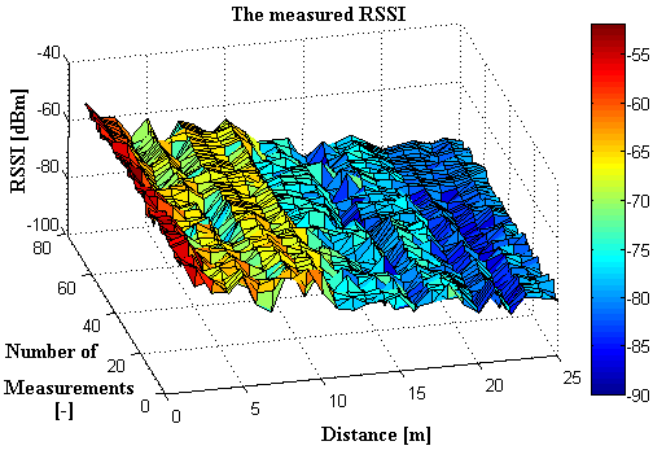


Figure 4. The measured RSSI values – the outdoor environment.

In the next figures (Figure 5. , Figure 6. and Figure 7. ), the measured characteristics of RSSI within distance for all scenarios are illustrated. In the displayed figures, the RSSI is the average value of 80 measured values (see (6)). Also, the maximum and the minimum values are shown in illustrated figures. It can be seen that the RSSI characteristic for the scenario one indicated higher values than the characteristic for the second scenario. Both scenarios were measured in the same building.

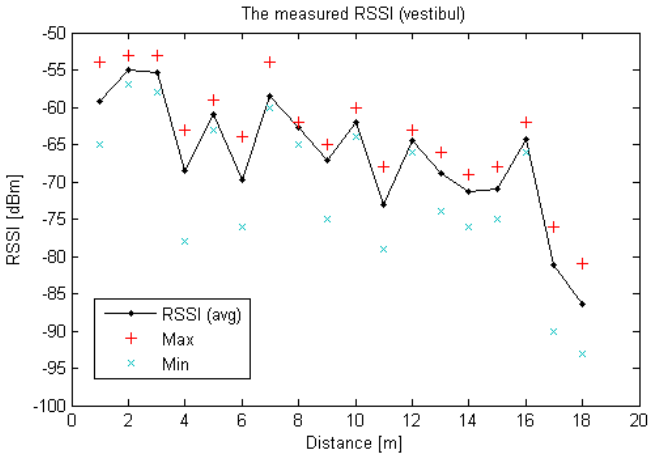


Figure 5. The fist scenario: The measured values of RSSI in the vestibule.

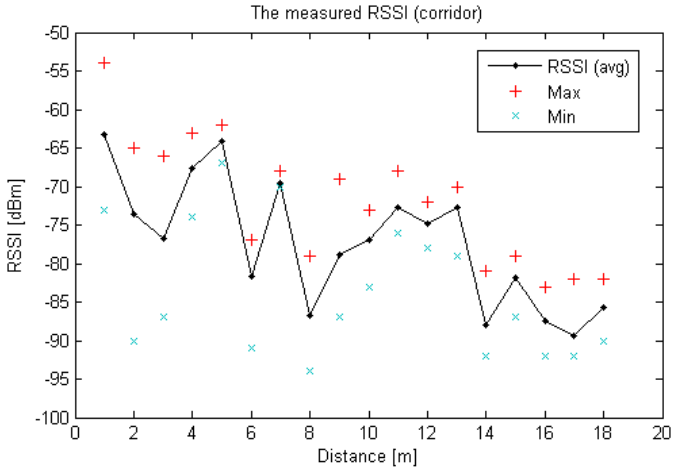


Figure 6. The second scenario: The measured values of RSSI in the corridor.

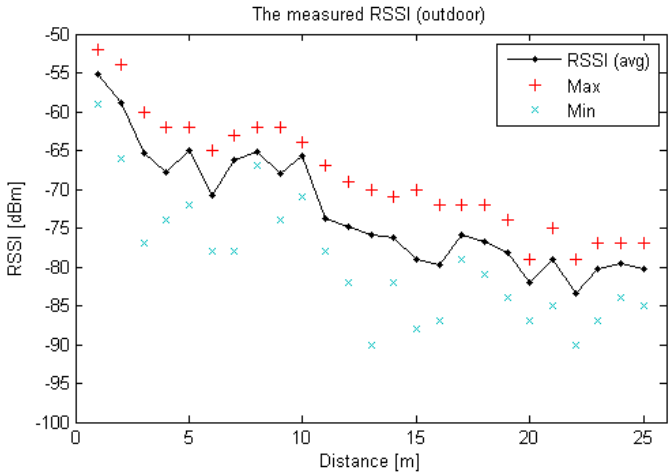


Figure 7. The third scenario: The measured values of RSSI for outdoor.

The path-loss exponent, reference distance and Gauss's constant were set on the basis of previous measurements of RSSI values in indoor and outdoor environments (see Figure 5. , Figure 6. and Figure 7. ). Also, the range of recommended values was considered (see TABLE I. ). The values of all parameters were adjusted so that the smallest error in the calculated distance was achieved. The parameters of the designed system were implemented for a long distance. The values set for three scenarios are shown in TABLE II. The values set for both indoor situations are equal.

TABLE II. THE VALUES OF PARAMETERS IN THE SYSTEM DESIGNED FOR (1) AND (4).

| Scenarios | The value of parameters | | |
|---|---|---|---|
| | ***n* [-]** | ***$d_0$* [m]** | ***Xσ* [-]** |
| Indoor | 4.9 | 7 | 4 |
| Outdoor | 3.4 | 7 | 5 |

Next figures (see Figure 8. and Figure 9. ) illustrate the measured distance (x-axis) with absolute and relative dis-

tance errors (y-axis) in meters and percentages for all measured situations.

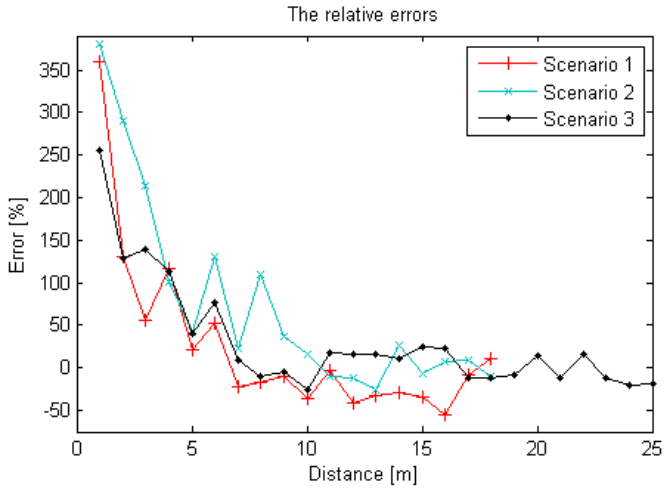


Figure 8. The measured distances for all scenarios – the absolute distance errors.

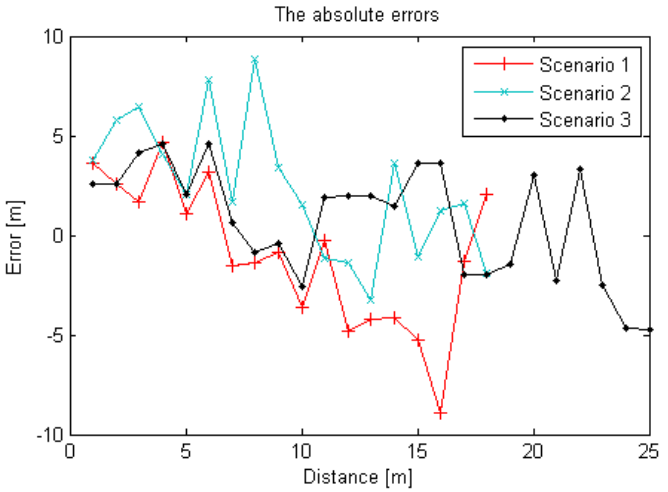


Figure 9. The measured distances for all scenarios – the relative distance errors.

The difference between the distances calculated by the designed system and their estimated (ideal) distance is illustrated in Figure 10.

The table (see TABLE III. ) shows the measured distance errors for all tested situations only for studied distances. The values of parameters (see TABLE II. ) were defined to measurement distances around 15 meters. If the length was less than the studied distance (7 m), the errors of computed distances were unacceptable for localization in WSN. Also, it can be seen that the scenario for outdoor environment indicated lower distance errors than the other scenarios.

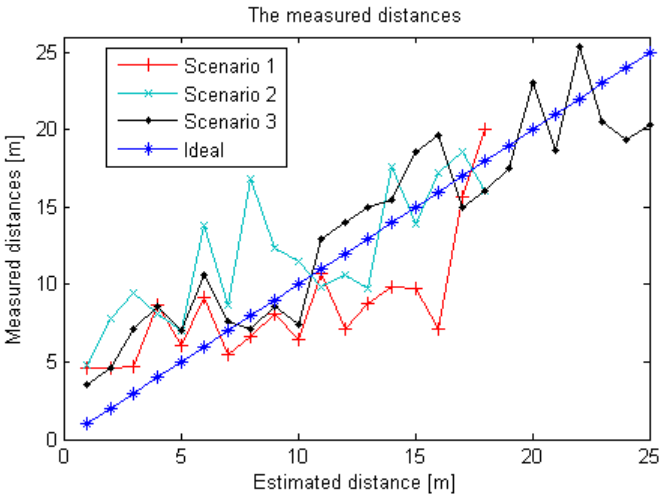


Figure 10. The measured and estimated distances for all scenarios.

TABLE III. THE VALUES OF DISTANCE ERRORS IN THE DESIGNED SYSTEM.

| Type of Scenario | Absolute errors [m] | | | Relative errors [%] | | |
|---|---|---|---|---|---|---|
| | *Max* | *Mean* | *Min* | *Max* | *Mean* | *Min* |
| Vestibule | 8.1 | 2.6 | 0.2 | 55.1 | 24.5 | 2.2 |
| Corridor | 8.2 | 3.0 | 1.1 | 110 | 31.9 | 7.1 |
| Outdoor | 4.7 | 2.3 | 0.4 | 25.1 | 14.0 | 4.4 |

The best results of computed and measured distance were indicated from 7 to 25 m in the outdoor environment. For the computed distances, the maximum relative error was slightly over 25%, the average below 15%. In case of absolute errors, the maximum absolute error was slightly below 5 m and the average was 2.3%. In the case of indoor, the average relative errors were over 30%.

### *B. Simulation of Trilateration*

The simulations of trilateration were tested with the help of the numerical computing program – Matlab. The distance errors (see TABLE III. ) were set in the simulated scenarios according to earlier measurements displayed in the previous part of the paper. The trilateration algorithm was launched in 20 iterations. The positions of all sensors were successfully detected during the localization process.

The results of localization are illustrated in Figure 11. Figure 12. and Figure 13. With the help of the x-axis and y-axis, the x and y-coordinates are described in the matrix where the sensors are situated. The localization error is illustrated by the z-axis. The errors of simulated scenarios are shown in TABLE IV.

The best results of localization error were indicated in the outdoor environment. In this case, the maximum error was slightly over 14 m. In the case of indoor, the maximum error was over 40 m.

TABLE IV. THE VALUES OF LOCALIZED ERRORS IN THE DESIGNED SYSTEM.

| Type of Scenario | Localization errors [m] | | |
|---|---|---|---|
| | ***Max*** | ***Mean*** | ***Min*** |
| Vestibule | 24.2 | 9.9 | 0.7 |
| Corridor | 43.1 | 16.1 | 0.9 |
| Outdoor | 14.1 | 6.6 | 0.5 |

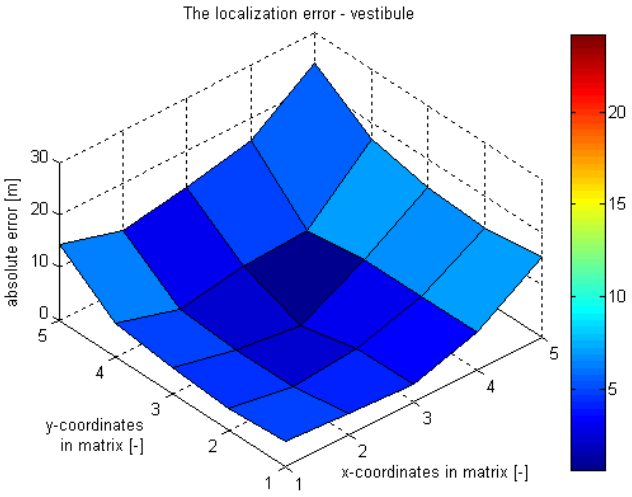


Figure 11. The first scenario.

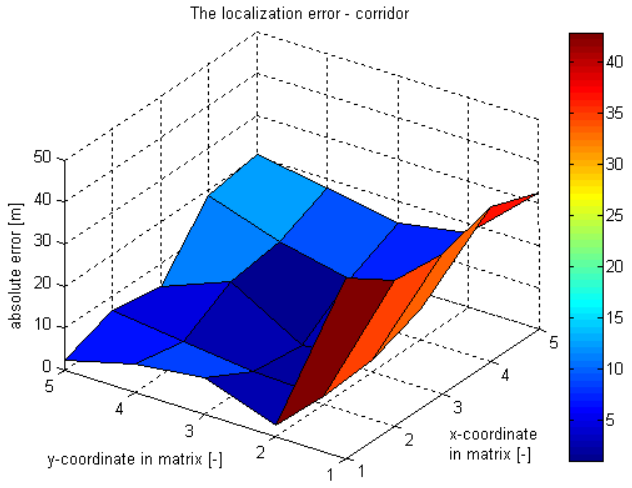


Figure 12. The second scenario.

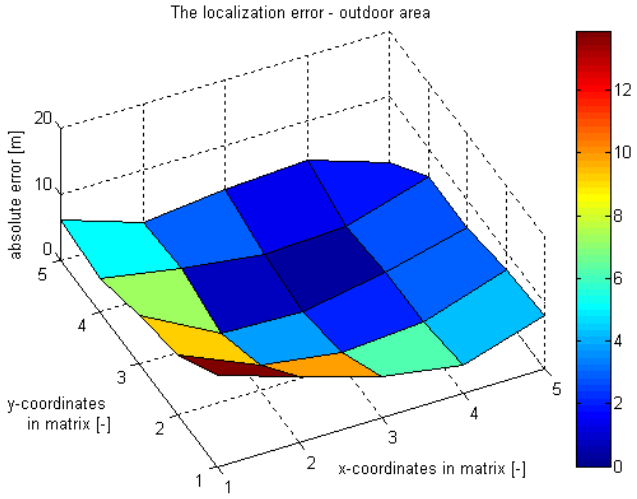


Figure 13. The third scenario.

## IV. CONLUSION

This paper describes the localization in WSN using trilateration algorithm with measurement distance based on RSSI method. In the article, three scenarios were tested to determine the error of designed system in the real environments. Two scenarios were situated in the indoor environments; one of them was tested in the corridor and second in the vestibule. The last scenario was measured in the outdoor environment. The system was designed to determine a distance around 15 m.

Also, these scenarios were simulated to estimate errors using localization algorithm with the help of MATLAB. The results of real measurements (the errors between measured and computed distances) were used to simulate localization errors.

The maximum measured distance for the building was 18 m. This length was affected by the dimension of indoor environment. In case of outdoor environment, the maximum tested distance was 25 m. For greater length than 25 m, the packet-loss parameter was too large.

The worse results were detected in the corridor scenario. In this measurement, the high error values could be affected by reflections of the radio signal in the narrow corridor. The measured errors in the first and second scenarios show that the designed system is unusable in indoor environments. In both scenarios, the high localization error was influenced by the high distance error. The maximum error was detected at small distances for which the purposed system was not designed. These errors are shown only in the displayed figures. The possible solution of the high error values is described in [5], where the authors separated the distance into smaller lengths and for each of these parts the values of parameters were set as shown in TABLE II.

## REFERENCES

[1] DU, Q.-L., SUN, X., DING, R., QIAN, Z.-H. , WANG, S.-X.: TOA-Based Location Estimation Accuracy for 3D Wireless Sensor Networks. *Wireless Communications, Networking and Mobile Computing 2009. WiCom '09. 5th International Conference*. 24.-26. Sept. 2009, p. 1-4. ISBN: 978-1-4244-3692-7.

[2] PARK, Ch.Y., CHO, H.S., PARK, D.H., CHO, S.E., PARK, J.W., LEE, Y.S.: AoA Localization System Design and Implementation Based on Zigbee for Applying Greenhouse. *Embedded and Multimedia Computing (EMC), 2010 5th International Conference.* 11.-13. Aug.2010, p. 1-4, ISBN: 978-1-4244-7710-4.

[3] LI, R., FANG, Z.: LLA: A New High Precision Mobile Node Localization Algorithm Based on TOA. *Journal of Communications, Vol. 5, No. 8 (2010)*. Aug. 2010. p. 604-611. ISSN: 1796-2021.

[4] STOYANOVA, T., KERASIOTIS, F., PRAYATI, A., PAPADOPOULOS, G.: Evaluation of impact factors on RSS accuracy for localization and tracking applications in sensors networks. *Telecommunication Systems: Mobility Management and Wireless Access*., 29. July 2009, Vol. 42, p. 235-248, ISSN: 1018-4864.

[5] JINPENG, T., HUICHANG, S., WENLIANG, G., YIFEI, Z.: A RSSI-Based Localization System in Coal Mine. *Microwave Conference CJMW 2008*. 10.-12. Sept. 2008, p. 167-171. ISBN: 978-1-4244-3821-1.

[6] SHEN, X., WANG, Z., JIANG, P., LIN, R., SUN, Y.: Connectivity and RSSI Based Localization Scheme for Wireless Sensor Networks. *International Conferences on Intelligent Computing, Lecture Notes on Computer Science - ICIC 2005*. Vol. 3645, p. 578 – 587.

[7] CHIA-YEN, S., MARRON, P.J.: COLA: Complexity-Reduced Trilateration Approach for 3D Localization in Wireless Sensor Networks. *Sensor Technologies and Applications (SENSORCOMM), 2010 Fourth International Conference*. 18-25 July 2010, p. 24-32. ISBN: 978-1-4244-7538-4.

# Scalar Measurement of Electromagnetic Shielding Efficiency of Carbon Textiles

Yunus Terzioglu
Department of Electric & Electronics Engineering
Middle East Technical University
Cankaya, Ankara
terziogluyunus@gmail.com

*Abstract*—**Electromagnetic shielding textiles are growing materials which indeed has numerous fields of applications today in tasks like increasing the safety of airborne systems, protection of electronic identifiers, protection suits for high voltage line workers and so on. This paper is focused on Electromagnetic Shielding Efficiency of carbon textile samples while illustrating a measurement principle and some basic information on shielding textiles.**

***Keywords-Carbon textile; Efficiency; ESE; Measurement; Shielding***

## I. INTRODUCTION

On the way ending up at the application of such technology, an objective observation on the material bears a grave significance, which will provide to developers very useful practical data that is not always possible to estimate using the calculations and equations, Fig. 1.

Figure 1. A simple application of shielding textiles [2].

There are many applications today in tasks like textiles products used for increasing the safety of airborne systems [1], protection of electronic identifiers [3] or protection clothing for high voltage line workers [4].

This article is a brief summary of the testing procedures of two different types of carbon fiber woven textiles primary designed for lamination applications.

## II. SHIELDING TEXTILES

The developed textiles in purpose of an electromagnetic shielding are based on regular textiles we get to see in our every-day life like cotton or polyesters. What makes them special is that they include certain amounts of copper, nickel, carbon microfibers or even silver particles in some samples, Fig. 2. Different compositions of these materials and different types of weavings make significant changes in the electromagnetic characteristics of the materials.

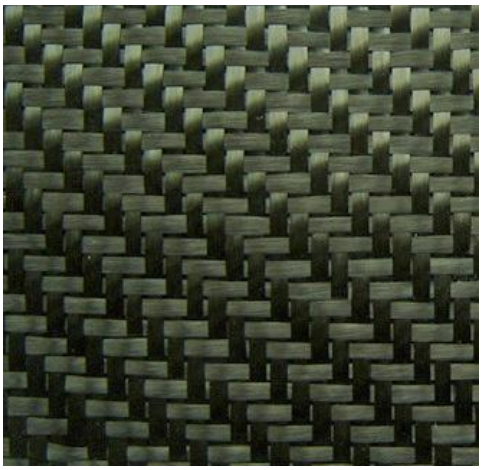

Figure 2. A sample of carbon fiber fabric [5].

The two samples that are handled during these experiments are carbon fiber fabrics. They are inscribed by no.54 and no.55. Both of these two textiles are woven only from carbon fibers. No.54 is woven like a cloth while no.55 is woven like a drill. This seemingly insignificant difference however alters the Electromagnetic Shielding Efficiency remarkably. The reason

is the changing sizes and the shapes of the pores on the cloth with different weaves.

## III. MEASUREMENT

In order to test the textile materials, a Rohde&Schwars FSL series spectrum analyzer and a Hewlett Packard 86222B microwave generator are used, Fig. 3.

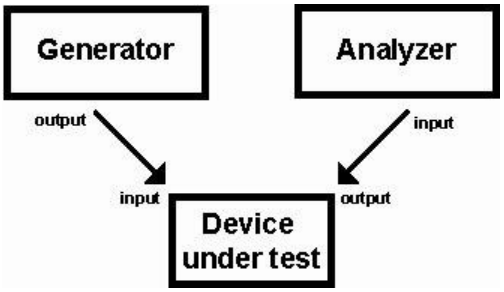


Figure 3. The general setup of the testing process.

### A. General Setup

A sweeping output, between 30 MHz and 1.5 GHz, is supplied by the generator to the spectrum analyzer through the device under test (DUT).

A circular coaxial flange with appropriate dimensions is used as a holder for the DUT. The holder is mainly designed to be used between 30 MHz and 1.5 GHz frequencies [6, 8] or from 9 kHz up to 1 GHz [7]. Electromagnetic shielding efficiency (ESE) of carbon fiber fabric is measured with respect to ASTM D 4935-99, Fig. 4.

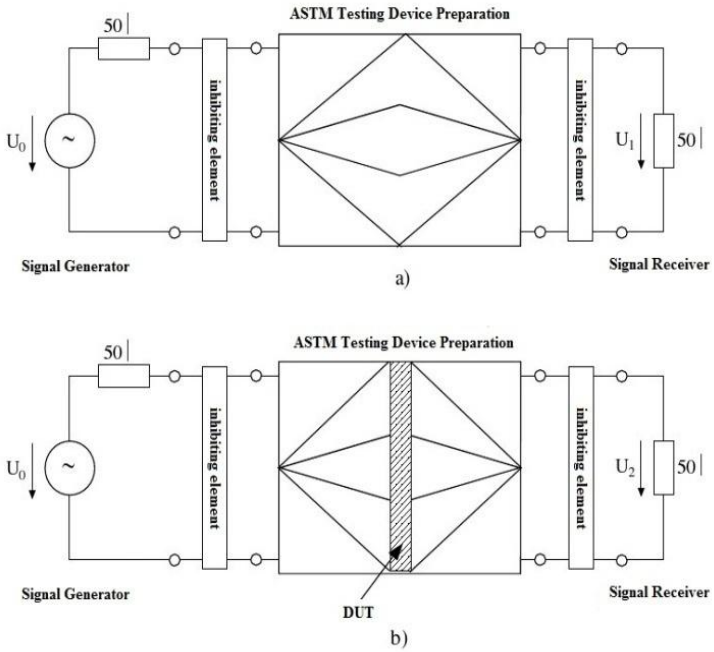


Figure 4. Measurement according to standard ASTM D 4935-99. Sample for reference measurement a), sample for load measurement b).

This device, coaxial flange, is to be used in two distinct sample forms during the testing process, Fig. 5. The first form is to make a reference reading before starting the actual test. In this phase only outer and inner shells (A) of the textile are placed within the flange and the readings taken this way are considered as a zero line. The second material form is a complete circular piece (B), which is placed into the flange as a whole. With the comparison of the two readings, a graph about the actual shielding values of the textile can be obtained.


Figure 5. Textile samples preparation for measurement with respect to ASTM D 4935-99.

### B. Measurement Principle

An output of microwave signals is supplied through the textile material to the analyzer and the power readings, which are observed on the analyzer screen, are used to observe the Electromagnetic Shielding Efficiency of different materials. Since we are interested in the reactions of the material in a considerably wide spectrum (30 MHz - 1.5 GHz), rather than a single frequency value, it is necessary for the generator to sweep that range continuously and get readings for those distinct frequency values in sequence.

It is critically important to obtain the synchronization between the generator and the analyzer, in order to get a clear graph of power level versus frequency. To achieve that, sweep time of the generator is held as short as possible (0.1 ms) and the reading sweep time of the analyzer is setting in considerably long time (7 s with 401 points, ~17 ms for each reading). It ensures that in the time interval which the analyzer gets a reading, the generator sweeps the whole frequency range at least once.

Due to all power losses within the connectors and probable errors in the outputs from the generator, it is clearly not reasonable to calculate the actual power values throughout the experiment.

Another and more practical approach lies on the comparison of two power readings on the spectrum analyzer rather than going for the actual powers. The first reading (Fig. 6.), which is to be taken without any DUT between the analyzer and the generator, is used as a reference to a second reading, which is to be taken while the shielding material is placed between the generator and the analyzer. The calculated power drop between the first and the second readings indicates how effective the tested material is, Fig. 7.

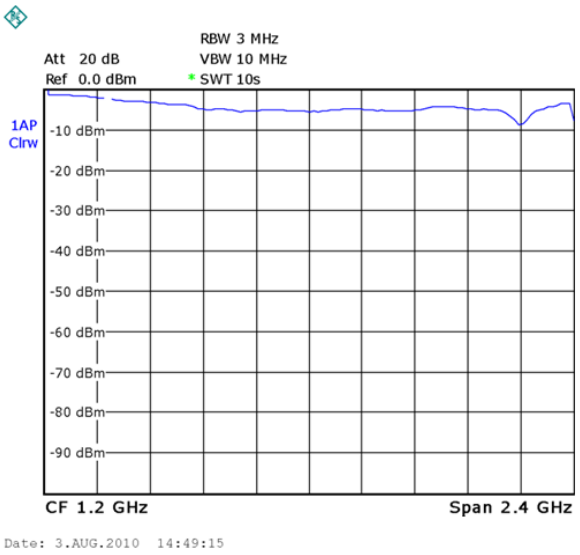


Figure 6. A reference reading.

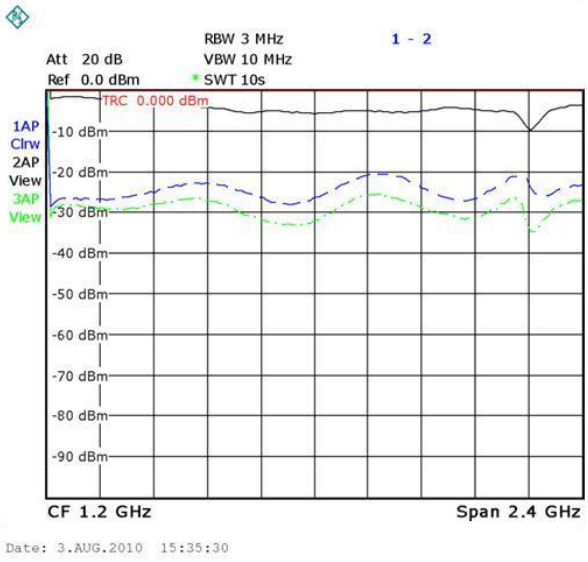


Figure 7. Reference reading (solid line), reading with the textile (dot-and-dashed line), actual power attenuation (dashed line).

### *C. Calibration and ASCII Data File Export*

The reference reading, which is obtained in the first place, is saved in one of the possible trace slots of the R&S FSL analyzer. So, it can be simply subtracted from the reading of the complete material (Fig. 7 Dot-and-dashed line) and this is achieved by using the analyzer's math function under 'trace menu'. By doing so the accuracy of the test is increased dramatically.

```
Type;FSL-6;
Version;1.60;
Date;10.Aug 10;
Mode;ANALYZER;
Center Freq;765000000.000000;Hz
Freq Offset;0.000000;Hz
Span;1470000000.000000;Hz
x-Axis;LIN;
Start;30000000.000000;Hz
Stop;1500000000.000000;Hz
Ref Level;10.000000;dBm
Level Offset;0.000000;dB
Ref Position;100.000000;%
y-Axis;LOG;
Level Range;100.000000;dB
Rf Att;20.000000;dB
RBW;3000000.000000;Hz
VBW;10000000.000000;Hz
SWT;8.000000;s
Trace Mode;CLR/WRITE;
Detector;AUTOPEAK;
Sweep Count;0;
Trace 1:;;
x-Unit;Hz;
y-Unit;dBm;
Values;401;
31832917.705735661;-35.286567687988281;7.3999252319335937
35498753.117206983;-32.211181640625;0.394805908203125
39164588.528678305;-33.522064208984375;-8.7475738525390625
42830423.940149628;-34.910873413085937;4.6818389892578125
46496259.35162095;-34.290351867675781;8.5218658447265625
50162094.763092272;-35.729904174804688;8.7887420654296875
53827930.174563594;-33.860252380371094;2.3614959716796875
57493765.586034916;-35.44464111328125;1.504989624023437 5
61159600.997506239;-33.930839538574219;7.3616943359375
64825436.408977561;-34.12567138671875;16.7496337890625
68491271.820448875;-36.0386962890625;6.342681884765625
72157107.231920198;-34.1741943359375;-4.6391983032226562
75822942.64339152;-33.465446472167969;4.2193832397460938
79488778.054862842;-34.882209777832031;2.2159423828125
83154613.466334164;-34.86895751953125;-7.6065216064453125
86820448.877805486;-35.940902709960938;-2.8283615112304687
90486284.289276809;-34.73883056640625;-4.03485107421875
94152119.700748131;-35.107902526855469;0.62786865234375
97817955.112219453;-34.666778564453125;9.217376708984375
```

Figure 8. Sample of ASCII code export of FSL Analyzer for 30MHz-1.5 GHz range.

After the actual result is obtained, the data of the resultant graph (Fig. 7 dashed line) is to be exported as a file of ASCII codes in order to process with MATLAB or such software, Fig. 8. The resultant ASCII code will be a 401x3 matrix with a 26 lines of header code. The items listed in the first column stands for the frequency values of the readings (from 30MHz to 1.5GHz in this test) and the magnitudes (20logH(jw)) of the power readings are to be listed on the second column. Once the data is successfully uploaded to MATLAB, skipping the first 26 lines, a graph of ESE can be drawn placing the frequency values on x-axis. The power readings on column 2 are multiplied by -1 and placed on y-axis. The resultant graph will show the Electromagnetic Shielding Efficiency of the material on test.

## IV. RESULTS

The resultant graphs are as shown in Fig.9 for both samples. And also a sheet of aluminum foil is tested under the same conditions and methods for a clear comparison of shielding efficiencies, Fig. 10. The graphs show the importance of the ways that the textiles are woven and how the size and shapes of the pores on the textiles can alter their shielding characteristics.

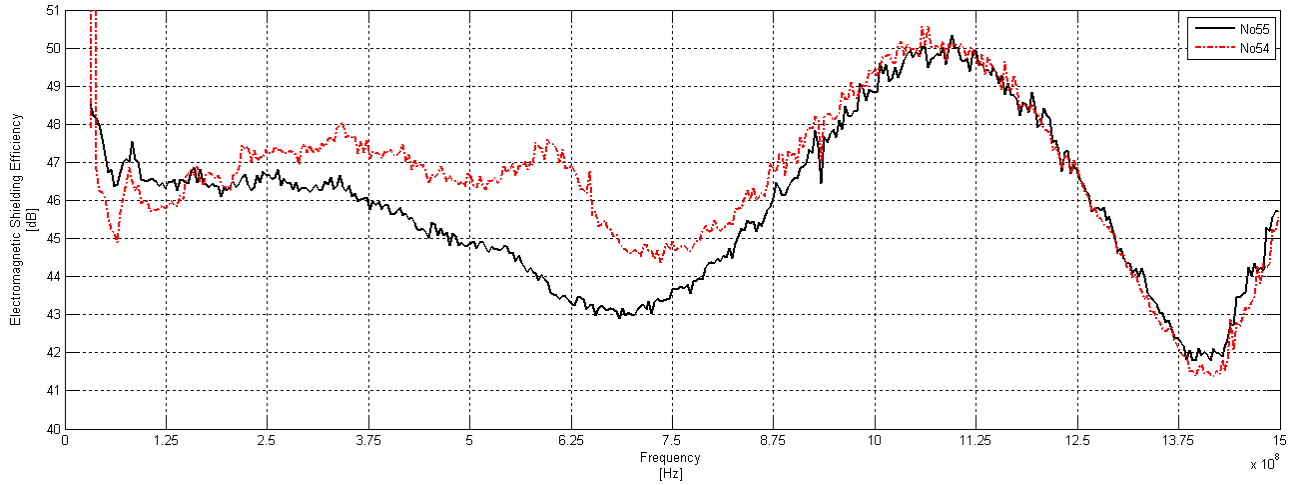


Figure 9. ESEs of the two samples no. 54 (cloth) and no. 55 (drill).

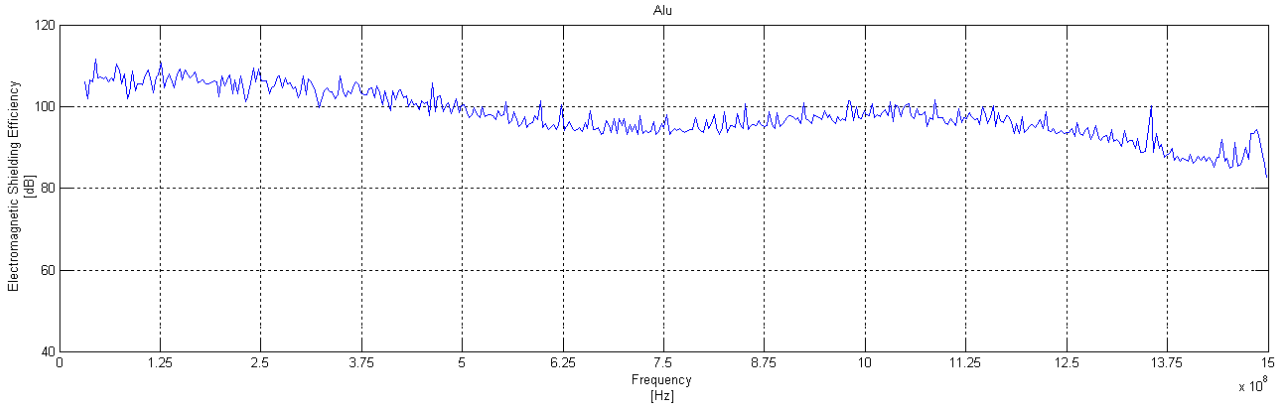


Figure 10. ESE of an aluminum sheet.

## V. CONCLUSION

Fig.9 illustrates the shielding efficiency of a pure aluminum sheet. Compared to it, the carbon samples No.54 and No.55 may seem quite inefficient at first. However, considering that those samples are woven material rather than a whole piece of sheet and they inevitably include pores, we can conclude that a spectacular amount of electromagnetic energy can be absorbed using textile material. Moreover, specifying the field of use for the material and deciding the frequency range that the material will be exposed to, the textiles handiness could be increased significantly.

## REFERENCES

[1] L. Vojtech, and M. Neruda, "Application of Shielding Textiles for Increasing Safety Airborne Systems - Limitation of GSM Interference," *The Ninth International Conference on Networks (ICM 2010)*, pp.157-161, July, 2010.

[2] Unknown Author, "SwicoFil AG textile services," Swicofil.com, August 2010. Available at: http://www.swicofil.com/swissshieldcanopy.html [Accessed 29 August 2010].

[3] L. Vojtech, M. Neruda, and J. Hajek, "Data hardware protection of electronic identifiers" *17th International Conference on Systems, Signals and Image Processing (IWSSIP 2010)*, p. Nr. 50, August, 2010.

[4] V. Arps, and M. Koch, "Personal safety in high frequency electromagnetic fields, Protective clothing, standards and measurements procedures", *EMC York 2004 International Conference and Exhibition*, July, 2004.

[5] F. S. Chuang, "Composite Materials Distribution Department," Fsfuhecailiao.Diytrade.com, July, 2010. Available at: http://fsfuhecailiao.diytrade.com/sdp/576972/4/pd-2969246/3094782-0/Carbon_Fiber_Fabric_cloth_-3k_2_2_twill.html [Accessed 20 July 2010].

[6] S. Helmers, and Jung, "Siemens – Center for Quality Engineering, Test Report No.: V09R0001," Kitigawa.de, July, 2010. Available at: http://www.kitagawa.de/database/testreport_engl_em65g_em70.pdf [Accessed 20 July 2010].

[7] J. Drinovsky, and Z. Kejik, "Electromagnetic Shielding Efficiency of Composite Materials," *Measurement Science Review*, pp. 109-112, July, 2010.

[8] T. W. Więckowski, and M. J. Janukiewicz, "Methods for Evaluating the Shielding Effectiveness of Textiles," Fibres & Textiles in Eastern Europe, vol. 14, No. 5 (59), January/December, 2006.

# GPRS transmission from short-circuit indicator

Petr Mlynek, Jiri Misurec
Department of Telecommunications, Faculty of Electrical Engineering and Communication, Brno University of Technology, Czech Republic
mlynek@feec.vutbr.cz, misurec@feec.vutbr.cz

Pavel Kubicek
MEgA - Měřící Energetické Aparáty, a.s.
Brno, Czech Republic
kubicek@e-mega.cz

*Abstract*— **The article deals with transmission of the information from short-circuit indicator. GPRS service of the GSM network was chosen as communication channel for this transmission. Primarily, the article is focus on testing GPRS communication for transmission of information from energetic indicator.**

***Keywords- GPRS; short-circuit; indicator***

## I. INTRODUCTION

At present, the electric line is disconnected during short-circuit indication until the electric line with short-circuit is exactly analyzed. After short-circuit is detected section on the line between the two electrical substations (ES) is disconnected and the power supply is restored. The detection of short-circuit is task of emergency squad, which goes along particular route of electric line and in particular ES to investigate, that indicator of short-circuit indicated the short-circuit current. The time period of short-circuit detection is dependent on configuration of affected line, placing of particular ES and at the traffic situation at the time. Acceleration of this process reduces the time of power supply cut, resulting in improved services received by the terminal customers. Powers companies can continue in distributing power supply without unnecessarily interrupt in distribution.

For these reasons it is necessary to integrate the short-circuit current indicator to the SCADA system [1]. PLC [2,3], GPRS [4] and Internet [5] were considered as possible communication channel. GPRS was chosen for its high availability and relatively simple installation process.

## II. LOCALIZATION OF SHORT-CIRCUIT AND POWER RESTORATION

Fig.1 shows the demonstrational situation of short-circuit indication on line, his localization and restoration of power supply. Individual ES contain indicators of short-circuit currents, the worker have to get to ES and find out state of the indication. In case, that the access to the ES is lengthy or complicated, the ES were equipped with remote signalization capabilities.

In cooperation with PRE distribution, a.s. [6], ES with installed short-circuit indicators [7] were chosen. Added to this ES was GPRS communication unit MEg 202.1, which sends out the message to the concentrator about change state of output detector IZP. This message is send through ČSN EN 60870-5-104 protocol. Concentrator forwards this message to the dispatch.

In ES area was measured the GSM signal strength and GPRS bit error rate. The measurement results are shown in Tab 2.

The following chapters provide more detailed description of particular part of communication string and summary of results.

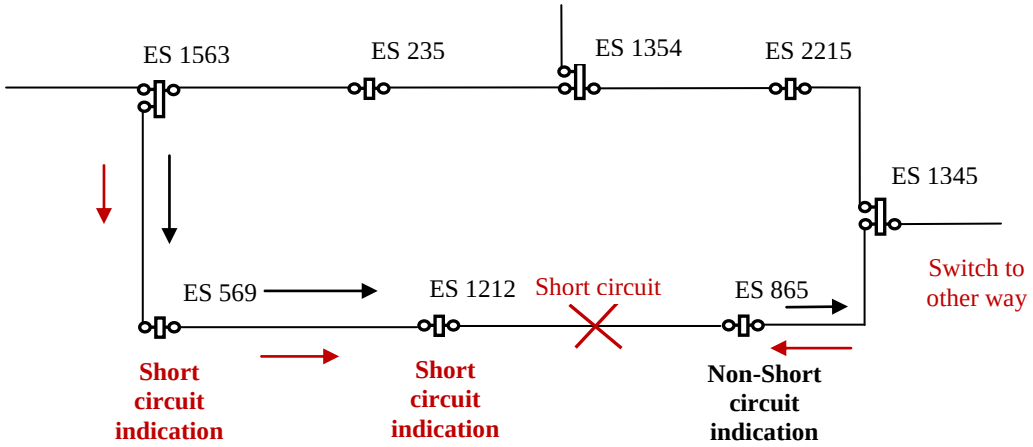


Figure 1. Example of short-circuit indication

The paper has been supported by Ministry of Industry and Trade of the Czech Republic the project No. FR—TI1/075 , Ministry of Education of the Czech Republic project No. MSM0021630513, and project *FEKT-S-10-16.*

## III. COMMUNICATION STRING

Schematic connection of particular parts of communication strings is shown in Fig. 2.

Hereinafter texts are describing individual parts of communication strings and their functions and together it provides an overview of functionality of the complete system. Communication string contains these parts:

### Indicator of short-circuit currents IZP

IZP is an indicator of short-circuit currents for MV and HV networks**.** It registers the passing of the short-circuit current through the phase conductor and, in this way, it facilitates and accelerates the identification of the faulty line section including the faulty phase. The IZP indicator has been designed for being used in radial or meshed networks supplied from one side. In cable networks with ground resistance it registers single-pole and multi-pole faults, in networks with a compensation coil it registers multi-pole short-circuits.

### Indicator of ground faults and short-circuit currents MEg61

The indicator of ground faults and short-circuit currents MEg61 has been designed for indicating the section of the overhead line of a compensated MV network with a ground fault and/or a short-circuit and for the telesignalization of relevant data. It may be also used in MV networks with grounded neutral point. The MEg61 are used for transmitting the state and/or the record of the development of the event.

### GPRS Communication unit MEg202.1

External GPRS module responds to signal from indicator. Module contain SIM card with fixed IP address and it is connected through private APN to the concentrator [8].

### Power source MEg101a

Communication unit need DC supply 12V, this ensure external module MEg101a [9].

### SCADA system in PRE distribution, a.s.

System in PRE distribution activates connection with concentrator and concentrator sends him status information of indication of particular IZP and state connection with communication unit, to that are indicators interconnected.

### Concentrator

Concentrator is mark for software application. Concentrator concentrates data of all indicators IZP and hand on this data to SCADA system.

In first phase testing (21 days) was way of continuation and maintenance connection configured according to specification CSN EN 60870- 5- 104 .The concentrator (TCP client) join on to particular communication unit (TCP server). However in this mode, cannot communication unit MEg202 in case of need initiate connection herself. If get to short-circuit at the time, when be connected interrupted, communication unit will send the message to the concentrator, which is not able to accept this message. Communication unit have to wait, than the concentrator resume connection. In this mode is treat, that delay of the short-circuit information transmission can be large.

In second phase testing, the communication unit initiates the connection. In case of short-circuit, the communication send the message to the concentrator. Communication unit receive the information, if the connection is cut off and immediately resume the connection and send the message again. In this mode is lower delay of information transmission, about 10-20 seconds.

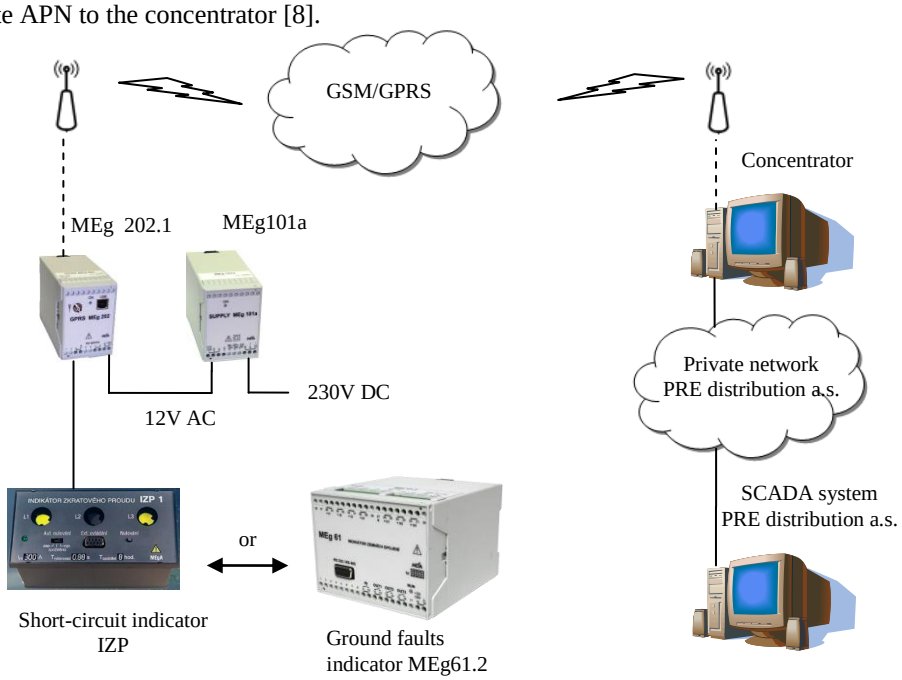


Figure 2. Communication string

## IV. TESTING OF GPRS CONNECTION

In cooperation with PRE distribution, a.s., ES with installed short-circuit indicators were chosen. In ES area was measured the GSM signal strength and GPRS bit error rate for installation the GPRS communication unit MEg 202.1. This unit ensures the remote data transmission from short-circuit indicators.

The evaluation of network running is carried out with the help of concentrator logs. The logs contain the information of break up and continuation connection between the concentrator and GPRS unit MEg202.1. In Tab. 1 are shown the numbers of break up connection in particular stations and approximate period of their durations.

TABLE I. THE NUMBER AND APPROXIMATELY TIME PERIOD OF BREAK UP GPRS CONNECTION IN PARTICULAR STATIONS

| | | First testing (21 days) | Second testing (167 days) | Total |
|---|---|---|---|---|
| **ES 1** | | | | |
| Time of failure | < 1min. | 118 | 6 | 124 |
| | < 5 min. | 26 | 1 | 27 |
| | < 30 min. | | 1 | 1 |
| | < 1 hour | 2 | | 2 |
| **ES 2** | | | | |
| Time of failure | < 1min. | 1 | 4 | 5 |
| | < 5 min. | | 1 | 1 |
| | < 30 min. | | | 0 |
| | < 1 hour | | | 0 |
| **ES 3** | | | | |
| Time of failure | < 1min. | 10 | 7 | 17 |
| | < 5 min. | | 1 | 1 |
| | < 30 min. | | | 0 |
| | < 1 hour | 1 | | 1 |

In first testing primary software proposal was used. This software was modified to reduce numerous short-term failure of connection. In second testing the SW was adjusted and therefore the number of short-term disconnections has declined significantly.

In case, that indication of short circuit current was during long-term disconnection, the information will be transmitted after regeneration of GPRS connection of communication unit.

Short-term disconnections with time period into one minute are probably caused by GPRS interference.

In disconnection lasting approximately 5 minutes it was found out that in some cases of TCP disconnection the reconnection is unattainable. This problem is caused by an unidentified fact of GPRS network. This problem can be solved by disconnecting of the GPRS and then repeated activation.

The results given in a Tab. 1 and Tab. 2 illustrate the connection between signal strength and number of disconnection in particular ES.

TABLE II. GPRS SIGNAL STRENGTH MEASUREMENT IN PARTICULAR ES

| Area of testing | type / technology HV | Data transmission test | Signal strength | Bit error rate |
|---|---|---|---|---|
| ES 1 | kiosk / classic | High bit error rate | -99.8dBm | 0,8 - 1,7% |
| ES 2 | kiosk / encapsulated | OK | -96.2dBm | 0 - 0,2% |
| ES 3 | block / encapsulated | OK | -85.8dBm | 0 - 0,2% |

## V. CONCLUSION

In terms of experimental network, real possibilities of data communication for transmission of energetic data between terminal energetic equipments trough GSM network using GPRS service were verified. During first implementation of ČSN EN 60870-5-104 protocol on GPRS service some problem were found and resulting in optimalization of connecting and connection maintenance.

Future development will focus on connection of current measuring device to the SCADA system with the help of communication unit MEG 202.1 and concentrator.

## REFERENCES


[1] DANEELS, A.; SALTER, W. WHAT IS SCADA?. *International Conference on Accelerator and Large Experimental Physics Control Systems*. Trieste, Italy. 1999

[2] HRASNICA, H., HAIDINE, A., LEHNERT, R. *Broadband Powerline Communications Network Design*. [s.l.] : Willey , c2004. 275 s. ISBN 0-470-85741-2

[3] Koutny, M.; Krajsa, O.; Mlynek, P. Modelling of PLC communication for supply networks. In *Proceedings of the 13th WSEAS International Conference on Communication.* Rhodos: WSEAS Press, 2009. s. 185-189. ISBN: 978-960-474-098- 7.

[4] KOUTNÝ, M.; HOŠEK, J. The system for real time measuring based on GPRS technology. In *Proceedings of 31th International Conference on Telecommunications and Signal Processing - TSP 2008.* 1. Budapest: Asszisztencia Szervezo Kft., 2008. s. 1-4. ISBN: 978-963-06-5487- 6.

[5] Mlynek, P.; Misurec, J.; Koutny, M. The communication unit for remote data acquisition via the Internet. In *Proceedings of the 7th WSEAS International Conference on Circuits, systems, electronics, control and signal processing (CSES'08).* Puerto de La Cruz, Spain: WSEAS Press, 2008. s. 168-173. ISBN: 978-960-474-035-2.

[6] *PRE – Pražská energetika, a. s.* Online: < http://www.pre.cz>.

[7] User manual Indikátoru zkratových prudů IZP1. *MEgA – Měřící Energetická Aparáty a.s.* [online]. 1.11.2008 , 1, [cit. 2010-11-21]. Online: <www.e-mega.cz >.

[8] User manual Communication unit Meg202.1. *MEgA – Měřící Energetická Aparáty a.s.* [online]. 1.11.2008 , 1, [cit. 2010-11-21]. Online: <www.e-mega.cz >.

[9] User manual Zdroj MEg101a. *MEgA – Měřící Energetická Aparáty a.s.* [online]. 1.11.2008 , 1, [cit. 2010-11-21]. Online: <www.e-mega.cz >.

[10] *PRE – Pražská energetika, a. s.* Online: < http://www.pre.cz>.

# Localization Techniques for Sensor Networks

Juraj Machaj, Peter Brida, Jan Duha
Department of Telecommunications and Multimedia
University of Zilina
Zilina, Slovakia
machaj@fel.uniza.sk, brida@fel.uniza.sk, duha@fel.uniza.sk

***Abstract*— This paper describes some of localization algorithms developed for wireless sensor networks. One centralized localization algorithm is compared to three decentralized localization algorithms based on Distance-Vector routing algorithm. Performance of localization algorithms was investigated in simulations, which were done in model created in Matlab. Simulation results show that decentralized algorithms may achieve less accurate results as centralized, but with much lower calculation complexity.**

***Keywords-Localization; Positioning; Sensor networks***

## I. INTRODUCTION

Distributed sensor networks have been discussed for more than 30 years, but the vision of wireless sensor networks (WSN) has been brought into reality only by the recent advances in wireless communications and electronics, which have enabled the development of low-cost, low-power and multi-functional sensors, that are small in size and can communicate on small distances using RF signals [1].

Localization is very important capability in most WSN applications. For example in environmental monitoring applications, bush fire surveillance or water quality monitoring data measured by sensors are meaningless without knowing where they were collected. In the other hand there are systems where localization availability may enable new applications like health monitoring, traffic monitoring or inventory management [2].

There are many ways how location of nodes in sensor networks can be achieved. One method is to determine the position of device thru manual configuration. This method is infeasible for large scale networks and for networks with mobile nodes. Another way is to use global positioning system (GPS) or another satellite positioning system. These systems may work well for outdoor positioning. Disadvantage is that they can not be used for example in indoor environments or dense urban environments. They also suffer from high hardware costs and high energy consumption.

These were reasons for development of local positioning systems. These systems relay on high density of reference nodes that knows their position. Sensors with unknown position – blindfolded nodes can determine its position using one of localization algorithms developed for WSN.

WSN localization algorithms can be divided based on data collected to range-based and range-free. Range-based algorithms use measurements of signal properties to achieve data for location estimation. In the other hand range-free algorithms can estimate position of blindfolded node using network information like proximity of nodes or hops between blindfolded node and reference nodes. In this paper only range-based algorithms will be described, because higher accuracy can be achieved.

Localization algorithms can be divided to centralized and decentralized based on estimation procedure and computation complexity. In decentralized algorithms framework, each node can compute its own position. These algorithms have lower complexity and can be used for networks with high mobility. In centralized algorithms position of all nodes in network is estimated in network coordinator and algorithms has high complexity. Performance and complexity of algorithms based on both frameworks will be compared.

Rest of paper is organized as follows. In section II data measurements used in localization algorithms will be introduced. Section III describes mathematical methods for position estimation. Localization algorithms used in simulation will be described in Section IV. Section V shows results of simulations and finally Section VI concludes the paper.

## II. DATA MEASUREMENT

In this section measurements of data used for localization are described. These measurements are used in range based localization algorithms in WSN.

### *A. Received signal strength*

Received signal strength (RSS) is basic data measurement used in localization. It is based on assumption that RSS depends on distance between transmitter and receiver.

Advantage of this measurement is that nodes don't need to have additional hardware to achieve data. Disadvantage is that accuracy depends on signal quality, is affected by signal fluctuation and of course propagation model needs to be very accurate.

### B. *Angle of Arrival*

Angle of arrival (AoA) is method that determines from which angle radio signal propagates, this method can be also called Direction of Arrival (DoA). AoA method is based on using properties of special uniform linear arrays (ULA). ULA consists from n elements with distance l, can be used to estimate direction of a RF signal based on the following relation:

$$\theta = \arcsin\left(\frac{c\Delta t}{l}\right), \quad (1)$$

where $\theta$ represents angle of RF propagation upon the ULA, $c$ is the speed of light, $\Delta t$ represents time difference between signal arrivals to consecutive array elements and $l$ is distance between consecutive elements of the ULA [1].

### C. *Time of Arrival*

Time of Arrival (ToA) is used to estimate distance between transmitter and receiver nodes. ToA is based on knowledge of RF signal propagation speed. In case of using ToA measurements in multipath condition is needed to accurately detect direct path between nodes and so estimate time accurately. From measurement of ToA distance can be computed using equation:

$$d = c.\tau_{DP}, \quad (2)$$

Where $d$ is distance between nodes, $c$ is speed of light and $\tau_{DP}$ is propagation time of direct path. Accurate measurement of ToA needs synchronization of nodes in network.

This measurement is not very popular in sensor networks, because of accurate synchronization and also additional hardware to achieve measurements is needed.

## III. POSITION ESTIMATION

In this section some of mathematical methods for position estimation are described. These mathematical methods were used in simulations together with localization algorithms, which will be described in next section.

### A. *Trilateration*

Trilateration is basic technique of estimation of position. It uses information about distances between reference and blindfolded nodes. Trilateration is used when distance from three reference nodes is known. Position is estimated as intersection of circles (Figure 1) given by equation:

$$(x - x_i)^2 + (y - y_i)^2 = r_i^2, \quad (3)$$

where $[x, y]$ are coordinates of blindfolded node, $[x_i, y_i]$ are coordinates of $i$-th reference node and $r_i$ represents distance from $i$-th reference node.

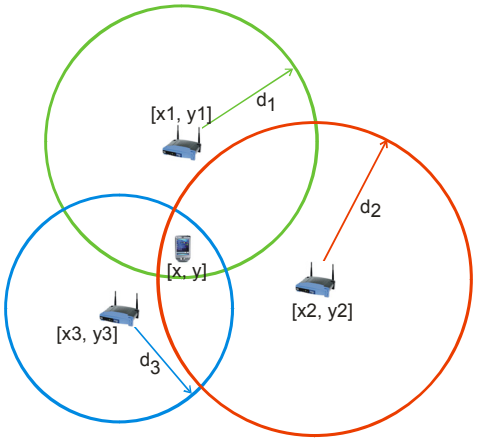


Figure 1. Trilateration

This method can be used in network and there is no need to have another localization algorithm. Problem is that in this case high number of reference nodes in network is needed.

### B. *Min-Max*

Min-Max was originally designed as part of multilateration technique. Compared to trilateration it has advantages that same or even better results can be achieved and calculation complexity is much lower [3].

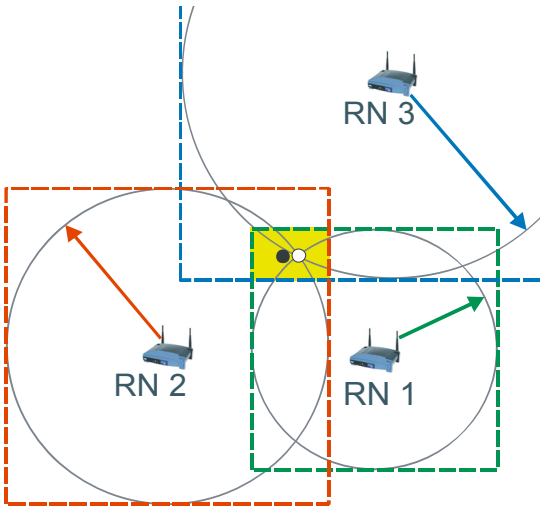


Figure 2. Min-Max position estimation

In Min-Max method circles are approximated with squares. Position of blindfolded node is estimated in center of square intersection, given by equation:

$$[\max(x_i - d_i), \max(y_i - d_i)] \times [\min(x_i + d_i), \min(y_i + d_i)], \quad (4)$$

where $[x_i, y_i]$ are coordinates of $i$-th reference node and $d_i$ represents estimated distance between blindfolded node and $i$-th reference node.

### C. *Transformation of coordinate systems*

Another way of estimation of blindfolded node position is use transformation matrix to convert local coordinate system, to coordinate system that can describe whole network, or global coordinate system.

In this method three different types of matrices can be used. First one is matrix of translation, this helps to move whole coordinate system to overlap with other one. Second type of matrix is rotation matrix, this helps to rotate coordinate system in desired angle. Last one is scaling matrix, this helps to scale coordinate system and is used when different metrics are used.

With combination of those three matrices we can find solution of transformation that has least sum of square errors.

## IV. LOCALIZATION ALGORITHMS

In this section some of localization algorithms that can be used in WSN are described. These algorithms are implemented in simulation model developed in Matlab. First three algorithms are based on Distance - Vector (DV) routing algorithm, which is widely used in Ad-hoc and sensor networks. These algorithms are distributed, so position is computed by blindfolded node itself. Last one is centralized algorithm called Multidimensional scaling. In this algorithm position of nodes should be calculated in central node.

### A. *DV-Euclidean*

In this localization method the true Euclidian distance between localized node *A* and reference node *N* is estimated. Blindfolded node *A* needs to have at least two neighbor nodes which have estimates to reference node *N* (Figure 3). Node *A* also measure distances *AB*, *AC* and *BC*, so there is condition that nodes *B* and *C* are neighbors to each other.

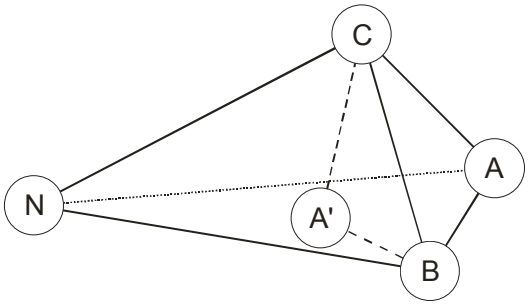


Figure 3. DV-Euclidean localization algorithm

If all the distances are estimated node *A* is allowed to compute the diagonal *AN*, with use of equations:

$$\cos(\alpha) = \frac{AB^2 - AC^2 - BC^2}{2 \cdot AC \cdot BC}, \quad \cos(\beta) = \frac{BL^2 - BC^2 - CL^2}{2 \cdot BC \cdot CL}, \quad (5)$$

$$AL^2 = AC^2 + CL^2 - 2 \cdot AC \cdot CL \cdot \cos(\beta \pm \alpha). \quad (6)$$

Diagonal *AN* is the Euclidean distance from blindfolded node *A* to the reference node *N*. It is possible that *A* is on the same side of *BC* as *N* in Figure 3 shown as *A'*. In this case the distance between *A* and *N* is different.

Choice between two possible solutions is made locally in node *A*. This can be done by voting, if node *A* have more neighbors with estimates to reference node *N*, or by examining relation with other common neighbors of nodes *B* and *C* [4], [6].

When choice between two possible solutions is done, position of blindfolded node A can be estimated using one of trilateration or multilateration techniques.

### B. *DV-Radial*

DV-Radial is localization algorithm based on AoA measurements. Position estimation process is similar to DV-Euclidean. Blindfolded node must have at least two neighbor nodes that know its position against reference node. Assuming that node *A* (Figure 4) knows angles to his neighbor nodes *B* and *C*, which knows angles to far reference node *L*.

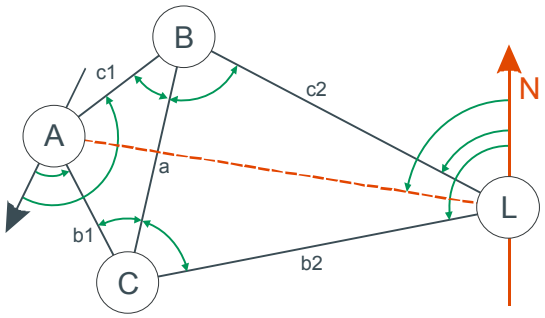


Figure 4. DV-Radial localization algorithm

Blindfolded node needs to calculate angle to reference node. If *B* and *C* are neighbors to each other, node *A* can determine all angles in triangles *ABC* and *BCL*. That allows node *A* to calculate angle *ALN*, which is in fact angle from reference node to blindfolded node [5].

Blindfolded node can achieve another estimation of angle *ALN* from other neighbour nodes in case they have fewer hops to reference node as nodes *A* and *B*. If blindfolded node has information about angle from at least two reference nodes, it can estimate its position using triangulation. Advantage of this algorithm is that it sends lower amount of data thru the network as Euclidean algorithm.

### C. *DV-Coordinates*

If nodes in network can measure distances and angles, it is possible to node establish its own coordinate system for which node is placed in the origin (position [*0*, *0*]). Axis can be chosen by bearing to one of the neighbor nodes. In Figure 5 for node *A* axis is chosen by node *E*. All neighbor nodes can be then added to local coordinate system.

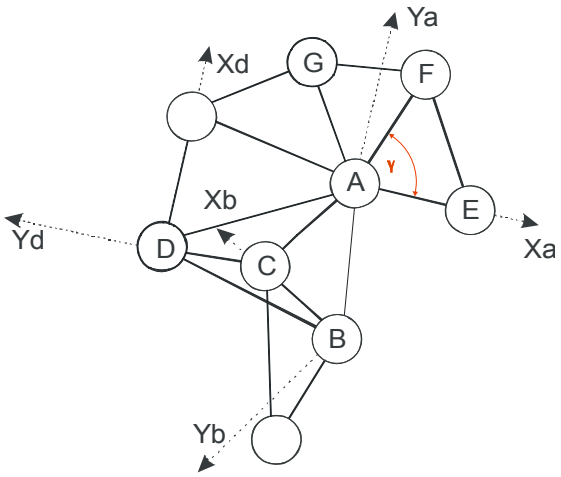


Figure 5. DV-Coordinates localization algorithm

Next step is called registration. In this step, nodes create transformation matrix to transform position of nodes from coordinate system neighbor nodes. For example nodes *A* and *B* have coordinates of nodes *A*, *B*, *C* and *D* in their coordinate systems, so transformation matrix can be calculated. Each coordinate achieved from neighbor node must be translated to local coordinate system [6].

Last step is localization of blindfolded node. If blindfolded node sends request for localization, neighbor nodes sends back positions of reference nodes in their coordinate system and their position in global coordinate system. If blindfolded node achieve positions of at least 3 reference nodes and translate them to its local coordinate system transformation matrix between global and local coordinate system can be achieved using registration procedure. The projection of [*0, 0*] through this matrix would yield global coordinates for the node. Other way is to use trilateration or multilateration to estimate position of blindfolded node.

### *D. MDS-MAP*

MDS-MAP is centralized localization algorithm based on multidimensional scaling (MDS). MDS can be described as data analysis techniques that display the structure of distance-like data as a geometrical picture [7]. It is usually used to find a placement of the points in a two- or three-dimensional, where the distances between points resemble the original similarities.

MDS-MAP algorithm consists from three phases. On first phase distances between all neighbor nodes are estimated using RSS or ToA methods, depending on nodes hardware. Nodes send estimated distances to network coordinator. Network coordinator constructs the distance matrix. In second step of this algorithm classical MDS is applied to distance matrix and relative local coordinate system with positions of all nodes is created. In last step of MDS-MAP algorithm transformation matrices can be used to transform relative coordinate system to global coordinate system in case that there is enough reference nodes in network.

## V. SIMULATION RESULTS

Simulations were performed in simulation model created in Matlab environment [8]. Precision of localization algorithms was evaluated as median of root square error, which represents Euclidean distance between real and estimated position of blindfolded node. Median is in fact center value of all errors achieved in simulations. Advantage compared to mean error is that median is not affected by extreme values.

Complexity of localization algorithms were evaluated by measurements of computing time during simulations.

First simulation scenario was proposed to evaluate impact of number of reference nodes in network on localization accuracy and complexity of localization algorithm. In this scenario network with 51 nodes was randomly deployed in area 100x100m. Radio range of nodes was 30m. Radio channel was affected with Additive White Gaussian Noise (AWGN), SNR was set to 3dB. Simulation results are shown in figure 6.

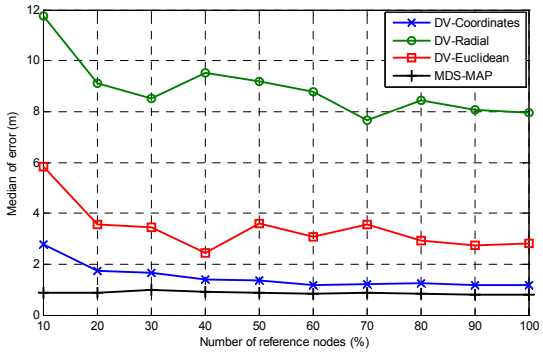


Figure 6. Median localization error

From the figure can be seen that localization error of DV localization algorithms is affected by number of reference points in network. MDS-MAP algorithm achieves best results from all the algorithms and its accuracy doesn't depend on number of reference points in network. In figure 7 cumulative distribution functions of errors for all simulated localization algorithms, when number of reference points was 30%.

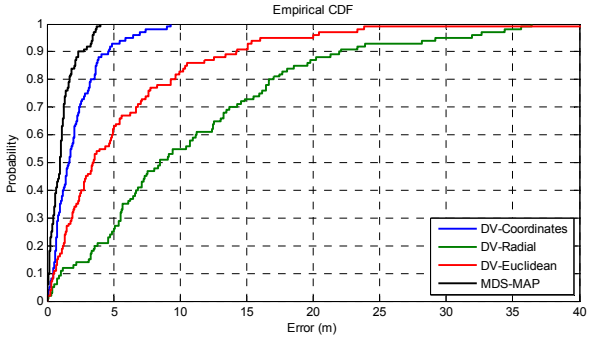


Figure 7. CDF of localization algorithms

From figure is clear that MDS-MAP achieves best results from all localization algorithms, when 90% of localization errors are lower than 2.5m. From DV based localization algorithms, best results were achieved by DV-Coordinates

algorithm. DV-Coordinates achieved over 90% of errors smaller than 5m. Variance of localization errors of DV-Euclidean and DV-Radial algorithms are much higher than errors achieved by DV-Coordiantes and MDS-MAP. Worst of all algorithms seems to be DV-Radial, which achieves for 90% probability error about 22m.

In next figure computation times of DV based algorithms are shown to compare complexity. Computation time of MDS-MAP is not shown, because it was much higher.

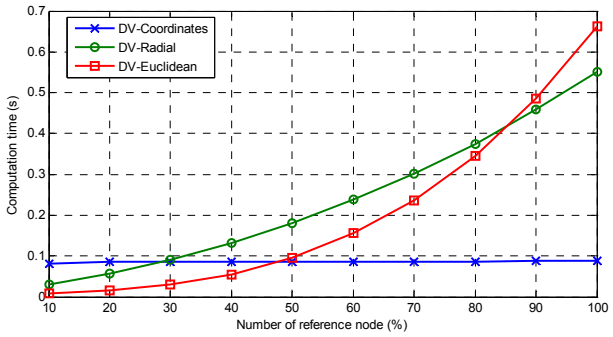


Figure 8. Computation times of DV based algorithms

From the figure can be seen that computation time of DV-Radial and DV-Euclidean grows up with higher number of reference nodes in network, while computation time of DV-Coordinates remains the same. For networks where small number of reference points is deployed DV-Radial and DV-Euclidean seems to be better solution from complexity point of view, but when number of reference nodes is higher than 30% and 50% complexity of DV-Coordinates is smaller than complexity of DV-Radial and DV-Euclidean respectively.

Computational time of MDS-MAP algorithm was similarly as computation time of DV-Coordinates constant, so complexity of these algorithms doesn't depend on number of reference points in network. As assumed computation time for MDS-MAP was much higher compared to decentralized algorithms. Mean computation time was 35.5 s for all number of reference nodes.

Second scenario was designed to find how computation complexity depends on nodes density. Number of nodes in network was changed and computation time of localization algorithms was measured. Results of this simulation can be seen in table 1.

TABLE I. COMPUTATION TIMES OF LOCALIZATION ALGORITHMS

| Number of nodes in network | Computation time [s] | | | |
|---|---|---|---|---|
| | DV-Coordiantes | DV-Radial | DV-Euclidean | MDS-MAP |
| 20 | 0,0211 | 0,0446 | 0,0164 | 1,7016 |
| 25 | 0,0191 | 0,0303 | 0,0134 | 3,3564 |
| 30 | 0,0240 | 0,0345 | 0,0157 | 6,1904 |
| 35 | 0,0306 | 0,0373 | 0,0149 | 10,2696 |
| 40 | 0,0479 | 0,0425 | 0,0116 | 16,7561 |
| 45 | 0,0673 | 0,0411 | 0,0134 | 25,3787 |
| 50 | 0,0808 | 0,0481 | 0,0150 | 36,2456 |

From the table can be seen that computation complexity of DV-Radial and DV-Euclidean localization algorithms doesn't depend on network density. In the other hand complexity of DV-Coordinates and MDS-MAP is affected by increasing number of nodes. In networks with small density, complexity of DV-Coordinates is lower than complexity of DV-Radial and achieves similar complexity as DV-Euclidean.

## VI. CONCLUSION

In this paper accuracy and complexity of several localization algorithms developed for WSN was compared. From results can be seen that centralized algorithm achieves most accurate position estimation, but complexity of this algorithm is extremely high, especially in networks with high number of nodes. Therefore centralized localization algorithm MDS-MAP should be used in networks with small density of nodes, or in networks where mobility of nodes is not allowed. On the other hand, decentralized algorithms has low computation complexity. DV-Euclidean and DV-Radial localization algorithms seems to be immune to increasing number of nodes in network, but its complexity grows up with higher number of reference nodes. DV-Coordinates achieved most accurate results from all investigated decentralized localization algorithms. Its complexity grows up with higher number of nodes in network, but it is still very small. Decentralized localization algorithms should be used in mobile WSN, because of small computation complexity.

## ACKNOWLEDGMENT

This work was partially supported by the Slovak Research and Development Agency under the contract No. LPP-0126-09 and by the Slovak VEGA grant agency, Project No. 1/0392/10 "The research of mobile nodes in wireless sensor networks".

## REFERENCES

[1] M. Guoqiang, F. Barış, "Localization algorithms and strategies for wireless sensor networks", Yurchak Printing Inc, ISBN 978-1-60566-396-8, 2009

[2] Krejcar, O.: User localization for large artifacts prebuffering and safety possibilities in mobile embedded systems. In: International Conference on Advanced Computer Control, Singapore, pp.: 41-46, ISBN: 978-0-7695-3516-6 (2009)

[3] K . Langendoen, N. Reijers, "Distributed localization in wireless sensor networks: a quantitative comparison", Computer Networks: The International Journal of Computer and Telecommunications Networking, v.43 n.4, p.499-518, 2003

[4] D. Niculescu, B. Nath, "Ad hoc positioning system (APS)," Global Telecommunications Conference, 2001. GLOBECOM '01. IEEE , vol.5, pp.2926-2931, 2001

[5] D. Niculescu, B. Nath, "Ad hoc positioning system (APS) using AOA," INFOCOM 2003. Twenty-Second Annual Joint Conference of the IEEE Computer and Communications. IEEE Societies, vol.3, pp. 1734- 1743, 2003

[6] D. Niculescu, B. Nath, "Dv based positioning in ad hoc networks," Telecommunication Sytstems 22 (14), pp. 267-280, 2003

[7] Sewoong Oh; A. Montanari, A. Karbasi, "Sensor network localization from local connectivity: Performance analysis for the MDS-MAP algorithm," Information Theory Workshop (ITW), 2010 IEEE , pp.1-5, 2010

[8] J. Machaj, J. Benikovsky, "Simulation model for localization in ad hoc networks", proceedings of Digital technologies workshopu 2009, ISBN: 978-80-554-0150-8.

# Direct Quadrature Frequency Synthesizer Implementation in VHDL

Daniel Kekrt, Milos Klima
Dept. of Radio Engineering
Faculty of Electrical Engineering
Czech Technical University in Prague
Prague, Czech Republic
kekrtd1@fel.cvut.cz,klima@fel.cvut.cz

Radek Podgorny, Jan Zavrtalek, Leoš Bohac
Dept. of Telecommunication Engineering
Faculty of Electrical Engineering
Czech Technical University in Prague
Prague, Czech Republic
radek@podgorny.cz,zavrtjan@fel.cvut,bohac@fel.cvut.cz

***Abstract*—In this article we describe a creation, modeling, implementation and simulation of a direct quadrature frequency synthesizer. It is very important functional block and has plenty of usages in the sphere of digital radio transmission systems. Firstly, as the core of frequency offset synchronizer at receiving side. Further, as the subcarrier source for digital frequency multiplexing in the base-band and as the instrument for channel transfer function measurement and Rayleigh fading Channel simulator. We describe the process of synthesizer modeling in Matlab in both floating and fixed point arithmetics for later implementation in the VHDL language for FPGA. The complete functional block was implemented in the Xilinx Virtex6 FPGA device attached to analog radio front-end built of Analog Devices evaluation boards. The results on the front-end output was measured, presented and compared with the Matlab model.**

**IndexTerms— Direct frequency synthesis, Frequency offset synchronization, Frequency multiplexing, Rayleigh Fading Channel simulator, Channel transfer function measurement**

## I. Introduction

With the improvement of performance of FPGA (Field-Programmable Gate Array) devices it becomes quite inviting to implement basic radio system parts in a digital domain. It brings simplicity of the circuit design and also offers numerous options of later adaptation of the entire system into specific real world scenarios. Multiple parts of the system can be implemented in a single chip thus bringing the overall efficiency in hardware design.

As a part of complex radio transmission system we have implemented an direct quadrature frequency synthesizer in VHDL language for the Xilinx Virtex6 FPGA device. Concretely, synthesizer with the fixed table (sine $1^{st}$ quadrant table). This paper is dedicated to precise description of synthesizer transformation to the fixed point arithmetics and consequent implementation of the designed synthesizer circuit structure in the VHDL language.

## II. Direct Frequency Synthesizer Model

The frequency synthesizer serves in the radio front-end of the digital transmission system a multiple functions. In particular on detection side it reduces the frequency offset that arises since transmitter $f^{(t)}(t)$ or receiver $f^{(r)}(t)$ carrier frequency is not absolutely stable and over time slightly fluctuates. The frequency difference causes received signal $r(t)$ to be parasitically modulated by harmonic signal $e^{j2\pi f_\Delta(t)t}$ of low frequency $f_\Delta(t) = f^{(t)}(t) - f^{(r)}(t)$ even after an analog quadrature demodulation. In the case of linear digital modulations it results in a rotation of constellation plane around its center. In order to cope with this problem it is necessary to mix a signal once more with the antiphase frequency $e^{-j2\pi f_\Delta(t)t}$ and since this frequency is low, it is possible to accomplish processing at easy digitally in FPGA or DSP directly in the receiver after sampling a signal $r(t)$ by the frequency $T_p$ that satisfies a sampling theorem.

The function block in the digital domain that suppresses undesirable parasitic modulation is called the frequency offset synchronizer, it is composed of three functional parts. The first is digital mixer, that is simply a pair of two multipliers, one multiplier is for in-phase signal component $r[n]$ a second for a quadrature component. Another block is an offset estimator that performs computation of $\hat{f}_\Delta[n]$ from the received signal using a knowledge of stochastic properties of an implemented modulation. The last block is just a frequency synthesizer. It takes on its input the phase increment samples of estimated parasitic frequency $\hat{\varphi}_\Delta[n] = 2\pi\hat{f}_\Delta[n]nT_p$ from the output of the digital integrator of the offset estimator and generates of them frequency $e^{-j\varphi[n]}$ which is then fed into a digital mixer.

Another area of application is a frequency multiplexing system for transmitting more signals. Here, a set of digital synthesizers in the digital domain creates a hierarchy of subcarriers that are modulated by different transmitted signals. A whole wave packet is then transferred outside of the digital domain and modulated onto a single carrier. In the receiver there is a complementary block of the same set of synthesizers that demodulate the received signal back to the original components.

The last major area of application is modeling of terrestrial flat or frequency selective Rayleigh channel with fading. The fading of a channel is simulated using Jake's simulator composed of a set of frequency synthesizers.

The output of the synthesizer can be described by a formula

$$y[n] = e^{j\varphi[n]}, \tag{1}$$

where $\varphi[n]$ is current content of the phase accumulator that

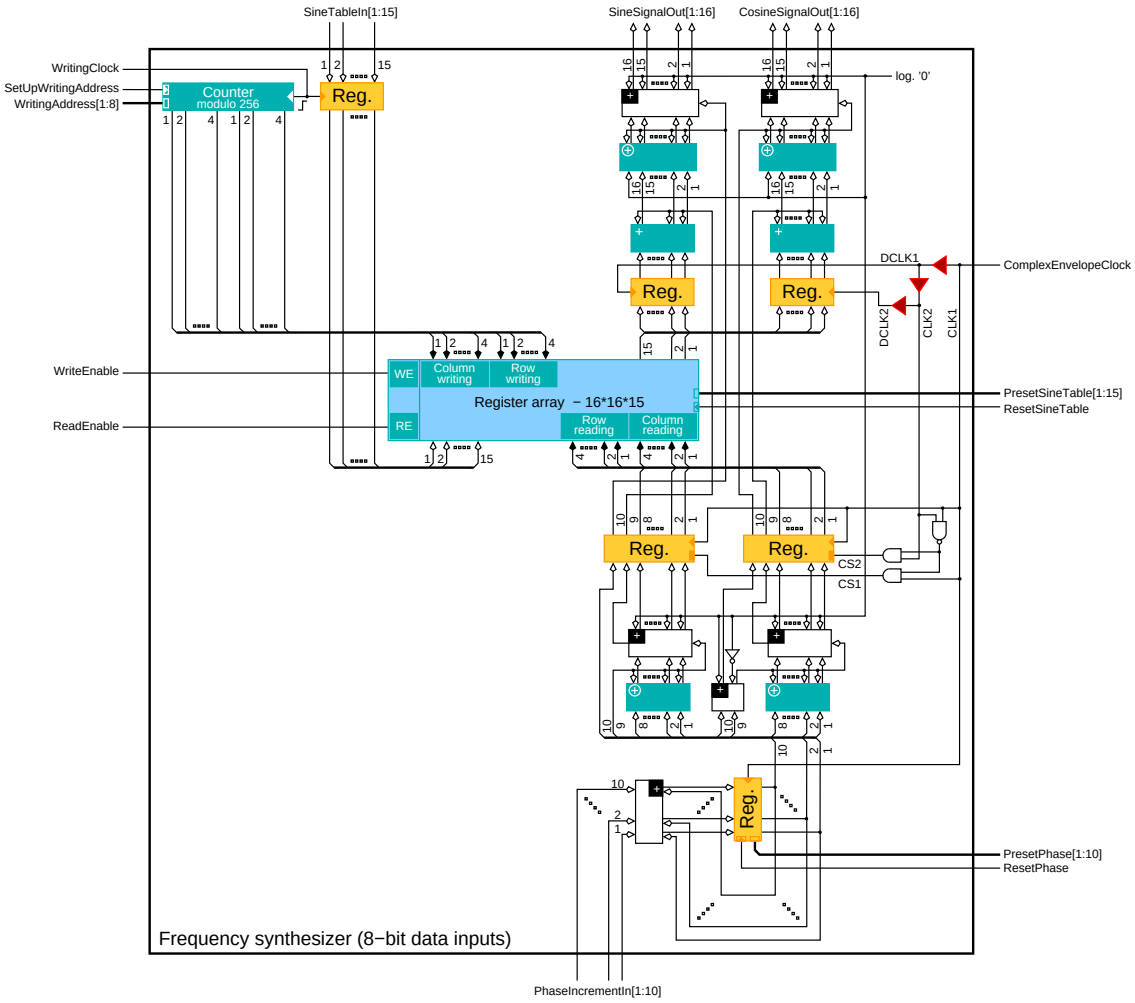


Figure 1. Synthesizer structure.

performs integration

$$\varphi[n+1] = \varphi[n] + \varphi_\Delta[n] \tag{2}$$

of the input phase increments $\varphi_\Delta[n]$. Let us denote initial accumulator value as $\varphi[0] = \varphi_0$. According to the method of calculating the nonlinearity $e^{j(.)}$ the direct synthesizers can be either the sine table or the polynomial based ones. In both cases, the entire period of the harmonic function parts of the nonlinearity of $e^{j(.)}$ is compiled using a quarter period of sine. Depending on the value of the highest two bit number $\varphi[n]$ , which is called as a quadrant indicator, a quarter period may be either mirrored or possible assigned a negative sign.

In the memory synthesizer the values of the quarter period sampled by specifically selected phase step are stored in the table. Benefit of this implementation is mainly in the speed and simplicity. On the other hand, disadvantages are higher memory requirements and certain restrictions on generated frequencies resulting from the fineness of the phase step. Exactly opposite it is in case of polynomial variant, where the sinus quarter period is replaced with a solid or semi-continuous polynomial approximation. There is a greater delay between sample $y[n]$ and $\varphi[n]$, since the calculation of the polynomial values takes some time, but the frequency accuracy is much bigger.

In this paper the implementation of simpler synthesizer with the sine table is discussed. Let us implement the synthesizer whose phase accumulator has a bit width of the $N_b^\varphi$. For the output then holds $\varphi_q \in \{0, \ldots, M_\varphi - 1\}$, where $M_\varphi = 2^{N_b^\varphi}$. When for a whole signal comes out a total of $M_\varphi$ values of the phase then a quarter period must have just $M = M_\varphi/4$. The ideal equation (2), in floating point operations can also be restated in analogous equation

$$\varphi_q[n+1] = (\varphi_q[n] + \varphi_{\Delta q}[n]) \bmod 4M, \tag{3}$$

for fixed point operation. The input $\varphi_{\Delta q} \in \{-2M, -2M+1, \ldots, 2M-1\}$, in form of phase increment then allows to change the current value of the phase $\varphi_q[n]$ in accordance with the sampling theorem, at maximum half period forward or backward. The values of the quarter sine table stored in the memory of the synthesizer are determined by the equation

$$b_q[\ell] = \left\lfloor (2^{N_b - 1} - 1) \sin\left(\frac{\pi \ell}{2M}\right) \right\rceil \text{ iff } 0 < \ell < M - 1, \tag{4}$$

where $N_b+1$ is a number of bits for quantization of the output signal

$$y_q[n] = g(\varphi_q[n])b_q[f(\varphi_q[n])]. \quad (5)$$

The functions $f(.)$ a $g(.)$ manipulate a stored quarter period $b_q[\ell]$ depending on what quadrant the synthesis is currently running at. The function $f(.)$ mirrors a table if necessary, and function $g(.)$ changes its sign.

## III. Circuit Structure

The memory synthesizer with a detailed description of its outputs is shown in Figure 2 and its circuit implementation is shown in Figure 1. There are two parallel sections in the design. The first one is used to generate the sine and second the cosine. Both branches share together one phase accumulator and a memory of the quarter sinus period, which is accessed $2\times$ per clock cycle ComplexEnvelopeClock (during this period, each of the sections read one sample from a memory). The memory size has been selected as $M = 256$ which corresponds to the minimum phase step $\varphi_{\Delta\,\min} = 0.00613592\,[\text{rad}]$. Hence the input of the block has a form of the phase increments signal in two's complement $\varphi^{tc}_{\Delta q}[n]$ with a maximum width of 10 bits (introduced scalar will be considered as a decimal representation of binary numbers in two's complement notation, i.e. as a whole positive number). In the scheme it is described as PhaseIncrementIn and subsequently it is added to the current content of the phase accumulator. Its 10 bits wide output is then split into two parts. Lower 8 bits are the basis for calculating the address of a sinus quarter period memory and upper two bits represent a quadrant pointer. Since the cosine is shifted to sine by one quadrant ($\pi/2$) it is necessary in its branch to increment its quadrant pointer. In contrast a quadrant pointer is left unchanged in the sine branch. The value of lowest bit of both quadrant pointers ($9^{\text{th}}$ bit) decides in the calculation of address whether or not the 8-bit base $a^{ub}[n]$ will be mirrored (the scalar will be considered as a decimal representation of an unsigned binary number, i.e. as an integer). If $9^{\text{th}}$ bit has log. '1' the 8-bit base $a^{ub}[n]$ is mirrored. The mirroring process is itself implemented using XOR gate, where the base is negated, and the adder that gets incremented. This will give the address $A^{ub}[n] = M - a^{ub}[n]$. If $9^{\text{th}}$ bit is log. '0 ' the base is left unchanged and becomes directly resulting address $A^{ub}[n] = a^{ub}[n]$. The upper bit of both quadrant pointers ($10^{\text{th}}$) indicates a sign. The top carry bits of adders that are generated by mirroring the base $a^{ub}[n]$, will be denoted as the saturation bits. If the saturation bit has log. '1'; the corresponding part is just in its maximum, i.e., in +1 or -1.

The calculated address pairs $A^{ub}_{\sin}[n]$ a $A^{ub}_{\cos}[n]$ together with the sign and saturation bits are buffered by a pair of 10 bits wide addressing registers. In one clock period CLK1 = ComplexEnvelopeClock both registers gradually deliver to the addressing input of the memory mentioned address pair through a common multiplexed bus, to which they are connected via the chip select input bits (CS) set on log. '1'. The clock CLK1 (or CLK2) in log. '1' state activates the CS input 1 (or CS 2) of addressing register.

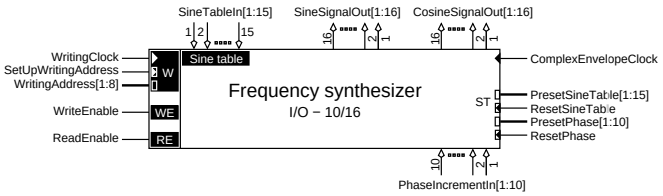


Figure 2. Synthesizer schematic sign.

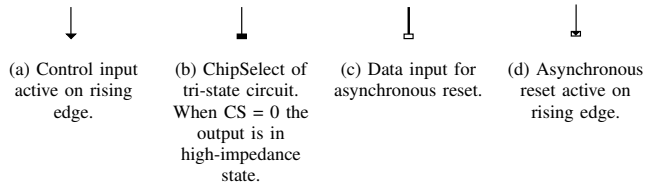

(a) Control input active on rising edge.

(b) ChipSelect of tri-state circuit. When CS = 0 the output is in high-impedance state.

(c) Data input for asynchronous reset.

(d) Asynchronous reset active on rising edge.

Figure 3. Signatures of control and data inputs and outputs of circuits used.

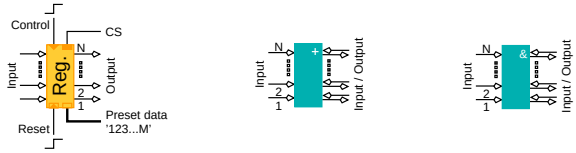


(a) Register active on rising edge with asynchronous reset on Reset signal rising edge.

(b) N-tuple OR logic elements.

(c) N-tuple XOR logic elements.


(d) Delay.

(f) Binary adder with no LSB carry and no MSB carry output.

Figure 4. Logic and arithmetic circuits used.

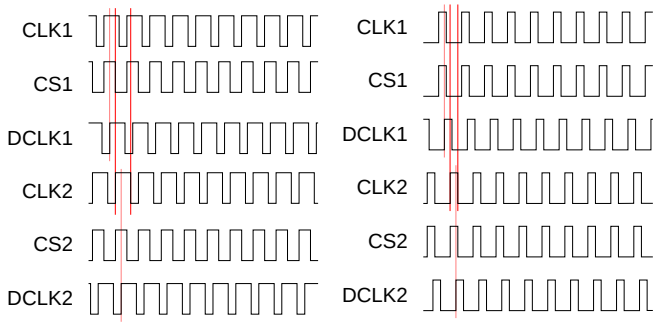


(a) The behaviour of timing and CS signals for clock with mark-space ratio 1:2.

(b) The behaviour of timing and CS signals for clock with mark-space ratio 2:1.

Figure 5. Timing and control (chip select) signals.

The length of log. '1' state of CLK1 must accordingly be set in such a way to allow enough time to successfully address a memory with both registers. A pair of AND and NAND gates condition CS1 and CS2 signals to avoid both to be kept simultaneously in log.1 state as duty cycle of CLK1 gets greater than 1:1, otherwise the three state output of addressing registers would be destroyed. Examples of the timing and activation signals for both possible conditions of clock duty cycle CLK1 are shown in Figure 5.

The memory data are then buffered by a pair of output registers with a width of 15 bits on the rising edge of DCLK1

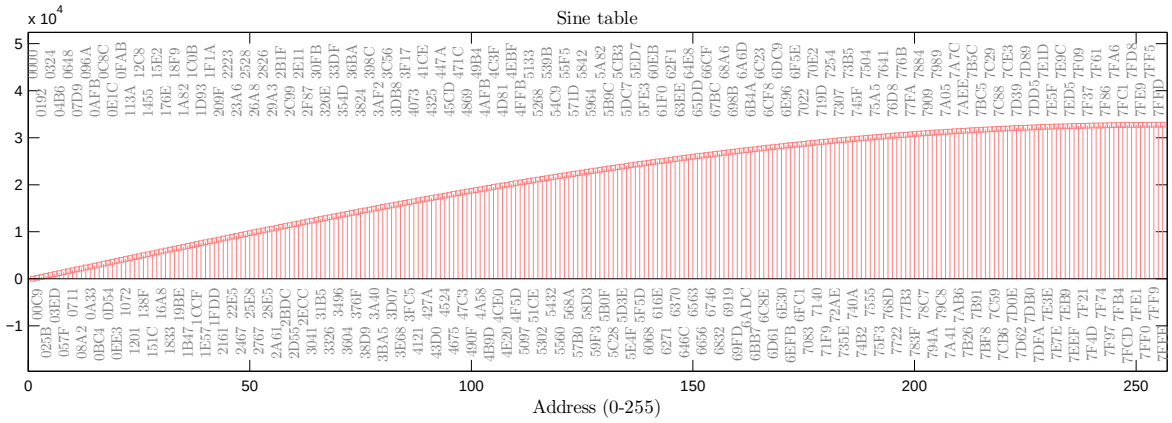


Figure 6. Sine 1st quadrant table with 16-bit quantization and phase accuracy $\varphi_{\Delta\,\min} = 0.00613592$ [rad].

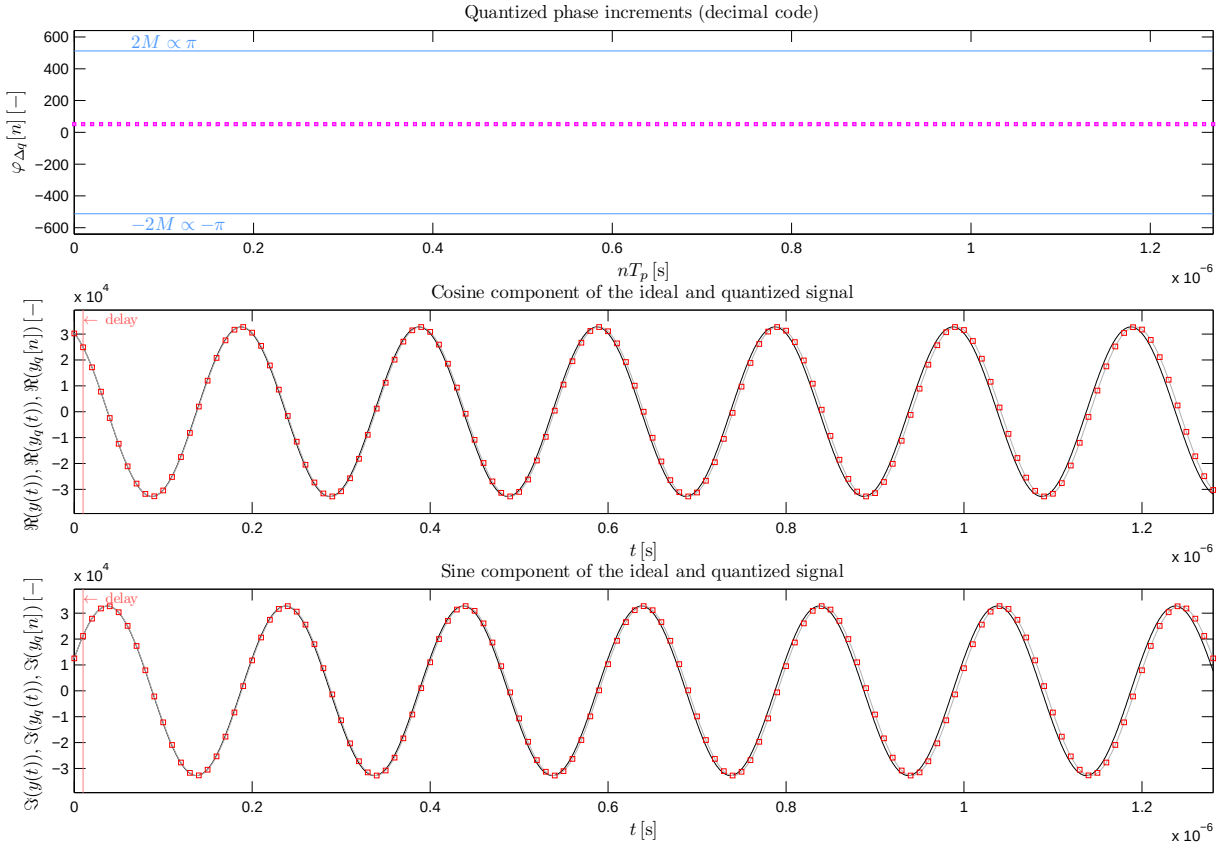


Figure 7. The synthesis of the constant frequency 5 MHz with 16-bit quantization and with initial phase $\varphi_{0q} = 64 \propto \pi/8$.

and DCLK2 clocks. The time delay between DCLK2 and DCLK1 clocks must be large enough allowing a memory to deliver a stored data in time to its output. It is clear from relation (4) that in the memory is stored only the sine table from 0 to $\pi/4 - \varphi_{\Delta\,\min}$ and the sine maximum $+1$ is missing there. It is therefore necessary to generate it if necessary. The saturation bits connected to a pair of OR gates behind the output registers are there for that purpose. The rest of the structure performs a sign change of a function if corresponding sign bit is in log. '1'. The total delay of the signal in the synthesizer is two clocks of ComplexEnvelopeClock.

## IV. MATLAB SIMULATION

The theoretical design will be demonstrated by the simulation of a synthesizer with a phase accuracy of $M = 256$ and its output quantized (including a sign) by $N_b + 1 = 16$ bits. Thus selected parameters correspond to the sine table in Figure 6. The sampling frequency in simulation was selected to $f_p = T_p^{-1} = 100$ MHz and the results for fixed and variable frequency can be seen on Figures 7 and 8, where comparison to ideal synthesis (solid black line) is also carried out. In case of a fixed frequency an offset of both is clearly seen being influenced by a phase quantizations.

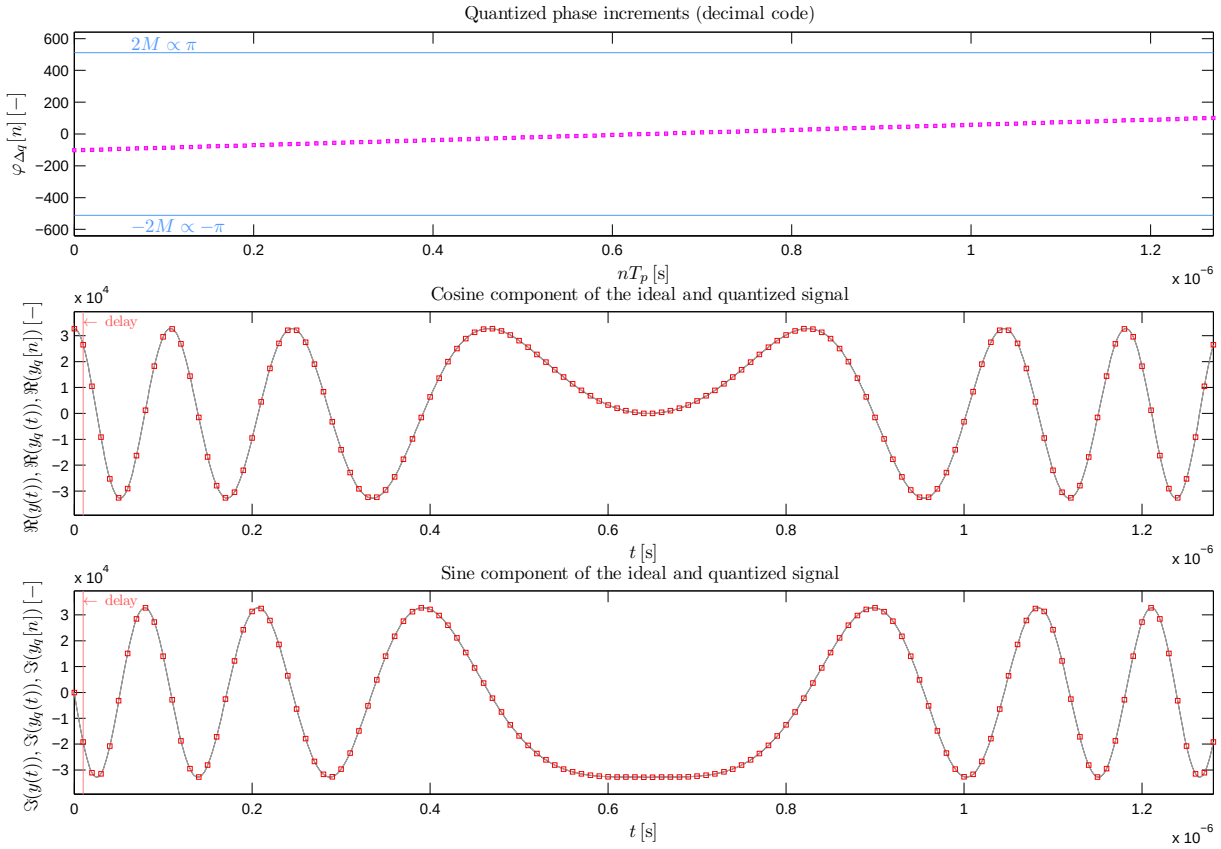


Figure 8. The synthesis of the linear increasing frequency from 0 to 10 MHz with 16-bit quantization and with zero initial phase.

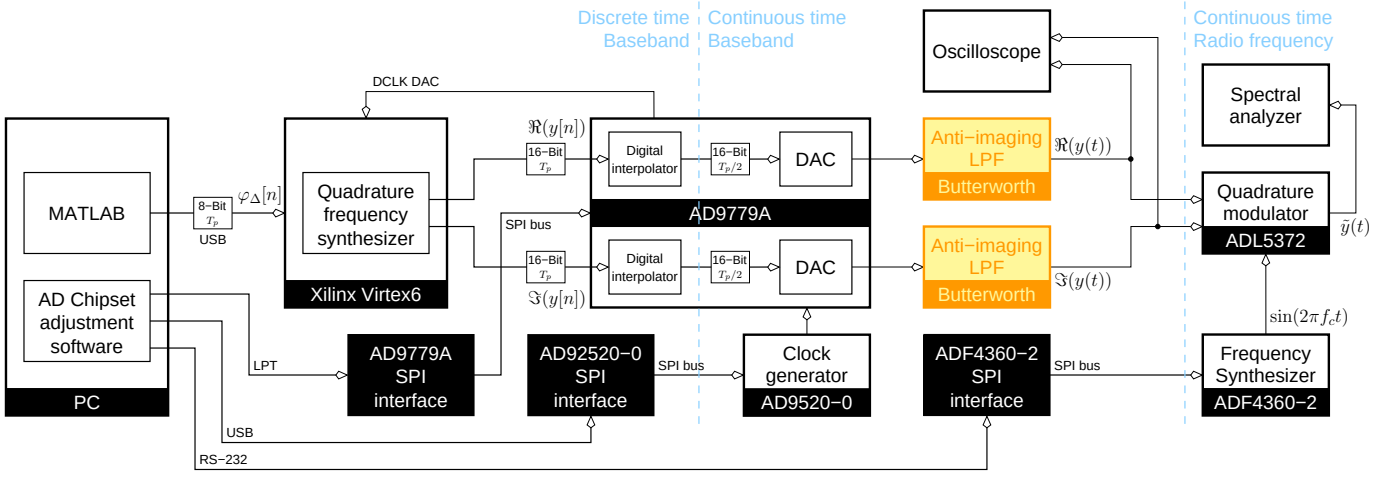


Figure 9. System structure.

## V. VHDL Implementation

We have implemented the design in VHDL [2], [3] and synthesized the design using the Xilinx ISE 12.3 design suite. In order to be able to communicate with the device, a set of memories and UART controller are also implemented. This of course raises the number of used flip-flops. The implementation contains memory made of FPGA slices for simplicity. In the final production-grade system the memory will be block-RAM. Also, in the final design, we plan to slightly change the structure so it can be implemented as single-clock synchronous system.

The prepared data set from Matlab has been downloaded to the synthesized design using a custom Python utility which communicates using our proprietary protocol over USB.

## VI. Results

The final design was synthesized for the Xilinx Virtex 6 FPGA and was tested on the actual hardware. The final design synthesizes to approximately 3000 slice registers, 10000 slice LUTs of which approximately 6000 is used as memory. These

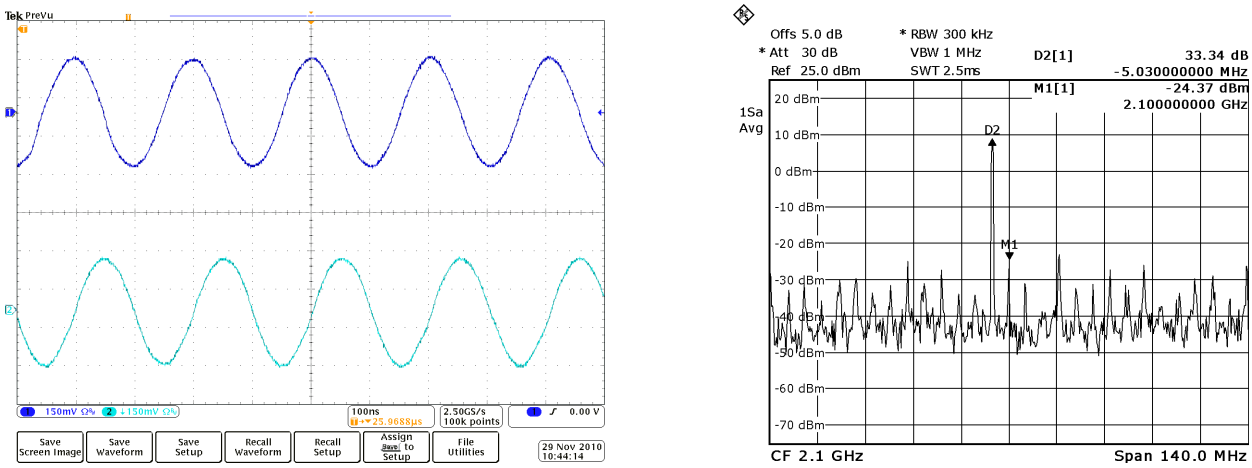


Figure 10. Oscilloscope and spectral analyzer snapshot of the constant 5 MHz frequency synthesis.

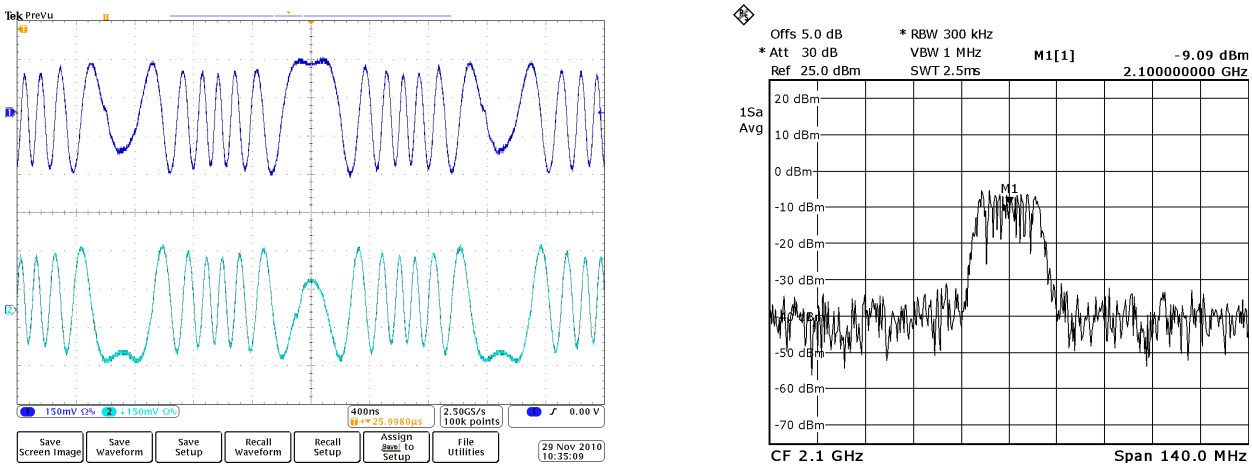


Figure 11. Oscilloscope and spectral analyzer snapshot of the linear increasing frequency synthesis from 0 to 10 MHz.

numbers are skewed because of the peripheral structures we had to implement as well in order to be able to communicate with the device and read/write memory contents. We have successfully verified the design using the measuring workbench shown in Figure 9 and consider it to be fully functional. The operating frequency was 100 MHz but the synthesizer in Xilinx ISE 12.3 timed the circuit to be able to run at up to 320 MHz. The measured waveforms and spectra are shown in Figure 10 and 11. The frequency $f_c$ of the analog carry wave was set up to 2.1 GHz. We have verified the circuit functionality using Tektronix DPO 4032 oscilloscope and Rohde&Schwarz FSL6 spectral analyzer.

## VII. Conclusion

The key benefit of the described direct quadrature frequency synthesizer with a sine table is the speed (overall structure delay is 2 clocks) and the frequency stability which is by the way a positive feature of all direct synthesizers. However, it requires large amount of memory. The memory should not only be big enough to accommodate a complete quarter period, but also sufficiently quick to be able to serve a double read requests on different addresses in one clock cycle. Another limitation arises from a selected minimum phase step $\varphi_{\Delta\,\min}$ that clearly set a range of the generated frequencies. So if the required memory size and corresponding frequency accuracy is not appropriate or speed is not crucial the polynomial implementation is more convenient. This structure has overall delay 3 clocks in case of quadrature approximation a 4 clocks with cubic approximation.

## Acknowledgment

This research work has been supported by the research project SGS10/204/OHK3/2T/13 "The hardware design and implementation of broadband transceiver with iterative synchronized Turbocode" of the Czech Technical University in Prague; by the research project P102/10/1320 "Research and modeling of advanced methods of image quality evaluation" of the Czech Grant Agency and by the FI-IM5/115 project of Ministry of Industry and Trade of the Czech Republic.

## References

[1] Petr Skalický, *Číslicové systémy v radiotechnice*, Vydavatelství ČVUT, 2004, ISBN 80-01-02854-2.
[2] Peter J. Ashenden, *The designer's guide to VHDL*, San Francisco: Morgan Kaufmann, 2002, ISBN 1-55860-674-2.
[3] Jiří Pinker, Martin Poupa, *Číslicové systémy a jazyk VHDL*, BEN-Technická literatura, 2006, ISBN 80-7300-198-5.
[4] John G. Proakis, *Digital communications, 5th ed.*, ISBN 978-0072957167, Boston : McGraw - Hill, 2008.

# Telecommunication systems

# Dependence of Far-end Crosstalk on Capacitive and Inductive Unbalances between Pairs in Cable

Pavel Lafata
Department of Telecommunication Engineering
Faculty of Electrical Engineering, Czech Technical University in Prague
Technicka 2, Prague 6, 166 27, Czech Republic
lafatpav@fel.cvut.cz

***Abstract*—The transmission speed of present xDSL digital subscriber lines is limited mainly by crosstalk. It appears in large metallic infrastructure between the symmetrical pairs and the digital systems operating within the same metallic cable. The capacitive and inductive unbalances between symmetrical pairs are the main source of crosstalk between them. Several models of far-end crosstalk using capacitive and inductive unbalances and their matrices have been already presented, or models using pseudo-randomly generated components, but these models are mathematically quite complex and require many parameters. Or, on the other hand, there are several models, which use only a few crosstalk parameters, and therefore they do not provide very accurate and realistic results. This paper presents initial mathematical formulas of far-end crosstalk's dependence on capacitive and inductive unbalances between two parallel pairs in a cable and a method of their derivation. These formulas will be subsequently implemented into new method for far-end crosstalk's simulation and modeling.**

***Keywords-Far-end crosstalk; Metallic cable; xDSL***

## I. INTRODUCTION

The elementary unit of a standard telecommunication cable is generally two insulated wires twisted uniformly to form a balanced pair. By twisting four insulated wires together a quad is formed. Several quads are typically twisted together to form a subgroup of pairs (or quads), these subgroups can be further twisted and gathered according to a cable internal structure. The resulting transmission parameters of a final cable are determined according to a method of construction, types of used materials and their processing [1]. During the process of cable's manufacturing, several parameters have to be measured and checked, and must meet specified tolerances. The major problem, which appears in large metallic networks, is crosstalk. It comes from unbalanced capacitive and inductive couplings between single copper pairs, their quads and multi-quads as well as from the ground unbalances [2]. The pairs in multi-pair or multi-quad cables usually demonstrate towards themselves small irregularities, which are caused by manufacturing tolerances, deformations and other specific reasons. The influence of near-end crosstalk (NEXT) can be well limited by separating transmission directions by using different frequency bands, but the elimination of far-end crosstalk (FEXT) is not so easy and therefore FEXT is a dominant disturbing source in current xDSL lines [3].

Several solutions for the reduction of FEXT influence have been already presented and tested. One of the most promising is Vectored DMT modulation (VDMT) [4]. This modulation is an upgrade of previous Discrete Multitone modulation (DMT) and it offers the elimination of FEXT crosstalk by coordinating the transmitted DMT symbols according to the transmission functions of all pairs and crosstalk in the metallic cable [5]. However, the practical implementation of VDMT modulation into the present DSLAMs multiplexors is not possible due to the overall complexity and computational demands of VDMT modulation for the full coordination of transmissions in large metallic cable systems. One of the possibilities how to simplify this process would be performing the VDMT modulation only for a limited number of pairs or even only for several xDSL sub-channels [6]. These pairs could be selected according to their contributions of crosstalk. This proposed method would require very accurate and realistic simulations of FEXT crosstalk and its prediction for each pair in the metallic cable. This model will come from the precise geometrical description of cable's internal structure, mathematical calculation of capacitive and inductive couplings and unbalances between metallic pairs. It will be necessary to implement specific functions and parameters to simulate cable's inhomogeneities, manufacturing tolerances, external and internal deformations, electrical parameters, etc., [7].

But first, it is necessary to derive initial mathematical formulas for calculation of FEXT from capacitive and inductive unbalances between two parallel pairs in a cable. These unbalances are typically based on the internal structure of a cable, its manufacturing tolerances, deformations and other inhomogeneities. According to these formulas, a new method for FEXT modeling could be proposed.

## II. THE GENERALL EXPRESSION OF CROSSTALK CURRENTS

The interstices between pairs, quads and subgroups of pairs in cable are usually filled with a gel or an air. These interstices form the internal deformations and inhomogeneities in a cable. There could be also several external deformations, which can be caused in process of cable's impropriate installation. These deformations form electrical unbalances between symmetrical pairs in a cable and together with tolerances and imperfections during the process of cable's manufacturing lead consequently into a crosstalk. The major part in resulting unbalance plays irregularities of conductors' diameters, insulation's thickness,

their positional differences and material's parameters. Several influences and parameters come also from the specific effects on internal inductivity and resistivity, effective permittivity of insulation and dielectric and important role also plays the internal structure and arrangement of a cable [1].

Capacitive and inductive unbalances and couplings are the main source of crosstalk between them. These capacitive and inductive couplings in a quad of four wires form an unbalanced bridge [7]. Using the star-polygon transformation it is possible to express resulting capacitive unbalance $C_{ub}$ and inductive unbalance $M_{ub}$ respectively. The calculation of these unbalances is based on the geometrical structure of the quad and other parameters, such as permittivity a permeability of the materials, as it was presented e.g. in [8], [9].

### A. The Calculation of Crosstalk Currents

The far-end crosstalk is caused by leaking currents, which penetrate from the disturbing pair to the parallel disturbed pair, thanks to the capacitive and inductive unbalances between them [2]. This situation is described in the next schematic.

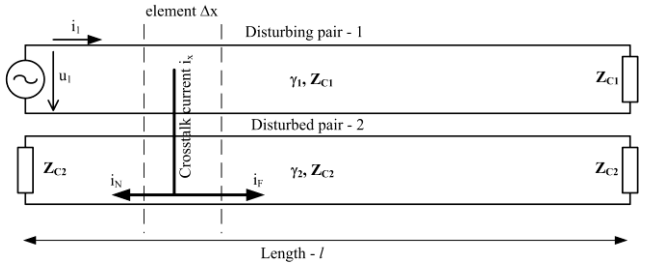


Figure 1. The schematic situation of disturbing and disturbed pairs.

We can assume the situation with two parallel pairs in a cable, where the near-end of the disturbing pair contains the source of signal $u_1$, which provides the total current $i_1$. The pair is correctly terminated on its far-end by the impedance $Z_{C1}$, which is close to the characteristic impedance of this pair. The disturbed pair is properly terminated on its both ends by its characteristic impedance $Z_{C2}$. The transmission function of disturbing pair is $\gamma_1$, while the transmission function of disturbed pair is $\gamma_2$. The length of both pairs is $l$. The infinite element $\Delta x$ contains total capacitive unbalance $C_{ub}\Delta x$, through which the capacitive crosstalk current $i_C$ propagates from the disturbing pair into the disturbed pair. This element also contains the inductive unbalance $M_{ub}\Delta x$, which causes the origination of inductive crosstalk voltage $u_M$ in the disturbed pair. The sum of both crosstalk disturbances is the total leaking current $i_x$, which propagates along the disturbed pair to its near-end as a current $i_N$ where it causes the near-end crosstalk NEXT and another part propagates also to the far-end as a current $i_F$ where it causes the far-end crosstalk FEXT.

The crosstalk current $i_{Cx}$, which comes from the capacitive unbalance $C_{ub}\Delta x$ can be expressed [8]:

$$i_{Cx} = \frac{u_{Cx}}{\frac{1}{j\omega C_{ub}\Delta x} + \frac{Z_{C2}}{2}} \tag{1}$$

The term with $Z_{C2}$ in the denominator can be neglected and the expression simplified:

$$i_{Cx} = j\omega C_{ub}\Delta x \cdot u_{Cx} \tag{2}$$

The voltage presented in the capacitive unbalance in the element $\Delta x$ is given:

$$u_{Cx} = Z_{C1} \cdot i_1 \cdot e^{-\gamma_1 x} \tag{3}$$

And therefore the equation (2) can be expressed:

$$i_{Cx} = j\omega C_{ub}\Delta x \cdot Z_{C1} \cdot i_1 \cdot e^{-\gamma_1 x} \tag{4}$$

This current is divided, one half propagates to the near-end, while the second half to the far-end of the disturbed pair. The current, which is caused by capacitive unbalance and appears at the far-end - $i_{CF}$, can be therefore calculated:

$$i_{CF} = \frac{1}{2} j\omega C_{ub}\Delta x \cdot Z_{C1} \cdot i_1 \cdot e^{-\gamma_1 x} \cdot e^{-\gamma_2 (l-x)} \tag{5}$$

It is also possible to express the crosstalk voltage $u_{Mx}$, which comes from the inductive unbalance $M_{ub}\Delta x$:

$$u_{Mx} = j\omega M_{ub}\Delta x \cdot i_{Mx} = j\omega M_{ub}\Delta x \cdot i_1 \cdot e^{-\gamma_1 x} \tag{6}$$

The crosstalk current coming from the inductive unbalance and appearing at the far-end - $i_{MF}$ can be calculated:

$$i_{MF} = -\frac{u_{Mx}}{2Z_{C2}} = -j\omega \frac{M_{ub}\Delta x}{2Z_{C2}} \cdot i_1 \cdot e^{-\gamma_1 x} \cdot e^{-\gamma_2 (l-x)} \tag{7}$$

Based on previous equations (5) and (7) it is possible to derive the summary far-end crosstalk current from both unbalances originating in the element $\Delta x$:

$$\begin{aligned} i_F &= i_{CF} + i_{MF} \\ i_F &= \frac{1}{2} j\omega \cdot i_1 \cdot e^{-\gamma_1 x} \cdot e^{-\gamma_2 (l-x)} \cdot \left( Z_{C1} C_{ub}\Delta x - \frac{M_{ub}\Delta x}{Z_{C2}} \right) \end{aligned} \tag{8}$$

### B. The Derivation of Standard FEXT Model

To obtain the standard FEXT model, it is necessary to adjust the equation (8) and to consider some simplifying assumptions, as described in [10]. Capacitive $C_{ub}$ and inductive $M_{ub}$ unbalances are generally various in the real metallic cable and are varying along the cable, so they can be expressed by analytic functions of the position $x$. But in the case of the

simplified standard FEXT model it is possible to assume the summary unbalances as their mean values for the whole length of a cable, so they are constant and independent on their positions *x*. Thanks to this assumption, it is possible to consider the element $\Delta x$ as infinitely short and to express it by using differential term *dx*. Another simplification considers the transmission parameters of both pairs within the same cable to be identical, therefore transmission functions of both pairs is $\gamma$, while their characteristic impedances are $Z_C$.

Based on these simplifications, the equation (8) can be modified:

$$i_F = j\omega \cdot Z_C \cdot i_1 \cdot e^{-\gamma x} \cdot e^{-\gamma(l-x)} \cdot \frac{1}{2}\left(\overline{C_{ub}} - \frac{\overline{M_{ub}}}{Z_C^2}\right) \tag{9}$$

The formula (9) can be further simplified:

$$i_{Fx} = j\omega \cdot u_1 \cdot e^{-\gamma l} \cdot \underbrace{\frac{1}{2}\left(\overline{C_{ub}} - \frac{\overline{M_{ub}}}{Z_C^2}\right)}_{\text{Total coupling constant - } C'} = j\omega \cdot u_1 \cdot e^{-\gamma l} \cdot C' \tag{10}$$

The transmission function of FEXT crosstalk is defined:

$$\left|H_{FEXT}(f)\right|^2 = \frac{P_{FEXT}(f)}{P_1(f)} \tag{11}$$

In which $P_{FEXT}(f)$ represents the power function of far-end crosstalk and $P_1(f)$ the input power function at the near-end of a disturbing pair. The FEXT power function can be obtained by an integration of crosstalk contributions (10) for the length *l*.

$$P_{FEXT}(f) = \left|Z_C\right| \cdot i_F^2 = \left|Z_C\right| \cdot \omega^2 \cdot u_1^2(f) \cdot C'^2 \cdot \int_0^l e^{-2\gamma x} \cdot dx \tag{12}$$

Assuming electrically long symmetrical pairs and thanks to the (12) it is possible to express transmission function of FEXT (11) as:

$$\left|H_{FEXT}(f)\right|^2 = \frac{P_{FEXT}(f)}{P_1(f)} = \frac{\left|Z_C\right| \cdot i_F^2}{\frac{u_1^2}{\left|Z_C\right|}}$$

$$\left|H_{FEXT}(f)\right|^2 = \frac{\left|Z_C\right| \cdot \omega^2 \cdot u_1^2(f) \cdot C'^2 \cdot l \cdot \left|H(f)\right|^2}{\frac{u_1^2(f)}{\left|Z_C\right|}} \tag{13}$$

$$\left|H_{FEXT}(f)\right|^2 = \left|Z_C\right|^2 \cdot \omega^2 \cdot C'^2 \cdot l \cdot \left|H(f)\right|^2$$

$$\left|H_{FEXT}(f)\right|^2 = K_{FEXT} \cdot f^2 \cdot l \cdot \left|H(f)\right|^2$$

Where $K_{FEXT}$ is a crosstalk parameter (a constant for the selected combination of pairs), which represents the summary rate of capacitive and inductive couplings between pairs. $|H(f)|^2$ is the transmission function of a pair, *f* is the frequency and *l* represents the length of both pairs.

Following the previous modifications, it is obvious, that:

$$K_{FEXT} = \left|Z_C\right|^2 \cdot 4\pi^2 \cdot C'^2 \tag{14}$$

Therefore $K_{FEXT}$ crosstalk parameter is expressed through the integration of capacitive and inductive unbalances in (12) along the cable. The equation (13) represents the standard simple FEXT model, which is presented in [10]. It is obvious that thanks to the previous simplifications and assumptions, this standard FEXT model with only one crosstalk parameter cannot be very accurate and that it provides only approximate results, which are presented as mean values of the summary crosstalk characteristics [13].

### *C. The General Model of Crosstalk Currents*

The previously derived standard FEXT model uses several simplifications and assumptions. The most severe condition is the consideration of constant capacitive and inductive unbalances and their independence on the position *x*. It is necessary to assume varying unbalances for accurate crosstalk modeling. However, analytical expression of these functions $C_{ub}(x)$, $M_{ub}(x)$, could be quite difficult. The values of these functions would probably vary pseudo-randomly in the interval given by manufacturing tolerances and other influences in the cable. It is possible to assume that the character of these functions would have probably the behavior of a normal distribution with the deviation given by these tolerances and imperfections of a cable. From this reason, it is not possible to use the operation of integration of the crosstalk contributions, but instead of that only simple summarization of the individual crosstalk currents.

The general expression is based on formulas (1)-(8) and the schematic illustration presented in the Fig. 2.

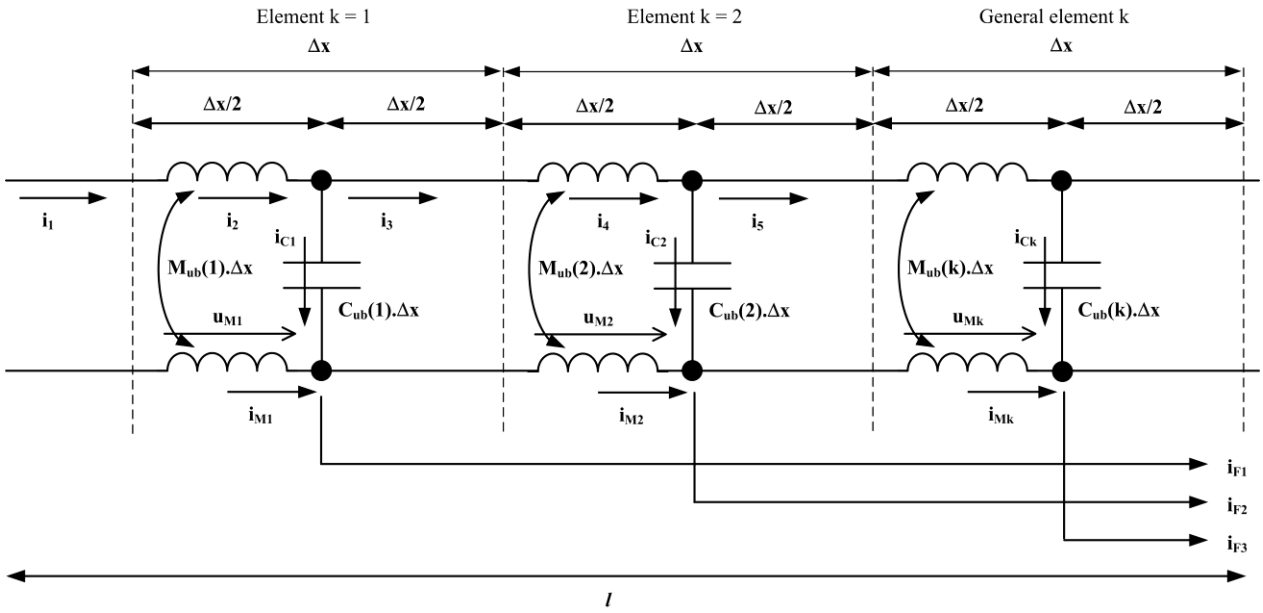


Figure 2. The illustration of crosstalk currents for the general model.

Both symmetrical pairs are divided into three basic elements. Each element contains its capacitive $C_{ub}(k)\Delta x$ and inductive $M_{ub}(k)\Delta x$ unbalance, in which the letter $k$ marks its position. The currents in the first element $k = 1$ can be expressed:

$$i_2 = i_1 \cdot e^{-\gamma_1 \frac{\Delta x}{2}} \tag{15}$$

$$i_{C1} = j\omega Z_{C1} C_{ub}(1)\Delta x \cdot i_2 = j\omega Z_{C1} C_{ub}(1)\Delta x \cdot i_1 \cdot e^{-\gamma_1 \frac{\Delta x}{2}} \tag{16}$$

$$i_{M1} = -j\omega \frac{M_{ub}(1)\Delta x}{Z_{C2}} \cdot i_2 = -j\omega \frac{M_{ub}(1)\Delta x}{Z_{C2}} \cdot i_1 \cdot e^{-\gamma_1 \frac{\Delta x}{2}} \tag{17}$$

$$i_3 = i_2 - i_{C1} = i_1 \cdot e^{-\gamma_1 \frac{\Delta x}{2}} - j\omega Z_{C1} C_{ub}(1)\Delta x \cdot i_1 \cdot e^{-\gamma_1 \frac{\Delta x}{2}} = i_1 e^{-\gamma_1 \frac{\Delta x}{2}} \cdot \left(1 - j\omega Z_{C1} C_{ub}(1)\Delta x\right) \tag{18}$$

The resulting far-end crosstalk current, which propagates to the far-end of the disturbed pair and which originates from the capacitive and inductive unbalances in the element $k = 1$, can be calculated:

$$i_{F1} = \frac{1}{2}\left(i_{C1} + i_{M1}\right) \cdot e^{-\gamma_2 (l - \frac{\Delta x}{2})} = \frac{1}{2} i_1 \cdot e^{-\gamma_1 \frac{\Delta x}{2}} \cdot e^{-\gamma_2 (l - \frac{\Delta x}{2})} \cdot \left( j\omega Z_{C1} C_{ub}(1)\Delta x - j\omega \frac{M_{ub}(1)\Delta x}{Z_{C2}} \right) \tag{19}$$

The crosstalk currents for the second element $k = 2$ can be expressed in the same way:

$$i_4 = i_3 \cdot e^{-\gamma_1 \Delta x} = i_1 \cdot e^{-\gamma_1 \frac{\Delta x}{2}} \cdot e^{-\gamma_1 \Delta x} \cdot \left(1 - j\omega Z_{C1} C_{ub}(1)\Delta x\right) = i_1 \cdot e^{-\gamma_1 \frac{3\Delta x}{2}} \cdot \left(1 - j\omega Z_{C1} C_{ub}(1)\Delta x\right) \tag{20}$$

$$i_{C2} = j\omega Z_{C1} C_{ub}(2)\Delta x \cdot i_4 = i_1 \cdot e^{-\gamma_1 \frac{3\Delta x}{2}} \cdot \left(1 - j\omega Z_{C1} C_{ub}(1)\Delta x\right) \cdot \left(j\omega Z_{C1} C_{ub}(2)\Delta x\right) \tag{21}$$

$$i_{M2} = -j\omega \frac{M_{ub}(1)\Delta x}{Z_{C2}} \cdot i_4 = -i_1 \cdot e^{-\gamma_1 \frac{3\Delta x}{2}} \cdot \left(1 - j\omega Z_{C1} C_{ub}(1)\Delta x\right) \cdot \left( j\omega \frac{M_{ub}(2)\Delta x}{Z_{C2}} \right) \tag{22}$$

$$i_5 = i_4 - i_{C2}$$

$$i_5 = i_1 \cdot e^{-\gamma_1 \frac{3\Delta x}{2}} \cdot \left(1 - j\omega Z_{C1} C_{ub}(1)\Delta x\right) - i_1 \cdot e^{-\gamma_1 \frac{3\Delta x}{2}} \cdot \left(1 - j\omega Z_{C1} C_{ub}(1)\Delta x\right) \cdot \left(j\omega Z_{C1} C_{ub}(2)\Delta x\right) \tag{23}$$

$$i_5 = i_1 \cdot e^{-\gamma_1 \frac{3\Delta x}{2}} \cdot \left(1 - j\omega Z_{C1} C_{ub}(1)\Delta x\right) \cdot \left(1 - j\omega Z_{C1} C_{ub}(2)\Delta x\right)$$

The summary far-end crosstalk current originating in the element $k = 2$ can be calculated:

$$i_{F2} = \frac{1}{2}\left(i_{C2} + i_{M2}\right) \cdot e^{-\gamma_2 (l - \frac{3\Delta x}{2})}$$

$$i_{F2} = \frac{1}{2} i_1 \cdot e^{-\gamma_1 \frac{3\Delta x}{2}} \cdot e^{-\gamma_2 (l - \frac{3\Delta x}{2})} \cdot \left(1 - j\omega Z_{C1} C_{ub}(1)\Delta x\right) \cdot \left( j\omega Z_{C1} C_{ub}(2)\Delta x - j\omega \frac{M_{ub}(2)\Delta x}{Z_{C2}} \right) \tag{24}$$

This current can be expressed by using general variable $k$:

$$i_{Fk} = \frac{1}{2} i_1 \cdot e^{-\gamma_1 \left(\frac{\Delta x}{2}\right) \cdot (2k-1)} \cdot e^{-\gamma_2 \left(\frac{l}{2k-1} - \frac{\Delta x}{2}\right) \cdot (2k-1)} \cdot \left(1 - j\omega Z_{C1} C_{ub}(k-1)\Delta x\right) \cdot \left( j\omega Z_{C1} C_{ub}(k)\Delta x - j\omega \frac{M_{ub}(k)\Delta x}{Z_{C2}} \right) \tag{25}$$

Based on the previous derivations it is possible to deduce the general expression of the far-end crosstalk current for general element $k$:

$$i_{Fk} = \frac{1}{2} i_1 \cdot e^{-\gamma_1 \left(\frac{\Delta x}{2}\right) \cdot (2k-1)} \cdot e^{-\gamma_2 \left(\frac{l}{2k-1} - \frac{\Delta x}{2}\right) \cdot (2k-1)} \cdot$$

$$\cdot \underbrace{\left(1 - j\omega Z_{C1} C_{ub}(1)\Delta x\right) \cdot \left(1 - j\omega Z_{C1} C_{ub}(2)\Delta x\right) \cdot \ldots \cdot \left(1 - j\omega Z_{C1} C_{ub}(k-1)\Delta x\right)}_{\text{generally } k-1 \text{ elements}} \cdot \underbrace{\left( j\omega Z_{C1} C_{ub}(k)\Delta x - j\omega \frac{M_{ub}(k)\Delta x}{Z_{C2}} \right)}_{\text{element } k} \tag{26}$$

$$i_{Fk} = \frac{1}{2} j\omega \cdot i_1 \cdot e^{-\gamma_1 \left(\frac{\Delta x}{2}\right) \cdot (2k-1)} \cdot e^{-\gamma_2 \left(\frac{l}{2k-1} - \frac{\Delta x}{2}\right) \cdot (2k-1)} \cdot \left( Z_{C1} C_{ub}(k)\Delta x - \frac{M_{ub}(k)\Delta x}{Z_{C2}} \right) \cdot \prod_{n=1}^{n=k-1} \left(1 - j\omega Z_{C1} C_{ub}(n)\Delta x\right) \tag{27}$$

The resulting far-end crosstalk current is given as a summary of all contributions expressed from (27):

$$i_{FEXT} = \sum_{k=1}^{m} i_{Fk}$$

$$i_{FEXT} = \frac{1}{2} j\omega \cdot \sum_{k=1}^{m} \left[ i_1 \cdot e^{-\gamma_1 \left(\frac{\Delta x}{2}\right) \cdot (2k-1)} \cdot e^{-\gamma_2 \left(\frac{l}{2k-1} - \frac{\Delta x}{2}\right) \cdot (2k-1)} \cdot \left( Z_{C1} C_{ub}(k)\Delta x - \frac{M_{ub}(k)\Delta x}{Z_{C2}} \right) \cdot \prod_{n=1}^{n=k-1} \left(1 - j\omega Z_{C1} C_{ub}(n)\Delta x\right) \right] \tag{28}$$

The main problem of this derivation represents the necessity of correct quantifying of capacitive and inductive unbalances and their values along the whole cable. One of the possible solutions is to divide the whole cable into isolated sub-sections and to use the cascade matrices for the calculations of the crosstalk currents. Several models of FEXT crosstalk using capacitive and inductive unbalances and their impedance matrices have been already presented, e.g. [11], or models using pseudo-randomly generated components [12], but these models are mathematically quite complex and require many parameters. Previous equation (28) represents the derivation of FEXT current in a disturbed pair. This equation could be used for an innovative FEXT model based on the simulation of capacitive and inductive unbalances between pairs in a cable. The best idea would probably be dividing the whole cable into the several sub-sections, which consist of the transmission lines, the crosstalk coupling and the bridge taps from the unused ends of both symmetrical pairs. Each section is described by its cascade matrix and the final crosstalk current is calculated by their multiplication.

## III. CONCLUSION

This paper presents several initial ideas and derivations of far-end crosstalk's dependence on capacitive and inductive unbalances between two parallel pairs in a cable. Equation (8) verifies the formula (13) for standard simple FEXT model. This standard model comes only from average crosstalk values for the whole cable and it takes into consideration only a mean value of capacitive and inductive unbalances. Therefore this simple model with only one crosstalk parameter cannot be very accurate, as was shown in [13].

Capacitive and inductive couplings can be described by the essential formulas for the net of capacitors and inductors between symmetrical pairs, quads and subgroups in a cable. It is necessary to implement functions for simulating manufacturing tolerances, inhomogeneities, deformations, etc. Several influences and parameters come also from the specific effects on internal inductivity and resistivity, effective permittivity of insulation and dielectric and important role also plays the internal structure and arrangement of a cable. It could be very complicated to express the values of capacitive and inductive unbalances mathematically. Moreover, these values are usually pseudo-random and are influenced by many internal and/or external effects. That is why a simple method by generating pseudo-random values using formulas of normal distribution and the proper statistical values could be used in the model. Resulting mathematical model for accurate FEXT simulations will be probably very complex, but will provide universal usage for various types of metallic cables and situations. The progress of its development will be presented in author's future publications and presentations. Some advances and derivations of cascade description of a cable for the purpose of FEXT modeling should be presented soon.

## ACKNOWLEDGEMENT

This work was supported by the Grant Agency of the Czech Technical University in Prague, grant No. SGS 10/275/OHK3/3T/13.

## REFERENCES

[1] Hughes, H.: Telecommunications Cables: Design, Manufacture and Installation. John Wiley&Sons Ltd., Chichester, England, June 1997. ISBN 0-471-97410-2.

[2] Rauschmayer, D., J.: ADSL/VDSL Principles: A Practice and Precise Study of Asymmetric Digital Subscriber Lines and Very High Speed Digital Subscriber Lines. Macmillian Technology Series, Indianapolis, USA, 1999. ISBN 1-57870-015-9.

[3] Starr, T., Cioffi, J. M., Silverman, P. J.: Understanding Digital Subscriber Line Technology. The Book. Prentice Hall PTR, Upper Saddle River, USA, Jan. 1999. ISBN 0-13-780545-4.

[4] Cendrillion, R., Ginis, G., Moonen, M., Acker, K.: Partial Crosstalk Precompensation in Downstream VDSL. Signal Processing 84. Elsevier (2004), pp. 2005-2019.

[5] Cendrillon, R., Ginis, G., Bogaert, E., Moonen, M.: A Near-Optimal Linear Crosstalk Canceller for VDSL. IEEE Transactions on Signal Processing. 2004.

[6] Vodrazka, J.: Multi-carrier Modulation and MIMO Principle Application on Subscriber Lines. Radioengineering, Vol. 16, No. 1, December 2007. ISSN 1210-2512.

[7] Lafata, P.: Modeling of Far-end Crosstalk in Multi-quad Cables Based on Capacitive and Inductive Unbalances Between Pairs. In TSP - 32nd International Conference on Telecommunications and Signal Processing [CD-ROM]. Budapest: Asszisztencia Szervező Kft., 2009, ISBN 978-963-06-7716-5.

[8] Schlitter, M.: Telekomunikační vedení. CTU Publishing, second release, Praha 1986. Publication number 5615.

[9] Nedev, N., H., McLaughlin, S.: Wideband Unshielded-Twisted-Pair (UTP) Cable Measurements and Modeling for Multiple-Input–Multiple-Output (MIMO) Systems. IEEE Transactions on Instrumentation and Measurement, Vol. 56, No. 6, December 2007.

[10] Chen, W., Y.: DSL: Simulation Techniques and Standards Development for Digital Subscriber Line System. Macmillan Technology Series, Indianopolis, USA, 1998. ISBN 1-57870-017-5.

[11] Clayton, R., P., McKnight, J., W.: Prediction of Crosstalk Involving Twisted Pairs of Wires-Part I: A Transmission-Line Model for Twisted-Wire Pairs. IEEE Transactions on Electromagnetic Compatibility, Vol. EMC-21, No. 2, May 1979.

[12] Cioffi, J., M., Fang, J., L.: A Temporary Model for EFM/MIMO Cable Characterization. IEEE 802.3 Standards Contribution, Los Angeles, CA, October 2001.

[13] Lafata, P., Vodrazka, J.: Simulations and Statistical Evaluations of FEXT Crosstalk in xDSL Systems Using Metallic Cable Constructional Arrangement. TSP - 31st International Conference Telecommunications and Signal Processing [CD-ROM]. Budapest: Asszisztencia Szervező Kft., 2008, ISBN 978-963-06-5487-6.

# Modeling of Aluminum Power Cables Network Containing Cascaded Taps

Jiří Vodrážka, Jaromír Hrad
Czech Technical University in Prague
Faculty of Electrical Engineering, Dept. of Telecommunication Engineering
Technická 2, Praha 6, Czech Republic
vodrazka@fel.cvut.cz, hrad@fel.cvut.cz

***Abstract*—This paper is dedicated to modeling of a power line network for applications of indoor high-speed data transmission. ZVRE network analyzer has been used for measurement of line parameters. We have defined models for specific types of power distribution cables with aluminum cores that have been used in older prefabricated apartment buildings. The model of the entire network uses the theory of line modeling with a cascade of several sections containing multiple taps.**

***Keywords-power line communication; high-speed transmission; modeling; topology inhomogeneities; bridged taps***

## I. INTRODUCTION

Many different technologies for data transmission are in use today for metallic or optical lines, as well as for radio or optical transmission over free space. This article deals with data transmission over power distribution lines known as PLC (Power Line Communication) or BPL (Broadband Power Line), which is not so common. The basic principle consists in transmission of digital signals in higher frequency band (from several hundreds of kHz up to approximately 36 MHz) using a multi-state modulation [2], [3], [4].

Among the advantages of PLC technology we can find the possibility to use the existing transmission media, the primary purpose of which, however, is not data transmission. Therefore this fact introduces also some disadvantages, including strong inhomogeneities of the line, electromagnetic emissions and the associated interference with other systems using the same frequency band. That is why much standardization effort in this area is paid to electromagnetic compatibility of PLC with other systems.

## II. MODEL OF THE TRANSMISSION ENVIRONMENT

Power line cables are designed to deliver electrical energy, but not high-frequency signals. Transmission parameters of this medium are not stable [6], [7]. When used for high-speed data transmission, the lines show inhomogeneities in the frequency band of units to tens of MHz. These inhomogeneities cause ripples in the attenuation characteristic and specific attenuation, and also substantial dissipation of energy into the ambient environment.

To approximate the measured specific attenuation values for the specific line in [dB.km$^{-1}$], we can use the modified function:

$$\alpha(f) = k_0 + k_1\sqrt{f} + k_2 f \tag{1}$$

that is, compared to the elementary model of a homogeneous line, supplemented with the linear term $k_2$ and the constant $k_0$. We can use linear approximation to describe the specific phase shift in [rad.km$^{-1}$]:

$$\beta(f) = b \cdot f \tag{2}$$

The characteristic impedance is real for high frequencies and its limit value is (3), but its actual curve is rippled as a result of reflections on the line (see Fig. 1).

$$Z_c = z \tag{3}$$

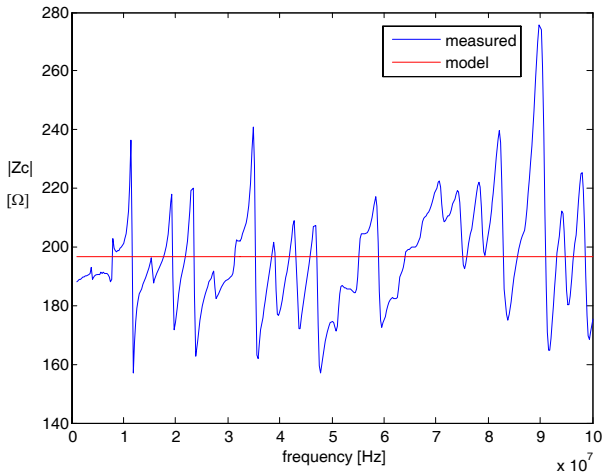


Figure 1. Absolute value of characteristic impedance, flat AYKY cable, 4 mm$^2$

TABLE I. PARAMETERS OF A MODEL FOR SECONDARY PARAMETERS

| Flat AYKY cable | | | |
|---|---|---|---|
| cross-section [mm$^2$] | | 2.5 | 4 |
| length [m] | | 20 | 14.5 |
| $\alpha(f)$ | $k_0$ | [illegible] | [illegible] |
| | $k_1$ | [illegible] | [illegible] |
| | $k_2$ | [illegible]-[illegible] | [illegible]-[illegible] |
| $\beta(f)$ | $b$ | [illegible]-[illegible] | [illegible]-[illegible] |
| $Z_c$ | $z$ | [illegible] | [illegible] |

In addition to inhomogeneities we can observe also other influences [1], such as parallel sections (taps) of power distribution lines, as well as other elements (circuit breakers, residual current devices, etc.).

The transmission function of a power distribution line may then be understood as that of an environment with multiple propagation paths. Measurements and modeling have proven that models of secondary parameters perform better than those of primary parameters for telecommunication lines [2].

The specific model has been designed for two flat cables AYKY having the cross-section of 4 mm$^2$ and 2.5 mm$^2$, respectively (see Table 1).

The attenuation reaches higher values than for copper cables, and the 100-ohm termination results in impedance mismatch.

## III. MODELING OF A LINE WITH CASCADED TAPS

The topology of local power distribution networks is similar to that of subscriber lines in access networks with metallic cables. They contain open-ended parallel sections (taps) that influence negatively their transmission parameters, limiting the achievable transmission speed.

At the point of branching, the signal propagating from the transmitter is split into two components. One portion of the signal passes through the tap, then it is reflected at the end, and at the branching point it is added to the signal on the main line.

For modeling of attenuation in a line composed of several sections with different parameters containing taps we use multiplication of matrixes representing the individual sections. A section of length $l_i$ may be described by matrix (4).

$$\begin{bmatrix} \cosh(\gamma_i(f)\cdot l_i) & Z_{Ci}(f)\cdot\sinh(\gamma_i(f)\cdot l_i) \\ \dfrac{\sinh(\gamma_i(f)\cdot l_i)}{Z_{Ci}(f)} & \cosh(\gamma_i(f)\cdot l_i) \end{bmatrix} \tag{4}$$

With respect to the properties of the model network it will be necessary to define matrix (5) representing an impedance connected in parallel (in shunt) with the input/output poles.

$$A=\begin{bmatrix} 1 & 0 \\ \dfrac{1}{Z} & 1 \end{bmatrix} \tag{5}$$

With respect to the input impedance of the tap and matrix (5), the matrix describing an open-ended tap of length $l_j$ will be defined as follows (6):

$$A_j=\begin{bmatrix} 1 & 0 \\ \dfrac{1}{Z_{Cj}(f)\cdot\coth(\gamma_j(f)\cdot l_j)} & 1 \end{bmatrix} \tag{6}$$

The resulting matrix representing the whole cascade of $n$ elements will be (7):

$$A=A_1\cdot A_2\cdot\ldots\cdot A_n=\begin{bmatrix} a(f) & b(f) \\ c(f) & d(f) \end{bmatrix} \tag{7}$$

Attenuation characteristic of the whole cascade will be inferred from matrix (7) – see formula (8), where $Z_n$ stands for impedance of signal generator and $Z_z$ for load impedance (i.e., terminating impedance of the line).

$$A(f)=20\cdot\log\left|\frac{a(f)\cdot Z_z+b(f)+Z_n\cdot(c(f)\cdot Z_z+d(f))}{Z_n+Z_z}\right| \tag{8}$$

The part of local power distribution network in a prefabricated apartment, which was chosen for modeling, has too many branches, and therefore it was necessary to simplify it, as shown in Fig. 2.

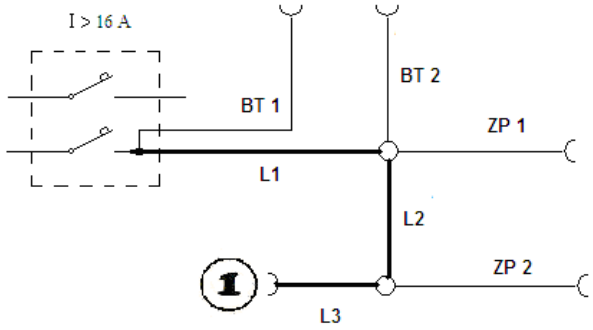


Figure 2. Simplified network diagram

There are 3 plain sections (L1, L2, L3), the properties of which are given by (4), then two simple open-ended taps BT 1 and BT 2 corresponding to matrix (6), and finally two compound open-ended taps ZP 1 and ZP 2, for which we have to determine their input impedance [7] at the branching point – see (9); then we can handle them as taps connected in parallel (5) for further considerations.

$$Z_{ZPi}(f)=\lim_{Z\to\infty}\frac{a(f)\cdot Z+b(f)}{c(f)\cdot Z+d(f)}=\frac{a(f)}{c(f)} \tag{9}$$

where *a(f)* and *c(f)* are the resulting elements from matrix (7) for the given compound tap ZP i (there is one matrix for each section of the line).

For the network presented in Fig. 2 we have to determine the input impedances for the compound taps ZP 1 and ZP 2. For example, in the case of ZP 1, as we can see in Fig. 3 and Fig. 4, the main path is composed of sections 1, 3, 5 and 7, for which we can use matrix (4); for sections 2, 4 and 6, on the other hand, we will use matrix (6).

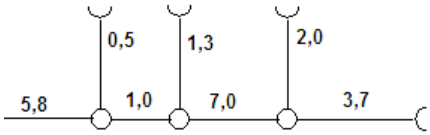


Figure 3. Compound tap ZP 1 with section lengths in [m]

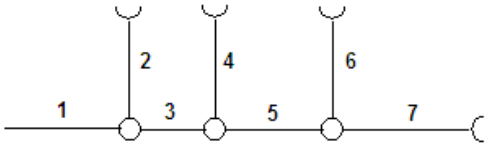


Figure 4. ZP 1 with marked sections

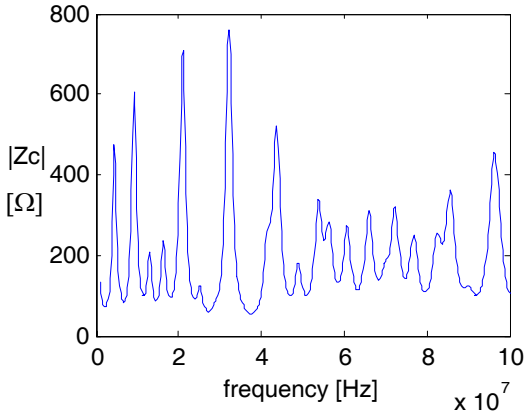


Figure 5. Absolute value of the input impedance for ZP 1

If, for example, section 6 would be longer than section 7, then the main path would be 1, 3, 5 and 6. After performing the multiplication (7) we get the elements *a(f)* and *c(f)* needed for calculation of the impedance according to (9). Subsequently, the calculated impedance can be put to matrix (5). We can apply the same procedure in the case of ZP 2 or any other one.

The curves of input impedances for ZP 1 and ZP 2 are illustrated in Fig. 5 and Fig. 6.

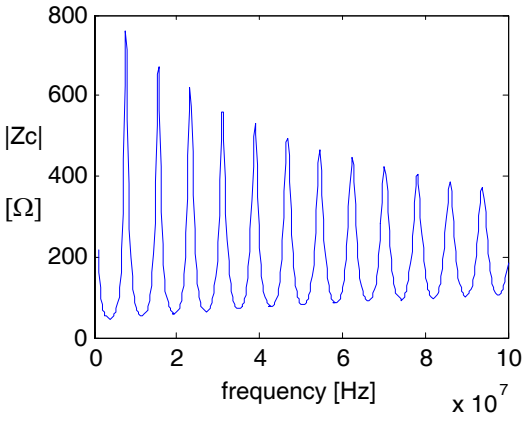


Figure 6. Absolute value of the input impedance for ZP 2

Modeling results for the whole cascade according to Fig. 2 are presented in Fig. 7. The displayed values refer to flat AYKY cable having the cross-section of 4 mm$^2$.

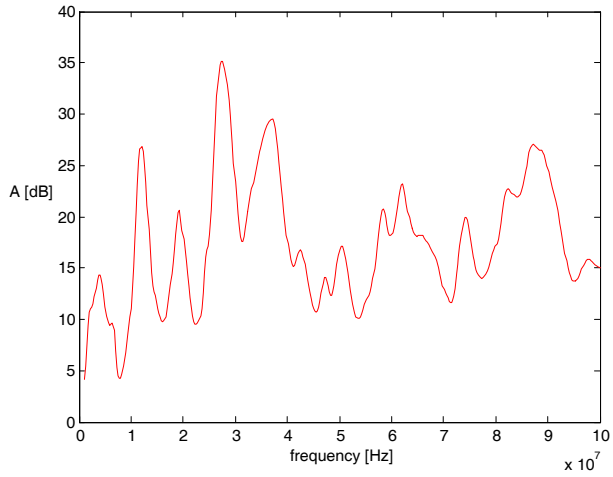


Figure 7. Attenuation of the modelled network (entire cascade)

## IV. Conclusion

Within the research presented hereinabove we have proposed a suitable configuration of a model network for PLC testing, inspired by a distribution network for electrical outlets in a prefabricated apartment. Since the primary parameters of the used cable (fat AYKY) were not available, it was necessary to perform the appropriate measurements. The measured values have been used to design models for the corresponding parameters, such as characteristic impedance and transmission function. Network analyzer Rohde&Schwarz ZVRE was used to measure the secondary parameters. The computed models of secondary parameters are applicable in subsequent work and/or simulations, including estimations of PLC throughput (transmission capacity).

## ACKNOWLEDGMENT

This paper has originated thanks to the support from the Czech Ministry of Education grant No. MSM6840770014.

## REFERENCES

[1] J. Vodrazka, "Modeling of low-voltage cable power parameters", Access server, on-line: http://access.feld.cvut.cz/view.php?cisloclanku=2006012901

[2] P. Vancata, „Standardization of Powerline Communication technology", Access server, on-line: http://access.feld.cvut.cz/view.php&cisloclanku=2005112801

[3] HomePlug Powerline Alliance – White papers on-line http://www.homeplug.org/tech/whitepapers/

[4] OPERA project, on-line: http://www.ist-opera.org

[5] T. Prokop, J. Vodrazka, "Modeling of transmission lines for digital subscriber lines". 15th International Conference on Systems, Signals and Image Processing, IWSSIP 2008. Bratislava, Pages: 53-56, Published: 2008.

[6] H. Hrasnica, "Broadband Powerline Communications Network". John Wiley & Sons, Chichester 2004. ISBN 0-470-85741-2

[7] S. Galli, T. Banwell, "A Novel Approach to the Modeling of the Indoor Power Line Channel—Part II: Transfer Function and Its Properties", IEEE Trans. on power delivery, vol. 20, no. 3, July 2005

# The use of simulation framework OMNeT++ in telecommunications

Petr Chlumsky, Zbynek Kocur, Jiri Vodrazka
Department of Telecommunication
Engineering
Faculty of Electrical Engineering
Czech Technical University in Prague
Prague, Czech Republic
chlumpet@fel.cvut.cz, kocur1@fel.cvut.cz, vodrazka@fel.cvut.cz

***Abstract*—Simulation has ability to determine the system behavior without being put into operation, even without costly and time consuming production. Especially in the field of telecommunications, where it is often demanded to handle a huge number of messages or terminals, the possibility to test the system before the real deployment is strictly appropriate. Simulation framework OMNeT++ provides very good resources for fast design such as large-scale models. For example, the hierarchical approach to model, scalability, aptitude of detailed analysis and a large database of pre-built models of protocols.**

***Keyword* - simulation; OMNeT++; telecommunication;**

## I. Introduction

There is very rapid development of new technologies and services in the field of telecommunications technology therefore an efficient use of time and money is needed. New system has to be properly tested before its deployment in a real environment, which could be a problem for example because of adequate load. Simulation tools are very good helper in this case, they allow to create a model corresponding to the real application with a diverse range of requirements. To build a sufficiently accurate model is needed to implement the actual function of the system parameters that define it, and also to consider other factors that may affect its operation. These factors should be also incorporated into the model. Behind each simulation is actually a mathematical foundation, which describes the physical nature of the problem. The type of simulation tool depends only on the level of model abstraction.

Simulation environment should offer fast development of such models by its own tools, model testing in various configurations and evaluation of given design. One of the frequently used simulation tools is OMNeT++, which fully meets these requirements and which even more eases development of models by its other properties, especially in the area of network simulation.

In the introductory article discusses the simulation in general, their benefits, but also disadvantages. Furthermore, the paper is focused on the area of telecommunication technology and presents an overview of selected, frequently used, network simulation tools.

## II. Benefits of simulation

Simulation allows the analysis of a system's capabilities, capacities, and behavior without requiring the construction of or experimentation with the real system [1]. When searching for an optimal configuration, it would be very costly to produce real-time system for each of the proposed alternatives. Through the simulation, it is possible to detect errors in the design early and localize them due to the ability to run the simulation at the accurately same conditions in each experiment which is very difficult in real practice. Gained knowledge can be used to build the final system and significantly cut costs associated with production. Simulated system can be decomposed into the smallest details and gives the opportunity to clearly move on from the simple to complex units, including the visualization option of them. Also there is no problem to determine the behavior of the boundary conditions that would otherwise be difficult to achieve, or could result in the destruction of the system, or even compromise human health. Another important advantage is to obtain the data from the testing of the appropriate model, because it is not necessary to be limited by availability of measuring devices or feasibility of the measurement during the data acquiring. Likewise, the simulation time can be completely controlled therefore otherwise; the data from model, which is difficult to access, could be obtained.

The results of the model are expected to confirm or refute the hypothesis. We can obtain outcomes from the simulation which are either numeric values as the data set of selected parameters (number of lost packets, frequency of collisions) or the simulation itself in the form of the recording of the entire simulation as a sequence of events and outcomes of individual entity. Possibility of suspending the running simulation and examine the current state of the simulation and the output of the module is useful, as well as the possibility of observing changes in the simulation step. Numeric values are stored in the scalar and vector (where each value is assigned by time stamp) data sets, which can be also displayed in the form of a chart or histogram.

Some frameworks provide their own tools for working with

data from simulations, bringing them together according to certain criteria and plotting the graph. Capacity of export to the format that offers extensive analysis and data visualization, such as MATLAB, Octave, Wireshark or Excel is also desired.

Fields of application of simulations are extensive, including telecommunications and computer networks, transportation networks, air systems, design of integrated circuits, natural sciences, medicine, construction, automation, modeling, economics and social relations. Simulations have its own place in education too because of their very effective illustrative features, they are fast, cheap to deploy and have an ability to influence any parameter regardless of the consequences.

However, the simulation is not always the solution, system that can be tested faster and cheaper in real world is useless to simulate. With increasing model complexity grows demands on computing power, on the other hand, the simplification of the model may lead to neglect too many parameters and thus to lower the value of the model quality. The models can not be used as the only solution; the simulation can not fully replace the real system as in some cases it is not possible to encompass all the factors involved in the real situation.

### *A. Simulation in telecommunications*

Many clients, terminals or data flows to be served perform the typical case in the telecommunication sector. Testing new systems and services, which is necessary to obtain optimal parameters, is therefore expensive and in many cases practically unfeasible. Simulation of the system is often the only way to ensure smooth deployment of the system into operation. For simulations in telecommunications, it is essential the modeling of network topology, transmission technology, simulating the function of various protocols or queuing systems. The simulation is typically well done used in the area of the research of the voice transmission via data network where a huge number of factors enters into the resulting quality of the transmitted call [2].

## III. Simulation tools

The basic way how to test a system is through reflection, pencil and paper. This approach, however, quickly loses its effectiveness and feasibility with increasing intensity of the modeled problem. There is a lot of hardware and software products that deal with this matter, they offer a platform for actual design of model. Hardware simulators are usually more specialized in a particular area compared with software tools, which is obvious due to their less flexible implementations. Their main advantage is speed and greater proximity to the real system. The downside is certainly the limitations of the model design, its size, range of available parameters and their limits, which are given by the hardware solution. Software tools offer the possibility to build a detailed model of a single element, as well as a model system with a large number of elements or services offered. Their limitation is often high computational complexity. Some issues, that may arise, could be neglected in the software simulators, such as the influence of electromagnetic interference. These simulators can be divided according to the behavior to continuous and discrete. The continuous simulator performs change of variable continuously by time variable function, discrete platform makes changes immediately at the time of the event. Currently, there is a number of simulation tools suitable for the area of telecommunications technology. Some of them are more specialized; others can be successfully used for solving a wide range of problems. Choosing the appropriate instrument hence rely mainly on the specific needs of the user. However, there are some general features that every simulation software should contain (according to [3]):

- Flexibility - not every model can be built from already prepared elements, which are, for example, part of a package for the system environment. Framework should allow creating new entities like a network nodes, links, messages or protocols.
- Modesty of the model creation - major part of the simulation should be results of the simulation, not its creation, hence the need for a rapid design to preserve as much time on analysis of the result as possible. Hierarchical approach to model creation is suitable for fast model creation, complex designs can be built from the basic elements. This is related to the possibility of reuse of already existing elements. Model parameters should be fast and easy to access, just like an option to run a whole batch of tests in which selected parameters changes automatically. As mentioned before, it is important to have an option to create models with huge number of clients; therefore simulation environment must be computional and memory-effective. Also good debugging skills of the framework are beneficial when the model is being created. Quick understanding of occurring phenomena often facilitates the visualization of simulation in the form of animation events which occurs among model elements or even within one node.
- Prearrange entities - availability of complete components for simulation fundamentally reduces the time required to create the desired model, it can be built-in modules (router model, PPP interface, propagation models) or the whole package covering an area of interest (wireless, IPv6, and so on).
- User support - every environment has its own specifics, thus a comprehensive installation and a user manual are necessary. For built-in modules or packages of models is fundamental an access to detailed documentation. Producer web site should provide the answers to frequently asked questions, sample tutorials, regular updating of the environment, contact to the technical support and links to projects dealing with the creation of models for the environment and links to mailing lists of the user community. Organization of conferences, seminars and publication of newsletters are also useful.
- Comprehensible outputs - simulation environment should allow associating of the selected data set and apply statistical functions, estimates, percentiles, confidence intervals

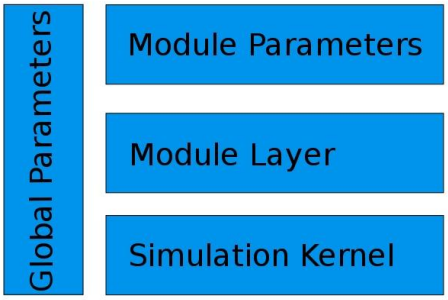


Figure 1. Architecture of network simulators

and basic mathematical operations on these groups. It should be able to plot the obtained data into different types of graphs (histogram, time series) and also to store data in a format acceptable for export to other tools suitable for analysis and visualization.

Although there are many differences between simulation tools, their architecture is similar. Its layers are shown in Figure 1. The lowest layer consists of simulation kernel, which provides a base class for running a simulation in which the user normally does not intervene. In the higher layer, the models of protocols, propagations, generally, the building blocks of desired model are already included. The highest layer covers the model variables, parameters of its elements. As the model can be affected by module parameters, the whole simulation can be changed by the global parameters.

### *A. A brief overview of commonly used software simulation tools in the field of telecommunications*

One of the most popular network simulator is NS-2 [4]. It is based on the processing of the discrete event models and provides many models of network protocols, including routing support, ad-hoc and wireless networks. The actual behavior of model components uses C++ language. For network topology, configuration and simulation control use OTcl scripts. So-called Network Animator (Nam) is a Tcl/TK based animation tool for viewing network simulation traces and real world packet traces. It supports topology layout, packet level animation, and various data inspection tools [5]. NS-2 is distributed as open source, it has a rich documentation and a large community of users.

J-Sim, formerly known as JavaSim, is an open-source framework programmed in Java, making it platform independent. Creating simulations it is, as in NS-2, in two languages. Basic, functional classes are entered in Java and configuration of network in Tcl-Java language. To develop network models can be used for example the INET package, but more specialized packages are available too [6]. Development of J-Sim seems to be suspended since 2006.

NS-3 [7] is the direct successor of NS-2, still is an open-source discrete-event network simulator but its interface is redesigned from the ground, hence is not backwards compatible. The kernel is modular, written in C++ language, models are written only in C++ (unlike NS-2 that used OTcl) or in Python. NS-3 is trying to work with real systems, such as sockets or device driver interfaces. It is designed for integration into virtual machines and testbeds.

OPNET Modeler is a part of products that support the entire life cycle of enterprise network management [8]. It is a software environment for design and analysis of communication networks. It is a commercial product, but is free for qualifying universities. It is hierarchical and object-oriented and offers a clear graphical interface that allows easy design and analysis of results. OPNET Modeler contains a very large database of network protocols based on C language. Source code of the simulation kernel is not available to users.

OMNeT++ [9] is an environment for creating hierarchically structured models of any system that can be described by discrete events. It offers interface based on Eclipse to the convenient user, graphical display and simulation tools for analyzing simulation results. Many packages with already completed models of protocols or network nodes are available. Notation of functional elements in the environment are carried out using C++, description of network topology is using the NED language (NEtwork Description). However, there are also extensions that allow the use of Java and C#. It is free for academic use; its commercial variant is called OMNEST.

MATALB Simulink despite massive popularity it has no support for simulation of networks [10]. But at least, it is used in conjunction with network simulators [11].

## IV. OMNeT++ FRAMEWORK

OMNeT++ as mentioned above, it is a development environment that enables the design of simulations for a wide range of areas. It can simulate any system whose functions are writable by discrete events, which can be decomposed into elements, along with communicating messages. Due to the hierarchical structure (illustrated in Figure 2) and the use of object-oriented approach designed simulations are very well scalable and limited only by computer performance on which the simulations runs. Creating simulations is very comfortable in this environment because of the graphical interface, leading to an easy and clear writing, and also the number of available libraries of ready models, for example wireless, sensors and ad-hoc networks, IPv4 and IPv6 networks, storage area and optical networks, MPLS, queuing networks, high-speed interconnections (InfiniBand) and others [12]. The basic element of simulations created in OMNeT++ framework is the creation of so-called simple modules. Their task is to carry out required functions and to form the core of the simulated system. Simple modules are entered in C++ language using simulation class library. These elements can communicate using messages that may represent frames or customers of service system. Messages may be generally very complex structures with many definable attributes. They are formed as a basic library class specialization. Messages are sent between modules either directly or more often through the gates. Gates realize input-output interface of modules and their interconnection is formed by the connection. It is possible to define various parameters

such as delay or error rate for each connection. Interconnected simple modules can be combined into compound modules, which can be further combine to create more complicated parts.

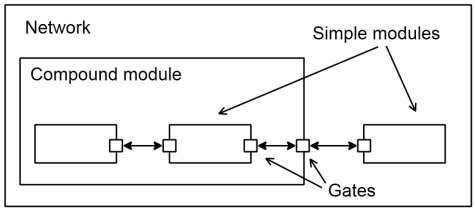


Figure 2. Hierarchical structure

The number of such nesting is not limited [13]. Individual modules, whether simple or complex, can be also used within other simulations. Interconnection of modules, namely the topology of simulated system is described in the NED language, which exhibit is at Figure 3. One can also easily write module parameters in NED and thus affect their behavior. The simulation environment provides entering of parameters as a numeric value, logical value, text, or XML structure. Parameters can be defined using different types of distribution too, or use the value entered by the user during the simulation.

```
network Example
{    submodules:
        Router: WirelessAP {
            parameters:
                routingFile = "AP.rt";
                mgmtType = default("Ieee80211MgmtAP");
                @display("p=135,119;i=device/accesspoint");
            gates:
                inout ethg[3];
                inout pppg[1];}
        MobileClient: CellPhone{
            parameters:
                numTcpApps = 1;
                tcpAppType="TCPEchoApp"}
        Client: WirelessHost {
            parameters:
                int numTcpApps = 1;
                tcpAppType="TCPSinkApp"
            gates:
                inout pppg[1];}
        Source: StandardHost {
            parameters:
                routingFile = "source.rt";
                int numTcpApps = 2;
                tcpAppType="TCPEchoApp"}
    connections:
        Client.pppg[0] <--> {datarate=100Mbps;} <--> Router.pppg[0];
        Router.ethg[0] <--> {delay=2ms;} <--> MobileClient.ethg[0];
        Router.ethg[1] <--> Source.ethg[0];}
```

Figure 3. An example of network topology in the NED language

Design simulation structure in OMNeT++ is facilitated by the possibility to use graphical interface, which already uses NED language for entry. Notation is possible both in the language of the NED and by visual editing, it possible to switch freely between these modes. Demonstration of visual editing mode is in the Figure 4.

The parameters of different runs of the same simulation can be configured in a shared ini file, which allows batch of different simulations to be run at once. An essential part of simulations is their evaluation and analysis. OMNeT++

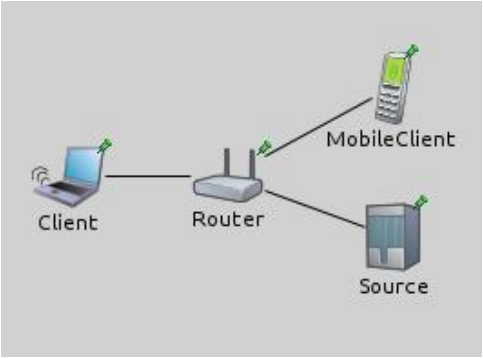


Figure 4. Sample graphic design model

provides tools that enable easy debugging of simulations, including the slowdown or complete suspension. This is possible through the implementation of the user interface Tkenv that provides tools to explore the simulation output of any object, to pass all the events in the system and clear animation of the entire simulation. Results of simulation are stored in scalar and vector data sets at the end of the simulation. For the consequent analysis and visualization the OMNeT++ framework has the Analysis Tool, which allows to compare data from different simulation runs, to clearly sort data and finally, to visualize them using graphs. For a precise analysis during the simulation exists in OMNeT++ tool EventLog. It allows, in addition, passing the detailed text, listing all the events for each module in the simulation, displaying them in the form of sequence chart. Such a view is very clear and allows thorough exploration of linkages and dependencies of simulated system. Simulation results can be also exported to a CSV file, Octave and MATLAB and thus enable more thorough analysis.

## V. Conclusion

As indicated in the article, simulations are a necessary tool in the field of telecommunications research. Many activities, that would be very hard to implement in real world, are feasible through the simulations. The paper discusses the basic structure of simulation tools and their principles that they describing the behavior of real systems. In addition, common simulation environments applicable in telecommunications are described. The end of article is devoted to demonstration of usage of simulation tools, especially on the OMNeT++ framework.

Thanks to OMNeT++ framework was successfully realized simulation of wireless communication between an aerobatic plane and a ground station. The goal was to optimize this wireless connection for increasing the throughput and resistibility of the wireless channel [14].

## Acknowledgment

This work was supported by grant MSMT: MSM6840770014.

## REFERENCES


[1] A. Law and W. Kelton, *Simulation Modeling and Analysis*. New York: McGraw Hill, 1991

[2] M. Voznak and F. Rezac and M. Halás, *Speech Quality Evaluation in IPsec Environment*, p. 49-53, In Proceedings of the 12th Inter. Conference on Networking, VLSI and Signal Processing - ICNVS 2010, University of Cambridge, ISBN 978-960-474-162- 5, ISSN 1790-5117, Cambridge, February 20-22,2010

[3] A. Law and M.G. McComas, *Simulation software for communications networks: the state of the art*, Communications Magazine, IEEE , vol.32, no.3, pp.44-50, 1994

[4] NS-2 home page, http://www.isi.edu/nsnam/ns/ [accessed on November 2010]

[5] Nam home page, http://www.isi.edu/nsnam/nam/ [accessed on November 2010]

[6] A. Sobeih, J.C. Hou, Lu-Chuan Kung, Ning Li, Honghai Zhang, Wei-Peng Chen, Hung-Ying Tyan and Hyuk Lim, *J-Sim: a simulation and emulation environment for wireless sensor networks*, Wireless Communications, IEEE , vol.13, no.4, pp.104-119, 2006

[7] NS-3 Reference Manual, version ns-3-dev 20 August 2010, http://www.nsnam.org/docs/release/manual.pdf

[8] OPNET home page, http://www.opnet.com/, [accessed on November 2010]

[9] OMNeT++ framework home page, http://www.omnetpp.org/, [accessed on November 2010]

[10] D. Henriksson, *Flexible Scheduling Methods and Tools for RealTime Control Systems*, Licentiate Thesis, 2003

[11] M.S. Hasan and H. Yu and A. Carrington and T.C. Yang, *Co-simulation of wireless networked control systems over mobile ad hoc network using SIMULINK and OPNET*, Communications journal, IET, 2009

[12] A. Varga and R. Hornig, *An overview of the OMNeT++ simulation environment*, 2008

[13] A. Varga, *OMNeT++ User Manual*, Version 4.0, 2010, http://www.omnetpp.org/doc/omnetpp40/Manual.pdf

[14] P. Chlumský, *Optimalizace chování bezdrátových datových protokolů pro mobilní aplikace*, Diploma Thesis, 2010

# Software Architectures for High Available Telecommunication Service Platforms

Jiri Hlavacek, Robert Bestak
Department of Telecommunication Engineering
Czech Technical University in Prague,
Prague, Czech Republic
hlavaj1@fel.cvut.cz, bestar1@fel.cvut.cz

***Abstract*—Today's mobile networks are built on IP and SIP technologies. Use of these technologies brings cost savings, but the reliability level usual for telecommunication systems can't be reached without use of availability specific configurations. This paper focuses on software implementation of telecommunication services using SIP. Three different types of applications are investigated: standalone SIP servers, stateless applications controlling SIP servers and stateful control applications. Requirements on context replication are identified for each type of application. Different software solutions improving the availability using context replication are analyzed. Comparison of these architectures is provided and their suitability for different application types is discussed.**

***Availability; context replication; software architecture; service development platforms; SIP***

## I. INTRODUCTION

One of the most important VoIP system's advantages is the ease of value-added services development. Many different development platforms are proposed, whether commercial or open source. As the use of VoIP systems grows, the availability is being more and more focused by users. First step is the adaptation of network architecture to the high availability requirements. Second one is the introduction of high availability principles in software implementations. In this paper we compare possibilities proposed by different frameworks and platforms with regard to the availability and the context replication. The focus is on development of value-added services. Although principles presented by this paper are protocol independent, software solutions discussed are working with the Session Initiation Protocol (SIP) [1].

The rest of paper is organised as follows. Section II introduces SIP based networks elements and functions. Section III describes different software architectures used for development of telecommunication services from the failover complexity perspective. Different methods of context replication implementation are presented by the section IV. Finally, section V presents our conclusions.

*This research work was supported by grant of Czech Ministry of Education, Youth and Sports No. MSM6840770014.*

## II. ARCHITECTURE OF SIP BASED NETWORKS

The SIP is a transaction based protocol for establishment and control of multimedia sessions. Basic elements of SIP networks are SIP terminals, registrar servers, proxy servers and redirect servers. The role of registrar server is to maintain associations between terminals and user's identification. Requests and responses are processed and routed by proxy servers. Redirect servers can reroute the request when needed, i.e. when a user redirects all calls to the voicemail service. The SIP standard defines two types of SIP entities processing call signalization: Proxy and Back-to-back user agent (B2BUA). The proxy can be stateless, transaction stateful or call stateful, whereas the B2BUA is always transaction and call stateful. Definition of the SIP proxy doesn't allow implementation of new services modifying standardized request processing. The term SIP server used in this paper refers to a B2BUA which can propose a call control Application Programming Interface (API).

In order to get a high available VoIP system it's necessary to use redundant network architecture and redundant SIP elements. Redundancy of stateless proxies is relatively simple to implement. All what's needed is a backup proxy and an IP takeover mechanism or an intelligent load balancer. General overview of the problem and some solutions for high availability network configuration are described for example in [2]. Stateful proxies can't be replaced without replication of contexts. Otherwise, calls can be lost. A solution for context replication needs to be found. Context replication is resources exigent, the choice of appropriated architecture is therefore important for overall system performance.

## III. ANALYSE OF APPLICATION ARCHITECTURES

One of software architecture's aims is modularity. In the telecom world it means, among others, to be network and protocol independent. Applications implementing value-added services usually use a high level service API. This kind of API is usually proposed by service development platforms, IPBX and by controllable SIP B2BUA.

There are two different levels of network abstraction: i) abstraction of protocol (stack) and ii) abstraction of service (session control). The former one is more suitable for half-call based applications like B2BUA whereas the latter one for high level services like call controller. Half-call based applications

needs to be stateful, whether call-control applications usually not.

The complexity of context replication implementation depends on the architecture of considered application. We identified three types of application depending on the level of interaction with the SIP server and the application complexity:

- Standalone SIP servers.
- Stateless applications controlling SIP servers.
- Stateful applications controlling SIP servers.

These types are depicted in Fig. 1. Next paragraphs describe each type in more details.

### A. *Standalone SIP Servers*

SIP servers without any control application can ensure transformation of calling and called numbers, topology hiding or protocol rectification. This type of application can also be used for routing purposes.

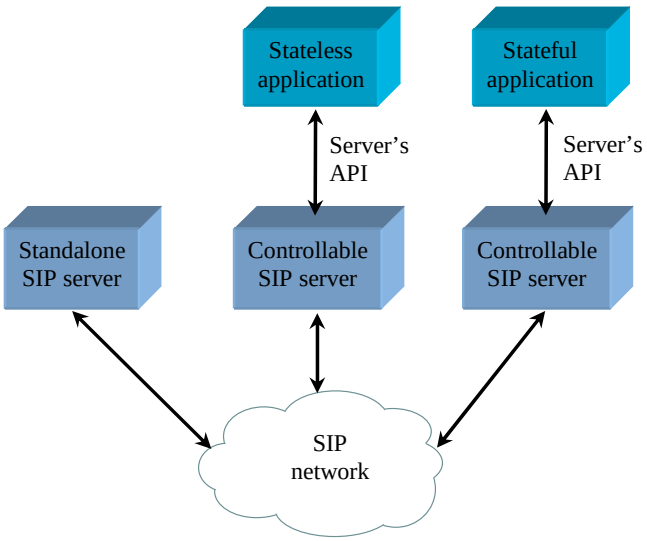


Figure 1: Application types

### B. *Stateless Applications Controlling SIP Servers*

In this case there's an application controlling the server behaviour via server's API. This application can interact with external data sources but it stays transaction and call stateless. Context's management is ensured by SIP server. An example of such application can be a policy enforcement application accepting or refusing calls in function of external directory or an implementation of applicative routing.

### C. *Stateful Applications Controlling SIP Servers*

This type of application is the most complex one. In the perfect world the SIP server should store only transaction context and the call context should be known just by application. Otherwise there's a risk of desynchronization between the server and the application and therefore a risk of memory leaks and other problems. As most servers manage calls, they store call contexts. Application is duplicating these contexts.

## IV. Facilities Proposed by Different Frameworks

In this paragraph properties of different software failover and replication solutions are analysed. Feasibility for each application type is discussed.

### A. *SIP Server*

SIP server can operate as standalone or it can be part of application. The SIP stack and logic of application servers can be seen as a specific case of SIP server. SIP implementations in application server usually use application server's replication mechanism (for more details see IV.D). Standalone SIP servers such as open source Asterisk IPBX [3] are focused on enriching the list of proposed services. High availability problems and particularly context replication becomes available just recently. The maturity of these solutions doesn't reach the maturity of application servers. SIP servers are normally used without any modifications. This paper focuses on user application development. SIP servers are considered as support functions and therefore they are not analysed in more details by the paper.

### B. *Application Level*

It's possible to implement a replication mechanism directly by application. The main difficulty is that contexts need to be replicated also in the network abstraction layer (e.g. in the IPBX). Synchronisation of these two entities needs to be ensured. There are many problems with this kind of developments. When replicating context independently to the application, it's hard to ensure synchronisation. The synchronisation is reliable if the replication is completely done at the application level and afterwards the application asks the IPBX to recreate contexts. The problem of such a solution is a low performance and complex API. An API that makes possible to create contexts in IPBX or SIP server in general is rare and therefore it is not as reliable as the standard ones. This solution is tricky and should be used only when there's no other choice. The advantage is that the whole process is completely mastered.

### C. *Clustering Using a Specific Framework*

The replication process can be ensured by more or less intrusive clustering software. An example of such a framework is a project called Terracotta Ehcache [4]. Terracotta Ehcache project is a Java Virtual Machine (JVM) level clustering solution based on dynamic bytecode modification techniques inserting replication functions at runtime. The configuration of replication data and method can be done using either XML files or Java annotations. This solution is efficient due to JVM level implementation. There's no impact on code itself as long as the code respect some base rules such as thread safe etc. This kind of framework focuses on performance and reliability aspects. Replication performances like throughput and latency are therefore usually better than the application server's one (see next paragraph). The disadvantage is that the implementation of the replication needs to be completely understood to find the right configuration for each application.

### D. *Application Server*

Application servers like the open source JBoss [5] or the commercial IBM WebSphere AS [6] integrate replication mechanisms. Both, SIP protocol contexts and application data can be replicated. An analysis of IBM WebSphere application server cluster availability can be found in [7]. A detailed availability model including hardware and software components is given and some numerical results are presented. Replication mechanisms are usually hidden to the application but for example the API of JBoss Cache [8] is documented and accessible to the developer. An example of application server based telecommunication platform is an open source project Mobicents [9]. The high availability support was integrated into Mobicents recently; it's based on services proposed by Jboss like Jboss Cache.

### E. *Network Level*

An interesting replication approach represents usage of load balancer at the network level. When using a load balancer based replication, all signalling messages are sent to all cluster nodes. Each node operates without knowledge of the other nodes. An external logic selects among them one active node.

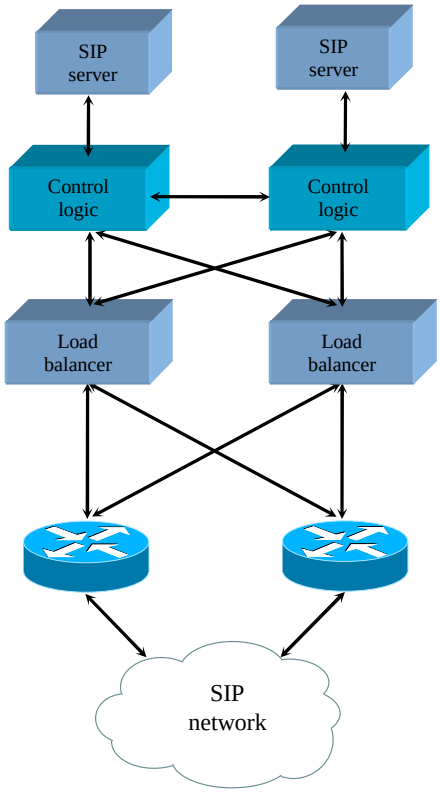


Figure 2: Network level replication implementation

Only the active node sends messages to the network, messages coming from other nodes are discarded by the external logic. This imposes some specific software solution, but the impact on performance is minimal. Specific components supervising the active node and discarding responses from the passive nodes need to be developed. The principle is shown in Fig. 2.

In order to eliminate single points of failure, all entities and network connections are redundant. More details concerning this type of solution can be found for example in [10] or [11].

The implementation of such solution is quite simple comparing with the other ones. It's an efficient and straightforward solution in case when there's no control application or when this application doesn't interact with any other application. Interaction with extern entities can overload external applications. External application charge increases as the number of requests is multiplied by the number of nodes in the cluster. In order to maintain the coherency in the cluster the response of external application needs to be the same to all nodes. Specific request dispatchers are needed to fulfil this condition for applications with external interaction. The complexity of this development needs to be estimated when this solution is considered.

## V. CONCLUSION

In this paper, we present a classification of telecommunication applications from the failover perspective. Three application types are discussed: i) standalone SIP server, ii) stateless application controlling SIP server and iii) stateful application controlling SIP server.

The standalone server is considered as a support function. The availability requirements and replication implementation should be considered during the choice of server for standalone use.

Comparing to stateful applications, stateless applications are simpler to implement in an environment requiring high availability. Replication of application data is not needed; only protocol state needs to be replicated. This case can be addressed by using SIP server replication approach, network level replication or by application server. These methods are efficient and scalable. Implementation using a SIP server avoids custom development needed by the replication at the network level. The advantage of network level solution is low impact on performances since the load balancer is a standard part of high available systems.

Clustering frameworks and application servers should be considered for stateful applications. These two concepts are comparable in terms of configuration complexity. Replication performances like throughput and latency are implementation dependent, but in general application servers propose to application more services with less performance. Specialised clustering frameworks usually scale and perform better.

## REFERENCES

[1] Rosenberg, J.; Schulzrinne, H.; et al. SIP: Session Initiation Protocol, June 2002. RFC 3261. http://www.ietf.org/rfc/rfc3261.txt (accessed Nov 18, 2010)

[2] J. Hlavacek, R. Bestak, "Improvements in the Availability of SIP Networks," In Proceedings of the 2010 Networking and Electronic Commerce Research Conference, Dallas, TX: American Telecommunications Systems Management Association Inc., pp.109-117, 2010

[3] Asterisk- The Open Source Telephony Project. http://www.asterisk.org/ (accessed Nov 18, 2010)

[4] Terracotta - High-Performance Scalability and High Availability for Enterprise Java Applications. http://www.terracotta.org/ (accessed Nov 18, 2010)

[5] JBoss AS. http://www.jboss.org/jbossas (accessed Nov 18, 2010)

[6] IBM - WebSphere Application Server - Software. http://www-01.ibm.com/software/webservers/appserv/was/ (accessed Nov 18, 2010)

[7] K. Trivedi, D.Wang, D. J. Hunt, A. Rindos, W. E. Smith, B. Vashaw, "Availability Modelling of SIP Protocol on IBM© WebSphere©," prdc, pp.323-330, 2008 14th IEEE Pacific Rim International Symposium on Dependable Computing, 2008

[8] JBoss Cache - JBoss Community. http://jboss.org/jbosscache (accessed Nov 18, 2010)

[9] Mobicents. http://www.mobicents.org/ (accessed Nov 18, 2010)

[10] Rajappa, B.; Motiwala, Y.; , "Message Based Redundancy Approach using Totem Protocol for Telecom Applications and Protocol Stacks," Communication Systems Software and Middleware, 2007. COMSWARE 2007. 2nd International Conference on , vol., no., pp.1-6, 7-12 Jan. 2007

[11] G. Kambourakis, D. Geneiatakis, S. Gritzalis, C. Lambrinoudakis, T. Dagiuklas, S. Ehlert, J. Fiedler, “High Availability for SIP: Solutions for Real-Time Measurement Performance Evaluation,” In International Journal of Disaster Recovery and Business Continuity, vol. 1, no. 1. pp.11-29, February 2010

# Analyze of Impulse Noise

Jaroslav Krejci,Tomas Zeman
Dept. of Telecommunication Engineering
Faculty of Electrical Engineering, Czech Technical University in Prague
Technická 2, CZ 166 27 Prague, Czech Rep
krejcja1@fel.cvut.cz, zeman@fel.cvut.cz

***Abstract*— The paper focuses on the impulse noise generated with a few home appliances under various conditions of their working. The experiment founds out a relationship between generating of impulse noise on the supply network line and on the telephone subscriber line. The paper describes comparison method of impulse noise which will serve for defining of impulse noise model.**

***Keywords- Impulse noise; Home appliances; PSD, capster; DSL***

## I. INTRODUCTION

The DSL technology, especially ADSL/ADSL2+ and VDSL/VDSL2 are currently most common; both of them preserve the primary function of the analogue (or ISDN) phone line and, in addition, they form data channels for high-speed services (e.g. IPTV).

IPTV is a multimedia service, which broadcasts television and radio signals over data networks based on the IP networking protocol. DSL technology is an option for implementation of access network that transmits digital TV signal to the end-users. The disadvantage of DSL is the distance between DSLAM unit and a modem, because the growing distance causes the transmission speed to decrease due to attenuation of the transmission environment and more interference.

## II. TYPE OF DISRUPTIVE EFFECT

There are many different sources of disturbance that influence the transmission properties of metallic lines in a negative way. If the system of an access network is well designed, the effects of internal system disturbances (mostly white noise of passive as active electric components) are relatively small. The real total information capacity of metallic line will be limited by external sources of disturbance, i.e.:

- Near-end crosstalk (NEXT)
- Far-end crosstalk (FEXT)
- Radio frequency interference (RFI)
- Impulse noise

While the first three listed types of external disturbance have been examined quite thoroughly, the study of impulse noise is not so usual.

Impulse noise is a non-stationary stochastic electromagnetic interference, which consists in random occurrences of energy peaks with random amplitudes. The source of impulse noise can be the electromagnetic radiation from power cables, high voltage power lines, power switching and control, and electrical discharges. The impulse noise, which is characterized by its short duration, is composed of peaks. These peaks occur in bursts, which cause so-called block errors in transmitted data.

## III. MODEL NOISE PULSE FOR EVALUATION OF IMPULSE NOISE INFLUENCE

With respect to the described nature of impulse noise, it is not easy to design an ideal methodology for evaluation of the impulse noise influence on high-speed data transmission systems. The basic problem is the definition of a model describing the impulse noise that would be suitable for testing of the said systems.

ITU-T recommendation for testing procedures of ADSL systems describes test impulses No. 1 and No. 2. It also proposes the basic methodology for determination of impulse noise influence on a system. The recommendation for HDSL defines Cook pulse (Eq. 1). Electromagnetic compatibility (EMC) standards describe specific bursts of pulses (European standard EN 61000-4-4).

$$\mathrm{f(x)} = \begin{cases} K|t|^{-3/4}, & \mathrm{t} \geq 0 \\ -K|t|^{-3/4}, & t < 0 \end{cases} \qquad (1)$$

Where K is a parameter which designates a shape of impulse.

## IV. EXPERIMENTAL SIMULATION MEASUREMENTS

Some specialized works show that the most significant influence on xDSL systems has the impulse noise that is injected in the closest proximity of the subscriber's xDSL modem (ATU-R).

This will be the case of disturbance in e.g. family houses or apartment buildings. Therefore we have chosen some very typical home appliances for testing of impulse noise effects.

Our testing workplace corresponds to the scheme described in ITU-T G.996.1 recommendation (with some minor modifications).

The proposed workplace is composed of a standard extension supply cable and a digital storage oscilloscope. There

is a very close parallelism of the supply cable and the local metallic subscriber line, the length of which is 2m (this value has been verified by numerous experiment and practical experience showing that for the lengths over 2m the increase of the induced interference is minimal). On the near end there is a common type of symmetric phone cable terminated by a balanced-unbalanced transformer that is connected with the 50-ohm input of the digital oscilloscope (see Fig. 1). This way we can measure the impulse noise disturbing the supply networks and the telephone subscriber line. Sampling rate was 50 MHz.

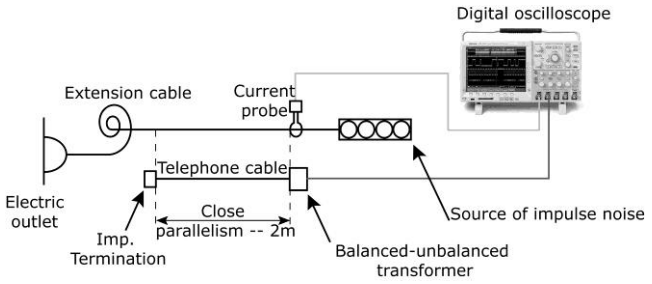


Figure 1. Setup of a workplace for impulse noise diagnostics

Sources of impulse noise will be represented by home appliances plugged in the electric outlet. The parallel cables should be as straight as possible and far enough from other sources of possible interference.

## V. Comparison Method of Impulse Noise

During measurement it has been occurred many impulses which were generated by every form home appliances. In terms of situation, it was suggested to create number of groups with similar power spectrum.

As a comparison method was chosen a method given on the basis cepstrum signal x.

$$\mathbf{C} = DFT^{-1}\left\{\log\left|DFT\left\{\mathbf{x}\right\}\right|\right\} \tag{2}$$

Cepster rate differences (including cepstral distance) is:

$$\mathbf{D_{i,k}} = \sqrt{\frac{1}{N}\sum_{i}^{C}\sum_{k}^{C}\left(\sum_{j}^{N}\left[\mathbf{Y_{j,i}} - \mathbf{Y_{j,k}}\right]\right)^2} \tag{3}$$

$$\mathbf{Y_{N,C}} = \left(y_{i,j}\right)_{N,C} \tag{4}$$

Where $\mathbf{Y_{N,C}}$ is matrix of cepster from matrix x signals. N – is number of samples and C – is number of signals

## VI. Results of Experimental Measurements

The testing was performed in five to six steps, depending on the specific device. The first step was always the measurement of disturbance without the respective appliance plugged, in order to minimize the bias in measured values. The total number of tested devices was 10; the extent of this paper allows summarizing of the testing results only for 3 of them, specifically:

- Universal charger HAMA,
- Handheld blender (SOFTmix ETA),
- High-speed drill with smooth regulation EXTOL (m. 404116).

In the idle condition during the experiment, the impulse noise was not observed at the oscilloscope input.

In the following figures the black curve represents the impulse noise in the supply network and the gray one the impulse noise in the telephone subscriber line.

### A. *Universal charger HAMA*

When the charger is plugged in, but without batteries, it does not produce any impulse noise. The behavior of the charging device is identical.

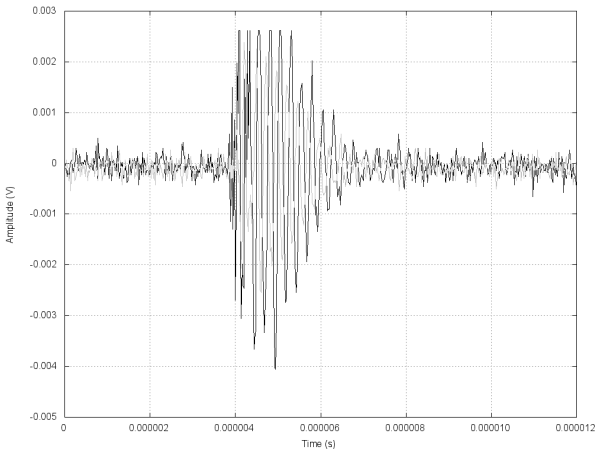


Figure 2. Batteries insertion

From Fig. 2 and Fig. 3 it is apparent that the impulse noise occurs in connection with transition states – i.e. when batteries are being inserted or ejected. The resulting impulse noise can be described by the following formula:

$$x(t) = \begin{cases} \hat{A}\cdot e^{-\frac{(t-t_0)}{\tau}}\cdot\sin(2\pi f(t-t_0)) & t_0 \le t \le t_0 + t_{in} \\ 0 & else \end{cases} \tag{5}$$

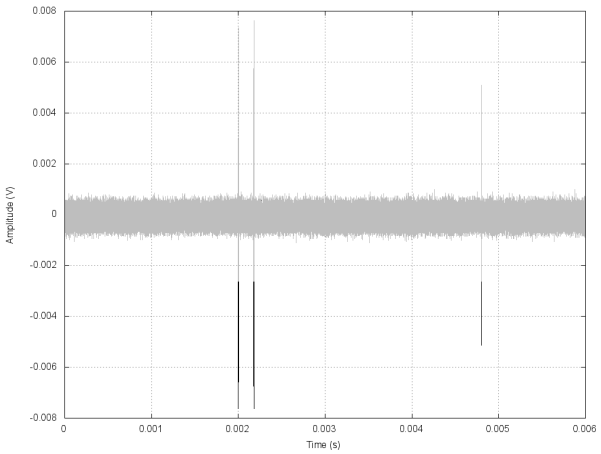


Figure 3. Batteries ejection

## *B. Handheld Blender*

The effects of the impulse noise generated by the blender in the steady state during normal operation towards the supply network are shown in fig.4.

There was occurred four type of impulse noise. The groups of impulses are shown in figs. 5 – 8. Every groups of impulses noise have PSD worse than -80 dBm. This noise can affect the VDSL and PLC communication

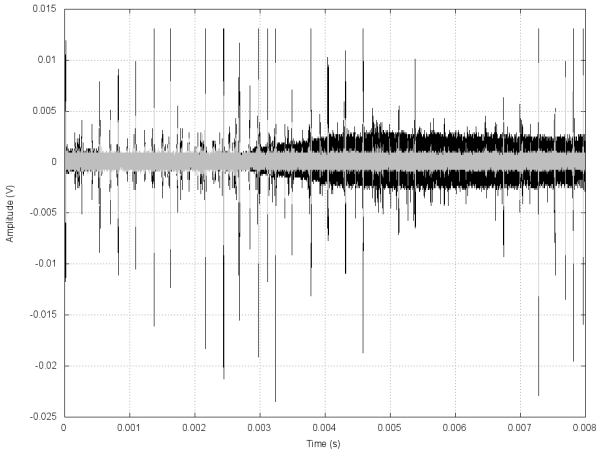


Figure 4. Blender running

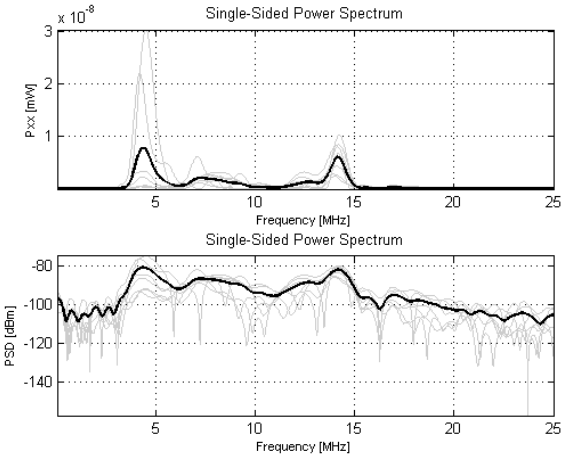


Figure 5. Blender running – 1. Type of impulse noise

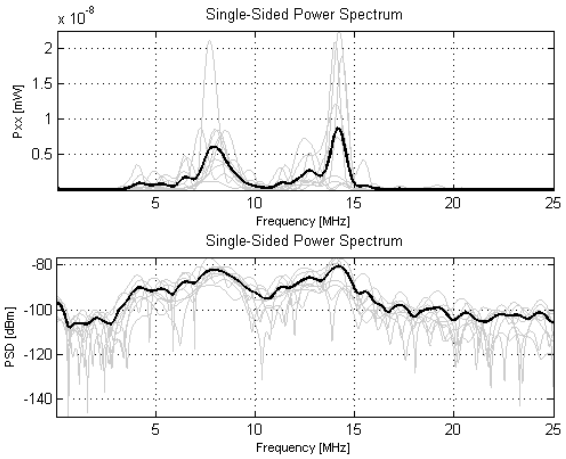


Figure 6. Blender running – 2. Type of impulse noise

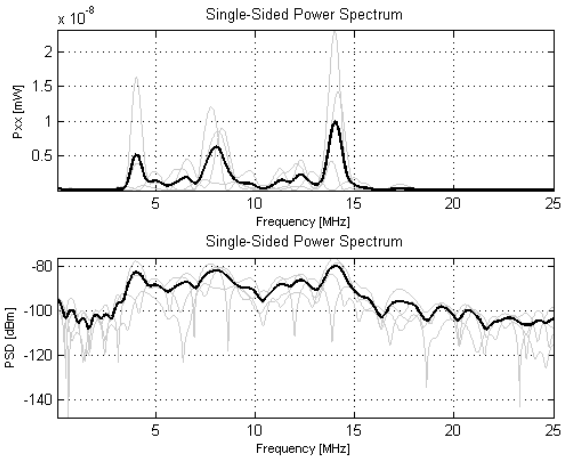


Figure 7. Blender running – 3. Type of impulse noise

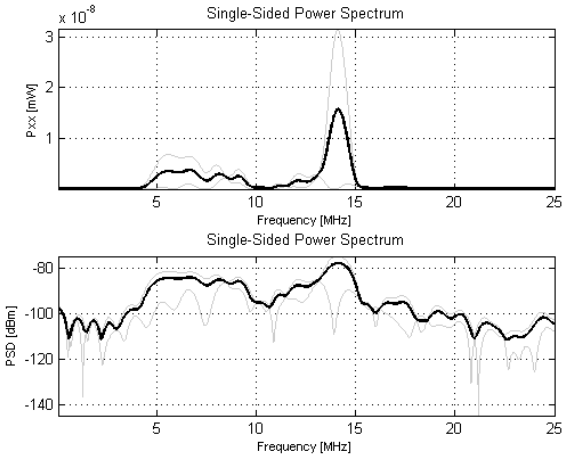


Figure 8. Blender running – 4. Type of impulse noise

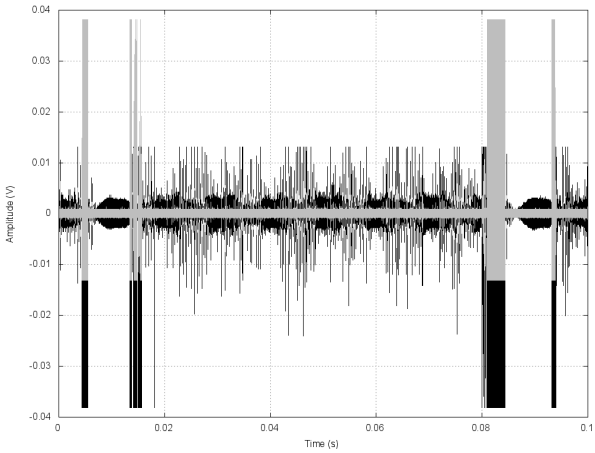


Figure 9. Seitching of blender speed

The fig. 9 illustrating the impulse noise generated by the blender show that the noise is rather random, with very high amplitude. There was occurred only one type of impulse noise. The type of impulse noise is shown in fig. 10.

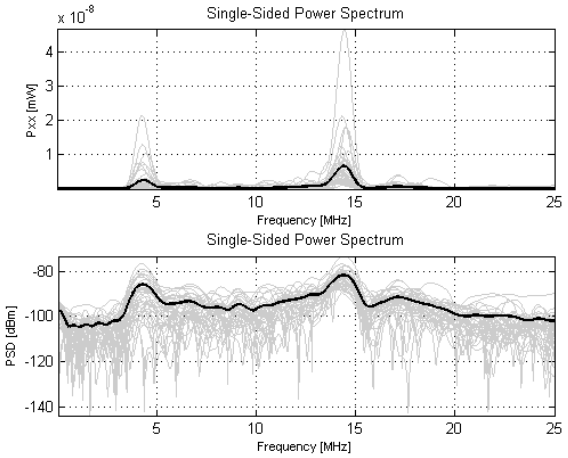


Figure 10. Switching of blender speed – type of impulse

### *C. High-speed Drill*

The highest values of impulse noise were obtained during the drill startup.

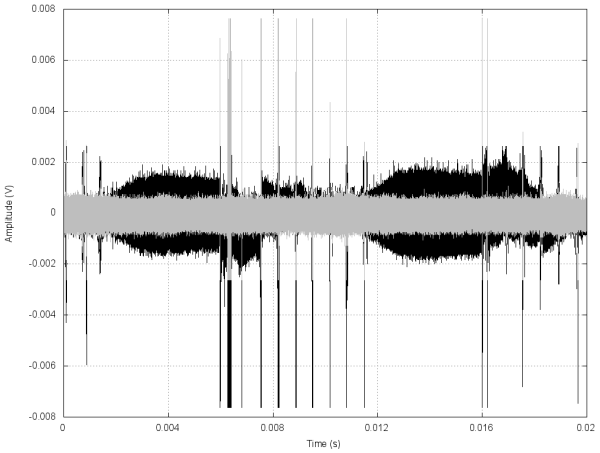


Figure 11. Drill running

The most frequent occurrence of impulse noise can be observed during regulation of the drill speed with maximum power. This is probably caused by switching to faster speed and subsequent transient states that generate impulse noise, and the electromagnetic radiation then induces impulse noise also in the telephone line.

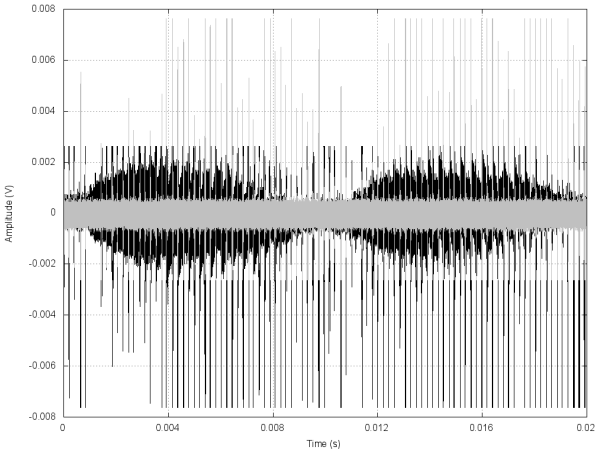


Figure 12. Drill speed regulation in operation – maximum power

There was occurred only one type of impulse noise. The type of impulse noise is shown in fig. 13. Every groups of impulses noise have PSD worse than -80 dBm. This noise can affect the VDSL and PLC communication.

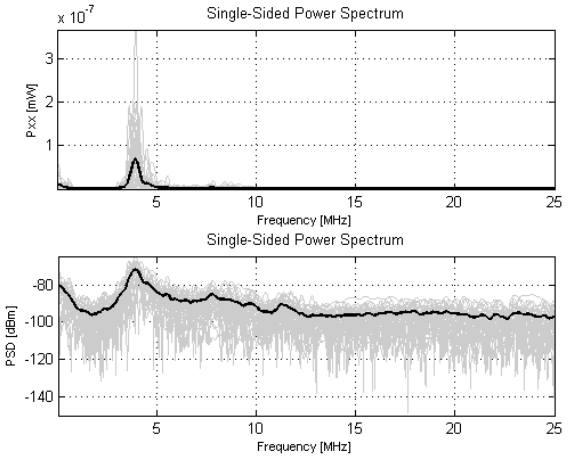


Figure 13. Drill – type of impulse noise

## VII. CONCLUSION

The measurements have proven that it is difficult to describe the impulse noise using universal models that use precisely defined test impulses.

The disturbance generated by small home appliances shows the influence on symmetric telephone lines in close vicinity of power lines caused by penetration (injection) of the interference into the telephone line. The disturbance is closely related to transient states, i.e. startup and shutoff of appliances or changing of their operational state (e.g. power or speed).

The disturbance in xDSL systems can be eliminated – to certain extent – with the help of suitable protective mechanisms. Data transmission can be protected using Reed-Solomon (RS) coding and interleaving.

In our future work we will focus on effects of disturbance from small appliances on video transmission in xDSL systems (especially ADSL2+ and VDSL), with respect to the distance between the power line and the metallic subscriber line, to the distance of the appliance, and also to the length of the cables. The quality (or level of corruption) of the video signal will be evaluated using objective methods that are commonly used for quality assessment of video.

In the future we will focus on analyse selected effects and influences of noise on the transmission of digital broadcasting signals (IPTV) and to simulate transmission systems and characteristics of telephone channels for the purpose of optimizing parameters of error-correction subsystems.

The most important result of the performed experiments will be a data bank of disturbing impulses that will serve for defining of impulse noise model.

## ACKNOWLEDGMENT

This research has been supported the Czech Universities Development Fund grant No. 1786/2010/G1.

## REFERENCES

[1] J. Krejci, T. Zeman, “Influence of Noise on IPTV over xDSL,” In IWSSIP 2009 - 16th International Workshop on Systems, Signals and Image Processing [CD-ROM]. Chalkida: TEI of Chalkida, 2009, p. 246151. ISBN 978-1-4244-4530-1.

[2] T. Prokop, J. Vodrazka, “Modeling of transmission lines for digital subscriber lines,” 15th International Conference on Systems, Signals and Image Processing, IWSSIP 2008. Bratislava, Pages: 53-56, 2008.

[3] John A. C. Bingham, “ADSL, VDSL, and Multicarrier Modulation.” 1 edition., Wiley-Interscience, 2000. 314 s. ISBN 978-0471290995..

[4] N. Nedev, “Analysis of the Impact of Impulse Noise in Digital Subscriber Line Systems.” Edinburgh, 2003. 185 s. Dissertation thesis. The University of Edinburgh

[5] Philip Olden, Herve Dedieu, Krista Jacobsen, “Fundamentals of DSL Technology.” Auerbach Publications, 2004. 1 edition s. ISBN 978-0849319136.

[6] ITU-T Recommendation G.996.1, Test procedures for digital subscriber line (DSL) transceivers [s.l.] : Telecommunication Standardization Sector of ITU, 02/2001.

# Security in Communications

# Protection of Web-based Applications

Radek Dolezel and Jan Humpolik
Brno University of Technology
Faculty of Electrical Engineering and Communication
Purkynova 118, Brno 612 00, Czech Republic
Email: {xdolez35,xhumpo03}@stud.feec.vutbr.cz

***Abstract*—The paper describes most frequent attacks aimed at web-based applications. Attacks elimination is a part of their description. We have built a web application and proved its protection for demonstration. Our web application represents an information system for sharing files among entered users. The web application contains all mentioned elements of protection. We have also secured a connection to the web application. Security advice and recommendations for protection of web-based applications are the main output of this paper.**

## I. Introduction

A web environment is the one of the most used environment in the whole Internet. There is a great number of web-based applications provided various services. These services are very often offered by information systems. Some data involved in information systems is accessible directly but some of it is available only after finished successful login process. Therefor each information system must satisfy suitable security level for processed user data. On the other hand there are some vulnerable or dangerous information systems and they could be attacked in the end. Reasons for attacks could be for example sensitive data (personal data, credit cards numbers, login information etc.) that users operate with and that is transfered via Internet routes. Hence it is necessary to protect both web-based applications and appropriate connection.

Our contribution is a description of most frequent web-based attacks and their elimination. We have built our own information system for demonstration. It is held in the web environment and all security advice and recommendations stated in this paper are applied.

The paper reflects some parts of Bachelor's thesis *Secured access for web applications* [1] written by Jan Humpolik and supervised by Radek Dolezel.

## II. Web-based attacks and their elimination

We have only chosen most frequent attacks aimed at web-based applications because there are a lot of these attacks and every moment could be invented the new one.

In the description of each attack is given its possible elimination. Based on our previous good experience, we used the XHTML, PHP and MySQL technology for our web application building. Apache HTTP Server represents a web server with proper configuration. The OpenSSL project is used for certificates issuing. Recommended protection corresponds with these technologies. We were using project documentation (PHP [2], MySQL [3], Apache HTTP Server [4], OpenSSL [5]) during our work. The following examples of most frequent web-based attacks are ordered alphabetically.

### A. ClickJacking

*Description:* ClickJacking attack seems like an invisible layer above the original web page. The user tries to click on real elements on the web page what he sees but in fact he clicks on hidden elements on the another web page located in the upper layer.

*Protection:* Disable an appearance of another layer on the web page with statement `X_Frame_Options` in the HTTP response header. The one of the possible way is to set up the statement in the `.htaccess` file.

### B. Cross-Site Request Forgery (CSRF)

*Description:* This attack is aimed at the entered user into the information system. During the session the user could be recommended (forced) to visit the another website. This another website contains hidden malicious forms sending dangerous data on the web page of the information system which the user is entered into. The attacker can also use modified URL directly without the another intermediate website.

*Protection:* Generate an authorization token, confirmation with an another element or channel, create a shorter time of the HTTP session.

### C. Cross-Site Scripting (XSS)

*Description:* Cross-Site Scripting attack focuses on inserting attacker's own malicious scripts on the web page through a user form situated on the attacked website.

*Protection:* Convert special characters in all inputs from users to HTML entities with the PHP statement `htmlspecialchars`.

### D. Session Fixation

*Description:* This kind of attack consists in forcing the user to use attacker's Session ID in login process.

*Protection:* Every time generate a new Session ID in each login process with the function `session_regenerate_id` in PHP.

### E. Session Hijacking

*Description:* If the connection between the web server and the user's computer is established a session for this connection is set up. The ID of the session is stored into a cookie file because of communication protocol HTTP is a stateless

protocol. The Session ID can be stolen from the cookie file by a dangerous script involved on the another website which the user is mystified (forced) to browse on.

*Protection:* Disable access of other scripting languages to the cookie files with enabling the parameter `$httponly` in the PHP function `session_set_cookie_params`.

### F. SQL Injection

*Description:* Execution of SQL (Structured Query Language) Injection attack is in connection with database engines. During this attack the attacker attempts to put malicious code contained in his SQL statement into the information system database.

*Protection:* Protection consists in escaping special characters in the SQL statement uploaded through the user form. It is possible to use `mysqli_real_escape_string` for MySQL. UTF-8 encoding is also recommended and `mysqli_set_charset` is used for UTF-8 set up in MySQL.

## III. Other threats

### A. Connection sniffing

*Description:* The HTTP protocol is used as default communication protocol for web-based applications. The HTTP protocol does not offer any security level for transfered data protection. If the attacker captures some parts of network traffic he can see transfered data in unsecured form.

*Protection:* Use the HTTPS protocol for all connections.

### B. Social engineering

*Description:* Social engineering is human-based threat. The attacker tries to deceive and persuade the ordinary user to give him important information. The attacker can abuse this information for another kinds of attacks [6].

*Protection:* Periodical training the users interested in using the concerned information system. Training can involve for example learning how to use the information system securely and which kind of information the users can give out.

## IV. Features of our web application

We have built our web application and in the following text we give the closer description of each part.

### A. Login process

Our web application represents information system. Information system is aimed at sharing files among entered users. If some user wants to share his own files or wants to access to other shared files, he must log into the information system. After the successful login process the user gets the user role. Appropriate access rights belong to each user role. The whole login process is divided into authentication and authorization. Authentication validates the user identity i.e. it compares the login name and the access password with data stored into the user database of the information system. Authorization represents the process of the user role assigning.

We use system CAPTCHA [7] for supply the login process, see Fig. 1. If the user put wrong login information for three times in the short period during the login process then he must type his password with combination of the original access password and the text displayed on the CAPTCHA field. This is protection against Internet bots (artificial scripts attempting to access into information systems).

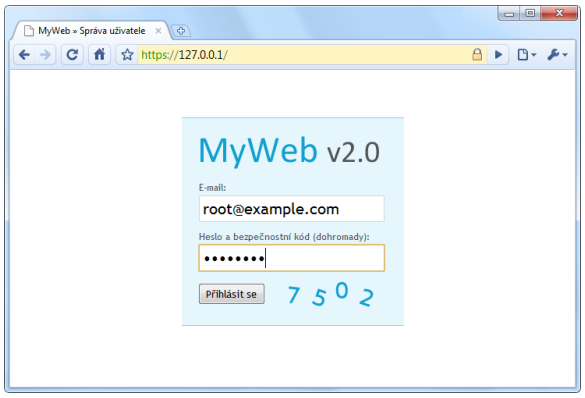


Fig. 1. Login form with CAPTCHA system

### B. Organization of users

During the login process the user role with appropriate access rights is given to the authenticated user. We divide the users participated in our information system into the three user roles.

The first role is an administrator. The administrator has unrestricted access rights. The administrator can create a user profile, change its properties or delete this profile. The administrator has also fully access to all shared files.

The second role represents a common user. This user has full access to his own files and can only download the files of the others but they must allow access for him. He can add comments to these files and evaluate them with points.

The third role is used for a guest. The guest can only download the files which the others share for him.

We use evaluation system for user popularity. The evaluation system is called Aura [8]. The Aura system consists in evaluation rating from 0 to 100 points. If the user gets 0 points then he loses ordinary access rights as the common user and becomes the guest. Only the administrator can give back default value of points to the user. The administrator does not have any points. The common user has 50 points in default. The guest has 0 points.

Summary of the user roles is in Table I. The user profile management is shown in Fig. 2.

### C. Secured connection

We have chosen the HTTPS protocol for the connection between the server and the user's computer. HTTPS is an application protocol and is based on the TLS/SSL protocol. TLS/SSL is situated between the application and transport layer of the TCP/IP layer model. The TLS/SSL protocol uses strong cryptographic functions for protection the whole connection (connection establishing, data transfer etc.). If the

TABLE I
ORGANIZATION OF USERS

| User role | Access rights | Aura (default) |
|---|---|---|
| Administrator | User management, full access to all shared files | – |
| User | Full access to own files, download allowed and shared files and add comments or evaluation to them | 50 |
| Guest | Only download allowed and shared files | 0 |


Fig. 2. User profile management

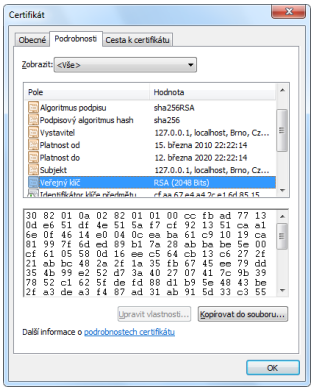


Fig. 3. Server certificate detail

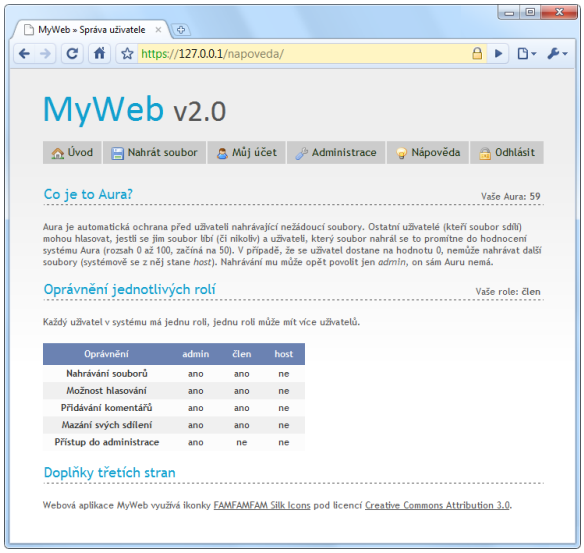


Fig. 4. Help panel

user uses unsecured connection via the HTTP protocol then the connection will be automatically forwarded to the secured connection via HTTPS. The server is authenticated to the user with its server certificate. We have issued our own self-signed server certificate. We used SHA-256 for signing and 2048 bits for RSA public key. The server certificate detail is depicted in Fig. 3.

During our project design and its building, we were aspiring to create a user-friendly application with easy-to-use functions, intuitive elements and eye-taking look. We implemented the help panel for better informedness of the users, see Fig. 4. Each part of our web application contains only relevant information for user needs. We have tried to decrease a number of redundant information according to keep the web application easy-to-use.

## V. APPLIED PROTECTION AND CONFIGURATION

We have protected our web application with applying following security advice and recommendations. Described attacks or threats which the protection is for are stated in brackets.

### A. Protection against described attacks

- The HTTP respond header is set up for blocking the another upper layer on the actual web page, see Fig. 5 (*ClickJacking*).

```
HTTP/1.1 200 OK
Date: Mon, 22 Mar 2010 21:01:18 GMT
Server: Apache
X-Frame-Options: deny
Set-Cookie: ID=efq32297u0j5j1s2rtptj91ci7;
  path=/; domain=127.0.0.1; secure; HttpOnly
Expires: Thu, 19 Nov 1981 08:52:00 GMT
Cache-Control: no-store, no-cache, must-revalidate,
  post-check=0, pre-check=0
Pragma: no-cache
Content-Length: 847
Keep-Alive: timeout=5, max=100
Connection: Keep-Alive
Content-Type: text/html; charset=UTF-8
```

Fig. 5. HTTP response header log

- The Session ID is only stored in the cookie file. The Session ID transfer via URL is disabled (*Cross-Site Request Forgery*).
- The cookie files are protected against scripting languages (*Cross-Site Scripting*, *Session hijacking*).
- Only the one session is possible for the connection. The old (original) session is closed with the new login process (*Cross-Site Request Forgery*, *Cross-Site Scripting*).
- Unique code confirmation is required during user data upload. Unique code is hidden in the user form. (*Cross-Site Request Forgery*).
- All the inputs from the users are converted to HTML entities (*Cross-Site Scripting*).
- The new Session ID is generated during each login process (*Session Fixation*).

### B. Protection of connection to the web application

- HTTPS is the communication protocol with server authentication to user and the server certificate is an authentication medium. The server certificate has been signed by SHA-256 and it contains RSA public key generated with 2048 bits length (transfered data attacks).

### C. Internal protection

- The Aura system is used inside of the information system for files evaluation. The evaluation rate belongs to the user who uploads the file. The rate is 0 – minimum, only download of files, 50 – default value for the new user, 100 – maximum, very popular user (deceitful users).
- Uploaded files are stored in the file system instead of the MySQL database. Into the database is only saved the SHA-256 hash created from the content of the uploaded file. The new file name is the same hash. Each user account has reserved 1 GB free space. Maximum size for the one uploaded file is 100 MB (database engine performance, deceitful users).
- Each user's password is saved as SHA-256 hash with salt. Hash of the password is stored into the database but salt is stored into the secret storage which is outside of the database (deceitful administrators, broken access to database).

### D. General protection and configuration

- The login process is protected with the CAPTCHA system for three wrong inputs of login information (Internet bots attack).
- After the successful login process, the IP address (IPv6 support), date and time, and the ID of a web browser are logged. Logged data could be used for statistics or for optimalization purposes.
- The whole information system uses UTF-8 encoding in each parts (web pages display, storing items into the database etc.). The output of the information system is in the `text/html` type. XHTML 1.0 Strict, CSS 2.1 and JavaScript are used but the information system is also accessible in a text mode (compatibility purposes).
- Sending the same form again is disabled during the web page refresh (comfort usage, database filling attacks).
- Extension `mod_rewrite` is applied for human-readable URLs.
- Web server output messages (warning, error etc.) are turned of (web page source code attacks).

We proved applied protection in our laboratory because our purpose is to maintain our web application in good condition and protected against most frequent and well-known web-based attacks. We also discussed some kinds of social engineering threats aimed at the users of web-based applications in general. Hence we recommend to train all the users.

## VI. Conclusion

We have studied and described most frequent web-based attacks in this paper. For these attacks we have recommended possible elimination. We discussed also social engineering threats. Based on our study we have designed and built our web application. The web application represents information system for sharing files among entered users. We give description of the information system and we also include some security advice and recommendations for better protection web-based applications against attacks.

For realization of our solution we have been using modern development technologies. The web application is considered as the whole complex unit with the secured connection based on strong cryptographic functions. During development of our web application we have emphasised security goals but on the other hand we have attempted to create the user-friendly and easy-to-use application. We have applied all mentioned security advice and recommendations. In our laboratory was proved applied protection. The web application contains the user roles with appropriate access rights. These roles are assigned to the entered users.

Our web application is in good condition under recent trends and standards. It is ready for real running.

## Acknowledgment

The authors would like to thank Ministry of Industry and Trade of the Czech Republic for financially support this research under grant no. FR-TI2/679.

## References

[1] J. Humpolik, *Secured access for web applications* (in Czech), Brno: Brno University of Technology, Faculty of Electrical Engineering and Communication, 2010. 56 pp. Bachelor's thesis supervisor Radek Dolezel.
[2] (2010, Nov.) PHP: Documentation. [Online]. Available: http://php.net/docs.php
[3] (2010, Nov.) MySQL :: MySQL Documentation: MySQL Reference Manuals. [Online]. Available: http://dev.mysql.com/doc/
[4] (2010, Nov.) Documentation: Apache HTTP Server – The Apache HTTP Server Project. [Online]. Available: http://httpd.apache.org/docs/
[5] (2010, Nov.) OpenSSL: Documents, Misc. [Online]. Available: http://www.openssl.org/docs/
[6] K. D. Mitnick, *The art of intrusion: the real stories behind the exploits of hackers, intruders & deceivers* Indianapolis: Wiley Publishing, 2006. 270 pp. ISBN 0-471-78266-1.
[7] (2010, Nov.) The Official CAPTCHA Site. [Online]. Available: http://www.captcha.net/
[8] (2010, Nov.) Co je Aura – Root.cz. [Online]. Available: http://www.root.cz/redakce/co-je-aura/

# EMV payment cards

Ondrej Morsky, Jan Karasek
Department of Telecommunications
Faculty of Electrical Engineering and Communication, BUT
Brno, Czech Republic
ondrej.morsky@phd.feec.vutbr.cz, karasek.jan@phd.feec.vutbr.cz

*Abstract*—***This paper is focused on smart cards and their use as authentication tokens in payment operations. It is a result of a research project of how to use EMV payment cards as authentication tokens in a standard home computer. This document describes standards and recommendations for payment cards and their implementation. First of all it is standard EMV which defines payment application, access to it, communication with the terminal and the way of authentication of the card and the user. This document is structured from electrical basics through communication protocol up to reading payment card specific data.***

***Keywords-Smart cards; EMV; Payment cards;***

## I. SMART CARDS

Smart card is a small plastic card with an embedded microprocessor. This microprocessor is capable of installing and running applications and communicating with the card reader. There are many types of smart cards differing in their performance, memory size, connection type etc. Contact smart cards in the form of classic cards are well-known. The cards are used for payments, for secure login to computer networks etc. [1]. The SIM card is also a smart card even if its size is very small in comparison with usual cards. There are also cards on the market that contain only a memory chip, but they are not capable of any computations. These cards are usually considered not to be smart cards because of missing a "smart" chip [1]. This article focuses on smart cards used for payments and especially in application protocol used for payments. Next chapters will describe how the card communicates with the reader and what is necessary to do before you can use your card for financial transaction.

## II. COMMUNICATION INTERFACE

Communication between the card and particular applications is based on ISO/OSI reference model [1].

Physical layer (voltage levels, signal timing, etc.) is defined in international standard ISO/EIC 7816 [1]. The card connected with the terminal is using a half-duplex serial interface. One of many procedures is the card initialization. After the card insertion, reset signal is raised. The card responds with a byte sequence called Answer To Reset (ATR). This sequence can be up to 33 bytes long. The reader can detect several basic information on the inserted card e.g. supported protocols and speeds, manufacturer or a card type [1].

Higher model layers are realized with transmission protocols T=0 and T=1. T=0 is a byte oriented protocol that can be used for calling functions stored on card, including parameters passing. The card always returns the function result, or error code in case of failure. Data units transferred by this protocol are so-called TPDUs (Transmission Protocol Data Units). T=1 protocol is, on the other hand, block oriented and is more complex and more complicated. This is the reason why it is not supported in all smart cards or readers [1].

For communication on a higher level Application Protocol Data Units (APDU) are transmitted. The structure of APDU corresponds to TPDU if T=0 protocol is used [1].

## III. OPERATING SYSTEM

Today's smart cards are capable of running multiple applications simultaneously. At the same time there is a demand on high security of these applications and their maximal separation, similarly as in desktop computers. These functions are ensured by operating system preinstalled on a smart card. Its main purpose is to mediate communication between particular applications and the reader and provide enough security so that no application is capable of reading data belonging to another application, intentionally or not. There are many operating systems differing in speed, security and orientation [1].

## IV. GLOBALPLATFORM

GlobalPlatform is a non-profit organization founded in 1999 to take responsibility for an older OpenPlatform specification. OpenPlatform was originally designed by VISA (a card issuing company) and it contained recommendations for the whole infrastructure of payment cards – cards, readers, terminals, and software. Today, GlobalPlatform has more than 60 members [2].

Recommendations for cards are mainly targeted on their operating system. GlobalPlatform does not specify an internal OS design, but only its security behavior and its programming API. The most important part is aimed at memory separation of particular running applications. This standard was developed so that multiple independent applications can be used on one smart card – e.g. payment, access and SIM applications. The operating system has to block reading or writing to memory not belonging to application. This is true for RAM memory and as well as for a smart card file-system. The standard also defines some optional functions, e.g. channels. This enables the reader

to create a couple of virtual connections to the card and use multiple applications simultaneously, or to run one application in multiple instances [3].

Part of this standard aims at software design, hardware parameters of readers, terminal networks, and a global system design as well [3].

## V. PAYMENT APPLICATION, EMV

As already said above, the smart card utilizes an operating system and applications running on it. The benefit of this approach is the ability to use one single card for many different purposes (e.g. as a payment card and an access control token together). Application intended for processing payment transactions is not defined in any standard. Only its behavior is defined, i.e. how it should be stored on a smart card, how to communicate with the reader or ATM etc. The company responsible for this specification is called EMVCo. This organization was founded by agreement of several card companies (EuroPay, MasterCard, and Visa). The main purpose was to ensure security and global interoperability of payment cards [4].

EMV specifications are freely available online. They are defined in four so-called books (Book 1 - Book 4). Each of them is targeted at one specific part of a complex proposal. The first book (Application Independent ICC to Terminal Interface Requirements) is aimed at mechanical and electrical characteristics of smart cards [5]. The second and third book (Security and Key Management and Application Specification) are focused on security algorithms and application protocol for communication of payment applications and terminals [6], [7]. The fourth book describes a global system behavior, network connections, payment terminal recommendations etc. [8]. The current version of this standard is 4.2, issued in June 2008. Also, there are several another recommendations, e.g. cards used for contactless payments etc. [9].

## VI. COMUNICATION PROTOCOL

For the communication on transport layer, T=0 protocol is being used. This protocol is defined in ISO/EIC 7816-3 [1]. Data units transmitted by this protocol are so-called Transmission Protocol Data Units – TPDUs. In case of T=0 protocol, Application Protocol Data Units (APDUs) are equal to TPDUs [1].

TPDU/APDU consists of a header and an optional data part. Protocol is designed with the view of a simple calling of functions stored on a smart card [1].

| **Header** | | | | **Data part (optional)** | | |
|---|---|---|---|---|---|---|
| CLA | INS | P1 | P2 | Lc | Data | Le |

Figure 1. Application Protocol Data Unit - APDU.

- CLA – Class byte – Represents a class of operation. Come classes are standardized, while others can be created by application developers [1].
- INS – Instruction byte – Specifies requested instruction/function.
- P1, P2 – Parameter byte – Indicated parameters for called function.
- Lc – Length of command – Contains the length of a data field.
- Le – Length of expected data – Contains the expected length of answer.

Answer received from the card always contains at least two bytes called SW1 and SW2. They are usually written as a 16bit number in hexadecimal form. This number indicates the result of called function. For example, the value 0x9000 usually means that the operation was completed successfully. Another optional part of the answer is a data field containing data returned by function [1]. As a returned data block usually contains a huge amount of structured information, TLV encoding is used in case of EMV standard [5].

A TLV object contains three data fields – tag, length and value. The following example is a TLV object representing language preferences in EMV protocol (Tag 0x5F2D) [7].

| **T** | **L** | **V** |
|---|---|---|
| 0x5F2D | 2 | 0x637A (cz) |

Figure 2. TLV encoding

- Tag – Describes the type of transferred data. Can be one or two bytes long.
- Length - Describes the length of data. Usually one byte, but can be more.
- Value – Contains data. It can contain another TLV objects inside.

It is possible to transfer structured data containing many different types of information using this format.

## VII. CONNECTING TO PAYMENT APPLICATION

Thanks to the EMV standard it is possible to install many different applications on one card and use them simultaneously. This was the purpose of the EMV standard. This feature does not allow you to have only different applications, but you can have many payment applications on card as well, e.g. issued by different banks. This is the reason why the terminal has to find the payment application first. Payment applications are stored in card, in the area called payment system environment – PSE. The reader has to find this area, select the application and process the transaction. EMV supports two types of connections to applications [5].

- The first method is opening a directory called "1PAY.SYS.DDF01" [5]. The reader can browse this folder, list all payment applications installed on the card and then select the compatible/supported one.
- The directory "1PAY.SYS.DDF01" is defined in EMV, but its implementation is optional [5]. In case

the directory is not present, the reader has to create a list of supported applications (so-called candidate list) and try all of them until he finds one supported by a card. The application existence is reported by return code 0x9000 – Application successfully selected [5].

According to unofficial information on the internet and our experience, the cards issued by MasterCard always implement the 1PAY.SYS.DDF01 directory while other card issuers do not utilize it. In case of using other than MasterCard cards, it is necessary to know application ID. They are not published, but some of them can be found on the internet. Some POS (Point Of Service) terminals also print-out ID of selected application to your bill after the payment, as you can see in Fig. 3.

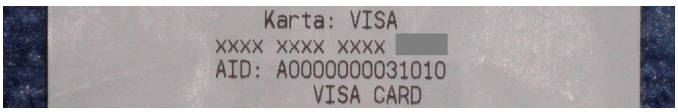


Figure 3. Photo of Application ID printed-out on a bill.

## VIII. Reading application information

The first step the terminal is supposed to do after selecting an application is calling a function GET PROCESSING OPTIONS [7]. This raises the initialization of current application. The standard also defines many status information and flags the terminal has to set or clear in its memory. This is however beyond the scope of this document. You can find more information in [7].

The second step is reading information on selected application. The terminal uses the READ RECORD function with a file ID as a parameter, until the card is returning data. In case of any failure (the card responds with another code than 0x9000), the payment transaction has to be interrupted.

After this step the terminal knows much important information on the card and cardholder. Here you can see examples of some tags. More tags can be found in [7].

*Cardholder Name (Tag 0x5F20)*
Name of a card owner. If the name exceeds the allowed maximum of 26 characters, it is split into more parts.

*Application Primary Account Number (Tag 0x5A)*
Account/Card number. The very same number is printed out on the front side of card (16 digits).

*Language Preferences (Tag 0x5F2D)*
Cardholder's preferred language. There can be more of these fields sorted by priority. The terminal should select the first language in the list it supports.

*Cardholder Verification Method (CVM) List (Tag 0x8E)*
Contains description of procedure which has to be used when authenticating a cardholder. (Online/offline PIN authentication, signature …)

## IX. Authentication

### A. Card authentication

The reader has to perform card verification. This procedure is necessary to prevent making duplicates and copies of cards or creating own cards with fake details [6]. There are several types of authentication, for example:

- Static data authentication (SDA). The terminal reads data from a card together with its signature and verifies it. This approach does not prevent "replay" attacks, because the signature is only statically stored on the card.
- Dynamic data authentication (DDA). In this case, the signature is computed on the card every time the terminal requests card verification.
- Combined dynamic data authentication/Application Cryptogram generation (CDA).

More information on the card verification can be found in [6].

### B. Cardholder verification

When reading application information, the terminal also gets a CVM (Cardholder Verification Method) list. It is a list of rules that will be used for user/cardholder verification. This data object is a relatively complicated structure, containing several different conditions which have to be fulfilled for a successful user's authentication. Verification method can differ based on a terminal type (ATM, POS), operation type (ATM withdrawal, payment, cash back …) or even based on a transaction amount [6] [7].

## X. Current and future work

EMV payment cards use a standardized interface and almost every PC card reader can be used for communicating with a card and simulating an ATM machine or POS terminal. Right now we are able to read all data from EMV cards with any ordinary PC/SC smart card reader. This application is written in C# using free Subsembly SmartCard API (http://www.smartcard-api.com) as a .NET wrapper for Win32 smartcard API. Currently, the program supports 18 different Application IDs and is capable of decoding and printing over 40 TLV objects. You can see application UI in Fig. 4.

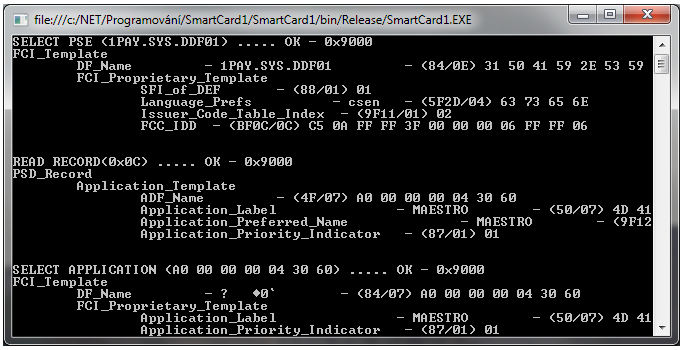


Figure 4. Screenshot of EMV card reading application

Now we are focusing on card authentications and later on cardholder verification using offline PIN authentication. The goal of this project is to create a library to allow using EMV payment card as an authentication token when using home PC. Instead of entering user name and password, the user will only insert a card and optionally enter PIN. Based on the inserted card, the library will find corresponding user and perform login.

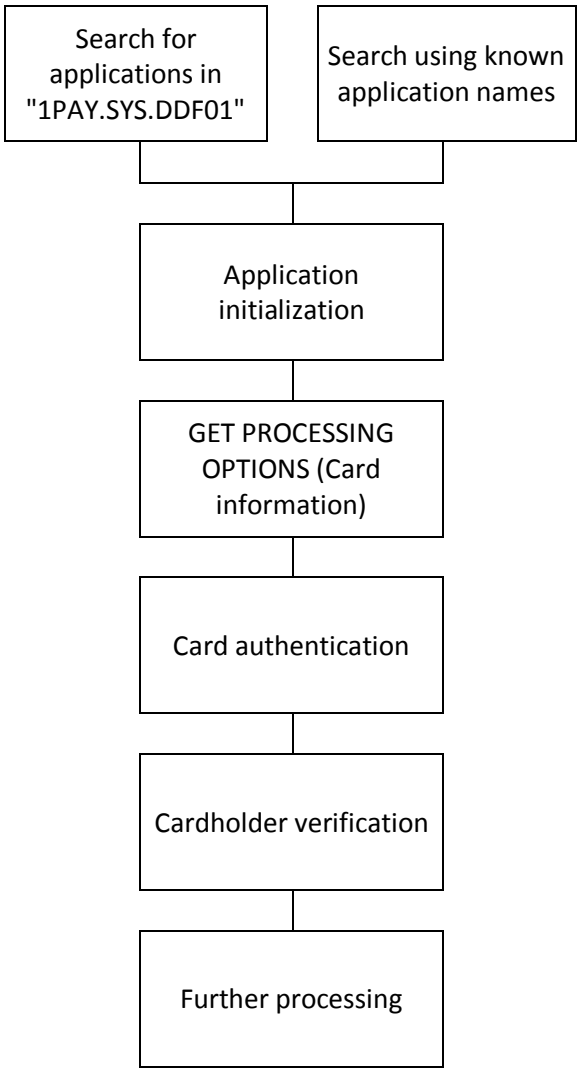


Figure 5. Simplified diagram of application flow.

## XI. CONCLUSION

The whole EMV specification is very widespread and complex. In addition, this specification makes some features only optional, while others are mandatory (e.g. Implementation of "1PAY.SYS.DDF01"). This means that there is no simple way of reading all data from EMV card. On the other side, this allows card issuers to select best option according to their needs. In this document only the basics of communicating with EMV payment card were described. However, this basic information is neccessary for further work with payment cards. The summary of application flow described in this document can be seen in Fig. 5.

## REFERENCES

[1] R. Wolfgang and E. Wolfgang, "Smart card handbook", 3rd edition, John Wiley & Sons, 2003, ISBN: 0-371-96720-3.

[2] -, "About GlobalPlatform", [Online] [Cited: 5th november 2010] http://www.globalplatform.org/aboutus.asp.

[3] -, "Card Specification Version 2.2", [Online] [Cited: 7th november 2010] [Published: March 2006] http://www.globalplatform.org/specificationscard.asp

[4] -, "About EMVCo". [Online] [Cited: 10th november 2010] http://www.emvco.com/about_emvco.aspx.

[5] -, "Book 1 - Application Independent ICC to Terminal Interface Requirements", ver 4.2, [Online] [Cited: 12th november 2010] http://www.emvco.com/specifications.aspx?id=155

[6] -, "Book 2 - Security and Key Management", ver 4.2, [Online] [Cited: 12th november 2010] http://www.emvco.com/specifications.aspx?id=155

[7] -, "Book 3 - Application Specification", ver 4.2, [Online] [Cited: 14th november 2010] http://www.emvco.com/specifications.aspx?id=155

[8] -, "Book 4 - Cardholder, Attendant, and Acquirer Interface Requirements", ver 4.2, [Online] [Cited: 14th november 2010] http://www.emvco.com/specifications.aspx?id=155

[9] -, EMV specifications, [Online] [Cited: 14th november 2010] http://www.emvco.com/specifications.aspx

# Broadcast Authentication Mechanism Optimization in Fully N-ary Tree Topology

Matej Rohlik
Department of Telecommunication Technology
Czech Technical University in Prague
Prague, Czech Republic
rohlimat@fel.cvut.cz

Tomas Vanek
Department of Telecommunication Technology
Czech Technical University in Prague
Prague, Czech Republic
tomas.vanek@fel.cvut.cz

*Abstract*—**Typical application of broadcast authentication protocols can be configurations where only one transmitter with multiple recipients exists (such as message exchange in sensor networks routing protocols, or the leader election process in sensors network). Authentication of every packet is very effective way to mitigate an attack, however, results in relatively increase in the end-to-end delay. To mitigate this drawback, the broadcast authentication protocols have been proposed. This paper deals with optimization of the broadcast authentication protocol DREAM parameters in a special case of fully N-ary tree topology.**

***Keywords- authentication; protocol; security; DoS; DREAM; N-ary tree***

## I. INTRODUCTION

One of the most impacting attacks targeting the selected server or the entire network is to accomplish a Denial of Service (DoS) attack. The most malicious is the Distributed DoS (DDoS) attack which is complicated to defend the overloading of the target. Such type of incident in the broadcasting communication can be prevented by verifying each packet's origin in the network. However, this method can influence and increase the time that the packets spent in the network and result into almost impossible communication. This issue can be resolved by using the DREAM (DoS-Resistant Efficient Authentication Mechanism) [1] protocol when broadcast communication network is in use.

## II. DREAM PROTOCOL

DDoS is so powerful since it uses multiple systems as resources of the attack and therefore is much stronger than a single source attack. DREAM mitigates the DDoS impact by involving analogous approach which the DDoS uses itself. The difference is that in the verification process, more stations are involved. The DREAM protocol can operate in two modes: normal and secure. Every incoming message is authenticated by the network node before being sent to the outgoing interface in the secure mode. In the normal mode, some of the messages are sent directly to the outgoing interface without being authenticated. This approach mitigates the potential single point of failure in the whole network since there is no single node where authentication occurs. The verification process is distributed among the neighboring nodes. The protocol functionality is influenced by the following parameters [2]:

- *NBR* – number of neighbors.
- *HT* – number of nodes that message passed without authentication. For such each node, the parameter is incremented by one. When the packet is authenticated *HT* is set to zero.
- *K* – maximum number of nodes, that can message pass without authentication.
- *b* – expected number of neighbors in unity distance from the source.
- *c* – expected number of neighbors in unity distance from the last node that forwards the message

The amount of messages to be sent or verified before sending out the interface is defined by the following decision rules (formulas):

$$Rand > \frac{b}{NBR} \tag{1}$$

$$Rand > \frac{2 \cdot c}{NBR} \tag{2}$$

where *Rand* is a random number generated by every node for every message in the range of 0 and 1 with the normal (Gaussian) distribution. The node decides for the first formula when the packet comes directly from a neighbor, the neighbor has been verified, or the parameter $HT = 0$. The node chooses the second formula in case when the message did not come from a neighbor, the neighbor has not been verified, or the parameter $HT > 0$

## III. MODEL OF THE DREAM MECHANISM

MATLAB environment has been used for the DREAM protocol simulation. The Figure 1 describes the DREAM protocol as a finite state machine using CPN-tools [3,4].

The general model of DREAM can be considered as compounded of six model fragments. By the assumption that the topology can be looped and every packet identified by the packet sequence number can be received repeatedly, the first model part provides a decision tool to detect whether a packet has been previously received or not. The source ID is verified in the second model part. Only messages sent by trusted neighbors are accepted. The third step sets the model mode to normal or secure state. In the secure mode all of messages are checked even if they were checked already. The mode is selected on the ratio of all the messages passing the system and forged ones. The next phase represents a decision process based on the number of nodes passed by the packet without being verified. If the current value is lower than the maximum allowed value, the message is directed into the verification queue before being sent to the following node. In this case, the HT value is set to zero after authenticated. Otherwise, the HT is increased by one a message sent. The sent packets which have not been verified prior to sending are additionally authenticated after being sent [2].

There are three ways how can the packet exit the model. The message is dropped (as duplicate, unverified neighbor, or a false signature), sent (without authentication), and counter count (number of true and false reports from the certification module).

The general DREAM model has been reduced according to considered assumptions which are explained in Simulation section. The modified model of the DREAM protocol is described in Figure 1.

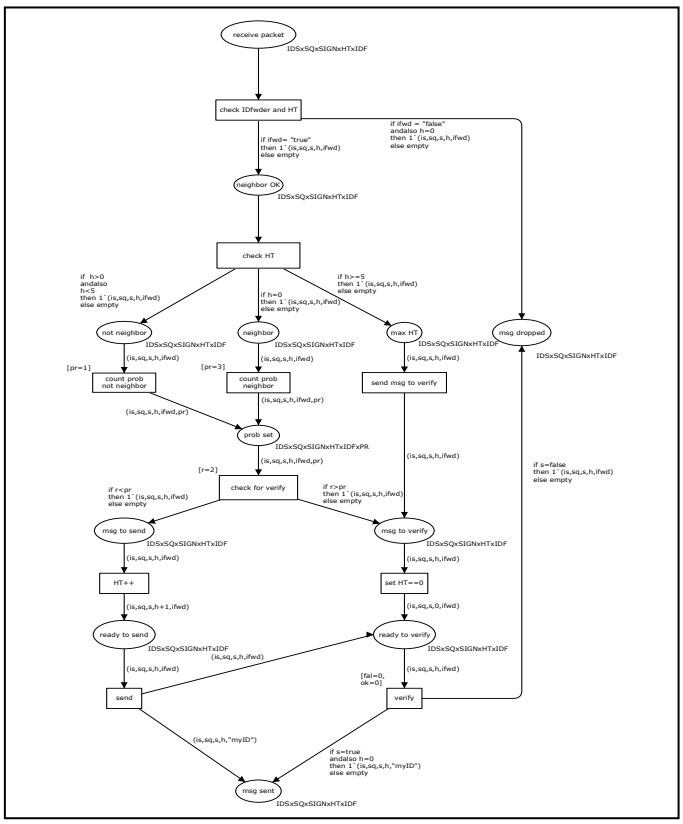


Figure 1. Model of the DREAM mechanism in an N-ary tree topology

## IV. SIMULATION

A time unit for authenticated and sent message has been determined as 100 % and the time unit for message sent without verification estimated as 20 % of the determined time unit. Since the duplicate message detection process checks only the received packet ID and a time unit of such procedure has been estimated as 1–2 %.

The simulation considers the following assumptions: if a duplicate packet is received, it is immediately dropped by the system. Such time is negligible compared to the verification and decision based times. Since a packet is being verified in every single node, a small amount of time is saved only by sending the packet before verification is executed. Such assumptions enable to change the general network topology into a loop free network scheme – into a tree and to omit the packet duplicity detection. Consideration that every single node of the tree topology is connected to the same number of neighboring nodes results into an N-ary tree topology.

For the simulation, the following expectations have been considered:

- The network contains only one transmitter. All other nodes are engaged into verification and forwarding processes only.
- The topology of the network is unchanged during the simulation, i.e., the number of neighbors does not change either.
- All the nodes are working in the normal (not the secured) mode during the whole simulation.
- Every node has exactly the same number of neighbors so the network topology represents a fully N-ary tree and resulting into the loop-free topology.
- Values *c* or *b* lesser that zero cause the model to enforce each node to work in the secure mode resulting in verification of all incoming messages before sending them. On the other hand, values $c \geq NBR/2$ and $b \geq NBR$ cause that each node sends the message without being verified. Therefore the parameters *b* and *c* have been selected with respect to the formulas (1) and (2) to ensure the random model behavior. This means that the parameters b and c must conform the following conditions (3, 4):

$$0 < b < NBR \tag{3}$$

$$0 < c < \frac{NBR}{2} \tag{4}$$

To limit the network topology and to respect the practical application of the simulation, a *length* variable has been determined and defined as follows: the *length* is the maximum number of nodes in a row to be passed by the message from the transmitter to the last node (a leaf of the tree). Since the total number of all nodes depends on *NBR* and *length* parameters, it can be counted as (5):

$$\sum_{i=0}^{length} \frac{NBR^i}{NBR-1} = \frac{NBR^{length+1}-1}{NBR-1}, \text{ where } NBR \neq 1 \quad (5)$$

To reflect the practical usage of this simulation, the *length* variable has been selected with respect to the *NBR* variable to generate at the most million of nodes in total.

The selection of the parameter *K* value higher than the *length* value does not affect the simulation. The packet cannot get further than the maximum network length.

$$0 \leq K \leq length \quad (6)$$

## V. RESULTS

Considering the previously mentioned parameters and simulation conditions, the results are shown as follows.

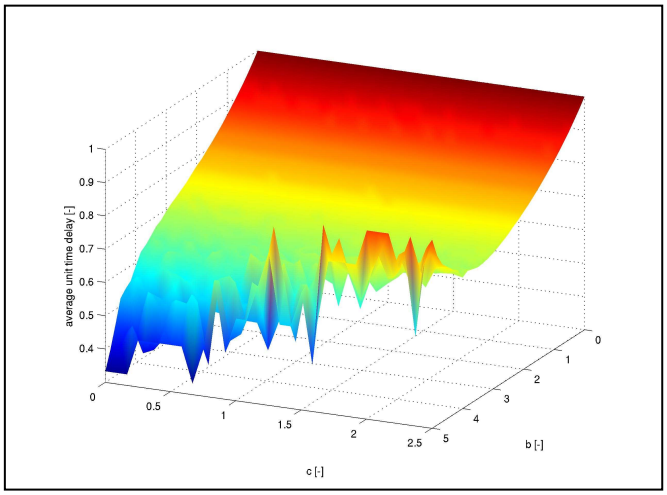


Figure 2. Average unit time delay, K=1, NBR=5, length=8

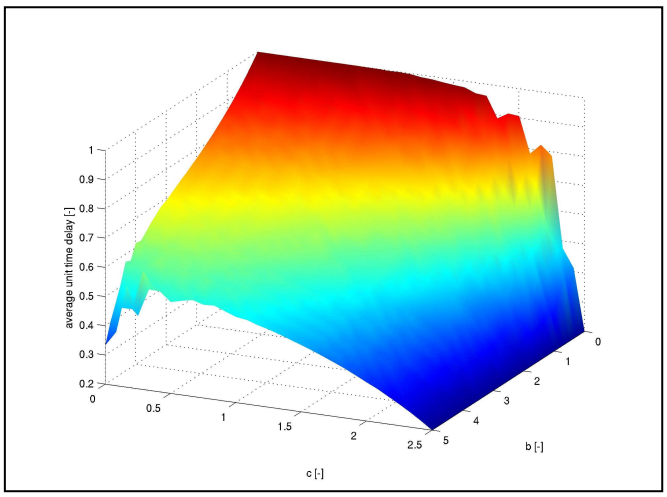


Figure 3. Average unit time delay, K=2, NBR=5, length=8

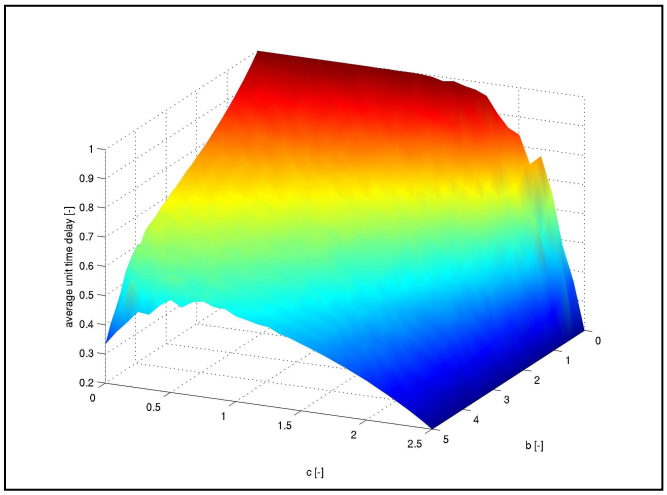


Figure 4. Average unit time delay, K=3, NBR=5, length=8

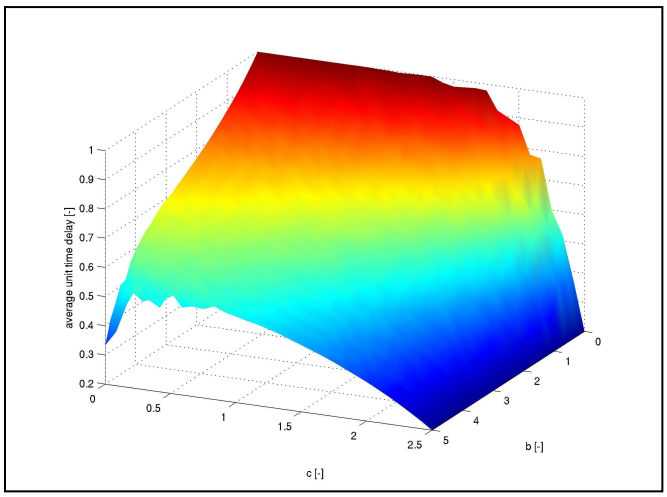


Figure 5. Average unit time delay, K=4, NBR=5, length=8

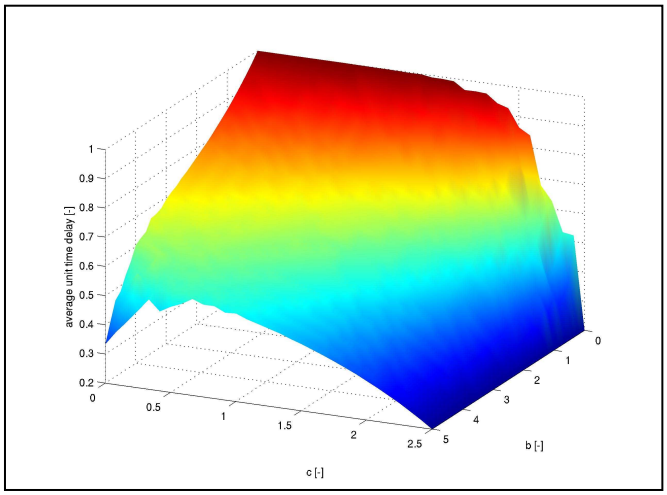


Figure 6. Average unit time delay, K=5, NBR=5, length=8

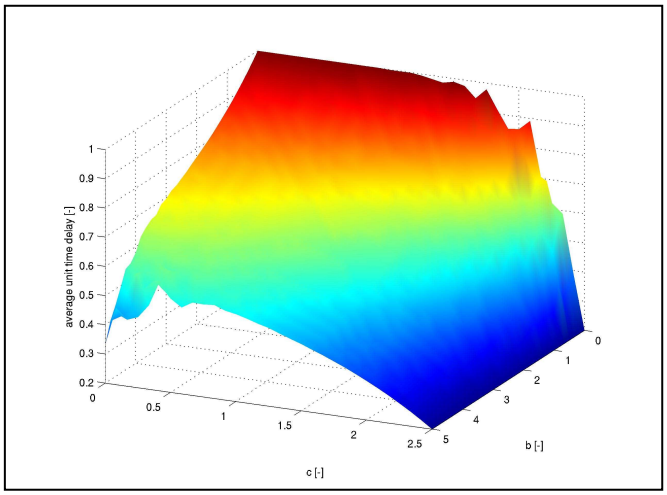


Figure 7. Average unit time delay, K=6, NBR=5, length=8

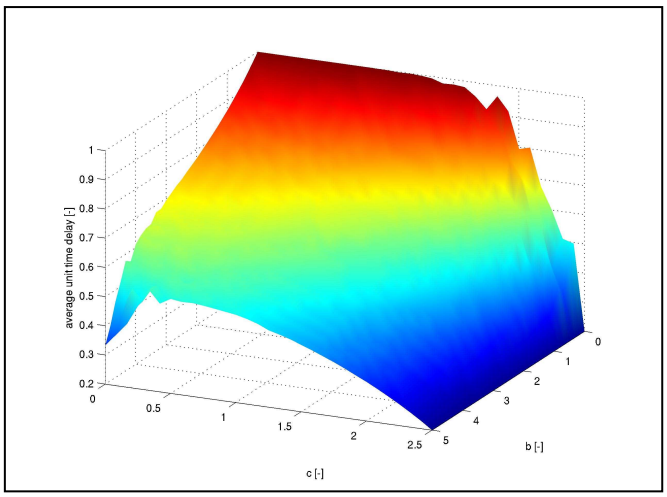


Figure 8. Average unit time delay, K=7, NBR=5, length=8

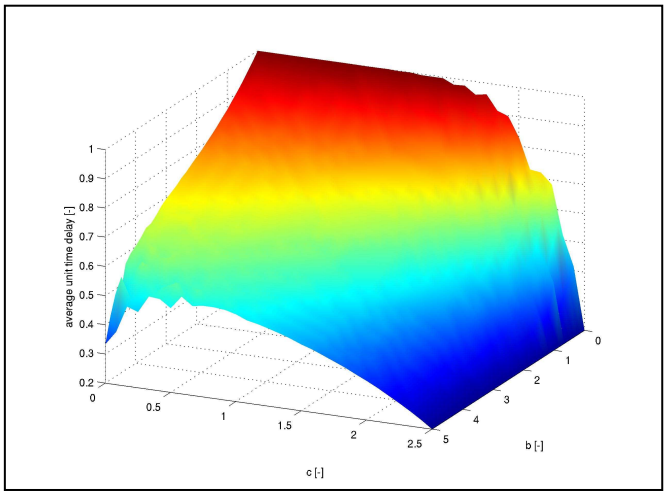


Figure 9. Average unit time delay, K=8, NBR=5, length=8

The simulation verified the importance of process selection of particular parameters. Incorrect choice of *b* a *c* parameters values can affect the protocol behavior. To ensure the model works correctly and retains the random character, these two parameters must be chosen with respect to the conditions (3) and (4). Similar recommendation applies to the parameter *K* which does not have sense to select otherwise than with respect to the condition (6).

Simulating the same network topology (equal *NBR* and *length* values), the average unit time delay tends to the value of unit time delay of model when no verification occurs in the nodes (Figures 2 – 9). The difference is only for K=0 (verification in every node is enforced) and K=1 when the verification process proceeds very often when compared to the total number of nodes (Figure 2). This behavior results into DREAM model independency on the *K* value (higher than 1) in the N-ary tree network topology.

Since there have been considered several assumptions resulting into the N-ary tree network topology, such topology has a practical drawback which is suppressed network redundancy and resiliency, and the message reaches several network nodes significantly faster than the others.

## ACKNOWLEDGMENT

This research work was supported by MSMT under the project no. MSM 6840770038.

## REFERENCES

[1] Huang, Y., He, W., Nahrstedt, K.; Lee, W.C. DoS-Resistant Broadcast Authentication Protocol with Low End-to-end Delay [online], 2008. <https://www.ideals.uiuc.edu/handle/2142/11432>

[2] Vanek, T., Rohlik, M. Model of DoS Resistant Broadcast Authentication Protocol in Colored Petri Net Environment, In *IWSSIP 2010 Proceedings* [CD-ROM]. Rio de Janeiro: EdUFF – Editora da Universidade Federal Fluminense, 2010, p. 264-267. ISBN 978-85-228-0565-5

[3] K. Jensen, "Coloured Petri Nets: Basic Concepts, Analysis Methods and Practical Use", Volume 1, Springer, 1996.

[4] ALY, Salah, MUSTAFA, Khaled. Protocol Verification And Analysis Using Colored Petri Nets [online], 2003. <http://facweb.cs.depaul.edu/research/TechReports/TR04-003.pdf >

# Random number generation

Jiri Sobotka
Department of Telecommunications
FECT, Brno University of Technology
Brno, Czech Republic
sobotkaj@feec.vutbr.cz

***Abstract*—Modern cryptographic algorithms deals with problem of generating true random numbers for the key creation. Each key has to be different from others and the level of differentness depends on the level of the randomness of the generated numbers. This article deals with problems of true random number generation and pseudo number generation. In our work, software for random number generation by user behavior was developed and the randomness of generated numbers was tested.**

***Keywords-Random number; True random number generator; Pseudorandom number generator, Cryptography***

## I. INTRODUCTION

Random numbers and their generation are part of our everyday life, although most people never heard of them. As an important part of cryptography, random numbers are used for example to key pair generation. Random number generations are important part of software simulators, electronic games and cryptographic algorithms.

In the field of random number generation are two important terms – PRNG (Pseudo-Random Number Generator) and TRNG (True Random Number Generator). Main difference is the way of implementation. Software RNG are generally considered as PRNG, because the randomness is calculated by some algebraic function or from specific tables, and the pattern of outputing numbers can be repeated. The sequence of the generated numbers only appears as random, thus is called pseudorandom. Generators of true random numbers are implemented in hardware form. Hardware random number generators usually use some physical phenomenon as a source of random numbers. As a TRNG can be considered a software application which is generating random numbers by unpredictable behavior of human operator, like mouse movement, pressing the keys of the keyboard and so on.

## II. PSEUDORANDOM NUMBER GENERATION

Common type of pseudorandom generator is Linear Congruent Generator, which is also one of the oldest types [2]. Pseudorandom generators are working with initialization numbers called seed. For example a system time can be used for a seed. The seed data are an initial value for the generating algorithm. Pseudorandom generators have a representative function in many programing languages.

### *A. Random numbers in C/C++*

C/C++ programing language has standardly defined function **rand ()**, which returns pseudorandom number between 0 and **RAND_MAX** [4]. In order not to generate still the same number, it is important to correctly setup the function by **srand(unsigne seed)** , which initialize the generator. In the case of inserting a constant number, the every run of the generator would produce the same random number. Thus is important to insert a variable. The correct operation of the function **rand()** is with this setup of srand: **srand(time(NULL))**. The **time()** method returns a number of seconds from 1st of January 1970 so the singularity at every run of the generator is ensured. The value of the number of seconds is an integer type and therefore when inserting the same values for initialization of the generator, same numbers are generated. In Borland C++ Builder is as other option a function **randomize()**, which performs a setting at system time **(srand(unsigned)time(NULL)))**.

One example of generating 5 numbers is the following source code. It hase been used in two development tools (Borland C++ Builder 6 and Microsoft Visual Studio 2008):

```
□include □stdli□h□
□include □stdio□h□
□include □time□h□
void main□void□
□
        int i□

        □srand□□□□□□□e□ample of initiali□ation □y constant value

        srand□time□NU□□□□□□initiali□ation □y system time value

        printf□□Five random num□ers from □ to □□n□□□

        for□i□□□i□□□i□□□

        printf□□□ d□n□□rand□□□ □□□□□calculation of modulo □□ from
        generated num□er
□
```

When setting the seed as constant number, with every generation the same numbers are generated. In C++ Builder its numbers 0;2;1;4;4 and in Visual Studio numbers 1;6;6;8;2. In both cases the generators are working in the same way and with same seed, but with different equations.

### *B. Random numbers in Java Language*

In Java language the situation is similar. The method used here is called **Random()**. The description can be made by a piece of source code:

```
□andom rand □ ne□ □andom□□□□initiali□ation □y a system time

□rand□setSeed□□□□□□setting of initiali□ation value
```

for□int i□□□i□□□i□□□System□out□println□rand□ne□t□nt□□□ □□□□

Initialization seed can be inserted directly into the constructor **Random(long seed)**, or by **setSeed(long seed)**, as is displayed in the code. If no initialization value is inserted, the system time is automatically used, which is done so by setup of initialization value at **System.currentTimeMillis()**.

## III. TRUE RANDOM NUMBER GENERATORS

True random generators depend on physical phenomenons as radioactive decay, atmospheric noise, photoelectric effect and others. TRNG can be also based on the human operator behavior, as mouse movement or the typing on the keyboard. In our work we have designed software application which generates random numbers by mouse clicking.

### *A. Generators based on physical phenomenons*

The random numbers are generated by physical phenomenon. Important part is transfer of the information to the computer. As an example can be described generation of random numbers by radioactive decay, because it is very reliable and tamper resistant. The time of the decay is completely unpredictable and easily detectable. One of the implementations of this kind of TRNG is HotBits [5]. As a source of radiation is used isotope cesium 137Cs, which has half-life 30,17 years. During decay is this isotope turned into metastable core of barium 137Ba, which has half-life 156 seconds. The barium 137 is a source of gama radiation.

For detecting the radioactive decay is used detector from Aware Electronics, model RM-80, which is connected by serial port. Captured data are the difference between two changes in radioactive decay, detected by Geiger-Müller counter.

The decay is taking place in random time and this unpredictability is used for generating numbers. The time between two impulses is measured ($T_1$) and then a time between two following impulses ($T_2$). If those times are the same, new measurement is done. If not, the values are compared. If $T_1>T_2$, the result is binary 1. If $T_1<T_2$, the result is binary 0.

### *B. Generators based on the human operator behavior*

The generator based on mouse movements can be used for generating short string of random numbers. During the movement of the mouse the coordinates are recorded and then, by certain algorithms, the number is generated. Example is Randomgen [3], which beside mouse movement uses system information, which changes frequently. In particular it is size of free memory and swap area. For using the keyboard as a source of input values, the keystrokes frequency, time between strokes or sequence of pressed keys can be used. But because the operating system is storing the keystrokes in buffer and sends them to the software once in a time, the result can be dissorted.

## IV. DESIGN OF THE SOFTWARE FOR RANDOM NUMBER GENERATION

In our work we have designed software for generating numbers based on mouse clicks in differ points of software window. Important part of our application is a hidden picture, associated with the area on the screen. The software can be set up to show the picture for presentation purposes. The area for clicks size of 800 x 600 pixels, according to the picture used. When the user click's somewhere in the area, a coordinates for X and Y axes are recorded together with the pixel at the point of click. The values of the color component (R,G,B) are extracted and the generated number is determined by following equation:

$$V = DM + (R + G + B) \bmod (HM - DM + 1)$$

Where V is generated number, DM and HM are bottom and top point of generated numbers range.

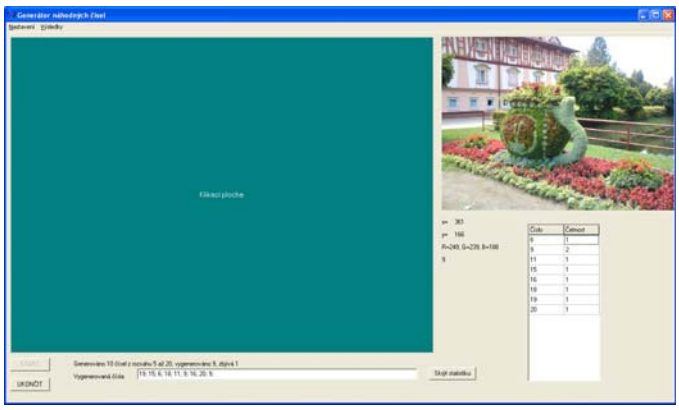

Fig. 1: Screen of the random number generator

### *A. Results*

Before start of the number generation, a quantity of generated numbers can be inserted. Then the user is asked to make clicks in the clicking area. For each click a one number is generated. The result is a table of generated numbers as displayed on Fig. 2.

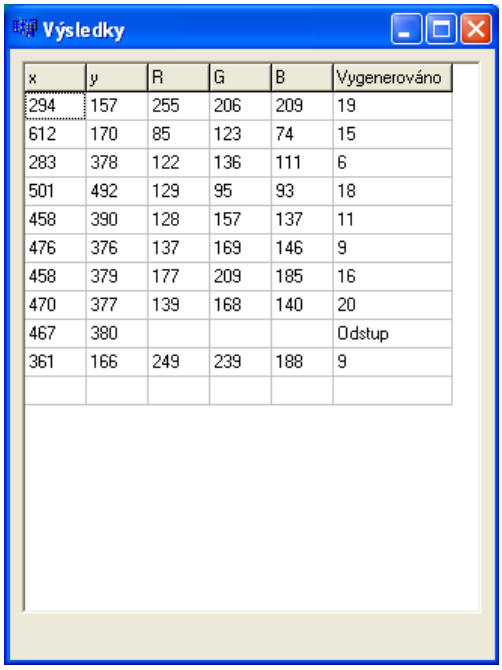


| x | y | R | G | B | Vygenerováno |
|---|---|---|---|---|---|
| 294 | 157 | 255 | 206 | 209 | 19 |
| 612 | 170 | 85 | 123 | 74 | 15 |
| 283 | 378 | 122 | 136 | 111 | 6 |
| 501 | 492 | 129 | 95 | 93 | 18 |
| 458 | 390 | 128 | 157 | 137 | 11 |
| 476 | 376 | 137 | 169 | 146 | 9 |
| 458 | 379 | 177 | 209 | 185 | 16 |
| 470 | 377 | 139 | 168 | 140 | 20 |
| 467 | 380 | | | | Odstup |
| 361 | 166 | 249 | 239 | 188 | 9 |

Fig. 2: Table of results

The application works with 12 pictures, which were modified for the used pixel range. In each run of the generator, one picture is pseudo-randomly chosen by **rand()** function.

We were analyzing the dependency of generated values on the image used. The pictures were randomly chosen from home archive. The results in the range of 0-9 generated values differ accordingly to used picture. All used pictures has resolution 800 x 600, which means, that each picture contains 48 000 pixels. Theoretically, the probability of generating each numeral should be the same in all pixels at all pictures. But accordingly to the Tab.1, the probability of generating each numeral is different at each picture. Pictures can be divided into 4 groups. Pictures 2,6,7,9 and 10 are in the tolerance 48 000 ± 1000 values of each numeral. Second group is with pictures 1 and 5, which are in the tolerance of 48 000 ± 2000 for each numeral. Third group are pictures 4 and 11, where the values are between 45 500 and 50 500. Last three pictures are in the fourth group, where some of the numeral has significantly higher values than the other numeral. For example pictures 3 and 12 have higher probability of generating numeral 5 than the other from the range 0-9.

| | 0 | 1 | 2 | 3 | 4 | 5 | 6 | 7 | 8 | 9 |
|---|---|---|---|---|---|---|---|---|---|---|
| 1 | 48860 | 48442 | 46569 | 48296 | 49384 | 49700 | 46817 | 47549 | 48059 | 46324 |
| 2 | 47049 | 48291 | 48839 | 48463 | 47744 | 48709 | 47963 | 47147 | 48381 | 47414 |
| 3 | 46805 | 46282 | 46223 | 46509 | 48160 | 61293 | 46130 | 46165 | 46510 | 45923 |
| 4 | 46862 | 49694 | 47758 | 47456 | 48099 | 48946 | 46693 | 46967 | 50165 | 47360 |
| 5 | 47039 | 47181 | 49367 | 48068 | 48077 | 49275 | 48229 | 47654 | 47218 | 47892 |
| 6 | 48167 | 47937 | 48062 | 47893 | 48524 | 47466 | 47763 | 47824 | 48247 | 48117 |
| 7 | 48115 | 48054 | 48491 | 48288 | 47543 | 48350 | 47930 | 47493 | 48144 | 47592 |
| 8 | 55872 | 54419 | 56443 | 42836 | 36737 | 40035 | 48594 | 40420 | 48734 | 55910 |
| 9 | 48950 | 48111 | 47410 | 48118 | 48250 | 47342 | 47777 | 48313 | 47830 | 47899 |
| 10 | 48607 | 47316 | 48037 | 48632 | 47795 | 47985 | 48578 | 47730 | 47136 | 48184 |
| 11 | 45582 | 47512 | 47813 | 47028 | 48687 | 48369 | 50281 | 47427 | 48544 | 48757 |
| 12 | 44521 | 45015 | 45578 | 45130 | 46245 | 74945 | 44648 | 44229 | 45130 | 44559 |

Tab. 1: Number of numerals 0 – 9, which can be generated at each picture

## V. RANDOMNESS OF THE GENERATED NUMBERS

The generated numbers were examined for the randomness, whether are really true random number, or just pseudorandom.

### *A. Randomness of the numbers*

For testing the numbers for the randomness can be test from several sources, classical tests [15] or theoretical [19].

Classical tests are frequency test, pairs, series, sequences and autocorrelation test. There are several testing batteries-software performing several different tests. Some examples:

- FIPS 140 – 1
- FIPS 140 – 2
- NIST Statistical Test Suit
- DIEHARD
- ENT

For example, the NIST contain 16 tests and DIEHARD 15 tests.

### *B. Testing of the numbers*

For our purposes we have used a test batery ENT [17]. Result of this test is the entrophy, arithmetic mean, Monte Carlo for π and serial corelation coefficient.

Results of the ENT test were slightly different accordingly to the used picture as in the previous test, but all of them past the tests for randomness with deviations less than 1%.

## CONCLUSION

There are two kinds of random number generators. In our paper we are presenting a software true random number generator based on the behavior of the operator. Numbers are generated accordingly to the clicking of the mouse in a field representing one of the 12 pictures. With each click a new number is generated. The numbers were then satisfyingly tested for the true randomness and aour application has been proved to be used as a source of true random numbers for creating certicates or keys for encrypting messages.

## REFERENCES

[1] ZOUHAR, Petr. Generátor náhodných čísel. Brno: Vysoké učení technické v Brně, Fakulta elektrotechniky a komunikačních technologií, 2009. 24 s. Vedoucí semestrální práce Ing. Jiří Sobotka.
[2] GLOMBÍKOVÁ, Viera Generování náhodných čísel : Pseudonáhodná čísla Přednáška [online]. 2008 [cit. 2009-11-21]. Available online: <http://www.kod.tul.cz/info predmety/Psi/prednasky 2007/prednaska 08/ Generovan 08.pdf>.
[3]BrotherSoft.com. Download True random number generator, True randomnumber generator 1.0 Download [online]. c2002-2009 [cit. 2009-11-21]. Available online:<http://www.brothersoft.com/true-random-numbergenerator-169743.html>.
[4]Srand - C++ Reference [online]. c2000-2009 [cit. 2009-11-21].Available online: <http://www.cplusplus.com/reference/clibrary/cstdlib/srand/>.
[5]WALKER, John. HotBits: Genuine Random Numbers [online]. May, 1996, last update: September 2006 [cit. 2009-12-08]. Available online: <http://www.fourmilab.ch/hotbits/>.

# Secured monitoring probe with highly redundant WAN connection

Lukas Macura, Jan Rozhon, Filip Rezac, Jiri Vychodil, Miroslav Voznak
Department of Telecommunications
VSB - Technical University of Ostrava
Ostrava, Czech Republic
jan.rozhon@vsb.cz, lukas.macura@vsb.cz, filip.rezac@vsb.cz, miroslav.voznak@vsb.cz

*Abstract*— **Many companies in the industry and automation often face the need to collect and send the data in a secure and highly reliable way. Starting with images taken by cameras in the remote storehouses, through voltage measurements in key areas of factory to connection quality monitoring in datacenters all the data must be processed and transmitted to the monitoring centre for further processing securely and reliably. Security is essential to prevent an unauthorized access to sensitive data while reliability is a keystone to maintain stable overview of the measured or monitored environment. This problem is solved by the highly reliable industrial computer design which provides very expensive solution though. In this paper, we will present the idea of a cheap secure and reliable monitoring probe design built upon mainstream router and open-source Linux platform OpenWRT. The whole solution is highly manageable, configurable and cost effective.**

***Keywords-ASUS WL-500g Premium router; OpenWRT;WAN redundancy; 3G connectivity***

## I. INTRODUCTION

To manage and control industrial processes, to allow surveillance data to be securely transmitted to the control center, or to monitor network purposes we need a device that would allow for reliable data transmission. This device could utilize a usual design based on the industrial computers, or it could utilize more general approach represented by a multipurpose hardware platform running some sort of open software. Although the first approach is used in the most of the cases the second one offers huge advantages including manageability and ease of enhancement because of the open software. Moreover, the usage of general hardware that on one hand is designed to reliably work for long periods of time and on the other hand is generally available to wide public can decrease the cost of the final solution making it highly cost-effective.

The main aim of this work is to present the general idea of the described device, name its most important components, provide some basic information about the possible software platforms and most importantly introduce the prototype of the final solution. In this paper the working example of the proposed monitoring probe will be introduced and described. The main reason for presenting this idea and concept is to support the cooperation among academic and industrial subjects and to prove such cooperation can result in the benefits of all sides.

The final goal of our work is to create the device that would be accepted by industry and used in some real installations.

## II. CONCEPTUAL DESIGN

First we need to decide what system we are going to use. This choice is highly important, because the system determines how freely we can proceed in choosing the hardware platform. To be more specific, if we decided to use for example an x86 system we would face serious troubles in finding suitable hardware, which would also be cost-effective. In this case we would create an industrial version of a personal computer and that is not our goal.

From the most commonly used operating systems Linux has the widest pallet of its variants. We can see numerous distributions for x86 platform, as well as for the RISC platform, which undergoes fast development drawn mainly by the smartphone industry now, therefore choice of hardware should not be an issue with Linux. There are variants of Linux-based operating systems that can be run on the hardware platform with limited performance and except of that Linux is considered to be stable, which is why it is used in many industrial installations (servers, datacenters, etc.). From the given we can assume some of the Linux-based operating systems could be used for our purposes making it stable, reliable and cost-effective. The big advantage of the Linux based operating systems is the open-source community, which provides support and development for the system.

Due to the initial idea of a probe it is clear that the final device will have limited hardware resources, therefore a minimalistic Linux distribution must be chosen. From the available software OpenWRT [1] operating system is the best choice because of its minimalistic design, huge hardware platform support and active community of developers. This operating system offers significant freedom in choice of the hardware, but to achieve two main points of our initial idea – redundant WAN connections and cost-effectiveness, we need to choose hardware that is generally available to wide public. This hardware should also be able to perform other tasks than just sending and receiving data securely, e.g. compression

capability could be also highly desired. The hardware design concept is depicted on the figure 1.

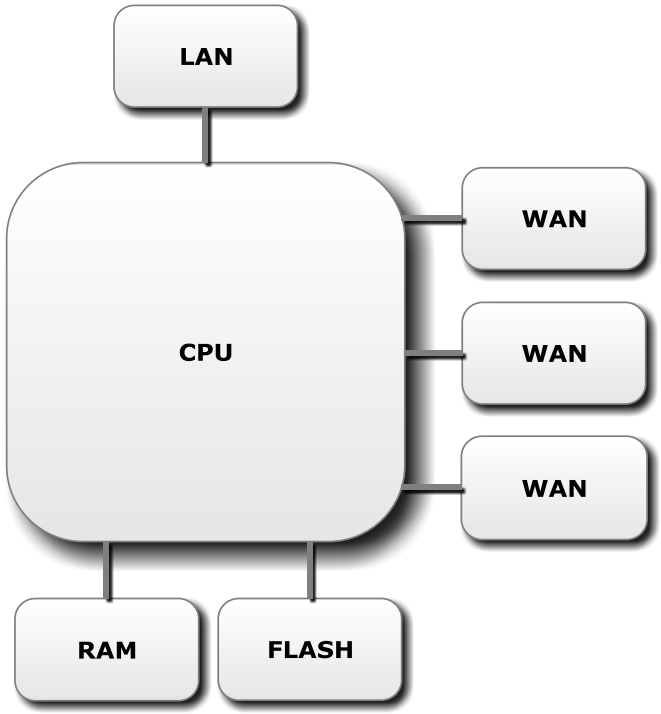


Figure 1. Basic Block diagram of the proposed device.

The figure shows two aspects that haven't been discussed yet. First, the shown LAN connectivity is required because of the need for connecting measuring device to the probe. Second, although the other type of a permanent storage could be used instead of the flash memory, the flash memory offers sufficient reliability, low power consumption and has no moving parts, which makes it more resistant to tremors.

## III. HARDWARE AND SOFTWARE REALIZATION

As a hardware platform we decided to use mainstream router ASUS WL-500g Premium, which is capable of running already mentioned OpenWRT system and has two possible WAN connections built in – Ethernet WAN interface and Wifi module. In addition it offers two USB ports, which can be used as connection to other WAN interfaces.

To perform routing this router accommodates 264 MHz processor of MIPS architecture, 32 MB of DDR memory and 8 MB of flash storage. All these parameters are sufficient to run the OpenWRT system [2] fluently and provide enough space for further enhancements. The limiting factor of this device is the Flash memory, which might be an issue when many packages are needed. If larger memory or higher performance is needed, there are also other platforms that could substitute ASUS router, e.g. RouterStation PRO, Mikrotik RB411U, etc. These options are however much more expensive.

The choice of software has already been outlined. The OpenWRT operating system is extremely efficient when utilizing hardware resources and only about 6 MB of disk space is sufficient for it. It supports common Linux shell system and the package management for installing additional software (packages). Because of the mentioned features the work in OpenWRT is very similar to work in any other Linux system. OpenWRT offers one advantage though. The configuration interface called UCI allows users to access and set most system variables in a unified manner.

In the package repositories of OpenWRT we can find vast number of packages, therefore an additional functionality can easily be implemented including encryption and compression algorithms.

The presented information gave us the base for creation of a more specific design. The probe will consist of a router running OpenWRT system and will be connected to the measuring device or devices if needed by its LAN ports, while secure transmission and reception of data will be performed by Ethernet WAN connection which in case of a malfunction will switch to WiFi link, or better some secured connection via USB port, for example 3G connectivity. This whole design is summarized and depicted on figure 2.

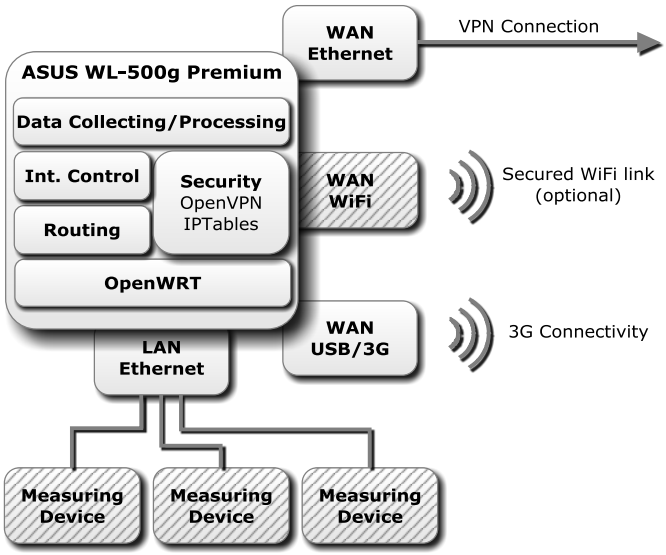


Figure 2. Hardware and Software diagram with possible physical connections to the control center.

To achieve secure connection and security in general a secure link to the control center must be established as well as internal security rules for communication between device and control center must be set. This is implemented by VPN connection over the Ethernet WAN link and internal mechanisms of the 3G connection protocol. WiFi connection is also possible but is not preferred because of the short range provided by the device. Internal security rules are implemented mainly by firewall restrictions, which are applied to the incoming, outgoing and forwarded connections.

In the final implementation two basic scenarios can be applied. First, the probe will function as the transceiver for the data measured or captured by another device. In this scenario the probe will ensure only the security elements and possible data processing algorithms, but will not be a source of the data.

Second, the probe will work as the source of data as well, e.g. for quality measurements in the data networks. In this case no special measuring or data collecting device is required, therefore the "Measuring Device" block in the figure 2 are marked as optional, which is represented by hatch fill of the block.

## IV. CONFIGURATION

In the previous sections the general design and choice of software has been presented. All of the presented ideas has been proved as functional and useful by other users of the OpenWRT system, which means the main contribution of the previous sections lies in applying of existing methods and resources to the new environment, but generally no new thoughts has been added. This is where this section differs. To be more specific, the configuration of the device so it is able to communicate over secure VPN connection and in the case of malfunction to switch to multiple 3G links has not yet been implemented successfully. Moreover, the provisioning system so that the probes can get most recent system and packages together with MAC address specific configuration has been developed. These two main contributions of our work will be presented in more detail in the following subsections, but except of that many partial modifications to the configuration scripts were applied, e.g. QoS settings were defined and tested, 3G modem scanning was linked to "ifup" function, multiwan support was modified, firewall setting were defined, easy-to-use compilation system was developed, etc.

### *A. Multiple WAN Configuration*

To ensure that the probe has the stable and reliable connection to the control center multiple WAN support was implemented. The physical connections were realized by VPN connection over the Ethernet WAN link and three 3G connections to three different providers. Each connection was assigned weight, which defined the preference of that particular connection based on available bandwidth and cost of the data transfer over the connection. Moreover, due to the extremely different bandwidth between Ethernet and 3G links the rules defining what data can be transferred over each link were defined to ensure that over slow and expensive 3G links sizeable data such as video transmissions won't be transferred. In addition, the system must be able to recognize that any interface was disabled, which makes the configuration even more complex.

All these features are defined in three configuration scripts, which can be found in */etc/config/*, namely *serialmodem*, *multiwan and qos*[3-5]. First one provides the means for scanning the interfaces and assigning them to individual providers using the CIMI identification. To ensure this a patch needed to be developed because by standard configuration the successful recognition of the provider-specific device was impossible. Of course, the static port assignment could have been used, but if the devices were connected to different port the whole functionality would be lost. Sample of the *serialmodem* script is depicted on the figure 3. While *serialmodem* ensures definition and assignment of interfaces to individual providers, *multiwan* defines the weight of each link and the behavior of the device in case of failure. The links are preferred in this order:

1. VPN connection over Ethernet,
2. 3G connection – T-Mobile,
3. 3G connection – Vodafone,
4. 3G connection - O2.

```
config globals
   option debug 3
   option prewait 30
   option regwait 15
   #option fork 0

config group vodafone
   option devices "/dev/ttyUSB0 /dev/ttyUSB1 /dev/ttyUSB2"
   option linkby comgt-cimi
   option cimi 23003
   option linkto /dev/gsm/vodafone
   option pin 1234
   option ifup wanvf
```

Figure 3. Sample of serialmodem script.

To achieve full functionality the new interface in the configuration script */etc/config/network* needed to be added for each secure connection – VPN and 3G. This allowed for passing the login information to the devices and linking the devices with "ifup" function. The example of an entry for T-Mobile 3G modem is depicted on the figure 4.

```
config interface wantm
   option proto    3g
   option apn apn-name
   option apncid 1
   option apnpdptype PPP
   option apnpdpaddr 0,0
   option initstring '&FE1Q0V1&C1&D2S0=0S7=60&K3N1'
   option hcomp 0
   option dcomp 0
   option username user
   option password pass
   option device   /dev/gsm/tmobile
```

Figure 4. T-Mobile "interface" in the network configuration script.

The definition of what data can be transferred over what link is done in *qos* and *firewall* scripts and follows general rules defined for OpenWRT system.

### *B. Provisioning*

The device which is in default configuration starts all the interfaces after the startup automatically. If the initiation of any WAN port is successful the device looks in the created online repositories for a newer version of system and key packages. If those exist the device downloads them and installs them. After the successful installation the device reboots and looks for the configuration scripts stored in online repositories under the name, which is the same as the device's MAC address. If this file exists the device downloads it using HTTPS protocol and using a unified configuration interface imports the configuration to the system and after another reboot the device is ready to use.

To ensure that no malicious packages are downloaded only the most trusted interface can be allowed to successfully accept the packages.

## V. CONCLUSION

The functional prototype of the monitoring probe was designed and tested. This device offers huge potential for usage in any industrial or network environment, where the data collection and processing takes place on many remote locations. It allows for secure connection with the control center and provides multiple communication channels in case of a failure, which together with its durable architecture and low-cost design makes it an ideal choice for mass deployment.

Our future work will aim at improving the proposed design so that the device could be used in the real environment in cooperation with a partner from industry to prove the competitiveness of our solution.

## REFERENCES


[1] OpenWRT, URL: http://openwrt.org/.

[2] "Asus WL-500g Premium", URL: http://oldwiki.openwrt.org/OpenWrtDocs(2f)Hardware(2f)Asus(2f)WL500GP.html.

[3] L. Macura, "Patch for serialmodem for OpenWRT", URL: https://forum.openwrt.org/ viewtopic.php?id=26539.

[4] "Simple MutliWAN configuration", URL: http://wiki.openwrt.org/doc/uci/multiwan.

[5] "Quality of Service configuration", URL: http://wiki.openwrt.org/doc/uci/qos .

[6] M. Pravda, Z. Kocur, "Time Synchronization through Network Time Protocol and Improvement of Its Accuracy", In Proceedings of the TSP 2009: 32nd International Conference on Telecommunications and Signal Processing, 182-186, 2009.

[7] Z. Kocur, M. Safranek, "High Speed Mobile Communication", In Proceedings of the TSP 2008: 31st International Conference on Telecommunications and Signal Processing, 164-166, 2008.

[8] Z. Kocur, V. Machula, J. Kulda, "Analysis of Influence of Disturbance Level on Data Transmission in Wireless Networks", In Proceedings of the TSP 2010: 33rd International Conference on Telecommunications and Signal Processing, 292-296, 2010.

# Network technologies and Services

# The New Unified Platform for Services and Applications in NGN with Regard to Quality of Services and Network Security

Milos Orgon, Marek Lednicky
Department of Telecommunications
STU Bratislava, Ilkovičova 3
812 19Bratislava, Slovak Republic
orgon@klt.elf.stuba.sk, marek.lednicky@gmail.com

*Abstract*— **Actual trend for creating telecommunication services is to use platforms to develop them and implement them in mobile and fix networks considering next generation network requirements NGN. This paper describes new unified platform for NGN Services and Applications with regard to quality of services (QoS) and network security.**

***Keywords-component: Next generation networks; Network security; Quality of services; Platform for NGN Services and applications***

## I. INTRODUCTION

A next generation network (NGN) is a network able to provide telecommunication services and applications to users and able to make use of multiple broadband, QoS-enabled transport technologies and in which service-related functions are independent of the underlying transport-related technologies. It enables unfettered access for users to networks and to competing service providers and services of their choice. It supports generalized mobility which will allow consistent and ubiquitous provision of services to users.

In NGN, the backbone of the overall network architecture will be packet network, supporting different access network technologies; this backbone will be attached with different gateways to integrate different access network technologies.

At present in NGN services and applications have diverse bandwidth and performance needs. User devices have improving but varied capabilities. Different access technologies are in use. Multiple providers and firewalls are involved end-to-end. Networks and communications are vulnerable, while some actors are malicious or non-trustworthy. Security may mean:

- Limitation of data disclosure
- Privacy
- Anonymous communications
- Prevention of changing data in transit
- Law enforcement
  - destruction of pirated content
  - tracking criminals
  - monitoring enemy's communications
- Base packet transport lacks inbuilt support for hard security and QoS

QoS may mean:

- Satisfactory bandwidth or network performance (e.g., delay, jitter, packet error ratio, and packet loss ratio)
- Satisfactory application performance, such as signal-to-noise ratio, lip sync, channel change delay, and post dialling
- Carrier-grade network reliability
- Robust communication security
- Quality of experience of a user .

Collective effect of service performance which determines the degree of satisfaction of a user of the service (as defined in E.800).

## II. NEXT GENERATION NETWORKS IN SLOVAKIA

General requirements for NGN networks are under WQ4/13 (ITU-T) as follows:

- Only legitimate requests are satisfied
- Ensure confidence transactions
- Allocate and de-allocate resources (e.g., bandwidth) based on established policy
- Hide the network topology (e.g., IP addresses of all but a few entities) as necessary
- Be able to handle remote network address/port translation devices and firewalls
- Mitigate relevant Denial-of-Service (DoS) attacks.

From end-user perspectives side, mobile users should be connected anytime, anywhere, for any requested service or application, with the best quality of service (QoS). From these perspectives we can imagine that, the centric management for the NGN is complex, and should support end-users mobility, security and QoS requirements.

Ensuring quality of service (QoS) is closely related to security, because they are placed higher demands on network security, increases demands on the quality of services (e.g. increase the use of encryption causes delays in the network.

In the near future, mobile users, will be able to connect to different telecommunication applications, ranging from normal voice calls, web browsing and e-mail services, on-line streaming data, real time video conferencing, interactive

network games, and etc. All these applications need specific quality of services requirements, for example voice traffic is sensitive to packets loss, packet delay and jitter, which will result in voice degradation, something similar to voice corruption in cellular phone when the coverage area is low. In NGN, the existence of multiple network access will ensure that all applications receive acceptable quality of service (QoS) [1, 2]. There are currently many projects and proposals to integrate heterogeneous network technologies, to support the management and monitoring of QoS parameters in centric architecture to offer application session with the best resources in mobile environments', both for inter-domain and inter a domain level. In most of these studies, the proposed architecture, depends on network class definitions for diffServ, each network QoS class ensure edge to edge QoS guarantees, described by parameters as delay, jitter, packet loss and bandwidth availability. These architectures deploy policies for SLA (Service Level Agreement), it acts like contracts between end user and service providers to specify the SLS (Service Level Specifications) that determine the required resources to be reserved for specific application QoS.

In 2006 was finalised the research work of next generation networks for the use in Slovakia. The task of State program of research and development was focused on development of telecommunication networks and services in liberalized environment for area of convergent technologies [3]. In the project, the network emphasis was placed on networks of IP telephony, numbering in converged network, communication security, network of service, modelling, network traffic simulation and verification, management of converged network, strategy of new technologies migration to NGN solutions (Next Generation Network) from the point of view of manufacturers and providers of public and private communication network and technologies.

Proposed architecture of NGN network was based on basis of infrastructure of convergent network and it was framed to differentiate functionality to four independent layers: access layer, transport layer, control layer and layer of services and applications.

These layers are communicating with each other by opened standardized interfaces. Core of the network consists of only one packet oriented layer which is used for different types of service requirements and it is accessible independently on used access network.

Recourses of access layer cover connectivity of end users (subscribers) to transport network. End-to-End connection is realized by this layer. Transport layer provides adaptation of incoming flows from access systems to packet environment and consequently processes (switching, routing) traffic. Besides switches and routers, the transport layer consists also of other types of gateways (Trunking Gateways, Access Gateways, Residential Gateways, Wireless Gateways, etc.). Gateways provide connectivity and full value of TDM devices and networks in global NGN architecture. In control layer of architecture of NGN is centralized the intelligence of the network. Management of connections and of all operations related to providing services are realized by devices such as Call servers, signalization gateways etc. General management of network (OSS system), resources of IN, etc. are in separated service layer.

Among separate layers of NGN architecture there are standard open interfaces. Open interfaces give wide variety of scalability and elasticity of telecommunication network, broader opportunities for realization, providing and maintaining of services and single supplier independence.

Compared to today's architectures of NGN conception brings decomposition of network nodes. Initial network nodes in circuit switched network were presented as blocs containing own switching matrices of links of circuit interfaces modules with control functions and modules for management. Decomposition of network nodes introduces separation and centralization of individual functions.

## III. NEW UNIFIED PLATFORM FOR NEXT GENERATION NETWORKS

Layer of services and applications was designed in the manner to provide function of basic services, which would be used to create more complex and more sophisticated services and applications. These level group platforms of service logics also known as applications servers and platforms for diffusion of content so-called media servers. By providing of services and applications there are generated two additional models: one of them is also known as web services inspired by internet with distributed intelligence supported by community of informatics and network people and second which is more centralized, more based on functions of management servers, is supported particularly by telecommunication community. By second model standardized interface is provided OSA/Parlay (Open Service Access) for controlled access to third party services. Third party are new type of service providers who do not have own network infrastructure and therefore they can not connect with own network to the transport layer. They are creating and offering only individual services and applications on other(s) operator's networks.

Layer of services and applications so provide main functional blocks of services, there are to be used for the design of composite services for transmission and routing, communication and provision of an information content, access and billing, and others.

PARLAY GROUP introduces a new vision into the area of development of services and applications and systematically develops unified open application programmable interfaces that depend not on the technology. By that independent programmable interface is then possible to integrate also services with IT (Information Technology) applications. Listed interface should be safely measurable and should make possible also account. These facilities have lead us to integrate this independent programmable interface in the model of ICT structure [4].

Parlay specifications are being developed by the Parlay Group, a consortium of member companies that include AT&T, BT, Cisco, IBM, Lucent, Microsoft, Nortel Networks, and others.

Use of the Parlay specifications is expected to make interface easier to add new cross-platform network applications so that users need not depend solely on the proprietary offerings of carriers. The Parlay Group is not a standards group itself, but sees itself as a facilitator of needed interfaces.

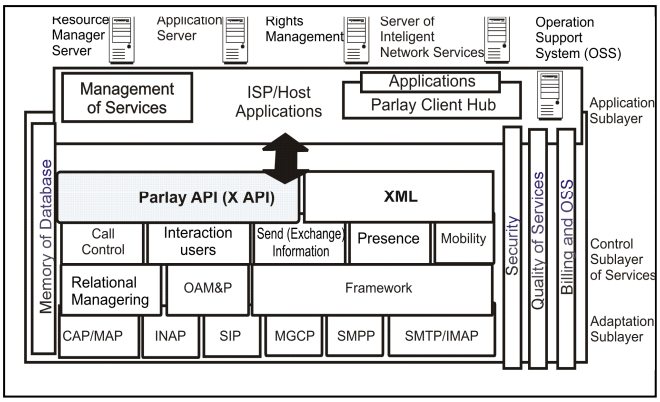


Figure 1. The Unified platform of services and applications, where ***CAP*** is CAMEL Application Part, ***MAP*** – Mobil Application Part, ***INAP*** – Intelligent Network Application Protocol, ***SIP*** – Session Interaction Protocol, ***MGCP*** – Media Gateway Control Protocol, ***SMPP*** - Small Message Peer-to-Peer Protocol, ***STMP/IMAP*** – Simple Mail Transfer Protocol/Internet Message Access Protocol, ***OAM&P*** – Operations Administration, Maintenance and Provisioning, ***OSS*** – Operation Support System, ***ISP*** Internet Service Provider

As Figure 1 describes consolidated platform (unified platform) of services and applications was divided to three sublayers – application sublayer, sublayer of control of services and applications and adaptation sublayer. A unified platform is based on OSA/Parlay structure (OSA – Open Service Access) and it creates solutions appropriate for fully secured services and applications in NGN networks.

Properties of unified platform of services and applications are following:

- It is a multiprotocol platform – supports CAP/MAP, INAP, CAMEL, WIN, SIP, MGCP etc. because it can support simultaneous providing of services of different networks.
- It isolates implementation of services through backbone, decreases investment into the network and also gives possibility to the continuous evolution of network.
- It allows modification of services due to user requests and provides more scalable services which were not possible to realize in traditional IN networks.
- It provides set of tools for development of standard services for third party service providers in consequence of better opportunities for both service provider and network provider.
- Application can be realized on multi application servers whereby higher reliability and continuous upgrade of system is introduced.

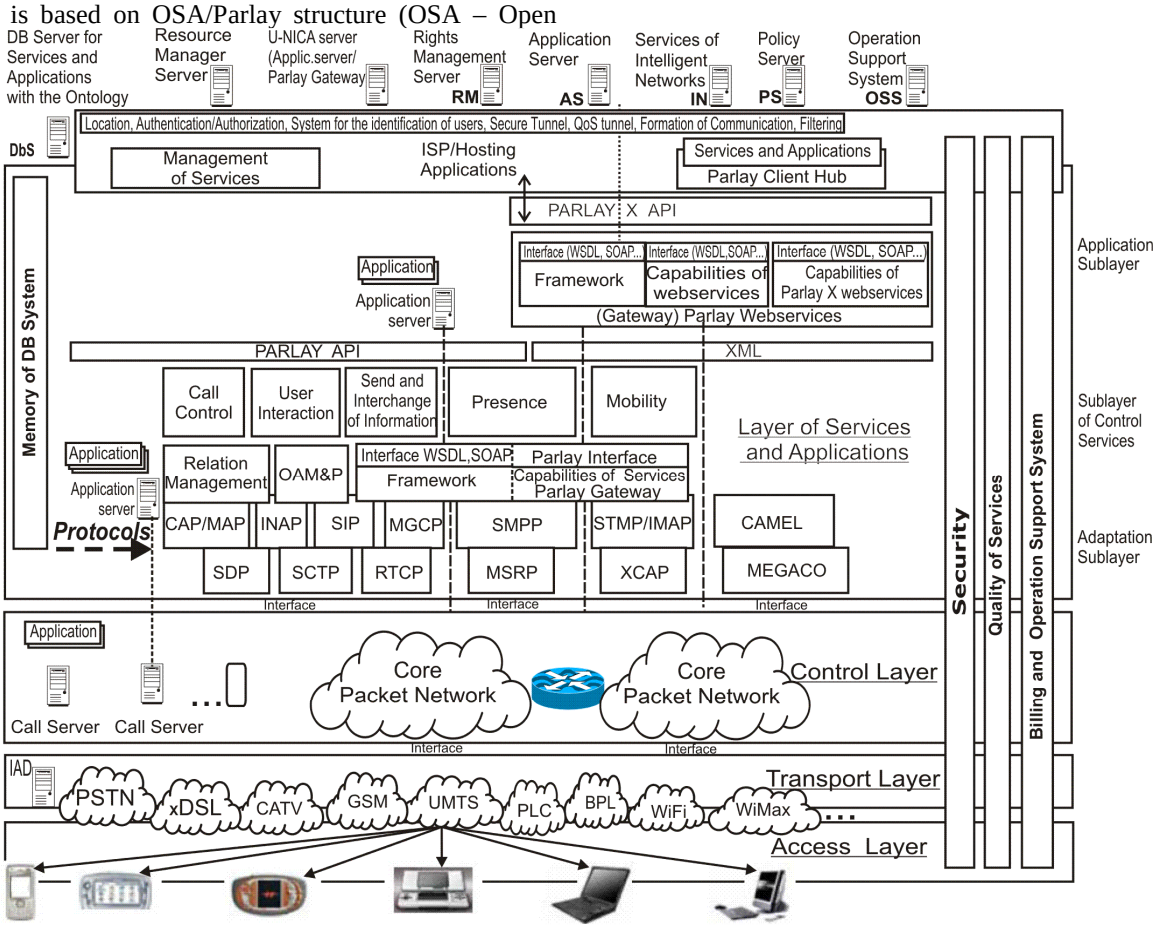


Figure 2. A new unified platform for NGN services and applications

Work on unified platform of services and application continued after finalizing of research and development [2] and result of this work was creating of the new unified platform of services and applications which is described on Figure 2.

API was enhanced to new web service usage which combines XML, WSDL and SOAP. These languages are considered as a main starting point needful for open mobile connection (OMA) to be able to research „cell“ web services. Individual sublayers have been also added – Application sublayer by Resource Manager Server, database

server for application with ontology interface for WSDL and SAOP, abilities of web services and Parlay X web services.

Sublayer of control of services was added by interface of Framework and Parlay gateway and Adaptation sub layer by CAMEL, XCAP, RTCP, STCP, SDP, MEGACO. Into the Application sublayer was also integrated: localization, system of identification of participants, authentication/authorization, possibility of creation of secured tunnel, QoS tunnel, establishing and filtering of communication. We can also see that application servers for different sort of applications segmented into the three sublayers and on the interface of transport layer – access layer IAD (Integrated Access Devices) were added.

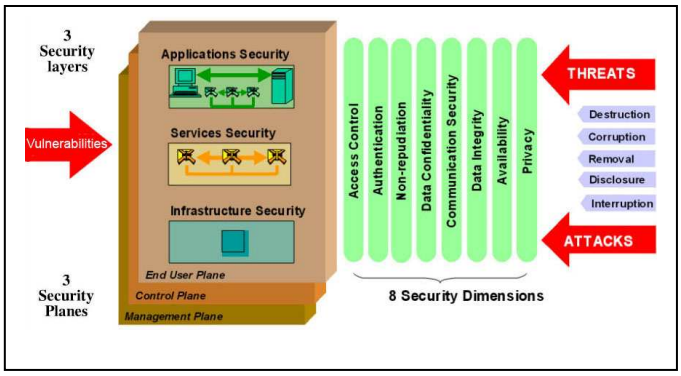


Figure 3. 72 Security perspectives (Rec. X.805 Security Architecture for End-to-End Communications)

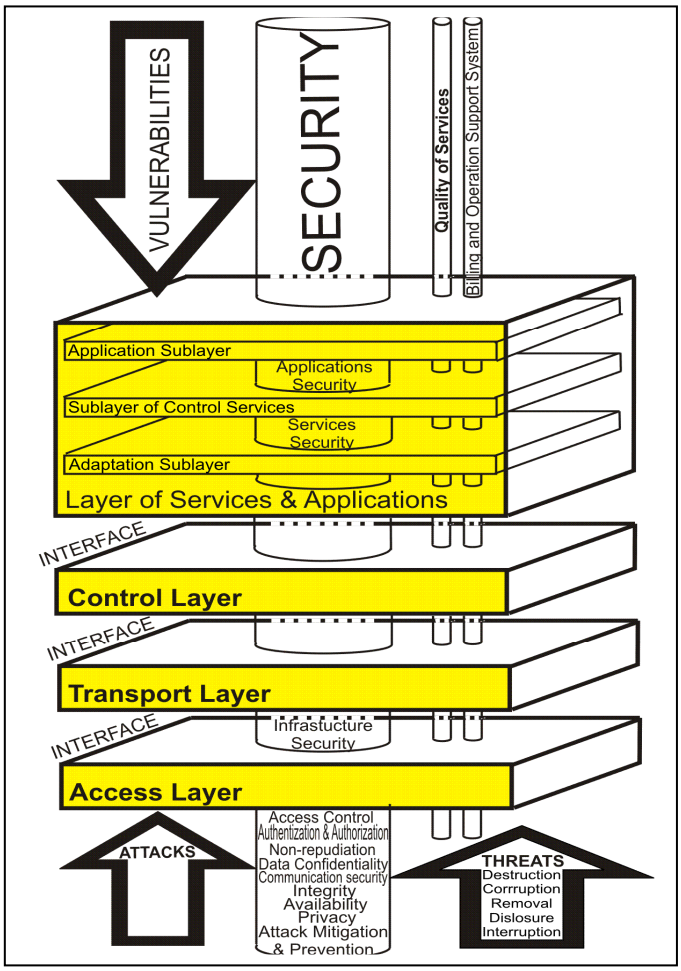


Figure 4. The security of NGN

The management for monitoring of each class QoS is a central manner for transport and access level networks. We propose to integrate QoS management architecture with dynamic access selector, allowing the end user to be always best connected on the best access network technologies, this to support end-users applications setup requirements, even while his roaming between different access networks, applications sessions should be supported continuously with soft handoff and without performance degrading.

In terms of security it should be noted that the security structure is much more complex than suggested by the rectangle in Figure 3 (see Figure 3 and 4).

shows the Network security, therefore, consists of 72 security perspectives (3 layers x 3 planes x 8 dimensions).

Access control is a major pillar of the security in the NGN architecture and as one of the most fundamental requirements for service delivery and business continuity. The security methodology provides an effective guide to developing a security architecture by helping to create a plan for defining, maintaining, and implementing security programs throughout the network.

The resulting architecture can then be applied to the service provider's security program through policies, procedures, and technologies.

The modern threats are following:

- **Reconnaissance threats** – Hackers scan network topologies to identify vulnerable devices and attack them.
- **Distributed-Denial-of-Service (DDoS) and infrastructure attacks** – These are IP packet-based attacks launched at the network infrastructure to compromise network performance and reliability.
- **Break-ins and Device Takeover** – These usually follow a reconnaissance and are the unauthorized access to a given device with the intention to compromise device security.
- **Theft of Service and Fraud** – This threat category pertains to the unauthorized use of network resources. Once the threats are identified, combating them requires the understanding of three basic principles, which include the following:
  - **Prevention** is the act of preparing a known defensive posture to prevent known threats. Prevention includes patching vulnerable systems, implementing standard and hardened system images, and implementing firewalls or other access control technologies.
  - **Monitoring** is the act of detecting potentially malicious and exploitative activities and differentiating between truly malicious activity and nuisance activity to understand the real-world threats that are encountered at key aggregation points. It involves deploying intrusion-monitoring technologies, conducting log analysis of servers and firewalls, and actively monitoring OS calls.
  - **Response** is the ability to act on the information discerned to control the impact of a confirmed real-world threat in near real-time.

Security in the NGN includes total visibility and complete control, based upon:

- **Identity and trust** – Identification of devices accessing to the network and inspection of credentials required to identify the state of trust
- **Telemetry** – Monitoring the effectiveness of security policies
- **Correlative intelligence** – Interpreting and transforming large data flows into meaningful operational information, which involves the contextualization of seemingly unrelated changes in posture, methods for determining violations of policies, or any combination of changes to posture that could affect guaranteed service delivery
- **Instrumentation** – Presenting the intelligence derived from audit logs, event monitoring, fault knowledge, and health and status information, and graphically displaying that understanding in the near real time
- **Virtualization** – Defining and interpreting policies for a logical device to a required posture
- **Policy enforcement** – Enforcing policies in response to an observation and how the policy defines the action required when that observation is contextualized Primary benefits of the Process Model for Service Provider Security include the integration of telemetry information, intelligent and collaborative management systems, cost efficiencies through virtualization, and a proactive and adaptive orientation for readiness against threats.

The NGN should allow a variety of authentication techniques to be used against the single user profile, such as name and password, SIM card, smart card, token etc. Thus the NGN may require an authentication broker and the NGN architecture may need to be expanded to support it. Whereas authentication provides a mechanism for ensuring that the user is who they claim to be, be it a person or a machine. Authentication does not, per se, allow the user access to the services of the NGN: this is the function of Authorization. The Authorization function provides information about what services an authenticated user may use within the NGN. Authorization may include not only the right to use basic communication functions, but also the authority to use Confidentiality services, priority service, etc. Access Controls are the mechanism that actually control access to an object based on whether the subject is authorized to access the object.

Non-repudiation is the ability to be able to prove that an action was performed - e.g., if a message is sent from an entity “a” to “b” and subsequently “a” denies having sent the message, with non-repudiation capability, “b” is able to prove that “a” did, in fact, send the message. This can be done by retaining records of all actions that were performed within the network by applications, management systems, or network services for a period of time. In the context of an NGN, an example of a situation requiring network support capability for non-repudiation is an action where the network triggers a billing event. User-to-user interactions may use other non-repudiation mechanisms and may not require network non-repudiation capabilities.

Confidentiality ensures that data is protected against unauthorized viewing in transit and that data is not disclosed to unauthorized parties. The application of data confidentiality mechanisms such as encryption and access control lists ensure that data cannot be understood by unauthorized entities and that information cannot be intercepted as it flows between authorized entities. The need for confidentially will vary depending on the network “plane” being considered and the particular security layer. For example, whereas as a service provider may consider confidentiality of signalling information a requirement to preserve the integrity of the network functions, confidentiality of user data may be considered a user responsibility. Thus, the requirements for confidentiality need to be specified across all “planes” of the network, across all security layers.

Communications Security refers to the need to ensure that communications between endpoints cannot be unlawfully intercepted or redirected. Availability is the need to ensure that the network infrastructure, services, and applications are available for use. This means protection from physical misadventures by the use of alternate routing and duplicated facilities, and also protection from such activities as DoS attacks and other malicious activities that would prevent access to facilities.

Integrity is the capability of ensuring that what goes in, comes out without having been modified. Integrity can be applied at different levels in a network. The requirements for integrity need to be specified across all layers of the network across all security layers.

Metrics for availability are discussed along with other performance metrics in the clause on QoS.

Privacy relates to preventing the unauthorized dissemination of information. For example, in the end of user plane, we need to ensure that network elements, services, or applications do not provide information pertaining to the end user’s network or use of services or applications to an unauthorized entity.

A next generation service provider should deploy mechanisms to mitigate attacks against its users and connected networks. It should also provide capabilities to shut down or prevent attacks originating from its network. To mitigate emerging threats when scaling to multi gigabit rates of traffic, service provider requirements have now shifted from using standalone security appliances to integrating security into the network infrastructure.

## IV. CONCLUSION

A new unified platform for services and applications in next generation networks with regard to quality of services and network security are presented in this paper. We have shown a possible platform which can be used by service providers in NGN networks The new platform was built so that in itself includes all the new specific requirements that need advanced services and applications designed for NGN networks, such as requirements for their security and ensure QoS (packets loss, packet delay and jitter, etc.).

## ACKNOWLEDGMENT

This work is a part of research activities conducted at Slovak University of Technology Bratislava, Faculty of Electrical Engineering and Information Technology, Department of Telecommunications, within the scope of the projects VEGA No. 1/0565/09 „Modelling of traffic parameters in NGN telecommunication networks and services“ and ITMS 26240120005 “Support for Building of

Centre of Excellence for SMART technologies, systems and services".

## REFERENCES

[1] Kavacký, M., Baroňák, I.: Quality of Service and Optimal Selection of Traffic Control Scheme in ATM Network. In: 5th International Conference on Electrical and Electronics Engineering ELECO 2007 : Bursa, Turkey, December 5 - 9, 2007. pp. 279-283. ISBN 978-9944-89-421-0.

[2] Chromý, E., Baroňák, I.: Utilization of 1st Erlang Formula in Asynchronous Networks, *Journal of* Electrical Engineering, FEI STU, vol. 58, no 6., 2007, pp. 342 – 346, ISSN 1335 – 3632.

[3] Baroňák, I.et all, "The Convergence of ICT Networks and Services in the Communication Infrastructure of SR", State Program of Research and Development - "Building of the Information Society", Report, STU Bratislava, 1456 pages, 2006, I. Baroňák (national coordinator)

[4] Orgoň, M., „Gnoseological, technological and methodic aspects of the design of electronic communication devices and applications, habilitation work, STU Bratislava, 93 pages, 2007

# VoIP and Converged Networks Controlled by ANN

Skorpil Vladislav, Novak David
Department of Telecommunication
Brno University of Technology
Brno, Czech Republic
skorpil@feec.vutbr.cz

***Abstract*—Technology of transfer voice by communications converged networks takes today the importance. Add a VoIP service to a well-functioning networks working on the IP protocol is neither difficult nor expensive operations, problems occur in the quality of the voice. Networks are often charged for other services, and often do not provide mechanisms to ensure the quality of the service. Switches controlled by classic sequential way can be ineffective. The paper studies and compares switches controlled using the artificial neural networks.**

***Keywords – Artificial Neural network (ANN), switch, Kohenen network, Converged network***

## I. I. INTRODUCTION

Converged networks are a range of information and multimedia technologies that connect not only the end points for the user but also the network elements to which the communication relates. From the point of multimedia content may the converged networks contain the following types of media types: text, audio, video, images, animation, interactivity. These multimedia forms may be included in the types of traffic such as VoIP, video conferencing, streaming video, and data. Tab. 1-4 summarizes the types of traffic and network requirements for the operation of these services. Services for voice and video communications are among the most demanding and any variations or complete loss of packets very declines quality of transmission [2,8]. The work builds on the [27, 28].

TABLE I. VOIP AND REQUIREMENT FOR COMMUNICATION

| | |
|---|---|
| Max. packet loss | 1% |
| Max. unidirectional delay | 200 ms |
| Max. jitter | 30 ms |
| Guaranteed bandwidth for the session | 12-106 kbit/s |

TABLE II. VIDEOCONFERENCE AND REQUIREMENT FOR COMMUNICATION

| | |
|---|---|
| Max. packet loss | 1% |
| Max. unidirectional delay | 200 ms |
| Max. jitter | 30 ms |
| Guaranteed bandwidth for the session | The volume of the session |

TABLE III. STREAMING VIDEO AND REQUIREMENT FOR COMMUNICATION

| | |
|---|---|
| Max. packet loss | 2% |
| Max. unidirectional delay | 5s |
| Max. jitter | - |
| Guaranteed bandwidth for the session | Depends on the encoding, and the speed of flow |

TABLE IV. DATA AND REQUIREMENT FOR COMMUNICATION

| | |
|---|---|
| Max. packet loss | various |
| Max. unidirectional delay | various |
| Max. jitter | various |
| Guaranteed bandwidth for the session | various |

For the correct function of the converged network it is necessary to keep the quality of service (QoS), traffic shaping, load balancing, security, and access to the simple administration of the network. [17]

## II. VOICE OVER IP

Voice communication using Ethernet and Internet, which uses the Internet Protocol is called VoIP (voice over IP). To transfer it uses TCP (Transmission Control Protocol), UDP (User Datagram Protocol) and the IP. It is necessary to ensure the quality of service (QoS) in the network for reliable and user-friendly telephone connection [12,17].

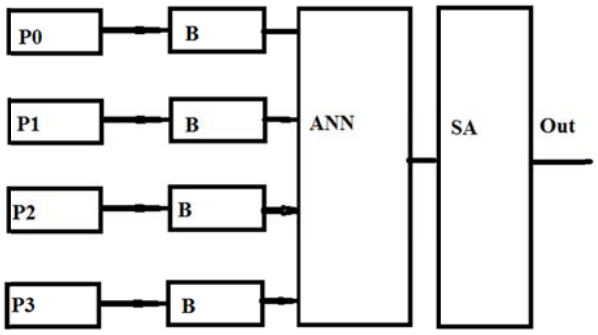


Figure 1. The switch controlled by Kohenen network

P0, P1, P2, P3 – inputs
B- Input Buffer
ANN – Artificial Neural Network
SA – Switching Area

## III. SIMULATION USING OPNET MODELER

The switch controlled by Kohenen ANN [1] – see Fig.1 and the classical switch are compared. The switch has four ports and its own QoS control. [13,16]. The details of the design of the switches and the details of the simulation using Opnet Modeler are listed in [27, 28].

For a VoIP service is not only important delays in the network, but also jitter in the network. Jitter for the whole network is illustrated in Fig. 2. In both cases, however, takes the low values but in the case using the ANN is after stabilization of the initial situations on ports up to half the jitter or null.

An important parameter of the switch is also a delay on individual ports. Delay on port P0, P1, is shown in Fig. 3 and Fig. 4. The delay on the remaining port P2 and P3 is not shown, takes a similar values as on ports P0 or P1. Delay on ports switches with ANN is in both cases, almost zero; this is for other network traffic very important.

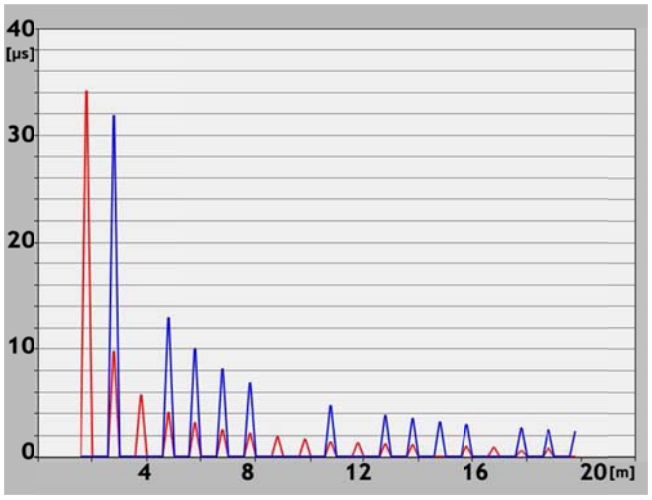


Figure 2. Jitter delay in a network with ANN (lower), classical (higher)

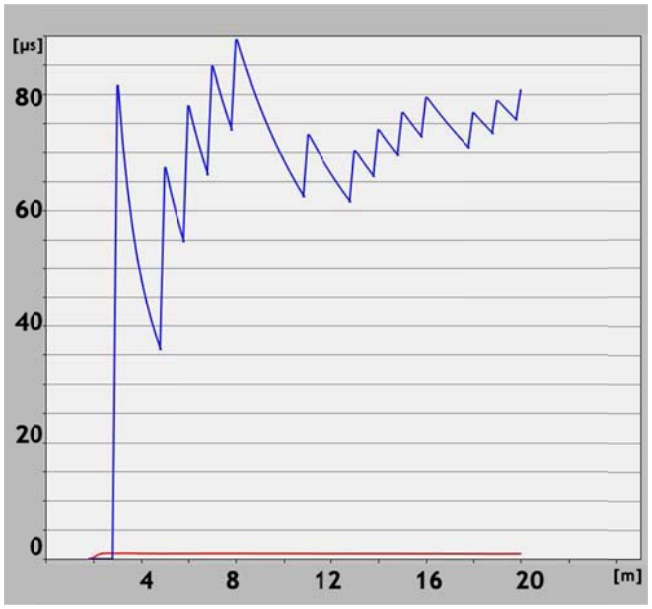


Figure 3. Delay on port P0 the with ANN (lower), classical (higher)


Figure 4. Delay on port P1 with ANN (lower), classical (higher)

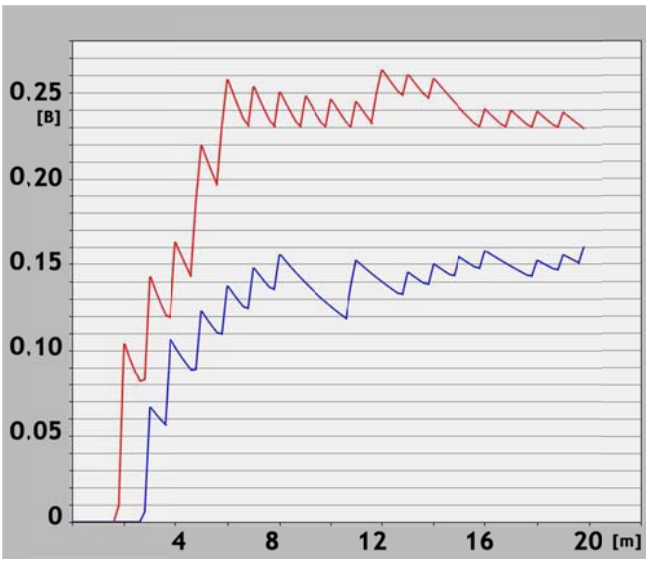


Figure 5. The use of stackes for the port P0 the with ANN (higher), classical (lower)

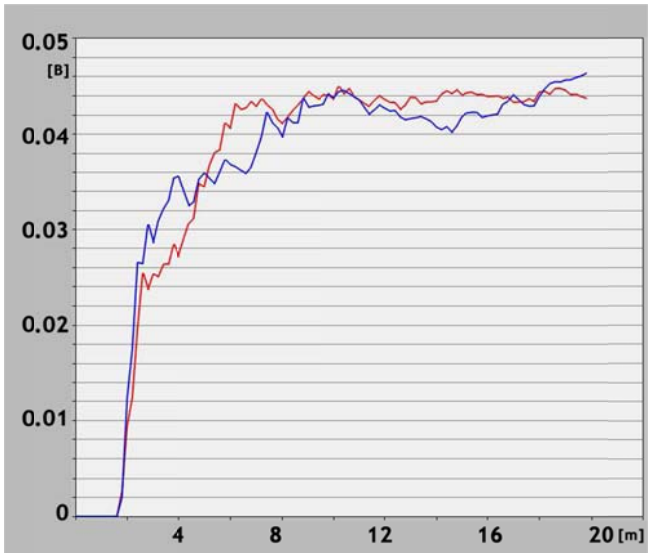


Figure 6. The use of stackes for the P1 port switches with ANN (higher), classical (lower)

The last parameter that loads a switch is an input switch buffer using. ANN's load input buffers on ports either to the same extent, or more than the classical switches. This load but it is not particularly high. These courses are given on the Figure. 5 port P0 and Figure 6 for the P1 port of the switch.

## IV. CONCLUSION

VoIP has as each technology advantages and disadvantages. The disadvantages are gradually very quickly rejected; there is the constant implementation of new services, protocols, security, etc.

The advantages include the ability to use the current infrastructure of the data network and the effective use of the capacity of the channel. A channel is the one used for more traffic and more services, low operating costs and the purchase price-are often lower than for a completely free of charge or classic ADSL, etc. To these costs, however, it is necessary to add the connection to the Internet service and to the provider that will guarantee the quality of the services so as to link the VoIP reliable and without other negative effects (echo, delay, etc.). Another advantage of the new services that do not provide the normal phone, telephony and data transmission at the same time.

Among the disadvantages of VoIP we can count lower quality in real time transmission. In the classical networks is this disadvantage rejected through alternative paths to failure and using quality of service in variations in the requirements for VoIP traffic. [12].

The disadvantage is the loss of a connection failure of the Internet. Failure of the Internet, but does not affect the internal Ethernet network (e.g. a company), but the call to the external network is impossible. Some problem is sending faxes, due to the software, and network restrictions in most households. This fixes the new Protocol T. 38.

## ACKNOWLEDGEMENT

This research was supported by the grant:

No MSM 0021630513 Research design of Brno University of Technology "Electronic communication systems and new generation of technology (ELKOM)"

## REFERENCES

[1] Novak, D. *Optimisation of a Voice Transmission in Communication Networks.* Diploma thesis. Brno University of Technology, Brno 2010

[2]Skorpil,V. Advanced Elements for Transmission Networks. *The Journal of the Institute of Telecommunications Professionals,* ISSN 1447-4739, Volume 2, Part2

[3]Skorpil,V. New Approach to Converged Networks. *Proceedings of the Seventh International Conference on Networking*. ICN 2008, April 13-18, Cancun, Mexico

[4] Skorpil,V. *Digital communication Technology.* Brno: VUT FEKT UTKO, 2002. 133 s. ISBN 80-214-2244-0.

[5]Drabek, O., Seidl, P., Taufer I. *Artifical Neural Networks – Basic of Theory and Application.* Pardubice: UP FEI, 2006.

[6]Tuckova, J. *An Introduction to theory and Application of the Artificial Neural Networks.* ČVUT, 2003. 103 s. ISBN 80-01-02800-3.

[7]Sima,J.,Neruda,R. *Theoretical Questions of Neural networks.* Praha: MATFYZPRESS, 1996. 390 s.

[8]Hamadoud, I., T., ITU-T Study Group 2, Teletraffic Engineering. 350 s.

[9]Raisanen,V. I*mplementing Service Quality in IP Networks.* John Wiley & Sons, New York, 2003.

[10] Peterka, J. *Bandwidth and its dividing.* Computerworld: e-archiv .1991. http://www.earchiv.cz/a91/a143c110.php3

[11] Held, G., *High Speed Digital Transmission Networking*. John Wiley & Sons, New York, 1999.

[12] Bazala, D. *Telecommunication and VoIP Technology.* Brno: BEN, 2006. 224 s., ISBN 80-7300-201-9.

[13] Raso,T., *Proposed application of neural networks in teleinformatics.* Diploma Thesis. Brno: BUT, 2006.

[14] Skorpil,V., Raso,T., Neural Networks for Communication Network Elements. *Proceedings of the International Conference on Instrumentation Communication and Information Technology 2007*, Technical University Bandung 2007.

[15] Krbilova, I., Vestenicky, P., *Use of Intelligent Network Services.* In Proc. of ITS, RTT, CTU Prague, 2004.

[16] Kral, M., *Design of a new network element architecture,* Diploma Thesis.Brno: BUT, 2006.

[17] Svoboda, J., *Telecommunication Technique 3.* Brno: BEN,2003. 136s. ISBN 80-901936-7-6.

[18] Horst, J., *Information and Telecommunication Technique.* Europa – Sobotáles, 2004. 399 s., ISBN 80-86706-08-7.

[19] Norgaard,M. *Neural Networks for Modelling and Control of Dynamic Systems.* Springer, London 2000.

[20] Stastny,J., Skorpil,V. Genetic Algorithm and Neural Network, *In Proceedings of the 7th WSEAS International Conference on Applied*

*Informatics&Communications,* pp. 347-351, Athens, Greece 2007, ISBN 978-960-8457-96-6, ISSN 1790-5117

[20] Fencl,T. and Bilek,J., Network Optimization. *In Proceedings of the 7th WSEAS International Conference on Applied Informatics&Communications,*

pp. 94-99, Athens, Greece 2007, ISBN 978-960-8457-96-6, ISSN 1790-5117

[22] Rivas,V.M., Arenas,M.G., Merelo,J.J., Prieto,A., EvRBF: Evolving RBF Neural Networks for Classification Problems. *In Proceedings of the 7th WSEAS International Conference on Applied Informatics&Communications*, pp. 100-105, Athens, Greece 2007, ISBN 978-960-8457-96-6, ISSN 1790-5117

[23] Benetazzo,L. Beni,M. Rullo,M., Fixed network Multimedia Messaging Services: protocols and Gateway. *In Proceedings of the 7th WSEAS International Conference on Applied Informatics&Communications*, pp. 168-175, Athens, Greece 2007, ISBN 978-960-8457-96-6, ISSN 1790-5117

[24] Bogdanov,I., Mirsu,R. Tiponut,V., Matlab Model for Spiking Neural Networks. *In Proceedings of the 13th WSEAS International Conference on Systems,* pp. 533-537, Rhodos, Greece 2009, ISBN 978-960-474-097-0, ISSN 1790-2769

[25] Takizawa,Y., Fukasawa,A. Novel Neural Network Scheme Composed of Prediction and Correlations. *In Proceedings of the 13th WSEAS International Conference on Systems*, pp.611 - 615, Rodos, Greece 2009, ISBN 978-960-474-097-0, ISSN 1790-2769

[26] Gacsadi,A., Tiponut,V., Gergely,E., Gavrilut,I. Variotional Based Image Enhancement Method by Using Cellular Neural Networks. *In Proceedings of the 13th WSEAS International Conference on Systems,* pp.396 - 401, Rodos, Greece 2009, ISBN 978-960-474-097-0, ISSN 1790-2769

[27] Skorpil,V. , Novak, D. Network Elements Controlled by Artificial Neural Network. In Proceedings of the 14th WSEAS International Conference on Communications. Corfu Island, Greece, 2010. pp. 145-148, ISBN: 978-960-474-200-4-0, ISSN 1792-4243

[28] Skorpil,V., Novak,D. Services for Advanced Communication networks. *Journal WSEAS Transactions on Communication.* ISSUE 10, Volume 10, October 2010, pp. 635-645, ISSN 1109-2742

# Functional safety in relation to fieldbus in industrial communication

Tomas Larys, Jiri Koziorek

Department of measurement and control, FEECS
VŠB-Technical University of Ostrava
Ostrava, Czech Republic
tomas.larys.st@vsb.cz, jiri.koziorek@vsb.cz

*Abstract* — **This paper deals with a present state of a functional safety in relation to fieldbus in industrial automation. At the beginning is shown summary of basic standards and norms used in functional safety. On a second part of this paper is described basic principle of safety profiles for standard communication fieldbus to use this existing fieldbus for safety functions.**

***Keywords - Functional safety; Safety Layer; Safety profiles; Standards***

## I. INTRODUCTION

At the present time two technical fields are discussed in engineering circles in industrial automation field. These technical fields are industrial control systems and industrial communication systems and their safety functions and characteristics. All of these are relevant with extend of general requirements for safety of industrial technological systems. These topics are being the most topical solved questions of contemporary development automation in advanced industrial countries. Industrial control systems and their communication bus based on electrical and electronical components have been used in many application areas for providing safety functions for a long time. If technologies, based on electronical and computer systems are to be effectively and safely used, it is necessary to satisfy some safety level. Failures and wrong functions of a technological establishment and machines can lead to risks for persons, environment and material values. Incidence of failures and probability of their occurrence determining necessary precaution to restriction risks by prevention of creation failures, their recognition and encompassment.

## II. BASIC OF FUNCTIONAL SAFETY

Common term "safety" has several meanings in principle. The system is safe in sense of the translation of word "safety", in case that it or its operation is not dangerous for its surroundings. The similar sense is security. The system is secure, if it is resistant against to unauthorized intervention against the unauthorized persons. Similar sense has word "reliability". It means rate of availability, then probability, that system will successfully finish its tasks before its breakdown. The last term which is mentioned with safety is Mean Time Between Failures (MTBF). This is statistic value indicating estimation of reliability of the systems. All of these terms are relevant directly or indirectly with SW and HW accessories of the industrial systems.

Safety of the industrial systems in its sense can mean protection against:

- Electric shock
- Accident by fire and heat
- Accident by dangerous radiation
- Risk caused by failure of correct function of a system

The last point of these safety aspects is more concrete and it is defined as: "Functional Safety". It means correct behaviour of safety control system and its parts. This is a part of total safety concerning of risk controlled equipment (*EUC-equipment under control*) and control system of the EUC. This part depends on correct function of safety control system, systems based on other principles, and outside instruments for decrease of the risk. For this kind of required behaviour it is necessary to achieve specific minimal level of standardization of these systems. [1]

## III. FUNCTIONAL SAFETY AND LEGISLATIVE LAW

Many countries on higher technological level created norms and legislative laws specifying requirements, functions, properties and process of development of system satisfactory functional safety during evolvement of industrial control systems and functional safety trends rise. Each country, dealing with these problems, created its own preview and methodology how to specify, standardize and introduce these safety technology systems. Discussion concerning unification of these different norms to one international standard began during evolution of international business and effort of many companies to expand to foreign markets. This unification would make expansion of companies to foreign markets easier and it would also simplify bureaucratic and legislative problems for system integrators, which are trying to apply their systems abroad.

The individual norms and standards from many countries were harmonized and still are harmonizing to one system at least within wider regions or continents by these reasons. We differ three main groups of the harmonized norms: Europe standards (IEC, EN), USA standards (UL, ANSI) and Asia standards (JIS). The most important and normative documents concerning the high function and high safety control were German norms **DIN V 19250/251** and US standard **ANSI/ISA S84.01-1996** and its international version **IEC 61508**. The aim of these standards has been definition of safety categories (in terms of risk for persons, environments and surroundings) and binding procedures to achieve safety behaviour systems in defined categories. *Siemens AG (2008)*

### *A. IEC EN 61508*

At the present time there exists a harmonized standard for how to design equipments in order to ensure functional safety. This standard for designers and users provides international norm IEC *EN 61508 Functional safety electrical/electronic/programmable electronic safety related system (E/E/PE).* Function safety according to norm IEC EN 61508 presents an international valid safety standard for equipments, where E/E/PE represents safety function. In other words this is a part of safety, which depends on correct function of equipment and control systems which ensure its safety.

IEC 61508 consists of 7 parts:

1) IEC 61508-1, General requirements;
2) IEC 61508-2, Requirements for electrical/electronic/programmable electronic safety-related systems;
3) IEC 61508-3, Software requirements;
4) IEC 61508-4, Definitions and abbreviations;
5) IEC 61508-5, Examples of methods for the determination of safety integrity levels;
6) IEC 61508-6, Guidelines on the application of IEC 61508-2 and IEC 61508-3;
7) IEC 61508-7, Overview of measures and techniques.

Some norms, which are being either published or prepared, are departmental implementations of IEC EN 61508. These are:

- IEC EN 61511 - Functional safety - Safety instrumented systems for the process industry sector
- IEC EN 62061 - Safety of machinery, Functional safety of safety-related electrical, electronic and programmable electronic control systems
- IEC 61513 Nuclear power plants - Instrumentation and control for systems important to safety - General requirements for systems

General norm of functional safety stands on two basic conceptions – safety life cycle and safety integrity level (SIL). Determination of appropriate level of requests of safety in dependence on rate pending risk is essential. For this are used qualitative (graph of risk) or quantitative methods. During choosing of components suitable for safety systems it is important to take into consideration except the aspect of safety also their real operational conditions and other requirements.

SIL is discrete level represented by a number from interval 1 to 4. Higher number determines higher safety integrity level. More dangerous can be the effects of the safety function errors, the higher must be the set safety integrity level. Afterwards the requests for a certain SIL of the safety systems and its components is determined, the acceptable risk is also determined and necessary reducing of risk is expertly estimated.

Safety integrity level, in practice in individual cases, can be determined in several ways. It depends on many aspects. These are:

- Complexity of a task.
- Kind of risk and its necessary reduction, which is necessary to be reached.
- Rate of parameters knowledge important for the formation of a risk.

[6]

### *B. EN ISO 13849*

On the next part of the text will be discuss standard EN ISO 13848 - Safety of machinery - Safety-related parts of control systems, which has a two parts. The part of norm EN ISO 13849-1 (Safety of machinery - Safety-related parts of control systems - Part 1: General principles for design) mentions safety requirements and instructions for construction and integration of the safety control system (SRP/CS - *Safety-Related Part of a Control System*), including software design. The norm specifies properties of these parts SRP/CS, which include properties level required for executing of safety functions. The norm is valid for SRP/CS without reference to type used technology and energy (electric, hydraulic, pneumatic, mechanic) for each type of machine equipment. The norm does not specify safety functions or properties levels, which have to be used in each concrete case.

EN ISO 13849-1 part does not specify requirements for the construction equipments, which are part of safety sections of control systems SRP/CS. Nevertheless, some of the introduced principles, such as categories or properties level, can be used. This part of the norm is established in order to give understandable details on the basis of which a construction

and properties of each SRP/CS application and machine can be judged for example by a third party, independent company or some testing station.

The part 2 - validation of the norm EN ISO 13849-2 specifies procedures and conditions, which has to be observed during verification which is done by the help of analysis and testing of enabled safety functions and achieved categories safety parts of control system according to EN ISO 13849-1. Some requirements for verifying are general and some of them are specific according to the used technology.

This norm defines performance level (PL). There are five discrete levels (a to e), which are used for determination of capability of SRP/CS to execute safety function at foreseeable conditions. These properties levels are defined by probability of dangerous failures per hour. This probability of dangerous failures of safety function depends on several aspects. These aspects are structure of HW and SW, detection of collision mechanism (DC), reliability of components (MTTF), common cause failure (CCF), construction process, service load, environment condition and work procedure. [3]

## IV. Industrial Communication systems - Fieldbuses

Within the evolution and extension of industrial control systems and their communication abilities more than twenty years ago also industrial communication systems – fieldbuses started to develop and extend a lot. There are many types of fieldbuses at the present time. Each type is discriminated by a kind of access on transfer medium, transfer protocol, security of transfer and application layer. The main parts of each fieldbus are physical layer and a transfer protocol. There are many types of physical layers, which specify data transfer on the level of physical media, as well as transfer protocol. Nonetheless different transfer protocols can operate under the same physical layer on totally different electrical transfer basis. Most of the fieldbuses are developed with direction on specific area of use. Physical layer construction and principle of transfer fieldbus protocol matches for this. There are three basic applications areas to which the fieldbus are divided by its assignment.

**0.** ***Level – Field instrumentation:*** This level includes actuators and sensors.

**1.** ***Level – Direct control:*** This level includes control and measurement systems, which are field instrumentation elements connected to. By the control system can be mean a relay circuit with fixed pre-programmed function up to complex programmable logic controllers (PLC) or PC based systems. Other groups are distributed control systems (DCS) or HMI/SCADA systems for visualization and control of controlled technology from process place or control room by an operator.

**2.** ***Level – Company control:*** This level is presented by a management or government of company. By physical preview these are a simple PC user with special SW for evaluating productivity of production, logistic, store government and other.

There are a lot of types of fieldbuses at the present time which are supported and developed by many producers and associations. Examples of these fieldbuses are: Foundation Fieldbus PROFIBUS, Profinet, ControlNet, WorldFIP, P-NET and others. These fieldbuses and more are defined in IEC 61158 and IEC 61784 norms. There are many others successful and extended fieldbuses, which are not defined in these norms. These are for example AS-I, CANopen LonWorks and others. Wireless communication fieldbus or wireless alternative for existing fieldbuses (no physical layer) are imprescriptible.

## V. Safety Profiles Of Fieldbuses Standards

The safety control system was separated from standard control system and safety communication was separated from standard communication from the start. If these systems are separated, risk of rise failure from common reason decreasing. Process systems can execute a service of second “safety” layer of the controlled system. If process control system and safety control system are separated, it is working correctly, but it is more expensive and complex.

The time has changed and today’s reality is different. Present safety and communication systems are integral part of the system for control technological process. This is assisting the whole system to simplify and reduce time needed for its design and putting in operation. New safety communication profiles were developed for existing standard communication fieldbus. These new safety profiles enable to realize standard and safety communication on the same physical channel. The costs of cableways were reduced and diagnosis of the control and controlled system was improved, too.

The basic common principle, used in many safety communication fieldbuses, is “*black channel*” principle (Fig.1). This principle comes out from practical and economical request – not to change anything on HW and SW of the standard communication technology (e.g. Foundation Fieldbus, PROFIBUS, Profinet, Ethernet Power Link, ControlNET), which are very well safe against failure from their principle of high operational reliability. This is principle, where functional safety is built up under the standard communication channel. Needed and required functional safety level of these communication systems is achieved by inserting safety layer above or into 7. Layer of OSI model and not by decreasing probability of communication failures on lower levels of the OSI model.

It was not necessary to trench on existing standard communication protocol, which was not designed with regard to future requests of functional safety. Modified 7th layer with implemented safety layer should in principle eliminate each possible transfer errors. These errors can be due to electromagnetic interference (EMI), errors and failures communication HW and errors of standard or safety HW and SW component.

On the following Fig. 1 there is shown the basic principle on which it is possible to realize functional safety communication on the ´black channel´ basis. The figure displays standard communication protocols extended with safety communication layer.

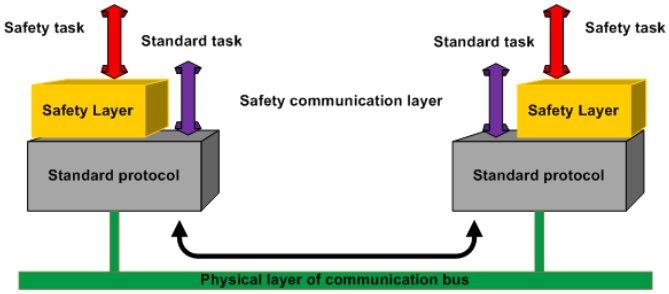


Fig. 1. The "black channel" principle of safety communication

Function of the safety layer consist in failures detections and perform precaution for elimination failure influence in conjunction with safety function of a communication entities (HW and SW precaution).

The Fig. 1 shows that standard communication and safety relevant communication are running on the same communication channel at the same time. Data, which are related to safety, are used for safety applications and data, which are not related to safety (standard data), are used for standard applications.

On the Fig. 2 the Fig. 1 is closely specified for whole safety chain. Contemporary operation of both standard and safety communication is evident from this figure. Safety and non-safety (standard) communication are absolutely independent. The simple communication channel should be sufficient for meeting requirements of the safety communication. Simple communication channel's doubling is not related with safety but with reliability.

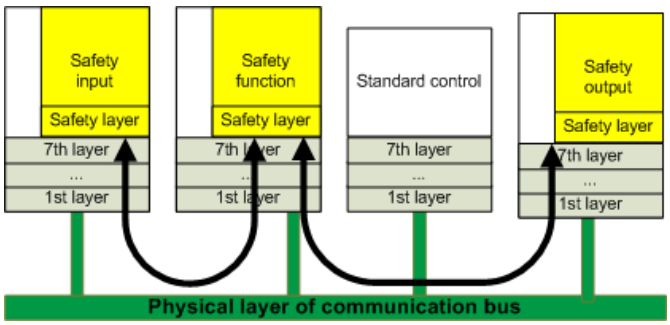


Fig. 2. Describe of standard and safety communication on the same fieldbus

Possible reasons for failures and errors which rise in communication fieldbuses are following:

**a) Repeating** – Repeated reception of the same data.

**b) Lost of data** - The data are not transmitted.

**c) Inserting** – Reception of data from another transmitter.

**d) Wrong sequence** – The data are received in another sequence, that in sequence, in which it was sent.

**e) Inconsistency** – The data are damaged or not full.

**f) Delay** – The data are delayed more than allowable interval between send and receive of the data.

**g) Overflow of a router's memory** – Router's memory is full.

These failures and errors are very similar as with standard communication (possibly same). Therefore the safety communication profiles are implemented into the current standard fieldbuses in order to eliminate these failures and errors. But there are also other failures, which can appear in consequences by implementation of these safety functions. These are:

a) **Interconnection of the safe and non-safe communication** – illegal communication between safe and standard sender/receiver.

b) **Entry to the safe memory area of an communication equipment** – illegal operation of the standard application under the safe data area

There are a several corresponding safety mechanisms, which could be implemented into nested safety layer of the communication protocol in order to eliminate these failures and errors

a) **Sequential numeration of data** – sender dispose a counter, its value is incremented by one with every sent package of data. And for each sent data is connected value of the counter.

b) **Time stamp of data** – sender connects to each sent data value of time, in which data was sent.

c) **Confirmation of data receives** – receiver sends to the sender information, that it has successfully received data.

d) **Identification of sender and receiver** – The data contain information about identification of sender and receiver.

e) **Data backup** – Backup of the sent data on the side of sender.

f) **Data redundancy** – Redundancy of sent data (multiple data sending, data coding).

g) **Check of data validity** – Into the sent data control data (e.g. CRC) are added.

In the Table 1. is noted how individual safety mechanisms inhibit to occurrence of individual communication errors.

TABLE 1. Possible data failures and methods of theirs elimination

| | Methods of elimination | | | | | | |
|---|---|---|---|---|---|---|---|
| **Possible data failures** | **Sequence number** | **Time stamp** | **Received data conf-irmation** | **Authe-nticat-ion** | **Data back-up** | **Data redun-dancy** | **Check of data validi-ty** |
| **Repeating** | X | X | | | | X | |
| **Data lost** | X | | X | | | X | |
| **Inserting** | X | | X | X | | X | |
| **Wrong sequence** | X | X | | | | X | |
| **Inconsist-ency** | | | X | | X | | X |
| **Delay** | | X | | | | | |
| **Safe and non-safe data overlap** | | | X | X | | | X |
| **Overflow of router's memory** | | X | | | | | |

The minimal request for safe communication protocol is that it has to be able to eliminate all failures and errors noted above. During designing a new type of safety profile for existing standard fieldbus it is very important to have knowledge about used physical layer, network topology and an outside environment. It is because each fieldbus has its own specification, properties and special errors mode. An example of implementation safety layer into the standard fieldbus is safety profile PROFIsafe for PROFIBUS or Profinet fieldbus. This principle is displayed on the Fig. 2. Analogous to standard data which are completed by supplemental byte, safe data are completed by completing bytes from used safety mechanism from Tab1 and these are inserted between dataflow of the standard frame. [2]

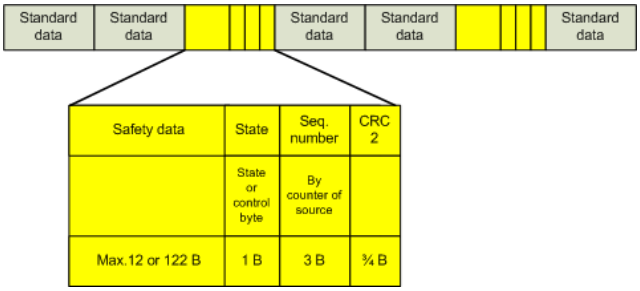


Fig. 3. Safety communication data inserted into standard communication data flow

## VI. CONCLUSION

Industrial communication systems – fieldbuses noted a giant success and boom from their origin before more than twenty years. It was in consequence theirs basic principle at first. Those were replaced by one cable complex cableways of great numbers of inputs/outputs of centralized systems by one cable – by fieldbus. Fieldbus enabled realize complex and extensive communication networks. By theirs basic principle was enabled diagnosis this networks and equipment connected to the fieldbus, too. The second main advantage was implementation safety profiles for developed standard fieldbus and integration standard and safety communication on to one fieldbus. At the present time continued development of safety profiles for wireless communication too. Over these achievements and advantages, these safety fieldbus are not relatively enough extensive. This problem is probably caused by fear and reluctancy of consumers to apply these systems. The reason can be higher initial costs. Unquestionable advantages of fieldbus with safety profiles, as more diagnostic functions, functional safety and reliability, are missing out. After some event, which could have negative influence to economics, environment or even people's lives, these functional safety systems are remembered too late. [4]

## ACKNOWLEDGMENT

This work is supported by grant of the Grant Agency of the Czech Republic GA102/08/1429 - Safety and security of networked embedded system applications.

## REFERENCES

[1] Adamski B. (2004), *Safety Bus Design Requirements for Process Industry Sector Applications*, Invensys- Premier Consulting Service, document available on: „http://www.safetyusersgroup.com/"

[2] Cernohorsky J., Koziorek J., Hrudka G. (2006), *The examples of implementation of two specialized case tools as extensions of a general framework*, Pages: 4909-4914, IECON 2006 - 32nd Annual conference on IEEE industrial electronics, VOLS 1-11 Book Series: IEEE Industrial Electronics Society, France.

[3] Composite authors (2008), *Functional safety of machine controls – application of EN ISO 13849. BGIA Report 2/2008e*, German Social Accident Insurance (DGUV), Berlin, ISBN: 978-3-88383-793-2

[4] Fialkowski Ch. M., Cusimano J. (2007), *Safety Fieldbus Taking Aim at the Process Industries*, Siemens Energy & Automation, USA

[5] Siemens AG (2008), *Easy implementation of the european machinery directive*, Siemens AG / Industr sector, Germany

[6] Smith, D. J., Simpson K. G. L. (2004) *Functional Safety: A Straightforward Guide to applying IEC 61508 and Related Standards, 2nd edition*, Elsevier Butterworth-Heinemann, Great Britain, ISBN: 0-7506-6269-7

# Testing and Comparison of Protocols for Desktop Virtualization

## RDP and PCoIP

Jiri Kouril, Jiri Hosek
Department of Telecommunications
Brno University of Technology
Purkynova 118, 612 00 Brno, CZECH REPUBLIC
kouril@feec.vutbr.cz, hosek@fees.vutbr.cz

***Abstract* — The article deals with the testing and comparison of virtualization techniques and protocols for desktop virtualization common available on Microsoft platforms, VMware and Citrix. The article is divided into three parts. The first part deals with the technical principles of virtualization and compares the benefits of individual technologies. The second part deals with the design of a methodology for testing the performance of virtualization protocols. Testing methodology consists of identifying key factors that describe the working process of client stations, which are subsequently used for the selection and design of hardware architecture. The third part is practically oriented and deals with the performance analysis and testing. The testing methodology is transformed into a scripting language and it is ready for automated testing. The performance characteristics of the RDP and PCoIP protocols are monitored and compared.**

***Keywords-Virtualization; Protocol; RDP; PCoIP; Analysis; Comparison***

## I. INTRODUCTION

A distribution of desktop virtualization is currently one of the most recent trends in IT infrastructure consolidation. This is the next logical step that builds on the virtualization of servers and it delivers savings to the client side. With this rediscover paradigm, where the computational burden is largely transferred to the server, it is possible to minimize the performance of client devices. The most important consequence of such a slimming bark applied to the client device is a significant reduction of energy consumption. The equipment that has been deliberately deprived on power parameters is known as a thin client.

This technology uses in principle two different approaches. The first, known as VDI, is based on a separate autonomous systems. Operating system images are stored in a centralized shared repository. In this repository, mentioned image is virtualized and ready for client connections. Access software on the client side connects to the virtualized system on the server, whole data transfer from peripherals client is redirected to a remote system. This process is hidden from the user and the system creates the impression that it is running locally. The second approach uses a single operating system which appears as a host. With every clients requirement to connect the host system creates isolated relation. From the perspective of the user, it is again a separate local system, but it is the same type as the host system and includes only those applications that are installed on the host. From the perspective of the host system, each session is running as another process, so it is not an autonomous system. This approach is known as Terminal Services TS [1], [2].

## II. ANALYSIS OF THE REQUIREMENTS FOR VIRTUALIZATION SYSTEM

Deployment of desktop virtualization technology to the production environment is an essential step over the use of traditional PC and it is necessary to implement appropriate analysis of requirements, which will be placed on such system. Systems of distribution of remote areas are generally the most difficult to use RAM. Right after the system memory has high demands on the storage subsystem. It is necessary to provide redundancy for images and virtual systems, while minimizing access times to data. The primary task in the planning of natural resource virtualization server is to set the number of users who such a server will connect [3]. Each user represents a session that represents some amount of the allocated memory. This memory mode must be added to the sum of all memory consumed by user applications. The value of this calculation is multiplied by the number of users and gets demands on memory. Determination of processor performance is very subjective according to the deployment location. There are general recommendations for the implementation of desktop virtualization system, but these are only a recommendation. Therefore, the establishments of appropriate stress tests are able to detect quantities of demands on the proposed virtualization environment.

Design of test methodology consists of the following points:

- Definition of monitored counter values
- Definition of requirements for virtualization architecture
- Definition of running client applications
- Selection of appropriate testing tools

- Evaluation of test results and their reflection in the design of physical resources.

Previous indicators can be summarized in a group designated as primary.

The secondary indicator can indicate the ability of the distribution protocol to adapt to the physical environment network and to deliver the expected result to the user in the expected time. One of the examples of the secondary parameter can be a response to a user's initiative in the WAN network.

### *A. Distribution Protocols*

Current users are demanding and in case of the deployment of distributed desktops, they expect the same comfort, what a local system provides them. Manufacturers of virtualization tools realized this fact and started to implement the tools ensuring high user experience into their systems and protocols. These improvements provide the use of hardware on the thin client computing for graphics data.

Microsoft uses for Terminal Services RDP protocol (Remote Desktop Protocol). The latest version of this protocol is labeled as RDP 7.The main benefit of this version is support for Microsoft Aero desktop environment [5]. Another new feature is the support for System Direct 2D and 3D 10.1., recorded and playback HD video without losing synchronization between video and audio.

Citrix is implemented extension of HDX (High Definition User Experience) in its distribution ICA protocol. This extension implements more effective bandwidth utilization for graphic data transmitting. Examples can be MediaStream HDX technology for Flash, which allows the streaming Flash video in its native compressed form. Video output is computed from the received data on the client side. HDX extension is able to dynamically adjust the bit rate according to the state transmission lines, which makes them suited for distribution of virtual desktops as trans-LAN (Local Area Network) and WAN (Wide Area Network).

VMware, of course, does not remain a party and in cooperation with Teradici created a new protocol called PC-over-IP. This technology can automatically identify the user's local device (for example, whether it is a thin client or projector) and accordingly is able to choose the optimal method of data delivery. Another criterion used to optimize the transmission is the status of data lines, which adapts the data transmission. PC-over-IP achieves excellent results in transmission of graphics and multimedia data, but it should be noted that to fully exploit the capabilities of this technology is necessary to have a hardware support Teradici technology.

## III. SELECTED TESTS AND TESTING PROCEDURES

The following text discusses the test performed with the RDP and PCoIP protocols that are mostly used in virtualization environment. For these tests was used both software and hardware implementations of thin client.

### *A. Performed Test*

During preparing of the test methodology the tests were divided into two groups to be able to cover both primary and secondary parameters. The first group of tests is intended to analyze primary parameters including monitoring the usage of memory and computer CPU time, depending on the scenario, which defines user's performance. The term “user’s performance” may represents the number of simultaneously running applications, used bit color depth of desktop, visual styles setting, etc.

Tests of the secondary group are divided into two types. The first type monitors bandwidth consumption depending on used protocol (RDP, PCoIP), session settings and user activity. The second type of test analyzes the operation system response to user command depending on physical parameters of the network, session setting, used protocol (RDP, PCoIP) and user activities.

Results of tests generated for one user under the above categories may be multiplied by the expected number of users working in a virtualized environment to obtain the physical parameters of virtualization server. This approach is not suitable for extreme situations that may arise, for instance the mass of users to log on virtualization server in a short time. Simulation of such a situation provides the scalability problem, which is not included among the tests because of its large extensiveness.

### *B. Created scenarios*

Depending on the type and number of simultaneously running applications different physical resources especially CPU and memory are used. For the analysis of the use of physical resources is necessary to define requirements of users working in a virtualized environment. From the view of group of user requirements it is appropriate to isolate the scenarios that significantly differ in consumption of physical parameters and can help to more accurately detect limitation in the design of virtualized infrastructure. For this analysis, two scenarios were developed representing users with low and high system requirements.

Created scenarios are shown in Fig. 1 and Fig. 2 in the form of flow chart.

Scenarios are designed to simulate the most common user activity on the computer. In a more detailed look at a scenario, it is possible to identify the blocks that fall into the categories of Text, PDF, Web, Presentations. This subcategories exclusion is particularly important for such type of test, which is monitoring the size of consumed bandwidth depending on the specific activities and the distinction is not important to the whole scenario. There are significant differences in the data stream for activities falling within the category of Text or Presentations.

Due to large number of configurable options for the RDP protocol, not all of these options are changed, but the created presets are used.

These presets correspond to the defined quality transmission lines and always provide the appropriate user

settings for the quality of the transmission lines. Created presets and their options are shown in the Table 1.

TABLE I. PARAMETER SETTINGS

| Parameters | Preset 1 | Preset 2 | Preset 3 |
|---|---|---|---|
| Desktop background | × | × | ✓ |
| Font smoothing | × | × | ✓ |
| Desktop composition | × | × | ✓ |
| Show window content while dragging | × | × | ✓ |
| Menu and window animation | × | × | ✓ |
| Themes | × | ✓ | ✓ |
| Bitmap caching | ✓ | ✓ | ✓ |
| Transmission line speed | 56 kbps | 256 kbps | LAN |

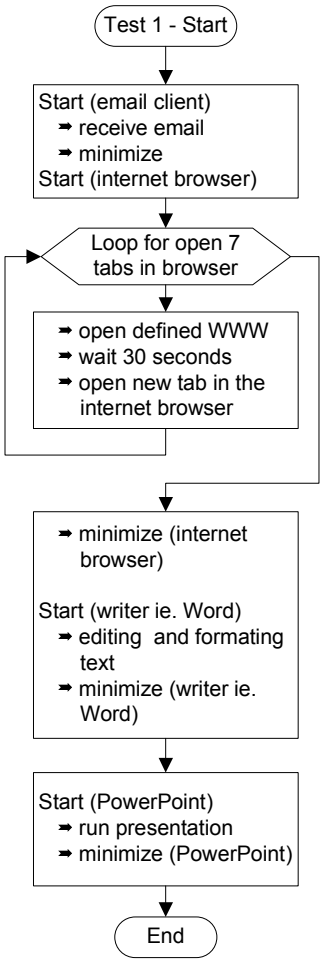


Figure 1. Test Sequence 1

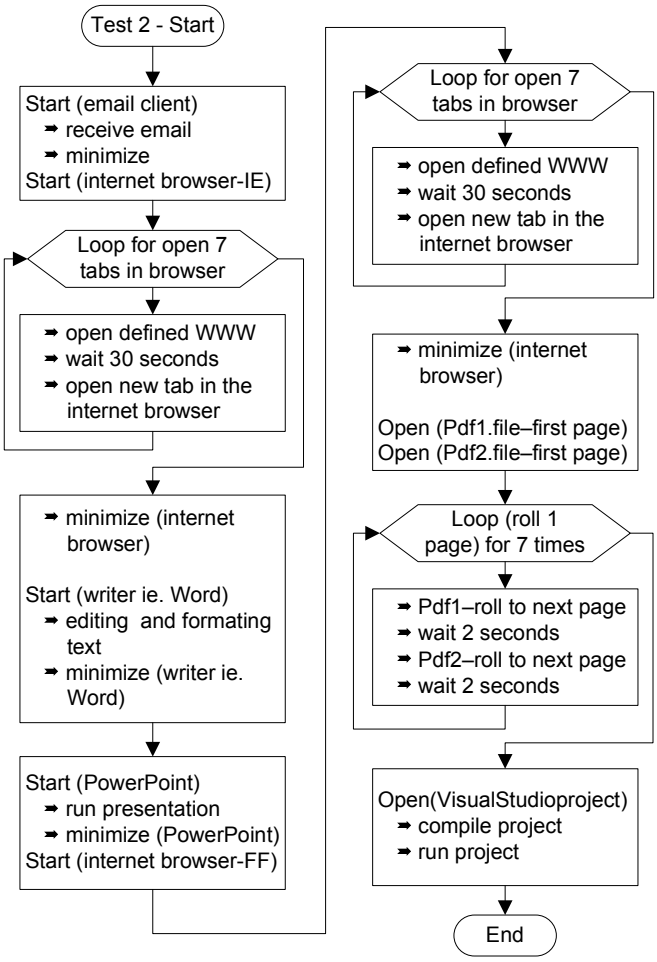


Figure 2. Test Sequence 2

PCoIP protocol in comparison with the RDP protocol offers significantly less parameters for the session setting. The absence of more detailed options settings can be attributed to the adaptive character of the protocol PCoIP. PCoIP protocol should be able to adapt to the physical condition of the line and offers the user maximum comfort comparable to the work on local system / desktop. For this reason, in the tests are defined only two groups of user settings. The first group is named as MIN and represents the minimum requirements and the second group is named as MAX and represents the maximum requirements (see Fig. 6).

### *C. Results*

The first type of tests (see Fig. 3) monitors a memory consumption during the establishment of terminal session using protocol RDP 7.0, depending on the parameters setting (see Table 1) of user sessions. The establishment of terminal session is considered the state when the user has successfully logged into the system and the desktop is displayed to the user.

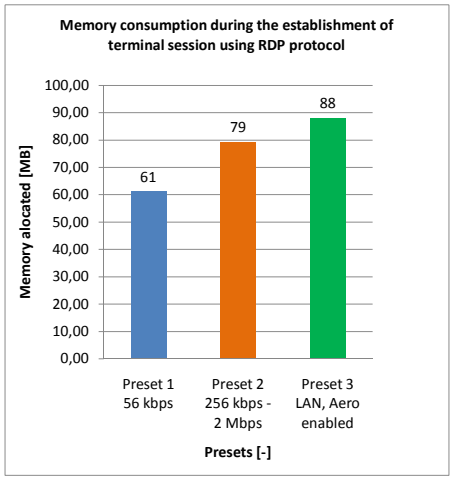


Figure 3. Memory consumption during establishment of terminal session using RDP

For parameters setting of Preset no.1 was consumed memory 61 MB. In the case of Preset no.2, where the parameters setting corresponds to the line speed of 256 kbps, increased memory is consumed by 18.82%. The increasing was mainly due to the use of visual styles. Activation of all the settings in Preset no.3 caused the value of consumed memory increased by 45.00% compared to the value of memory consumed in Preset no.1. In this case, the increase was caused by the use of Microsoft Aero environment.

The next test (see Fig. 4) is focused on the system memory requirements, depending on the user scenarios. By the selection of Preset no.3 the value of consumed memory was higher by 55.80 % for the chosen scenario of user with low system requirements (see Fig. 1, Test Sequence 1) compared with the value of Preset no.1. In the case of the selection of scenario of user with high system requirements (see Fig. 2, Test Sequence 2) the consumed memory increased by 26%. These values point to the fact that in the case of using more memory by the chosen scenario is to reduce the impact of user settings to memory consumption.

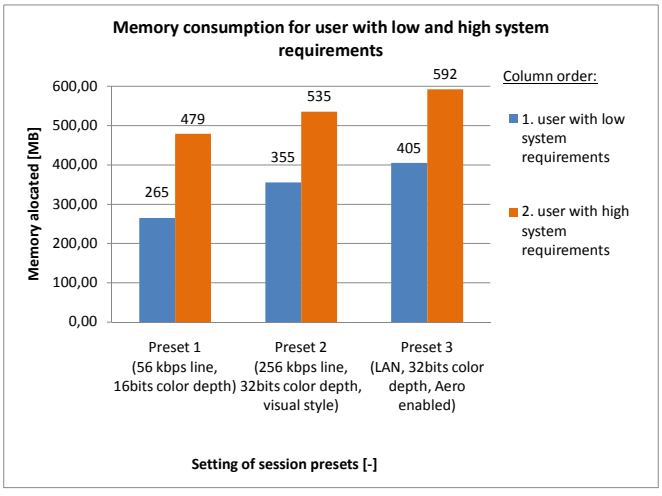


Figure 4. Memory consumption for users with low and high system requirements

Bandwidth consumption of RDP 7.0 compared with bandwidth consumption of PCoIP brought interesting results which shows that the protocol PCoIP used for its activity significantly more of bandwidth than the protocol RDP. For comparison the values obtained for the Preset No.1 and selected scenario Test Sequence 1 (part "text") PCoIP protocol used 4.32 times more bandwidth than RDP.

Specific measured values are 2.15 kbps for RDP and 9.27 kbps for PCoIP. This trend was similar for the other test scenarios (see Fig. 5 and Fig. 6). PCoIP protocol is designed as an adaptive protocol, and because of this feature could be a disadvantage in this test. Adaptive protocol is adapting to state of lines and trying to use the most of its potential for maximizing user requirements. If this happens at network with low load (low traffic), there may be situations where the protocol will use more network bandwidth than necessary.

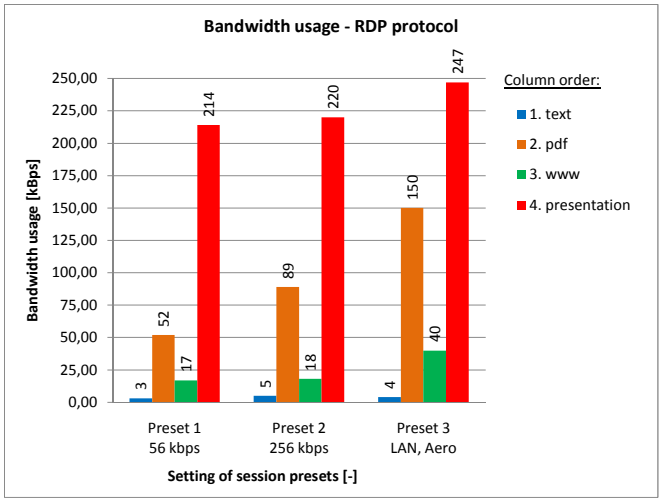


Figure 5. Bandwidth usage – RDP

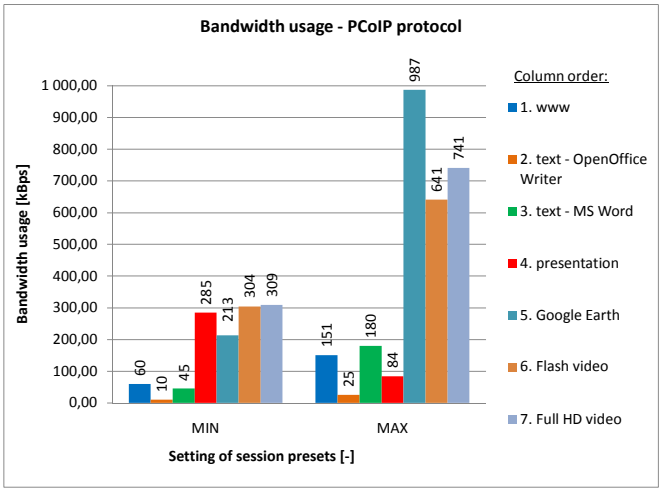


Figure 6. Bandwidth usage – PCoIP

Fig. 7 and Fig. 8 show the system response time to user request, depending on the quality parameters of transmission lines. In this test the response time was much better for protocol PCoIP only selected scenarios "Desktop" gave worse

results than the protocol RDP. It was not too difficult a rendering operation and therefore in the case of RDP, the most data could be stored in the cache, where could be loaded more quickly and without limitation caused by the setting of transmission lines.

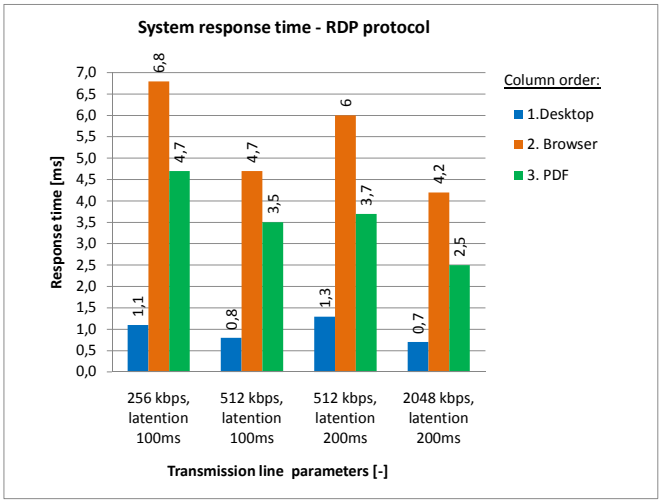


Figure 7. System response time – RDP

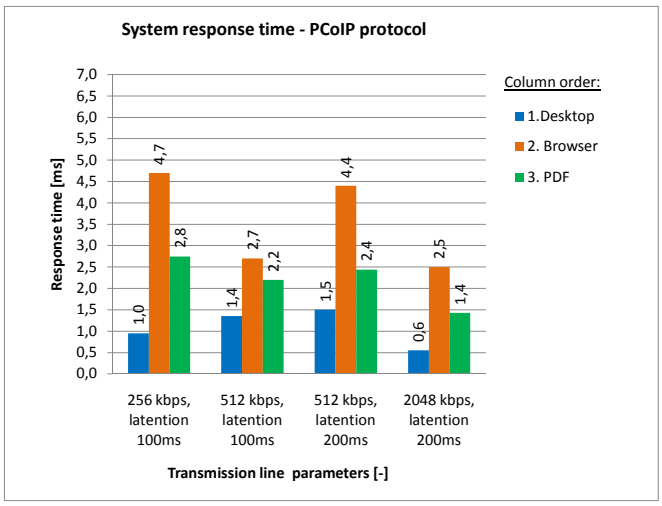


Figure 8. System response time – PCoIP

Last test is called Scalability test which is focused on simulation of the critical usage of system resources. Test is used for capture extreme situation, which can occur in case of the mass users are logged together at the same time (e.g. beginning of the lessons, beginning of working day etc).

Using a script every one second new connection session was gradually generated to a total of 18 users. A result of the scalability test is shown in the Fig. 9.

The monitored counters were:

- Available memory (in the Fig.9 is plotted red),
- CPU load (plotted green),
- Page Faults (plotted yellow),
- Number of active sessions respectively the number of connected users (plotted blue).

In the Fig. 9 the green curve shows CPU load which is at maximum from the start and this value is kept almost constant to end of the logging process.

According to recommendation in [5], each start of new connection session can load the CPU, so that the peak of CPU load curve can reach the maximal value of 100%. Immediately after this peak state the curve must fall below the maximum.

Applying the trend line (moving average of 30%) on the CPU load curve, in ideally case this curve should increase with a smaller slope than the curve of the number of connected users and reach a constant; value (ideally not reached) later than the curve of the number of connected users (all users have already logged in).

The coefficient multiplying the number of potential users, to multiply the number of processor cores corresponds to a coefficient of 1.5. This means that doubling the number of CPU cores will increase the number of acceptable users 1.5 times. Looking at the curve representing the available memory (red curve) shows that immediately after a steep decline, the curve starts to grow slowly until it reaches the maximum point. At this point it is appropriate to focus on the yellow curve representing the Page Faults. Page Faults indicates the need to read data from hard disk / storage. This situation usually indicates a lack of memory, but in this case the memory grows.

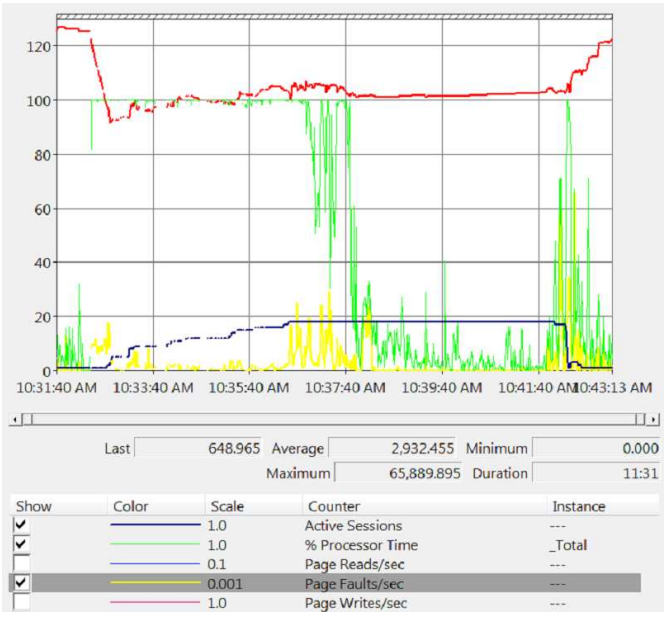


Figure 9. Scalability test

If an application is allocated memory, this memory is considered to be used, although it may be used only half. The amount of memory actually used is called the working set.

The graph in Fig. 10 obtained from reference [6] shows the three zones.

**Zone 1** represents the abundant memory stage. This is when physical memory is greater than the total amount of

memory that applications need. In this zone, the operating system does not page anything to disk,

**Zone 2** represents the stage when unused portions of the working sets are trimmed. In this stage the operating system periodically trims the unused pages from the processes' working sets whenever the amount of available memory drops to a critical value. Each time the unused portions are trimmed, the total working set value decreases, increasing the amount of available memory, which results in a significant number of pages being written to page files.

**Zone 3** represents the high pressure zone. The working sets are trimmed to a minimal value and mostly contain pages that are frequented by the greater number of users. Page faults will likely cause the ejection of a page that will need to be referenced in the future, thus increasing the frequency of page faults.

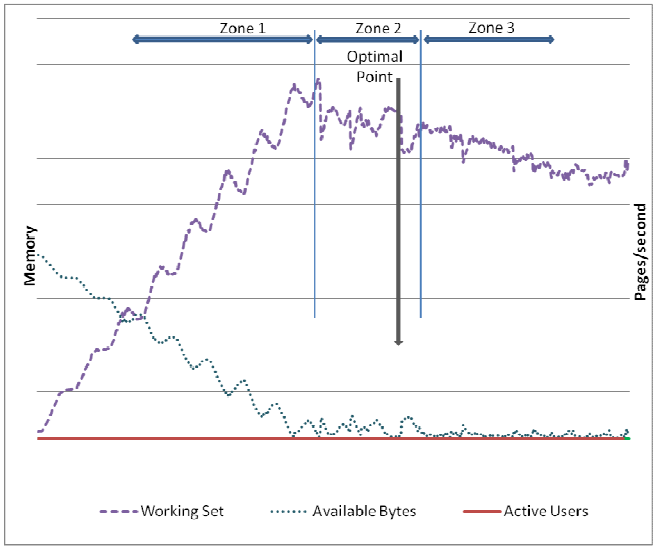


Figure 10. Stages of memory usage

## IV. CONCLUSION

Creating a test methodology consists of the definition of monitored parameters. Based on these parameters were developed tests monitoring the server load, bandwidth consumption, depending on the transport protocol, the reaction time elapsing between the user's request and reactions of the system, the ability of a server to process user requests for utilization of critical hardware resources.

After a testing methodology different test scenarios to define user behavior and hence the server load that causes are following. For the realization of test scenarios was necessary to select appropriate automated testing tools. In this work, we used primarily the programs Wintask and Remote Desktop Load Simulation Tools. Wintask allows interactive user record business, which is then converted into a scripting language like Visual Basic. Load Remote Desktop Simulation Tools is a toolset designed specifically for stress testing the Microsoft Remote Desktop Services.

The above tests were used to compare the performance characteristics and RDP protocols PCoIP that are used by VMware View and Microsoft Remote Desktop Services. The test results showed that the protocol PCoIP has much faster response system while passing through the WAN than RDP. Based on theoretical and practical knowledge, we prepared two case studies on the deployment of virtualization technology into production environments.

## ACKNOWLEDGMENTS

This article has been supported by projects No.MSM0021630513 of the Ministry of Education, Youth and Sports of the Czech Republic.

## REFERENCES

[1] Anderson, CH. K. L. Griffin. Windows Server 2008 Terminal Services. Microsoft Press, 2009, Paperback. ISBN: 978-0-7356-2585-3

[2] Microsoft TechNet. Microsoft Virtual Desktop Infrastructure (VDI) Explained. WWW: <http://edge.technet.com/Media/Microsoft-Virtual-Desktop-Infrastructure-VDI-Explained/>

[3] Remote Desktop Protocol Performance: Presentation and Hosted Desktop Virtualization. Microsoft Corporation, WWW: <http://download.microsoft.com/download/4/d/9/4d9ae28534314335a86e969e7a146d1b/RDP_Performance_WhitePaper.docx>

[4] Stanek, W. R., Mistrovstvi v Microsoft Windows Server 2008. CPRESS, 2009. ISBN: 978-80-251-2158-0.

[5] Remote Desktop Protocol Performance Improvements: in Windows Server 2008 R2 and Windows 7. Microsoft Corporation, 2009. WWW: <http://www.microsoft.com/downloads/details.aspx?displaylang=en&FamilyID=e4d25d08-ae40-4c5c-ac81-eaacdc9923d3>

[6] Remote Desktop Session Host Capacity : Planning in Windows Server 2008 R2 [online]. [s.l.] : Microsoft Corporation, 2010 [cit. 2010-04-19]. WWW: <http://www.microsoft.com/downloads/details.aspx?FamilyID=CA837962-4128-4680-B1C0-AD0985939063&displaylang=en>.

# Voice Messaging System as Measure to Distribution of Urgent Information

Filip Rezac, Miroslav Voznak, Jan Rozhon, Jiri Vychodil, Karel Tomala, Jan Diblik, Jaroslav Zdralek
Department of Telecommunications
VSB–Technical University of Ostrava
Ostrava, Czech Republic
fillip.rezac@vsb.cz, miroslav.voznak@vsb.cz, jan.rozhon@vsb.cz, jiri.vychodil@vsb.cz, karel.tomala@vsb.cz, jan.diblik@vsb.cz, jaroslav.zdralek@vsb.cz

*Abstract*— **Systems aimed at warning a large population against danger or serving as information sources are rather numerous these days and are used in many areas of human activity. Most of these systems, however, are based on sending text messages or distributing messages using a central device (siren horn, radio broadcasting). The paper deals with developed system based on VoIP enabling a user to distribute a voice message on mobile phones. It can be used not only for the purpose of warning in case of disasters but generally to notify people and announce an important message. Article also describes individual technologies which the application uses for its operation as well as issues relating to hardware requirements and transfer line bandwidth load.**

***Keywords: Voice message; VoIP; Disaster warning; Asterisk, Sipp***

## I. INTRODUCTION

Our system is based on using SIP call generator to generate and distribute voice messages directly to the end device (IPphone, cellphone, fixed line, etc.) [1]. The benefit of such communication compared to the others is the fact that it uses a phone call and therefore it is possible to get feedback who accepted the message and to improve efficiency of alert system. The whole system will be based in the data centre of a telecommunications operator and will be accessible to the crisis centre's staff. A staff member logs into the system created by us, loads the pre-recorded alert and other parameters and sends the request. The output of the application are SIP messages which are sent into communication server, it can be based on open-source softswitch, such as Asterisk or OpenSIPS [2], [3]. The softswitch processes the messages and starts initiating calls to the end users according to the pre-defined parameters. The end user obtains a better understanding and sufficient information to solve the situation. If the end user does not answer the call (missed call, phone switched off), the system arranges to re-send the message and re-initiate the call with the end user concerned.

## II. TECHNOLOGY

Primarily, the system is designed to alert population to dangerous situation. Naturally, it can be used in other areas of activities. The system has been de-signed as LAMP server [4], [5], [6]. The crisis centre' staff can operate it through a web interface.

We suppose a cooperation with mobile operators, they are able to deliver the list of numbers located in target area. The list which the staff members enter is saved in the XML format and contains three columns - telephone number of the end user, BTS station where the subscriber is registered and a throughput rate of the BTS station [7]. The number of rows in the list equals the number of end users. The messages are entered in the system in the .wav or .pcap format [8]. This voice message is then sent out to all end users and played once the phone is answered. We have developed the conversion of a WAV container into a PCAP format using the Web application (see figure 1). The file is fed in using the input file field. Once the file is fed in by a user, the programme reads the file's header. Based on the header, the codec used; number of channels, mono/stereo record, etc. are determined. The application supports up to two channels which can be converted into a mono record, μ-LAW, A-LAW and PCM codecs, 8 and 16 byte sample. The web server contains a simple form to input a file, to set up output codec and source and target IP address. Once these data have been filled in, the programme first reads the header and establishes whether the input codec is supported, the number of channels, etc. If a certain parameter does not correspond, the application returns an error message and the file is not converted. If everything is order, the file is converted and immediately offered for download by users.

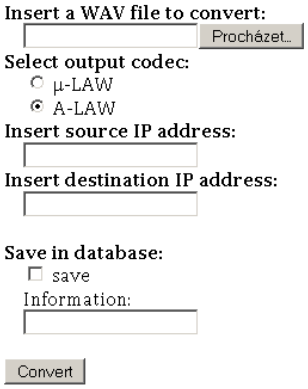


Figure 1. Web form of converting tool.

The conversion source code, and the implementation of web pages are written in PHP. This allows for easy portability between systems and operation systems' independence and wide-spectrum of utilization. Our solution uses an Apache open source server. Data about samples stored are saved in a MySQL database. Database example is shown on figure 2.

| # | Information | Lenght | Codec | Size | Source IP | Destination IP |
|---|---|---|---|---|---|---|
| 1 | Hello | 0:05 | A-LAW | 300kB | 158.196.244.2 | 196.168.142.8 |
| 2 | This is echo test | 0:53 | $\mu$-LAW | 600kB | 196.168.142.5 | 158.196.344.4 |
| 3 | Alarm | | | | | |
| 4 | Dangerous | | | | | |
| 5 | Warning | | | | | |

Figure 2. Database of saved files.

Users can define for a file to be saved in a database [9]. To achieve that, the user needs to fill in the Information field. The file is saved under the name indicated in this field and is ready for further processing. The system contains a list of files saved together with information about the files. The files can still be reconverted after they have been saved.

The staff members may set the duration of the ringing. The call is not regarded as executed unless the end user answers the call. The remaining parameters entered into the system will be described further along with other algorithms which used these parameters. The system uses the open-source generator Sipp with pre-set call schemes in the XML format [10].

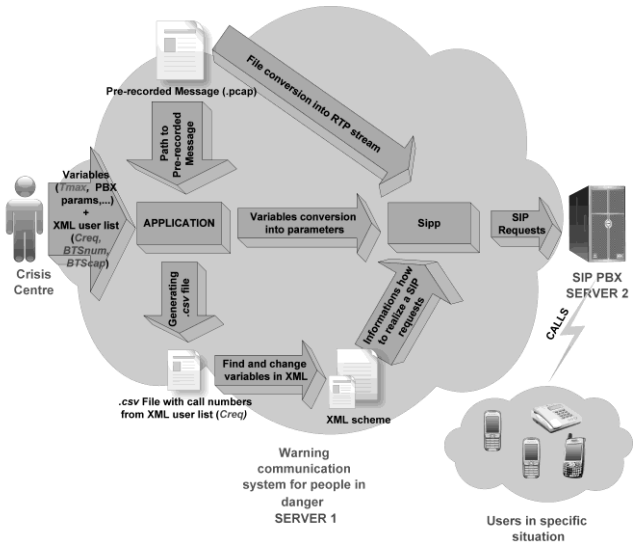


Figure 3. Alert System Scheme.

We met with Sipp in a research project in CESNET association and the acquired experience proved to be invaluable for this research [11], [12]. To be able to process parameters entered into Sipp and XML dynamically, we applied two methods.

Using the first one, a correct parameter is assigned to the values entered into the forms by the crisis centre staff, and it is then sent to Sipp. In order to dynamically switch the telephone numbers based on the loaded list of end users, values in the XML scheme for Sipp need to change dynamically too. This is the purpose of the .csv file which is generated by the application directly after the list of end users has been loaded. This is where the XML scheme gets the telephone numbers and Sipp creates the SIP message for the softswitch. Figure 3 illustrates the scheme. Another issue addressed while developing the system was how many messages and subsequent calls are we able to generate at a particular moment.

As mentioned above, via Sipp application are calls generated based on XML schemes, so it has been necessary to create a suitable template, satisfactory SIP ITU-T recommendation. Created scheme serves as instructions according to how Sipp generates the calls. In an XML scheme a variables are dynamically changed for each SIP request (called number). These numbers are imported from the generated .csv file. Figure 4 shows an INVITE request in XML scheme for Sipp.

```
<send retrans="500">
 <![CDATA[

   INVITE sip:2717@[remote_ip] SIP/2.0
   Via: SIP/2.0/[transport] [local_ip]:
   [local_port];branch=[branch]
   From: [service] <sip:[service]@
   [remote_ip]>;tag=[call_number]
   To: 2717 <sip:2717@[remote_ip]>
   Call-ID: d///[call_id]
   CSeq: 3 INVITE
   User-Agent: Grandstream GXP2000
   1.1.6.37
   Contact: <sip:[service]@[local_ip]:
   [local_port];transport=[transport]>
   Max-Forwards: 70
   Allow:INVITE,ACK,CANCEL,BYE,NOTIFY,
   REFER,OPTIONS,INFO,SUBSCRIBE,UPDATE,
   PRACK,MESSAGE
   Supported: replaces, timer, path
   Subject: Performance Test
   Content-Type: application/sdp
   Content-Length: [len]

   v=0
   o=[service] 8000 8001 IN
   IP[local_ip_type] [local_ip]
   s=SIP Call
   c=IN IP[media_ip_type] [media_ip]
   t=0 0
   m=audio [auto_media_port] RTP/AVP 0
   a=rtpmap:0 PCMU/8000
   a=ptime:20
   a=sendrecv

 ]]>
</send>
```

Figure 4. Message INVITE in XML schme.

INVITE message initiates a call to the SIP server but before Sipp sends the registers on dedicated account on SIP

server, over which the calls will be initiated. Figure 5 shows code in a XML scheme, that is used for sending prerecorded voice message in .pcap format. This message is sent by a Sipp as RTP flow to the called party.

```
<nop>
 <action>
  <exec play_pcap_audio="/home/filip/
      Desktop/SPITFILE/pcap_examples/
      danger.pcap" />
 </action>
</nop>
```

Figure 5. Sending .pcap message over Sipp.

## III. METHOD

During application development it was necessary to find out, where are the limits of the number of requests which the Sipp is able to sent. While testing, we established that Sipp is the biggest constraint of the whole system. This open-source tool can generate a maximum of 700 SIP requests at a particular moment without a fault. For higher values, the generated INVITE requests contain errors in structure or length. This is why we set the maximum amount of calls generated at a particular moment to 500. In order to be able to distribute even to sets of end users exceeding 500, it was necessary to divide the total amount of requested calls into subsets of 500 requests. We refer to these subsets as groups and set the interval between individual groups to 60 seconds. If we take into account that the maximum length of a pre-recorded voice message is 30 seconds and staff can only set the maximum duration of ringing to 15 seconds, the resulting time is 45 seconds. This means that the call length never exceeds 45 seconds. This indicates that our system can generate 500 calls every 60 seconds.

In the text and figures below, this value of maximum calls - 500 is referred to as *Cmax*. Once the staff member logs in s/he can enter the XML list of end users into the system. The system immediately calculates the total number of calls to be generated *Creq*, number of groups to which the calls will be divided *Gn* and the estimated time to send all calls *Tsnd* [s].

$$Gn \cong \frac{Creg}{Cmax} \tag{1}$$

The number of groups *Gn* is determined using formula (1), estimated time *Tsnd* using formula (2).

$$Tsnd \cong \left(\frac{Creg}{Cmax}\right) \cdot 60 \tag{2}$$

If, for instance, staff member enters a list with 6800 end users, we will obtain the following values: *Creq*=6800, *Gn*=14 and *Tsnd*=816s.

In case the threat of danger or natural disaster becomes real, staff have exact time models setting the maximum time limits in which all end users should be alerted. This time value is inserted into the system form and is described as the maximum time to send all planned calls *Tmax* [s]. Figure 6 illustrates two situations which can arise after the value is inserted. In the first case where $Tsnd \le T\max$, there is time remaining to re-send unanswered calls *Trem* [s] after all calls have been sent for the first time. In this case, the system generates the value of time remaining *Trem* and notifies the staff that during this time, the system is to automatically re-initiate calls which have not been answered in the first wave. Where the end user does not answer the call for the second time either, the calls are being re-initiated until $Trem = 0$. In the latter case, where $Tsnd < T\max$, the system returns information that the time required to initiate all calls *Tsnd* is longer that the maximum time for sending requests set by staff *Tmax* and therefore it is not possible to guarantee that all end users will be contacted and requests for unanswered calls re-generated. If staff want to contact all end users, or even set aside time to re-initiate unanswered calls, they need to increase *Tmax* so that $T\max > Tsnd$. This is how the staff get an idea of the time plan to generate calls and can thus make further steps to address the situation.

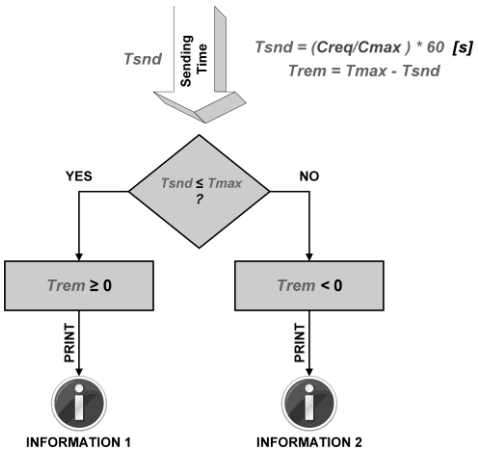


Figure 6. Time Diagram.

Other values which staff need to enter into the ready-made forms before calls can actually start to be generated is the duration of the ringing at the end user's side, login name and password to the SIP account and of course the location of the pre-recorded voice message.

Once all forms have been filled, the system can start initiating calls according to pre-set parameters. Staff members launch the call generation by pressing the SEND button. At first, the system logs into the IP switchboard and the SIP account created for this purpose and then it starts to generate SIP requests using the *Sipp* application (Figure 7).

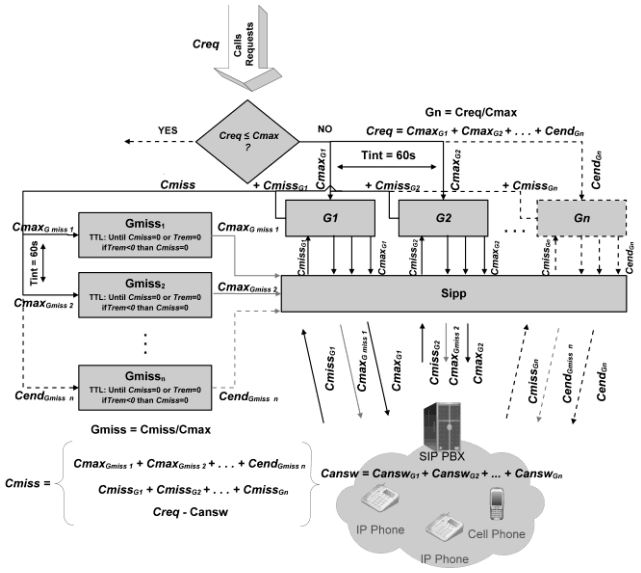


Figure 7. Calls Diagram, Creq > Cmax.

Generating is carried out across individual groups (*G1-Gn*) with 60 seconds interval. Each group contains *Cmax* call requests, the last group contains the remaining requests (*Cend*). By adding together all *Cmax* and *Cend,* we obtain a total number of call requests *Creq* (3). Requests are dispatched to the switchboard in sequence and the switchboard starts to initiate individual calls.

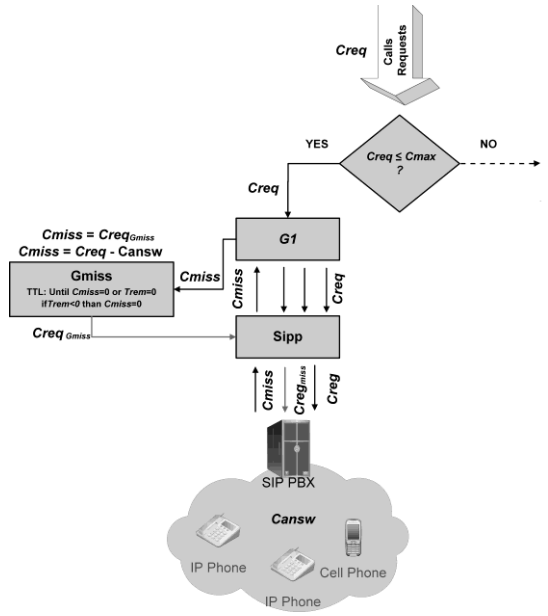


Figure 8. Calls Diagram, Creq ≤ Cmax.

At this stage, the end device (cellphone, fixed line, etc.) of the end user starts to ring and keeps ringing for the time defined by staff in the system form. If the end user answers the call within this time span, a voice message containing information about the danger and how to address it is played to him/her. This call is marked as answered (*Cansw*). If the end user fails to answer the call during the defined period of ringing, or the end device is not available, the call is marked as unanswered (*Cmiss*). Once all requests across all groups have been generated, the system adds together all unanswered calls (4). If *Trem*>0, the system starts to generate SIP requests for call previously unanswered. Where *Cmiss*>*Cmax*, such calls are again subdivided into individual groups (*Gmiss1 – Gmissn)*. The number of these groups can be determined using formula (5). Unanswered calls are re-initiated until *Trem*=0 or until there is no unanswered calls *Cmiss*=0.

## IV. FEATURES

While generating, the system indicates the total number of requests *Creq*, number of groups *Gn* and *Gmiss*, total number of answered calls *Cansw*, number of unanswered calls *Cmiss* and times *Tsnd* and *Trem*. If an unexpected situation occurs, the whole process can be aborted by pressing the ABORT button.

$$Creq = Cmax_{G1} + Cmax_{G1} + ... + Cend_{Gn} \tag{3}$$

$$Gmiss \cong \frac{Cmiss}{Cmax} \tag{4}$$

$$Cmiss = \begin{Bmatrix} Cmax_{Gmiss1} + Cmax_{Gmiss2} + ... + Cend_{Gmissn} \\ Cmiss_{G1} + Cmiss_{G2} + ... + Cmiss_{Gn} \\ Creg - Cansw \end{Bmatrix} \tag{5}$$

Figure 7 illustrates the situation where $Creq \leq Cmax$ and values of *Gn* and *Gmiss* equal 1. The definition of individual variables is the same as for figure 8.

The whole system was designed to distribute pre-recorded voice messages to alert people to danger or natural disaster. Its aim is to provide sufficient information to large population on how to address a particular situation in the shortest time possible in a form which cannot be missed or disregarded. Depending on the content of the pre-recorded message, the system may not only function as a part of the early warning scheme, but it can also function as the basic infrastructure for other areas of human activities. Below we provide an overview of situations in which the system could be used:

- Alert system for population safety during natural disasters (floods, fires, earthquakes, wind storms, snow breaks, dangerous substance leakages), conflicts (attacks, wars, raids, army drills).
- Information system: during traffic congestion, to distribute poll results, to distribute election results, to announce sports competition results, to broadcast news (e.g. for visually impaired).
- Advertising system: to distribute advertisements, to address voters, to announce lottery winners.

TABLE I. SENDING TIME FOR DIFFERENT POPULATION

| **Status** | **Example** | **Population** | **Sending Time - *Tsnd* [h] aprox.** |
|---|---|---|---|
| Village | Drnovice | 435 | 0,015 |
| Small Town | Kyjov | 11 597 | 0,39 |
| City | Brno | 371 399 | 12,38 |
| Big City | Prague | 1 285 995 | 43 |
| University | VSB-TU students | 24 058 | 0,8 |

Whatever situation the system is applied for, we can always reliably calculate the time necessary to address the target group of end users (Table 1). We use formula (2) where *Creq* is the total number of end users to be targeted and *Cmax* is set to 500. If it was necessary to inform all students at our university (24 058) about a certain event within 1 hour, our system would manage it. The same applies in case a natural disaster should occur – the system is able to advise community population within a certain time span depending on the population size.

## V. CONCLUSION

We developed a system which can distribute voice messages in the form of telephone calls using VoIP technology and SIP protocol fast and efficiently. It uses open-source application *Sipp* and any compatible softswitch enabling for registration of an SIP account. The benefit of using voice message to transfer information as opposed to other forms of information systems is that the information can be easily perceived by target audience, thus reducing the probability of it being missed. The system is controlled through a web interface, which makes it accessible from any machine with an Internet browser.

At present, the system is subject to intensive beta testing. We plan to implement several enhancements in the future, such as VoiceXML schemes for creating an interactive media dialog or a more user-friendly installation tool available through the web interface. As the *Sipp* application develops, we expect to increase the maximum amount of generated SIP requests at a particular moment.

## ACKNOWLEDGMENT

The research leading to these results has received funding from the European Community's Seventh Framework Programme (FP7/2007-2013) under grant agreement no. 218086.

## REFERENCES

[1] M. Voznak, F. Rezac, J. Zdralek, “Danger Alert Communication System”, The 17th International Conference IWSSIP 2010, June 17-19, 2010, Rio de Janeiro, Brazil, pp.231-234.

[2] J. Meggelen, J. Smith and L. Madsen, “Asterisk The Future of Telephony”, 2nd edition, O'Reilly Media, 2007.

[3] F. E. Goncalves, “Building Telephony Systems with OpenSIPS 1.6”, Packt Publishing, 2010.

[4] R. Scoular, “Apache: The Definitive Guide”, O'Reilly Media; 3rd edition, 2002.

[5] P. DuBois, “MySQL Cookbook”, O'Reilly Media; 2nd edition, 2007.

[6] R. Lerdorf, „Programming PHP”, O'Reilly Media; 1st edition, 2002 .

[7] R. Bestak, “Evolution of 3GPP Core Network”, 15th International Conference on Systems, Signals and Image Processing, JUN 25-28, 2008 Bratislava, Slovakia, pp: 25-28 .

[8] J. Vychodil, M. Voznak, K. Tomala, J. Rozhon, F. Rezac, “Converting audio WAV container to PCAP format”, In conference proceedings RTT 2010, Velké Losiny, September 8-10, 2010.

[9] P. DuBois, “MySQL, “ 4th ed., Addison-Wesley Professional, September 2008, 1224 p.

[10] M. Voznak, F. Rezac, “11th International Conference on Research in Telecommunication Technology (RTT 2009)”, SEP 02-04, 2009 Czech Tech Univ, Dept Telecommun Engn, Srby, Czech Republic, pp. 119-121.

[11] F. Rezac, M. Voznak, J. Ruzicka, “Security Risk in IP Telephony”. In proceedings CESNET Conference 2008, 25-26.2008, Prague, pp.31-38.

[12] M. Voznak, F. Rezac, “Implementation of SPAM over Internet telephony and a defence against this attack,” Asszisztencia Szervező Kft. Budapest: 32nd International Conference TSP, Dunakiliti, 2009, pp.200-203.

[13] M. Voznak, F. Rezac, M. Halas, “Speech Quality Evaluation in IPsec Enviroment. Recent Advances in Networking”, VLSI and Signal Processing: 12th ICNVS’10, University of Cambridge, UK, February 20-22, 2010, pp. 49-53.

[14] I. Pravda, J. Vodrazka, “Voice quality planning for NGN including mobile networks”, 12th International Conference on Personal Wireless Communications (PWC 2007), Prague, Book Series: International Federation for Information Processing, vol. 245, 2007, pp: 376-383.

# Applied Electronics in Telecommunications

# Detection of Negative Impact of Radio Relay Communication on the Weather Radar Measurement by Using Hough Transform

Ladislav Chmela, Jaroslav Burcik
Department of Telecommunication Engineering
FEE, Czech Technical University in Prague
Prague, Czech Republic
chmellad@fel.cvut.cz, burcik@fel.cvut.cz

*Abstract*—**The paper deals with the issue of detection of negative impact of radio relay communication on the weather radar measurement. Described methods are on the basis of image processing, as a main tool was chosen Hough transform.**

***Keywords-Radio Relay Communication; Meteorological Measurement; Weather Radar; Radar Image; Image Processing; Hough ransform***

## I. INTRODUCTION

Weather impacts and determines almost every human activity, activity of people and all society, in personal life and in work. Knowledge of current state of meteorological conditions and capability of its development prediction allows effective use of time and resources in weather-dependent activities. It is advantageous if the meteorological conditions are analyzed automatically, because autonomous work of monitor and evaluation systems is enabled.

We continue with previous solutions of this issue [1], where different sources of meteorological information were described (basic thermometers, sophisticated meteorological stations, satellite atmosphere images, radar precipitation clouds measurements or visual sky monitoring from ground). Automatic evaluation of numerical data (e.g. temperature) is generally simple. It is watching of exceeding of certain thresholds or in some cases with combination of simple numeric operations. But automatic evaluation of meteorological image data [2] brings lot of complications because image data are very divers and it takes complicated (intelligent) algorithms to detect possible errors. One of these complications is negative impact of radio relay links on meteorological radar measurements [3]. This negative impact takes effect in introducing errors on radar measured data and moreover causing errors in radar image.

## II. WEATHER RADARS AND ITS IMAGES

### A. Weather Radars

Weather radars serve to detection of rainfall cloudiness and are used for estimation of immediate rainfall intensity. Principle of the radar function is based on the reflexive dispersion of microwaves on the water drop and ice crystals in rainfalls and cloudiness. Radar measuring provide immediate review about the motion and structure of rainfall systems, enable very short-term prediction (for few minutes or hours in advance) and warning before dangerous phenomena, that are linked to convective cloudiness (storms, hailstones etc.).

At present time Radar Department of the Czech Hydrometeorological Institution (CHMI) [4] controls two weather radars: radar Gematronik in Drahanská highlands (hill Skalky) for central Moravia and radar EEC in Brdy highlands (hill Prague) for central Bohemia. Weather radars serve for detection of precipitation clouds (storms up to about 250 km from the radar). They can be used for estimation of instantaneous precipitation intensity up to approximately 150 km from the radar.

### B. Weather Radar Measurement

Typically, weather radar measurements are composed of approximately 10 to 20 azimuth rotations of antenna with various elevation angles. These volumetric measurements are repeated every 5 minutes [4].

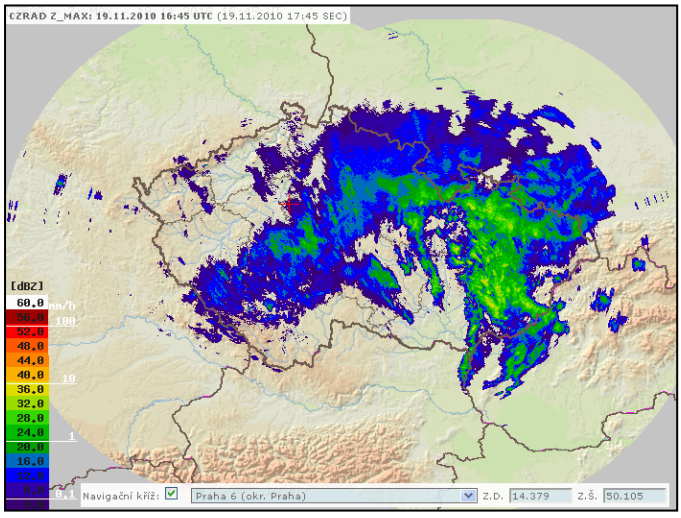


Figure 1. Weather radar image [5].

Creation of consolidated Czech Republic radar information is made centrally every 5 minutes on server in workplace in Prague-Libuš. Every 15 minutes there are publically disposable images on CHMI website [5] in lower resolution; example is on the fig. 1.

### C. *Weather Radar Data*

Volumetric radar data are stored in spherical coordinate system to RVD files (RVD format is universal open format independent on radar producers) [6]. File consists of text header (basic volumetric measurements parameters) and binary data (intrinsic measurement volumetric radar data).

Volumetric data are written by individual elevations (according to the order entered in the header, mostly from the lower to the highest elevation). Each elevation is composed of beams with fixed azimuthal step (step must be calculated from the number of beams in the elevation – usually 1 step = 1 °). Data are written beam by beam clockwise. The first beam starts to the north (azimuth 0 °). Each beam is recorded away from the radar to the maximum distance. The number of samples per beam and the number of beams in the elevation is written in the text header separately for each elevation. Each value (spherical pixel) is recorded by 1 byte (8 bits). Data is encrypted by SIGMET RVP6 convection. Fig. 2 illustrates the data as image information in the so-called B-display [7]. This is a representation of radar reflectivity $Z$ for the lowest elevation ($\theta = 0.1$ °).

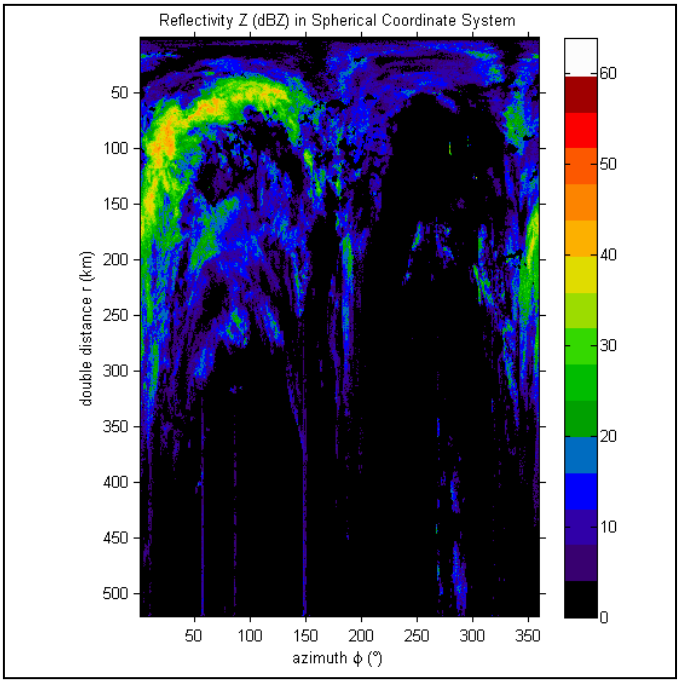


Figure 2. Illustration of reflection Z for the lowest elevation in spherical coordinates.

### D. *Weather Radar Images*

For practical application radar data are transferred from spherical coordinates ($r$, $\theta$, $\varphi$) to 3D Cartesian coordinates ($x$, $y$, $z$). To simplify the transformations between the two-dimensional images (matrices) systems, it is possible to not consider the specific elevation angle ($\theta = 0$ °). However, this is only work simplification and distorts the three-dimensional relationship between data from different elevations. Then for every combination of Cartesian coordinates $x$ and $y$ we calculate origin polar coordinates $r$ and $\varphi$ by next equations:

$$r = \sqrt{x^2 + y^2} \tag{1}$$

$$\varphi = \operatorname{arctg}\left(\frac{y}{x}\right) \text{ for } \varphi \in \langle 0, 90 \rangle \tag{2}$$

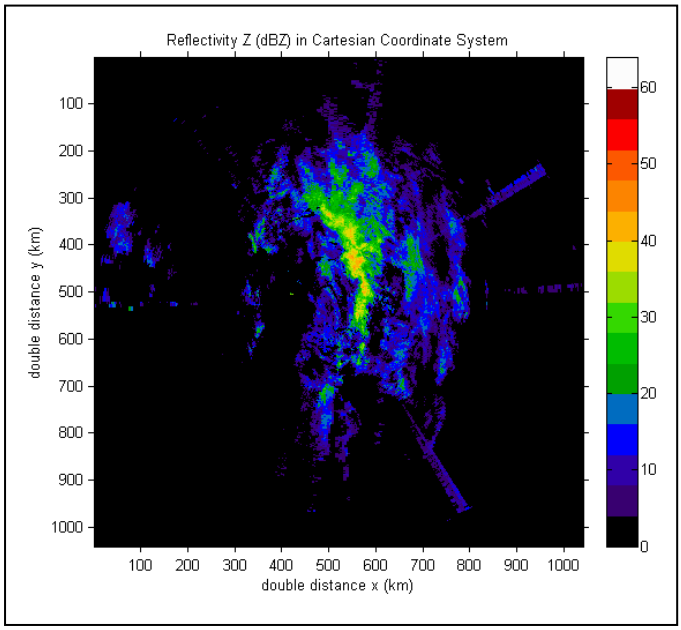


Figure 3. Illustration of reflection Z for the lowest elevation in Cartesian coordinates.

In fig. 3 is shown the same situation as in fig. 2, this time in Cartesian coordinates, in the so-called P-display (PPI: Plan-position indicator) [7]. This representation can be already easily used e.g. as link with map for context of detected precipitation clouds with the territory over which it is located; see fig. 1.

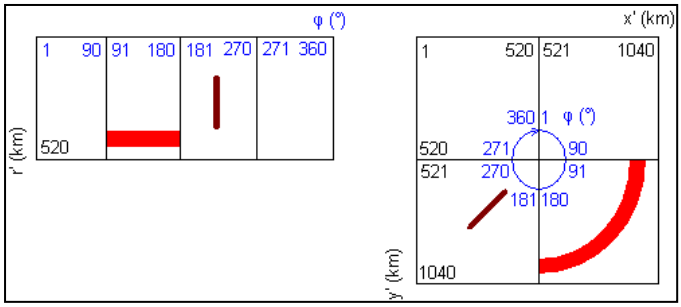


Figure 4. Scheme of related areas in the polar system coordinates with the individual quadrants of the Cartesian system of coordinates.

For illustration, scheme of related areas in the polar system coordinates with the individual quadrants of the Cartesian system of coordinates, is shown in fig. 4. This scheme is particularly useful when working with azimuth φ as the functional formula in the form set out above applies only to a certain interval of angles.

## III. Negative Impact of Radio Relay Communication on the Weather Radar Measurement

Since the beginning of weather radars operating in the Czech Republic the radio relay connections have not had on radar measurements any influence, because both systems operate in different frequency bands. In 2005 there was a significant change in the potential uses of free frequency band [8].

Based on the general authorization VO-R/12/08.2005-34 [9] issued by the Czech Telecommunication Office (CTO) is now allowed to operate in 5 GHz. Band from 5.15 to 5.35 GHz can be used only indoors, band from 5.470 to 5.875 GHz even outdoors. However, the CHMI weather radars have been operating in the latter interval since 1995. Radars have such sensitive receivers, that they capture even very distant radio relay communications that the radar images show as radial units with tip in the source of interference, directed away from influenced radar (see fig. 5) [10].

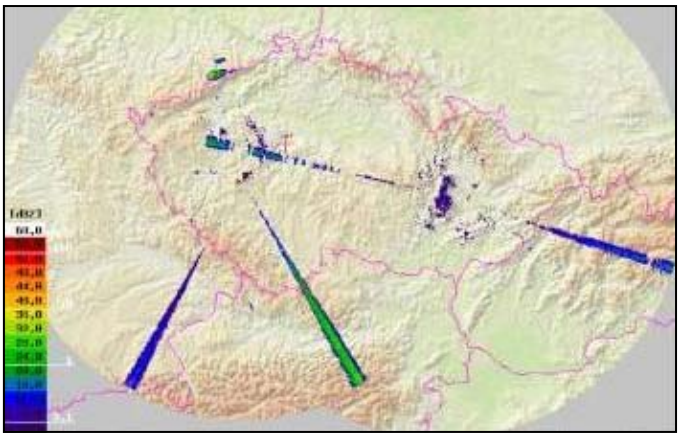

Figure 5. Example of interference of weather radars by radio relay communications [10].

While CTO requires operators who post on the same frequency as the weather radars to move their operations to another frequency, the noise is still so common that CHMI even tried to retune their radars because of constant dissatisfaction with interference radar measurements [11]. Initial frequencies were changed from 5.652 GHz (Skalky) and 5.660 GHz (Brdy) to 5.645 GHz (Skalky) and 5.630 GHz (Brdy) on 21.05.2009 [4]. But the problem persists even with this change.

## IV. Detection of Negative Impact of Radio Relay Communication on the Weather Radar Measurement

The negative impact of radio relay communication on the weather radar images is seen as the line objects. Image processing methods [12, 13, 14] offer different ways to approach the line detection, e.g. using Laplacian or Kernel line finding operators. Another way is to use Hough transform.

Main advantage of Hough transform is that it is tolerant of gaps in feature boundary descriptions and is relatively unaffected by image noise. The fundamental idea of the Hough transform is based on the polar coordinate representation of the line. If a line exists in the image, it will be in accordance with a polar equation given by [12]:

$$\rho = m\cos\theta + n\sin\theta\,, \tag{3}$$

where $\rho$ is the length of a normal vector from the origin to this line and $\theta$ is the orientation of $\rho$ with respect to the $x$-axis. For any point $(m,n)$ on this line, $\rho$ and $\theta$ are constant. Hence, for every $(m,n)$ coordinate pair on the line, there exists a value of $\theta$ and $\rho$ that is an entirely different manifestation of the image [12]. This is shown in fig. 8.

In the case of using Hough transform process of detection of negative impact of radio relay communication on the weather radar measurement we proceeded according to these steps:

*1) Conversion of radar image to the binary image.* It is necessary to set threshold of reflection $Z$ for conversion of radar image to the binary image.

*2) Application of the mathematical morphology (especially closing).* It is important to use proper structuring element.

*3) Using edge detection (Canny).* It is necessary to set value of Canny detection threshold.

*4) Applying the Hough transform.* It is important to have properly prepared the input image.

*5) Show result in original radar image.*

### A. Preparing Image for Edge Detection

The radar image in the original state (as in fig. 2 and 6a) is difficult to process with Hough transform, that´s why it is necessary to prepare it. First step is convert image to binary value state as in fig. 6b. Threshold in this case is zero. Second step is using mathematical morphology to prepare image for edge detection. Because the lines that are sought are vertical, we use the structural element linking the narrow points vertically above each other in closing mathematical morphology. Result is in fig. 6c.

### B. Edge Detection

Image processing methods [12, 13, 14] offer different ways to approach to the edge detection, e.g. using Sobel or Prewitt operator. Another way is the edge detection with Canny operator.

Calculate Canny edges takes a lot longer than usual convolutional edges. On the other hand the edges obtained by the Canny operator are much more smooth and clear and hence more tolerant to noise [12]. Fig. 6d, 7a and 7b show results with three different values of a threshold.

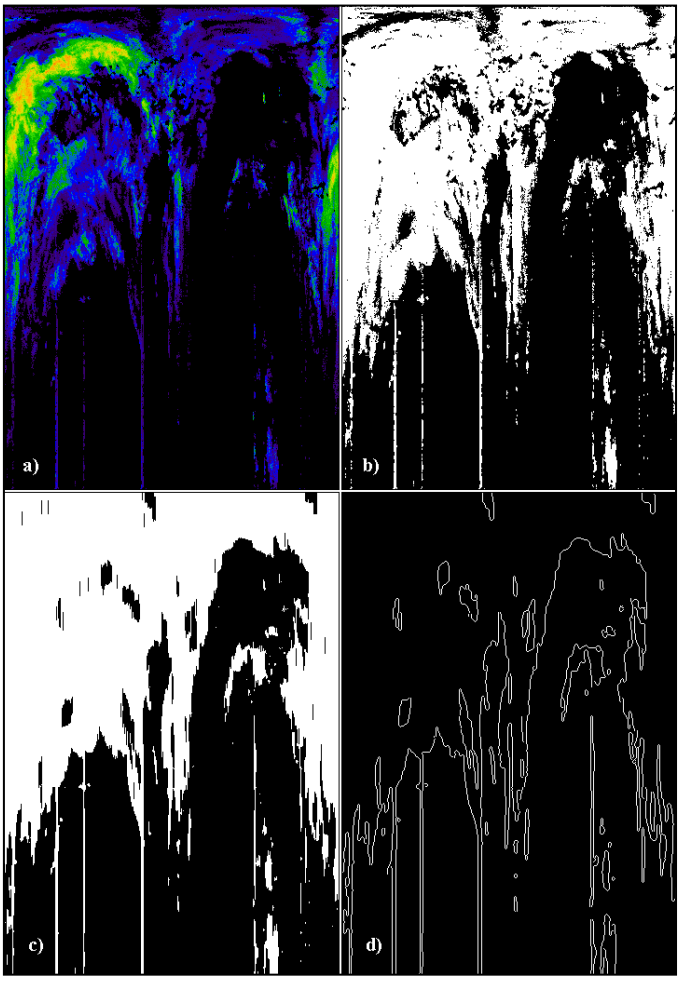


Figure 6. Original image (a), binary image (b), closing (c) and Canny edge detection with a threshold of 0.6 (d)

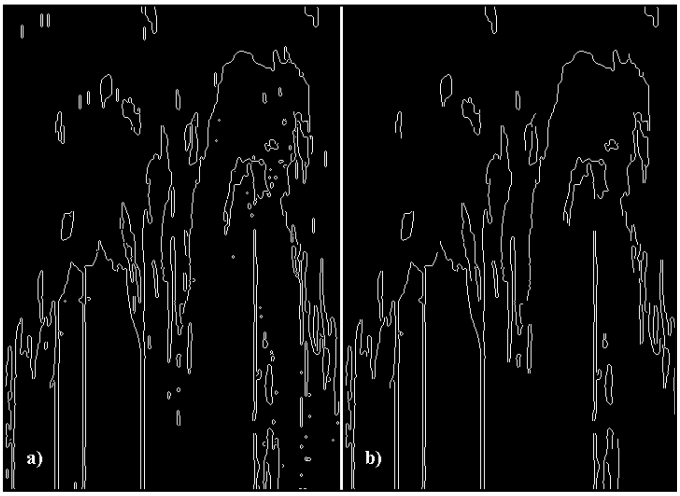


Figure 7. Canny edge detection with a threshold of 0.1 (a) and 0.9 (b).

### C. *Line Detection Using Hough Transform*

Finally is used Hough Transform for detecting vertical lines. In both fig. 9a and 9b is used parameter *theta* ($\theta$) from –0.5 to 0.5 by steps 0.5. The reason for the limited spread of $\theta$ is expected vertical direction of the line search. This is shown in Figure 8, where highs are just about $\theta = 90$ degrees.

Results are accurate and represent the fundamental basis for continuing in elimination of negative impact of radio relay communication on the weather radar measurement.

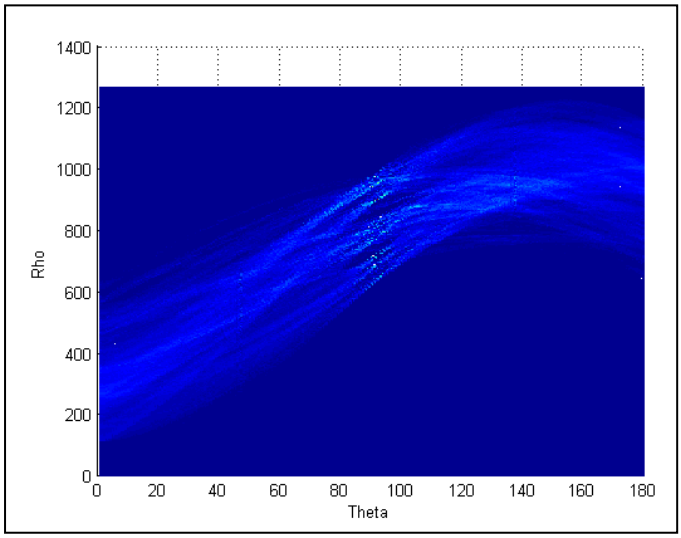


Figure 8. Mesh plot for the Hough transform. From Canny edge detection with a threshold of 0.6 (b).

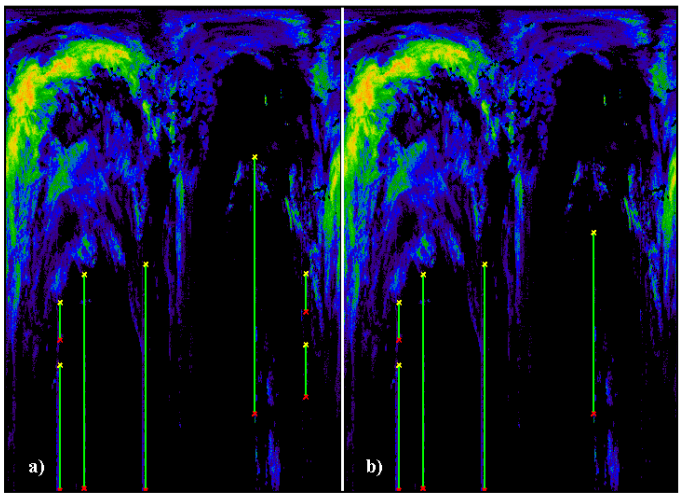


Figure 9. Line detection using Hough transform. From Canny edge detection with a threshold of 0.1 (a) and 0.9 (b).

## CONCLUSION

We introduce basic and simple way of the detection of negative impact of radio relay communication on the weather radar measurement by using Hough transform.

In the case of using Hough transform is necessary important to have properly prepared the input image. Our solution consists of a few relatively simple steps (conversion of radar image to the binary image, application of the mathematical morphology, using edge detection, applying the Hough transform.

Elimination of the detected errors will be the next stage of the solution. After the successful design of the whole algorithm will follow the algorithm testing on continuous set of radar data for statistical evaluation of the success of our method. The results of our efforts will be implemented in a real processing of current CHMI meteorological data.

## ACKNOWLEDGMENT

The data used in this paper was provided for research purposes by the Radar Department of the Czech Hydrometeorological Institute.

## REFERENCES

[1] L. Chmela, "Automatická analýza meteorologické situace" (Automatic Analysis of Meteorological Situation), Diploma theses. Prague: Czech Technical University in Prague, 2008.

[2] L. Chmela and J. Burčík, "Meteorological Image Processing in Automated Systems," Proceedings of IWSSIP 2008. 15th International Conference on Systems, Signals and Image Processing. Bratislava: Slovak University of Technology, 2008, p. 527–530. ISBN 978-80-227-2856-0.

[3] L. Chmela and J. Burčík, "Negativní vliv radioreléových spojů na meteorologická radarová měření" (Negative Impact of Radio Relay Communication on Radar Measurement), Sborník příspěvků konference KRÁLÍKY 2009. Brno: Brno University of Technology, FECT, 2009, p. 109–112. ISBN 978-80-214-3938-2.

[4] "CHMI Radar Network" [online], Prague: Radar Department of the Czech Hydrometeorological Institute, 2010 [cit. 2010-11-21]. WWW: http://portal.chmi.cz/files/portal/docs/meteo/rad/info_czrad/index.html.

[5] "Aktuální radarová data" (Actual Radar Data) [online], Prague: Radar Department of the CHMI, 2010 [cit. 2010-11-21]. WWW: http://portal.chmi.cz/files/portal/docs/meteo/rad/data_jsradview.html.

[6] P. Novák, "Definice formátu radarových dat ČHMÚ-OR. verze 1.2" (Definition of Radar Data Format), Prague: CHMI, 2006.

[7] "IEEE Std 686™-2008: IEEE Standard Radar Definitions," New York: IEEE Aerospace and Electronic Systems Society, 2008.

[8] M. Wimmer and J. Čížek, "Soudobé trendy v oblasti moderních bezdrátových spojů" (Contemporary trends in modern wireless communications) [online], Prague: CESNET, 2005 [cit. 2010-11-21]. WWW: http://www.cesnet.cz/doc/techzpravy/2005/trendy.

[9] "Všeobecné oprávnění ČTÚ č. VO-R/12/08.2005-34 k využívání rádiových kmitočtů a k provozování zařízení pro širokopásmový přenos dat na principu rozprostřeného spektra nebo OFDM v pásmech 2,4 GHz a 5 GHz" (General Permission CTO n. VO-R/12/08.2005-34) [online], Prague: CTO, 2005 [cit. 2010-11-21]. WWW: http://www.ctu.cz/1/download/Opatreni%20obecne%20povahy/VO_R_12_08_2005_34.pdf.

[10] P. Havránek, T. Žejdlík and P. Novák, "Systematické rušení české meteorologické radarové sítě CZRAD zařízeními RLAN" (Systematic Interference Czech Weather Radar Network CZRAD with Devices RLAN) [online], Prague: CHMI, 2007 [cit. 2009-06-09]. WWW: http://www.chmi.cz/meteo/olm/Let_met/_tmp/ruseni_radaru.htm.

[11] P. Moš, "Meteorologové museli přeladit radar, kvůli internetu" (Meteorologists Had to Tune the Radar, because of the Internet) [online], Prostějov: Prostějovský deník, 2009 [cit. 2010-11-21]. WWW: http://prostejovsky.denik.cz/zpravy_region/meteorologove-museli-preladit-radar-kvuli-internet.html.

[12] U. Qidwai and C. H. Chen, "Digital Image Processing: An Algorithmic Approach with MATLAB," Boca Raton: Chapman & Hall/CRC, 2010. ISBN 978-1-4200-7950-0.

[13] R. C. Gonzalez and R. E. Woods, "Digital Image Processing," New Jersey: Pearson Education, Inc., 2008. ISBN 978-0-13-168728-8.

[14] M. Sonka, V. Hlavac and R. Boyle, "Image Processing, Analysis and Machine Vision," Toronto: Thomson, 2008.

# Bluetooth Based Body Sensor Network

Martin Cerny , Marek Penhaker
Department of Measurement and Control
VSB – Technical University of Ostrava
Ostrava, Czech Republic
martin.cerny@vsb.cz, marek.penhaker@vsb.cz

*Abstract* – **Bluetooth is commonly used technology for plenty applications. The aim of this work is to utilize advantages of Bluetooth for biosignal data transmission, to design functional and useful body senosor network . The design has been influenced by economical crisis, the price of bluetooth modules and biosignal sensors has been minimalized.**

## I. INTRODUCTION

The Bluetooth is one of the modern telecommunication technologies, which is used in many branches so often now. This young and dynamically developed technology is used in many applications, which we are using every day. It is used in mobile telecommunications, for wireless connection of computer peripheries, for wireless connections of various sensors and regulators in industry regulations [1].

So why don't to use this technology in biomedical engineering. This work treats of usage the Bluetooth technology in biomedical engineering. The Bluetooth technology is used for wireless transmission of some biological signals from measuring device to computer. Measuring devices including Bluetooth could be more mobile, the manipulation with these devices could be easier and there couldn't be emplacement problems. To check on possibility of usage of Bluetooth technology in biomedical engineering it was used for transmission data from blood pressure monitor, from device for pulse oximetry and ECG data[5],[6].

Cable replacement is benefit for user. User get more comfort, the manipulation with device is easier. The device is more flexible and more useable. There is the possibility to create wireless network set up from more devices. It is possible to communicate with notebooks, PDA or mobile phones [2].

## II. MATHERIALS AND METHODS

It was used OEM modules from refurbished produces for measure. Such OEM modules are often included in many diagnostics devices. Because such OEM modules are created for using at built-in systems, it was necessary to solve problems with power supply and optimize communication interface to can those OEM modules communicate with computer by standard serial interface or by Bluetooth. There was for both selected OEM modules designed and realized circuits for power supply stabilization, circuits for conversion communication interface of modules to RS232 standard and circuits which allow connections with modules for realize Bluetooth connections[4].

The first chose OEM module is OEM module named ChipOx from EnviteC Company. ChipOx is a pulse oximeter module for the non-invasive determination of the functional oxygen saturation in human arterial blood (SpO2) and for measuring the pulse frequency. ChipOx has very small dimensions (31mm x 14mm x 5mm), which allows it to be easily installed in medical products. It also has low energy consumption, is equipped with ESD and EMC protection and can be easily mounted on a carrier printed circuit board (host PCB).

ChipOx offers 3 inputs with maximal input voltage 2400 mV for the measurement of other parameters, which are each sampled with a maximum of 100 Hz, 12 Bits.

The sampling rate and the input voltage ranges are freely configurable over the communication protocol.

The second chose OEM module is module ECG 100 from MCC Company. It is created for electrocardiography with standard bipolar limbs leads. It can communicate by UART protocol. It sends to host device values of II and III Einthoven leads. Measured pulse frequency range is between 30 and 245 beats per second and it is measured as sliding average from last eight measured values. Module can detect pacemaker impulses and when leads are not connected.

For blood pressure measuring was used blood pressure monitor UA-767PC, which include standard serial interface. This interface was used for Bluetooth communication too. The Bluetooth module was connected to that interface. It was necessary to connect Bluetooth module to serial connector and provide power supply. The blood pressure monitor can save measured values from last 126 measurements. It is saving these four basic values: systolic pressure, diastolic pressure, pulse frequency and time. It is possible to start a new measuring by defined command from connected computer too. In this case the monitor sends to computer measured values immediately after end of measuring process.

Figure 1 Blood pressure monitor

Bluetooth module, which was chosen for realisation Bluetooth communication, can be used as a component in many types of systems allowing them to communicate wirelessly with other Bluetooth products such as PC-cards, laptops, handheld computers and mobile phones. It allows with an RS232 port or UART interface to communicate wirelessly via Bluetooth with other Bluetooth devices. The module can be configured using the Windows based configuration wizard or using AT commands. It supports Generic access profile, Serial port profile, Dial-up profile and LAN access profile. The module is qualified according to the Bluetooth 1.1 specification. Next function of this module is Wireless multidrop. This feature allows the module to simultaneously communicate with up to three remote Bluetooth devices depending on application and cases. The module automatically forms a wireless multidrop network and distributes all data to all connected devices.

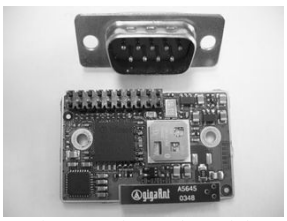

Figure 2 Bluetooth module

## III. TREATMENT

The first was tested communication between referenced devices and computer by standard serial line. It was good for test of functionality of devices and ability of communication [3]. Then can be designed, realized and tested Bluetooth communication. The first it was point-to-point communication afterwards the point-to-multipoint communication. It was created wireless network of all referenced devices.

It is necessary to set up correct communication protocol of serial communication between device (computer) and Bluetooth module the first. Afterwards could be set up the parameters of Bluetooth communication.

At the basic settings were set up name of Bluetooth device and selected possibility to set up the Bluetooth parameters by Bluetooth. Next was selected operation mode connectable and discoverable. The other devices can connect to it and it can be found when other devices are performing searches. It was necessary to decide on a client or a server role of Bluetooth module. Used Bluetooth modules can be set up client and the server at the same time. It is very profitable at point-to-point communication.

For point-to-point communication were designed three versions of Bluetooth communications parameters. Referenced Bluetooth modules at the computer and device side realized the Bluetooth communication too.

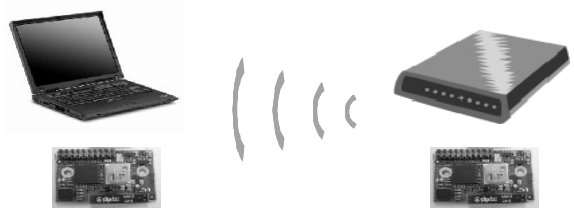

Figure 3 Point-to-point communication

For point-to-multipoint communication was possible to use on computer side USB Bluetooth dongle or referenced Bluetooth module and its function for creating point-to-multipoint network - Wireless multidrop. But after tests it was clear that this function (Wireless multidrop) isn't accordant with engaged wants. As a consequence was chosen USB Bluetooth dongle BT-600 from ACER Company. This USB dongle can work by standard driver for Bluetooth communications included in operating system WindowsXP (2nd service pack). This driver provides to create more than one virtual serial port.

The first was tested point-to-point communication between computer with USB Bluetooth dongle and measuring devices via Bluetooth. Afterwards was designed and realized point-to-multipoint connection between referenced USB Bluetooth dongle and all other referenced devices. After the far devices with Bluetooth module were found by the USB Bluetooth dongle (more precisely by drivers in operating system), were these devices added to list of Bluetooth devices. Each of found devices gets own virtual serial port. In the visualisation software, which was created too, was set up only correct name of virtual serial port for each device, and communication could start.

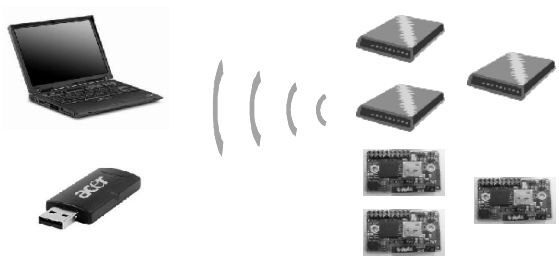

Figure 4 Point-to-multipoint communication

The Bluetooth communication is realized in RFCOMM standard. Every used module will be represented in the PC by virtual serial ports. User has

to find correct serial port, can connect device properly to PC. There could be find problem with connection establishing, because each driver for Bluetooth dongles has other structure. The standard Bluetooth driver in windows was tested and original software for ACER Bluetooth dongles too. The official driver was better; the communication had more parameters which could be changed, the security settings was better. After any tests the driver was changed. It was possible to establish, but user had to know that only serial port marked as outgoing is right.

Part of this work is the software for visualisation and saving measured data too. This software, named BIOMONITOR is developed in development system Labview from National instruments, version 6.1. The most important demands were easy intuitive control and very good lucidity of user interface.

It was designed and realized user interface, where each group of measured values has own colour of chart or more precisely colour of background. The part of final software is the Terminal too. Terminal allows to user select, which values would to measure at that time. Depending on it the user interface is changed and user can see only that charts and groups of indicators, which are need to indicate measured data.

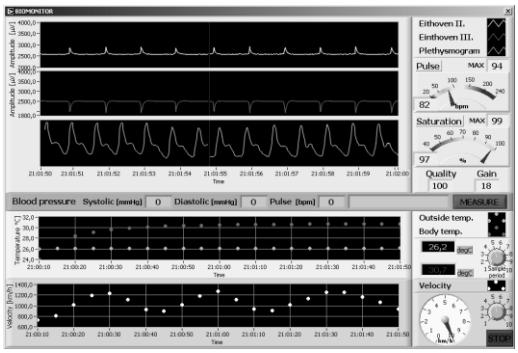

Figure 5 BIOMONITOR user interface

## IV. RESULTS

It was realized wireless network of medical devices. The network was realized by Bluetooth technology. For Bluetooth communication was used Bluetooth modules created for serial cable replacement on the device side. On the computer side was used USB Bluetooth dongle. All the system is mobile and can be used in every computer, which can cooperate with USB Bluetooth dongle. It can be used in computer which include anything else for realize Bluetooth communication. Accumulators can supply realized devices. It is very good, because such devices are flexible and mobile.

It was created software for visualisation and saving measured data. Software is very easy to control and it is very well designed. Software displays all the measured biosignals at the time. It means, there are visible values electrical activity of hearth - Eithoven I and Eithoven III, plethysmogram, quality and gain of measured signal of plethysmography. The next part of user interface of software displays values of blood pressure measurement – values of systolic and diastolic blood pressure. There is a filed which displays a status of measurement of error messages. The last part of user interface displays values which are measured by analog inputs of ChipOx module. In this case there are measured two values of temperature and velocity of car, where entire measuring system could be used. All measured values are saved to structured files, to be used for next data processing.

## IV. CONCLUSION

The results of this work can be used in implementation of wireless communication in branch of medical technique. Realized network of devices can be used in many applications of telemedicine, mainly as the system of monitoring base life functions. This network can be used in the field of telemonitoring for example long ill people, elderly people and other. Displayed version of software is suited for visualisation values which are measured in frame of project of Biomedical laboratory VSB-TU Ostrava.

## ACKNOWLEDGMENT

The work and the contribution were supported by the project Grant Agency of Czech Republic – GAČR 102/08/1429 “Safety and security of networked embedded system applications”. The work was in part supported by the Ministry of Education of the Czech Republic under Project 1M0567.

## REFERENCES

[1] Cerny M., Penhaker M. Biotelemetry In *conference proceedings 14th Nordic-Baltic Conference an Biomedical Engineering and Medical Physics,* JUN 16-20, 2008 Riga, LATVIA, Volume: 20 Pages: 405-408 Published: 2008, ISSN: 1680-0737, ISBN: 978-3-540-69366-6

[2] V. Kasik FPGA based security system with remote control functions. In *5th IFAC Workshop on Programmable Devices and Systems*, NOV 22-23, 2001 GLIWICE, POLAND, IFAC WORKSHOP SERIES Pages: 277-280, 2002, ISBN: 0-08-044081-9

[3] Krejcar, O., Cernohorsky, J., New Possibilities of Intelligent Crisis Management byLarge Multimedia Artifacts Prebuffering. In *I.T. Revolutions 2008, December 17-19,2008 Venice, Italy*. Lecture Notes of the Institute for Computer Sciences, Social-Informatics and Telecommunications Engineering, LNICST Vol. 11. pp. 44-59. M. Ulieru, P. Palensky and R. Doursat (Eds.). Springer, Berlin, Heidelberg. ISBN 978-3-642-03977-5, ISSN 1867-8211 (Print) 1867-822X (Online), DOI 10.1007/978-3-642-03978-2_2008/01

[4] Bernabucci, I., Conforto, S., Schmid, M., D'Alessio, T. A bio-inspired controller of an upper arm model in a perturbed environment, In proceedings The 2007 International Conference on Intelligent Sensors, Sensor Networks and Information Processing Pages: 549-553 ISBN: 978-1-4244-1501-4

[5] Simsik,D., Galajdova,A., Majernik,J., Busa,J., Zelinsky,P.: Grundtvig training on technical advisory in assistive technology. Lekar a technika. Czech Republic,Volume 35, 2004, ISSN 0301-5491, pp. 111 - 113.

[6] Majerník, J., Svida, M., Majerníkova, Z.: Medicínska informatika. 1. vydanie, Univerzita Pavla Jozefa Šafárika v Košiciach, Košice, 2010, Equilibria, s.r.o., ISBN 978–80–7097–811–5, 200 s.

# Implementation of Incremental Controller into a Single Chip Microcontroller

Robert Frischer, Ivo Spicka, Milan Heger
dept. of Automation and Computing in Metallurgy
Technical University of Ostrava
Ostrava, Czech Republic
robert.frischer@vsb.cz, ivo.spicka@vsb.cz, milan.heger@vsb.cz

***Abstract*—The goal of article is to provide a basic mathematical description of incremental controller and suggest structure of single blocks so that be able to implement into single chip microcontroller. Individual blocks are analyzed as far as elementary operation's level. From hardware description resulting, that selected structure is suitable for implement into similar MCU especially if they are able to configure I/O pins as with ours MCU.**

**Keywords- Incremental; Proportional; PIC; Controller; Handled Limit States**

## I. INTRODUCTION

The PID controller algorithm involves three parameters: the proportional, the integral and derivative values, denoted P, I, and D. The proportional value determines the action to the current error, the integral value determines the action as the sum of recent errors, and the derivative value determines the action based on the rate at which the error has been changing. The sum of these three actions known as action value adjust the system state via a action element such as a control valve.[2]

Note that the use of the PID algorithm does not guarantee optimal control strategy of the system or system stability.

Some applications may require using only one or two modes, a PID controller will be called a PI, PD, P or I controller.

Note: Due to the diversity of the field of control theory and application, many naming conventions for the relevant variables are in common use.

### Control loop basics

A familiar example of a control loop is mixing hot and cold water by using corresponding valves to maintain the water at the desired temperature. This typically involves the mixing of two streams, the hot and cold water. The person tests the water or measure its temperature. Based on this knowledge - feedback they perform a control action to adjust the hot and cold water valves until the process temperature stabilizes at the desired value.

## II. PID FUNCTION

In the absence of disturbances, pure proportional control will not settle at its target value, but will retain a steady state error (droop) that is a function of the proportional gain and the process gain. Only the drift component (long-term average, zero-frequency component) of process gain matters for the droop – regular or random fluctuations above or below the drift cancel out.

### *A. Proportional term*

The proportional term (sometimes called gain) makes a change to the output that is proportional to the current error value. The proportional response can be adjusted by multiplying the error by a constant Kp, called the proportional gain [5].

### *B. Integral term*

The contribution from the integral term (sometimes called reset) is proportional to both the magnitude of the error and the duration of the error. Summing the instantaneous error over time (integrating the error) gives the accumulated offset that should have been corrected previously [5].

### *C. Derivative term*

The rate of change of the process error is calculated by determining the slope of the error over time (i.e., its first derivative with respect to time) and multiplying this rate of change by the derivative gain Kd [5].

### *D. Integral windup*

One common problem resulting from the ideal PID implementations is an integral windup, where a large change in setpoint occurs (say a positive change) and the integral terms accumulates a significant error during the rise (windup), thus overshooting and continuing to increase as this accumulated error is unwound. This problem can be addressed by:

- Initializing the controller integral to a desired value
- Increasing the setpoint in a suitable ramp
- Disabling the integral function until the PV has entered the controllable region
- Limiting the time period over which the integral error is calculated
- Preventing the integral term from accumulating above or below pre-determined bounds

- Freezing the integral function in case of disturbances

Many PID loops control a mechanical device (for example, a valve). The rate of mechanical wear is mainly a function of how often a device is activated to make a change. Where wear is a significant concern, the PID loop may have an output deadband to reduce the frequency of activation of the output (valve).

The proportional and derivative terms can produce excessive movement in the output when a system is subjected to an instantaneous step increase in the error, such as a large setpoint change. In the case of the derivative term, this is due to taking the derivative of the error, which is very large in the case of an instantaneous step change. As a result, some PID algorithms incorporate the following modifications:

*E. Derivative of output*

In this case the PID controller measures the derivative of the output quantity, rather than the derivative of the error. The output is always continuous (i.e., never has a step change). For this to be effective, the derivative of the output must have the same sign as the derivative of the error.

*F. Setpoint ramping*

In this modification, the setpoint is gradually moved from its old value to a newly specified value using a linear or first order differential ramp function. This avoids the discontinuity present in a simple step change.

*G. Setpoint weighting*

Setpoint weighting uses different multipliers for the error depending on which element of the controller it is used in. The error in the integral term must be the true control error to avoid steady-state control errors. This affects the controller's setpoint response. These parameters do not affect the response to load disturbances and measurement noise.

*H. Noise in derivative*

A problem with the Derivative term is that small amounts of measurement or process noise can cause large amounts of change in the output. It is often helpful to filter the measurements with a low-pass filter in order to remove higher-frequency noise components. However, low-pass filtering and derivative control can cancel each other out, so reducing noise by instrumentation means is a much better choice. Alternatively, a nonlinear median filter may be used, which improves the filtering efficiency and practical performance [1].

## III. PID CONTROLLER THEORY

The PID control scheme is named after its three correcting terms, whose sum constitutes the control variable $u$. A difference between desired value of controlled system output $w$ and real system output $y$ give an error $e$ as an input of the controller. Its output control value is signed as $u$.

$$e(t) = y(t) - w(t) \tag{1}$$

In the time space the controller can be described by the following equation

$$\mathrm{u(t)} = \mathrm{r_0 e(t)} + \mathrm{r_I} \int_0^{\mathrm{t}} \mathrm{e(t)dt} + \mathrm{r_d} \frac{\mathrm{de(t)}}{\mathrm{dt}} \tag{2}$$

There $r_0$ is the proportional gain, $r_I$ is the gain of the integral part and $r_D$ is the gain of the derivation part of controller equation.

The transfer function $G_r$ of the controller in complex space can be written as

$$G_r = \frac{U(s)}{E(s)} = r_0 + \frac{T_I}{s} + T_D\, s \tag{3}$$

where $U(s)$ is an controller output, $E(s)$ is error function $T_I$ id the time constant of integral part, $T_D$ is the time constant of derivate part of the controller. This equations is not very suitable for make a sense how to program a discrete controller using microcontroller unit. So it is necessary to find some discrete equivalents of integral and derivation. Some good substitution are a sum and a difference. So the equations (x) can be rewritten using following terms

$$\int_0^t e(t)dt \approx T \sum_{i=0}^{k-1} e_i \tag{4}$$

$$\frac{de(t)}{dt} = \frac{e_k - e_{k-1}}{T} \tag{5}$$

In the difference from the basic representation of the summation controller can be written as

$$u(k) = u_0 + r_0 e_k + \frac{r_0}{T_I} \sum_{i=1}^{k} e_i + r_0 T_D \frac{(e_k - e_{k-1})}{T} \tag{6}$$

This mathematical form has one basic problem - it can be known all errors $e_k$ from the beginning time to present time. Next form, where only last tree error values for step $k, k-1$ and $k-2$ are necessary. In the equation () $I_k$, , $D_k$ and $D_{k-1}$ are sums and differences from equation ().

$$\Delta u_k = u_k - u_{k-1} = r_{0(e_k - e_{k-1})} + \frac{r_0}{T_I}(I_k - I_{k-1}) + r_0 T_D (D_k - D_{k-1}) = r_0\, \Delta e_k + \frac{r_0}{T_I} \Delta I_k + r_0 T_D \Delta D_k \tag{7}$$

$$\Delta u_k = u_k - u_k - 1 = q_0 e_k + q_1 e_{k-1} + q_2 e_{k-2} \tag{8}$$

Here $\Delta u_k$ is a change of controller output in step k-1 and k, $q_0$, $q_1$, $q_2$, are controller parameters, $e_k$ , $e_{k-1}$, $e_{k-2}$ are errors in the corresponding steps. The parameters $q_0$, $q_1$, $q_2$ are in the following correspondence with the time constants and gain of the PID controller

$$q_0 = r_0 + \frac{r_0 T_D}{T} \tag{9}$$

$$q_1 = -r_0 - 2\frac{r_0 T_D}{T} + \frac{r_0 T}{T_I} \quad (10)$$

$$q_2 = \frac{r_0 T_D}{T} \quad (11)$$

In the absence of disturbances, pure proportional control will not settle at its target value, but will retain a steady state error (droop) that is a function of the proportional gain and the process gain. Only the drift component (long-term average, zero-frequency component) of process gain matters for the droop – regular or random fluctuations above or below the drift cancel out.

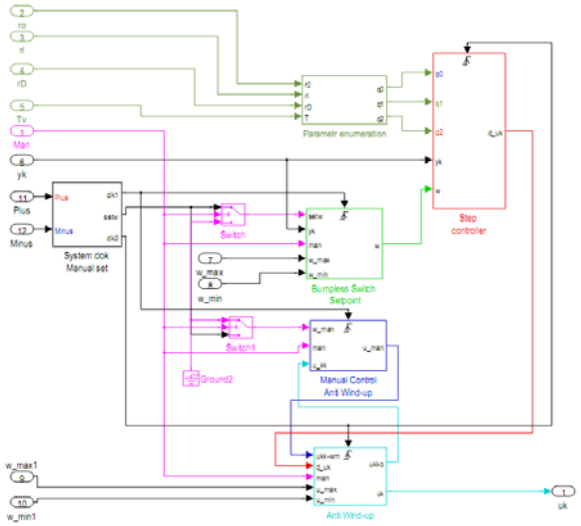


Figure 1. Controller's inner block diagram

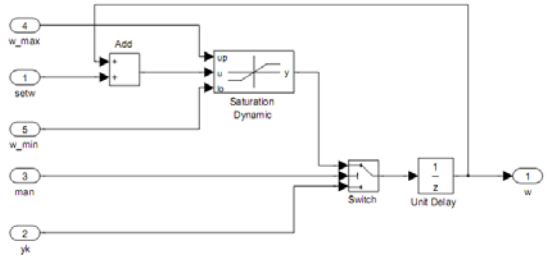


Figure 2. Bump less switch set point

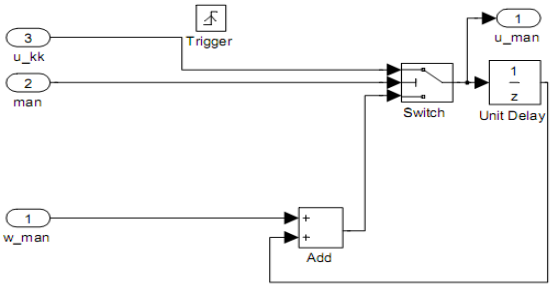


Figure 3. Manual control and anti windup block

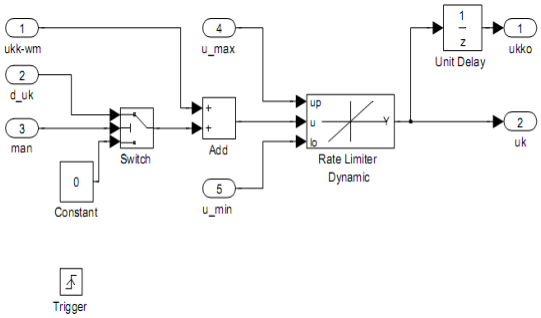


Figure 4. Anti windup block inner scheme

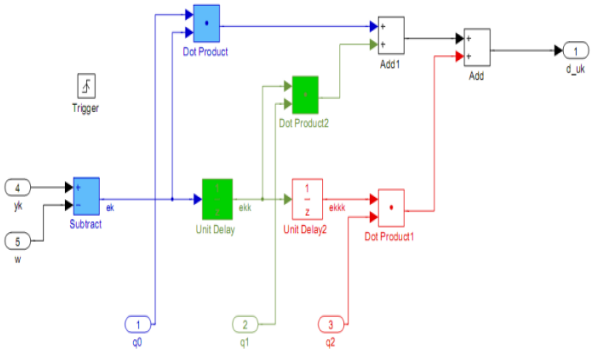


Figure 5. Step controller block

**Chyba! Nenalezen zdroj odkazů.**describe I/O configuration of one block of the controller. Inner structure represents Figure 1. Here we can see individual blocks. It is very important to timing counting operations. This timing signal coming-out from block called "STEP CONTROLLER" (Figure 5. ). These blocks have to work in interactive mode. Variable conversion block recalculating classic PID values into values useable in incremental controller form. The Anti windup block serve to prevent step changes when "Demand values" change occur (Figure 4. ). The bump less switch ensure unharmed switch of controller from manual into automatic control. Introduced concept is making basic controller's body. It is possible to add some other features like demand value limitation, derivative part filtration and last but not least implementation of Takahashi's controller form, where control loop participate on proportional signal size only.

## IV. HW PART

The heart of the system is 16-bit single chip microprocessor (MCU) by MICROCHIP company with type symbol PIC24FJ64GB106 (Figure 6. ). It is powerful microprocessor with many integrated interfaces and remapable pins. This MCU connect to old series of 8-bit processors but offers much more extend instruction suite and many other improvements. Previous PSD controller suffer from some inadequacies resulting from restrictions of simple, 8-bit MCU. We are minimized these issues thanks

to power of the unit (CPU) and also with hardware support for multiplying and dividing.

### A. MCU PIC24FJ64GB106

This is very advanced, 16-bit MCU with modified Harvard architecture disposing with about 16MIPS power with clock rate of 32MHz. It's contain PLL, A Phase Lock Loop frequency multiplier, available to the external oscillator modes and which allows clock speeds of up to 32MHz. With PLL we can achieve full speed even with internal, 8MHz oscillator. The instruction's executed time is reduced to 125ns compared to 200ns of previous model. Most single-word instructions are executed in a single instruction cycle, unless a conditional test is true or the program counter is changed as a result of the instruction. In these cases, the execution takes two instruction cycles, with the additional instruction cycle(s) executed as a NOP. We can do difficult computing operations thanks to native support for multiplying and dividing. All of these operations has a minimum affect to a total program execution time (compared to 8-bit version, where were necessary to design software tools for dividing and multiplying). Supply voltage is no critical, suggested 3.3V is used with withdrawal of about 15mA. As a part of the chip is 32kHz secondary oscillator which is used for RTCC (Real-Time Clock/Calendar). Main benefits are integrated two-way USB communication interface eventually native support for SPI and IIC serial communication. Another useful component of the MCU are five, independent 16-bit timers for time-critical applications (e.g. presented PSD controller). The analog variables can be read by integrated 10-bit A/D converter witch 16 multiplexed inputs with 500ksps sampling rate. Along with remapable pins, big amount of RAM (16K) and instructions set optimized for using C language we can use this MCU as a powerful tool for real-time applications like modern PSD controllers are.

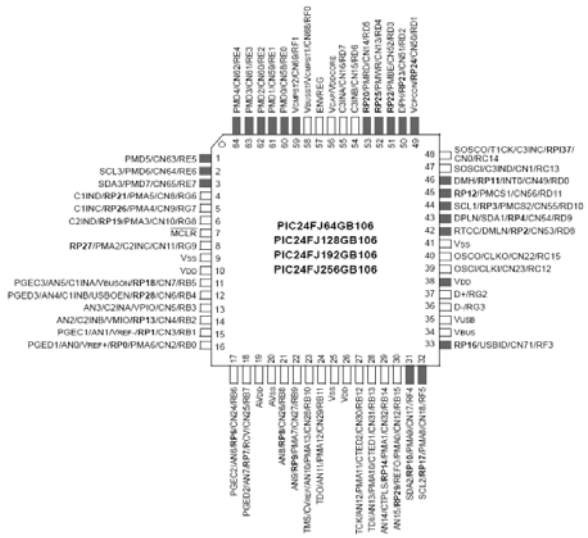


Figure 6. The PIC24FJ64GB106

### B. Controller's PCB

Great advantage are 29 remapable pins. The PCB design is then quite simple. Whole controller make one-sided PCB with exposed system's pins. Controller has 8 analog and 8 digital inputs. The action interventions can be generated by 8 digital outputs and with one (five max) power PWM output. a PWM native support of this MCU make it best for direct control of AC or DC motors or servo mechanisms. A PWM output server as driver for power N-MOS-FET transistor IRF7413. Thanks to its low on-state resistance, $R_{DS(on)}$=0.011Ω is possible to drive bigger motors without power switch cooling. If we drive 5A load, the total power dissipation on power transistor is only about 0.28W. A maximum allowed current load is 13A continuously, if we keep blocking voltage up to 30V. On Figure 7. we can observe the PCB including text notes. Finished controller is presented on Figure 9.

Following code represent an implementation of PID in microcontroller code (ASM):

```
;----------------------------------P-------------------------------------
movfw   kp              ;computed constant
movwf   k1              ;k1, k3 are multiplicators
movfw   et
movwf   k2
movwf   k3
call    nasobeni;e(t) * kp = P
movfw   k2
banksel STATUS
movwf   P               ;result to P

;----------------------------------I-------------------------------------
movfw   ki              ; computed constant
movwf   k1              ;k1, k3 are multiplicators
movfw   it
movwf   k2
movwf   k3
call    nasobeni;i(t) * ki = I
movfw   k2
banksel STATUS
movwf   I               ; result to I

;----------------------------------D-------------------------------------
movfw   kd              ; computed constant
movwf   k1              ;k1, k3 are multiplicators
movfw   dtt
movwf   k2
movwf   k3
call    nasobeni;d(t) * kd = D
movfw   k2
banksel STATUS
movwf   D               ; result to D

;----------------------------------nasobeni-----------------------------
        banksel STATUS
```

```
decfsz   k1,f
goto     $+2
return
movfw    k3
addwf    k2
btfss    STATUS,C
goto     nasobeni
movlw    .255
movwf    k2
return
```

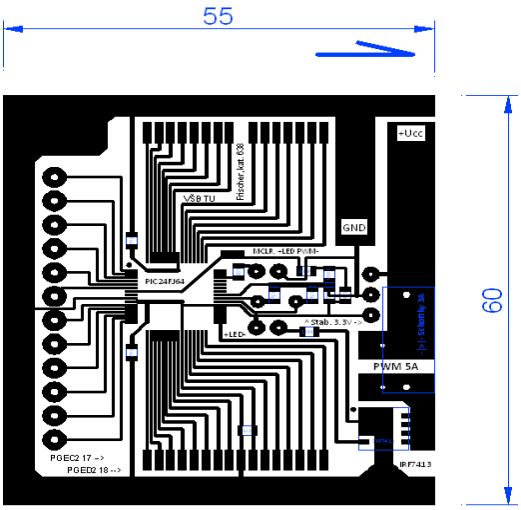


Figure 7. Controllers PCB design with I/O interface

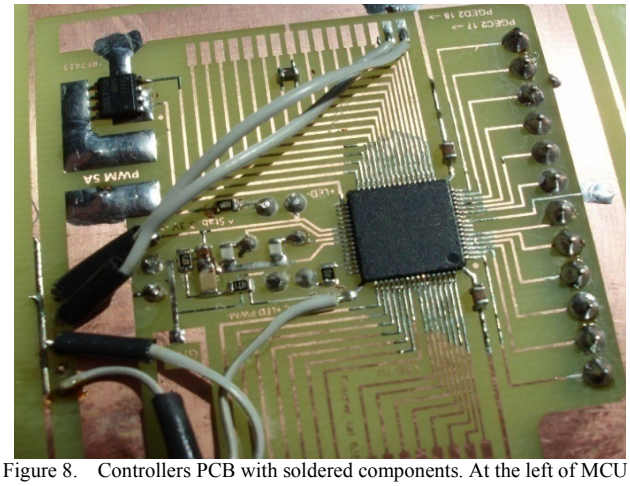

Figure 8. Controllers PCB with soldered components. At the left of MCU a capacitor network for oscillator and special RESET RC network is.

## V. Result Discussion

We describe a solution based on single chip microcontroller design and implementation. Solution is targeted to sector of low priced electronics. Possibilities of using a single chip with price under one dollar (in large series of company production line) are in many areas from home automation to fully equipped factory automation, where a connection to some PLCs can be made.

## VI. Tuning of Proposed Solution

The academic control community has developed many new techniques for tuning PID controllers. Often these methods try to stretch the capabilities of PID control to match the performance of the advanced controller design. In some of these methods the control signal of advanced technique will be approximated by PID respect to a cost function which is usually the norm of error between output of PID controller and advanced controller. These methods, which are called optimal control signal matching methods, have been discussed in details [8].

We would like to enhance our solution by tuning of genetic algorithm. For deriving the new tuning formula, the genetic algorithm is applied to design the PID controllers for a test batch of processes. We then derive the tuning formula by finding simple formulas that describe the correlation between the process characteristics and the controller parameters. In this section, the genetic based PID controller design method and the way to derive the tuning formula will be described more in [7].

## VII. Conclusion

The article had to task to show basic mathematical describe of incremental controller and suggest structure of single blocks so that be able to implement into single chip microcontroller. Individual blocks are analyzed as far as elementary operation's level. From hardware description resulting, that selected structure is suitable for implement into similar MCU especially if they are able to configure I/O pins as with ours MCU.

## Acknowledgment

This research has been carried out under the financial support of the research grants "Centre for Applied Cybernetics", Ministry of Education of the Czech Republic under Project 1M0567 and "Safety and security of networked embedded system applications", GACR, GA 102/08/1429, Grant Agency of Czech Republic.

## References

[1] Ang, K.H., Chong, G.C.Y., and Li, Y. (2005). PID control system analysis, design, and technology, IEEE Trans Control Systems Tech, 13(4), pp.559-576. http://eprints.gla.ac.uk/3817/

[2] Bennett, Stuart (November 1984), "Nicholas Minorsky and the automatic steering of ships", IEEE Control Systems Magazine 4 (4): 10–15, ISSN 0272-1708

[3] Li, Y. and Ang, K.H. and Chong, G.C.Y. (2006) PID control system analysis and design - Problems, remedies, and future directions. IEEE Control Systems Magazine, 26 (1). pp. 32-41. ISSN 0272-1708

[4] Yang, T. (June 2005). "Architectures of Computational Verb Controllers: Towards a New Paradigm of Intelligent Control". International Journal of Computational Cognition (Yang's Scientific Press) 3 (2): 74-101.

[5] http://en.wikipedia.org/wiki/PID_controller

[6] Krejcar, O., Spicka, I., Frischer, R., Heger, M., Incremental PIC Controller with Handled Limit States and Manual Settings, In Proceedings of 2nd International Conference on Mechanical and Electronics Engineering, ICMEE 2010, 01. -03. August 2010, Kyoto, Japan, Volume 1, NJ. IEEE Conference Publishing Services, 2010 pp. 379-383, ISBN 978-1-4244-7480-6, DOI 10.1109/ICMEE.2010.5558526

[7] Jing-Chung Shen; , "New tuning method for PID controller," Control Applications, 2001. (CCA '01). Proceedings of the 2001 IEEE International Conference on , vol., no., pp.459-464, 2001, doi: 10.1109/CCA.2001.973908

[8] Moradi, M.H.; , "New techniques for PID controller design," Control Applications, 2003. CCA 2003. Proceedings of 2003 IEEE Conference on , vol.2, no., pp. 903- 908 vol.2, 23-25 June 2003, doi: 10.1109/CCA.2003.1223130

[9] Liptak, Bela (1995). Instrument Engineers' Handbook: Process Control. Radnor, Pennsylvania: Chilton Book Company. pp. 20–29. ISBN 0-8019-8242-1.

[10] Tan, Kok Kiong; Wang Qing-Guo, Hang Chang Chieh (1999). Advances in PID Control. London, UK: Springer-Verlag. ISBN 1-85233-138-0.

[11] Idzkowski A., Walendziuk W. (2009) Evaluation of the static posturograph platform accuracy, Journal of Vibroengineering, Volume 11, Issue 3, 2009, pp.511-516, ISSN 1392 - 8716

[12] Idzkowski A., Walendziuk W. (2009) Portable acquisition system for domiciliary uroflowmetry, Journal of Vibroengineering, Volume 11, Issue 3, 2009, pp.592-596, ISSN 1392 – 8716

[13] Vasickova, Z., Augustynek, M., New method for detection of epileptic seizure, Journal of Vibroengineering, Volume 11, Issue 2, 2009, pp.279-282, (2009) ISSN 1392 - 8716

[14] Dondio, P., Longo, L., Barrett, S. (2008) A translation mechanism for recommendations", IFIP Proc., Vol. 268, IFIPTM 2008/Joint iTrust and PST Conference on Privacy, Trust Management and Security Trondheim, Nórway, Jun 18-20, 2008, pp. 87-102

[15] Peterek, T., Zurek, P., Augustynek, M., Penhaker, M (2009) Global courseware for visualization and processing biosignals, WORLD CONGRESS 2009 - MEDICAL PHYSICS AND BIOMEDICAL ENGINEERING, Munchen

[16] Krejcar, O., Janckulik, D., Motalova, L., Complex Biomedical System with Biotelemetric Monitoring of Life Functions. In Proceedings of the IEEE Eurocon 2009, May 18-23, 2009, St. Petersburg, Russia. pp. 138-141. ISBN 978-1-4244-3861-7, DOI 10.1109/EURCON.2009.5167618

[17] Cerny M., Penhaker M. The Circadian Cycle Monitoring In Konference proceedings Conference Information: 5th International Summer School and Symposium on Medical Devices and Biosensors, JUN 01-03, 2008 Hong Kong, PEOPLES R CHINA, Pages: 41-43, 2008, ISBN: 978-1-4244-2252-4

[18] Krejcar, O., Frischer, R., Use of Accelerometers for Material Inner Defect Detection, In Proceedings of International Conference on Applied Electronics, AE 2010, 08. -09. September 2010, Pilsen, Czech Republic, 2010 pp. 179-182, ISBN 978-1-4244-6818-8, ISSN 1803-7232

[19] Krejcar, O., Jirka, J., Janckulik, D., Proactive User Adaptive System for Windows Mobile Devices – Processing of Sound Input Signal for Sleep State Detection, In Proceedings of 2nd International Conference on Mechanical and Electronics Engineering, ICMEE 2010, 01. -03. August 2010, Kyoto, Japan, Volume 1, NJ. IEEE Conference Publishing Services, 2010 pp. 374-378, ISBN 978-1-4244-7480-6, DOI 10.1109/ICMEE.2010.5558525

[20] Krejcar, O., Adamec, O., RT Visualisation using aJile aJ-80 Real Time Embedded Platform, In Proceedings of 9th RoEduNet IEEE International Conference, RoeduNet 2010, 24. – 26. June 2010, Sibiu, Romania, NJ. IEEE Conference Publishing Services, 2010 pp. 79-84, ISBN 978-1-4244-7335-9, ISSN 2068-1046

[21] Krejcar, O., Adamec, O., Evaluation and Testing of RT-Java Parameters on aJile aJ-80 Real Time Embedded Platform, In Proceedings of International Conference On Networking and Information Technology, ICNIT 2010, 11. – 13. June 2010, Manila, Philippines, NJ. IEEE Conference Publishing Services, 2010 pp. 540-544, ISBN 978-1-4244-7579-7, DOI 10.1109/ICNIT.2010.5508456

[22] Kromer P, Snasel V, Platos J, Husek D. GENETIC ALGORITHMS FOR THE LINEAR ORDERING PROBLEM, NEURAL NETWORK WORLD, Vol. 19, Issue 1, pp. 65-80, 2009 ISSN: 1210-0552

[23] Gono R., Kratky M., Rusek S., Analysis of Distribution Network Failure Databases, PRZEGLAD ELEKTROTECHNICZNY, Vol. 86, Issue 8, pp. 168-171, 2010 ISSN: 0033-2097

[24] Krejcar, O., Frischer, R., Spicka, I., Simple Discrete Controller with PWM Power Output. In Proceedings of 5th International Conference on Systems, ICONS 2010, April 11-16, 2010, Menuires, France. NJ: IEEE Conference Publishing Services, 2010. pp. 181-185. ISBN 978-0-7695-3980-5, DOI 10.1109/ICONS.2010.38

[25] Litschmannova M., The methodology for the evaluation of energy savings' states of the public lighting, PRZEGLAD ELEKTROTECHNICZNY, Vol. 84, Issue 8, pp. 65-67, 2008 ISSN: 0033-2097

[26] Krejcar, O., Tutsch, M., Frischer, R., Spicka, I., Design and Realization of Low Cost Discrete PSD Controller for Power Electronics Applications, In Proceedings of Second International Conference on Computer Engineering and Applications, ICCEA 2010, 19. – 21. March 2010, Bali Island, Indonesia, Volume 2, NJ. IEEE Conference Publishing Services, 2010 pp. 439-443, ISBN 978-0-7695-3982-9, DOI 10.1109/ICCEA.2010.234

[27] Brad, R., Satellite Image Enhancement by Controlled Statistical Differentiation, In INNOVATIONS AND ADVANCED TECHNIQUES IN SYSTEMS, COMPUTING SCIENCES AND SOFTWARE ENGINEERING, International Conference on Systems, Computing Science and Software Engineering, ELECTR NETWORK, DEC 03-12, 2007, pp. 32-36

[28] Popovici, Z. O., Brad, R., Stoica E. A., Web based conference management system, In 5th RoEduNet IEEE International Conference, Proceedings, Sibiu, ROMANIA, JUN 01-03, 2006, pp. 239-243 (2006)

[29] Tutsch, M., Machacek, Z., Krejcar, O., Konarik, P., Development Methods for Low Cost Industrial Control by WinPAC Controller and Measurement Cards in Matlab Simulink, In Proceedings of Second International Conference on Computer Engineering and Applications, ICCEA 2010, 19. – 21. March 2010, Bali Island, Indonesia, Volume 2, NJ. IEEE Conference Publishing Services, 2010 pp. 444-448, ISBN 978-0-7695-3982-9, DOI 10.1109/ICCEA.2010.235

[30] Machacek, Z, Srovnal, V., "Automated system for data measuring and analyses from embedded systems", In 7th WSEAS International Conference on Automatic Control, Modeling and Simulation, Mar 13-15, pp. 43-48, Prague, Czech Republic (2005)

[31] Srovnal, V., Machacek, Z, Srovnal, V., "Wireless Communication for Mobile Robotics and Industrial Embedded Devices", In 2009 EIGHTH INTERNATIONAL CONFERENCE ON NETWORKS, Mar 01-06, pp. 253-258, Gosier, France (2009)

[32] Kotzian J, Srovnal V., Can based distributed control system modeling using UML, 2003 IEEE International Conference on Industrial Technology, VOLS 1 AND 2, Proceedings, pp. 1012-1017,2003 , ISBN: 0-7803-7852-0.

[33] Kotzian J, Srovnal V., Methodology of designing embedded control systems, Programmable Devices and Systems, IFAC Workshop Series, pp. 133-137, 2002, ISBN: 0-08-044081-9

# Battery-less Remote Sensors with Reversed Peltier Power Source based on Energy Harvesting Principle

Robert Frischer
dept. of Automation and Computing in Metallurgy
Technical University of Ostrava
Ostrava, Czech Republic
robert.frischer@vsb.cz

Ondrej Krejcar, Jindrich Cernohorsky
dept. of Measurement and Control
Centre for Applied Cybernetics
Technical University of Ostrava
Ostrava, Czech Republic
ondrej.krejcar@remoteworld.net,
jindrich.cernohorsky@vsb.cz

***Abstract*— Special events (oceanobiologist, seismic activities detection, detection of chemical substances in huge reservoirs etc.) requiring special electrochemical power sources, which are much more expensive of course. In this article we will present a modern way of powering intelligent sensors. Gaining the energy to supply sensors is possible even from immediate sensor's environment. The energy harvesting term is way, how to obtain this ubiquitous energy. Our application is using sophisticated circuit from Linear Technology, which is capable to use even small energy bursts to discontinuous intelligent sensors operations. The heat energy is converted into electric energy which is stored in very high capacity capacitor (about 1F). In case, that accumulated energy is sufficient, the signal "Power Good" is generated. This signal is sign to sensor to perform measuring and data archiving.**

**Keywords- Energy Harvesting; Reversed Peltier; Remote Sensors; Autonomous Sensor Network**

## I. INTRODUCTION

Advances in low power technology are making it easier to create wireless sensor networks in a wide range of applications, from remote sensing to HVAC (Heating, Ventilating, and Air Conditioning) monitoring, asset tracking and industrial automation. The problem is that even wireless sensors require batteries that must be regularly replaced. It is a costly and cumbersome maintenance project. A better wireless power solution would be to harvest ambient mechanical, thermal or electromagnetic energy from the sensor's local environment. This technique is called energy harvesting. It is process, by which free ambient energy is derived, captured and stored.

Typically, harvestable ambient power is on the order of tens of microwatts to tens mill watts, so energy harvesting requires careful power management and sophisticated circuits with latest technology design in order to successfully capture a few microwatts of ambient power and store it in a useable energy reservoir. As a reservoir usually serve a capacitor with huge capacity (order of farads). One common form of ambient energy is mechanical vibration energy, which can be caused by motors running in a factory, airflow across a fan blade or even by a moving vehicle. A piezoelectric transducer can be used to convert these forms of vibration energy into electrical energy, which in turn can be used to power wireless sensors. To manage the energy harvesting and the energy release to the system, the LTC3588 piezoelectric energy harvesting power supply. It uses an efficient energy harvesting algorithm to collect and store energy from high impedance piezoelectric elements, which can have short-circuit currents on the order of tens of micro amps (1).

$$I_{delivered} = \frac{P_{delivered}}{U_{delivered}} \; [A] \qquad (1)$$

Advantage of mechanical-vibration energy is relatively high output voltage, which is suitable for another processing. On the other hand, thermal environmental energy has a great disadvantage just in value of output voltage (order of tens mill volts). This very low voltage is very difficult to transform up to the useable level (order of volts). Losses, which originates by conversion are relatively high and deteriorate whole circuit efficiency. Nevertheless, thanks to the new technology new types of MOSFET transistors and control circuits with extremely low quiescent power appear. This MOSFET transistors with very low RDS(on) and control circuits are key blocks in power sources design which are utilizing ambient environmental energy. Further described power source is intended to supply intelligent sensors with using surrounding thermal energy from immediate sensor's surroundings. Thermal energy is very suitable because there is no need of vibrations or intensive electromagnetic radiation. TEG (thermo electric generator) device acts as source of electricity. Output voltage level is in order of tens mill volts (hundreds mill volts at max). Low voltage disadvantage is compensated by relatively high supply current in order of hundreds of milliamps (1). Using thermal ambient energy is very gainful when supplying sensors which are monitoring oxygen content in the water, because during the day is the air temperature usually higher than the water temperature and at night vice versa. In addition in winter time is thermal gradient between frozen air and liquid water constant and relatively high. Another indisputable advantage against mechanic-vibration energy is

lack of any moving parts. Regarding to its character, thermal power sources are stable during a long time period.

Basic common feature of the power sources which using free environmental energy is discontinuous operation. Many wireless sensor systems require only low average power, which make from them front candidates for powering by energy harvesting technique. Many sensors in addition are monitoring variables with very slow process system type (for example oxygen content in water, slow temperature process etc.). That's why the measurement can proceed discontinuously, resulting on a low duty cycle of operation correspondingly low average power requirement. For example, if a sensor system requires 3.3V at 50mA (165mW) while awake, but is only active for 100ms out of every second, then the average power required is only 16.5mW, assuming the sensor system current is reduced to micro amps during the inactive time (sleep time) between transmit bursts. If the same wireless sensor only samples and transmits once per a minute instead of once a second, the average power plummets under 30μW. This difference is significant, because most forms of energy harvesting offer very little steady-state power. In case of utilizing TEG, we have got about tens of mill watts but only in case of thermal gradient in order of few degrees. The less average power required by an actual application, the more likely it can be powered by harvested energy. A typical wireless sensor system powered by harvested energy can be broken down into five fundamental blocks, as illustrated in (Fig. 1).

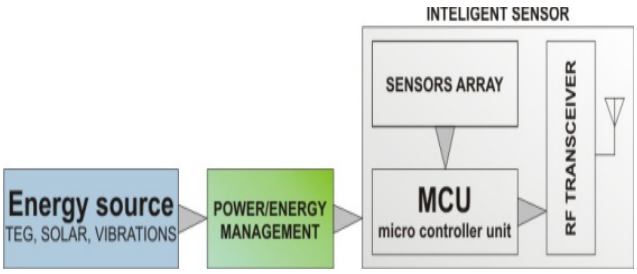


Figure 1. Typical scheme of measuring chain with intelligent wireless sensor

With the exception of the power management block, all of these blocks have been commonly available. For example, microprocessors that run on microwatts of power (MICROCHIP nanoWAT technology), and small RF transmitters and transceivers (MICROCHIP's MRJ24J40) that also consume very little power are widely avail-able. Low power analog and digital sensors are also ubiquitous. The missing link in completing this energy harvesting system chain has been the power converter/power management block that can operate from one or more of the common sources of free energy. This block wasn't able to realized until the new special MOSFET transistors with very low RDS(on) appears. These transistors has merit in rocket boost of new technologies, which are engaged in using surroundings residual energy. MOSFET transistors have no undesirable voltage decay called UCE. That's why is possible to use power sources with voltage level about tens mill volts and accumulate little energy bursts.

## II. TEG (THERMO ELECTRIC GENERATOR)

Thermoelectric generators (TEGs) are simply thermoelectric modules that convert a temperature differential across the device, and resulting heat flow through it, into a voltage via the Seebeck effect. The polarity of the output voltage is dependent on the polarity of the temperature differential across the TEG. Reverse the hot and cold sides of the TEG resulting to changes output voltage polarity. TEGs are basically Peltier's cells, only utilized in reversed mode. These Peltier's cells are made from many small semiconductor blocks connected together with copper tape. Output power is directly proportional to the cells surface and output power is directly proportional to number of semiconductor blocks. Inner structure of Peltier's cell is presented on (Fig. 2).

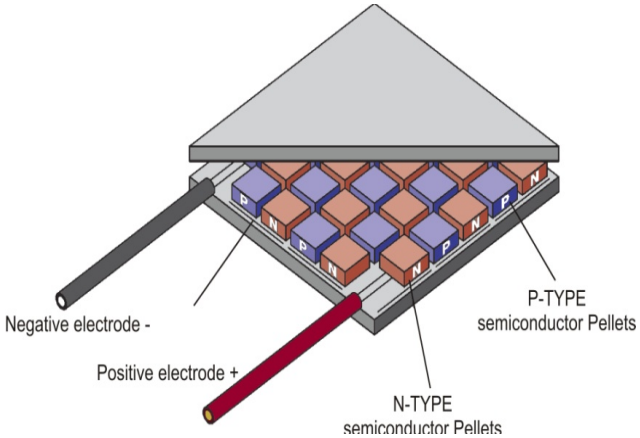


Figure 2. Inner structure of TEG

We have made several tests of selected TEGs, which have to tell us relation between the thermal gradient to TEG output power. TEG worked into constant load (power resistor with value 0R27). Results can be compared on (Fig. 3.).

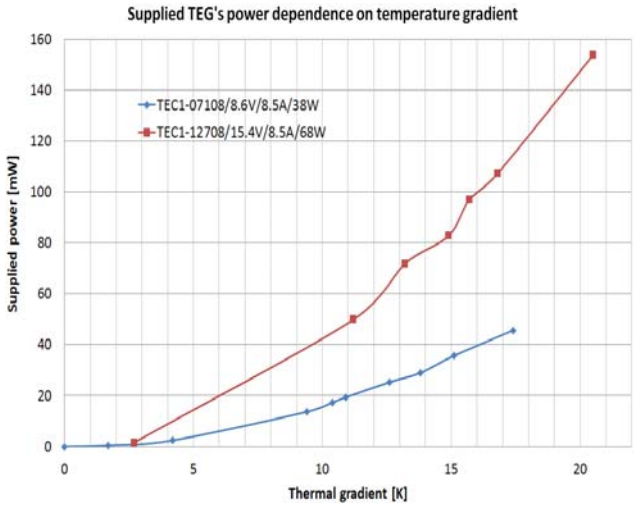


Figure 3. Supplied TEG's power dependence on temperature gradient

There were compared two Peltier's cells. Both of them were tested in reverse mode. The first one has nominal supply voltage 8.6V, the second one double the voltage, 15.4V. Purpose of this test was to tell, how wide difference in output power will we notice. From (Fig. 3). We can assume that cell with higher nominal voltage report better results. Measuring chain and temperature lay-out is presented on figure 4.

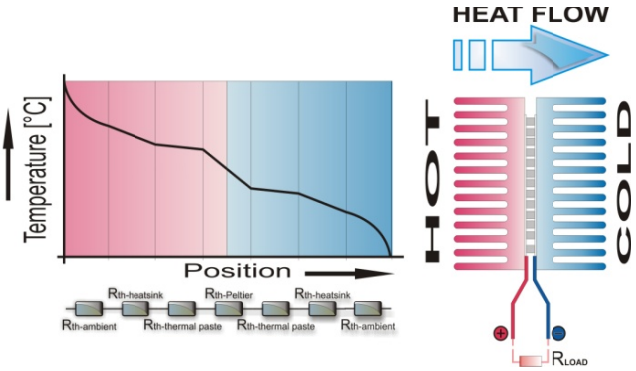


Figure 4. Measuring chain and temperature lay-out

## III. HW PART

As a power management component were chosen an integrated circuit from LINEAR TEHCNOLOGY [1], LTC3108. The LTC3108s self-resonant topology steps up from input voltages as low as 20mV. This energy harvester power source is designed for applications which are using very low average power, but requiring periodic pulses of higher load current [2]. This is typical for intelligent sensors, which are continuously measure oxygen content in water and transmit data into superior system. Oxygen content in water is very slow varying variable. Therefore one measure per minute or even hour is sufficient. Oxygen content in water is very important parameter with regard to life under the ice in winter season. Continuous thick ice cover may result into decreasing oxygen dissolved in water and mean risk for life under the water surface. Thermal gradient which is among the air and water is sufficient to power simple sensor and successive components. Blocks schematic of used power source is shown on (Fig. 5).

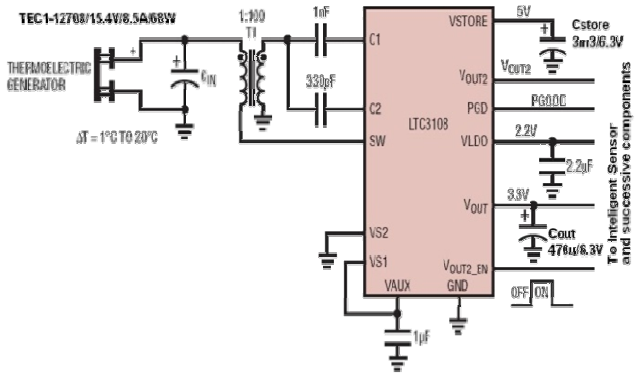


Figure 5. Circuit diagram of TEG power source with two level outputs

The main advantage rest on self-oscillating design. Feedback loop consist of secondary transformer windings, capacitor Cosc and resistor Rosc. Without these the circuit would scarcely do its job. If the TEG generate a proper voltage spike, or the leading edge is sufficiently slope (2), the secondary winding generate much more higher voltage spike (3), (4), which opens the gate of switching MOSFET. So through the primary winding flow maximum obtainable current defined by TEG type and environment conditions. Steady state on primary side lead to no energy is flow to the secondary side, so there is no energy to power up the MOSFET's gate (the $C_{osc}$ is acting as differentiator). Transistor will switch off and the residual energy stored in primary winding creates another spike which will make the loop infinite. It is very simple and clever idea.

$$\frac{\Delta U}{\Delta t} > k_{critical} \rightarrow \frac{\Delta I}{\Delta t} > j_{critical} \quad (2)$$

So if

$$\Delta I \rightarrow \Delta\Phi$$
$$u_{pri} = \frac{\Delta\Phi_{\Sigma 1}}{\Delta t};\ u_{sec} = \frac{\Delta\Phi_{\Sigma 2}}{\Delta t} \quad (3)$$

$$\text{If } \Phi_{\Sigma 1} = \Phi_{\Sigma 2} = \Phi \text{ then} \quad (4)$$
$$\Phi_{\Sigma 1} = N_1 \cdot \Phi;\ \Phi_{\Sigma 2} = N_1 \cdot \Phi;$$
$$u_{pri} = N_1 \cdot \frac{\Delta\Phi}{\Delta t};\ u_{sec} = N_2 \cdot \frac{\Delta\Phi}{\Delta t}$$

Where

- N represent number of turns
- $\frac{\Delta U}{\Delta t}$ voltage slope (TEG parameter)
- $\frac{\Delta I}{\Delta t}$ current slope (TEG + Primary winding parameter + environments)
- $\Phi$ magnetic flux
- $\Phi_\Sigma$ scattering magnetic flux
- $k_{critical}$ and $j_{critical}$ is minimum slope value

DC-DC power conversion isn't very efficient, because of very low voltage input. So the output power can be easily calculated by (5).

$$W_{load} = P_{load} \cdot t_{ON}\ [J]$$
$$W_{COUT} = \frac{1}{2} \cdot C_{COUT} \cdot U_{out}^2$$
$$but\ U_{out}\ is\ in\ range\ 3 - 3.3V\ so$$
$$W_{COUT} = \frac{1}{2} \cdot C_{COUT} \cdot \Delta {U_{out}}^2\ [J] \quad (5)$$
$$t_{run} = \frac{W_{COUT}}{W_{load}}\ [s]$$

Where

- $P_{load}$ is average sensor consumption [Ws]
- $C_{cout}$ is output capacitor capacity [F]
- $t_{ON}$ is average sensor ON-time [s]

$t_{RUN}$ is maximum ON-time, before output voltage fall below acceptable level. [s]

Where

$P_{load}$ is average sensor consumption [Ws]

$C_{cout}$ is output capacitor capacity [F]

$t_{ON}$ is average sensor ON-time [s]

$t_{RUN}$ is maximum ON-time, before output voltage fall below acceptable level. [s]

## IV. Smart Mobile User Adaptive System

A smart mobile user adaptive system can be developed based on previously discussed solution [7]. The usage of such created system can be founded in areas like large ocean remote monitoring of water quality or water currents. For example a use of remote sensor networks for monitoring of expansion of oil after sea damage (in Mexican gulf in 2010).

For continental areas a similar usage can be found in monitoring of content of oxygen in fish ponds or lakes to be informed about a need to increase oxygen content in water to fish survive in winter periods.

For both mentioned usage areas a 24 hours monitoring cycle is needed. Use of battery for power in such remote sensors HW solution is uneconomical because there is a need of hundreds or thousands of sensors with a final price of several dollars.

Development of Smart User Adaptive System (Smart UAS) is strongly based on information from remote sensors powered by proposed system with energy harvesting. Based on these information a recommendations are made in server part of Smart UAS by special developed algorithms [6], [9]. Especially for presentation issues satellite images [10] with pointed data from remote sensors stations are very useful. All data are needed to be stored in some type of database system [8].

The last part of Smart UAS is remote sensors stations, which are distributed in large areas as described before. To develop a control system some special architecture from [11], [12], [13] can be suggested to use. For data processing issues a source articles [3], [4], [5] are suggested to follow.

## V. Conclusion

Problems examined above reflect the possibilities which we have, when designing energy harvester. Water environment is suitable for heat based energy harvesters. Relatively constant thermal gradient and high heat capacity of water guarantee good conditions to running sensors array. Described power source can supply one intelligent sensor with measure frequency about one per minute. By using more powerful TEGs or their cascade connection we can achieve much more power. Power management basis will stay the same, with few minimum modifications.


## Acknowledgment

This research has been carried out under the financial support of the research grants "Centre for Applied Cybernetics", Ministry of Education of the Czech Republic under Project 1M0567 and "Safety and security of networked embedded system applications", GACR, GA 102/08/1429, Grant Agency of Czech Republic.


## References


[1] Technology, Linear. WIRELESS REMOTE SENSOR APPLICATION POWERED FROM A PELTIER CELL. LT Journal of Analog Innovation. April 2010.

[2] Ultralow Voltage Energy Harvester Uses Thermoelectric Generator. LT Journal of Analog Innovation. October 2010, pp. 1-11.

[3] Idzkowski A., Walendziuk W. (2009) Evaluation of the static posturograph platform accuracy, Journal of Vibroengineering, Volume 11, Issue 3, 2009, pp.511-516, ISSN 1392 - 8716

[4] Idzkowski A., Walendziuk W. (2009) Portable acquisition system for domiciliary uroflowmetry, Journal of Vibroengineering, Volume 11, Issue 3, 2009, pp.592-596, ISSN 1392 – 8716

[5] Vasickova, Z., Augustynek, M., New method for detection of epileptic seizure, Journal of Vibroengineering, Volume 11, Issue 2, 2009, pp.279-282, (2009) ISSN 1392 - 8716

[6] Dondio, P., Longo, L., Barrett, S. (2008) A translation mechanism for recommendations", IFIP Proc., Vol. 268, IFIPTM 2008/Joint iTrust and PST Conference on Privacy, Trust Management and Security Trondheim, Nórway, Jun 18-20, 2008, pp. 87-102

[7] Krejcar, O., Janckulik, D., Motalova, L., Complex Biomedical System with Biotelemetric Monitoring of Life Functions. In Proceedings of the IEEE Eurocon 2009, May 18-23, 2009, St. Petersburg, Russia. pp. 138-141. ISBN 978-1-4244-3861-7, DOI 10.1109/EURCON.2009.5167618

[8] Gono R., Kratky M., Rusek S., Analysis of Distribution Network Failure Databases, PRZEGLAD ELEKTROTECHNICZNY, Vol. 86, Issue 8, pp. 168-171, 2010 ISSN: 0033-2097

[9] Litschmannova M., The methodology for the evaluation of energy savings' states of the public lighting, PRZEGLAD ELEKTROTECHNICZNY, Vol. 84, Issue 8, pp. 65-67, 2008 ISSN: 0033-2097

[10] Brad, R., Satellite Image Enhancement by Controlled Statistical Differentiation, In INNOVATIONS AND ADVANCED TECHNIQUES IN SYSTEMS, COMPUTING SCIENCES AND SOFTWARE ENGINEERING, International Conference on Systems, Computing Science and Software Engineering, ELECTR NETWORK, DEC 03-12, 2007, pp. 32-36

[11] Machacek, Z, Srovnal, V., "Automated system for data measuring and analyses from embedded systems", In 7th WSEAS International Conference on Automatic Control, Modeling and Simulation, Mar 13-15, pp. 43-48, Prague, Czech Republic (2005)

[12] Srovnal, V., Machacek, Z, Srovnal, V., "Wireless Communication for Mobile Robotics and Industrial Embedded Devices", In 2009 EIGHTH INTERNATIONAL CONFERENCE ON NETWORKS, Mar 01-06, pp. 253-258, Gosier, France (2009)

[13] Kotzian J, Srovnal V., Methodology of designing embedded control systems, Programmable Devices and Systems, IFAC Workshop Series, pp. 133-137, 2002, ISBN: 0-08-044081-9

# Surface conductance of textile materials modeling

Marek Neruda, Lukas Vojtech
Department of Telecommunication Engineering
Czech Technical University in Prague
Czech Republic
nerudmar@fel.cvut.cz, vojtecl@fel.cvut.cz

*Abstract*— **Production and application of textile materials with the ability of electric charge value control on its surface find extensive use in the field of protective clothing protection. Equipage of assembly line workers in electrical industry by these protective clothing ensures ESD (ElectroStatic Discharge) requests and thereby it protects producing components. Price optimization and production parameters setting in production process relate to modeling of resultant electrical characteristics. Surface conductance is one of the most important parameters. This paper is focused on description of standardized measuring methods, state-of-the-art of surface conductance modeling methods and charge pattern in textile structure. Main contribution of this paper is in description of a new model of surface conductance and its numerical solution.**

***Keywords-Conductance; ESD; Measuring method; Modeling; Resistivity; Rextile***

## I. INTRODUCTION

Protection against effects of electrostatic charge is the important part of many technological procedures. Some of the textile materials enable to control intensity and surface charge pattern. One of the main outlets of these textiles is the field of protective clothing for workers in electrical components production, equipment production or service. Interesting applications are also luxury applications for managers who come through the spaces with prescribed ESD (ElectroStatic Discharge).

Production process of these textiles is based on implementation of conductive grid into classical textile structures. A grid is composed of fibers with electric conductivity. These electric conductivity fibers are formed by metal materials or by composite materials based on carbon structures. Perspective method of electric fibers production is also applicable modern physical methods based on plasma or laser [1].

This grid is placed in warp and woof direction in dimensions of several millimeters. It ensures suitable surface charge pattern. A sufficient electric conductivity of grid fibers and its density influence surface electric conductivity (surface resistance). Therefore it also influences surface electrostatic charge pattern, which can originate from activity of workers. Originated electrostatic charge is staggered on the textile surface of products. It prevents from accumulation of the charge and also from a possibility of discharge origination, which can damage electrical apparatuses.

A production of described types of textile materials requires an optimization of production process and consumption of electrical conductive fibers in comparison with competition of present manufacturing corporation. A design of new types of textile materials and also cost optimization require an ability of modeling of surface conductance. It has to follow for example requirements of standards IEC (EN) 61340 [2].

Section 2 describes two most important standardized measuring methods called Test methods for measurement of charge decay according to EN 1149-3:2004 and Test method for measurement of surface resistivity according to EN 1149-1:2006. A described method of electric charge pattern modeling come up to the first method called Test methods for measurement of charge decay. The main contribution of this paper is a new model for description of surface conductance of textile materials, which come up the method called Test method for measurement of surface resistivity. This model leads to mathematical problem of Infinite Grid of Resistors. Consequently a new procedure is implied and shows a possible solution of this problem. Conclusion is described in section 7.

## II. STANDARDIZES MEASURING METHODS

The most important standardized measuring methods are Test methods for measurement of charge decay according to EN 1149-3:2004 and also Test method for measurement of surface resistivity according to EN 1149-1:2006.

Test methods for measurement of charge decay describe two standardized methods. The first one is focused on measurement based on tribological charging. The principle of this method depicts Fig. 1. No. 1 describes a device for measuring of electrostatic field intensity. Mounting clamp is shown under No. 2. No. 3 is a sample. No. 4 and 5 show initial and final position of slider. No.6 is a cam chain guide. A weight under No. 7 stretches the sample. A cylindrical rod shows No. 8. An electrostatic charge is generated by a grinding of the sample through the cylindrical rod at uniformly retarded motion in a direction of free fall between 4 and 5 positions.

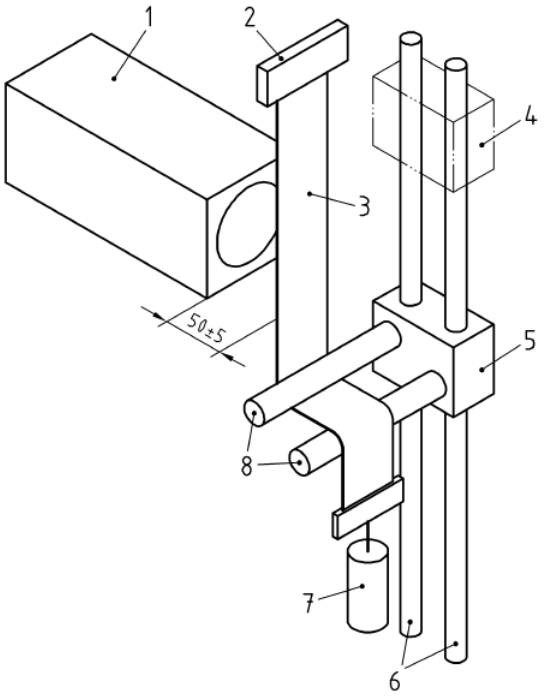


Figure 1. Tribological charging of measured sample [3].

The second method describes using a system of toroidal electrodes for measuring charge reduction in the sample of surface textile, Fig. 2. A generator (marked G) charges an electrode (No. 8) by high-voltage impulse. Intensity of electrostatic field is distributed between the electrodes No. 8 and No. 3 and 4 and is deformed by the sample (No. 6). This intensity is reduces by down-lead of the sample. Time response of the intensity of electrostatic field is recorded by recorder (No. 2). No. 1 describes charge amplifier.

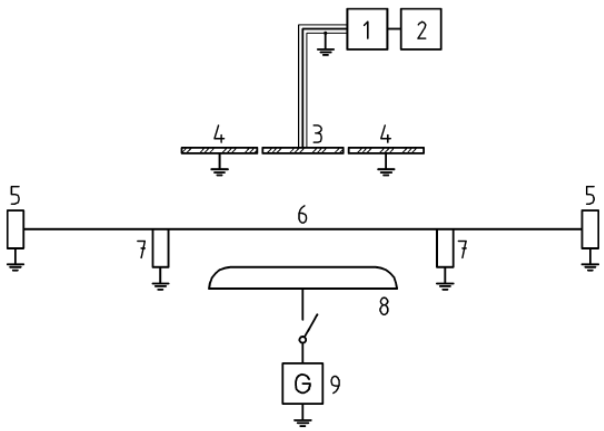


Figure 2. Method of inductive charging [3].

Test method for measurement of surface resistivity according to EN 1149-1:2006 describes Fig. 3 [4]. The method is based on measurement of surface resistivity of measured sample (No. 10) in the circular ring of coaxially ordered electrodes (No. 5). The electrode (No. 1) serves as ground and stabilization of intensity of electrostatic field distribution.

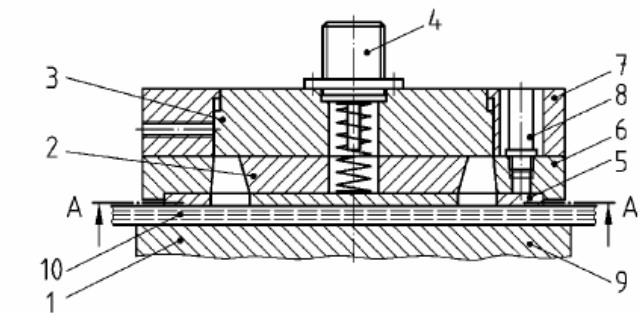


Figure 3. A gauging fixture for measuring of surface resistivity via coaxial electrodes [4].

## III. Modeling of Electric Potential Distribution – Present Models

An interesting work in the field of modeling of electrostatic field distribution is published in dissertation thesis [5]. It rather corresponds to measuring method of inductive charging. An interesting example of the model is the output from Femlab software. The results of realized models and experiments show that present published models (Geometic-Nielsen and Static) are not possible to use for textile materials with antistatic characteristics. These models do not take into account porosity of the textiles. Therefore they neglect the very important component of electrostatic conductivity, the down-lead of electrostatic charge in dielectric formed by the air with specific humidity [5].

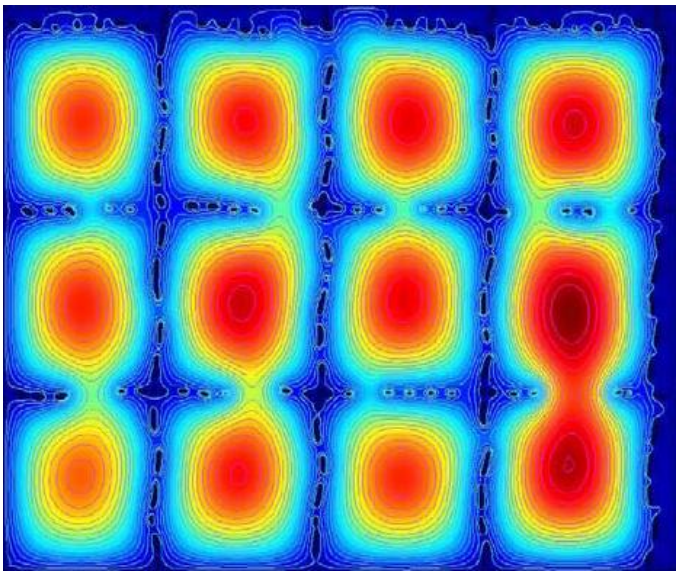

Figure 4. Example of electric potential distribution on the surface of modelled textile sample [5].

## IV. MODEL OF SURFACE CONDUCTANCE

New designed model is inspired by the method called Test method for measurement of surface resistivity according to standard EN 1149-1:2006 [4]. The structure of textile materials with antistatic characteristics can be seen from electrical point of view as a structure of resistors of finite grid of resistors. The finite field of resistors is limited variety of well know mathematical puzzle „Infinite Grid of Resistors“, which is composed of network of resistors with common nodes [6]. It is necessary to reflect upon more complicated structure for the purpose of equivalent diagram. Individual resistors are formed by resistivity of used fiber per unit of length in considered grid of resistors. The resistivity of used fiber per unit of length is given by distance of warp and woof of functional (electrically conductive) fiber. Individual nodes cannot be considered as ideal connection because of the influence of textile weaving and used textile weave. This connection resembles to transition resistor. It is not possible to consider ideal electrical connection composed of nodes, which is known from theory of electric circuit. In the first step the simplification can calculate with almost ideal connection.

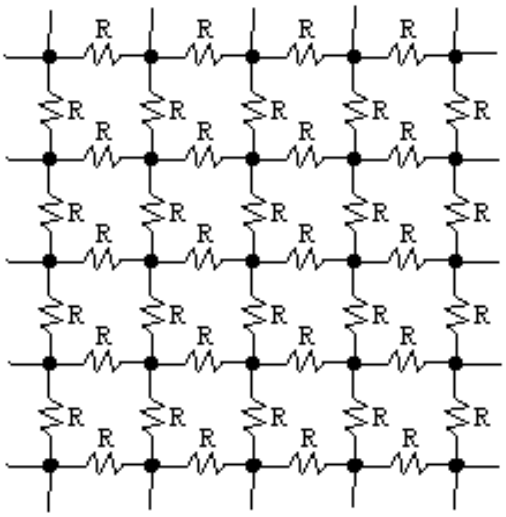


Figure 5. Well-known mathematical puzzle based on the premise of an Infinite Grid of Resistors [6].

A pass between infinite and finite grid of resistors can be implemented by described standardized measuring method, which uses coaxial electrode, Fig. 3. If the profile of electrode is placed on the profile of infinite grid of resistors (macro view on the structure of antistatic textile), the infinite grid of resistors pass on to finite grid of resistors, Fig. 6.

Realized limitation simplifies a solution of original mathematical puzzle with infinite grid of resistors. A calculation takes into account the resistors, which are placed in circular ring formed by circle electrodes.

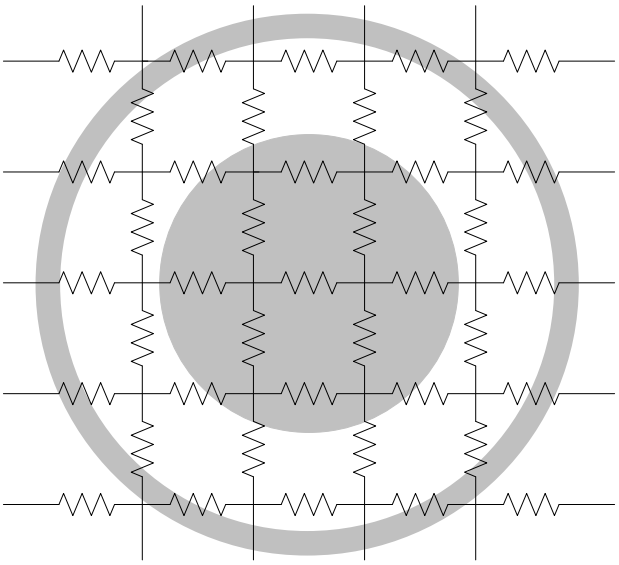

Figure 6. Origination of finite grid of resistors.

## V. CALCULATION PROCESS

Infinite grid of resistors is limited by the shape of cylindrical electrode. Therefore this grid is simplified into finite grid of resistors. The finite grid of resistors can be seen as several resistors connected between two electrodes. The first one is in the inner cylindrical electrode and the second one is the outer cylindrical electrode. The potential is changed from the inner to outer electrode because of resistivity.

A numerical solution of the model results from the fact that distribution of electric potential forms patterns with the same level of intensity of electrostatic field and also patterns with the same values of resistors. As a consequence the structure of patterns can be seen as serial-parallel connection of resistors.

The serial-parallel connection of resistors can be calculated as several sums of resistors. Every sum contains the specific number of resistors, which are connected between the points with the same potential. The points with the same potential create a pattern similar to squares.

The pattern depicted in Fig. 7 shows the idea of the calculation. The initial point of the calculation is the potential in the middle of the circle. It is possible to mark this initial point by variable n. In this case, n is equals to 1, because only 1 resistor R is considered as a side of the square. The next potential level is at the n=3, where 3 resistors are considered as a side of the square. This idea can further continue. If the same potentials are marked, serial-parallel connection of the resistors is more obvious from the Fig. 7 and Fig. 8.

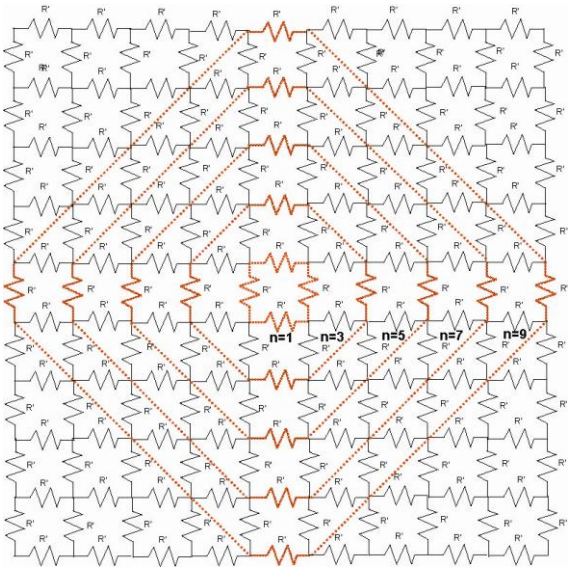


Figure 7. Points with the same potential of the textile material.

If n=3 is considered, a total number of resistors is equaled to number 8 (R' = 8). R' is the value of fiber length between two nodes. It is also possible to consider (1).

$$R'=\rho \cdot l / S \quad (1)$$

R' is a constant for specific type of the fiber (textile), ρ is specific conductance, l is length and S is size of conductor.

In this case (n=3), the resistors are parallel connected. If R'=8, total resistivity R is equaled to R=R'/8.

If n=5 is considered, a total number of resistors of the next value of the potential is equaled to number 16. If a square is considered for the calculation, it is necessary to add other value of potential, because it is present. The number of resistors is now equaled to 8. Equation (2) is got for n=5. The result for n=3 has to be also involved. These resistors are also parallel connected. Different values of potential cause serial connection of resistors.

$$R=R'/8 + R'/16 + R'/8 \quad (2)$$

For n=7, R'=24 for the next value of potential. The value R'=16 has to be also added to complete the calculation of the original square shape of the textile. Result is shown in (3).

$$R=R'/8 + R'/16 + R'/24 + R'/8 + R'/16 \quad (3)$$

Fig. 8 depicts a calculation of serial-parallel connection of resistors, where n=9.

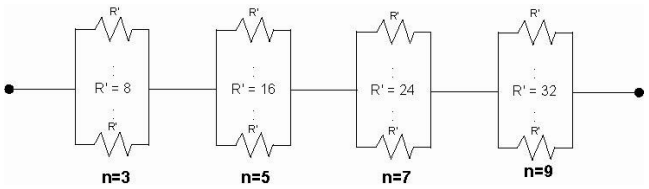


Figure 8. Serial-parallel connection of resistors.

This idea can further continue. This calculation leads to summation formula, which is described in (4).

$$R = R'/8 + 1/4 \sum_{n=5}^{r} \frac{R'}{n-1} + 1/4 \sum_{n=5}^{r} \frac{R'}{n-3}, n \in \langle 5, r \rangle, r \; is \; odd \quad (4)$$

where r and n are connected resistors R' in horizontal direction.

Equation (4) contains 3 expressions. The first one is a resistivity of n=3. The second one is the resistivity of sums of places with the same potential. It is depicted in Fig. 7 by dashed line. The third expression is the resistivity of the rest of the resistors, which form the "corners" of the original square.

This calculation is the first approach. It is further necessary to specify exact end of the cylindrical electrode in comparison with this pattern of resistors. It leads also to summation formula, which considers some same summands and differences of consecutive potentials.

## VI. Future Work

A numerical exact model of surface conductance requires control measurement and optimisation. Optimisation of this model uses a standard gauging fixture according to standard EN 1149-1:2006 [4]. It is also necessary for measurement of modelled samples to realize a gauging fixture for length resistor of used fibers. It is based on several measurement of resistor value and evaluation of individual sections of measured fiber. A base condition is the same mechanical effort of the fiber, which corresponds to tension force. This tension force effects on inside the fiber. Mechanical effort is supposed with the use of textile brake or weight at the both end of the measured fiber.

## VII. Conclusion

Modeling of surface resistivity (conductance) of new designed antistatic textile materials enable to optimise production process and reduces costs of used antistatic fibers. Optimisation of technological parameters is the other possible application. It considers a change of technological parameters such as density of antistatic fibers, i.e. warp and woof direction of different types of antistatic fibers.

## Acknowledgment

This work was supported by project BE-TEX (FI-IM5/202) "Human and technology protection against high frequency radiation – research and development of new textiles",

supported by Ministry of Industry and Trade of the Czech Republic in Impuls program.

## REFERENCES

[1] S. Shahidi, J. Wiener, and M. Štěpánková, "Influence of Dielectric Barrier Discharge Treatment on Adhesion Properties of Platinum Coated PP and PET Fabrics," *23rd Symposium on Plasma Physics and Technology (SPPT 2008)*, pp.164-165, June, 2008.

[2] Standard IEC 61340-4-4:2005: Electrostatics -- Part 4-4: Standard test methods for specific applications - Electrostatic classification of flexible intermediate bulk containers (FIBC). Available at: http://www.iso.org/iso/catalogue_detail.htm?csnumber=42806 [Accessed 20 July 2010].

[3] Standard BS EN 1149-3:2004: Protective clothing. Electrostatic properties. Test methods for measurement of charge decay. Available at: http://shop.bsigroup.com/ProductDetail/?pid=000000000030049226 [Accessed 20 July 2010].

[4] Standard BS EN 1149-1:2006: Protective clothing. Electrostatic properties. Test method for measurement of surface resistivity. Available at: http://shop.bsigroup.com/en/ProductDetail/?pid=000000000030112375 [Accessed 20 July 2010].

[5] M. Maršálková, and J. Militsky, „Electric Behavior of Textiles with Antistatic Properties and Methods of Their Evaluation," Ft.Tul.cz, October. 2009. Available at: http://www.ft.tul.cz/bulletin/statni_doktorske_zkousky_a_obhajoby/teze-Marsalkova.pdf [Accessed 15 July 2010].

[6] UnknownAuthor, "Infinite Grid of Resistors," MathPages.com, March, 2010. Available at: http://www.mathpages.com/home/kmath668/kmath668.htm [Accessed 15 March 2010].

# Electromagnetic Compatibility Implantable Pacemaker Testing

Radovan Hajovsky, Marek Penhaker, Ondrej Capek
Jindrich Cernohorsky, Jan Skapa
Department of Measurement and Control, Departement of Telecommunications
Faculty of Electrical Engineering and Computer Science
VSB–Technical University of Ostrava, 17. listopadu 15, 708 33, Ostrava-Poruba
Ostrava, Czech Republic
radovan.hajovsky@vsb.cz, marek.penhaker@vsb.cz,
ondrej.capek@vsb.cz, jindrich cernohorsky@vsb.cz,
jan.skapa@vsb.cz

David Korpas
Faculty of Medicine,
Palacky University Olomouc, Křížkovského 8, 771 47
Olomouc, Czech Republic
david.korpas@seznam.cz

***Abstract*—The aim of the work was to assess the influence of electromagnetic non-ionizing radiation to cardiac pacemaker. The electromagnetic field can influence the pacemaker functionality and also the wireless communication between programmer and device. Electromagnetic compatibility is tested by direct induction of interference signal to the inputs of cardiac pacemaker according to technical specification. The tests were also made by generating of interference radio frequency signals to disturb the wireless telemetry communication. For testing purposes a circuit of artificial tissue has been designed and assembled, to which a cardiac pacemaker has been connected, as well as the antenna for short radio distance band. It has been proved that the cardiac pacemaker is resistant to co-phasally fed modulated electromagnetic field and also to the circuit of artificial tissue with the connected cardiac pacemaker. It has also been proved that the wireless telemetry communication is sensitive to the interference and disturbances. The non-proper cardiac pacemaker behavior change can endanger the patient's health during the diagnostics and therapeutics procedure. The results can help the physician in decision of patients with implantable pacemaker to dauntless medical procedure.**

***Keywords-Electromagnetic Compatibility, Implantable Pacemaker, Measurement, Disturbing Signal***

## I. INTRODUCTION

The ever increasing number of electronic devices, appliances and systems also brings other problems related to electromagnetic disturbance and resistance regarding these and other objects against disturbance. The level of the disturbance grows in the frequency bands 0 Hz to hundreds of GHz. Electronic devices can contain signal generators working on several different frequencies, whereas each device or its particular part can be the source as well the receiver of the disturbance. [1]

Electromagnetic compatibility is the ability of the device, system or appliance, to function properly even in an environment, where there are other sources of electromagnetic signals (natural or artificial) operating, at the same time, they must not affect their environment in an illegal way, and thus may not produce signals, which would illegally disturb other appliances and other living beings. [1] [3]

## II. IMPLANTABLE PACEMAKERS

An implantable pacemaker is an electronic device, generating electrical impulses, which should replace the regulating system of the heart in case of a heart defect. This defect can result in an irregular activity of the heart or a decreased pulse rate, which leads to reduced oxygen supply in the tissue and subsequent dyspnoea, giddiness, blackouts, and sometimes even death. Implantable pacemakers can also be combined with defibrillators called cardioverters.

Modern multi ventricular pacemakers today are highly integrated electronic devices with many pacing modes and circuits to enhance the quality of the heart pulse rate regulation during the patient's physical activity.

Signals measured by the pacemakers from the heart are usually within the range of 0,1 – 30 mV. The pacemaker on the contrary stimulates the heart muscle using electrical discharge of 1 - 10V if needed, using implanted lead. [1] [9]


Figure 1. *The Guidant INSIGNIA™ I Entra 1294 DDDR Pacemaker and Cognis 100-D Pacemaker*

Pacing modes VVI, AAI, DDD, and rarely also the VDD mode are used with cardiac pacemakers today. Using one lead, a dual chamber pacemaker reads the P wave from the right heart atrium, the detection of which is followed by an adjustable AV delay interval, usually about 120 ms long, and then a pacing impulse is sent into the right ventricle through another lead. During unipolar pacing, the metal case of the pacemaker forms the indifferent electrode for scanning and stimulation. During a bipolar pacing, two electrodes are placed on both leads. The DDD mode basically substitutes the disrupted transfer system, thereby retaining the synchronous activity of the atrium.and ventricle. When the activity of the heart decreases under the set limit, the pacemaker works at the set speed of the atrium and ventricle stimulation.

## III. EXPERIMENTAL MEASUREMENTS

A set of two types of measurement were carried out within the testing of the EMC parameters of pacemakers. First of them dealt with the issue of measuring the effect of the electromagnetic non-ionizing radiation on the pacemaker activity itself and the second measurement was carried out with the aim to analyze the effect of the electromagnetic RF radiation on the communication between the pacemaker and the programmer. [5] [6]

### *A. Electromagnetic Non-Ionizing Radiation Effect of the Pacemaker Activity*

The CSN EN 45502-2-1 standard (furthermore "standard") was used as the theoretical base, which describes in detail, how the pacemakers should be build to ensure their correct operation and, at the same time, the safety of the patients and users - it defines the tests, which the appliances have to pass in order to conform to this standard.


Figure 2. The Artificial Tissue Module

The testing method of the EMC pacemaker was selected in accordance with the standard - to find out, if the pacemaker is not likely to change its therapeutical behavior during the common mode induction of the moduled electromagnetic field, i.e. to bring testing signals with the course, frequencies and amplitudes as defined below, to the circuit of the artificial tissue with the connected pacemaker. The pacemaker shall be in the synchronized mode set by a signal from an operating generator. [2] [4]

### *B. The circuit of Artificial Tissue*

In order to follow the measuring procedures defined in the above mentioned standard, it was necessary to design a circuit using artificial tissue. The basic scheme is shown in Figure 2.

A measuring chain was created for the measurement, and the following devices were used in it. The measurement was perform on the Guidant INSIGNIATM I Entra 1294 DDDR pacemaker programmed to Guidant ZOOM® LATITUDETM 3120 Programming System. Furthermore, the digital oscilloscope Tektronix TPS 2014 (Figure.4 oscilloscope 1) and digital oscilloscope Tektronix TPS 2024 (Figure.4 oscilloscope 2) were used in the measuring circuit. Two functional generators Agilent 33220A (Figure.4 generator 1 and 2) were used as the functional generators. The main element of the measuring circuit was the Artificial Tissue Module specified and defined in the standard, where all the above mentioned devices were connected.

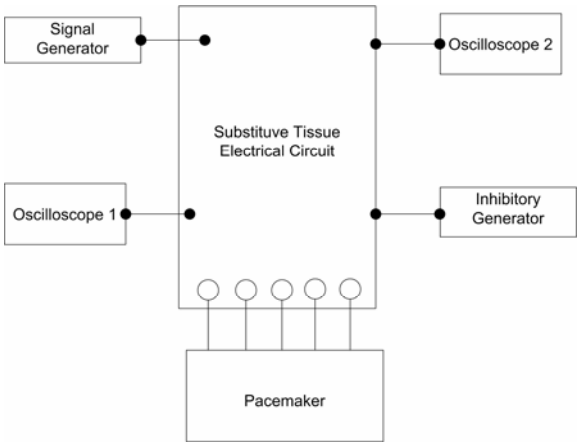


Figure 3. The Experimental Measurement Chain

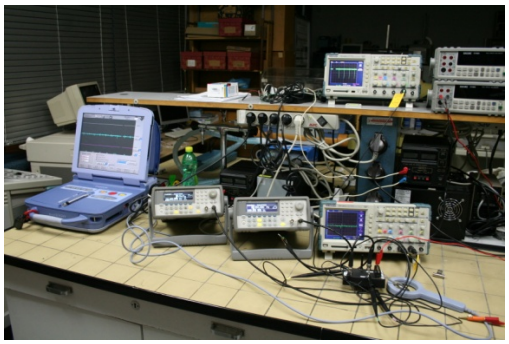

Figure 4. Measuring Workplace for Electromagnetic Radiation Influence

Firstly, the sensitivity threshold of the pacemaker was measured and the required amplitude of inhibitory impulses was set for the pacemaker to change into the inhibited mod. The oscilloscope 2 was then switched over to point K and the processes at both points were measured with the test signal generator set with a carrier frequency of 20 Hz, 200 Hz, 2 kHz, 20 kHz and 150 kHz and the amplitudes according to Chart 2.

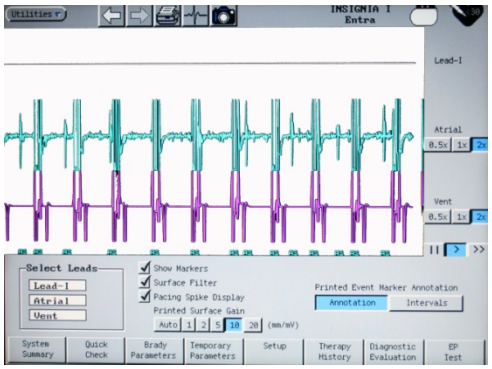


Figure 5. Form of Tested Carrier Frequency with 150 kHz Frequency on the Programer's Screen

### *C. The effect of the electromagnetic RF radiance on the communication between the pacemaker and the programmer.*

The wireless telemetry among the programmer and the patient devices was developed by the Boston Scientific Corporation to have the possibility to program patient devices at longer distances, to decrease the risk of disturbing the operative field sterility during the implantation, as well as to maximize the patient's comfort, e.g. during follow-ups or during the device re-setting, contrary to induction telemetry with the help of a circular probe. [10]

The presetting of the patient's device is secured through acknowledgement signals after a successful transfer of the programmed data as it works in a no-license ISM zone SRD on the frequency of 869,85 MHz, which is not reserved only for the communication between these devices, and practically anybody including the often used mobile phone GSM technology can use it for radiation (when meeting the transmission performance and other transmission parameters), thus causing a communication failure. An incomplete or incorrect device setting is therefore out of the question. [7]

No methodology for this kind of measurement has been cited in the literature. Therefore, the following procedure was selected. A half-wave of a dipole aerial was created and a disturbing signal with the frequency, which is used for the wireless telemetry communication, i.e. 869,85 MHz and the signal shape of a clear unmodulated sines with the help of an RF signal generator. Furthermore, the relation of the radiated output of the aerial in the moment of the failure of telemetric connection (when raising the transceiver output) as well as when the connection was restored (when reducing the transceiver output) was measured at the distance of the aerial placed:

- on a straight line, formed by the pacemaker and the programmer (position and – Figure. 8) aerial – pacemaker – programmer as well as b – Figure. 9) aerial – programmer – pacemaker)
- on a vertical line, which passes through the centre of the join of the pacemaker and programmer

Figure 6. Measuring Workplace for Electromagnetic RF Radiation Influence

The pacemaker was connected with the programmer using the wireless telemetry, and it was left in a default setting - to measure the disturbance effect on the telemetry connection, the pacemaker had to only transmit the signal (noise in this case) from the electrodes into the programmer - when the transmission was interrupted, the noise disappeared from the programmer monitor as well. In order to express the total effective radiated output of ERP, the total inhibition of the lead and the aerial was taken into account.

**Measurement in Placement 1**

For the a) and b) position, the pacemaker and the programmer was placed at the distance of 2,5 m. The aerial was placed on a straight line at the distance of 1 to 5,5 m after 0,5 m steps. The output of the generator was set and recorded from the minimum to the telemetric connection failure and again from the maximum till restoring the connection during each placement of the aerial.

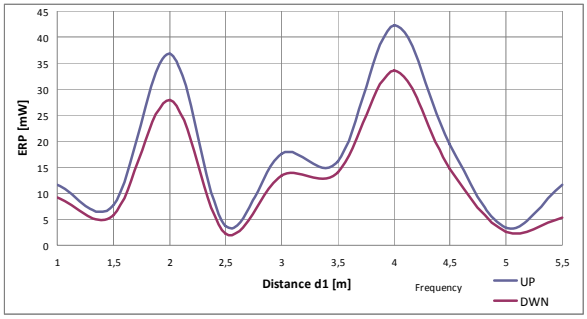


Figure 7. ERP to Antenna Distance Dependence Placement a

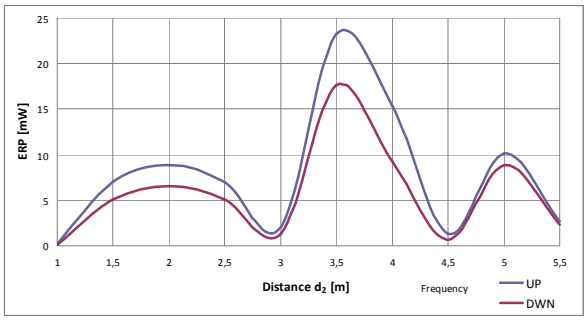


Figure 8. ERP to Antenna Distance Dependence Placement b

### D. Measurement in Placement 2

The pacemaker and programmer were placed at a distance of 3 m. The aerial was placed on a vertical line, which goes through the centre of the pacemaker and programmer join at the distance of 1 to 8 m after 1 m steps. The output of the generator was set and recorded from the minimum to the telemetric connection failure and again from the maximum till restoring the connection during each placement of the aerial.

## IV. CONCLUSION

The result of the test measurement shows, that the pacemaker complies with the standard except for the carrier frequency of the test signal of 150 kHz, when the pacemaker stayed inhibited, however on the monitor of the programming device could be seen the fact that the oscillation burst of the test signal detected the activity of the heart chamber to be spontaneous. Practically, this could mean, that the pacemaker would inhibit through the interfering signal, however, if the patient's heart did not produce spontaneous pulses, the pacemaker would not generate pacing pulses and its main function would thus not be fulfilled, which is unacceptable. This false detection was nevertheless probably caused by inaccuracies of measurements and the measuring devices as well as by the noise on the circuit parts.

The wireless telemetry connection failed to work at ERP values in units up to tens of mW. These are relatively low values, which show, that this telemetry can tend to fail when there is a device near the pacemaker, working on this or a close frequency with relatively poor performance, such as wireless phones, headsets, patients' monitors, electrosurgical devices and other devices working in the UHF range.

## ACKNOWLEDGMENT

The work and the contribution were supported by the project Grant Agency of Czech Republic – GAČR 102/08/1429 "Safety and security of networked embedded system applications". Also supported by the Ministry of Education of the Czech Republic under Project 1M0567. Students Grant Agency SGS SV450021" Biomedical Engineering Systems VI"

## REFERENCES

[1] Korpas, D., Psychological Intolerance to Implantable Cardioverter Defibrillator, In Biomedical Papers-Olomouc, Volume 152, Issue: 1 p.: 147-149 , June 2008 , ISSN: 1213-8118

[2] Vasickova, Z., Augustynek, M., New method for detection of epileptic seizure, Journal of Vibroengineering, Volume 11, Issue 2, 2009, pp.279-282, (2009) ISSN 1392 – 8716

[3] Cerny, M. Movement Activity Monitoringof Elederly People – Application in Remote Home Care Systems In Proceedings of 2010 Second International Conference on Computer Engineering and Applications ICCEA 2010, 19. – 21. March 2010, Bali Island, Indonesia, Volume 2NJ. IEEE Conference Publishing Services, 2010 p. ISBN 978-0-7695-3982-9

[4] Cerny, M.: Movement Monitoring in the HomeCare System . In IFMBE proceddings. Ed. Dossel-Schleger, Berlin:Springer, 2009, issue. 25, ISBN 978-3-642-03897-6; ISSN 1680-07

[5] Skapa, J., Siska, P., Vasinek, V., Vanda, J. Identification of external quantities using redistribution of optical power - art. no. 70031R In Book OPTICAL SENSORS 2008 Volume 7003, p. R31-R31, 2008,ISSN: 0277-786X , ISBN: 978-0-8194-7201-4

[6] Palan, B., Roubik, K., Husak, M., Courtois, B. CMOS ISFET-based structures for biomedical applications In Proceedings Medicine & Biology at 1st Annual International IEEE-Embs Special Topic Conference on Microtechnologies, Pages: 502-506 Published: 2000, ISBN: 0-7803-6603-4

[7] Kašík, V.: The Laboratory for PLD Education - Technical Equipment Design and Development. In conference proceedings PDS 2003, Oxford: IFAC, Pergamon, 2003, p. 391 – 394, ISBN 0-08-044130-0, ISSN 1474-6670

[8] Skapa, J. Vasinek, V., Siska, P. Analysis of Optical-Power Redistribution for Hybrid Optical Fibers In Book Fiber Optic Sensors and Applications Volume 6770, 2007 ISSN: 0277-786X, ISBN: 978-0-8194-6930-4, DOI: 10.1117/12.752587

[9] Krejcar, O., Janckulik, D., Motalova, L., Complex Biomedical System with Biotelemetric Monitoring of Life Functions. In Proceedings of the IEEE Eurocon 2009, May 18-23, 2009, St. Petersburg, Russia. pp. 138-141. ISBN 978-1-4244-3861-7, DOI 10.1109/EURCON.2009.5167618

[10] Krejcar, O., Cernohorsky, J., Fojcik, P., Janckulik, D., Martinovic, J., Smartphone, PDA and mobile Embedded device clients of Biotelemetric System for monitoring of life functions. In 5th International Conference on Innovations in Information Technology, Innovations 2008, December 16-18, 2008, Al Ain, United Arab Emirates. pp. 145-149. ISBN 978-1-4244-3396-4, DOI 10.1109/INNOVATIONS.2008.4781761

# Implantable Defibrilator Testing

Marek Penhaker, Jiri Kotzian, Vladimir Kasik, Jiri Sterba, Jindrich Cernohorsky
Department of Measurement and Control, Faculty of Electrical Engineering and Computer Science, VSB–Technical University of Ostrava, FEI, 17. listopadu 15, 708 33, Ostrava-Poruba
Ostrava, Czech Republic
marek.penhaker@vsb.cz,

David Korpas
Faculty of Medicine,
Palacky University Olomouc, Křížkovského 8, 771 47
Olomouc, Czech Republic
david.korpas@seznam.cz

***Abstract*—The article deals with problems of Implantable Cardioverter-Defibrillators testing. A part of the study was a proposal and realisation of a metering circuit that replaces a human body and setting of electric quantities values at input of an implantable defibrillator for testing of qualitative features of defibrillation discharges. For measurement of these discharges a measuring desk was designed and arranged by means of which also defibrillation discharges in the whole range of the defibrillator were measured (0.1- 41J). Designed testing procedures will verify both correctness of programmed parameters and functionality of electronic circuits' part of the defibrillators. Resultant procedures used in this project might be used for testing of parameters for various types and for various producers of defibrillators before their implantation.**

***Keywords-ImplantablebCardioverter-Defibrillator, Defibrillation Shock, Testing, Programmer***

## I. INTRODUCTION

Technique in biomedicine has been continuously developing. Steps that lead to new technological applications and searching of new procedures how to improve these applications have been related to it. The heart is one from the most important organum of the human body. Therefore also cardiology does not stay behind in development of these applications. Modern methods especially in care for patients with atrial fibrillation require not only difficult diagnostic procedures but also treatment by means of cardiostimulator implantation or by implantation of cardioverter-defibrillator. Therefore it is important to improve continuously these therapeutic devices in order that they make better quality of life possible, respectively they make immediate rescue of endangered people possible. The target of this project is to measure features of defibrillation discharges by means of a created appliance, to analyse obtained data, and to evaluate results and energetic losses. [5] [10]

## II. IMPLANTABLE DEFIBRILLATORS

Electronic equipment capable to generate electric pulses that have a task to replace heart's own control system in the case of cardiac insufficiency is called a cardiostimulator. The equipment tends to be implanted into a human organism in the case of important bradypragia of cardiac frequency, respectively in the case of burning creation or conduction of cardiac pulses (bradycardia) out. By means of stimulation electrodes the implantable cardiostimulator not only monitors but also stimulates function of the heart. In fact they are combination of a cardiostimulator and actual defibrillator. Such appliance is able to detect ventricular tachycardia or ventricular fibrillation with a help of very complicated internal algorithm and it is able to suppress this arrhythmia by electric discharge usually by energy of 20 J. After this discharge a brachycardia might come next and here cardiostimulator function is applied.

Figure 1. Implantable Defibrillator COGNIS 100-D

Newer ICD generation is able not only to make a detection and discharge but according to setting during detection of ventricular tachycardia it might apply also antitachycardia program (ATP) when it suppresses arrhythmia by means of quick stimulation. The discharge is applied by the appliance no sooner than in the situation when ATP fails. By that the appliance energy is saved and the patient is not exposed to the discharge that is sometimes perceived unpleasantly.[1]

The whole system consists of the appliance and from one or two flexible electrodes conducted through the subclavian vein in to the heart. Inside the appliance there are a battery, a microprocessor processing all the information and appropriate electric circuits (see Fig. 1). ICD monitors continuously electric activity of the heart. In the case of slow rhythm of the heartbeat it operates as a cardiostimulator and keeps the hearts action regular with preset frequency. In the case of creation of a quick life-threatening rhythm of the heartbeat, it starts the appropriate care during a few seconds. [3] [2]

## III. MEASUREMENT OF IMPLANTABLE DEFIBRILLATOR PARAMETERS

For function verification and designation of discharges features of the implantable defibrillators a specific metering application was created.

### *A. Measuring Chain*

For measuring purposes we use PRM programmer, model 3120 by means of which we will program ICD. PRM programmer task is to set individual discharges in the range (0.1 - 41J). For defibrillation discharges measurement Cognis 100-D Model P107 ICD was used. Because an amplitude of such discharge achieves at maximal discharge not less than a few hundreds Volts, it is important to reduce this voltage, respectively to reduce it on measurable values (0-10V) by means of a developed gauging fixture.

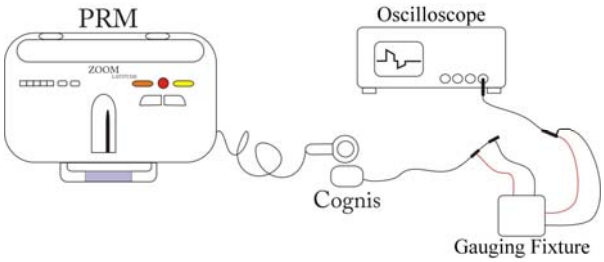


Figure 2. Defibrillation Discharge Measurement Engagement

For recording and evaluation of the measured discharges TEKTRONIX TPS 2024 oscilloscope was used. A working place layout for discharges measurement is stated in Fig. 2.

### *B. Gauging Fixture for Defibrillation Discharges Measurement*

The main function of this fixture is to substitute natural impedance load of the defibrillator which is human texture on current conditions and further to decrease the amplitude of defibrillation discharge on measurable values (0- 10V) with possibility of digitalization. The circuit is solved as a resistor divider. It is equipped with protective elements for the case of failure. The input voltage is decreased, that is in the ratio of the voltage divider. [4] The circuit is equipped with protective elements from the safety reason and reduction of high input voltage break down risks to JP3 output. One from these protective elements is a varistor that serves as a protection in the case of R1, respectively R2 resistor damage. Another protective element is a revertible fuse "Polyswitch" that serves as the current protection.

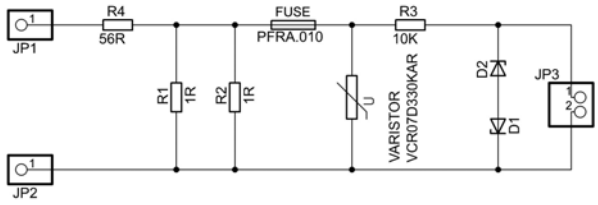


Figure 3. Gauging Fixture Electric Diagram

That is necessary to rectify a biphasic discharge, two Zener diodes are required. The output is stabilised on the voltage (0-10V). The circuit diagram of the gauging fixture is stated in (Fig.3) and its real construction in (Fig.4) [6]


Figure 4. Gauging Fixture

### *C. Measuring of Defibrillation Discharges*

For measuring of defibrillation discharges it is necessary to connect individual elements according to the circuit diagram (Fig.2). A telemetric programming head is attached to ICD. Consequently the electrodes are connected to individual ports of the pulse generator. Input connector of the fixture with conductors and testing hooks designated on the gauging fixture "defib" are connected to the electrode on coils (RV, RA Coils). Connect a test tip with the hook (black) to RV Coil. Connect a test tip with the hook (red) to RA Coil. Connect the output connector of the gauging fixture designated as "Card" to the oscilloscope then. Resulting interconnection is showed in (Fig.5). [7][8]

It is necessary to set ICD on these parameters by means of the programmer SW environment:

- Tachy-Mode: "Monitor + Therapy".
- SETTINGS – VENTRICULAR TACHY THERAPY SETUP : RV Coil to RA Coil
- Lead Polarity: Initial.
- After setting the parameters, it is possible to invoke a discharge: TESTS – EP TESTS - COMMANDED SHOCK - tick off.
- Coupling interval and energy in the range of (0.1-41J)
- Enable
- Deliver
- Defibrillation discharge waveform is consequently recorded on the oscilloscope

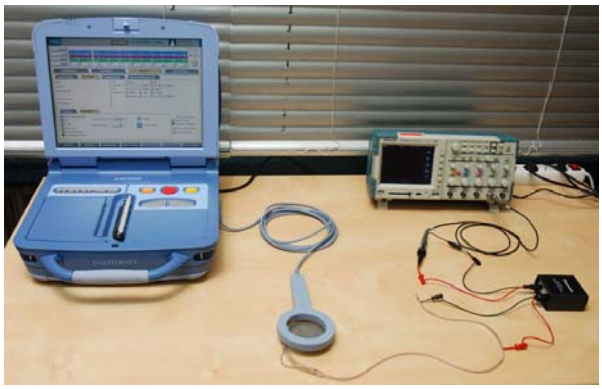

Figure 5. Measurement Photo Documentation

## IV. Measurement Results

Defibrillation discharges were set and measured in the range of (0.1-41J) step by step. During discharges measurement the data were recorded dealing with individual amplitudes level values and with individual pulses width values. (See Fig. 6)

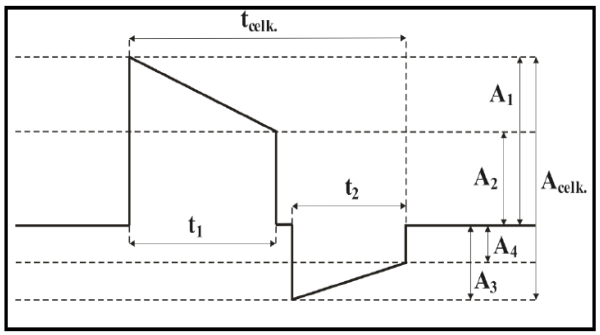


Figure 6. Measured Discharge Parameters

## V. Enumeration of Defibrillation Discharge Real Value

For purposes of the defibrillation biphasic discharge measurement it was necessary to decrease its voltage level on the values measurable by an ordinary oscilloscope.

Real value of the defibrillation discharge voltage amplitude ranges in hundreds of Volts. Accordingly during the highest discharge of 41J it amounts to 706.8V. The measured waveform of defibrillation discharge voltage in time is displayed in Fig. 7. [9]

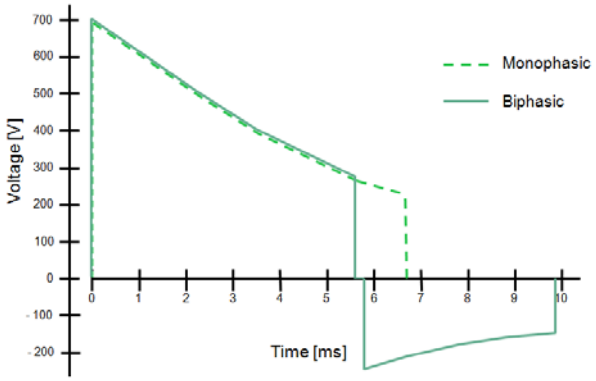


Figure 7. Measured Voltage Curve at 41J

Considering the way of gauging fixture connection by means of the voltage divider, the input voltage amplitude value can be calculated by multiplication of the measured amplitude value from Table 2 by the dividing ratio D. The voltage divider dividing ratio is designated according to the formula (1).

$$D = \frac{U_{in}}{U_{out}} \quad (1)$$

The dividing ratio must be designated from the immediate voltage values after the input voltage Uin connection because the gauging fixture is getting warmer quickly and the dividing ratio changes depending on it. Obtained results of the real discharge amplitude value are stated in Table 1.

TABLE I. Measured Amplitude of Bi Phased Discharge

| Discharge energy [J] | A1 [V] | A2 [V] | A2 [V] | A2 [V] | Acelk, [V] |
|---|---|---|---|---|---|
| 0,1 | 33,48 | 18,04 | 17,11 | 11,90 | 50,59 |
| 0,3 | 58,03 | 28,27 | 26,78 | 16,36 | 84,07 |
| 0,6 | 81,84 | 37,2 | 35,34 | 22,32 | 117,1 |
| 0,9 | 100,4 | 42,78 | 42,78 | 26,04 | 145,0 |
| 1,1 | 111,6 | 44,64 | 44,64 | 26,04 | 158,1 |
| 1,7 | 139,5 | 59,52 | 57,66 | 35,34 | 197,1 |
| 2 | 146,9 | 65,1 | 61,38 | 37,2 | 206,4 |
| 3 | 182,2 | 74,4 | 74,4 | 40,92 | 252,9 |
| 5 | 238,0 | 93,0 | 93,0 | 52,08 | 331,0 |
| 6 | 256,6 | 104,1 | 104,1 | 63,24 | 357,1 |
| 7 | 275,2 | 115,3 | 111,6 | 66,96 | 386,8 |
| 9 | 316,2 | 130,2 | 130,2 | 74,4 | 442,6 |
| 11 | 357,1 | 148,8 | 133,9 | 81,84 | 483,6 |
| 14 | 386,8 | 163,6 | 156,2 | 81,84 | 550,5 |
| 17 | 438,9 | 178,5 | 163,6 | 89,28 | 595,2 |
| 21 | 483,6 | 200,8 | 186,0 | 104,1 | 662,1 |
| 23 | 513,3 | 200,8 | 200,8 | 111,6 | 699,3 |
| 26 | 550,5 | 215,7 | 215,7 | 126,4 | 751,4 |
| 29 | 572,8 | 223,2 | 223,2 | 133,9 | 781,2 |
| 31 | 587,7 | 230,6 | 230,6 | 133,9 | 810,9 |
| 36 | 639,8 | 245,5 | 245,5 | 148,8 | 870,4 |
| 41 | 706,8 | 279 | 260,4 | 148,8 | 930,0 |

It results from the obtained data that the highest value of A1 amplitude for the discharge energy of 41J is 706.8V. The parameters importance again comes from Fig. 6. Figure 8 shows the result of imported data for the defibrillation discharge of 41J energy to Matlab program.

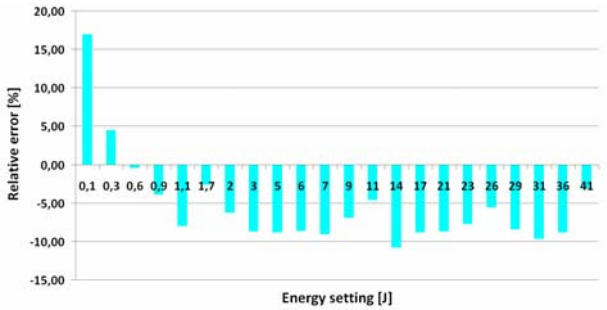


Figure 8. Abnormalities in Energy Supplied by Defibrillator

It ensures that in the course of too low energy of the defibrillation discharge (0.1J and 0.3J), RPM programmer delivered higher energy than the set one was, respectively approximately by 16.9% higher for 0.1J energy and by 4.47% higher for 0.3J energy. For the other set energies of the discharges only losses were found out, respectively the set energy was higher than the delivered one.

### *A. Evaluation of Measured Amplitude, Pulse Width and Discharge Impedance*

The obtained measured data of the individual amplitude values and defibrillation discharge correspond to requirements that were put on the gauging fixture. The lowest measured value was on the level of A4 amplitude in the course of discharge energy of 0.1J that is 0.128V. On contrary the highest measured value was on the level of A1 amplitude in the course of discharge energy of 41J that is 7.6V.

As regards the discharge impedance the difference between the real impedance value and the measured impedance value is 7.114 Ohms then. This difference might be caused by the electrode that might have low impedance.

## VI. CONCLUSION

Before the actual measurement proposal and realisation, the know-how of used implantable devices had to be analyzed especially as regards Cognis 100-D cardioverter-defibrillator.

The problem of defibrillation discharge measurement consisted in high voltage that had to be reduced for measuring purposes by appropriate digital equipment. At first a circuit with operation amplifiers was designed. This circuit did not meet with demands of the high voltage pulses. The requirement to measure and reduce this discharge to measurable values was met only with the circuit solved as a voltage divider. During work with these high voltage pulses, the circuit had to meet with both the demands of operators' safety and safety of the gauging fixtures connected to this circuit. It meant to add protective elements to the circuit for the case of failure.

The other step was a proposal of a measuring chain by which it would be possible to ensure quality measuring of the defibrillation discharges and from which it would be possible to evaluate the measured discharges. The measuring chain for defibrillation discharges measurement consisted of four main parts. That is RPM programmer, model 3120, the cardioverter-defibrillator (ICD), the gauging fixture for defibrillation discharges measurement and TEKTRONIX TPS 2024 oscilloscope.

The last step was the appropriate measuring of defibrillation discharges according to the measuring chain, a consequent analysis and evaluation of the obtained data. The results were evaluated and processed in MATLAB program. The gauging fixture meets requirements for defibrillation discharges measurement at Cognis 100-D cardioverter-defibrillator. In spite of that it is important to keep maximal safety especially while setting parameters for defibrillation discharge vector at RPM programmer and correct connection of the gauging fixture to a cardioverter-defibrillator (ICD) electrode. The gauging fixture output is standardised on voltage ±10V and by it for measuring of discharges' parameters it makes usage of measuring card for PC possible.

In future the used gauging fixture will be completed with A/D and D/A converters that make direct semi automated measuring and evaluation with usage of computer technology or with independently working built-in device possible.

## ACKNOWLEDGMENT

The work and the contribution were supported by the project Grant Agency of Czech Republic – GAČR 102/08/1429 "Safety and security of networked embedded system applications". Also supported by the Ministry of Education of the Czech Republic under Project 1M0567. Students Grant Agency SGS SV450021" Biomedical Engineering Systems VI"

## REFERENCES

[1] Korpas, D., Psychological Intolerance to Implantable Cardioverter Defibrillator, In Biomedical Papers-Olomouc, Volume 152, Issue: 1 p.: 147-149 , June 2008 , ISSN: 1213-8118

[2] Bernabucci, I., Conforto, S., Schmid, M., D'Alessio, T. A bio-inspired controller of an upper arm model in a perturbed environment, In proceedings The 2007 International Conference on Intelligent Sensors, Sensor Networks and Information Processing Pages: 549-553 ISBN: 978-1-4244-1501-4

[3] Skapa, J. Vasinek, V., Siska, P. Analysis of Optical-Power Redistribution for Hybrid Optical Fibers In Book Fiber Optic Sensors and Applications Volume 6770, 2007 ISSN: 0277-786X, ISBN: 978-0-8194-6930-4, DOI: 10.1117/12.752587

[4] Garani, G., Adam, G. K. Qualitative modelling of manufacturing machinery In Book - 32nd Annual Conference on IEEE Industrial Electronics, IECON 2006 VOLS 1-11 p. 1059-1064, 2006 , ISSN: 1553-572X, ISBN: 978-1-4244-0135-2

[5] Majernik,J., Molcan,M., Majernikova, Z.: Evaluation of posture stability in patients with vestibular diseases, SAMI 2010, 8th IEEE International Symposium on Applied Machine Intelligence and Informatics, Óbuda University, Budapest, Hungary, 2010, ISBN 978-1-4244-6423-4, pp. 271-274.

[6] Palan, B., Roubik, K., Husak, M., Courtois, B. CMOS ISFET-based structures for biomedical applications In Proceedings Medicine & Biology at 1st Annual International IEEE-Embs Special Topic Conference on Microtechnologies, Pages: 502-506 Published: 2000, ISBN: 0-7803-6603-4

[7] Kašík, V.: The Framework for Parallel Computing Systems Design. In conference proceedings PDS2004, Gliwice, Poland. IFAC WS 2004 0008 PL, 2004, p. 238-240, IFAC, ISBN 83-908409-8-7

[8] Kasik, V.: Implementing of fast graphic functions in FPGA programmable logic. In PDES 2009, IFAC Workshop on Programmable

Devices and Embedded Systems, pp.63-66, Roznov pod Radhostem, Czech Republic, (2009)

[9] Cerny, M.: Movement Monitoring in the HomeCare System . In IFMBE proceddings. Ed. Dossel-Schleger, Berlin:Springer, 2009, issue. 25, ISBN 978-3-642-03897-6; ISSN 1680-07

[10] Cerny, M. Movement Activity Monitoringof Elederly People – Application in Remote Home Care Systems In Proceedings of 2010 Second International Conference on Computer Engineering and Applications ICCEA 2010, 19. – 21. March 2010, Bali Island, Indonesia, Volume 2NJ. IEEE Conference Publishing Services, 2010 p. ISBN 978-0-7695-3982-9

# Measurement and Diagnosis Assessment of Plethysmographycal Record

Marek Penhaker
Department of Measurement and Control
VSB– Technical University of Ostrava
Ostrava, Czech Republic
marek.penhaker@vsb.cz

***Abstract*— The aim of this work is the measurement and evaluation of plethysmographycal records giving important information about the blood vessel function. Part of this work was design and creation of measurement chain with the possibility of gathering and storing records to the PC. Result of this work is to present the methodology for classifying the records by means of mathematical methods that would contribute to systematic evaluation of what has been found by finger plethysmography. Thereafter the experimental expert system based on framework systems serves to determine the diagnosis on the basis of previous mathematical processing is introduced.**

***Keywords: Plethysmohgraphy, Measurement, Diagnosis, data transfer***

## I. INTRODUCTION

The finger plethysmography is a noninvasive method for recording pulse waves from fingertips of human extremities. Pulse wave is created by the heart activity and by penetration of blood through the vascular system. The variability of particular plethysmographycal records is rather wide, therefore till now the definite criterions, that determine limit between physiological and pathological trace, were not established. It is why the analyses of records is a time consuming process and the evaluation is before all subjective and it depends on the knowledge and skill of physicians. The aim of this study is to find out the most used methods of evaluation of plethysmographycal record till this time and a proposal for evaluation with the use of new methods of processing by the help of computers and new mathematical methods. [2]

## II. TIME DOMAIN PROCESSING

Evaluation of pulse waves was done by a skilled physician visually or with the help of the most used criterions. Some of that criterion did not take in question the possibility of a change of pulse frequency during examination and from it arose an error in reading of parameters of pulse wave. The error was bigger with more quick pulse frequency. The advantageous was to use criterions, which express the ratios of individual parameters of the pulse wave. We used such parameters, which could better define relations between single parts of pulse wave and limit the influence of the change of pulse frequency and magnitude of amplitude.

The parameters ratio between peaks distance of pulse wave could easier determine the location placement of particular parts with respect for the magnitude of pulse wave, which could be at every single measurement variable.

## III. FREQUENCY DOMAIN PROCESSING

The advantage of this evaluation is looking on the pulse wave in whole not only on its parts. The most effective method today is Fourier transform but during the systematic research of arteries elastic reactions with the help of analysis problems arose because still we do not have systematically methodical unified research of these reactions of the arterial system to various stimulus. In this area the evaluation is orientated more on comparison of records obtained from more measurements done on a lot of patients of the same category of findings and evaluated record, it means on particular harmonic components, than on evaluation of frequency spectrum of the waveform alone. The experienced physician (expert) during the analysis of pulse wave in time domain decides about the possible pathological findings and will file into group according the kind of illness. The larger the group of patients is examined in this way, the more exact the consequent ranges among particular groups are. [1]

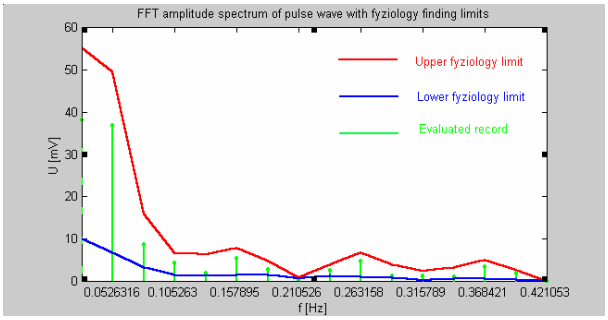


Figure 1. Amplitude FFT Spectrum of Pulse Wave Displayed with Physiological Ranges

## IV. TESTING RESULTS AND EVALUATION

The expert system creates the entire elaboration of plethysmographycal records and it is able to simulate the work of doctors at the determination of diagnosis.

In the final summary the evaluation by the expert system will include the evaluation in time domain with the help of existing and supplementary criterions and it will contain the evaluation of parameters obtained during the evaluation in frequency domain.

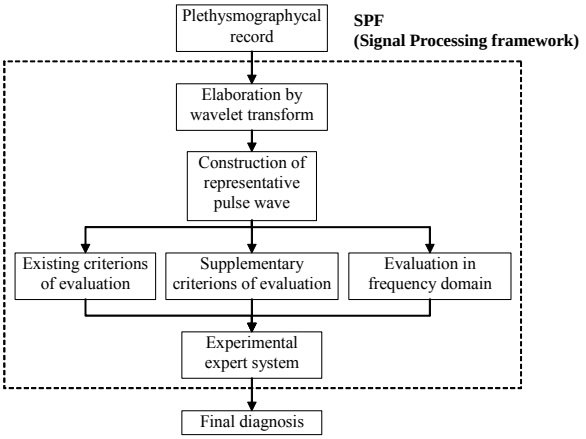


Figure 1: Model of Evaluation Method SPF

The experimental testing of proposed expert system for support of diagnoses on the basis of analysis of plethysmographycal record was realized by problem orientation of fuzzy rule based interactive expert system LMPS v 3.02 (Linguistic Model Processing System).The problem orientation of fuzzy model system LMPS is done on the basis of expert evaluation of the real data measured by analyses of real plethysmographycal records and supplemented with diagnosis declared by doctor. In the present the system is able to recognize two chosen diagnoses II and I.The set of 28 measurements was used for testing method SPF. [3] [7]

Experimental verification of diagnostic effect of suggested method for evaluation of plethysmographycal records was done on four real records.These test records serve for verification of predicative abilities of suggested bases and for verification of estimation accuracy of diagnostic effect.

TABLE I. RATE OF POSSIBILITIES OF EXPERT SYSTEM OUTPUTS FOR PARTICULAR BASES

| n. of record | SPF diagnosis | | Diagnosis of physician | Results agreement |
|---|---|---|---|---|
| | *I* | *II* | | |
| 1 | 1 | 0 | I | OK |
| 2 | 1 | 0,5 | I | OK |
| 3 | 0 | 0,9 | II | OK |
| 4 | 0,17 | 0,83 | II | OK |

The expert system proved in use good results TABLE I. The size of patient's set influenced the number of output diagnoses. Not all-possible diagnoses were found because they were not at this set of patients present.The infliction of vascular system will be characterized by amplitude expansion on particular frequencies that were created from groups of spectrum of the same type of damage. The evaluation of measured record will be done by comparison its spectral components from amplitude expansion of particular groups of findings.

The actual study of the evaluation of plethysmographycal record enables to give criterions in frequency domain. These criterions represent from first to forth harmonic parts of amplitude spectrum of the signal. These criterions will be subsequently used as input variable of linguistic model for the diagnosis estimation.Today is usual to use wavelet transform which serve for before all to time frequency analysis of data and generalization of filtration. The wavelet transformation has been also used to eliminate eventual disorders and errors in scanning of the plethysmographycal record. [9]

## V. HARDWARE REALIZATION

For our purposes the pletysmographycal records was needed. First Criticare USP-504 was used for measurement. For possibility of transferring data from pulse oximeter to computer, where the records was gathered and stored, it was necessary first to connect the output of pulse oximeter and input of computer. Pulse oximeter contains two analog outputs and one digital output with interface RS-232. Computers have usually two interfaces RS-232, so the easiest way of realization would be just using this interface. This solution has, except the simplicity and low price, the advantage, that we would gather data taken by pulse oximeter – pletysmographycal curve, saturation and beat – over one cable. However the disadvantage of this solution is too low quality of transferred curves, which is probably caused by insufficient sampling rate of device. So it was necessary to use another solution with using of already mentioned analog outputs, where we can route signals with help of configuration menu. The output signal is continual and is on the BNC connectors on the rear panel of device. [4] [5]

It is possible to route to analog outputs all signals, which the device processes. Output signal level is between 0 – 1 VDC. For exact setting of device measuring analog outputs, it is possible to use testing signal.

Figure 2: Telemetry Chain

Connection design is the following: On one of the analog outputs is pletysmographycal curve and on the interface RS-232 are beat and saturation. Beat and saturation progress in time isn't important, a doctor is interested only in steady-state value, so the sample rate is irrelevant there and therefore these values may be transmitted over RS-232 interface. On the contrary the sample rate is very important for pletysmographycal curves, because it is necessary to know

their waveform and therefore their progress in time and with regard to insufficient sample rate of device internal A/D converter, these values must be sampled and converted outside device. However computer isn't usually equipped with analog inputs and purchasing of A/D conversion card is too expensive and in addition it isn't possible to put this card into notebook. So first it was necessary to create some interlink, which would convert analog signal to digital and then send it to any standard computer input. As an ideal interlink appears a simple microprocessor, which would receive signals from one analog output and one RS-232 interface and then all of these received data transmit to computer RS-232 interface. [6]

Figure 3: Communication device with embedded micro-processor

As interlink for transferring data from pulse oximeter to computer, it was created a circuit, whose main component is microprocessor PIC16F873 of firm Microchip (Figure 3). This microprocessor is, with regard to its architecture and accessories, very cheap. It is equipped with five-canal ten-bit A/D converter and one USART interface, which is able to communicate with RS-232 interface

### *A. Measuring Device for Terrain Use*

Later the ENVITEC PO 300 pulse oximetry module was used. The PO 300 (Figure 4) features pulse oximetry technology in a very small and low powered design. The board consists of a multilayer PCB with surface-mounted components with a total size of 77 x 65 x 12 mm. Power requirements of the module are limited to approximately 0.15 W. Depending on the application 3 different response modes are available: sensitive, normal and stable. The sensitive mode provides best accuracy with sensitive artefact rejection. To achieve very stable values the stable mode is offered. During each mode fast changes of oxygen saturation and pulse rates will be detected and transmitted. Every second current values of oxygen saturation and pulse rate will be transmitted for all response modes. For each measurement a quality signal is given to evaluate the measured oxygen saturation and pulse rate. This quality reaches from 0 to 10 and indicates the degree of artefacts. The serial transmission is based on TTL level with 9600 Baud, 8 data bits, 1 stop bit and no parity. Every second a new pulse rate, oxygen saturation and quality value is transmitted. Pulse wave values (7 Bit, 0 - 127) are sent with 100 Hz. The PO300 can receive data to adjust the response mode and select the transmission of the plethysmogram curve. For receiving signals and transmitting control signals with computer's RS232 port, the MAX232 circuit was used for converting voltage levels. An analog output of data is an available (in our case unused) option. [8]

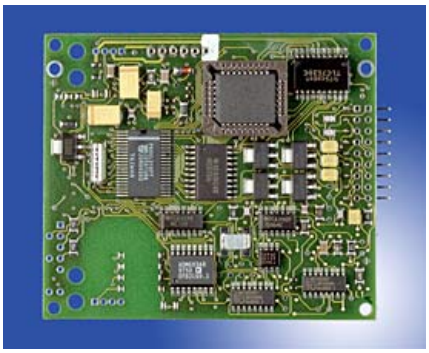

Figure 4: PO300 module

PO 300 wasn't designed as stand-alone device. It hasn't any visual output or data storage possibility. The first solution of this problem was simple interconnection via RS 232 (using MAX 232) to computer, where data was gathered and stored. Later a new mobile device was created using PO 300 module, microprocessor PIC16F874, LED displays, bargraf, piezo-beeper and few buttons, which was all powered by rechargeable battery. Also there was an output for interconnection with computer via RS 232. This device may be used in terrain showing pulse and saturation on LED displays, pulse wave amplitude on bargraf and there may be set alarm values for minimum and maximum pulse and saturation, which is indicated by piezo-beeper. Altough this device is now stand-alone, it may be not used in clinical praxis without interconnection with computer (this possibility is still included), because there is no display showing pulse wave (only pulse wave amplitude) as well as no output for printing or achieving records. But for terrain use it is enough.

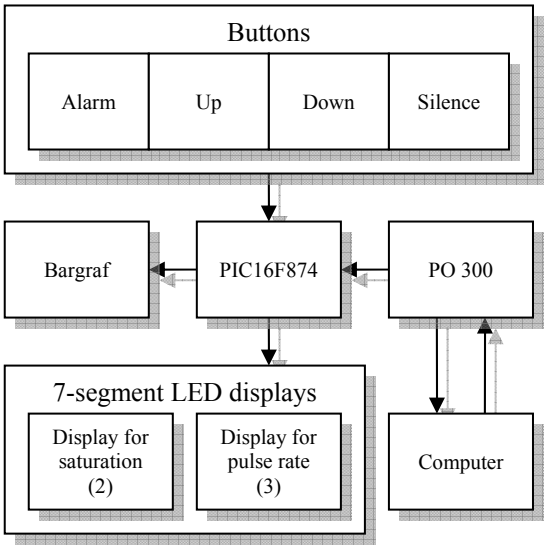


Figure 5: Plethymographycal Device Architecture

The serial output of PO 300 module is connected to serial input of microprocessor and to MAX 232 (providing output to computer). The serial input of PO 300 is connected only to MAX 232. There is no need to connect it also to microprocessor, because to PO 300 may be sent signals for change response mode, send software version, serial number of PO 300 module and actual response mode, toggle sending of

pletysmographycal curve and reset. Except the reset, which may be also invoked by sending logical 1 to another input pin (for this was assigned one "reset" button), all answers to signals to PO 300 are unimportant for terrain use, therefore the input is connected only to computer and not to microprocessor. All output data was processed in microprocessor and then sent to LED displays and bargraf to show proper values. For showing pulse rate and saturation, five seven-segment LED displays were used (two for saturation, three for pulse rate). The special circuit for changing the decimal value between 0-9 represented by binary number (three inputs) to proper output for showing the proper value on seven-segment LED display (seven outputs) was used. The ten-LED bargraf is showing the amplitude of pletysmographycal curve. (Figure 5)

There is also the possibility for adjusting alarm values. By pressing button "alarm", the showing of all data was halted, only the most up LED on bargraf is lighting and the three seven-segment LED displays for pulse rate is blinking, indicating that now may be adjusted high alarm value for pulse rate. The actual alarm value is showed on display and may be changed by pressing "up" and "down" buttons. After second pressing of "alarm" button, the high alarm value for pulse rate is stored, the lowest LED on bargraf is lighting and three seven-segment LED displays for pulse rate is still blinking, but now is showing the lower alarm value for pulse rate, which may be again changed by using "up" and "down" buttons. After another press of "alarm button" may be changed the lower alarm value for saturation (the upper alarm value for saturation isn't used). The way of changing is the same as mentioned before. After next press of "alarm" button is all returned to normal mode, showing all measured data again. When pulse rate or saturation is not between set alarm values, then the piezo-beeper is beeping and the value, which invoked the alarm, is blinking. The piezo-beeper may be silenced by pressing "silence" button, but the exceeding value will be still blinking, until the value returns to interval between alarm values (or by changing alarm values).

## VI. DISCUSSION

This measuring hardware and evaluating method were already successfully proved on the small tested group of people. But we need to perform more explorations on much bigger set of patients to find out the answer to the question if this method is really effective for elaboration of correct diagnosis, monitoring of a development of diseases of the vascular system and effect of the treatment.Thereafter will be done the final appraisal of this method. For the present we still cannot to enunciate definitely if the answer is positive or negative. But even the negative conclusion could have an informative value.

## VII. CONCLUSION

The aim to make the evaluation of plethysmographycal records more accurate leads to an idea to create the systematic apparatus (named SPF) for evaluation of pulse wave. In order to filtration and storage of modified signal was taken an advantage of possibilities of the new mathematical means of wavelet transform and the final conclusion was made by expert system based on framework. The hardware used for measuring data was improved during this work to meets our requirements as much as possible. First we used Criticare 504 USP plethysmograph, which has own monitor. This fact means the possibility to see the pletysmographycal curve without using other devices (e.g. computer), but also it means higher price and larger device. For our purposes we needed to gather the records to computer, so the own monitor wasn't necessary. Therefore later the PO 300 module based device (which is much smaller) without own monitor (only LED displays, bargraf and buttons was present) was used.

## ACKNOWLEDGMENT

The work and the contribution were supported by the project Grant Agency of Czech Republic – GAČR 102/08/1429 "Safety and security of networked embedded system applications". Also supported by the Ministry of Education of the Czech Republic under Project 1M0567. Students Grant Agency SGS SV450021" Biomedical Engineering Systems VI"

## REFERENCES

[1] Idzkowski A., Walendziuk W. (2009) Evaluation of the static posturograph platform accuracy, Journal of Vibroengineering, Volume 11, Issue 3, 2009, pp.511-516, ISSN 1392 - 8716

[2] Idzkowski A., Walendziuk W. (2009) Portable acquisition system for domiciliary uroflowmetry, Journal of Vibroengineering, Volume 11, Issue 3, 2009, pp.592-596, ISSN 1392 – 8716

[3] Vasickova, Z., Augustynek, M., New method for detection of epileptic seizure, Journal of Vibroengineering, Volume 11, Issue 2, 2009, pp.279-282, (2009) ISSN 1392 – 8716

[4] Cerny, M.: Movement Monitoring in the HomeCare System . In IFMBE proceddings. Ed. Dossel-Schleger, Berlin:Springer, 2009, issue. 25, ISBN 978-3-642-03897-6; ISSN 1680-07

[5] Krejcar, O., Cernohorsky, J., Fojcik, P., Janckulik, D., Martinovic, J., Smartphone, PDA and mobile Embedded device clients of Biotelemetric System for monitoring of life functions. In 5th International Conference on Innovations in Information Technology, Innovations 2008, December 16-18, 2008, Al Ain, United Arab Emirates. pp. 145-149. ISBN 978-1-4244-3396-4, DOI 10.1109/INNOVATIONS.2008.4781761

[6] Gono R., Kratky M., Rusek S., Analysis of Distribution Network Failure Databases, PRZEGLAD ELEKTROTECHNICZNY, Vol. 86, Issue 8, pp. 168-171, 2010 ISSN: 0033-2097

[7] Bernabucci, I., Conforto, S., Schmid, M., D'Alessio, T. A bio-inspired controller of an upper arm model in a perturbed environment, In proceedings The 2007 International Conference on Intelligent Sensors, Sensor Networks and Information Processing Pages: 549-553 ISBN: 978-1-4244-1501-4

[8] Cerny, M. Movement Activity Monitoringof Elederly People – Application in Remote Home Care Systems In Proceedings of 2010 Second International Conference on Computer Engineering and Applications ICCEA 2010, 19. – 21. March 2010, Bali Island, Indonesia, Volume 2NJ. IEEE Conference Publishing Services, 2010 p. ISBN 978-0-7695-3982-9

[9] Izakian, H., Abraham, A., Snasel, V., Metaheuristic Based Scheduling Meta-Tasks in Distributed Heterogeneous Computing Systems In Journal SENSORS Volume: 9 Issue: 7 Pages: 5339-5350 , Juyl 2009, ISSN: 1424-8220, DOI: 10.3390/s90705339

# FPGA-supported Diagnostics of Digital Systems in Biomedicine

Vladimir Kasik
Department of Measurement and Control, Faculty of
Electrical Engineering and Computer Science,
VSB–Technical University of Ostrava, FEI,
17. listopadu 15, 708 33, Ostrava-Poruba
Ostrava, Czech Republic
vladimir.kasik@vsb.cz

***Abstract*—A classic approach to perform a diagnostics of digital systems is to use logic analyzer in any form. Unfortunately, today's digital systems in biomedicine often have more logic lines needed to analysis than possible in standard logic analyzers. Furthermore a simple graphical and/or textual view of measured signals can be insufficient for the diagnosis. The paper introduces a module for ON-LINE diagnostics of the FPGA (Field Programmable Gate Array) based and other logic systems in biomedicine. The diagnostic system includes a VGA interface for data visualization on the monitor. Contained VGA controller doesn't use a video-memory for separate pixels. A Dual-port Block RAM inside FPGA is used instead to store the captured data.**

***Keywords- FPGA; Diagnostic system; VGA; Logic analyzer***

## I. INTRODUCTION

A classic approach to perform a diagnostics of digital systems is to use logic analyzer in any form. Unfortunately, today's digital systems in biomedicine often have more logic lines needed to analysis than possible in standard logic analyzers [3]. A second problem is usually an impossibility of connecting the analyzer probe to the Unit Under Test (UUT). In the following text an FPGA-supported method for diagnostics is presented. In fact, the described design is also a kind of the FPGA-powered logic analyzer with specific features. A majority of the functions are contained in the FPGA device, thus the description of the principles is concentrated in a FPGA digital design.

The result of the work is a set of function modules targeted to programmable FPGA digital logic. It includes data acquisition unit, video (VGA) output unit, clock generator units and others. The design is usable in two ways. One of them is for diagnostics of others embedded FPGA-based digital systems. It supposes, that the diagnostic FPGA is the same device as for the primary logic. Of course, that method is applicable for designers of the product only. A significant advantage of that is a possibility of higher data width of the logic analyzer inputs. The second way is to connect the necessary number of FPGA lines to inputs and/or outputs of the UUT.

The main part of the project is the digital FPGA design with the possibilities of flexible adaptation to many embedded systems in biomedicine and other measuring/control applications. In most cases that design is utilized with the VGA output for checking the diagnostic results.

Biomedical instruments, in which the method can be applied, are ECG and other signal simulators, Medical imaging instruments, Data storage application, etc. [2], [3], [4], [5].

## II. STRUCTURE OF THE DIAGNOSTIC MODULE

The structures of the FPGA design for both the methods as mentioned above are shown in Fig. 1 and Fig. 2. A common feature of the designs is an absence of a video memory. A Dual-Ported Block RAM for samples is used instead. Due to the possibilities of today's FPGAs, that memory is also contained in that programmable chip. The processes inside the FPGA like Triggering, Sampling, Data Storage and Samples Viewing, are concurrent and run in real-time.

A design entry of the modules is made in schematic drawings, VHDL code and also a state diagrams. The targeted platform in the project is a Xilinx Spartan3 FPGA with some specific resources used in the design, like BRAM, DCM and others.

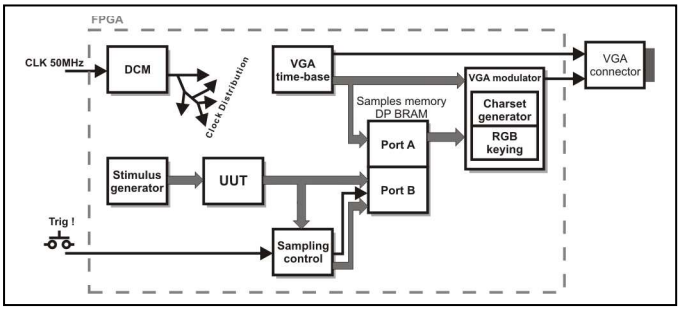


Figure 1. Diagnostics of the design inside FPGA

Beyond the FPGA device, the diagnostics project should include any controls for triggering, options selecting, initialization and others.

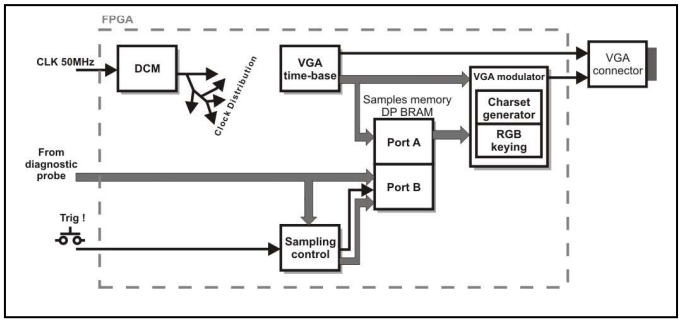


Figure 2. Diagnostics of the design outside FPGA

One basic block in the design, which is used in all the applications, is the Time-base module, see Fig. 3. The module generates regular VGA signals, especially a light beam coordinates on the screen, horizontal and vertical synchronization pulses and some status signals.

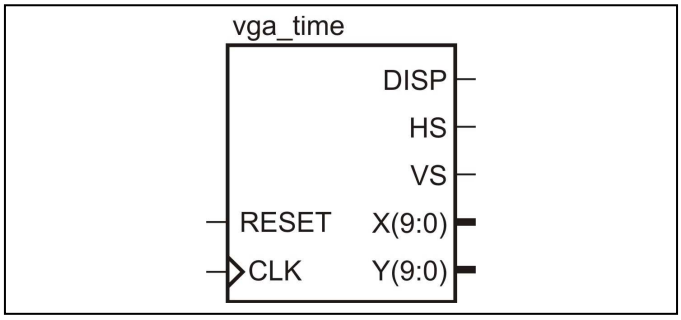


Figure 3. Schematic symbol of the time-base module

The module is made of two finite state machines (FSMs), where one FSM controls the light beam in the horizontal direction and the second one in the vertical direction.

Although the video resolution in the project is VGA 640x480, the time-base module is customizable for any other video resolution of course. It depends on timing specification constants in the FSM description. The logic analyzer is designed for digital systems implemented in the same FPGA by default, nevertheless it is easily applicable for the systems outside FPGA. For that case, plenty of FPGA devices have from tens to hundreds of I/O lines compatible with the most of the logic standards.

The logic analyzer design on the Fig. 1 measures output signals outgoing from the analyzed UUT module, which is stimulated with specified logic signals. Since the trigger is launched, the sampled data is stored in port A of the dual-ported block memory. On the other hand, an automatic data reading process from port B of that block memory runs independently on the previous data acquisition. Data stream obtained from the memory is then converted into videosignal. The style of the data view is configurable in the VGA modulator block.

A DCM block (Digital Clock Manager) is a hard implemented module inside the Spartan3 and many others modern FPGA devices of the Xilinx company. The DCM is used for the clock signal generation and thus for controlling all the logic system. The designed logic analyzer is able to perform both the Timing analysis and also the State analysis, pursuant to the clocking signal source. When used internal DCM for clocking, then the Timing analysis is performed. When the clocking signal inside FPGA is connected to corresponding clock signal in the tested instrument, then the State analysis can be proceed. The maximum clocking / data sampling frequency is influenced by the timing parameters of the logic design in the FPGA.

## III. Memory Dump Function With The Diagnostic Module

Additional function of the designed analyzer is a real-time memory dump on the VGA output. The memory dump view in hexadecimal radix is shown in Fig. 4.

The character set as well as the type of displaying depend on the VGA modulator unit. The video time base generates the periodic sequence of X-Y coordinates on the screen. These coordinates then passes to the combinatorial logic, which produces the brightness/color information of the light beam.

Figure 4. Detailed view of the Memory Dump on the VGA monitor

Thus the combinatorial logic is used for modulation of the video signal. Probably the simplest character generator uses an 8 x 8 character set including inter-character spaces. The screen view arrangement and columns / rows highlighting are both specified in the VGA modulator logic.

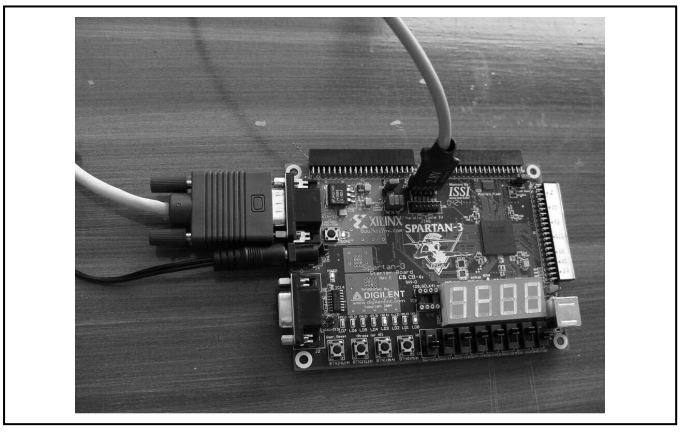

Figure 5. Spartan3 Starter Kit with Xilinx FPGA

The project has been tested on a Spartan3 Starter Kit with a Xilinx XC3S200-FT256 FPGA. The board includes the VGA connector with simple connection to the FPGA through simple resistor triplet.

## IV. Application Specific Diagnostics Of The Biomedical Instruments

In many cases, the simple use of the logic analyzer is not sufficient for a full-valued diagnosis of the digital systems [7], [8]. Various Application Specific Diagnostic Modules (ASDM in the following text) for FPGA digital logic can be the right thing to resolve that task. Following example demonstrates the utilization of ADSM for an ECG Signals Simulator diagnosis [1].

There is an 8-channels DAC converter generating the analog signals in the example. Considering the multichannel DAC with serial SPI data input, the simple data acquisition doesn't give any readable results. The highly specific "dack" module in Fig. 6 performs all needed data conversions to final refined view.

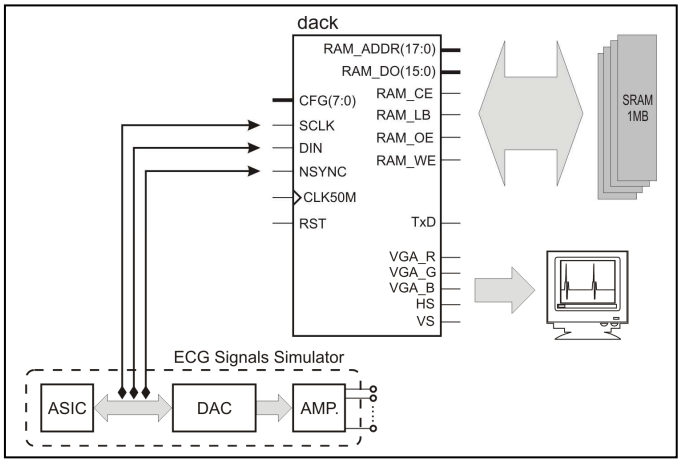


Figure 6. Application Specific Diagnostics of an ECG Signals Simulator

The module recognizes the input serial data stream and stores the word-aligned data samples in a fast Static RAM.

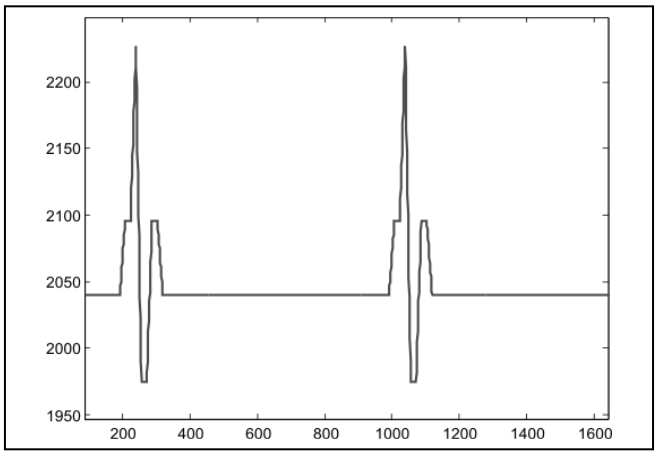


Figure 7. Graphic representation of captured data

Those data are concurrently read from that SRAM and viewed in any VGA output device. That process requires fast memory device and powerful SRAM driver for a dual-ported connection.

The video output can be either in the graphical or in the textual form as shown in Fig. 7 and Fig. 8.

Data in Fig. 8 are displayed after recognition by the ASDM module. Separate columns represent: hexadecimal sample index, system time in the clock ticks after start of data acquisition, type of the specific SPI word, DAC channel number or command, value included.

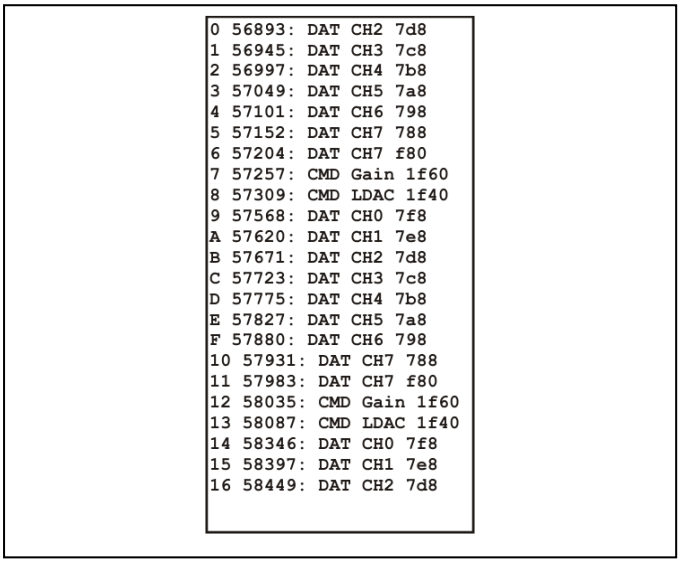


Figure 8. Textual representation of captured data

## V. Conclusion

The great advantage of the FPGA devices is the wonderful design flexibility. Thus the described diagnostic systems can be fitted to plenty of digital systems in biomedicine without extensive changes in the hardware [12], [13], [14], [16]. However, the principles can be easily used in other industrial [6], [7], [8], wireless [10], [15] and especially real-time systems [9], [11], [17]. The features of the Application Specific Diagnostic Modules are hardly realizable with common diagnostic instruments.

## Acknowledgment

The work and the contribution were supported by the project Grant Agency of Czech Republic GACR 102/08/1429 "Safety and security of networked embedded system applications".

This work was supported by the Ministry of Education of the Czech Republic under Project 1M0567.

This work was partially supported by the faculty internal project "Biomedical engineering systems V".

## REFERENCES


[1] Bernabucci, I., Conforto, S., Schmid, M., D'Alessio, T. A bio-inspired controller of an upper arm model in a perturbed environment, In proceedings The 2007 International Conference on Intelligent Sensors, Sensor Networks and Information Processing Pages: 549-553 ISBN: 978-1-4244-1501-4

[2] Cerny, M. Movement Activity Monitoringof Elederly People – Application in Remote Home Care Systems In Proceedings of 2010 Second International Conference on Computer Engineering and Applications ICCEA 2010, 19. – 21. March 2010, Bali Island, Indonesia, Volume 2NJ. IEEE Conference Publishing Services, 2010 p. ISBN 978-0-7695-3982-9

[3] Cerny, M. Movement Monitoring in the HomeCare System. In IFMBE proceddings. Ed. Dossel-Schleger, Berlin:Springer, 2009, issue. 25, ISBN 978-3-642-03897-6; ISSN 1680-07

[4] Cerny, M., Penhaker, M. Bed Vibration Measurement and Evaluation for Maintenance Health Systems. In Proceedings of 2nd International Conference on Mechanical and Electronics Engineering, ICMEE 2010, 01. -03. August 2010, Kyoto, Japan, Volume 1, NJ. IEEE Conference Publishing Services, 2010 pp. 372-373, ISBN 978-1-4244-7480-6

[5] Cerny, M., Penhaker, M., Mobile Embedded Biotelemetry System for Humans. In Proceedings of International Conference on Applied Electronics, AE 2010, 08. -09. September 2010, Pilsen, Czech Republic, 2010 pp. 253-256, ISBN 978-80-7043-865-7, ISSN 1803- 7232, DOI In Print

[6] Gono R., Kratky M., Rusek S., Analysis of Distribution Network Failure Databases, PRZEGLAD ELEKTROTECHNICZNY, Vol. 86, Issue 8, pp. 168-171, 2010 ISSN: 0033-2097

[7] Idzkowski A., Walendziuk W. Evaluation of the static posturograph platform accuracy, Journal of Vibroengineering, Volume 11, Issue 3, 2009, pp.511-516, ISSN 1392 - 8716M.

[8] Izakian, H., Abraham, A., Snasel, V., Metaheuristic Based Scheduling Meta-Tasks in Distributed Heterogeneous Computing Systems In Journal SENSORS Volume: 9 Issue: 7 Pages: 5339-5350 , Juyl 2009, ISSN: 1424-8220, DOI: 10.3390/s90705339

[9] Korpas, D., Psychological Intolerance to Implantable Cardioverter Defibrillator, In Biomedical Papers-Olomouc, Volume 152, Issue: 1 p.: 147-149 , June 2008 , ISSN: 1213-8118

[10] Krejcar, O., Janckulik, D., Motalova, L., Complex Biomedical System with Biotelemetric Monitoring of Life Functions. In Proceedings of the IEEE Eurocon 2009, May 18-23, 2009, St. Petersburg, Russia. pp. 138-141. ISBN 978-1-4244-3861-7, DOI 10.1109/EURCON.2009.5167618

[11] Penhaker, M., Cerny, M. The Circadian Cycle Monitoring. Conference Information: 5th International Summer School and Symposium on Medical Devices and Biosensors, JUN 01-03, 2008 Hong Kong, PEOPLES R CHINA, Pages: 41-43, 2008, ISBN: 978-1-4244-2252-4.

[12] Penhaker, M., Cerny, M., Martinak, L., et al. HomeCare "Smart embedded biotelemetry system". Book Series IFMBE proceedings World Congress on Medical Physics and Biomedical Engineering, AUG 27-SEP 01, 2006, Seoul, SOUTH KOREA, Volume: 14 Pages: 711-714, 2007, ISSN: 1680-0737, ISBN: 978-3-540-36839-7.

[13] Penhaker, M., Cerny, M., Martinak, L., et al.: HomeCare - Smart embedded biotelemetry system. In Book Series IFMBE proceedings World Congress on Medical Physics and Biomedical Engineering, AUG 27-SEP 01, 2006 Seoul, SOUTH KOREA, Volume: 14 Pages: 711-714,2007, ISSN: 1680-0737, ISBN: 978-3-540-36839-7

[14] Penhaker, M., Cerny, M., Rosulek, M. Sensitivity Analysis and Application of Transducers. 5th International Summer School and Symposium on Medical Devices and Biosensors, JUN 01-03, 2008 Hong Kong, PEOPLES R CHINA, Pages: 85-88 Published: 2008, ISBN: 978-1-4244-2252.

[15] Prauzek, M., Adamec, O., Penhaker, M., Testing of Portable Tele-Medical Power Supply. In Proceedings 2nd International Conference on Signal Processing Systems, ICSPS 2010, 05. - 07. July 2010, Dalian; China, 2010 Volume 2, pp. 380-382, ISBN: 978-142446891-1, DOI: 10.1109/ICSPS.2010.5555532

[16] Stankus, M., Penhaker, M., Cerny, M., Low Cost Data Acquisition System for Biomedical Usage. In XII Mediterranean Conference on Medical and Biological Engineering and Computing 2010, MEDICON 2010, May 27-30, 2010 Chalkidiki, Greece. Springer, IFMBE Proceedings, Vol. 29, Part 2. pp. 883-885. Panagiotis D. Bamidis and Nicolas Pallikarakis, (Eds.). Springer, Berlin Heidelberg. ISBN 978-3-642-13038-0 (Print) 978-3-642-13039-7 (Online), ISSN: 16800737, DOI: 10.1007/978-3-642-13039-7_223

[17] Vasickova, Z., Augustynek, M., New method for detection of epileptic seizure, Journal of Vibroengineering, Volume 11, Issue 2, 2009, pp.279-282, (2009) ISSN 1392 - 8716

# FPGA based ZigBee Interface for Biomedicine Applications

Vladimir Kasik
Department of Measurement and Control, Faculty of
Electrical Engineering and Computer Science,
VSB–Technical University of Ostrava, FEI,
17. listopadu 15, 708 33, Ostrava-Poruba
Ostrava, Czech Republic
vladimir.kasik@vsb.cz

***Abstract*—The paper deals with design and implementation of a ZigBee interface for a "Cerberos" biomedical telemetric system. The design is targeted into FPGA programmable logic and it covers SCI to ZigBee module communication interface with specific "Cerberos" communication protocol. The interface is register – oriented and is designed for full-duplex connection due to SCI. A FIFO buffer is also included in FPGA design to meet the "Cerberos" specification. In spite of this, the design methodology can be utilized also for common SCI to ZigBee interfaces. The ZigBee module on the other side is based on a CC2480 ZigBee transceiver. Detailed description of communication controller design and FPGA implementation details are described in the following chapters.**

***Keywords- FPGA; ZigBee; Biomedical; Communication interface***

## I. INTRODUCTION

The "Cerberos" project [1], [3], [4], [6], [7], [14] is framed to telemetry systems in biomedicine and it uses several ZigBee modules for transferring the biometric data between patient's telemetry modules and a central data acquisition module (DAM in the text). Due to specific communication protocol and hardware interfaces used the data must be converted and framed.

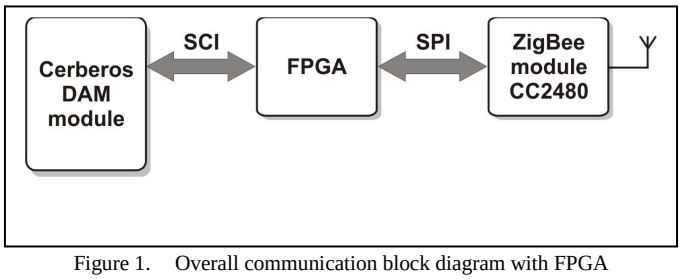


Figure 1. Overall communication block diagram with FPGA

The interface is register – oriented and is designed for full-duplex connection due to SCI connection, which is used on the DAM side. The ZigBee module on the other side is based on a common CC2480 transceiver [16] with use of an AREQ protocol. The communication must meet the specific requirements for transferring the biometric data, which includes temperature, pressure, weight and ECG data with up to 100 Hz bandwidth. The data are transferred from the DAM in 253 bytes long packets with up to 19200 Bd. Transmission rate of the CC2480 is then set to 4 Mb/s, however the communication speed can be notably reduced by communication errors of the wireless transfer depending on the application environment. In addition the FPGA proceeds some requested integrity checking and data processing before start of the communication with CC2480.

## II. COMMUNICATION PROTOCOL DESIGN

A byte oriented protocol is used for the communication between DAM and FPGA modules. It consists of seven parts, see Figure 2. The Header and Footer are constant unique symbols and when they are to be included in transferred data, then they must be replaced with other two-byte constants. Packet ID identifies the type of the packet according to "Cerberos" system, which defines several data packets and some command packets [3], [4], [6]. DLen byte stands for Data Length with value up to 253.

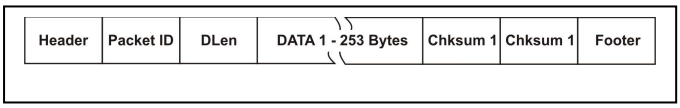


Figure 2. DAM to FPGA communication protocol

Double checksums are included in the packet because of the increased communication reliability in biomedical applications [11], [12], [13]. The FPGA calculates the checksum validity in designed hardware and just in the time the bytes income to the chip. The same protocol is used for the FPGA to DAM direction except some commands specifications. Then the FPGA can be used in more applications using SCI to any other wireless technology [2], [5], [8], [9], [10].

## III. DIGITAL LOGIC DESIGN

The digital logic design for FPGA consists mainly of communication transceivers, Dual FIFO buffer and controllers, see Fig. 3. It also includes clock generators (not shown in the Figure) for communication transceivers and for general clocking. The SCI and SPI transceivers provide serialization and deserialization of the data, bit recognition at the SCI and appropriate frame handling at the SPI. The Dual FIFO buffer is based on a Dual-Ported Block RAM, which is included in a Xilinx's Spartan3 architecture used with advance in the project. Both the DPRAM ports have separated address and data buses, referenced A and D in the Figure, and separate clock and control signals.

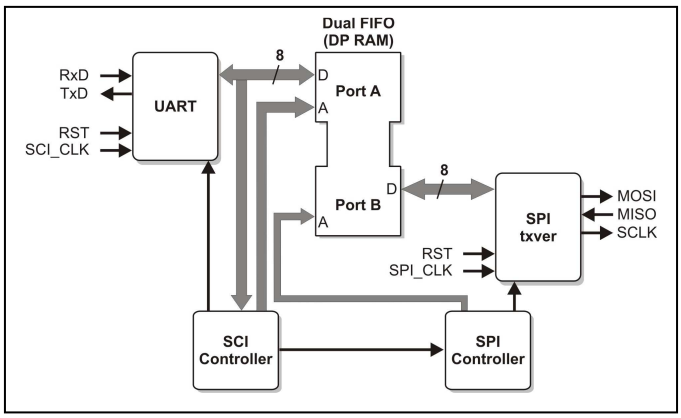


Figure 3. Simplified logic design in FPGA

The SCI Controller operates also as an instruction decoder for commands incoming from the DAM module and received by SCI.

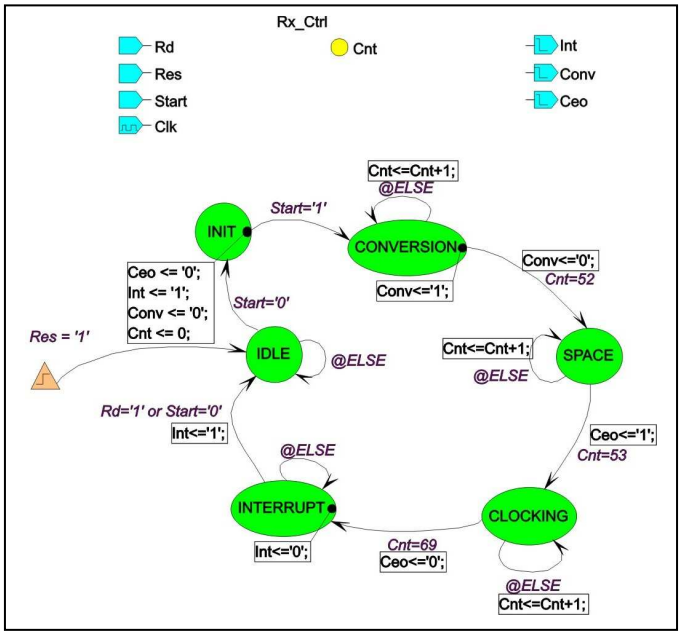


Figure 4. FSM diagram for SCI receiving

Generally, both the controllers work independently except some control commands to SPI Controller. Both the controllers are designed as Finite State Machines – FSMs. Then they are converted to VHDL description, synthetized and implemented together with rest of the logic into FPGA. One controller in the design contains three FSMs which are usually for Rx, Tx and overall control operations. A partial FSM for SCI receiving is shown in Fig 4.

## IV. FUNCTIONAL VERIFICATION OF THE DESIGN

Major part of the functional verification has been concentrated to the FPGA digital logic. First stage of the verification has been carried out in a functional simulator. After some essential debugging the design results are functional and reliable.

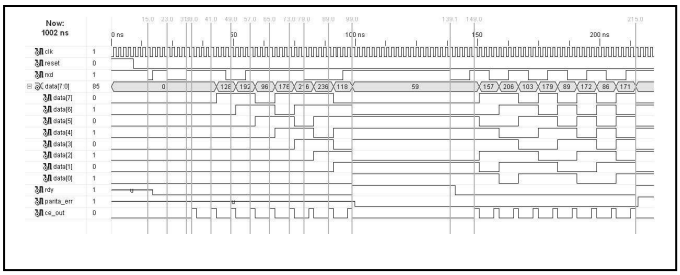

Figure 5. Functional verification in the simulator

Next, the design has been tested on a logic analyzer with the same positive results. The timing specifications can be demonstrated on reasonably low latency of the command response at 32µs [16].

## V. CONCLUSION

Described architecture of ZigBee interface is primarily projected for a "Cerberos" application in biomedicine, however it can be utilized also for common SCI to ZigBee interfaces [14], [15]. The benefit of the FPGA usage is the flexibility of the hardware design and data processing speed-up for parallel decomposition of the functions into independent blocks. The FPGA design is relatively very small and then the device can involve many others logic functions.

TABLE I. DEVICE UTILIZATION SUMMARY

| Logic Utilization | Resources | | |
|---|---|---|---|
| | *Used* | *Available* | *Utilization* |
| *Slice Flip-Flops* | *236* | *3840* | *6%* |
| *Number of 4 input LUTs* | *1095* | *3840* | *28%* |
| *Number of occupied Slices* | *647* | *1920* | *33%* |
| *Number of Block RAMs* | *2* | *12* | *17%* |
| *Total equivalent gate count for design* | | | *23451* |

## ACKNOWLEDGMENT

The work and the contribution were supported by the project Grant Agency of Czech Republic GACR 102/08/1429 ”Safety and security of networked embedded system applications”.

This work was supported by the Ministry of Education of the Czech Republic under Project 1M0567.

## REFERENCES

[1] Cerny M., Penhaker M. Biotelemetry In conference proceedings 14th Nordic-Baltic Conference an Biomedical Engineering and Medical Physics, JUN 16-20, 2008 Riga, LATVIA, Volume: 20 Pages: 405-408 Published: 2008, ISSN: 1680-0737, ISBN: 978-3-540-69366-6

[2] Cerny, M. Movement Activity Monitoring of Elederly People – Application in Remote Home Care Systems In Proceedings of 2010 Second International Conference on Computer Engineering and Applications ICCEA 2010, 19. – 21. March 2010, Bali Island, Indonesia, Volume 2NJ. IEEE Conference Publishing Services, 2010 p. ISBN 978-0-7695-3982-9

[3] Cerny, M. Movement Monitoring in the HomeCare System. In IFMBE proceddings. Ed. Dossel-Schleger, Berlin:Springer, 2009, issue. 25, ISBN 978-3-642-03897-6; ISSN 1680-07

[4] Cerny, M., Penhaker, M. Personal System of Remote Health Care In Proceedings of 2nd International Conference on Mechanical and Electronics Engineering, ICMEE 2010, 01. -03. August 2010, Kyoto, Japan, Volume 1, NJ. IEEE Conference Publishing Services, 2010 pp. 413-415, ISBN 978-1-4244-7480-6

[5] Cerny, M., Penhaker, M. Plethysmography Bluetooth Measurement. In Proceedings of 2nd International Conference on Mechanical and Electronics Engineering, ICMEE 2010, 01. -03. August 2010, Kyoto, Japan, Volume 1, NJ. IEEE Conference Publishing Services, 2010 pp. 337-339, ISBN 978-1-4244-7480-6

[6] Cerny, M., Penhaker, M., Mobile Embedded Biotelemetry System for Humans. In Proceedings of International Conference on Applied Electronics, AE 2010, 08. -09. September 2010, Pilsen, Czech Republic, 2010 pp. 253-256, ISBN 978-80-7043-865-7, ISSN 1803- 7232, DOI In Print

[7] Cerny, M.: Movement Monitoring in the HomeCare System . In IFMBE proceddings. Ed. Dossel-Schleger, Berlin:Springer, 2009, issue. 25, ISBN 978-3-642-03897-6; ISSN 1680-07

[8] Krejcar, O., “Localization by Wireless Technologies for Managing of Large Scale Data Artifacts on Mobile Devices”. In The 1st International Conference on Computational Collective Intelligence - Semantic Web, Social Networks & Multiagent Systems, ICCCI 2009, October 05-07, 2009 Wroclaw, Poland. Lecture Notes in Artificial Intelligence, LNAI Vol. 5796. pp. 697-708. N.T. Nguyen, R. Kowalczyk, and S.-M. Chen (Eds.). Springer-Verlag, Berlin, Heidelberg. DOI 10.1007/978-3-642-04441-0

[9] Krejcar, O., “Problem Solving of Low Data Throughput on Mobile Devices by Artefacts Prebuffering”, In EURASIP Journal on Wireless Communications and Networking, Article ID 802523, 8 pages. Hindawi publishing corp., New York, USA, DOI 10.1155/2009/802523 (2009)

[10] Krejcar, O., Janckulik, D., Motalova, L., Musil, K., Penhaker, M., Real Time ECG Measurement and Visualization on Mobile Monitoring Stations of Biotelemetric System. In The 2nd Asian Conference on Intelligent Information and Database Systems, ACIIDS 2010, March 24-26, 2010 Hue City, Vietnam. Springer, Advances in Intelligent Information and Database Systems, Studies in Computational Intelligence, SCI Vol. 283. pp. 67-78. N.T. Nguyen et al. (Eds.). Springer-Verlag, Berlin, Heidelberg. ISBN 978-3- 642-12089-3, ISSN 1860-949X (Print) 1860-9503 (Online), DOI 10.1007/978-3-642-12090-9_6 (Paper quality rate: 66.5%, 66.5/100) (Acceptance rate: 36 %, 32/348)

[11] Penhaker , M. Cerny, L. Martinak, et al. HomeCare Smart embedded biotelemetry system. Book Series IFMBE proceedings World Congress on Medical Physics and Biomedical Engineering, AUG 27-SEP 01, 2006 Seoul, SOUTH KOREA, Volume: 14 Pages: 711-714, 2007, ISSN: 1680- 0737, ISBN: 978-3-540-36839-7

[12] Peterek, T., Prauzek, M., Penhaker, M., A New Method for Identification of the Significant Point in the Plethysmografical Record. In Proceedings 2nd International Conference on Signal Processing Systems, ICSPS 2010, 05. - 07. July 2010, Dalian; China, 2010 Volume 1, pp. 362-364, ISBN: 978-142446891-1, DOI: 10.1109/ICSPS.2010.5555642

[13] Prauzek, M., Peterek, T., Adamec, O., Stankus, M., Penhaker, M. Simple Data Acquisition System for Photopletysmography and Electrocardiography. In Proceedings 2nd International Conference on Signal Processing Systems, ICSPS 2010, 05. - 07. July 2010, Dalian

[14] Srovnal, V. Penhaker, M., Architecture and Infrastructure of Health Maintenance Systems. In Proceedings of 9th RoEduNet IEEE International Conference, RoeduNet 2010, 24. – 26. June 2010, Sibiu, Romania, NJ. IEEE Conference Publishing Services, 2010 pp. 341-345, ISBN: 978-142447335-9, ISSN 2068-1046, DOI In Print

[15] Stankus, M., Penhaker, M., Cerny, M., Low Cost Data Acquisition System for Biomedical Usage. In XII Mediterranean Conference on Medical and Biological Engineering and Computing 2010, MEDICON 2010, May 27-30, 2010 Chalkidiki, Greece. Springer, IFMBE Proceedings, Vol. 29, Part 2. pp. 883-885. Panagiotis D. Bamidis and Nicolas Pallikarakis, (Eds.). Springer, Berlin Heidelberg. ISBN 978-3-642-13038-0 (Print) 978-3-642-13039-7 (Online), ISSN: 16800737, DOI: 10.1007/978-3-642-13039-7_223

[16] Texas Instruments. Transceiver CC2480 Data Sheet. <http://focus.ti.com/docs/prod/folders/print/cc2480a1.html>.

# Speech and Image Processing

# Speckle Noise Supression in Ultrasound Medical Images

Radek Benes, Kamil Riha
Department of Telecommunications
Brno University of Technology
Brno, Czech Republic
radek.benes@phd.feec.vutbr.cz, rihak@feec.vutrb.cz

***Abstract*—The paper deals with ultrasound image de-noising methods. Firstly, the speckle noise phenomenon in ultrasound images is described. Then, various methods for the reduction of such noise are presented such as Kuan, Lee, and Frost filters, SRAD. Moreover, the improvement of Kuan method is proposed that is based on algorithm suggested by Lopes [1]. All presented methods and the proposed one were tested on synthetic and real ultrasound image data. Testing with synthetic images allows us the precise quality comparison of particular methods, but the results are slightly dependent on chosen noise model. Thus, the tests were also performed on real data, which will show the suitability for practical usage.**

***Keywords- speckle noise; de-noising; kuan; frost; lee; wavelets***

## I. INTRODUCTION

Ultrasound is widely used in medicine for imaging internal organs like liver, kidney, spleen, uterus, heart, artery, etc. This type of medical examination is very popular due to its speed, scanner portability, non-invasive principle, cheapness, etc. On the other hand, ultrasound images are often low-contrast; they contain a lot of artifacts and noise. Moreover, the noise in ultrasound images (the speckle noise) has a multiplicative character, so its removing from the observed ultrasound image is more complicated than for example removing of Gaussian additive noise.

The speckle noise problem is very specific; so many de-noising methods were tailored just for this purpose. The most common methods are briefly described in related work section. There are also mentioned some general de-noising methods, which are slightly adjusted to remove just speckle noise.

This paper is organized as follows. Section II is consists of the introduction to the speckle noise problematic and its mathematical description. Section III contains an overview of speckle de-noising methods and other common modified de-noising methods. The next section describes our proposed improvement of Kuan method. The rest of the paper is focused on the evaluation of described methods and also to the discussion of their suitability for usage in echocardiography images.

## II. SPECKLE NOISE MODEL

Speckle noise [2] is a common phenomenon in ultrasound imaging system. This noise arises from random interference between the coherent returns issued from scatters present on surface. Speckle noise in ultrasound images is often undesirable, especially when the further image processing is automatic. Thus, the speckle noise filtering (speckle de-noising) is important pre-processing step.

Mathematically, the speckle noise can be assumed as pure multiplicative model [3]

$$I(t) = R(t) \cdot u(t), \tag{1}$$

where $t = (x, y)$ represents spatial coordinates in the image, $I(t)$ is the observed image, which is corrupted by multiplicative speckle noise $u(t)$, with mean value $\overline{u}$ and variance $\sigma_u^2$. The $R(t)$ represents the reflection of investigated region. Due to multiplicative character of speckle noise, this noise can be better observed in high intensity regions. Some authors, for example Kaur [4], extend the pure multiplicative noise model with additional Gaussian noise.

$$I(t) = R(t) \cdot u(t) + \mu(t). \tag{2}$$

In our paper the simple multiplicative model from Eq. 1 is assumed.

## III. RELATED WORK

The speckle noise is undesirable especially in automatic ultrasound image processing, because it complicates further image processing. The character of speckle noise is different from the most common additive character of Gaussian noise, and therefore speckle de-noising requires special methods. So, several methods for speckle noise suppression have been proposed so far. All methods were designed to remove as much noise as possible, while preserving important features (like strong edges, important small spots, etc.). De-noising methods can be based on adaptive principle [5], [6], [7], partial differential equations (PDE) [8], multi-scale approach, etc. The

most common adaptive methods designed so far are Lee [5], Frost [9], and Kuan [10] filter.

*A. Lee filter* [5]

Lee filter (more precisely Lee MMSE filter) is based on linear speckle noise model and the minimum mean square error (MMSE). The image data enhancement comes from the basic filter equation

$$\hat{R}(t) = I(t) \cdot W(t) + \overline{I}(t) \cdot \big(1 - W(t)\big), \qquad (3)$$

where $\hat{R}(t)$ is the de-noised image, $I(t)$ is the image corrupted with speckle noise and $\overline{I}(t)$ is the mean image intensity within the filter window. $W(t)$ is weighted coefficient determined as

$$W(t) = 1 - \frac{C_u^2}{C_I^2(t)}, \qquad (4)$$

where $C_u$ and $C_I(t)$ are variation coefficients of speckle $u(t)$ and image $I(t)$ respectively

$$C_u = \frac{\sigma_u}{\overline{u}}, C_I(\mathrm{t}) = \frac{\sigma_I(t)}{\overline{I}(t)}. \qquad (5)$$

*B. Kuan filter* [10]

This approach transforms the multiplicative noise model into signal dependent additive noise model, and then the minimum mean square error (MMSE) is applied. Resulting equation is similar to the Eq. 3 for Lee filter, but the weight factor $W(t)$ is different

$$W(t) = \frac{1 - \frac{C_u^2}{C_I^2(t)}}{1 + C_u^2}. \qquad (6)$$

*C. Frost filter* [9]

The Frost filter is an adaptive filter that convolves pixels in a fixed window with impulse response $m(t)$ given by

$$m(t) = \exp(-K \cdot C_I(t) \cdot |t_0|), \qquad (7)$$
$$C_I(t) = \frac{\sigma_I(t)}{\overline{I}(t)},$$

where $K$ is the filter parameter and $|t_0|$ is distance measured from pixel located at coordinates $t$.

*D. Improved Lee filter* [1]

The improvement of Lee filter is based on the presumption that the areas in the image can be classified into one of three classes. First class contains all homogenous areas, where the speckle noise is suppressed by application of simple low pass filter. Second class contains all heterogeneous areas, where the Eq. 3 for Lee filter is used to reduce speckle noise. Finally, the third class contains isolated points and other important image features with high image variance. For the third class, the improved filter retains original pixels from observed image. These cases can be written by equation

$$\hat{R}(t) = \begin{cases} \overline{I}(t) & C_I(t) \le C_u \\ I(t) & C_I(t) > C_{max} \\ I(t) \cdot W(t) + \overline{I}(t) \cdot W'(t) & \text{otherwise} \end{cases} \qquad (8)$$
$$W(t) = \exp\left(\frac{-K \cdot (C_I(t) - C_u)}{C_{max} - C_I(t)}\right).$$

Similar principle can be used for Frost and Kuan filters.

*E. Wavelet based de-noising* [12], [13]

Speckle noise is a high-frequency component of the image and naturally it affects wavelet coefficients. Thus, wavelet base de-noising uses thresholding of wavelet coefficients to suppress such noise.

The procedure starts with Discrete Wavelet Transform (DWT) calculation, then the coefficient thresholding is performed and finally the image is reconstructed via Inverse Discrete Wavelet Transform (IDWT) computation. The main goal of wavelet thresholding consists of the determination of the most suitable mother wavelet, the best threshold method and the appropriate threshold levels. The most common threshold methods are soft and hard thresholding. *Hard thresholding* sets all coefficient less than or equal to the threshold $x_{\mathrm{thr}}$ to zero

$$x = \begin{cases} x & \text{for } |x| > |x_{\mathrm{thr}}| \\ 0 & \text{for } -x_{\mathrm{thr}} \le x \le x_{\mathrm{thr}} \end{cases} \qquad (9)$$

*Soft thresholding* method subtracts the threshold value from any coefficient that is greater than the threshold. This moves the time series toward zero

$$x = \begin{cases} x - x_{\mathrm{thr}} & \text{for } x > x_{\mathrm{thr}} \\ 0 & \text{for } -x_{\mathrm{thr}} \le x \le x_{\mathrm{thr}} \\ x + x_{\mathrm{thr}} & \text{for } x < -x_{\mathrm{thr}} \end{cases} \qquad (10)$$

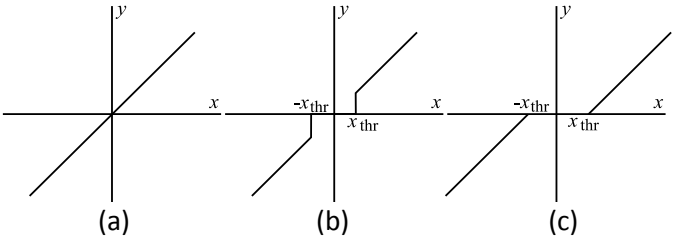


Figure 1. The demonstration of hard (b) and soft (c) thresholding method processed the original signal depicted in figure (a).

Due to the multiplicative nature of speckle noise, the logarithmic transformation (more precisely $\log(I + 1)$ ) of original image $I$ must be performed before wavelet decomposition. This homomorphic transformation changes the multiplicative character of the noise to additive which can be easily suppressed according to [12].

In this study, the *db2* mother wavelet and the soft thresholding with universal threshold estimation [13] was utilized.

### F. *Speckle reduction anisotropic diffusion (SRAD)* [8]

This method was tailored directly for ultrasound and radar imaging applications (both contain speckle noise). SRAD method uses instantaneous coefficient (similar to the coefficient of variation in Lee and Frost filter), which is a function of local gradient, magnitude and Laplacian operators. Authors claim, that this method is better than classical anisotropic reduction method when the image is corrupted by speckle noise.

This method is based on partial different equation (PDE) which involves the image gradient, Laplacian and image intensity.

### G. *Wiener filtration* [14]

Wiener filter is designed especially for removing of additional Gaussian noise, so it is not possible to use this method directly for multiplicative speckle noise.

To solve this issue, Jain [15] developed a homomorphic approach which converts the multiplicative noise into additive noise by computing of the logarithm of the image. Subsequently, the Wiener filter can be applied to this additive noise.

## IV. Enhanced Kuan filter by sigmoid weighting factor (KuanS)

The proposed improvement of the Kuan filter is based on the same region classes as shown in Improved Lee filter described above in section II. The main difference consists in the processing of the heterogeneous regions. Our proposed method comprises the sigmoid function to the modification of weighted function $W(t)$. The modified weighted factor $W'(t)$ can be calculated by using

$$W'(t) = \frac{1}{1+\exp(-K\cdot(W(t)-0.5))}. \quad (11)$$

This approach enables smoother transition between extreme values within the heterogeneous areas. De-noising of homogenous regions remains the same as de-noising with improved Kuan method. Also, the de-noising of isolated points and other significant image properties is the same as in improved Kuan.

## V. Test images and de-noising quality evaluation

All speckle noise filters are highly sensitive to particular image quality, so it is very difficult to evaluate the performance of particular methods. For the utilisation in medicine, it is required to achieve the best ratio between the capability of noise supression and the preservation of details in image.

In this paper, the quality of particular de-noising methods was evaluated with two types of images – synthetic images and real ultrasound image data. The phantom image availible in Matlab (Fig. 2 (a)) was used as a synthetic image. This phantom image was corrupted with speckle noise in accordance to the presented noise model (Eq. 1). In this experiment, the de-noising quality can be accurately evaluated, because both the original (the ground truth) and de-noised images are known.

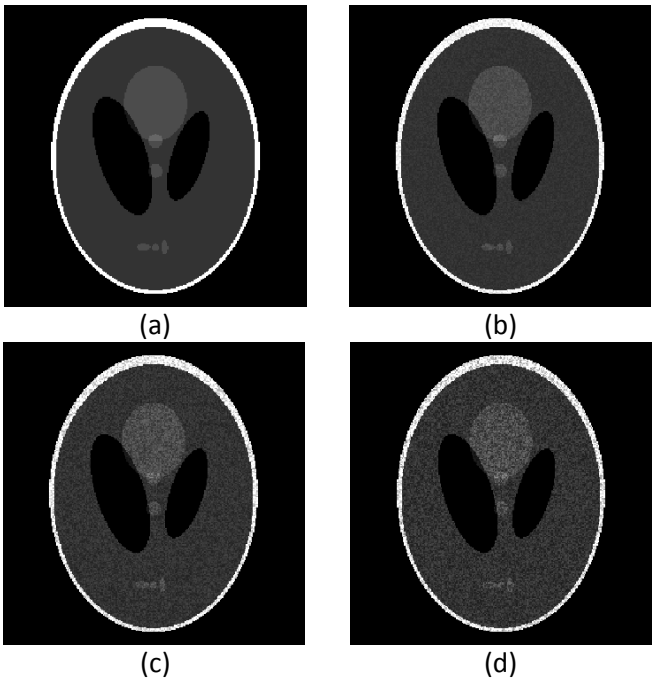


Figure 2. (a) The phantom image. (b) – (d) The phantom image corrupted with different levels of scpekle noise (σ=0.04, σ=0.07, σ=0.10).

As mentioned, real ultrasound images were also used. The evaluation of quality of de-noising on real images is more complicated, because only observed (image corrupted with noise) and de-noised images are availible. On the other hand, in this experiment we can compare particular methods in real conditions in this experiment, and select the most suitable one from the perspective of further processing of real images. Therefore, the parameters for evaluation of particular de-noising methods can be for example slope of edges, or standard deviation of selected homogenous regions. The de-noising quality can be also compared visually.

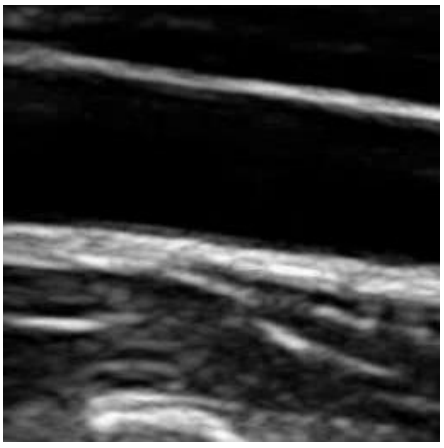

Figure 3. The real B-mode ultrasound image of comon carotid arthery in longitudal scan.

The following subsections describe some qualitative parameters that can be used for evaluation of quality of de-noising methods.

### A. Peak signal to noise ration (PSNR)

According to [12], the PSNR can be evaluated as

$$PSNR = 10 \cdot \log_{10}\left(\frac{I_{\max}}{MSE}\right), \quad (12)$$

$$MSE = \frac{1}{M \cdot N \sum_{m=0}^{M-1} \sum_{n=0}^{N-1} (R(m,n) - \hat{R}(m,n))^2}.$$

The *MSE* is Mean Square Error between the original and de-noised image.

### B. Approximation of linear slope of edge $m$ [13]

The linear slope of an edge can be determined by using equation 13 aplyed to selected strong edges. It is suitable to transform such edges to one-dimensional signal before the computation of slope of the edge.

$$m = \frac{\Delta y}{\Delta x}, \quad (13)$$

where $\Delta y$ and $\Delta x$ represents the edge parameters, as shown in Fig. 4.

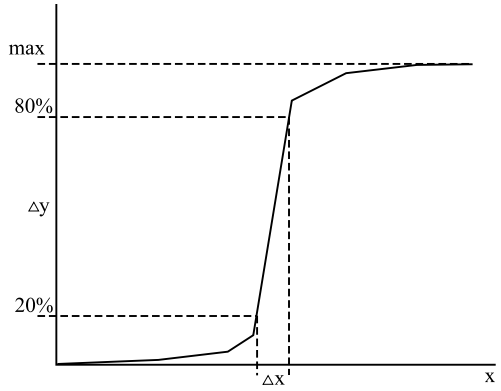


Figure 4. Linear slope of edge aproximation estimation.

All values $m$ obtained from de-noised images are related to the reference value estimated from original images if it is possible.

### C. The standart deviation of important regions

In both synthetic and real ultrasound images, it can be found such regions, where the texture should be homogenous. The standard deviation of pixels in such regions can be also used to compare the quality of de-noising methods. Better de-noising methods guarantee lower value of standard deviation in homogenous regions.

### D. Mean Value Preservation

In synthetic data, where the original image is known, the mean value in homogenous regions in original image and in image after de-noising can be calculated. Good methods have to preserve the mean value in homogenous regions.

## VI. RESULTS

The results of de-noising methods are summarized in the following tables and graphs. The values of slope of edge approximation are related to the reference value estimated from original images.

### A. Synthetic data

In this experiment, the "phantom" image (Fig. 2 (a)) available in Matlab was used and was corrupted with different levels of speckle noise. The variance of speckle noise was chosen in range from 0.01 to 0.1 (Fig. 2 (b) – (d)).

Table I shows the peak signal to noise ratio (PSNR) for all tested methods for chosen levels of speckle noise. For all chosen speckle noise levels, the PSNR values are the best when using the Wavelet based de-noising, Wiener filtration and our proposed improvement of Kuan filter (KuanS). All values are plotted in Fig. 5.

Table II summarizes the standard deviation of selected homogenous regions and slope of edges for all tested methods. Also, the best results were achieved while using Wavelet based de-noising, Wiener filtration and proposed Kuan improved method. Fig. 7 shows the slope of edge approximation for chosen variance of noise.

### B. Real data

In this experiment, the real echocardiography images (Fig. 3) have been used. These images contain the speckle noise from the nature of the ultrasound imaging, so is not necessary to corrupt these images with artificial speckle noise. Only observed and de-noised images are available, thus the quality evaluation of particular methods is quite limited.

In table III, the standard deviation of selected homogenous regions and slope of edge, can be seen. The values in this table confirm the results achieved with synthetics data. Again, the Wavelet based de-noising, wiener filtration and proposed improvement of Kuan achieve the best results among the tested methods.

## CONCLUSION

When evaluating the results, all measured parameters have to be considered. According to the presumption, within the group of tested methods, the one based on Wavelets achieves the best results in most of measured parameters (the highest PSNR, the lowest standard deviation). Only the preservation of edges in real ultrasound images is surprisingly not as good in comparison to other methods. Methods like SRAD and Homomorphic Wiener, tailored to remove of speckle noise, also gives very good results. On the other hand, these methods are quite computationally complex and thus, the simpler methods, such as Lee, Kuan, and its improvements are also appropriate for some applications where the fast processing is important. The time requirements of presented methods were not compared in detail, because they are dependent on the implementation language. Some methods were implemented in C and thus their processing is naturally faster than for methods implemented in Matlab.

The proposed improvement of Kuan filter (KuanS) achieved better results in all measured parameters in comparison with presented standard Kuan filter and its improved variant. Especially the standard deviation of selected homogenous regions is better while the edge preservation remains satisfactory.

TABLE I. PARAMETERS MEASURED ON SYNTHETIC ULTRASOUND IMAGES

| | PSNR | | | |
|---|---|---|---|---|
| | ***σ=0.01*** | ***σ=0.04*** | ***σ=0.07*** | ***σ=0.10*** |
| **Kuan filter** | 20,71 | 18,58 | 17,51 | 17,07 |
| **Improved Kuan** | 26,59 | 25,41 | 24,24 | 21,83 |
| **KuanS** | 27,13 | 26,23 | 25,44 | 22,83 |
| **Lee** | 20,71 | 18,49 | 17,46 | 17,07 |
| **Frost** | 25,03 | 22,63 | 21,67 | 20,41 |
| **Wavelet** | 27,14 | 26,88 | 24,34 | 22,99 |
| **Wiener** | 24,66 | 22,51 | 21,99 | 21,73 |
| **SRAD** | 26,29 | 24,78 | 23,85 | 22,29 |

TABLE II. PARAMETERS MEASURED ON SYNTHETIC ULTRASOUND IMAGES

| | Standard deviation | | | | slope of edge |
|---|---|---|---|---|---|
| | ***σ=0.01*** | ***σ=0.04*** | ***σ=0.07*** | ***σ=0.10*** | ***σ=0.07*** |
| **Kuan filter** | 0.012 | 0.029 | 0.037 | 0.053 | 0.63 |
| **Improved Kuan** | 0.009 | 0.013 | 0.017 | 0.021 | 0.70 |
| **KuanS** | 0.009 | 0.013 | 0.017 | 0.020 | 0.70 |
| **Lee** | 0.012 | 0.029 | 0.037 | 0.053 | 0.65 |
| **Frost** | 0.022 | 0.033 | 0.043 | 0.051 | 0.50 |
| **Wavelet** | 0.007 | 0.011 | 0.021 | 0.027 | 0.69 |
| **Wiener** | 0.014 | 0.022 | 0.030 | 0.042 | 0.63 |
| **SRAD** | 0.012 | 0.017 | 0.023 | 0.027 | 0.62 |

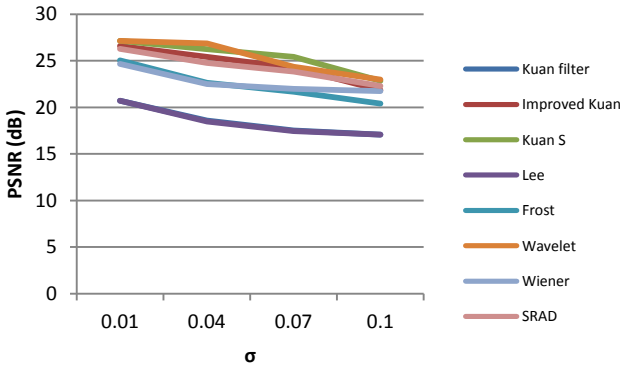


Figure 5. PSNR measured on phantom de-noised by particular method.

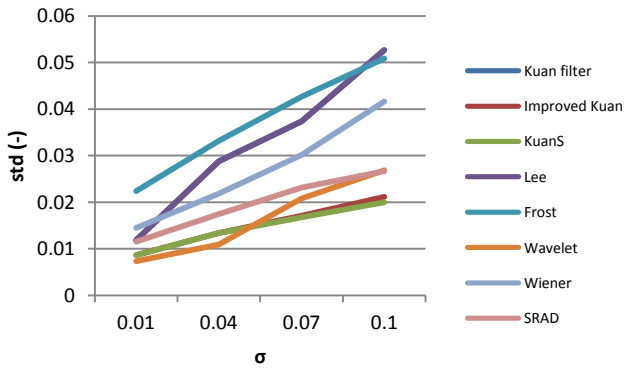


Figure 6. Standard deviation measured on phantom image de-noised by particular method

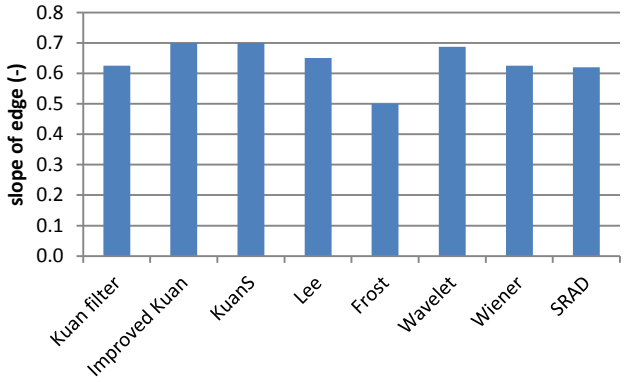


Figure 7. Slope of the edge for particular methods on phantom image.

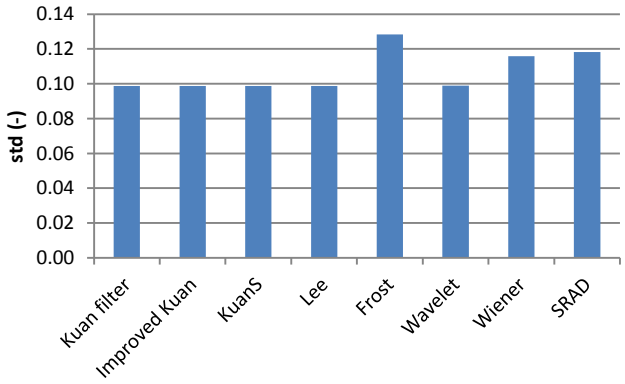


Figure 8. Standard deviationd of selected regions for particular method on real ultrasound images.

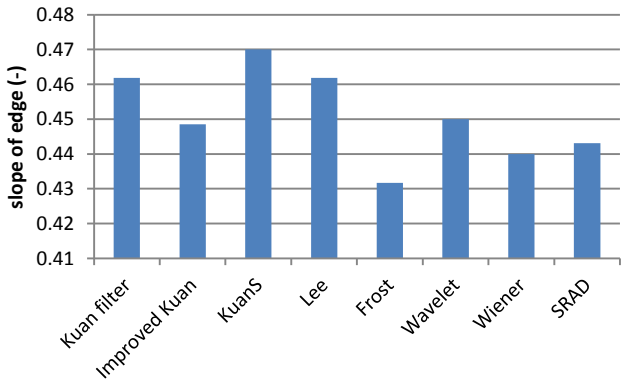


Figure 9. Slope of the edge for particular methods on real ultrasound images.

TABLE III. PARAMETERS MEASURED ON REAL ULTRASOUND IMAGES

| | Standard deviation | slope of edge |
|---|---|---|
| **Kuan filter** | 0.0987 | 0.462 |
| **Improved Kuan** | 0.0987 | 0.448 |
| **KuanS** | 0.0987 | 0.470 |
| **Lee** | 0.0987 | 0.462 |
| **Frost** | 0.1284 | 0.432 |
| **Wavelet** | 0.0990 | 0.450 |
| **Wiener** | 0.1158 | 0.440 |
| **SRAD** | 0.1183 | 0.443 |

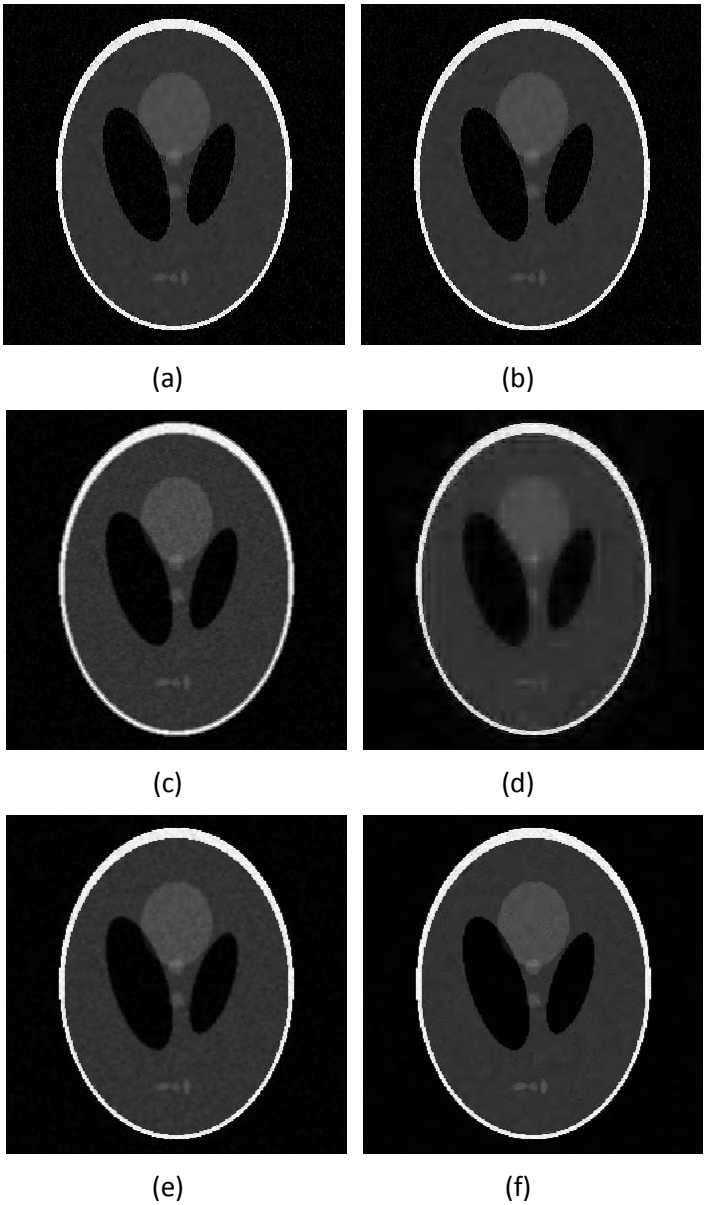


Figure 10. De-noised images after using (a) Kuan filter, (b) KuanS, (d) Frost, (e) Wiener, (f) SRAD.


## ACKNOWLEDGMENT

This work was prepared with the support of the MSMT projects No. 2B06111 and MSM 0021630513.


## REFERENCES


[1] A. Lopes, R. Touzi, and E. Nezry, "Adaptive Speckle Flters and Scene Heterogeneity," IEEE Trans. Geosci. Remote Sens., vol. 28, pp. 992–1000, 1990.

[2] T.R. Jeyalakshmi, and K. Ramar, "A Modified Method for Speckle Noise Removal in Ultrasound Medical Images", International Journal of Computer and Electrical Engineering, Vol. 2, No. 1, February, 2010.

[3] S. Zhenghao, and K.B. Fung, "A Comparison of Digital Speckle Filters," Geoscience and Remote Sensing Symposium, 1994. IGARSS '94. Surface and Atmospheric Remote Sensing: Technologies, Data Analysis and Interpretation., International , vol.4, no., pp.2129-2133 vol.4, 8-12 Aug 1994 doi: 10.1109/IGARSS.1994.399671

[4] A. Kaur, and S. Karamjeet, "Speckle Noise Reduction by Using Wavelets". NCCI 2010-National Conference on Computational Instrumentation CSIO Chandigarh, India, 19-20 March 2010.

[5] J. S. Lee, "Digital Image Enhancement and Noise Fltering by Use of Local Statistics," IEEE Trans. Pattern Anal. Mach. Intell., vol. PAMI-2,pp. 165–168, 1980.

[6] P. Coupe, P. Hellier, C. Kervrann, and C. Barillot, "Nonlocal Means-Based Speckle Filtering for Ultrasound Images," Image Processing, IEEE Transactions on , vol.18, no.10, pp.2221-2229, Oct. 2009 doi: 10.1109/TIP.2009.2024064.

[7] T. R. Crimmins, "Geometric Filter for Speckle Reduction", Applied Optics, 1985.

[8] Y. Yongjian and S. T. Acton, "Speckle Reducing Anisotropic Diffusion," Image Processing, IEEE Transactions on , vol.11, no.11, pp. 1260- 1270, Nov 2002. doi: 10.1109/TIP.2002.804276

[9] V. Frost, J. Stiles, K. Shanmugan, and J. Holtzman, "A Model for Radar Images and its Application to Adaptive Digital Fltering of Multiplicative Noise," IEEE Trans. Pattern Anal. Mach. Intell., vol. PAMI-2, pp. 157–65, 1982.

[10] D. Kuan, A. Sawchuck, T. Strand, and P. Chavel, "Adaptive Noise Smoothing Flter for Images with Signal-dependent Noise," IEEE Trans. Pattern Anal. Mach. Intell., vol. PAMI-7, no. 2, pp. 165–177, Feb. 1985.

[11] R. D. Nowak, "Wavelet-based Rician Noise Removal for Magnetic Resonance Imaging ," Image Processing, IEEE Transactions on , vol.8, no.10, pp.1408-1419, Oct 1999 doi: 10.1109/83.791966

[12] S.Sudha, G.R.Suresh and R.Sukanesh, "Speckle Noise Reduction in Ultrasound Images by Wavelet Thresholding based on Weighted Variance". International Journal of Computer Theory and Engineering, Vol. 1, No. 1, April 2009.

[13] J. Prinosil, Z. Smekal, and K. Bartusek, "Wavelet Thresholding Techniques in MRI Domain," Biosciences (BIOSCIENCESWORLD), 2010 International Conference on , vol., no., pp.58-63, 7-13 March 2010 doi: 10.1109/BioSciencesWorld.2010.143

[14] R.C. Gonzales, R.E.Woods. Digital Image Processing. Prentice Hall, Upper Saddle River, NJ, 2001.

[15] Anil K.Jain, "Fundamentals of Digital Image Processing" first edition, 1989, Prentice – Hall, Inc.

# Grammar Guided Genetic Programming for Automatic Image Filter Design

Jan Karasek, Radim Burget, Radek Benes, Lubos Nagy
Department of Telecommunications
Faculty of Electrical Engineering and Communication, Brno University of Technology
Brno, Czech Republic
karasek.jan@phd.feec.vutbr.cz; burgetrm@feec.vutbr.cz; lubos.nagy@phd.feec.vutbr.cz, radek.benes@phd.feec.vutbr.cz

*Abstract*—**This paper presents a new innovative technique for high level image filter design. At first, the evolution framework has been designed and implemented. This framework should maximize reusability and robustness of source code and performance of proposed filters. This article describes part of the framework which deals with grammar-guided genetic programming and its use case. The use case shows how it is possible to make an image filter design by automatic process of evolution. The concrete example is shown on the recognition of artery in medical screening. The main contribution of this work is not to substitute the human work, but to facilitate and improve the productivity of image filter design.**

***Keywords-Evolutin Framework; Genetic Algorithms; Genetic Programming; Context Free Grammar; Image Filter Design***

## I. INTRODUCTION

Evolutionary computing (EC) techniques are used in many commercial or scientific areas of interest. Fields of application of these techniques lie mainly in the optimization of processes, procedures or in achieving even better results for complex and computationally demanding tasks, which are hardly solvable by current algorithms or are unsolvable with them at all. The application areas where EC is applicable include computer science, mathematics, physics, medicine, engineering, construction, economics, and many others. If more specific, in commercial area, evolutionary techniques in economics are applied in production planning, travelling salesman problem solving, in engineering - circuit design, optimization of parameters of antennas, materials design and aerodynamic shape design of racing cars and other vehicles, etc. In the field of scientific practice, evolutionary techniques are used in cryptographic algorithms, design of synthetic drug molecules, materials, packet routing in the network infrastructure, etc.

During the past years many different techniques and algorithms, which have been gradually improved and supplemented by additional computing concepts and functions, appeared in this area. Although, there are many different evolutionary concepts, all these techniques share the basic idea, which is derived from the common algorithm. This idea is inspired by biological evolution. [1] In its basic principle, the idea involves several operations: the evolution of the population, potentially the best individuals, the selection of individuals chosen by selection method, and a recombination operator - the operator is simulated by crossing the genes of two individuals, also called crossover, and gene mutation in one individual is also used.

Evolutionary computing techniques are divided into several basic groups. Four basic groups can be derived from various literary sources [2]: genetic algorithms (GA) [2], genetic programming (GP) [2], evolutionary programming (EP) [2], and evolutionary strategy (ES) [2]. As mentioned before, all techniques are based on the common ground. First, the fitness function is given to be optimized. Also, a randomly generated set of candidate solutions entering the evolutionary process is given. This set is evaluated by the fitness function. The candidate solution, which is closest to the desired result, is top rated. Because of selection process, the candidate solutions which have better ranking are more likely to get into the next generation, where the candidates are reproduced by reproduction operations such as crossover and mutation. When diversification of the population is small, the rate of mutation has to grow. The process of selection, crossover and mutation is repeated in each generation of the population until the termination criterion is met. The termination criterion may be an individual's fitness value, the algorithm running time, number of generations, etc. In this article we focus just on genetic programming and its application in practice.

The rest of the paper is structured as follows. The second chapter gives an overview of articles related to the topic discussed in this article. The third chapter discusses proposal of an evolutionary framework (EF) developed at the Department of Telecommunications, Faculty of Electrical Engineering and Communication, Brno University of Technology. The fourth chapter shows a case study where the EF is utilized. The fifth chapter summarizes the existing knowledge and results achieved through the framework and further ways of EF development are outlined.

## II. RELATED WORK

In the last decade, many frameworks and libraries have been designed using a computational kernel based on evolutionary techniques. Computing frameworks have been implemented in various languages as well as various support of evolutionary techniques and different operators.

Starting by the language C where, unfortunately, object oriented concepts could not be used, the library SGA-C [3] has been implemented for experimenting with genetic algorithms and the project GENESIS [4] – which also uses only the GAs. As far as GP can be used, the lilGP system was implemented in C, based on the Lisp expressions.

The best known implementation in the C++ language is the GAlib [5] library that offers many functions related to GAs. GAlib is modular in terms of representation of chromosomes and operators and can be further enhanced thanks to well-defined interfaces. In this group we can also mention the EO library [6] and GAGS [7] which are also advanced implementations of GAs. Among the frameworks, implemented in the C++ language which also uses the technique of GP, the EO framework [6], the Open BEAGLE [8], and GAlib [3] can be included.

Perhaps, the best known systems implemented in JAVA are the ECJ [9], JGAP [10], and JCLEC [11]. The ECJ system was designed to by highly flexible, easily modifiable, and with an eye toward efficiency at George Mason University under the direction of Dr. Kenneth De Jong. The ECJ provides genetic algorithm and genetic programming with or without elitism, evolutionary strategies, very flexible architecture, many selection operators, multithreading and asynchronous island model over TCP/IP and many other functions. JGAP is a genetic algorithm and a genetic programming component provided as a JAVA framework. JGAP provides basic genetic mechanisms which can be easily applied to problem solutions. Another evolutionary computation research system is JCLEC. JCLEC provides a high-level software environment for GA, GP and EP. The architecture of JCLES is strongly based on object oriented principles. The main features of this framework are: opened source under the GPL license, elegant and robust architecture, it is a portable software, user friendly and its main contribution is generic, which allows to execute any kind of problem with minimum requirements. Evolvica [12], using the kernel eaLib implemented in the C++, which is quite extensive and quite complicated for beginners in the field of evolutionary computing, has been implemented as the JAVA programming framework .

There are a lot of frameworks and libraries implemented in other languages, such as .NET (JGAP ported to .NET for example), MATLAB (GPLAB and GPTIPS toolboxes), and even in languages such as Ruby, Perl, and Python.

In the paper [13], there are many of these frameworks compared with the result that none of them does not set a general view of evolutionary computation, but most of them specialize in only one of the evolutionary techniques and only provide support for normal operators, such as selection, crossover, and mutation. Thus, if a framework meets at least half of the demands imposed on it in terms of evolutionary computing techniques, it is often implemented in an appropriate language for our purposes or released under a license that would not be usable for both scientific and commercial applications. It was decided to implement own framework for these reasons, which would be used in all our future projects.

## III. EVOLUTION FRAMEWORK

It is not easy to make a robust and flexible design to meet all the demands of the group of evolutionary computation, since it is possible to look at this issue from several perspectives. An important building block is to propose the representation of candidate solutions, evolutionary operations, such as recombination (crossover), mutation, selection and other operators that can take many forms and must meet various criteria and comply with restrictive conditions, as for example when crossover and mutation are used in the grammar-guided computational techniques. Some operations, such as selection, can be designed globally for all evolutionary techniques, while others, such as recombination and mutation operators must be specialized specifically for one kind of evolutionary technique.

The first development phase of the framework was to implement two evolutionary techniques, namely genetic algorithms and genetic programming with the tree represented chromosome, controlled by a context-free grammar. The framework has been designed so that it can be extended easily in future with other elements, such as the representation of genetic algorithms chromosome and genetic programming chromosome, with implementation of Cartesian and linear chromosome, with the possibility of using other evolutionary operators, automatically defined functions and various retrieval algorithms.

### *A. Tree Based Genetic Programming*

Genetic programming [14] is a domain-independent problem-solving approach in which computer programs are evolved to solve, or approximately solve, problems. GP is an extension of GA. The main difference between them is the representation of the structure they manipulate and the meanings of the representation. GAs usually operates on a population of fixed-length binary strings. GP typically operates on a population of parse trees which usually represent computer programs [15]. In applying genetic programming to a specific problem, there are five major preparatory steps. These five steps involve determining [1]:

- the set of terminals - such as numbers, constants, samples of voice or image etc.
- the set of primitive functions (non-terminals) – arithmetic and logic functions etc.
- the fitness measure
- the parameters for controlling the run
- the method for designating a result and the criterion for terminating a run

The primary genetic operators which are used in proposed EF are crossover and mutation. In principle, the crossover operation is used to create new offspring from two parents selected based on the fitness. The crossover is based on selecting a crossover point in both parents and swapping the sub-trees. The mutation operation is an asexual operator; it means that it operates only with one parent. The mutation point is randomly selected and the sub-tree is replaced by

a completely newly generated sub-tree. These techniques are the basic approaches and many variants of these operators exist in practice.

### *B. Grammar-Guided Genetic Programming*

The grammar-guided genetic programming (GGGP) is an extension of traditional GP systems. The GGGP goals are to provide knowledge about the problem to be solved to simplify the search space and to solve the closure problem and to always facilitate generating of valid individuals. This extension of genetic programming concerns the crossover operation, the mutation and also the initialization method, which has to be adapted. The evolution framework uses the grammar-based crossover (GBX) and the grammar-based mutation (GBM) based on the research in [16] [17].

A context-free grammar G is defined as 4-tuple G = (T, F, S, P), where T is the set of terminals, F is the set of non-terminal symbols (functions) and $T \cap F = 0$, S is the start symbol and P represents the set of production rules, written in BNF (Backus-Naur Form). Based on the grammar defined in [16] and [17], the individuals are defined as derivation trees with the root S, the internal nodes from the set F and the external nodes (leaves) from the set T.

### *C. Design of Evolution Framework*

This part of the paper presents a designed structure of evolution framework. The framework design is introduced in the way how the framework can be used in a practical application and the demonstration of the proposal is accompanied with class diagrams.

The first step to be done when it is intended to use the GGGP is to define terminal and non-terminal symbols and the rules for grammar. This part of framework is depicted in Fig. 1. The Class Grammar defines the grammar for genetic programming. The grammar describes structures of programs. For example, the grammar defines that the only follower of the non-terminal ROOT can be non-terminal E (expression) and the possible non-terminal followers of E can be "E+E", "E-E" or just terminal "T". The grammar class includes rules and input parameters. The class Action resp. ActionTree defines an action which can be performed on a tree node in a chromosome. The proper implementations are inherited from ActionTree and extended with new methods, similarly to the attributes and methods inherited for nodes that represent terminal nodes, such as DoubleTerminal, IntegerTerminal, DoubleTerminalConstant, and IntegerTerminalConstant. The Rule class represents rules contained in the grammar.

The second step of genetic program design is to define a configuration of whole program which means, crossover and mutation rate, max depth for tree, population size and number of evolutions, which is an end criterion in this case. The Config class serves for the manipulation with configuration parameters.

The third step is to define the fitness function and to create a new instance of DefaultEvolutionSpecifier. The interface IFitnessEvaluator orders how to design a fitness function. The interface IEvolutionSpecifier defines the way how the population is being processed (i.e. how the crossover, mutation and clone operators are used) in single evolution. The class EvolutionSpecifierAdapter performs a sequence of reproductions, crossovers, mutations and selection operations. The class DefaultEvolutionSpecifier defines the way how the population is processed in each evolution. This is the key class which contains information on a defined grammar, configuration and fitness function. Fig. 2 also shows the class DefaultEvolutionSpecifierTreeGP which demonstrates how the type of genetic programming can be implemented.

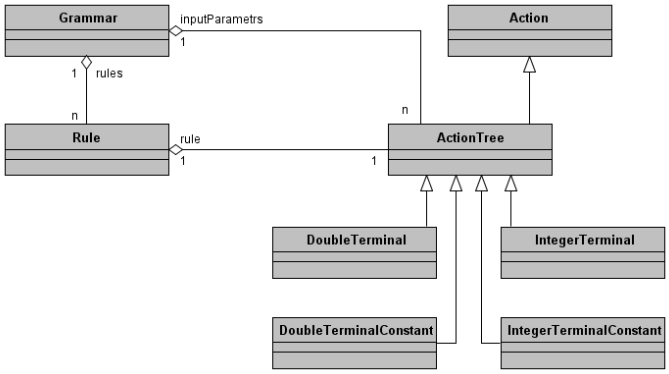


Figure 1. Class diagram of grammar part

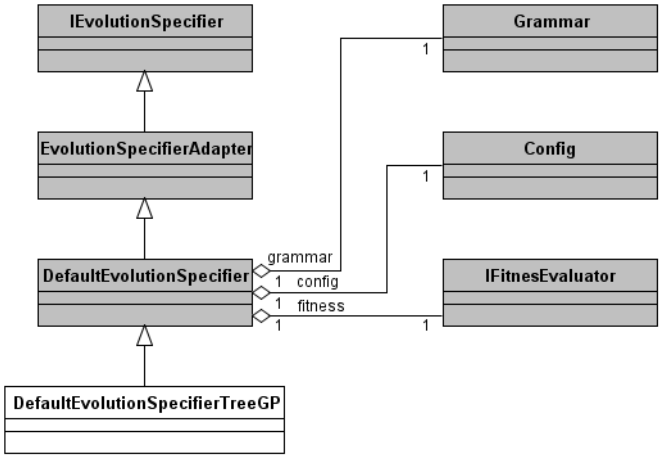


Figure 2. Class diagram of evolution specifier and fitness part

The fourth and last step is to create a new instance of genetic program and run the evolution process. Fig. 3 presents a class diagram where the basic classes of evolution framework are depicted. The class Program is the core of evolutionary framework which evolves population. The overall insight in the structure of genetic program is depicted in the figure below. The program takes as an input configuration the file specifying the information on population (i.e. population size, number of evolutions, mutation and crossover rates etc.) – class Config. At the start of an evolution the population (class Population) is initialized with a required number of chromosomes. These chromosomes (class Chromosome and concrete inherited class TreeChromosome) are represented as a tree of nodes in this

example (class Node). All the chromosomes are initialized randomly with a maximum height in configuration. The evolution specifier defines the way how the chromosomes are mutated and crossovered. The IFitnessEvaluator stands for a class for evaluation of chromosome fitness.

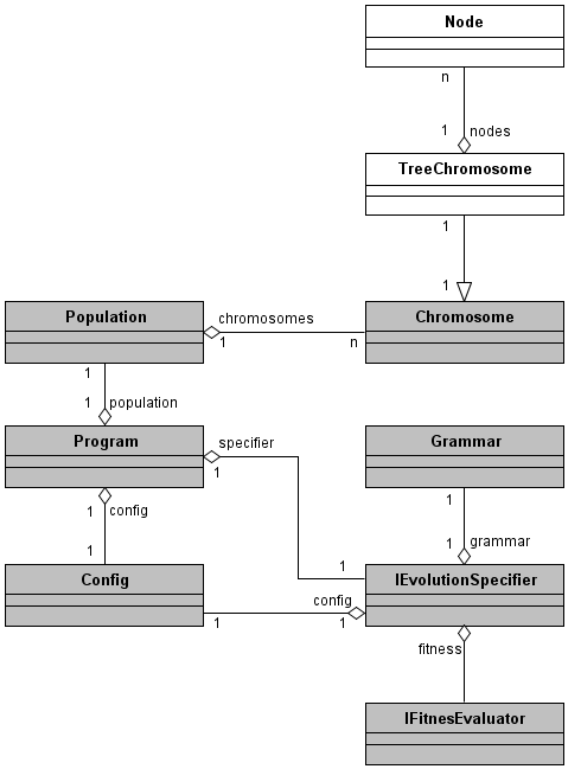


Figure 3. Class diagram of evolution framework, and the part of grammar guided genetic programming

## IV. USE CASE – IMAGE FILTER DESIGN

In this chapter image filter design utilizing evolution framework will be described as a use case example. Image filter design is a time-consuming process and can easily get stuck in a suboptimal solution when it is designed by the human programmer. The aim of this example is to facilitate and improve the productivity of image filter design in many scientific and engineering applications.

E.g. object recognition is a very complex process and has to be extremely accurate. The quality of recognition depends on the quality of image and design of the algorithm. In this point we are building on experiences gained in research [18]. Almost all image filters are designed by conventional ways. The most common approach for a new image filter design is a static design by a human programmer. The problem of such approach is that the process is very time-consuming and is quite easy get stuck in a suboptimal solution.

The main contribution of this example is to propose an innovative approach to the image filter design using evolutionary techniques and to show its use. The following text presents an illustrative example and its results achieved by the proposed evolution method – GGGP. In this example, the filter for artery recognition from the medical screening has been designed. Robustness design of the resulting filter is dependent on the number of plug-ins. In this project, a limited set of plug-ins is used, nevertheless it is possible to trace the good functionality of the proposed program. Defined grammar in this use case example:

T = (Image, Integer)

F = (Hough Transform, Erode, Dilate, Open, Close, Threshold, Entropy Treshold, Histogram Equalization, Watershed, Hessian, Blur, Logarithm, Sobel, Laplace)

S = Root

P = { Root ::= HoughTransformation,

HoughTransformation ::= Erode Integer Integer Integer | Dilate Integer Integer Integer | Open Integer Integer Integer | Close Integer Integer Integer,

Open | Close | Erode | Dilate ::= Treshold | EntropyTreshold

Treshold | EntropyTreshold ::= Sobel | Laplace | HistogramEqual. | Watershed,

HistogramEqual. ::= Hessian,

Sobel | Laplace | Hessian | Watershed ::= Blur | Logarithm,

Blur ::= Logarithm Integer | Image Integer,

Logarithm ::= Image }

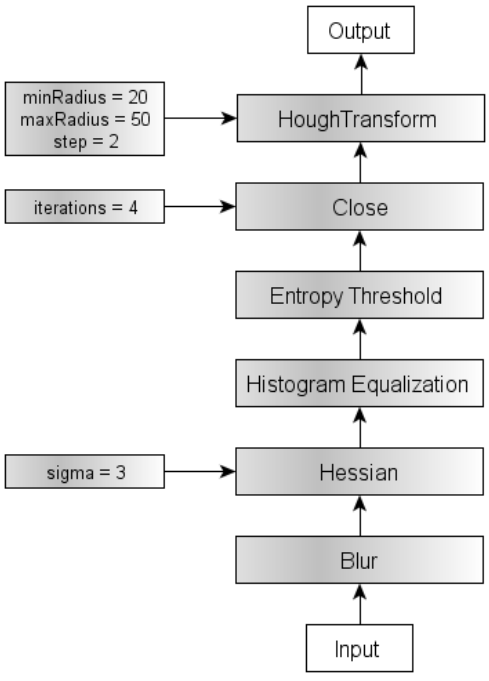


Figure 4. Proposed image filter designated by evolution framework with grammar-guided genetic programming

Fig. 4 shows the filter proposed by evolution framework. Fig. 5a-5f shows outputs of the individual filters in the generated filter. The filter was designed in 40 evolutions with initialization population which contained 100 chromosomes, with crossover rate 80% and mutation rate 30%. The total time of the final filter design was 12h 11m. The detection of artery by an individual chromosome (filter) takes from 1.2s to 1.8s in individual images.

The fitness function was designed for the evaluation of individual chromosomes based on calculation of the accuracy of detection of centres in all the arteries from the image training set containing 9 frames. The resulting filter was tested on a set of test images, comprising 147 images. The success of the artery detection on images of the testing set was approximately 75%. The success at this stage of development is very good and it may be even higher in the future, when additional plug-ins will be implemented.

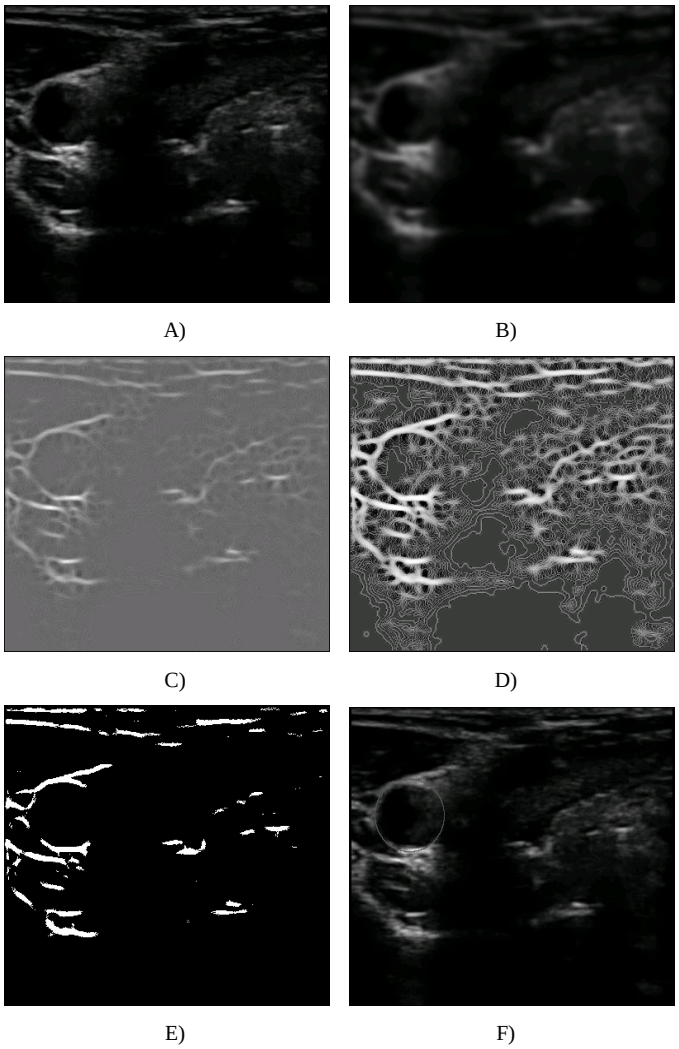


Figure 5. Output of the individual filters in the generated filter a) input image, c) output of Gaus-sian smooth, d) output of Hessian, e) output of histogram equalization, f) output of thre-shold, g) final output - recognized artery.

As we can see the image under consideration is given to the entry of Gaussian blur. This filter is one of the linear smoothing filters and its main task is to reduce noise. Blur must not be chosen too large to prevent the filter to remove some important properties of the picture. The blurred image then enters the block which analyzes the degree of curvature in the image using the Hessian. The operator indicates with a light color the areas where a certain curvature is apparent. This can be used with advantage to find circular shapes as required by assignment. The proposed filter then performs histogram equalization which enhances the image contrast. This is followed by binary thresholding. Specifically, thresholding based on entropy is used. [19] The accepted method comes out of the assumption that the input image is generated from two signals: the foreground and background signal. An ideal thresholding occurs at the moment when the sum of entropies of the two signals reaches the maximum. Based on this premise, a formula is established to determine the ideal threshold, which is then used for binary thresholding. Over the binary images, the morphological operations of erosion and dilation, constituting together the operation Close, were performed. They ensure improving of images for further processing.

The last step, strictly prescribed by grammar, is Hough transformation. Besides the input image, other parameters enter the plug-in: the minimum and maximum size of the circle and the step to analyze this range. The method will search the specified number of best-rated circuits and will return their parameters. The principle of Hough transformation lies in the transformation of the original image into a new multi-dimensional space. The maximum, which coordinates correspond to the parameters of sought element, is localized in the new space. There are modifications to find lines, circles, as well as methods for other shapes. The proposed structure of the resulting plug-in achieves the best fitness function across a training set and gains a certain optimality of found solution. The resulting filter can then be applied to many other similar images.

## V. CONCLUSION

The proposed framework is implemented in the JAVA programming language with a view to design patterns and object oriented programming concepts. The main contribution of this framework is that it can be used in scientific and commercial areas without restrictions. The framework is designed as a modular, robust and flexible system, so other functions and techniques can be added later. Its main advantage is the use of grammar, because the state space to be searched is simplified. In the future we plan to extend this framework in other areas of evolutionary computing. At the first step the Cartesian chromosome will be implemented and tested and genetic algorithms will be completed. The release of this evolution framework is planned to take place in one year after proper testing. As a use case the new approach to image processing filter design was proposed, implemented and basically evaluated. It is clear that the evolution cannot substitute the human in the process of a new image filter design; however it can definitely significantly facilitate and improve the productivity of human work.

## ACKNOWLEDGMENT

This work was supported within the framework of the research plan MSM 0021630513 and by the internal grant of the Faculty of Electrical Engineering and Communication, Brno University of Technology, registration number FEKT-S-10-16.

The access to the MetaCentrum supercomputing facilities provided under the research intent MSM6383917201 is appreciated.

## REFERENCES

[1] J. R. Koza, "Survey of genetic algorithms and genetic programming," WESCON Conference, IEEE, pp. 589 – 594, 1995.

[2] W. B. Langdon, R. Poli, N. F. McPhee, and J. R. Koza, "Genetic Programming: An Introduction and Tutorial, with a Survey of techniques and Applicatons," Springer-Verlang Berlin Heidelberg, vol. 115, pp. 927–1028, 2008.

[3] R. Smith, D. Goldberg, and J. Earickson, "Sga-c: A c-language implementation of a simple genetic algorithm," 1994.

[4] J. J. Grefenstette, "Genesis: A system for using genetic search procedures," In Proceedings of a Conference on Intelligent Systems and Machines, pp. 161–165, 1984.

[5] M. Wall, "Galib: A C++ library of genetic algorithm components," Technical report, Massachusetts Institute of Technology, Mechanical Engineering Department, April 1996.

[6] J. J. Merelo, "Eo evolutionary computation framework," http://eodev.sourceforge.net/.

[7] J. J. Merelo, and A. Prieto, "Gags, a flexible object-oriented library for evolutionary computation," In P. Isasi D. Borrajo, editor, MALFO96, Procs. of the First International Workshop on Machine Learning, Forecasting and Optimization, pp. 99–105, 1996.

[8] C. Gagné, and M. Parizeau, "Open BEAGLE: A New Versatile C++ Framework for Evolutionary Computations," GECCO 2002, pp. 161–168, 2002.

[9] S. Luke, L. Panait, G. Balan, S. Paus, Z. Skolicki, J. Bassett, and R. Hubley, "ECJ: a Java based evolutionary computation research system," Chircop A, 2006.

[10] JGAP home page, Java Genetic Algorithms Package. http://jgap.sourceforge.net/, 2010.

[11] S. Ventura, C. Romero, A. Zafra, J. A. Delgado, and C. Hervás, "JCLEC: a Java framework for evolutionary computation," Springer-Verlang, vol. 12, pp. 381–392, 2007.

[12] Evolvica – Evolutionary Algorithms Framework in Java. Technical report, Technical University Ilmenau, Germany. http://www.evolvica.org/.

[13] R. Ványi, "Object Oriented Design and Implementation of a General Evolutionary Algorithm," Springer-Verlang Berlin Haidelberg, GECCO 2004, LNCS 3103, pp. 1275–1286, 2004.

[14] J. R. Koza, "Genetic Programming II: Automatic Discovery of Reusable Programs," Cambridge, Massachusetts: MIT Press, p. 768, 1994.

[15] J. R. Koza, D. Andre, F. Bennett, and M. Keane, "Genetic Programming 3: Darwinian Invention and Problem Solving," Morgan Kaufman, p. 1154, 1999.

[16] M. García-Arnau, D. Manrique, J. Ríos, A. Rodríguez-Patón, "Initialization method for grammar-guided genetic programming," ScienceDirect, vol. 20, pp. 127–133, 2007.

[17] J. Couchet, D. Manrique, J. Ríos, A. Rodríguez-Patón, "Crossover and mutation operators for grammar-guided genetic programming," Springer, vol. 11, pp. 943–955, 2006.

[18] R. Burget, J. Karásek, Z. Smékal, V. Uher, and O. Dostál, "RapidMiner Image Processing Extension: A Platform for Collaborative Research," International Conference on Telecommunications and signal processing, Baden Austria, 2010.

[19] P. K. Sahoo, S. Soltani, A. K. C. Wang, and Y. C. A. Chen, "Survey of The Thre-sholding Techniques," Computing Vision Graphics Image Process, pp. 233–260, 1988.

# Algorithm Calculating the Ratio of Cerebrospinal Fluid to the Skull

Radka Pustkova, Frantisek Kutalek, Marek Penhaker, Jindrich Cernohorsky
Department of Measurement and Control, Faculty of Electrical Engineering and Computer Science, VSB–Technical University of Ostrava, FEI, 17. listopadu 15, 708 33, Ostrava-Poruba
Ostrava, Czech Republic
radka.pustkova@vsb.cz, frantisek.kutalek@vsb.cz, marek.penhakersb.cz, jindrich cernohorsky@vsb.cz

Vilem Novak
Children's Neurology Clinic
Faculty Hospital Ostrava
Ostrava, Czech Republic
vilem.novak@fnspo.cz

***Abstract*— The results presented in this article introduce the possibility of software processing by image data from CT and MRI in clinical practice. It is important to work with the most accurate data in the diagnosis and further monitoring of the patient. Especially in the case of birth defects or post-traumatic conditions of head called Hydrocephalus, it is necessary to work with this data. A production increase of the cerebrospinal fluid, called cerebrospinal fluid (CSF), causes bring intracranial pressure up. The oppression of the brain tissue has resulted of this. The determination of CSF ratio to the skull in medical practice is used to improve diagnosis and monitoring before and after surgery in patients with Hydrocephalus diagnosed. The evaluation is done by individual doctor experience. The proposed method brings a new opportunity to more accurate evaluation of medical data in this area. Software was implemented in Matlab2006b using Image processing Toolbox. Input data format is JPEG images.**

***Keywords- CT; MRI; Liquor; Skull; Image Processing; Hydrocephalus; MATLAB***

## I. INTRODUCTION

The diagnosis and further monitoring of a patient, it is necessary to analyze continuously the available data. Especially in congenital defects and traumatic conditions head, due to the overproduction of cerebrospinal fluid increases intracranial pressure, and thus repression of brain tissue.

The results presented in this article provide a means of software processing data from CT and MRI in clinical practice. The main goal is to determine the ratio of CSF to intracranial volume, which is vital for determining the progression of therapy.

## II. METHODS

To calculate used by the single-frame semi-automatic selection masks. Input data are in JPEG format of 512 x 512 PX. JPEG format is sufficient for this application.From the images there are also obtained data as the number of frames in the series, the distance between cuts, the number of PX per mm and the calculated conversion factor. These data are important for further processing. In the block diagram are represented by data.

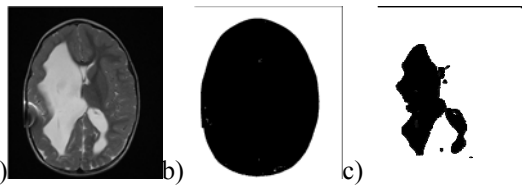


Figure 1. a) Original MRI image, b) mask oft the skull and c) mask of the liquor.

Some tissues share the same luminance value even though not in the selected choice, must be removed from the image. Conversely, some tissues, especially the cranial bones in pediatric patients were not due to lack of calcification and displays must be manually added. Individual functions and methods for proper selection of masks were processed in MATLAB. In the scheme of this procedure constitutes a block correction. The output is a series of mask data for cerebrospinal fluid and skull mask. Method of processing input images is shown in Figure.2).

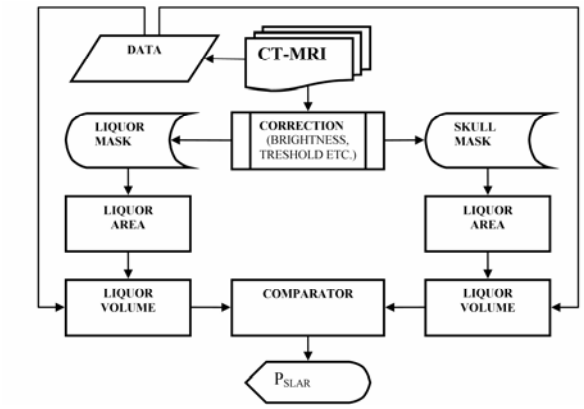


Figure 2. Calculating scheme of the ratio of CSF to the skull.

Input data were first regulated in the block luminance brightness. The removing noise from the input data is in charge of block noise correction. There was also needed manual correction perform. Now the data are ready for segmentation of objects in the picture and create and save the masks.

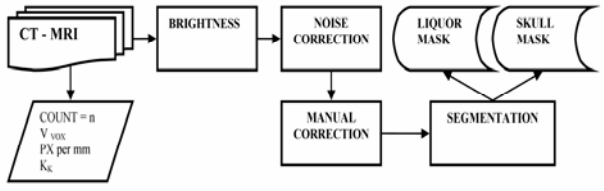


Figure 3. Diagram shows the individual mask preparation.

The blocks liquor area and skull area are sorted data from cerebrospinal fluid and skull masks. Content area masks $S_L$, calculated for the area of cerebrospinal fluid in one section, are determined by the number of black points in the mask. Entered by equation (1):

$$S_L = \sum_{i=0}^{i}\sum_{j=0}^{j} x_{i,jPRK} + \sum_{i=0}^{i}\sum_{j=0}^{j} x_{i,jNPRK} \qquad (1)$$

The area is represented by a point in the masks of images. These points are overlap each other, when comparing the two images, marked $x_{i,jPRK}$ for points respectively $S_{PRK}$ for the area, or not overlap, marked $x_{i,jNPRK}$ respective $S_{N\,PRK}$. This information is important for the calculation rounded. The scheme Figure.3) shows the function block Liquor area. Ranking data for talc CSF, as is the scheme for overlapping and overlapping area is responsible for block comp. The procedure is applied to all data in the series. Then performed to calculate the volume represented by block Liquor volume.

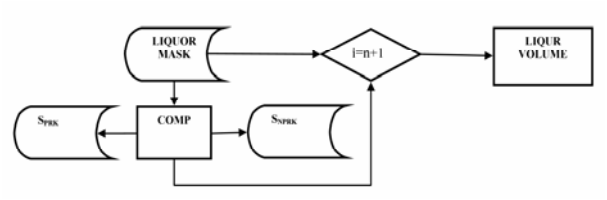


Figure 4. Function of liquor area diagram block.

To calculate the volume it is needed to know the distance $v_{vox}$ of individual cuts. It was found analysis of input data. The resulting volume $V_L$, calculated for the volume of CSF is the sum of the volumes. Shows equation (2):

$$V_L = \sum_{n=1}^{n}\left(S_{LNPRK}\cdot K_k + S_{LPRK}\right)\cdot v_{vox} \qquad (2)$$

The calculation should be calculated separately with data for the overlapping area and not overlapping areas. The not overlapping area is included in the calculation of the conversion factor $K_k$, which aims to refine the calculation of the radius edges. The principle of calculating the volume of liquor is shown in Figure.4).

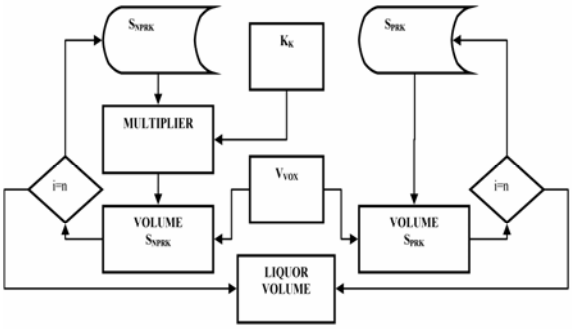


Figure 5. Diagram shows the principle of the computation of the cerebrospinal fluid volume.

The input data include information on the overlapping and not overlapping areas of two compared images. In case of no overlapping image is required overlapping area multiplied by the conversion factor. When using the conversion factor is the final volume of distorted error 6.86%. Provides block multiplier. Using aliasing filters can then move the value of distortion $\Delta V_L = 0{,}62 \pm 0{,}36\%$.

Multiply distance of each area $v_{vox}$ is the task blocks volume $S_{PRK}$ and volume $S_{N\,PRK}$. All data in the series applied. The function liquor volume block is findings the final volume of liquor. The same procedure is applied to the skull mask.

Data are ready to compare the different volumes. Compare two volumes between as is an Comparator block, see.

Figure.1), tasks. Determination of the ratio of CSF to the skull $P_{SLar}$ is the most important output of the software since it indicates the current status of the patient. Entered by equation (3):

$$P_{SLar} = \left( \frac{V_L}{V_S} \right) \cdot 100\% \quad (3)$$

Where $V_S$ is the volume of the skull. The $V_L$ is the cerebrospinal fluid volume.The resulting ratio is automatically calculated by the program.

## III. RESULTS PRESENTATION

Presented solution was tested on a set of patient images of children with congenital hydrocephalus, a total of ten.

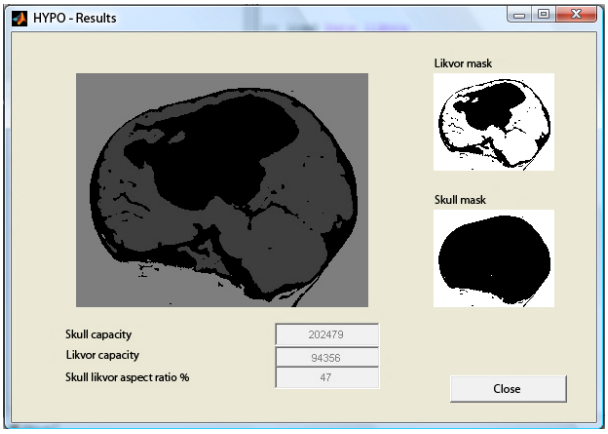


Figure 6. Display ratio of CSF to mask skull cut before surgery.

A data of patients were tested before and after surgery at intervals of several years with respect to increasing the volume of the skull in pediatric patients due to natural growth. The tested data showed change in the volume of cerebrospinal fluid before and after therapy. From the records that were taken at intervals of four years after the operation shows that the volume before $9{,}3cm^3$ and after $8{,}4cm^3$ surgery reduced the overall CSF volume by 10%. This in the case of subjective assessment of the doctor could not be determined. In all cases the proposed algorithm successfully used and tested.

To solve this problem there was designed and implemented software, to semi automatic selection of images extracted from the processed desired area. Software was developed in Matlab2006b using Image Processing Toolbox, and uses knowledge in the field of image processing. The open design allows the software solutions developed.

Ratio determination of cerebrospinal fluid in the skull determined by the doctor based on subjective impression. The method used software processing more accurate.

TABLE I. REAL DATA OF KIND PATIENT WITH HYDROCEPHALUS USED BY THE SAME AREA BEFORE AND AFTER SURGERY. THIS DATA ARE BEFORE CALCULATING.

| cut | 2004 before surgery | | 2008 after surgery | |
|---|---|---|---|---|
| | *Liquor (PX)* | *Skull (PX)* | *Liquor (PX)* | *Skull (PX)* |
| 1 | 374341 | 2832128 | 345482 | 2596897 |
| 2 | 461426 | 2821788 | 436422 | 2542564 |
| 3 | 668928 | 2814429 | 517746 | 2524663 |
| 4 | 713404 | 2774935 | 672970 | 2450053 |
| 5 | 757437 | 2666283 | 633301 | 2411929 |
| 6 | 647723 | 2598683 | 636403 | 2401602 |
| 7 | 593565 | 2479986 | 620638 | 2343522 |
| 8 | 587979 | 2335049 | 562504 | 2256987 |
| 9 | 578149 | 2136652 | 541435 | 2210403 |
| 10 | 535405 | 2832128 | 532907 | 2035211 |
| 11 | 484295 | 1901501 | 473203 | 1830127 |
| 12 | 374341 | 1677214 | 383150 | 1570817 |
| 13 | 272873 | 1394122 | 169350 | 1312851 |

The results indicate that decreased CSF and at the same time to decreased the patient's.

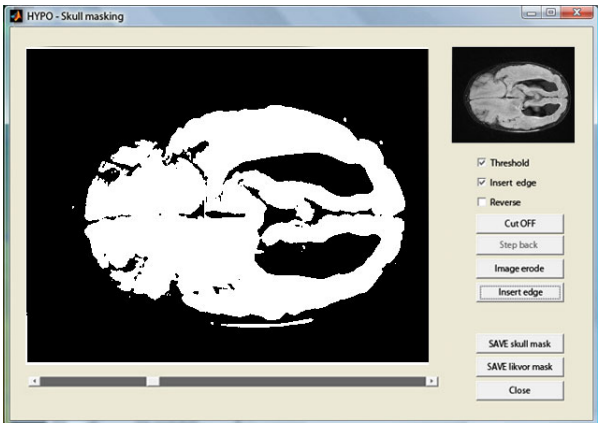


Figure 7. Picture of the preparation of skull mask using liquor mask as input.

## IV. CONCLUSION

It is a completely new method of calculating the volume of cerebrospinal fluid in the skull of the patients that is being developed. Using the analogy to a sphere to achieve are better results than comparing individual images. It is better than without taking into account a rounding. Data processing is more automated, which eliminates error introduced by the user.

The results helped to make explicit decisions on the progression of treatment and the therapeutic techniques that were previously difficult objective.Further improvements algorithms will eliminate errors in the semi automatic selection of masks, which currently can be up to 10%. Applications will aliasing filters, more precise calculation and reduce distortion.


## ACKNOWLEDGMENT

The work and the contribution were supported by the project Grant Agency of Czech Republic – GACR 102/08/1429 “Safety and security of networked embedded system applications”. Also supported by the Ministry of Education of

the Czech Republic under Project 1M0567. Students Grant Agency SGS SV450021" Biomedical Engineering Systems VI"

## REFERENCES


[1] Krejcar, O., Janckulik, D., Motalova, L., Complex Biomedical System with Biotelemetric Monitoring of Life Functions. In Proceedings of the IEEE Eurocon 2009, May 18-23, 2009, St. Petersburg, Russia. pp. 138-141. ISBN 978-1-4244-3861-7, DOI 10.1109/EURCON.2009.5167618

[2] Idzkowski A., Walendziuk W. (2009) Evaluation of the static posturograph platform accuracy, Journal of Vibroengineering, Volume 11, Issue 3, 2009, pp.511-516, ISSN 1392 - 8716

[1] Vasickova, Z., Augustynek, M., New method for detection of epileptic seizure, Journal of Vibroengineering, Volume 11, Issue 2, 2009, pp.279-282, (2009) ISSN 1392 - 8716

[3] Cerny, M.: Movement Monitoring in the HomeCare System . In IFMBE proceddings. Ed. Dossel-Schleger, Berlin:Springer, 2009, issue. 25, ISBN 978-3-642-03897-6; ISSN 1680-07

[4] Gono R., Kratky M., Rusek S., Analysis of Distribution Network Failure Databases, PRZEGLAD ELEKTROTECHNICZNY, Vol. 86, Issue 8, pp. 168-171, 2010 ISSN: 0033-2097

[5] Bernabucci, I., Conforto, S., Schmid, M., D'Alessio, T. A bio-inspired controller of an upper arm model in a perturbed environment, In proceedings The 2007 International Conference on Intelligent Sensors, Sensor Networks and Information Processing Pages: 549-553 ISBN: 978-1-4244-1501-4

[6] Cerny, M. Movement Activity Monitoringof Elederly People – Application in Remote Home Care Systems In Proceedings of 2010 Second International Conference on Computer Engineering and Applications ICCEA 2010, 19. – 21. March 2010, Bali Island, Indonesia, Volume 2NJ. IEEE Conference Publishing Services, 2010 p. ISBN 978-0-7695-3982-9

[7] Izakian, H., Abraham, A., Snasel, V., Metaheuristic Based Scheduling Meta-Tasks in Distributed Heterogeneous Computing Systems In Journal SENSORS Volume: 9 Issue: 7 Pages: 5339-5350 , Juyl 2009, ISSN: 1424-8220, DOI: 10.3390/s90705339

[8] Majernik,J., Molcan,M., Majernikova, Z.: Evaluation of posture stability in patients with vestibular diseases, SAMI 2010, 8th IEEE International Symposium on Applied Machine Intelligence and Informatics, Óbuda University, Budapest, Hungary, 2010, ISBN 978-1-4244-6423-4, pp. 271-274.

[9] Simsik,D., Galajdova,A., Majernik,J., Busa,J., Zelinsky,P.: Grundtvig training on technical advisory in assistive technology. Lekar a technika. Czech Republic,Volume 35, 2004, ISSN 0301-5491, pp. 111 - 113.

[10] Majerník, J., Svida, M., Majerníkova, Z.: Medicínska informatika. 1. vydanie, Univerzita Pavla Jozefa Šafárika v Košiciach, Košice, 2010, Equilibria, s.r.o., ISBN 978–80–7097–811–5, 200 s.

[11] Zivcak, J., Kneppo, P., Hudak, R., Methodics of IR imaging in SCI individuals rehabilitation In Book 27th Annual International Conference of the IEEE Engineering in Medicine and Biology Society, Vols 1- p.: 6863-6866, 2005 ISSN: 1094-687X, ISBN: 0-7803-8740-6

[12] Skapa, J. Vasinek, V., Siska, P. Analysis of Optical-Power Redistribution for Hybrid Optical Fibers In Book Fiber Optic Sensors and Applications Volume 6770, 2007 ISSN: 0277-786X, ISBN: 978-0-8194-6930-4, DOI: 10.1117/12.752587

[13] Skapa, J., Siska, P., Vasinek, V., Vanda, J. Identification of external quantities using redistribution of optical power - art. no. 70031R In Book OPTICAL SENSORS 2008 Volume 7003, p. R31-R31, 2008,ISSN: 0277-786X , ISBN: 978-0-8194-7201-4

[14] Palan, B., Roubik, K., Husak, M., Courtois, B. CMOS ISFET-based structures for biomedical applications In Proceedings Medicine & Biology at 1st Annual International IEEE-Embs Special Topic Conference on Microtechnologies, Pages: 502-506 Published: 2000, ISBN: 0-7803-6603-4

[15] Rozanek, M., Roubik, K., Influence of the changes in pulmonary mechanics upon the suitability of artificial lung ventilation strategy In Proceedings of the Second IASTED International Conference on Biomedical Engineering, p. 474-477, 2004 , ISBN: 0-88986-408-X

[16] Hozman, J., Zanchi, V., Cerny, R., Marsalek, P., Szabo, Z. Precise Advanced Head Posture Measurement In Book Challenges in Remote Sensing - Proceedings of the 3rd Wseas International Conference on Remote Sensing (REMOTE '07) p. 18-26, 2007, ISSN: 1790-5117, ISBN: 978-960-6766-17-6

[17] Kasik, V., "FPGA based security system with remote control functions", In 5th IFAC Workshop on Programmable Devices and Systems, Nov 22-23, pp. 277-280, Gliwice, Poland (2001)

[18] Kašík, V.: The Framework for Parallel Computing Systems Design. In conference proceedings PDS2004, Gliwice, Poland. IFAC WS 2004 0008 PL, 2004, p. 238-240, IFAC, ISBN 83-908409-8-7

[19] Kasik, V.: Implementing of fast graphic functions in FPGA programmable logic. In PDES 2009, IFAC Workshop on Programmable Devices and Embedded Systems, pp.63-66, Roznov pod Radhostem, Czech Republic, (2009)

[20] Garani, G., Adam, G. K. Qualitative modelling of manufacturing machinery In Book - 32nd Annual Conference on IEEE Industrial Electronics, IECON 2006 VOLS 1-11 p. 1059-1064, 2006 , ISSN: 1553-572X, ISBN: 978-1-4244-0135-2

[21] Adam, K. A., Garani, G., Samaras, N., Srovnal, V. Koziorek, J. Kasik, V., Kotzian, J. Design and Development of Embedded Control System for a Lime Delivery Machina In Proceedings of the 10th Wseas International Conference Mathermatical Methods and Computational Techniques MMACTEE' 08: p. 186-19,2008, ISBN: 978-960-6766-60-2

[22] Voznak, M. Rezac, F., Halas, M., Recent Advances In Networking, Vlsi And Signal Processing In Book Mathematics and Computers in Science and Engineering p. 49-53, 2010, ISBN: 978-960-474-162-5

# Face recognition on ORL and YELL database using PCA method

Dominik Jelšovka, Róbert Hudec
Department of Telecommunications and Multimedia
University of Zilina
Zilina, Slovakia
jelsovka@fel.uniza.sk, hudec@fel.uniza.sk

*Abstract*— **This paper provides an example of the face recognition method using PCA. Principle component analysis (PCA) is a multivariate technique that analyzes a face data in which observation are described by several inter-correlated dependent variables. The goal is to extract the important information from the face data, to represent it as a set of new orthogonal variables called principal components. The paper presents a proposed methodology for face recognition based on information theory approach of coding and decoding the face image. The algorithm has been tested on 200 images (20 subjects). A recognition score for test lot is calculated by considering almost all the variants of feature extraction. The proposed methods were tested on Olivetti and Oracle Research Laboratory (ORL) face database and own YELL database. Test results gave a recognition rate of about 95% for ORL database and 99, 75% for our YELL database.**

***Keywords-Face recognition; PCA-principal component analysis; ORL database;YELL database;***

## I. INTRODUCTION

Face recognition has been studied extensively for more than 20 years. Since the beginning of 90's the subject has became a major issue; mainly due to its important real-world applications in areas like video surveillance, smart cards, database security, internet and intranet access [1]. The face is the primary focus of attention in the society, playing a major role in conveying identity and emotion. Human face recognition plays a significant role in security applications for access control, real time video surveillance systems, and robotics. Today, there are many unimodal biometric personal identification systems, e.g., fingerprint, palm print, retinal, iris, face, voice, ear, signature, DNA, as well as multi modal biometric based on hybrid unimodal ones. The most imperative sub-topics in the domain of face research is face recognition [1], [2]. Face recognition is a technology which recognize the human by his/her face image. The problem of automatic human face recognition can be stated as follows: given an image of a human face (test set), compare it with pre-stored models of a set of face images labeled with the person's identity (the training set), and report the matching result [1]. Face recognition can be divided into two core approaches namely, content-based and appearance based [1]. Content-based recognition is based on the relationship between facial features like eyes, mouth & nose etc. In appearance based recognition the face is treated as a two dimensional pattern of intensity variation. The face matching is done through its underlying statistical regularities. The problem of human face recognition is a complex and highly challenging one having a variety of parameters including illumination, pose orientation, expression, aging, head size, image obscuring (eye glass effect), disguise, and face background [2, 3, 4]. This paper employed a new feature projection approach based on PCA method, doing the optimum transformation for the differences between the classes. Section 2 presents related work. The Proposed methodology is discussed in section 3 and experimental results are listed in section 4. Finally, sections 5 conclude and suggest the future scope.

## II. RELATED WORK

Basically, there are two approaches in face recognition, appearance-based (holistic) and feature-based (structural). Both approaches are designed to use previous knowledge, obtained from feature extraction, to recognize human faces. The appearance-based approach is based on statistical approaches, where the holistic features of the face image are extracted from the whole image, and therefore use global information instead of local information. Under the appearance-based holistic approach, many techniques are commonly used: (a) the eigenfaces, known as the Principle Components Analysis (PCA) [3, 4, 10], (b) the Fisherfaces known as the linear Discriminant analysis (LDA) [1] , and (c) the Independent Component Analysis (ICA) [5, 6]. PCA is a dimensionality reduction technique; it searches for directions in the dataset that have the largest variance and defines a projection matrix to project the data onto it. This leads to a lower dimensional presentation of the data, and therefore removes some of the noisy directions. In PCA, a 2-dimensional face image with a size p rows and q column pixels can be viewed as a one dimensional vector of dimension $m$ x $n$. The key idea of the PCA approach is to find the vectors that best account for the distribution of face images within the entire $m$ x $n$ image space. These vectors define the subspace of face images, they are called face space. These vectors are the eigenvectors of the covariance matrix. Optimal reductions in dimensionality of the eigenspace, as well as the influence of the training set of faces were studied in [7,8]. In the eigenface, every face in the database is represented as a feature vector of weights. The

weights are obtained by projecting the image onto eigenface components of the projection matrix. For a new test image whose identification is required, the new image is also represented by its vector of weights. The identification of the test image is done by locating the image in the database whose weights are the closest to the weights of the test image [4, 5, 8,]. Although the eigenface/PCA technique shows optimal dimensionality reduction of the face recognition problem, yet it fails to recognize faces when they are viewed with different levels of light or angles or different facial expression. But it is primary problem for all 2D face recognition methods and this problem is caused by capturing facial images for faces databases. The next problem is that, how we reduce face dimension. When the reduction is too large, a lot of important face information is lost and recognition is poor. Although PCA approach has best recognition rate from all 2D face recognition methods. However, eigenfaces have the advantages of speed and efficiency. Any human face can be considered to be a combination of these standard eigenfaces. On the other hand, the feature-based approach deals with local structural information of the face and the relationship among them. It models the face in terms of its geometric descriptors that include distance, angles, and areas between elementary face features such as eyes, mouth, eyebrows, nose, chin, etc [3, 4, 9,].

## III. PROPOSED PCA METHODOLOGY

Basically, PCA approaches typically include two phases: training and classification. In the training phase, an eigenspace is established from the training samples using PCA and the training face images are mapped to the eigenspace for classification. In the classification phase, an input face is projected to the same eigenspace and classified by an appropriate classifier.

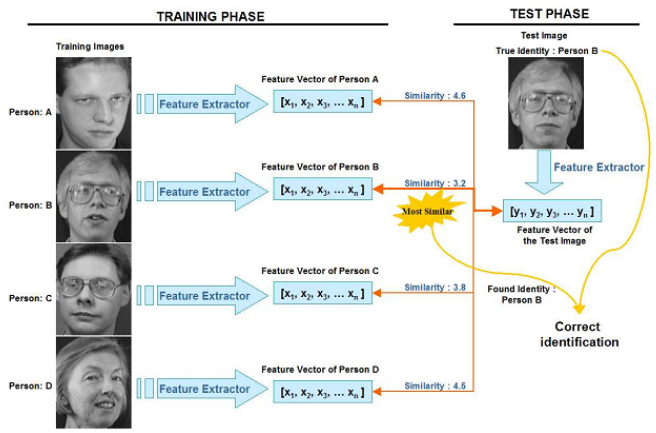


Figure 1. Principle face recognition system using PCA

In the following, a brief description is outlined for the algorithms used more details on the standard eigen-faces approaches may be found in [1, 2, 3, 6, 9].

### A. *Principal Component Analysis PCA –Eigenfaces approach*

PCA, the basis of standard eigenface technique [1, 7] is widely used in face recognition. PCA is mapping data to new space. PCA allows us to compute a linear transformation that maps data from a high dimensional space to a lower dimensional sub-space. The goal of PCA is to reduce the dimensionality of the data while retaining as much as possible of the variation present in the dataset. Traditionally each image is first converted to a vector by row (or column) concatenation. Then PCA is applied for dimensionality reduction. The key idea of the PCA method is to find the vectors that best account for the distribution of face images within the entire *m* x *n* image space. These vectors define the subspace of face images, they are called face space. Because these vectors are the eigenvectors of the covariance matrix corresponding to the original face images, and because they are face-like in appearance, they are called eigefaces. We make this transformation images into the low subspace due to the speed up the computational time and recognition time. PCA subspace is defined by the eigenvectors of the covariance matrix and in this subspace PCA algorithm examines the images. For each eigenvector belong to non-zero eigenvalues of covariance matrix forming the ortonormal base. Examples of PCA subspace is illustrated in next figure 2.

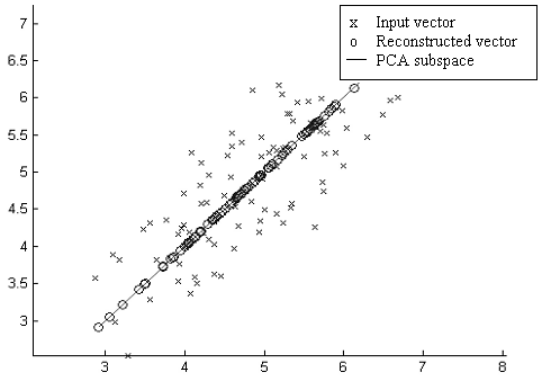


Figure 2. PCA subspace

The following steps summarize the process:

- Let a face image X(x, y) be a two dimensional *m* x *n* array (8-bit Gray Scale) of intensity values. An image may also be considering the vector of dimension *mn*, so that a typical image of size 112x92 becomes a vector of dimension 10304. Let the training set of images {X1, X2, X3… XN}. The average face of the set is defined by

$$\overline{X} = \frac{1}{N}\sum_{i=1}^{n} X_i . \qquad (1)$$

- Calculate the covariance matrix to represent the scatter degree of all feature vectors related to the average vector. The covariance matrix C is defined by

$$C = \frac{1}{N}\sum_{i=1}^{n}(X_i . - \overline{X}).(X_i - \overline{X})^T \quad (2)$$

- The Eigenvectors and corresponding eigenvalues are computed by using

$$C.V = \lambda.V, (V \in R_n, V \neq 0) \quad (3)$$

where $V$ is the set of eigenvectors matrix C associated with its eigenvalue λ.

- Each of the mean centered image project into eigenspace using

Figure 3. Example eigenfaces.

- Next step is to classify eigenvectors (only those with non-zero eigenvalues)

$$W = [V_1, V_2, V_3 ... V_i] \quad (4)$$

where $W$ is linear transformation matrix.

- Project all the training images of $i^{th}$ person to corresponding eigen-subspace

$$y_k^i = w^T(x_i), (i = 1,2,3,...N) \quad (5)$$

- In the testing phase each test image should be mean centered, now project the test image into the same eigenspace as defined during the training phase.
- This projected image is now compared with projected training image in eigenspace. Images are compared with similarity measures. The training image that is the closest to the test image will be matched and used to identify.
- Calculate relative Euclidean distance between the testing image and the reconstructed image of $i^{th}$ person

## IV. EXPERIMENT AND RESULTS

### A. Datasets

The Olivetti Research Lab (ORL) Database of face images provided by the AT&T Laboratories from Cambridge University has been used for the experiment. For some subjects, images were taken at different times varying the lighting, facial expression (open / closed eyes, smiling / not smiling) and facial details (glasses / no glasses). All the images were taken against a dark homogeneous background with the subjects in an upright, frontal position (with tolerance for some side movement).It contains slight variations in illumination, facial expression (open/closed eyes, smiling/not smiling) and facial details (glasses/no glasses). It is of 400 images, corresponding to 40 subjects (namely, 10 images for each class). Each image has the size of 112 x 92 pixels with 256 gray levels. Some face images from the ORL database are as follows:

Figure 4. Some Face images from ORL Database

The ESSEX Yale Face database contains 10 frontal face images of 20 subjects, giving a total of 200 images. Each image has the size of 92 × 112 pixels with 256 RGB levels. Lighting variations include left-light, center-light, and right-light. Spectacle variations include with-glasses and without-glasses. Facial expression variations include normal, happy, sad, sleepy, surprised, and wink. Some face images from the Yale face database are as follows:

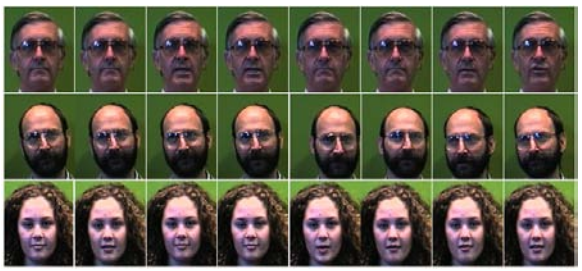

Figure 5. Some Face images from YELL Database

### B. Experiment

The experiment has been done on face databases ORL with different number of training subjects i.e. five, ten, fifteen and twenty. For testing all the images in the database has been considered. Eigenfaces are calculated by using PCA algorithm and experiment is performed by varying the number of eigenfaces used in face space to calculate the face descriptors of the images. The PCA developed in MATLAB. For calculating the recognition rate for PCA with five training images of each subject, 200 images tested for ORL and essex YELL database. It is important to say, that as input for this

algorithm is used gray level images from the ORL database and images are stored with .pgm suffix. Images from YELL database is used for algorithm as RGB level and stored with .pnm suffix. This means that after loading the entire database of face images are all stored as column vectors, with which the algorithm works next.

Examples proposed PCA technique is illustrated in next block diagram.

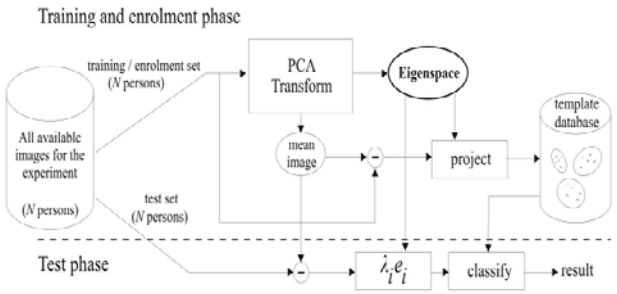


Figure 6. Block diagram PCA method

## C. *Results*

In the first part of our experimental study, first image of 5 subjects from ORL database and next YELL database are selected as prototype; the rest construct the test set. Next we increased up number of subjects on 10, 15, 20 and made recognition experiment again. The results of the experiment on ORL database and YELL database has been shown in next two figures 7 and figure 8 respectively. The first figure 7 show incorrect face recognition result and second figure 8 illustrate correct recognition result.

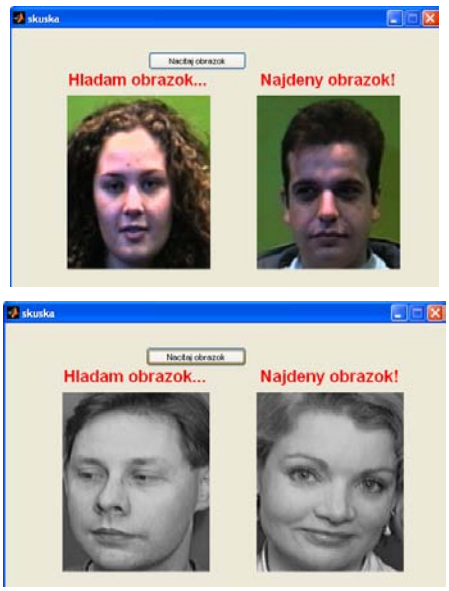


Figure 7. Incorrect face recognition result for ORL (gray level) database.

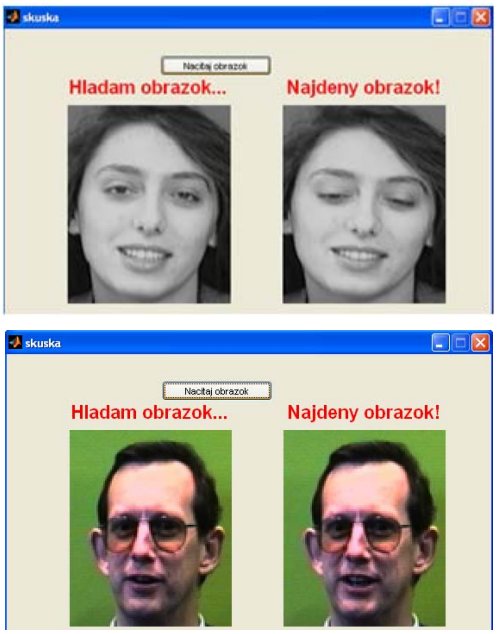


Figure 8. Correct face recognition result for ORL (gray level) database and YELL (RGB level) database.

The corresponding graphical representation of face recognition result has been shown in next diagram.

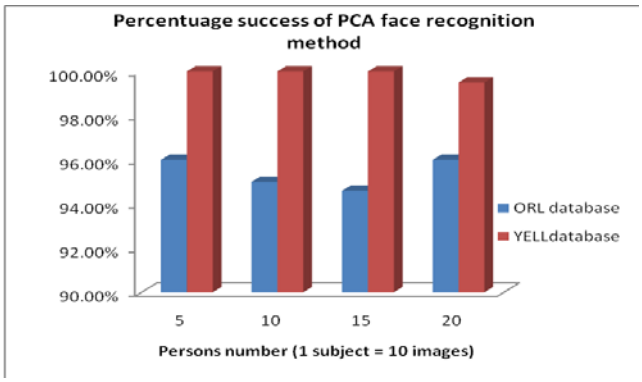


Figure 9. Face recognition success for different number of subjects.

From this diagram we can analyze that the PCA method for face recognition gives quite the good recognition rate. Average recognition rate is about 95% for ORL database and 99, 75% for YELL database. We can say, that for RBG images from YELL database is the result better. This is due to, that gray level images is characterized only one value and RGB level image is characterized using three component values. Thus the result fare recognition is more accurate.

# V. CONCLUSIONS

The paper presents a face recognition approach using PCA. The PCA is the basis of standard eigenface technique [3, 6] is widely used in face recognition .We have introduced a feature extraction technique from still images, which have been

evaluated on well-known database ORL and our YELL database. This technique has been found to be robust against extreme expression variation as it works efficiently on ORL database and YELL database. In the figure 9 can see the recognition rate by varying the number of subjects and the average recognition rate for the ORL dataset is about 95% and for the YELL database is 99, 75%. Future work is suggested towards exploring the combination with LDA, CCA etc.

## ACKNOWLEDGMENT

This paper has been supported by the Slovak Scientist project VEGA grant agency, project no. 1/0570/10, "Algorithms research for automatic analysis of multimedia data" and Slovak Scientist project VEGA grant agency no. 1/0655/10, “Algorithms for capturing, transmition of 3D image for 3D IP television”.

## REFERENCES

[1] P. N. Belhunmeur, J. P. Hespanha, D. J. Kriegman, Eigenfaces vs Fisherfaces Recognition Using Class specific linear projection, IEEE Trans Pattern Analysis and Machine Intelligence, 1997

[2] W. Zhao, R. Chellappa, A. Rosenfeld, and P. J. Phillips. “Face recognition: a literature survey” ACM Computing Surveys, Vol. 35, No. 4, December 2003, pp. 399–458

[3] F. M. H. Yang, D. J. Kriegman, and N. Ahuja, “Detecting Faces in Images: A Survey” IEEE Transactions On Pattern Analysis And Machine Intelligence, Vol. 24, No. 1, January 2002

[4] M. Kirby, L. Sirovich, “Application of the Karhunen-Loeve procedure for the characterization of human faces”, IEEE Trans. Patt. Anal. Mach. Intell. Vol. 12, No. 1, pp. 103-107 1990.

[5] K-C. Kwak, W. Pedryez, “Face Recognition:A Study in Information Fusion using Fuzzy Intrgral,” Pattern recognition Letters, vol. 26, pp. 719-733, 2005.

[6] H. Bernd, T. Koshizen, “Components for Face Recognition ” Proceedings of the 6th International Conference on Automatic Face and Gesture Recognition, Seoul, Korea, pp.153–158, 2004.

[7] A. Pentland, B. Moghaddam, T. Starner, “View-based and modular eigenspaces for face recognition”, Proceedings of IEEE, CVPR, 1994.

[8] A. S. Tolba, A.H. El-Baz, A.A. El-Harby “Face Recognition: A Literature Review”, International Journal Of Signal Processing Volume 2 Number 2 2005 ISSN 1304-4494.

[9] S. Makdee, C. Kimpan, S. Pansang, “Invariant range image multi - pose face recognition using Fuzzy ant algorithm and membership matching score” Proceedings of 2007 IEEE International Symposium on Signal Processing and Information Technology,2007.

[10] H. Bernd and T. Koshizen, “Components for Face Recognition, ” Proceedings of the 6th International Conference on Automatic Face and Gesture Recognition, Seoul, Korea, pp.153–158, 2004.

[11] F. Samaria and A. Harter. “Parameterisation of a stochastic model for human face identification”, In 2nd IEEE Workshop on Applications of

# The Architecture of 3D Reconstruction Algorithm Through Segmentation of Stereo Image Sequence

Patrik Kamencay, Peter Lukáč
Department of Telecommunications and Multimedia
University of Zilina
Zilina, Slovakia
kamencay@fel.uniza.sk, lukac@fel.uniza.sk

***Abstract*—Stereo vision refers to the ability to infer information on the 3D structure of scene from two images taken from different viewpoints. In this paper, architecture for 3D scene reconstruction from stereo image sequence through segmentation is presented. The reconstruction of real objects is one of the most widely known computer vision applications. It is the process of capturing the shape and appearance of real objects. The resultant 3D model have wide application in virtual reality, computer aided design (CAD) and engineering.**

***Keywords-Segmentation; Stereo vision; 3D reconstruction; Markov Random Field; Belief propagation; Graph cut.***

## I. INTRODUCTION

This paper describes a set of algorithms for structure, motion automatic recovery and visualization of a 3D image from a sequence of 2D images. The important step to perform this goal is matching of corresponding pixels in the different views to estimate the depth map. The depth of an image pixel is the distance of the corresponding world point from the camera center. Detecting objects, estimating their pose, geometric properties and recovering 3D shape information are a critical problem in many vision application domains such as robotics applications, high level visual scene understanding, activity recognition, and object modeling [1]. The structure and motion recovery system follows a natural progression, comprising the following phases:

- image acquisition,
- feature matching,
- segmentation,
- feature detection,
- epipolar geometry,
- rectification,
- disparity,
- recovery of 3D structure.

A lot of applications in computer vision are based on a pixel-labeling problem, such as stereo matching, image restoration or object segmentation based on MRF (Markov Random Field) [1], [2], [3]. An important component of an MRF-based approach is the inference algorithm used to find the most likely setting of each node in the MRF. In this paper Belief propagation and Graph cut algorithms are used. In the last years, great advances have been achieved in dense disparity estimation, being Graph cuts and Belief Propagation two of the most outstanding algorithms [1], [4]. Particularly, Belief Propagation has some characteristics which make it very interesting to deal with, i.e. powerful message passing and high flexibility.

These stereo algorithms differ in both the inference algorithm used and the formulation of the MRF. A comparison between these two different approaches for the image segmentation (Graph Cut and Belief Propagation) is described in [2], [3].

The outline of the paper is as follows. In the next section, an overview of basic principle of camera model is introduced. Markov random field based on segmentation is described in Section III. The methods Graph cut and Belief propagation are presented in the Section IV. In Section V the architecture of recovery algorithm is proposed. Finally the experiment results are introduced in Section VI and brief summary is discussed in Section VII.

## II. CAMERA MODEL

The simplest form of real camera comprises a pinhole and imaging plane. A pinhole camera model is used in most of camera calibration methods and is an approximation suitable one for many computer vision applications. This camera model is based on the principle of colinearity, where each point in object space is projected by a straight line through the projection center into the image plane. Model (Figure 1) describes the transformation from world coordinate system (X, Y, Z) to ideal camera image coordinate (x, y).

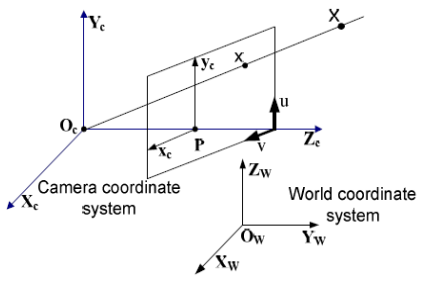


Figure 1. The Pinhole camera model

The camera performs linear transformations from the 3D projective space to the 2D projective space [4]. In order to understand how points in the real world are related mathematically to points on the imaging screen two coordinate systems are of particular interest:

- the external coordinate system,
- the camera coordinate system.

The external coordinate system is denoted by "W" and the camera coordinate system denoted by "C". The point $O_c$, called a central or a focal point, together with the axes $X_c$, $Y_c$ and $Z_c$ determine the coordinate system of the camera.

## III. MARKOV RANDOM FIELD – BASED SEGMENTATION

MRF models are often used for image segmentation, because of their ability to capture the context of an image (i.e., dependencies among neighboring image pixels) and deal with the noise. A typical MRF model for image segmentation, as shown in Figure 1, is a graph with two kinds of nodes: hidden nodes (circles in Figure 2, representing region labels) and observable nodes (squares in Figure 2, representing image pixels). Edges in the graph depict relationships among the nodes.

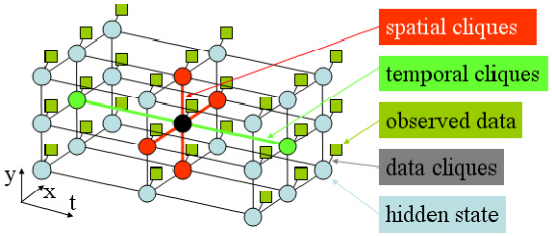


Figure 2. MRF Model

The problem of detecting moving objects in the current image is equivalent to determining whether each pixel is or is not a motion pixel based on the given video observations. In other words, we need to estimate each pixels motion likelihood state, given observed image data. Belief Propagation is a powerful algorithm for making approximate inferences over joint distributions defined by MRF models.

## IV. SEGMENTATION

The goal of image segmentation is to group image pixels into logical groups or segments which may represent objects in the scene. In 3D Segmentation, the grouping is done on voxels in volumetric data as is typically encountered in medical imaging. Segmentation is typically posed as a binary labeling problem where *foreground* and *background* constitutes the set of labels typically assigned to pixels or voxels.

### A. Belief Propagation

Belief propagation is an iterative inference algorithm for graphical models such as MRF which is based on a message passing principle that propagates messages in the network [1], [5].

The above model contains only pairwise cliques, and the joint probability over the 3D volume is

$$P(s_1,..,s_N,d_1,...,d_N)=\prod_{i\neq j}\psi_{i,j}(s_i,s_j)\prod_k\phi_k(s_k,d_k), \quad (1)$$

where $s_i$ and $d_i$ represent state node and data node separately. $\Psi$ is the state transition function between a pair of different hidden state nodes and $\phi$ is the measurement function between the hidden state node and observed data node. $N$ represents the total number of state or data nodes in the 3D volume. Under the squared loss function, the best estimate for node $s_j$ is the mean of the posterior marginal probability (minimum mean squared error estimate, MMSE estimate):

$$s_{jMMSE}=\sum_{s_j}s_j\sum_{s_i,i\neq j}P(s_1,..,s_N,d_1,...,d_N), \quad (2)$$

where the inner sum gives the marginal distribution of $s_j$ [5].

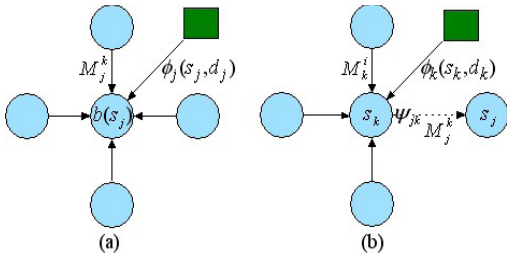


Figure 3. (a) Computing belief; (b) Computing message.

Since the joint probability involves all the hidden state nodes and data nodes in the 3D volume, it is hard to compute the MMSE estimate based on the implicit multivariable probability distribution. However belief propagation messages are effective to compute the MMSE estimate recursively. Each hidden state node has a **belief**, which is a probability distribution defining the node's motion likelihood. Thus the MMSE estimate of one node is computed as:

$$s_{jMMSE}=\sum_{s_j}s_j b(s_j), \quad (3)$$

where

$$b(s_j)=\phi_j(s_j,d_j)\prod_{k\in Neighbor(j)}M_j^k, \quad (4)$$

is the belief at node $s_j$ and $k$ runs over all neighboring hidden state nodes of node $s_j$. The belief at node $s_j$ is the product of all the incoming messages $M$ and the local observed data message $(\phi_j(s_j, d_j))$. The computation is shown in Figure 3 (a). The passed messages specify what distribution each node thinks its neighbors should have. Figure 3 (b) shows how to compute the message from node $s_k$ to $s_j$:

$$M_j^k=\sum_{s_k}\psi_{jk}(s_j,s_k)b(s_k). \quad (5)$$

After substituting $b(s_k)$ by equation (4), we have

$$M_j^k = \sum_{s_k} \psi_{jk}(s_j, s_k)\phi_k(s_k, d_k) \prod_{i \in Neighbor(k)\setminus j} M_k^i, \quad (6)$$

where $i \in Neighbor(k)\setminus j$ denotes all the neighboring nodes of $k$ other than $j$. After multiplying all the incoming messages $M$ from neighboring nodes (except from the node $s_j$) and the observed data message $(\phi_k(s_k,d_k))$, the product is evolved from the message-sender to the message-receiver by transition function $\psi_{jk}(s_j,s_k)$ [5].

### B. Graph Cuts

Segmentation by graph cut is a very interesting approach. The basic idea of this approach is the following:

- each image pixel is viewed as a vertex of a graph,
- the similarity between two pixels is viewed as the weight of the edge of these two vertices,
- segmentation is achieved by cutting edges in the graph to form a good set of connected components.

A graph $G = (V, E)$ can be partitioned into two disjoint sets, $A, B, A \cup B = V, A \cap B = 0$ by simply removing edges connecting the two parts. A directed weighted graph $G = (V, E)$ consists of a set of nodes $V$ and a set of directed edges $E$ that connected them [6].

A graph normally contains some additional special nodes that are called terminals, usually called the source $s \in V$ and the sink $t \in V$ [7].

The degree of dissimilarity between these two pieces can be computed as total weight of the edges that have been removed. In graph theoretic language it is called the cut:

$$cut(A,B) = \sum_{u \in A, v \in B} w(u,v) \quad (7)$$

Graph cut provide:

- for less interesting $V$, polynomial algorithm for global minimum,
- for a particulary interesting $V$, approximation algorithm,
- for many choices of $V$, algorithms that find a strong local minimum,
- good experimental results.

In Figure 4 we show a simple example of a two terminal graph.

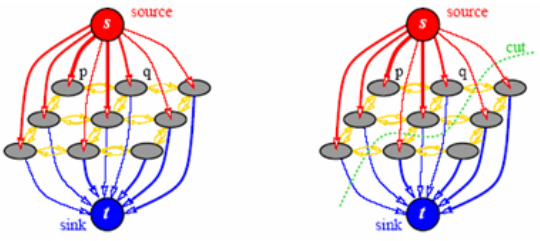


Figure 4. (a) A graph $G$; (b) A cut on $G$.

## V. The Proposed Architecture of Reconstruction Algorithm Based on Segmentation Method - Belief Propagation

The input to the 3D reconstruction algorithm is a stereoscopic pair images. The images are captured using a pair of digital cameras. The 3D reconstruction will be based on extracting dense depth information from the input image pair. In the heart of the 3D reconstruction procedure lies a stereo matching algorithm. The proposed 3D reconstruction architecture is illustrated at Figure 7.

Camera calibration is a necessary step in 3D computer vision in order to extract metric information from 2D images. We have used the Camera Calibration Toolbox for Matlab in our 3D reconstruction [8]. With this toolbox, we can determine camera properties, position and orientation. The parameters of a stereo system: intrinsic and extrinsic parameters.

Intrinsic parameters:

- focal length,
- principal point,
- skew coefficient,
- distortions.

These parameters characterize the transformation mapping an image point from camera to pixel coordinates, in each camera.

Extrinsic parameters:

- relative 3D rotation, 3x3 matrix $R$,
- relative 3D translation, 3x1 vector $T$.

Describe the relative position and orientation of the two cameras.

The corner detection is the first step in the camera calibration process.

The coordinates of the all corners point was used during the calibration. We compute the intrinsic and the extrinsic parameters from this coordinates. In this experiment we used Harris corner detector.

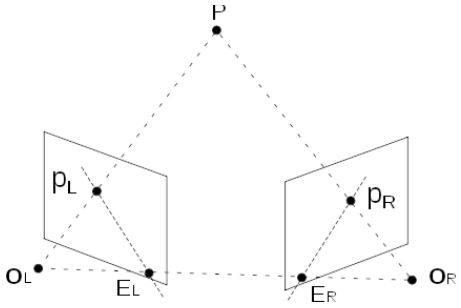


Figure 5. Epipolar Geometry

Epipolar geometry (EG) is the geometry of stereo vision. When two cameras view a 3D scene from two distinct positions, there are a number of geometric relations

between the 3D points and their projections onto the 2D images that lead to constrains between the images points [9], [10].

Example of epipolar geometry is shown on Figure 5. Two cameras, with their respective focal points $O_L$ and $O_R$, observe a point P. The projection of P onto each of the image planes is denoted $p_L$ and $p_R$. Points $E_L$ and $E_R$ are the epipoles.

All epipolar lines go through the cameras epipole. Corresponding points must lie on conjugate epipolar lines. The search for correspondences is reducing to a 1D problem.

Rectification is a transformation which makes pairs of conjugate epipolar lines become collinear and parallel to the horizontal axis. Searching for corresponding points becomes much simpler for the case of rectified images [9].

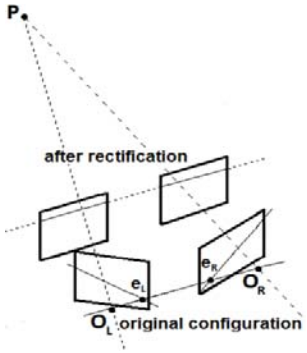


Figure 6. Image rectification

Disparity is the distance between corresponding points when the two images are superimposed. The disparities of all points form the disparity map [6].

The proposed architecture of 3D reconstruction algorithm:

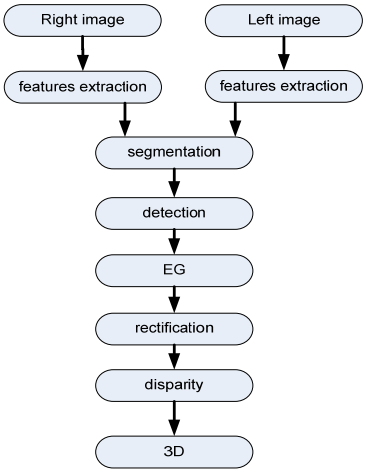


Figure 7. Architecture of reconstruction algorithm

## VI. EXPERIMENTS

This section describes the experiments that verify the earlier sections.

### A. *Belief Propagation versus Graph Cuts*

For the images shown in Figure 8, Belief propagation is superior. The primary reason for this superiority appears to be that the Graph Cut algorithm assigns portions of the background to have very small disparity.

An example of segmentation can be seen in Figure 9. Belief Propagation (b) does preserve some structures that Graph Cuts (a) does not.

Figure 8. Input images

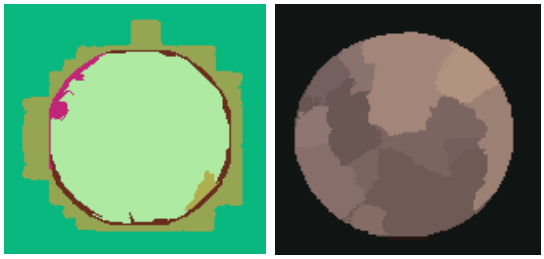

Figure 9. Graph Cut versus Belief Propagation

These two segmentation algorithms were compared using automatic algorithm evaluating the precision of segmentation This plays important role for two reasons: (1) it can be placed into a feedback loop to enforce another run of segmentation algorithm that may include more sophisticated steps for high precision segmentation and (2) the outcome of this evaluation can be treated as a quality factor and thus can be used to design a quality driven adaptive recognition system.

TABLE I. PRECISION BELIEF PROPAGATION VERSUS GRAPF CUT

| PRECISION | |
|---|---|
| **BP** | **GC** |
| 0,5872 | 0,3735 |
| 0,5725 | 0,4353 |
| 0,5765 | 0,3743 |
| 0,6092 | 0,4053 |
| 0,5833 | 0,3795 |
| 0,5993 | 0,3902 |
| 0,6107 | 0,3704 |
| 0,5162 | 0,3217 |
| 0,5688 | 0,3673 |
| 0,6069 | 0,4066 |
| 0,5831 | 0,38241 |

The presented algorithms were implemented in MATLAB environment. The final comparison was made by using the evaluation criterion. The criterion used for comparing

segmentation algorithms presented in this article in chapter IV. This evaluation criterion is based on computing precision. Each of the algorithms is compared with segmentation by a human. Average value of segmentation precision for Belief Propagation algorithm was approximately 58 percent. For Graph Cut average value of segmentation precision was 38 percent.

### *B. Corner detection*

The corner detection is the first step in the camera calibration process. The coordinates of the all corners point was used during the calibration. We compute the intrinsic and the extrinsic parameters from this coordinates.

Corner detection:

- Harris corner detector,
- Canny detector.

In this experiment we used Harris corner detector. The basis for image reconstruction is to find outstanding corners in images and compare them. This detector is today the most commonly used. The Harris corner detector is based on the local autocorrelation function. The principle of the algorithm consists in calculating the auto-correlation matrix for each image point.

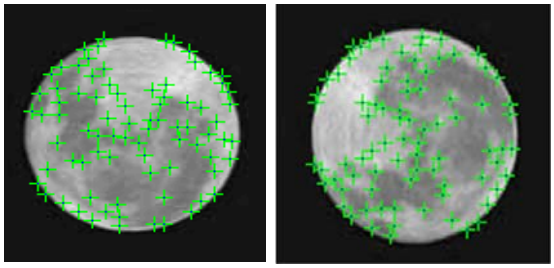

Figure 10. Corner detection

### *C. Disparity map and Creating 3D model*

A disparity map codifies the distance between the object and the cameras: closer points will have maximal disparity and farther points will get zero disparity. For short, a disparity map gives some perception of discontinuity in terms of depth. The 3D model is obtained from each pixel of the disparity map.

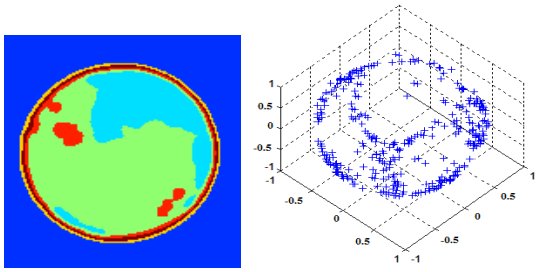

Figure 11. Disparity map, 3D object

The final reconstructed 3D is seen in figure 11. This model represents a 3D object using a collection of points in 3D space, connected by various geometric entities such as lines, curved, surfaces. 3D model can be created by algorithmically (procedure modeling) or scanned.

## VII. CONCLUSION

The method for reconstructing a 3D scene from two input images was presented. We mentioned some manners allowing a three - dimensional reconstruction of picture or object in this article. The proposed system is based on 3D reconstruction solution using stereo images. This system works with common cameras. The applications of these methods of 3D picture processing are very usefull in sphere of medicine, for example detection and identification of tumor in brain and also in other branches as physics, astronomy, biology or geography. Future task we could speed up computation time and improve precision of Belief propagation algorithm.

## ACKNOWLEDGMENT

This paper has been supported by the Slovak Scientist project VEGA grant agency, Project No. 1/0655/10 “Algorithms for capturing, transmition and reconstruction of 3-D image for 3-D IP television”.

## REFERENCES

[1] J. S. Yedida, W. T. Freeman, Y. Weiss, J., “Understanding belief propagation and it is generalizations” Exploring Artificial Intelligence in the New Millennium, Chap. 8, pp. 239-236, January 2003.

[2] J. Sun, N. N. Zhang, H. Y. Shum, Stereo matching using belief propagation. In IEEE Transactions on Pattern Analysis and Machine Intelligence, 25(7):787-800, 2003.

[3] M. F. Tappen, W. T. FREEMAN, Comparison of graph cut with belief propagation for stereo using identical MRF parameters. In IEEE International Conference on Computer Vision, 2003.

[4] J.B. Frey, R. Koetter, N. Petrovic, *Very loopy belief propagation for unwrapping phase images.* In T. G. Dietterich, S. Becker, and Z. Ghahramani, editors, *Advances in Neural Information Processing Systems 14*, Cambridge, MA, MIT Press, 2004.

[5] Z. Yin, R. Collins: *Belief Propagation in a 3D Spatio - temporal MRF for moving object detection,* Department of Computer Science and Engineering, The Pennsylvania State University, University Park, PA, 2007.

[6] M. Benco, R. Hudec, The advanced image segmentation techniques for broadly useful retrieval in large image database, Zborník z medzinárodnej vedeckej konferencie "Nové smery v spracovaní signálov IX.", Tatranské Zruby, Slovak Republic, pp. 40-44, May 2006, ISBN 978-80-8040-344-7.

[7] Y. Boykov, O. Veksler, R. Zabih, Fast Approximate Energy Minimization via Graph Cuts, Proc. IEEE Trans. Pattern Analysis and Machine Intelligence, vol. 23, no. 11, pp. 122-123, 2005.

[8] Bouguet, J. Y.: Camera Calibration Toolbox for Matlab, http://www.vision.caltech.edu/bouguetj/calib_doc/

[9] A. Fusiello and L. Irsara. Quasi-euclidean Uncalibrated Epipolar Rectification. International Conference on Pattern Recognition (ICPR), Tampa, FL, 2008.

[10] T. Azevedo, J.M. Tavares, M.A. Vaz, Development of a computer platform for object 3D reconstruction using computer vision techniques, 2007.

# Summary

The KTTO 2010 Conference was held in the aula of the Technical University of Ostrava on 9th and 10th December 2010. The authors of about fifty papers, which passed through reviews and were accepted, were invited to present them. During the opening ceremony, the contribution to the field of telecommunications by professor Divis was appreciated, namely his efforts in establishing this branch at the Technical University of Ostrava. Looking back at those fifteen years, it is evident that a major progress was achieved under his leadership. Prof. Divis then reminded the first sad anniversary of prof. Blunar's death and his crucial role in establishing telecommunications in Ostrava.

The subsequent lectures were divided into two days and nine sections. The individual parts of the conference program were moderated by chairmen who also managed discussions on presented topics. The KTTO 2010 Conference was accompanied by a workshop on TriplePlay testing. The social evening, taking place in several venues at the famous Stodolni street in Ostrava, was no less successful. Next year, KTTO 2011 will move one hundred kilometres to Polish Szczyrk. It will be held on 22nd - 24th June 2011 and we will be co-organisers together with our partners of the University of Bielsko-Biala.

In conclusion, I would like to thank my colleagues from conference committee who actively participating in the preparations and made the success of the conference possible. I would also like to thank all lecturers, authors of papers and their reviewers. Last but not least, I would also like to thank our media partner Averia and ProfinetTest.

Miroslav Voznak
KTTO 2010 chairman
In Ostrava, December 11th 2010